GEOLOGY OF THE ARABIAN PENINSULA

Shield Area of Western Saudi Arabia

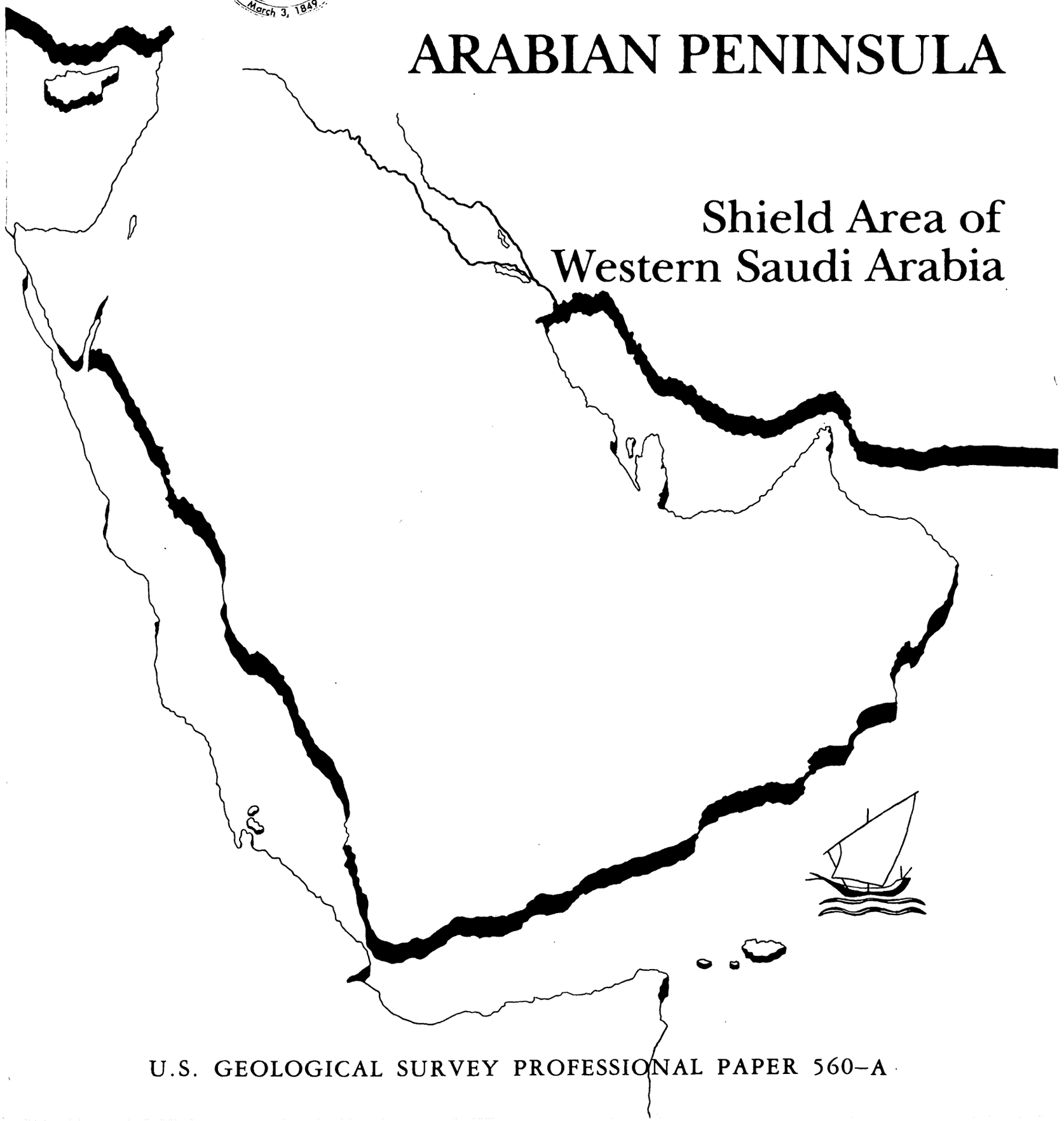

U.S. GEOLOGICAL SURVEY PROFESSIONAL PAPER 560–A

The Earth from space. Africa and Arabia lie north of the Indian and Atlantic Oceans, cloud-draped from the Antarctica Ice Cap to the Equator.

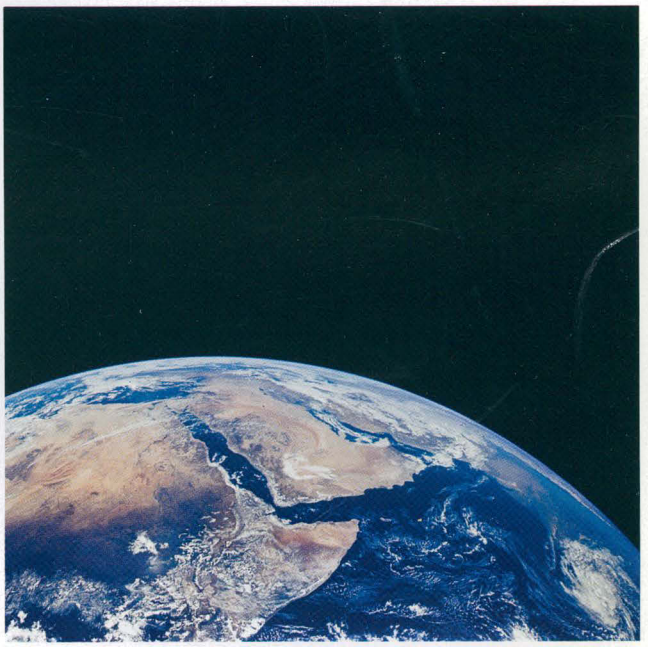

A closer view shows northeast Africa, the Arabian Peninsula, and the Arabian Sea. Photographs from Apollo 17 spacecraft at about 100,000 nautical miles from Earth.

GEOLOGY OF THE ARABIAN PENINSULA

SHIELD AREA OF WESTERN SAUDI ARABIA

FRONTISPIECE.—The Arabian Shield. As seen from space, the shield appears as a red crescent on the west side of the Arabian Peninsula and as a continuation of the Sahara Desert extending across north Africa. Photograph from Apollo II spacecraft at about 98,000 nautical miles from Earth.

Geology of the Arabian Peninsula

Shield Area of Western Saudi Arabia

By GLEN F. BROWN, DWIGHT L. SCHMIDT, *and* A. CURTIS HUFFMAN, JR.

U.S. GEOLOGICAL SURVEY PROFESSIONAL PAPER 560–A

Prepared in cooperation with the Ministry of Petroleum and Mineral Resources, Deputy Ministry of Mineral Resources, Jiddah, Kingdom of Saudi Arabia

A review of the geology of western Saudi Arabia as refined from U.S. Geological Survey Miscellaneous Geologic Investigations Map I–270A, "Geologic Map of the Arabian Peninsula", 1963

UNITED STATES GOVERNMENT PRINTING OFFICE, WASHINGTON: 1989

DEPARTMENT OF THE INTERIOR

MANUEL LUJAN, JR., *Secretary*

U.S. GEOLOGICAL SURVEY

Dallas L. Peck, *Director*

Library of Congress Cataloging in Publication Data

Brown, Glen Francis, 1911–
Shield area of Western Saudi Arabia.

(U.S. Geological Survey professional paper ; 560–A)
"A review of the geology of western Saudi Arabia as refined from U.S. Geological Survey miscellaneous geologic investigations map I–270–A, 'Geologic map of the Arabian Peninsula,' 1963."
Bibliography: p.
Supt. of Docs. no.: I 19.16:560–A
1. Geology—Saudi Arabia. I. Schmidt, Dwight Lyman, 1926– . II. Huffman, A.C. III. Title. IV. Series: Geological Survey professional paper ; 560–A.
QE291.S28B76 1989 555.3'8 87–600038

For sale by the Books and Open-File Reports Section, U.S. Geological Survey, Federal Center, Box 25425, Denver, CO 80225

FOREWORD

This volume, "The Geology of the Arabian Peninsula," is a logical consequence of the geographic and geologic mapping project of the Arabian Peninsula, a cooperative venture between the Kingdom of Saudi Arabia and the Government of the United States. The Arabian-American Oil Co. and the U.S. Geological Survey did the fieldwork within the Kingdom of Saudi Arabia, and, with the approval of the governments of neighboring countries, a number of other oil companies contributed additional mapping to complete the coverage of the whole of the Arabian Peninsula. So far as we are aware, this is a unique experiment in geological cooperation among several governments, petroleum companies, and individuals.

The plan for a cooperative mapping project was originally conceived in July 1953 by the late William E. Wrather, then Director of the U.S. Geological Survey, the late James Terry Duce, then Vice President of Aramco, and the late E.L. deGolyer. George Wadsworth, then U.S. Ambassador to Saudi Arabia, and Sheikh Abdullah Sulaiman, then Minister of Finance of the Government of Saudi Arabia, lent their support to the plan. In November of the following year, 1954, Director Wrather approved the U.S. Geological Survey's participation and designated G.F. Brown responsible for the western Arabian shield region in which he had previously worked under U.S. foreign-aid programs. In January 1955, F.A. Davies, Chairman, Board of Directors, Arabian-American Oil Co., approved Aramco's participation and appointed the late R.A. Bramkamp, chief geologist, responsible for compilation of the area within the Kingdom where the sediments crop out. This responsibility fell to L.F. Ramirez following the death of R.A. Bramkamp in September 1958.

R.A. Bramkamp and G.F. Brown met in New York in February 1955 and planned the program, including scales of maps, areas of responsibility, types of terrain representation, and bilingual names. Thus there was established a cooperative agreement between the Kingdom of Saudi Arabia, the U.S. Department of State, and the Arabian-American Oil Co. to make available the basic areal geology as mapped by Aramco and the U.S. Geological Survey.

The agreement specified publication of a series of 21 maps on a scale of 1:500,000, each map covering an area 3° of longitude and 4° of latitude. Separate geologic and geographic versions were to be printed for each of the quadrangles; both versions were to be bilingual—in Arabic and English. A peninsular geologic map on a scale of 1:2,000,000 was to conclude the project.

High-altitude photography, on a scale of 1:60,000, of the Kingdom of Saudi Arabia was initiated during 1949 by the Aero Service Corp. and completed in 1959. Both third-order vertical and horizontal control and shoran were utilized in compiling the photography. This controlled photography resulted in highly accurate geographic maps at the publication scale which then served as a base for the geologic overlay. The topography of the sedimentary areas was depicted by hachuring and that of the shield region by shaded relief utilizing the airbrush technique.

The first geographic quadrangle was published in July 1956 and the last in September 1962. While preparation of the geographic sheets was in progress, a need arose for early publication of a 1:2,000,000-scale peninsular geographic map. Consequently, a preliminary edition was compiled and published in both English and Arabic in 1958. The second edition, containing additional photography and considerable new topographic and cultural data, was published in 1963. The first of the geologic map series was published in July 1956 and the final sheet in early 1964. The cooperative map project was completed in October 1963 with the publication of the 1:2,000,000-scale "Geologic Map of the Arabian Peninsula" (Miscellaneous Geologic Investigations Map I–270 A).

As work on the quadrangles progressed, geologists, companies, and governments working in areas adjacent to the Kingdom of Saudi Arabia were consulted by Aramco and invited to participate in the mapping project. The number of cooperating participants was expanded to 11, which included the operating oil companies in the peninsula and which are identified elsewhere in this text; the Overseas Geological Surveys, London; the Government of Jordan; F. Geukens, who had worked in Yemen; and Z.R. Beydoun, who had studied the Eastern Aden Protectorate. With the close cooperation of the authors, the new data were added to data already plotted on the base map of the Arabian Peninsula.

As the geological coverage of the peninsular map grew, the need for a text to accompany the map became

apparent to both the U.S. Geological Survey and the Aramco geologists. Exploratory conversations were begun by Aramco with companies working in the other countries of the Arabian Peninsula for their participation in the preparation of a monograph on the geology of the Arabian Peninsula. Each author prepared a description of the geology of the area for which he was responsible, as shown in the sources of geologic compilation diagram on the peninsular map. The U.S. Geological Survey undertook the publishing of the volume as a professional paper, and the Government of Saudi Arabia was to finance its printing. It was early agreed that there would be no effort to confine the contributions to a standard format and that no attempt would be made to work out an overall correlation chart other than shown on the "Geologic Map of the Arabian Peninsula." Thus, the individual style of authors of several nationalities is preserved.

Cooperation and relations have been of the highest order in all phases of the work. The project would not have been possible without the full support of the U.S. Department of State, the Kingdom of Saudi Arabia, and all contributors. In fact, the funds which made publication of this volume possible were contributed by the Saudi Arabian Government.

The data provided by the maps and in the professional paper provide information for an orderly scientific and economic development of a subcontinent.

O. A. SEAGER,
Arabian-American Oil Co. (Retired)

W. D. JOHNSTON, JR.,
Former Chief, Foreign Geology Branch,
U.S. Geological Survey (Deceased)

CONTENTS

ILLUSTRATIONS

[Plates are in pocket]

FIGURES

TABLES

GEOLOGY OF THE ARABIAN PENINSULA

SHIELD AREA OF WESTERN SAUDI ARABIA

By GLEN F. BROWN, DWIGHT L. SCHMIDT, and A. CURTIS HUFFMAN, JR.

"Nay, the very slate beds of Snowdonia have not forced their way up from under the mountain without long and fearful struggles. They are set in places upright on end, then horizontal again, then sunk in an opposite direction, then curled like sea-waves, then set nearly upright once more, and faulted through and through...."

Charles Kingsley, *in* Town Geology (1873)

ABSTRACT

Western Arabia lies within the low-latitude desert of north Africa and the Middle East, the core being the Arabian segment of the African Shield. The core of complex basement rocks accounts for about 670,000 km^2, or one-third of the Arabian Peninsula. Reconnaissance mapping of these crystalline rocks, together with bordering sedimentary rocks and volcanic flows, begun in 1950, resulted during the next 13 years in a series of geologic and geographic maps without extensive texts. The maps served as general guides for development of natural resources, including water supplies, ore deposits, and building materials. An intensive exploration program that began in 1963 and involved numerous geologists has vastly increased geologic information.

Rainfall in Arabia is meager and episodic, and vegetation is sparse except in isolated copses on the crest of the Hejaz Range. Comparison of flora with similar species in the Sudan, where records of rainfall have long been kept, allows evaluation of mean annual precipitation. Wandering bedouin following fodder created a delicate balance between population and water supply—now disturbed by wells drilled in alluvium and lava fields.

A trapezoidal region of Precambrian crystalline rocks lies along the northeast flank of the Red Sea, with two long prongs extending northwest and southeast for a total of 1,800 km. These basement rocks of the Arabian Shield are well exposed on the uplands, scarp mountains, and coastal pediments where the Phanerozoic cover rocks have been stripped as a result of Paleozoic epeirogeny and Tertiary ramping. The shield outcrops are divided into three tectonic provinces by N. 45° W.- trending shear zones of the Najd fault system of latest Proterozoic and possibly earliest Paleozoic time. The southwestern province, the 'Asīr[1] upland, was sharply uplifted and tilted to the northeast during the Neogene. The northwestern province, consisting of the Ash Shifā'- Hismā upland as well as Jabal Shammar farther east, similarly was uplifted and tilted. These two provinces are separated by the flat-lying median Najd province, which is chiefly bounded by the principal Najd faults.

The outcrops of the shield rocks are of the Late Proterozoic Eon—upper Riphean to Vendian or Infracambrian epochs, including the Ediacarian System. The most reliable isotopic ages range from about 900 to 560 m.y., but some Middle Proterozoic rocks may be present in the easternmost shield. The rocks are divided into six lithostratigraphic sequences, two plutonic suites, and an ophiolitic suite. The mafic and ultramafic volcanic and plutonic rocks of the ophiolitic suite everywhere were emplaced tectonically and are probably of different ages in different places. Some ophiolite occurs as obducted blocks, but most is highly deformed and altered to serpentinite in fault zones that mostly define sutures between different tectonic blocks or terranes within the shield.

Three of the lithostratigraphic sequences consist of mafic to silicic volcanic rocks and volcanic-derived clastic rocks which, with their subvolcanic plutonic rocks of a dioritic suite, probably formed in oceanic island arcs during convergent plate tectonism. These rocks make up the primary, or first-formed, crust of the shield. Chemical analyses show that the primary shield rocks, regardless of age, are principally calc-alkalic with some associated tholeiitic varieties. Most of the layered rocks are andesitic, but they range from basalt to dacite and in places contain intercalated pillow basalt, marble, chert, and carbonaceous or graphitic schist. Most of the plutonic rocks of the dioritic suite are dioritic, but they range from gabbro to trondhjemite and rarely contain potassium feldspar. The sequences and an associated dioritic suite become younger toward the eastern shield, that is, the primary crust of the shield youngs toward the east.

Two western sequences consist of the Jiddah (Samran) and Baish-Bahah Groups and range in radiometric age from about 900 to 800 m.y.; the eastern sequence consists of the Halaban (Hulayfah) Group and ranges from 800 to about 700 m.y. During subsequent orogeny, most of the rocks were intensely deformed and mostly metamorphosed to upper greenschist facies, but rising in places to the almandine-amphibolite facies.

Two other lithostratigraphic sequences with an associated plutonic granitic suite are the products of two mountain-building episodes during which the primary crust was greatly thickened and converted into craton. The two sequences, including largely the Ablah (Al Ays) and Murdama (Shammar) Groups, consist of abundant sedimentary rocks, commonly arkosic, that are the erosional products of the

[1]Geographic place names follow, in general, the U.S. Board on Geographic Names "Official Standard Names Gazetteer, Saudi Arabia, 1978," except where new names are introduced and where general usage has anglicized the spelling. Diacritical marks are added to help transliteration into Arabic. Local usage is followed for practicality as comprehended.

Manuscript approved for publication October 30, 1986.

orogenic mountains. They are several thousand meters thick. Less abundant calc-alkalic to alkalic volcanic rocks, commonly dacitic and rhyolitic, are intercalated with the sedimentary rocks. The plutonic rocks of the granitic suite in association with both sequences have syntectonic and posttectonic phases, are products of the orogenies, and are the principal new ingredients making up the craton.

Gneiss domes were a significant part of these cratonization orogenies. In association with orogenic crustal heating, some of the low-density, more silicic tonalitic and trondhjemitic rocks of the primary crust rose as gneiss domes. Partial melting in the middle or lower crust below the gneiss domes produced large volumes of granitic magma that intruded the gneiss domes as granodioritic batholiths.

The Ablah Group and the older part of the granitic suite are about 775 to 740 Ma old and are associated with the Ablah orogeny and early cratonization in the western and earlier formed half of the shield. The Murdama (Shammar) Group and the younger part of the granitic suite are about 660 to 580 Ma old and are associated with the culminant orogeny and late cratonization that was shieldwide. The granitic suite during both orogenies consists of early, syntectonic granodiorite batholiths associated with the gneiss domes and late, posttectonic monzogranite plutons. Only during the culminant orogeny, late magmatic evolution produced syenogranite and alkali-feldspar granite commonly in circular and ring-structured plutons and with associated explosive volcanic deposits (Shammar Group); final products, some of which have economic potential, were peralkalic and peraluminous. The late plutonism of the culminant orogeny was distinctly bimodal in that subordinate gabbroic rocks are associated with the granites.

Various building blocks or terranes of the andesitic and dioritic primary crust were collisionally agglomerated during the Ablah orogeny, early cratonization, whereas the entire shield as currently exposed was further collisionally accreted and compressionally consolidated during the culminant orogeny, final cratonization. Thousands of kilometers of oceanic crust had to be subducted in about 300 m.y. to form the large primary crust of the Arabian Shield. The inevitable collisional events during consumption of such a large volume of oceanic crust invariably led to numerous collisional orogenies that collectively encompass the widely known Pan African tectonic episode.

The youngest lithostratigraphic sequence, the Jubaylah Group, is essentially postcratonic, although it is the end product of the collisional culminant orogeny. Final east-west compression of the entire shield from about 580 to 560 m.y. caused the craton to fracture along the large northwest-trending, left-lateral faults and elsewhere along lesser, northeast-trending, right-lateral, conjugate faults of the Najd fault system. Erosional products of this more localized deformation were the sedimentary rocks of the Jubaylah Group, which also includes intercalated andesitic to basaltic volcanic rocks of a mafic alkalic compositional trend.

The collisional edge of an old continental plate (or tectonic fragments thereof), suspected on the eastern edge of the Arabian Shield, has not been shown with certainty to be exposed. Presumably, widespread contamination from such an old continental crust affects U/Pb, Sm/Nd, Rb/Sr, and common lead ratios in the young plutonic rocks of the easternmost shield. One mass of anorthosite near Jabal Khidā' on the central eastern edge of the shield may be a fragment of this old continental plate in that associated granodiorite may be as old as 1,600 to 1,800 Ma.

Epeirogenic uplift, erosion, and cooling of the uppermost shield during Early and Middle Cambrian time is indicated by an average fission track age of 510±52 m.y., on sphene from diorite (hornblende K-Ar age of 615±12 m.y.) in the southwestern part of the shield. The hiatus was followed by extensive deposition of the Cambro-Ordovician Saq Sandstone in the north and northeast and the Wajid Sandstone in the southeast and south of the shield. The Cambrian Siq Sandstone had already been deposited in the northern part. During the middle and late Paleozoic, broad epeirogeny caused further erosion of the shield until marine transgression deposited the Upper Permian Khuff Formation at least in the eastern part of the shield. In the southwestern shield, the nonmarine Upper Triassic Khums Sandstone was deposited variably on Wajid or Precambrian rocks and is overlain by limestone of the middle Upper Jurassic Amran Formation.

Except for shallow marine sandstone of problematic Cretaceous age deposited on the Amran Formation in the southwestern shield and on Precambrian rocks in the northwestern shield, the younger beds on the shield are Paleocene and younger, with the possibility that the lowermost are upper Maestrichtian. The early Tertiary beds contain vertebrate fossils of coastal marine or estuarine environment 250 km east of the Red Sea in the central shield. Marginal marine sediments were deposited in a western tongue of the latest Tethys Sea as late as Eocene on the western shield and at least as far south as Jiddah.

The great harrats of flood basalt erupted on the western shield during late Oligocene and early Miocene at the same time a 2,000-km-long continental rift valley developed along the future Red Sea axis. Within this rift valley, Baid freshwater tuffaceous lakebeds were deposited between mafic and silicic volcanoes. During late early Miocene time, the Red Sea opened at a rate of 4.4 cm/yr in a first-stage movement while continental dikes and swarms of oceanic tholeiitic dikes, gabbro, and granophyre plutonic rocks were intruded into the rift sedimentary and volcanic rocks at the newly formed continental margin. The continental margin was deformed and greatly extended at this time. About 14 or 15 m.y., as the first-stage spreading stopped, the Red Sea Escarpment rose; its erosion caused deposition of coarse conglomerate of the Bathan Formation. About 3,000 m of evaporite was deposited on the young Red Sea oceanic crust during the late Miocene desiccation crisis.

A second stage of sea-floor spreading about 4–5 m.y. produced the Red Sea axial trough, consisting of oceanic crust, as well as renewed uplift and tilting of the three tectonic provinces in response to compression from counterclockwise rotation against the Dead Sea Rift. This late movement caused widespread major stream capture, especially along the wadis that formerly drained southwesterly or northwesterly, the channels turning westward through narrow gorges to the coastal plain and the Red Sea.

INTRODUCTION

The mapping of the geology of the Arabian Shield of Saudi Arabia during the period 1950 to 1958, as shown on Miscellaneous Geologic Investigations Map I–270A by the U.S. Geological Survey and the Arabian-American Oil Company (USGS–ARAMCO, 1963), was part of a larger program undertaken by the Kingdom of Saudi Arabia and the Government of the United States (see "Foreword" for details). The geology shown on the geologic map of this report (pl. 1) is a revision of part of Map I–270A and represents a compilation of geologic mapping done as part of the USGS-Saudi Arabian program from 1963 to the present. As chapter A of USGS Professional Paper 560, this report synthesizes and brings up to date a large amount of geologic data gathered by many individuals.

Prior to the inception of USGS fieldwork in 1950, almost no geologic studies of the western part of the Arabian Shield (fig. 1, pl. 1) had been made. This lack

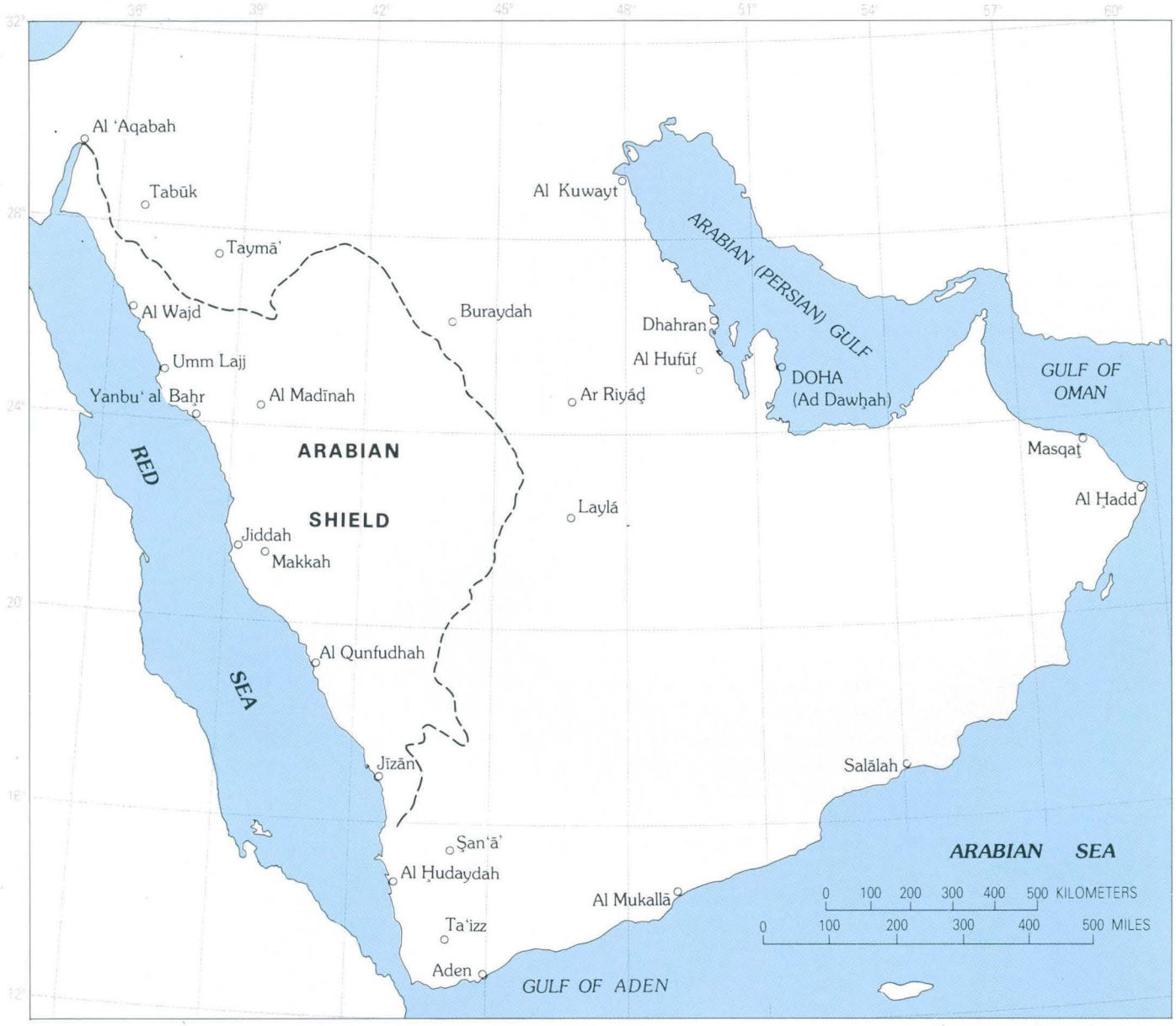

FIGURE 1.—Location of the Arabian Shield, Arabian Peninsula.

contrasted sharply with the wealth of data available for central and eastern Arabia, where petroleum companies have been actively exploring for nearly 50 years. Fieldwork from 1950 to 1958 contributed information for the western part of the geologic map of the Arabian Peninsula (USGS–ARAMCO, 1963) and for a series of 20 quadrangle maps. As a base for geologic mapping, the USGS field party used aerial photography and necessarily described petrologic units in field terms because it was soon recognized that the shield rocks that could be classified into lithostratigraphic groups ranged from nonmetamorphosed facies through greenschist and amphibolite metamorphic facies. These Precambrian rocks are intricately folded and faulted, and in addition are intruded by numerous hypabyssal and plutonic igneous rocks. Nonetheless, from 1950 to 1963 the USGS laid the groundwork for economic development in the Arabian Peninsula of other than hydrocarbons by completing and publishing reconnaissance maps of 670,000 km^2 of complex basement rocks—and also by accomplishing its primary purpose of evaluating the economic, principally hydrologic, possibilities of the region. The resulting maps were published as a series of quadrangle maps at 1:500,000 scale (geologic

I–200 to I–220A, geographic I–200 to I–220B) and a geologic map of the entire peninsula published at 1:2,000,000 scale (I–270A). Beginning in 1963, emphasis was placed on economic mineral resource evaluation of the shield as well as continued mapping of the shield rocks.

The economic boom in Saudi Arabia since 1970 has led to more detailed mapping by many geologists from several nations, besides a growing number of Saudi Arabian geologists, with the result that the quality of geologic knowledge and interpretation of the western part of the shield now approaches that obtained by earlier petroleum exploration in the area of sedimentary cover of the shield. This report describes the layered and massive igneous rocks of the Arabian Shield area in western Saudi Arabia and traces the evolution of the geologic nomenclature from 1950 to the geologic names as they are currently being used (1984). Data from geophysical and geochemical field studies have aided these intensified surveys, as have results of chemical and petrographic analyses prepared in laboratories in Jiddah and abroad. Diamond-drilling at encouraging prospects has added some third dimension. Perhaps the most important studies have been isotope measurements for determining radiometric ages (Baubron and others, 1976; Fleck and others, 1976, 1980; Aldrich and others, 1978; Cooper and others, 1979) which supply the "pegs" on which the Precambrian geologic history hangs, because fossils in the Arabian Shield are limited to stromatolitic and related forms of debatable value as time markers. Fortunately, the Arabian segment of the African megacraton is well exposed, and ideas on the outcrop can and have been challenged. The diversity of geologic concepts from various disciplines and many cultural backgrounds has done much to elucidate the geology of the segment.

Like chapter D of Professional Paper 560 (Powers and others, 1966), this report is essentially a compilation which, without the chronological data and the large volume of work done by many geologists since the preliminary map was published, would be less useful. This report discusses the stratigraphic and tectonic history of the shield area and relates the stratigraphic terminology of the 1963 map to current concepts.

PREVIOUS GEOLOGIC WORK

The first areal geologic descriptions of western Arabia (fig. 1) in modern times are those of Charles Doughty (1888), who prepared a general geologic map colored in along the routes of his trips during the period 1875 to 1878 and described in "Travels in Arabia Deserta." He separated the granites and traps, most of which crop out in what he called the central plutonic country extending from Jabal Shammar (Ḥā'il) to Makkah, from the overlying sandstone and limestone of the Great Nefud and the Qasim and from the still younger volcanic eruptions, the extensive basaltic lava fields (harrats) of Tertiary and Quaternary age.

Concurrent with Doughty's travels and 4 yr later, though their trails never crossed, Charles Huber traveled in central and northern Arabia as far as Jabal Shammar and Al Qaṣīm (Huber, 1891). His map, published posthumously, carries scant geologic information, but he collected rock specimens which were later studied by S. Meunier (1891) and P. Lamare (1923), who quotes Meunier. The distribution of alkalic granite plutons and peralkalic rhyolite in the Shammar region was noted by Lamare (1923, 1930a, 1930b).

During the period 1908–1915, Alois Musil (1926) explored and mapped much of northwestern Arabia. L. Kober (1911) accompanied him in 1910 to make geologic observations that gave the first general sequence, mostly of the Phanerozoic, of that part of Arabia.

Although Richard Burton (1978) briefly explored and searched for gold mines in northwestern Arabia along the Red Sea coast from near lat 27°30′ N. to lat 28° N., the first serious mineral exploration following the expansion period of the Abbasid Caliphates (750–833 A.D.) was that of K.S. Twitchell on behalf of King Abdul Aziz ibn Sa'ud. Twitchell, an American mining engineer, made many reconnaissance trips in search of water supplies and mineral prospects (Twitchell, 1958). His work led to the development of a gold mine 400 km northeast of Jiddah at Mahd adh Dhahab, which produced 643,817 ounces of gold and 1,003,131 ounces of silver from 1939 to 1954. Recent work by the USGS has led to the discovery of an extension of the veins (Luce and others, 1976; Worl, 1978). During the development period of this mine, G.A. Dirom and T.P. Larken visited several ancient prospects in the Najd and in the northern Hejaz in the vicinity of Al Wajh and Yanbu' an Nakhl. Some prospecting was also done in the southern Hejaz south of Aṭ Ṭā'if.

In 1944, Max Steineke and E.L. Berg of the Arabian-American Oil Company and Lt. G. Wadsack of the American Military Mission mapped about 10,000 km^2 by reconnaissance methods along the Red Sea coast, covering Jiddah, 'Usfān, and Wādī Fāṭimah, to choose drilling sites for a water supply for Jiddah (Steineke and others, 1944). The crystalline rocks were not subdivided, but Tertiary and Quaternary sediments and lavas were mapped.

NATURE AND SCOPE OF RECENT WORK

The USGS began a systematic reconnaissance of western and central Arabia in 1950 at the request of the

late King Abdul Aziz ibn Sa'ud. R.O. Jackson and G.F. Brown started in the 'Asīr province of southwestern Arabia, assisted by Sharif Kasem and Hisham Farouki, and joined by R.G. Bogue and G.H. Goudarzi in the fall of 1953. D.F. Dougherty spent one year studying the surface-water possibilities. The reconnaissance was extended northward and eastward, with Bogue visiting the northwestern and southeastern portions of the shield.

Because no adequate maps for western Arabia existed, W.E. Wrather, then Director of the U.S. Geological Survey, obtained sufficient funds to contract for aerial photographs covering 55,000 km^2 of the 'Asīr Province in the southwestern part of the country. These flights were conducted in 1951. Subsequently, the U.S. Foreign Economic Administration contracted for aerial photography covering an additional 68,500 km^2 along the Red Sea coast north of the 'Asīr; and finally, in 1955, on the advice of H.E. George Wadsworth, the American Ambassador, H.R.H. Faisal ibn Abdul Aziz, then viceroy of the Hejaz, requested aerial photography of the remainder of the western provinces. This covered about 810,000 km^2 and included the western part of a belt of trimetrogon photography taken earlier that extended from Jiddah to Dhahran on the east coast. The aerial photographs served as a base for compilation of the series of geographic and geologic maps, at scales of 1:500,000 and 1:2,000,000, published between 1956 and 1963.

In 1954, under the direction of Dr. F.K. Kabbani, the Saudi Arabian Directorate General of Petroleum and Mineral Affairs began geologic work, much of which was done by D.F. Schaffner and W.H. McLean, assisted by Hashim Shigdar and Ahmed Al-Shanti; G.F. Brown assisted in this work in 1957–58. In 1954, the Bundesanstalt fur Bodenforschung sent four geologists, G. Richter-Bernburg, H.R. von Gaertner, W. Schott, and H. Schurenburg, who made a rapid reconnaissance along the major roads and trails. In 1955, Roman Karpoff of the Societe Lyonnaise des Eaux et de l'Eclairage, Paris, made two trips across the shield and traveled to the vicinity of Al Madīnah and Al Līth. In 1956–58, G.F. Brown made a reconnaissance of the northeastern part of the shield, and in December 1962 he traveled from Tabūk westward to Wādī 'Ifāl and south to Al Wajh in the company of Dr. F.K. Kabbani.

Following this early geological reconnaissance, more intensive geological surveying was begun in 1963 under the direction of G.F. Brown, USGS, for Sheikh Ahmed Zaki Yamani, Minister of Petroleum and Mineral Resources. The areal work was extended in 1963, in 1965–67, and to the present (1984) to include airborne magnetic and total-gamma radiation measurements. In 1963, the USGS sent W.C. Overstreet, Richard Goldsmith, R.F. Johnson, J.W. Mytton, J.W. Whitlow, C.L. Hummel, and V.A. Trent to carry out reconnaissance and geochemical sampling, and W.E. Davis and R.V. Allen to introduce ground geophysical exploration, all under the direction of G.F. Brown. G.H. Sultan, Abdullah Ankary, Hashim Hakim, and Jamil Kouther, of the Saudi Arabian Directorate General of Mineral Resources, assisted and mapped areas on their own responsibility. The early fieldwork was supported by limited geochronological laboratory work by the Carnegie Institution, Washington, D.C.

Early in 1964 the Japanese Geological Survey sent a team of seven geoscientists to Arabia under the direction of Dr. Shizuka Okumi, and then, in 1966, under Dr. Ken Kirayama. These scientists concentrated their activities on specific mineral occurrences, with emphasis on geochemistry and detailed mapping.

In 1965 the French Bureau des Recherches Geologiques et Minieres (BRGM) began work for the Ministry, consisting mostly of areal mapping and prospecting, when they were given responsibility for a 140,000-km^2 region that was subdivided into three areas of the Arabian Shield. Under the direction of Jacques Reneaux, and later under J.J. Altmann, much of the mapping has been directed by G. Eijekelboom, J. Delfour, M. Bertucat, and currently C. Pellaton, as Chief Geologists. Under their direction and with their participation, quadrangle mapping has been accomplished by 25 geologists, supported by K-Ar and Rb-Sr isotopic dating in France (Baubron and others, 1976).

ACKNOWLEDGMENTS

Thanks are due many members of the Government of Saudi Arabia who helped in the field, financed the work, and made the surveys possible. The work was started under the guidance of the late Sheikh Abdullah Sulaiman, former Minister of Finance, was continued under Sheikh Abdullah Tariki, former Minister of Petroleum and Mineral Resources, and was completed under Sheikh Ahmed Zaki Yamani, former Minister of Petroleum and Mineral Affairs. Dr. Fadil Kabbani, former Deputy Assistant Minister of Petroleum and Mineral Affairs, directed much of the early phases and accompanied G.F. Brown in the field in northwestern Arabia and east of Jiddah. Sheikh Ghazi H. Sultan followed Dr. Kabbani as Deputy Minister, and both he and Sheikh Mohammed Qusai Assad provided assistance vital to the completion of this report. G.H. Sultan, Abdullah Ankary, A.Y. Bagdady, Haskim Hakim, A.M. Helaby, F.M. Kana'an, Ziad-al Koulak, M.M. Mawad, Mohammad Naqui, J.H. Kouther, Ghanum Jeri, Misfir bin Yam, A.O. Ankary, R.G. Bogue, Gus Goudarzi, and Wallace McLain spent many arduous months in the

desert. K.S. Twitchell kindly made his field notes available, and Daniel Schaffner supplied his mine examination reports and the geologic reports written by members of the Saudi Arabian Mining Syndicate. Dr. Kabbani supplied the reconnaissance reports of the Bundesanstalt fur Bodenforschung, the notes of Sheikh Ahmad Fakhry, who had earlier searched extensively for lost mines with Twitchell, and various unpublished reports prepared by the Directorate of Mineral Affairs.

Viktor Kahr, working for the Ministry of Petroleum and Mineral Affairs, mapped 7,650 km^2 in northwestern Arabia and 1,500 km^2 along the eastern edge of the shield. In addition, A. Al-Shanti mapped 2,000 km^2 of the eastern shield and areas near Jiddah, W.K. Liddicoat mapped 10,000 km^2 north of Jiddah, and F.M. Kana'an mapped 2,850 km^2 adjacent to Liddicoat's map, as did J. Kouther. Karl Nebert mapped 2,400 km^2, also north of Jiddah, and 1,500 km^2 at the eastern edge of the shield, and also directed work by students of the Saudi Research Center for Applied Geology along the northern flank of Wādī Fatimah between Jiddah and Makkah. These areas have been incorporated in our compilation, as has later work, where available, from BRGM, Ministry geologists, the Japanese Geologic Survey, and members of the geological department of King Abdulaziz University.

The French oil company AUXERAP studied the coastal strip under the direction of Dr. Michel Gillmann in 1966 and 1967. They made their report available and gave permission for incorporation of the measured stratigraphic section of the Khums and Amran Formations.

P.K. Theobald, Jr., and Charles Thompson, USGS, beginning in 1963 gave support in geochemical prospecting and chemistry. W.J. Dempsey expanded the geophysical program and initiated diamond-drilling. Concurrently in 1963, the Topographic Division, USGS, sent G.W. Harbert, J.S. Crabtree, and T.E. Taylor to prepare the base maps and supervise aerial photography. Later this work was continued by F.G. Lavery, K.S. McLean, R.C. Nixon, G.C. Myers, C.M. Robins, and R.H. Tucker. A special team composed of R.E. Kenfield, G.E. Morrison, Jr., R.C. Nixon, A.A. Shands, W.E. Smith, and D.J. Winstead came to prepare topographic maps of the phosphate-bearing area in Wādī as Sirḥān near the Jordan frontier. More recent topographic map control has been continued by F.J. Fuller and D.J. Faulkender.

Under a 3-yr extension, 1966–1969, of the 1963 agreement, which ended essentially in 1966, and subsequent to the earlier reconnaissance photogeologic mapping and search for mineral deposits, the work became more intensive in areas considered of greatest economic potential. It consisted of geological mapping, mostly at a scale of 1:100,000 (some more recently has been compiled at a scale of 1:250,000), using helicopters and support by geophysical, geochemical, and drilling activities as well as petrographic, chemical, and geochronological support in the laboratory. A second 3-yr extension of the working agreement began in 1969, continuing the work initiated in 1966 under the direction of G.F. Brown. This new extension was directed first by J.J. Norton, later by T.H. Kiilsgaard, followed by F.S. Simons and D.G. Hadley, all assisted by R.O. Jackson. Currently (1984), R.O. Jackson is continuing direction of the field party. The program has continued to the present; the last 9 yr of work has been part of the Saudi Arabian first and second Five Year Development Plans as directed by Sheikhs Ahmed Zaki Yamani and Ghazi Sultan. USGS geologists who contributed to the geologic and economic knowledge during the extended time include D.L. Schmidt, D.B. Stoeser, J.C. Cole, and P.L. Williams as chief geologists, and G.H. Allcott, R.E. Anderson, W.R. Brock, D.A. Brobst, R.W. Bailey (deceased), F.W. Cater, J.C. Cole, R.G. Coleman, H.R. Cornwall, F.C.W. Dodge, J.L. Doebrich, E.A. DuBray, R.L. Earhart, J.E. Elliott, G.M. Fairer, D.J. Faulkender, W.D. Fenton, D.L. Gaskill, Louis Gonzalez, R.C. Greene, W.R. Greenwood, D.G. Hadley, F. Hershey, K.S. Kellogg, R.W. Luce, Conrad Martin, C.R. Meissner, J.S. Pallister, W.C. Prinz, J.S. Ratte, R.J. Roberts, L.F. Rooney, D.L. Rossman, E.G. Sable, R.P. Sheldon, C.W. Smith, J.S. Stuckless, P.K. Theobald, F.V. Tompkins, A.E. Weissenborn, J.W. Whitney, K.L. Wier, and R.G. Worl. R.V. Allen, G.E. Andreasen, H.R. Blank, W.F. Davis, V.J. Flanigan, M.E. Gettings, Andrew Griscom, S.A. Hall, D.L. Hase, D.R. Mabey, and J.A. Pitkin gave geophysical support. R.W. Girdler served as consultant. After L.T. Aldrich's and T.W. Stern's pioneer work in geochronology, C.E. Hedge, R.F. Marvin, H.H. Mehnert, V. Merritt, B.R. Doe, and R.J. Fleck analyzed shield rocks for isotopic ratios and estimates of age. J.A. Cooper and J.S. Stacey analyzed zircon by the U, Th-Pb method for dating (Cooper and others, 1979). J.F. Sutter measured $^{40}Ar/^{39}Ar$ of a sample from the youngest flows in the craton. Chemical analyses were made under the direction of M. Gonshor, and later of W.L. Campbell and K.J. Curry. Petrographic work was first directed by D.H. Johnson, followed by R.W. Luce, F.C.W. Dodge, and J.J. Matzko.

As regards geologic mapping, regional compilation of the geology of the shield, using the 1:100,000-scale geologic maps, was begun in 1977 on a scale of 1:250,000. These smaller scale maps were used in the preparation of this report as they became available. Jacques Delfour, Robert Dhellemmes, Yves Gros, John Kemp, J. Letalenet, Claude Pellaton, and Jean-Pierre Prian of the Bureau des Recherches Geologiques et

Minieres prepared 1:250,000-scale maps in the central and northern part of the shield. H.R. Blank, G.M. Fairer, M.E. Gettings, W.R. Greenwood, R.O. Jackson, W.C. Prinz, and F.S. Simons of the U.S. Geological Survey prepared similar maps of the southern part of the shield. And finally, larger areas at scales of 1:500,000 and 1:1,000,000 were compiled first in 1983 by J.Y. Calvez, C. Aloac, J. Delfour, J. Kemp, and C. Pellaton of the French Bureau for most of the northern part of the shield (Calvez and others, 1983), followed by plutonic rock compilations of the southern part of the shield below lat 20° N. by D.B. Stoeser of the U.S. Geological Survey at the larger scale (Stoeser, 1985). Stoeser, together with J. Elliott, also prepared a similar maps of the northeastern corner of the shield north of lat 25° N. (Stoeser and Elliott, 1985).

For this report, Salman Bloch assisted with petrographic work and geologic compilation from March 1975 until April 1977, continuing petrographic work begun earlier by the late Dr. Carl Brodel, R.O. Jackson, G.F. Brown, and R.G. Coleman. Subsequently, Richard Hoeksema recalculated the geochronological data to new constants published by the International Subcommission on Geochronology (Steiger and Jager, 1977) and plotted the histograms. Thanks are due W.C. Overstreet and M.E. Gettings for their technical review and constructive suggestions. Elizabeth J. Tinsley typed and assembled the manuscript, and Audrey G. Schmidt prepared many of the illustrations. Final geologic map preparation was accomplished by Neal Maxfield, Jewel A. Dickson, Jerry M. Russell, and Will R. Stettner.

And finally, it is impossible to give sufficient credit to Wenonah Bergquist, who edited the report and supervised preparation of the illustrations at an early stage. Her sustained counsel and encouragement made completion possible, as did family support during the long years of fieldwork and separation, especially support of Laura Cameron Brown, late wife of the senior author.

GEOGRAPHY

CLIMATE

Saudi Arabia lies in the center of the great trade-wind desert that extends across northern Africa into Asia. In Saudi Arabia, important modifications of the hot, dry, desert climate are due to the effect of the Red Sea and the flanking mountain ranges of Ash Shifā', Hejaz, and 'Asīr.

Rainfall is meager and episodic, ranging from a minimum mean annual of less than 2 cm in the north to a maximum of about 30 cm along the southern crest of the 'Asīr range in the southwest. Most of the region probably has an average annual rainfall of 10 cm (see fig. 2), but systematic records have been kept only in recent years. At Mahd adh Dhahab, in west-central Saudi Arabia, a 14-yr record shows a range from a minimum of 1.2 cm to a maximum of 13.1 cm, with an average of 6.2 cm. At Jiddah, on the Red Sea coast, where the average is about 8 cm, infrequent rains during the last 15 yr have been as much as 15 cm, falling within a few hours, although there are some years when no rain falls. Indeed, parts of the vast interior region, particularly north of Al Madīnah and east of the 'Asīr, have had no rain for periods of several years, according to bedouin accounts and as attested by the sparseness of the vegetation. The northern regions, within the belt of westerly planetary winds, have winter precipitation. In the southern region, the monsoon season of late summer is marked by moisture-laden winds which, blowing from the southwest against the western rim of the high plateau of Yemen and Hejaz ('Asīr), are forced upward to furnish the greatest precipitation along the crest. Records kept at Ṣan'ā' in the Yemen, east of the crest, show an average of 30.2 cm (minimum 15.4 cm, maximum 49.5 cm), with the heaviest precipitation in July and August and a secondary peak in April. At Ar Riyāḍ, in central Saudi Arabia, a 7-yr record shows an average of 10 cm (minimum 2.8 cm, maximum 23.8 cm), almost all precipitation falling in the winter and spring months.

Even if rainfall had been recorded for many years, the episodic and local nature of most precipitation makes averages of doubtful value. A better guide has been provided by the late Dr. John Tothill's study of the vegetation along the Red Sea coast and in the 'Asīr. Drawing on his knowledge of the vegetation in the Sudan, where rainfall records have been kept, he correlated precipitation with various index genera and floral groups common to the Sudan and western Arabia. Figure 2 is based mainly on his work; also included in figure 2 is a record compiled by Ali H. Al-Shalash, University of Riyadh, from 60 stations for a period of 3 to 14 yr (Ministry of Agriculture and Water, written commun., 1974).

Temperatures range from below freezing during the winter months in the mountains and high plateaus to summer maxima of about 120 °F (44.5 °C). Temperatures have large diurnal ranges (table 1)—sometimes as much as 60 °F (16 °C)—caused by the rapid transmittal of heat from the bare rock surfaces as the desert passes from day to night.

Relative humidity during the day is low away from the seacoast—in the summer about 10 percent and in the winter 45 percent, according to the fragmentary records. The large diurnal range of temperature often produces an early morning dew when the rock surfaces

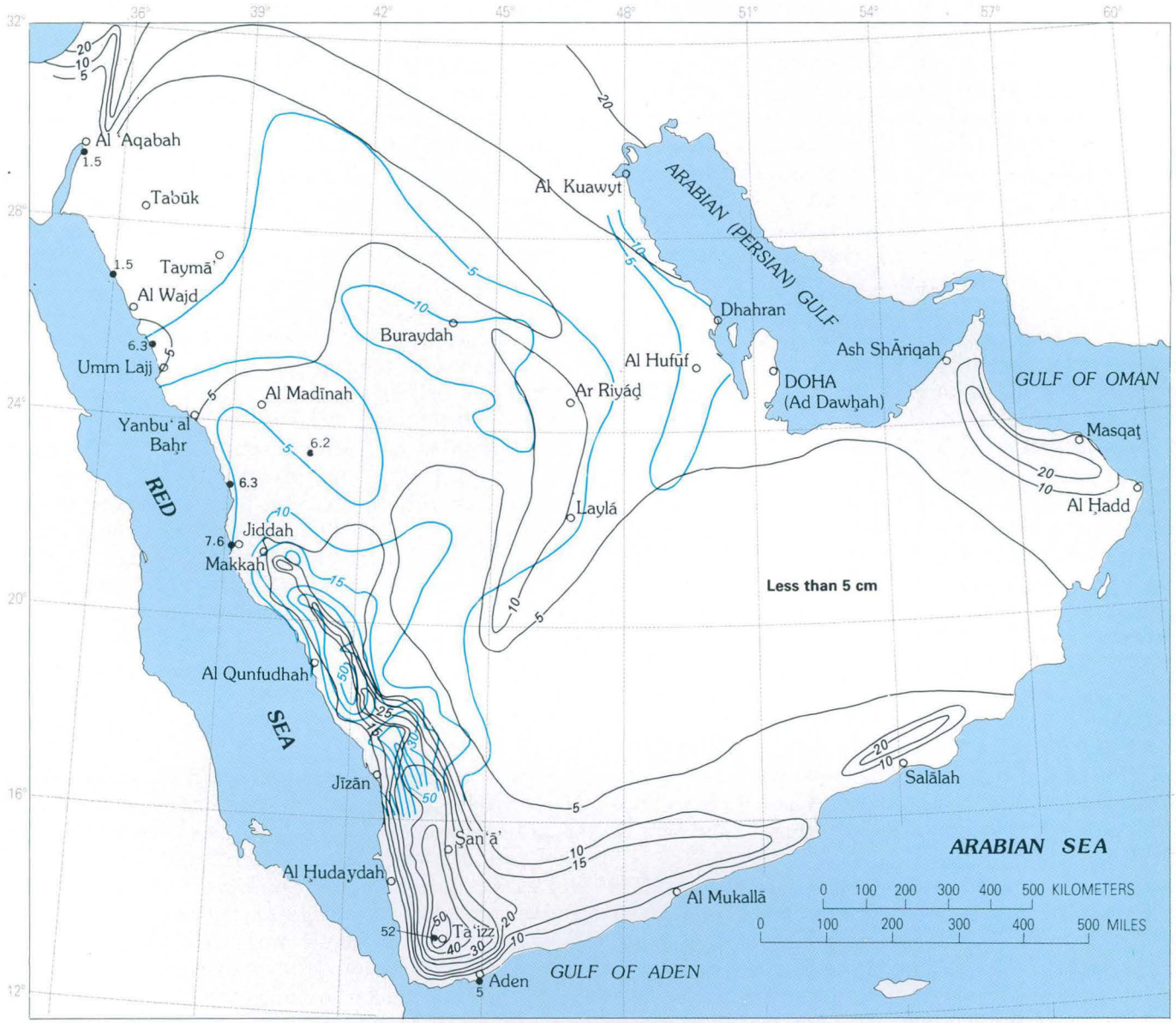

EXPLANATION

Annual Rainfall

10 — Based on vegetation studies of J. D. Tothill and on records of precipitation. Isohyetal contour interval 5 and 10 centimeters

50 — Based on records for 3 to 14 years (average 5 years) at 60 stations. Compiled by Ali H. Al-Shalash, University of Riyadh, from weather stations of the Ministry of Agriculture and Water. Isohyetal contour interval 5, 10, and 15 centimeters

7.2 Locality where precipitation was recorded or estimated on the basis of vegetation studies

FIGURE 2.—Estimated rainfall distribution in the Arabian Peninsula.

TABLE 1.—*Air temperatures and relative humidities at selected sites in western Saudi Arabia*

[Air temperatures in degrees Celsius, relative humidities in percent. After Saudi Arabian Ministry of Agriculture and Water]

Month	Abhā[1] Alt. 2,200 m; lat 18°13′ N., long 42°29′ E.				Al Mindak[2] Alt. 1,920 m; lat 20°06′ N., long 41°17′ E.				Belesmer[2] Alt. 2,250 m; lat 18°46′ N., long 42°13′ E.				Biljurshī[2] Alt. 2,040 m; lat 19°51′ N., long 41°34′ E.			
	Air temperature			Mean rel. hum.	Air temperature			Mean rel. hum.	Air temperature			Mean rel. hum.	Air temperature			Mean rel. hum.
	Max.	Min.	Avg.		Max.	Min.	Avg.		Max.	Min.	Avg.		Max.	Min.	Avg.	
Jan	22.2	1.2	11.2	68	20.2	-1.2	10.9	61	23.1	-2.2	8.7	60	21.8	2.2	12.1	50
Feb	20.0	4.8	13.3	67	22.0	-5.8	11.6	63	22.8	-2.0	10.5	59	22.6	-2.0	12.7	55
Mar	23.0	2.8	14.8	64	23.6	4.0	14.8	64	21.4	0.5	11.7	66	24.0	3.8	15.8	54
Apr	25.8	9.2	17.8	56	27.0	6.4	17.1	63	22.6	4.8	13.1	66	26.0	9.0	17.2	54
May	29.6	8.8	20.3	40	32.2	6.8	19.5	54	27.6	5.0	14.6	64	32.1	10.0	20.0	40
Jun	31.0	13.6	22.4	34	31.2	6.5	20.9	51	26.0	4.2	17.1	43	31.2	10.4	23.2	35
Jul	29.4	11.6	21.3	42	33.0	11.0	22.5	54	28.2	8.1	19.0	43	32.8	11.2	23.6	41
Aug	29.4	14.0	21.7	40	32.2	11.2	23.2	56	27.8	9.8	19.0	51	32.6	14.6	24.1	43
Sep	29.0	10.0	19.4	40	32.0	10.2	21.7	50	27.3	3.6	16.8	46	31.9	11.7	22.4	43
Oct	25.4	7.0	16.6	39	28.2	5.7	18.5	50	23.0	0.4	12.6	47	27.8	8.4	18.7	42
Nov	23.0	5.0	14.0	46	26.6	4.0	14.5	66	22.0	-0.8	10.5	71	24.0	6.4	14.7	58
Dec	18.8	2.3	11.6	53	22.8	-1.8	11.1	62	19.8	-3.0	8.0	([3])	22.6	1.0	11.7	58
Ann.	31.0	1.2	17.0	49	33.0	-5.8	17.2	58	28.2	-3.0	13.5	([3])	32.8	-2.0	18.0	48

Month	Qal'at Bīshah[2] Alt. 1,040 m; lat 20°00′ N., long 42°36′ E.				Ḥā'il[2] Alt. 1,010 m; lat 27°28′ N., long 41°38′ E.				Jiddah[4] Alt. 17 m; lat 21°30′ N., long 39°12′ E.				Al Madīnah[4] Alt. 648 m; lat 24°31′ N., long 39°42′ E.			
	Air temperature			Mean rel. hum.	Air temperature			Mean rel. hum.	Air temperature			Mean rel. hum.	Air temperature			Mean rel. hum.
	Max.	Min.	Avg.		Max.	Min.	Avg.		Max.	Min.	Avg.		Max.	Min.	Avg.	
Jan	30.2	3.8	16.9	45	23.6	-3.0	10.1	54	26.6	19.4	23.0	55.5	23.9	13.3	18.6	46
Feb	34.0	5.0	19.9	43	27.0	-4.4	12.0	45	26.6	18.9	22.8	52.5	25.0	13.3	19.1	42
Mar	35.0	9.0	22.4	36	30.4	1.6	17.2	31	28.9	20.5	24.7	52	28.9	16.1	22.5	32
Apr	36.4	13.0	24.8	41	33.1	7.0	19.3	30	31.0	22.8	26.9	54.5	35.5	23.3	29.4	29
May	39.1	16.8	27.9	40	38.8	12.4	25.2	23	32.7	24.4	28.6	54	37.7	24.4	31.1	37
Jun	40.0	14.8	28.0	27	38.0	15.0	26.6	15	34.4	25.5	30.0	56	40.5	27.8	34.2	16
Jul	41.0	18.0	30.3	26	41.0	18.0	30.1	13	34.4	27.2	30.8	53.5	37.7	26.1	31.9	26
Aug	41.1	19.4	30.8	30	41.0	19.0	30.1	15	35.0	27.8	31.4	55.5	40.0	27.8	33.9	22
Sep	39.0	10.0	26.4	28	40.2	13.2	27.7	13	33.9	26.6	30.3	63.5	40.5	26.1	33.3	25
Oct	32.6	6.6	20.0	23	34.2	8.0	21.6	16	32.7	24.4	28.6	61.5	36.1	23.3	29.7	26
Nov	33.6	5.1	20.9	37	31.0	2.2	16.4	32	30.5	23.3	26.9	57	28.3	27.8	28.1	43
Dec	31.0	2.0	16.7	44	27.2	-5.0	9.8	45	28.3	21.1	24.7	54	25.5	13.3	19.4	47
Ann.	41.1	2.0	23.8	35	41.0	-5.0	20.5	28	31.1	23.3	27.2	55.5	33.3	21.1	27.2	33

Month	An Nimās[2] Alt. 2,600 m; lat 19°06′ N., long 42°09′ E.				As Sulayyil[2] Alt. 600 m; lat 20°28′ N., long 45°34′ E.				Aṭ Ṭā'if (Howiyah)[2] Alt. 1,530 m; lat 21°24′ N., long 40°27′ E.				Turayf[4] Alt. 850 m; lat 31°41′ N., long 38°40′ E.			
	Air temperature			Mean rel. hum.	Air temperature			Mean rel. hum.	Air temperature			Mean rel. hum.	Air temperature			Mean rel. hum.
	Max.	Min.	Avg.		Max.	Min.	Avg.		Max.	Min.	Avg.		Max.	Min.	Avg.	
Jan	12.6	-5.6	3.3	36	27.6	2.3	13.9	47	26.6	3.2	14.2	36	17.2	4.4	10.8	56
Feb	17.0	-4.4	8.6	40	35.6	2.0	17.5	39	27.8	1.8	16.6	37	15.5	3.3	9.4	49
Mar	20.2	1.8	10.8	41	37.2	5.8	21.7	27	28.6	9.8	19.5	42	20.0	6.7	13.4	48
Apr	24.0	4.0	13.2	58	39.2	14.0	26.5	26	30.4	10.0	20.2	34	26.6	19.4	23.0	26
May	27.8	7.2	16.4	51	43.7	18.4	31.7	18	36.0	8.0	22.9	29	32.7	15.4	24.1	17
Jun	27.0	6.8	18.1	40	45.0	18.4	32.5	11	35.2	14.8	26.1	15	37.7	20.0	28.9	21
Jul	29.0	10.2	19.0	43	45.0	22.6	34.8	10	35.8	16.8	27.2	18	35.5	20.0	27.8	19
Aug	28.0	12.0	19.0	41	45.0	21.1	34.5	9	35.8	18.8	27.3	20	37.7	20.5	29.1	18
Sep	28.0	6.0	18.0	43	44.0	14.1	30.3	10	35.2	13.0	25.0	18	32.7	16.7	24.7	16
Oct	23.8	3.0	13.8	44	37.0	10.0	24.0	13	30.8	10.2	20.8	24	28.9	14.4	21.7	26
Nov	20.0	1.4	10.6	65	35.0	6.1	19.5	26	28.6	8.2	18.0	36	18.9	9.4	14.2	41
Dec	19.7	-0.2	8.0	70	29.9	3.6	16.6	35	27.8	-1.4	13.6	36	17.2	4.4	10.8	53
Ann.	29.0	-5.6	13.2	48	45.0	2.0	27.6	25	36.0	-1.4	21.0	29	26.6	12.2	19.4	33

[1] 1970.
[2] 1971.
[3] No record.
[4] More than 10 years.

and nearby air have cooled below the dewpoint; however, the low humidity and the first rays of the morning sun quickly evaporate it. The high humidity and heat along the Red Sea cause much discomfort and lethargy, especially as the dampening effect of the sea often holds the air temperature at a high level throughout the night.

Winds range widely in direction and velocity. A prominent northwesterly, the "shimal," blows strongly in spring and early summer in the central and eastern parts of the country. A southwestern wind direction in northwestern Arabia has produced prominent yardang troughs north of lat 24° N. Sand storms and dust storms are common, and eolian landforms and deposits are conspicuous in the younger terranes (see fig. 68).

SETTLEMENT[2]

Long the home of wandering bedouin who traditionally follow the rains for forage, Saudi Arabia is changing rapidly as the few larger populated places grow at the expense of nomadic groups and smaller agricultural communities. Makkah, the religious center of the Moslem world, now (1980) has a permanent population of at least 200,000, and its population increases manyfold during the annual pilgrimage, as does that of Jiddah, the port for Makkah, which has a permanent population of more than 1,300,000 (1980). Al Madīnah, the second holy city, had a permanent population of perhaps 40,000 before current expansion but has grown substantially in recent years; it also experiences a very large influx during the annual pilgrimage. Aṭ Ṭā'if, the summer capital near the crest of the Hejaz Range east of Makkah, is comparable in size to Al Madīnah and is likely to grow at an increasing rate, provided there is sufficient water. The only large inland city is Riyadh, the political capital, which has a population of about 1,000,000 (1980). An important industrial complex is being built near Yanbu' al Baḥr at the terminus of the east-west double pipeline for oil and gas from Al Ḥasā.

A series of small agricultural communities extends southward from Aṭ Ṭā'if along the mountain crest through the southern Hejaz and the 'Asīr into Yemen. They include the districts of Bilād Ghāmid, 'Asīr, As Sarāt, and Ẓahran, settlements increasing in size and number southward. Starting from about lat 20° N., a similar series of villages and cultivated tracts extends toward the south at the seaward base of the range, culminating in several large villages in the Jizan coastal plain just north of the Yemen frontier. The topographically higher communities practice terrace cultivation, whereas the Red Sea coastal plain (the Tihāmat) valleys and the inland valleys are cultivated by flood diversion, supplemented in the Jīzān area by a modified terrace or basin type of irrigation where there is sufficient rainfall. A new dam on Wādī Jīzān supplies irrigation water to the area around Abū 'Arīsh.

About 90 percent of all cultivated land and most of the predominantly agrarian communities in Saudi Arabia lie within two belts in the southern Hejaz, 'Asīr and the southern Tihāmat; the seaports of Al Līth, Al Qunfudhah, and Jīzān serve as outlets for the area. Going eastward toward the desert, the villages are replaced by seminomadic and nomadic groups.

Small ports and fishing villages are situated along the Red Sea north of Jiddah at Rābigh, Yanbu' al Baḥr, Umm Lajj, Al Wajh, and Ḍubā, in general decreasing in size and importance northward. The small village of 'Aynūnah is situated at the northeastern corner of the Red Sea, and Maqnā and Ḥaql are on the eastern shore of the Gulf of Aqaba. A string of settlements are in Wādī Fāṭimah east of Jiddah; several other small communities lie in the larger wadi valleys north of Jiddah. These extend as far north as Yanbu' an Nakhl, directly west of Al Madīnah, beyond which there are almost no permanent settlements except on the coast; the most important of the inland villages near the coast are Madrakah, Khulayṣ, Buraykah, Ḥaqqāq, Ar Rayyān, Badr Ḥunayn, Al Ḥamrā', and Al Musayj'īd. In the upland of the Ḥismā, the only settlements of any size are Taymā' and Tabūk, although Khaybar and Al 'Ulā are on the edge of the upland. Al Bad' in Wādī 'Ifāl, which forms a valley in the Shifā' east of the Gulf of Aqaba in northwesternmost Saudi Arabia, has a small settled community.

Inland on the crystalline desert plateau are palm oases and farms at Qal'at Bīshah, Turabah, Khurmah, and Ranyah, all separated by wide expanses of stony desert. Farther north, in the northern Hejaz, the populated places are smaller and more widely spaced. Of these, Al Muwayḥ, Ad Dafīnah, 'Afīf, Al Qā'īyah, and Ad Dawādimī lie along the Aṭ Ṭā'if-to-Riyadh road; Ḥādhah, Ṣufaynah, Al Ḥanākīyah, Al Khalf, Al Ḥuwayyiṭ, Al Ḥāyiṭ, and Zarghaṭ are small villages along the eastern edge of the lava fields (where water is available) that extend from near Aṭ Ṭā'if northward to lat 27° N. The ancient community of Khaybar occupies a similar position on the western edge of the lava fields north of Al Madīnah. East of Qal'at Bīshah, beyond the four small villages that extend northward up the wadi for 40 km, there are no permanently inhabited settlements until the constriction of Wādī ad Dawāsir at the east edge of the crystalline plain, some

[2]Demography as of 1980.

200 km distant. Northeastward from Bīshah no villages are found until Ṣabḥā', some 400 km away, is reached. To the north beyond Ṣabḥā', several villages—Sanām, Ar Ruwayḍah, and 'Arwā'—lie at wadi constrictions, where there are slight local increases in ground-water supply.

Ḥā'il, the capital of the Jabal Shammar province, has a population of about 5,000 and is located where dikes and a wadi constriction impound some ground water beneath a grus plain. Toward Ḥā'il, in the northeastern corner of the crystalline shield, the most important villages are Ḍarīyah, Miskah, An Nabhānīyah, Al Fawwārah, Samīrah, Ṭābah, Fayd, Al 'Uqaylāt, Ghazzālah, Mawqaq, and Qufār.

FLORA

RELATION TO GEOGRAPHIC SETTING AND HUMAN USE

Acacia, or camel thorn, is the most widespread, and in many places almost the only, shrub and small tree of the western desert. The acacia "samr" (*Acacia tortilis* (Forsk) Hayne), perhaps the hardiest, may be found growing along the wadis or, where rainfall is slightly higher, on the desert plains as isolated flat-topped trees or copses. The acacia "sallam" (*Acacia ehrenbergiana* Hayne) is also widespread, growing in clumps or thickets along wadi floors, as it requires more water than the samr. In the high mountains the acacia locally called "talh" (*Acacia seyal*?) probably includes more than one species; it grows into trees larger than samr or sallam. There are several other species, but none of the acacias is a true phreatophyte, indicating land without a permanent water table; most vegetation away from the mountains and seacoast is mesophytic, growing only when rain falls (Vesey-FitzGerald, 1957).

The most important of the Arabian phreatophytes are the date palm "nakhla" (*Phoenix dactylifera L.*), the "sidr" (*Zisyphus spina-christi* L. Willd.; fig. 3*A*), with its lacy foliage and haw-shaped fruit rich in vitamins, the two tamarisks "tarfa" and "ithil" (*Tamarix orientalis* Forsk and *Tamarix macrocarpa* (Ehrenb.) Bunge; fig. 3*B*), the "dom" palm (*Hyphaene thebaica* (Del.) Mart.), and the "rak" (*Salvadora persica* L.), or "toothbrush shrub," which forms rings of dense vegetation, often growing on small dunes and maintaining a root system below the sand. The halfa grass (*Desmostachya cynosuroides* Stapf) is common in the upper stretches of wadis in the southern part of the country.

A distinct flora grows where salty or saline ground water is present, especially along the Red Sea coast, dominant plants being the succulent salt bush *Suaeda* (represented by two or three species) and the sea lavender (*Statice axillaris*); the mangrove-reef-fringing copses (*Rhizophora* sp., *Bruguiera* sp., or *Avicennia marina*) are prominent only south of Al Qunfudhah at lat 18°30′ N. (Vesey-FitzGerald, 1955).

In vast stretches of the western desert, where many of the acacias have been burned for charcoal, vegetation is limited to forage shrubs and grass which spring into foliage and flower after rains. The hamdh vegetation is largely *Salsola tetrandra* Forsk, which grows in saline conditions, but there are also at least five other shrubs. The rimth vegetation is largely *Haloxylon schweinfurthii* Ascherson, which is favored for camel grazing. Another widely scattered bush is the harmal (*Rhazya stricta*), or African rue (*Peganum harmala*). The grasses *Panicum turgidum* Forsk and *Lasiurus hirsutus* (Boiss) Monro are widespread, growing in clumps that furnish forage for camels, sheep, and goats and are often gathered for hay.

Many unusual plants and trees grow in the Hejaz and the 'Asīr. Of these, the juniper "ar'ar" (*Juniperus macropoda* Boiss. or *Juniperus procera* Hochst.) (Mandaville, 1973) is the only important conifer in Arabia. It grows in small forests or groves along the crest of the 'Asīr where rainfall is 12 in (30.5 cm) or slightly higher. The largest indigenous tree in Saudi Arabia, *Acokanthera deflersii* Schwein, grows only in the upper foothills east of Jīzān (fig. 3*C*). The wild fig (*Ficus salici folia* Vahl), the tamarind (*Tamarindus indica* L.; fig 3*D*), the poinciana (*Delonix elata* L. Gamble), the dragon's blood tree (*Dracaena ombet* Kotschy and Peyr), the sandalwood (*Osyris compressa* Berg.), the aloes, the 'ishr (*Coloptropis* sp.), with its milky, rubber-producing sap, and the *Adenium* sp., or poison bush, with its beautiful pink or red flowers, are of special interest. The cactuslike *Euphorbia* is represented by several species, there being no indigenous cacti on the peninsula, although the prickly pear, *Opuntia* sp., has been imported for its fruit.

Food crops in Saudi Arabia are grown mostly in the 'Asīr where the mountain slopes are terraced to hold the rain, along wadis draining the 'Asīr and the Hejaz, and in scattered isolated oases where ground water sustains the date palm, grains, fruit trees, vegetables, and hay. The most important food crops by far are dates, wheat and barley, the nonsaccharine sorgums (dhura and dukhn), corn, and alfalfa. Fruits besides dates include olive, fig, orange, lemon, lime, pomegranate, grape, cactus apple, apricot, banana, and guava. The vegetables currently cultivated include beans, squash, eggplant, okra, tomato, lettuce, cabbage, onion, carrot, pepper, and potato. Three varieties of truffle grow wild in the desert following fall and winter rains, and several varieties of melons are hauled to the markets in season.

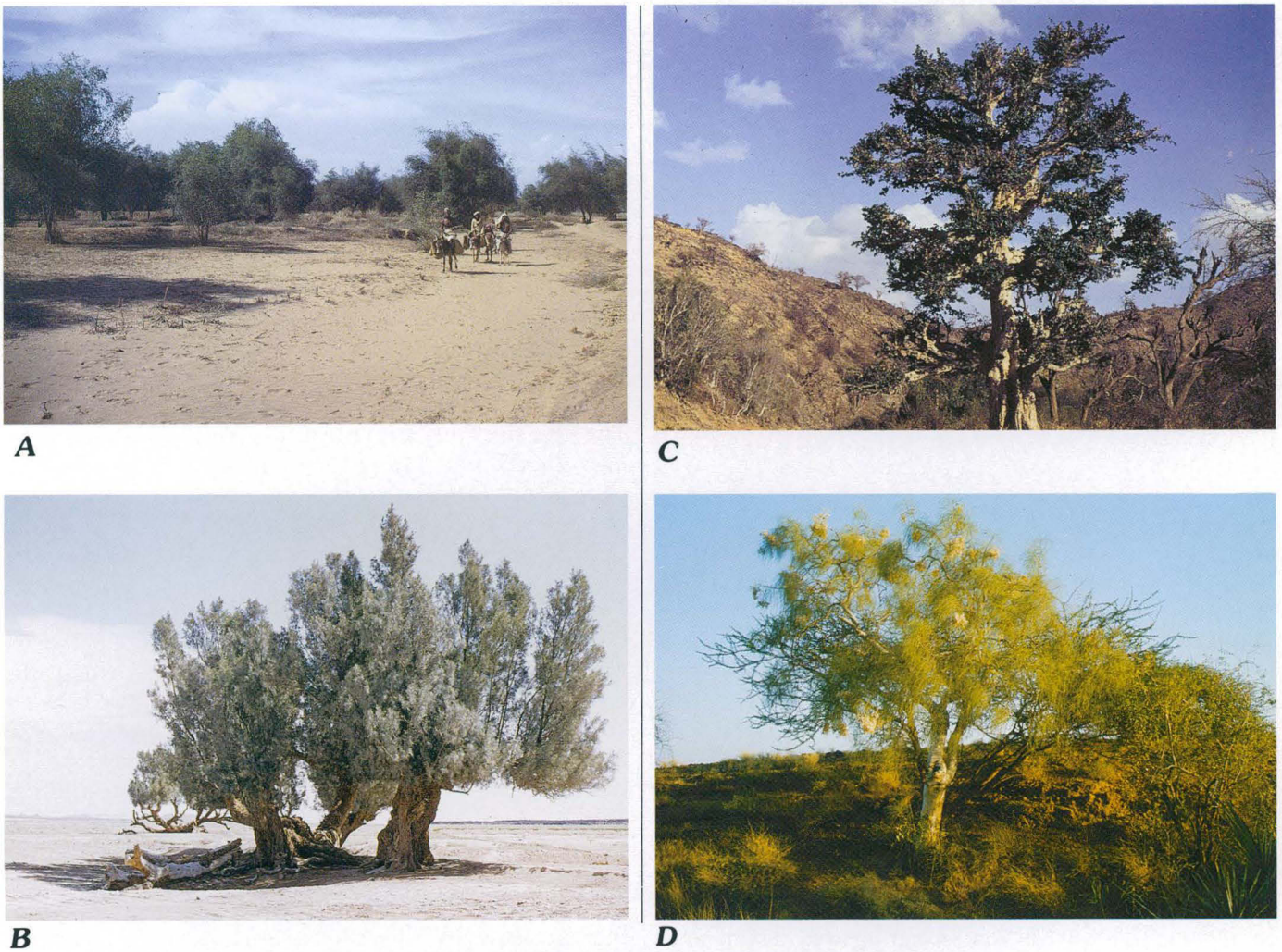

FIGURE 3.—Examples of a few phreatophytes, indicating permanent ground water. *A, Zisyphus spina-christi* L. Willd. *B, Tamarix macrocarpa* (Ehrenb.) Bunge. *C, Acokanthera deflersii* Schwein., the largest indigenous tree in Saudi Arabia, photographed at the junction of Wādī Qa'ah (Yithrib) and Wādī Shini near Jallat al Mawt. *D, Tamarindus indica* L.

RELATION OF FLORA TO RAINFALL

By J.D. Tothill[3]

Fieldwork for a study of the floral zones of the coastal plain, or Tihāmat, between Jiddah and the Yemen frontier, and of the 'Asīr Mountains was done in 1950 and 1951 when the Food and Agriculture Organization of the United Nations was examining the possibility of supplementing the existing irrigation systems of the coastal plain in Jīzān province. From time immemorial, primitive to well-developed irrigation systems were employed on the principal rivers that rise in the 'Asīr Mountains and form desert deltas on the Tihāmat. With the increase of population and the need for more food, both for humans and for domestic animals, some reinforcements by means of barrages had become necessary.

The size and number of barrages that would be required would depend on rainfall in the catchment areas, and an estimate of rainfall accurate enough to use as a basis for determining the size of the barrage projects was urgently needed. No rainfall records for the area had ever been kept, and it was not practical to wait a decade or longer for meteorological observations to be made. In these circumstances it was decided to test the possibility of defining natural floral zones and using these as the basis for estimating rainfall on the mountains. Seven zones were eventually distinguished, and the rainfall estimate made for each was used for figure 2 (see table 2).

The plan was to make three widely separated traverses down the face of the mountains, to establish as

[3]Deceased.

TABLE 2.—*Summary of annual rainfall estimates for and characteristics of floral zones*

[Rainfall in inches]

Floral zone	Estimated rainfall at—		
	Dry edge	Wet edge	Mean
Ar Rub' al Khālī	Trace	2	1
Samr desert	2	4	3
Sallam desert	4	5	4.5
Asak-Commiphora desert	5	7	6
Kleinia-pastoral	7	10	8.5
Euryops-barley	10	12	11
Rose-juniper-agricultural	12	16.8	14.4

Floral zone	Characteristic	Distribution
Ar Rub' al Khālī	Plant growth insufficient to produce camel forage.	The Empty Quarter. Parts of coastal range north of Jiddah.
Samr desert	Rain sufficient for samr but not for sallam.	On coastal plain from Jiddah to Al Wajh.
Sallam desert	Samr and sallam both common. Good growth of the tufted forage grasses *Lasiurus hirsutus* Boiss. and *Panicum turgidum* Forsk. *Commiphora* and *Euphorbia cuneata* absent.	On coastal plain from Jiddah to Wādī 'Itwad. East of Scarp Mountains, a narrow strip from near Aṭ Ṭā'if to the Yemen.
Asak-Commiphora desert	Samr and sallam attain optimum growth and both common. On Tihāma, *Commiphora africana* and *Euphorbia cuneata* definitive. On foothills, *Acacia asak* and *Anisotes trisulcus* definitive.	On Tihāmat from Wādī 'Itwad to the Yemen. On 'Asīr foothills up to 5,000 ft.
Kleinia-pastoral	On western face of 'Asīr, *Anisotes, E. cuneata,* and juniper all absent. *Acacia etbaica,* or qarad, common as bush, becoming bigger and better near the upper limit. Occasional *Kleinia.*	On western slopes of 'Asīr extends from 5,000 to 7,000 ft.
	On plateau above scarp, *Kleinia violacea* common. *Acacia etbaica* finds optimum conditions and has become well-grown tree.	On 'Asīr plateau from Abhā and Khamīs Mushayṭ north to Ṣaḥrā and south to El Qa'am; and generally up to 7,500 ft.
Euryops-barley	*Kleinia* has disappeared. *Euryops* has become definitive plant. Wheat and barley grown regularly as rain crops.	A fragment on Jabal Fayfā.
	Acacia etbaica common as a tree, and conditions for it remain optimum.	A fairly extensive area commencing 35 mi south of Abhā and extending to Aqabat al Alb.
	Juniper and *Dodonaea* absent.	Another fragment between Abhā and Jabal as Sūdah starting at 7,500 ft and ending at 8,200 ft.
Rose-juniper-agricultural	Many definitive plants, but *Rosa abyssinica* and *Juniperus macropoda* conspicuous. Juniper becomes 40-ft tree in favorable sites. The only acacia is *etbaica,* which has shrunk to become a bush. *Euryops* has faded out. Good crops of wheat, barley, lentil, and alfalfa regularly grown. A number of permanently flowing, spring-fed streams.	Confined in the 'Asīr region to Jabal as Sūdah above 8,200-ft contour and to traces at heads of Wādī Baysh.

many zones as could be easily recognized by the coming in or disappearance of readily identified definitive, or index, plants, and then to determine rainfall for each zone. The area of each zone would be calculated from an aerial survey map by joining the zone contours for the three traverses.

Despite the wild ruggedness, precipitate steepness, and inaccessibility of the upper 2,000 ft (610 m) of the western face of the mountains, the plan worked quite well. Seven easily recognized zones were eventually defined; their definitions, extent in the 'Asīr area, and probable rainfall are given below. The project proved to be of considerable practical value, as its findings were used as the rainfall basis for designing the required barrages.

The traverses of the western face of the 'Asīr were made by the ascent of Jabal Fayfā, Wādī Baysh, and Wādī 'Itwad.

During the fieldwork on the coastal plain, I had the stimulating companionship of Dr. Van der Plas. For the three traverses of the 'Asīr, I was most happily accompanied by Thomas Smallwood[4], a specialist in water supplies for irrigation purposes. For the journey down Wādī Qa'ah and into the main Wādī Baysh I am deeply indebted to Dr. Glen Brown, a geologist of the U.S. Geological Survey whose friendship and stimulating ideas I came to value greatly.

The Saudi Arabians were both our hosts and our friends, and it is a pleasure to acknowledge the many acts of courtesy and kindness shown us by a long list of local residents, from the late King Abdul Aziz ibn Sa'ud and his sons, the late Kings Saud and Faisal, down through all walks of life to humble folk who helped us in our daily tasks.

Plant specimens were determined through the kindness of Dr. Taylor, then Custodian of the Herbarium and Head of the Botanical Department of the British Natural History Museum. Miss D. Hillcoat did most of the determinations, and to her I owe a special debt of gratitude.

Basic plant collections in southwest Arabia were made by Hugh Scott and E.B. Britton of the expedition sponsored by the British Natural History Museum, and in recent years D.F. Vesey-FitzGerald added important collections from both the coastal plain and the mountains. My own collection of some 170 named species supplements the collections made by Scott, Britton, and Vesey-FitzGerald and was made from the somewhat narrower point of view of discovering and delineating floral zones. In a few cases, material was insufficient or inadequate for sending to the museum and it was necessary to make provisional determinations. This applies particularly to the free form of *Acacia etbaica* Schweinf. and to *Commiphora africana* (A. Rich.) Engler.

[4]Deceased.

THE SEVEN FLORAL ZONES

As there are no names in general use that fit the seven zones, it seemed best to use names that could easily be learned and understood by anyone working in Arabia. The country people of Saudi Arabia are good botanists and have Arabic names for all the index plants used, and they will naturally use these names instead of the few Latin names that have seemed necessary here.

The zone-defining plants were identified as a result of making a collection of every species that was in blossom or in seed or in a recognizable condition of any kind. This was done on all the journeys, and the distribution of each plant was noted. The collection was eventually handed to the Botanical Department of the British Natural History Museum for determination, because its Herbarium is particularly rich in material from Arabia and the Middle East; this proved to be a most happy arrangement.

The rainfall estimates are based partly on the known isohyet limits of definitive plants that also happen to grow in the Sudan, where there is a long history of botanical collecting, culminating in the three fine volumes on "The Flowering Plants of the Sudan" by Dr. F.W. Andrews (1950, 1952, 1956), and where rainfall statistics have also been compiled for many years.

For the barley zone, the estimates are based on the known minimum requirements for crops in the Soluch area near Bengazi; for the agricultural zone, the estimates represent the writer's personal opinion of the rainfall required to produce regular good yields of barley, wheat, lentil, and alfalfa on that sort of soil and in that climate. In all cases, the definitive plants or crops are supposed to be growing as pure rain crops unblessed by added water from a dry wadi or by runoff water collected naturally or by human wit.

To fit the seven zones into their places, it seems both logical and useful to commence the discussion with three of the driest zones in Arabia, which, however, are not represented on the western face of the 'Asīr Mountains.

AR RUB' AL KHĀLĪ ZONE

The driest of all zones in Arabia coexists with the geographical Ar Rub' al Khālī, or, literally, The Empty Quarter; as this name is so widely known, it seems proper to use it for the driest of the floral zones. It is too dry to support trees or shrubs, and vegetation is limited to grasses and other plants that spring to life

after receiving rain from one of the rare and sporadic showers that may occur.

Throughout the zone there are dry wadis, and the large ones may carry ground water for many miles. The best of these intruding tongues support the vegetation of wetter zones; although these tongues occur in the geographical Ar Rub' al Khālī, they are here excluded from the floral zone of that name.

The rainfall for the zone can be estimated to be only a trace in the driest part and ranging to a shade less than 2 in at the boundary with the next zone. The 2-in limit is fixed by the fact that in the northern Sudan the boundary-defining shrub, samr (*Acacia tortilis*), disappears as one proceeds northward into the Sahara at approximately the 2-in isohyet.

The zone occurs in many pockets outside Ar Rub' al Khālī of the maps, as for instance in the hills behind the port of Al Wajh which include the ancient mine workings of Al Hurayrah.

SAMR DESERT ZONE

This zone is marked by the fact that the conspicuous bush *Acacia tortilis* (Forsk) Hayne, known universally by Arabs on both sides of the Red Sea as samr, is dominant. It grows sparingly to abundantly depending on soil, but there is no other bush that remotely resembles it. The zone is extended into wetter areas to the point where the bush *Acacia ehrenbergiana* Hayne, universally known to Arabs as sallam, puts in an appearance.

In the Sudan the northern limit of distribution of sallam practically coincides with the 4-in isohyet, so the samr zone extends from the 2-in to the 4-in isohyet. The zone is widespread in Saudi Arabia, but on the coastal plain it does not occur south of Jiddah.

SALLAM DESERT ZONE

This zone is characterized by the presence of the two well-known acacias samr and sallam, and by the absence of *Commiphora* and *Euphorbia cuneata*. The acacias are about equally common.

On the Tihāmah, the dry edge of the zone begins a few miles south of Jiddah, where sallam comes, at first sparingly, onto the scene. For the next 200 mi (322 km) there are many samr but few sallam, indicating a continuation of the dry edge. Between Wādī Ḥalī and Wādī 'Itwad, however, the rainfall increases so that sallam becomes well grown and as abundant as samr. The zone extends another 10 mi south until it becomes wet enough for *Commiphora africana*, or qaffal, and *Euphorbia cuneata*, known locally as maz.

Nowhere in this zone can the grain "dukhn," *Pennisetum purpureum*, be grown as a rain crop. In the Sudan 6 in of rain are required for the poorest crop of dukhn that is worth growing, and this affords a basis for assessing the wet boundary of this zone at a little less than 6 in or perhaps 5 in.

ASAK-COMMIPHORA-DESERT ZONE

The name of this zone calls attention to two of the index plants—*Acacia asak*, one of the thorn bushes called "hashab" by Arabs, and, on the coastal plain, *Commiphora africana*, or qaffal. The other two index plants are *Anisotes trisulcus* of the foothills and the nonprickly *Euphorbia cuneata* of the Tihāmah, which is widely used for supporting the thatch of village houses.

The two acacias samr and sallam reach their maximum development in this zone, as do the two important tufted grazing grasses of the samr and sallam zones, *Lasiurus hirsutus* Boiss. and *Panicum turgidum* Forsk. On the coastal plain this zone commences a little south of Wādī 'Itwad and extends through Jīzān province to beyond the Yemen frontier. As to rainfall, the northern boundary was estimated to receive 5 in.

Nothing in the vegetation indicates the rainfall at the southern boundary, but as one proceeds south through the zone, one finds that the millet "dukhn," *P. purpureum*, is grown as a rain crop at about the latitude of Port Jīzān, thus indicating a rainfall of 6 in there. As this comes at about the middle of the zone, the southern boundary can be assessed by proportion as having rainfall of 7 in.

A check on these estimates is that in the Sudan *Commiphora africana* first appears as one proceeds south in Andrews' (1950, 1952, 1956) acacia-desert-scrub region, fairly close to the northern boundary at about the 5-in isohyet. This *Commiphora* is probably the same as, and certainly the ecological representative of, the coastal plain species of the Jīzān.

KLEINIA-PASTORAL ZONE

This is a well-marked zone commencing on the western escarpment at about 5,000 ft (1,524 m), varying a little with aspect, where *Anisotes* and *Acacia asak* fade out. At this boundary the succulent composite herb *Kleinia violacea*, locally "thuriya," becomes an index plant, but it is not as common on the steep mountain slopes as on the plateau lands above.

Associated with it, however, is *Acacia etbaica*, or "qarad" of the Arabs. On the escarpment this takes the form of a vigorous bush or small tree as much as 15 ft high, but on the better lands above the scarp it takes the form of a well-grown tree as much as 30 ft high.

The upper limit of the zone, at about 7,500 ft (2,287 m), is marked both by the appearance of *Euryops* and

by the point at which barley comes to be grown as a purely rain crop. This zone is important, as it embraces the finest pastoral lands in southwest Saudi Arabia. The rainfall at the upper limit of the zone is that required for growing barley as a rain crop. Statistics are available for the Soluch area of Cyrenaica, Libya, situated on the coastal plain to the west of Bengazi. The precipitation at this place is 7 in, some 5.8 in of which fall during the barley growing season. Barley is here regularly grown as a subsistence crop, and this seems to show that 6 in of rain is the minimum needed for this crop in a Mediterranean climate. In tropical Arabia where barley is similarly grown on marginal lands, the sun is hotter and it seems reasonable to raise the estimate to 8 in.

Barley is grown in this zone only during long rains, and for 8 in of long rains one must add 2 in for short rains, making a total of 10 in. On this basis, the *Kleinia*-pastoral zone begins at the 7-in isohyet and extends to the 10-in isohyet.

EURYOPS-BARLEY ZONE

This is preeminently the zone in which barley and wheat, where suitable lands are available, are regularly grown as subsistence crops on true rain lands that receive no additional subsoil or runoff waters. It is also marked by the conspicuous presence of the composite *Euryops arabicus* Steud, locally "jabur," which can be recognized from a distance even when not in bloom because it bears remarkable resemblance to a 2-ft-high seedling of Scotch or similar pine. The herb is as stiff as a pine and has a similarly symmetrical arrangement of branches, and it completes the deception by having 2-in long leaves so narrow as to suggest needles. The dominant, and only, acacia, *Acacia etbaica* Schweinf., finds optimum conditions in this zone and becomes a well-grown(?) tree as much as 30 ft tall.

The upper limit of the zone is sharply marked by the lower altitude limit of the conspicuous and only conifer, *Juniperus macropoda* Boiss., which is likewise the lower limit for the bush *Dodonaea viscosa* Jacq.

We came upon fragments of this zone on Jabal Fayfā at what we estimated to be 4,000 to 4,500 ft (1,219 to 1,372 m), at El Qa'am on top of the escarpment 35 mi south of Abhā at 7,500 ft (2,286 m) by altimeter, near Aqabat al Alb on the Yemen frontier at 7,700 ft (2,347 m), and, finally, between Abhā and Jabal as Sūdah, where it began and ended at 7,500 ft (2,286 m) and 8,200 ft (2,499 m), respectively.

As to rainfall for the zone, the dry edge coincides with the minimum required for the regular cultivation of wheat and barley as rain crops, which was estimated above to be 10 in annually.

The wet edge is the boundary line for juniper. In the account by Hugh Scott and Everard B. Britton (1941) in the British Natural History Museum's "Expedition to South West Arabia 1937–38," this species is recorded as occurring on Jabal Gelal some 25 mi south of Ṣan'ā', Yemen. The rainfall at Ṣan'ā' averaged 11.78 in from 1938 to 1947, inclusive, and this suggests a minimum moisture requirement of 12 in for this bush or tree.

At the same edge the ubiquitous shrub *Dodonaea* makes its appearance. At Erkowit in the Sudan, this Erkowit privet, as it is there called, makes a first appearance as one approaches from the desert. The Kassala isohyet of 300 mm, or 12 in, passes through or very close to Erkowit, which also suggests the 12-in isohyet as being the upper limit for this zone.

ROSE-JUNIPER-AGRICULTURAL ZONE

The rainfall in this zone affects the flow of water to the coastal plain to only a minor extent, both because the zone is so very limited in extent and because the plateau waters from a line usually about half a mile from the edge of the scarp flow eastward to Ar Rub' al Khālī. Wādī Baysh and wadis to the south of it receive practically no water from this zone. Wādī 'Itwad receives a little, and Wādī Ḥalī receives a substantial quantity.

Literally dozens of definitive plants could be used for index purposes, but *Rosa abyssinica* R.Br. and *Juniperus macropoda* Boiss. are outstanding and suffice for practical purposes. The zone is confined in the 'Asīr region to the top of Jabal Fayfā, to a trace at the heads of Wādī Qa'ah, and to Jabal as Sūdah from above the 8,200 ft (2,499 m) contour up to the summit at 9,425 ft (2,873 m). There is no precise method of estimating rainfall for this zone, but for reasons given above the lower limit can with some degree of confidence be estimated at 12 in.

At an elevation of 9,200 ft (2,804 m) was a field owned and farmed by Sheikh Mohammad bin Mohammad bin Said, who was a brother of the "naib," or headman, of the village of Sūdah on Jabal as Sūdah. Mohammad gave me the following cropping history for the field, sown in December and harvested in May:

Year	*Crop*	*Yield*	*Average*
1952	Wheat	Fair	—
1951	Barley	Good	240 kg, or 528 lb, per feddan, or acre
1950	Wheat	Fair	—
1949	Barley	Fair	—
1948	Wheat	Good	—

Mohammad stated that during his 50 yr of active farming at the village, there had never been a crop failure, that the crops could be grown only in the long rains, and that in the short, or monsoon, rains moisture was sufficient only for the freshening of forage grasses and for the healthy maintenance of the widely grown alfalfa. The Sheikh also said that when crops of wheat and barley began to deteriorate, it was the custom to alternate with a crop of *Lens esculenta*, or lentil, as a rejuvenator.

As on Jabal Fayfā, the effectiveness of the rainfall must be substantially enhanced by the regular appearance of moist cloud, or shabura, which we experienced on several occasions during our 10-day visit. The area covered by shabura is as much as a mile wide on the plateau and is marked by festoons of Spanish moss that drape the branches of the juniper trees.

This is a good agricultural area that has very regular rainfall sufficient for the production of a fair to good crop of barley, wheat, lentil, or alfalfa. It is believed that such crops, together with juniper trees, some of which attain a height of 40 ft, seem to require rainfall of at least 14 in. The village land has an altitude of 9,200 ft (2,804 m), so the upper limit would have, by proportion, an annual rainfall of 15 in. For total rainfall, one must then add a correction of 12 percent at the Jabal as Sūdah latitude for the summer, or monsoon, rains, making a total annual rainfall of 16.8 in at the top of the mountain.

The error, in my opinion, may not be very great because Mr. Eric Mackinnon, after a very long experience in the Sudan, records for the Blue Nile Province (see Tothill, 1948, p. 804) that, "In general it may be said that the production of successful rain crops requires a rainfall of 400 mm, 16 in., or more." The hotter sun at the lower elevation of that province, coupled with the absence of shabura (mist), would tend to equate the 16 in with a little less on Jabal as Sūdah.

The estimates of rainfall for the zone are therefore 12 in at the lower boundary and 16.8 in at the top, with an average of 14.4 in.

PRECAMBRIAN LAYERED ROCKS OF THE ARABIAN SHIELD

The rock units mapped in reconnaissance fashion on the geologic map of the Arabian Peninsula (USGS–ARAMCO, 1963) were at that time described mostly in field terms, and the map was based in part on interpretation of aerial photographs. Although the map was planned only as a general guide for ore and water search, at an early stage lithostratigraphic groups were recognized to range from unmetamorphosed sediments and volcanics to greenschist and amphibolite metamorphic facies, and to change lithologically in short distances along the strike of the volcanogenic and related rocks. Because the resolution of stratigraphic problems would require detailed work over many years, the units were described only in general terms on the map legend. We have attempted to correct and amplify the earlier reconnaissance mapping with current knowledge from numerous contributors (see annotated bibliographies, Ministry of Petroleum and Mineral Resources, 1977, 1980, 1981).

HISTORIC GEOLOGIC DIVISIONS

In the first published attempts at division of the basement rock, Karpoff (1955, 1957a) described two series—the Medina and the Wadi Fatima, in the central part of the shield. We had begun our reconnaissance study 5 yr earlier at the Yemen border and had worked northward. By 1960, general rock assemblages had been extended into the areas described by Karpoff (1960), wherein we tentatively recognized eight units exclusive of plutonic rocks. Of these, six were equivalent to parts of the older Medina Series of Karpoff and two were equivalent to and coordinate with his younger Wadi Fatima Series. By 1963, after mapping seven quadrangles (3°×4° at a scale of 1:500,000) and segments of three others—about 36 percent of the Kingdom of Saudi Arabia—we compiled a map at 1:2,000,000 scale which was combined with the mapping of the Arabian-American Oil Company (ARAMCO) and various others into the composite map of the Arabian Peninsula (USGS–ARAMCO, 1963). At that time we recognized a total of 33 units among the basement rocks, of which 19 were given rock-term names without formal reference to geographic localities. Of the 14 names based on geographic localities, 2 were regional, namely the Halaban and the Shammar. The Halaban was named for Ḥalabān Ridge and the region around Ḥalabān Pass near the southern end of the ridge in the east-central part of the shield, and the Shammar was named for Jabal Shammar, the regional name for the area around Ḥā'il in the northeastern part of the shield.

Some explanation of the first use of these names is desirable. The first geologist to describe layered rocks near Ḥalabān Ridge was Bogue (1953) of the USGS. He thought that the dioritic and andesitic greenstone and related rocks of the region were probably the same as the "Shawaq volcanics" he had earlier described at Wādī Shawāq in the Jabal ash Shifā' region 900 km northwest of Ḥalabān and near the northwestern edge of the shield. We felt that even though the lithology and metamorphism appeared to be similar, the units were separated by too great a distance of unmapped terrain to justify correlation until the areas were

mapped in more detail. Accordingly, G.F. Brown and R.O. Jackson (1960) chose the name "Halaban Andesite" for Bogue's "Shawaq volcanics"; later the term "Halaban formation" was used, because it was known that rock types other than andesitic greenstone were in the section and that an assemblage of at least group rank would be found if it were mapped in any detail (Eijkelboom, 1969).

Likewise, the name "Shammar rhyolite" was used (Brown and Jackson, 1960) to designate the largely unmetamorphosed and silicic volcanic rocks associated with sedimentary rocks cropping out in the northern part of the shield, to distinguish these younger rocks from older rhyolite and related volcanogenic beds farther south.

The six other names published in 1960 (Brown and Jackson, 1960) were, from oldest to youngest, the Hali Schist, Baish Greenstone, and Lith Complex below the Halaban, and the Murdama, Fatimah, and Ablah Formations above the Halaban and below the Shammar rhyolite. Later we described (USGS–ARAMCO, 1963) the Jiddah Greenstone, which is intruded by the Mecca Granite, the Hibshi Formation, dominantly a clastic-volcanic formation that disconformably overlies a gray biotite granite and underlies at least part of the Murdama phyllite in the Jabal Shammar region, the Hadiyah slate in the northwestern part of the shield, and the iron-bearing Silasia Formation. Units were individually named because field information was insufficient to warrant closer correlation over large areas. Names of large wadis or coastal towns were used to avoid giving a specific type locality until the units could be mapped in detail and the best type sections and localities could be chosen. The Murdama and Hibshi Formations are exceptions; both have excellent sections on the mountains of those names.

CURRENT GEOLOGIC DIVISIONS

During the past 17 yr, more detailed mapping by numerous geologists has begun to elucidate structural complexities, chronologic episodes and sequences, sedimentary and volcanogenic facies changes, and metallogenic epochs. Computer-enhanced imagery from satellite signals supplied a new tool that supplements aerial photographs and standard color composites of satellite-derived scenes (Blodget and Brown, 1982). Airborne magnetic and digital gamma-radiation surveys also helped in interpreting the geology.

As a result of the more detailed mapping, some formations of the USGS–ARAMCO map (1963) were raised to group rank (Schmidt and others, 1973) to include various formations named for specific localities and type sections. Also, because many more radiometric ages have been determined and structural control is better understood, the sequence of groups has been changed somewhat. The rock units, as currently (1982) mapped and named, are shown in plate 1.

ULTRAMAFIC AND OPHIOLITIC ROCKS

Ultramafic and serpentine rocks and associated mafic volcanic and plutonic rocks, chert, slate, and marble are widespread but are sparsely distributed throughout the shield. Ultramafic rocks associated with the older marine beds of the Baish-Bahah were described by Hadley (1975a) as an ultramafic complex in part "conformably interbedded in the Baish group and in part intrusive into it" (Qunfudhah quadrangle, lat 19°10′ N.). Greenwood (1975b) has mapped a serpentine-talc belt at the base of the Baish Group farther northeast in the Biljurshī' quadrangle at lat 19°55′ N. At Jabal Rayyan (Wask) (Al 'Ays area) a mafic-ultramafic dome has been studied intensely for its chromite potential (Kahr, 1961; Johnson and Trent, 1967; Bakor and others, 1976; Kemp and others, 1980; Kemp, 1981). Samples collected by Viktor Kahr, who recognized the domal rocks as belonging to the ophiolitic suite, were studied by T.P. Thayer, who identified peridotite, alpine gabbro (with alteration to prehnite and other minerals of the rodingite suite), and "...albitized volcanic breccia commonly associated with albite granite of the end member of the alpine mafic magma stem," all identified with ophiolite. Kemp and others (1980) report a Pb/U age of 882±12 m.y. from zircon in plagiogranite of the ophiolitic complex. Bakor, Gass, and Neary (1976) consider the ophiolite dome to have formed in a back-arc environment. As these ultramafic rocks are on the southwest flank of the youngest fault zone (part of the Najd fault system of the shield) and on the northeast flank of the Wādī Kamāl domal complex, it appears that the upper mantle-basal oceanic layers of the Wask ophiolite were exposed either by Najd faulting and subsequent erosion or by uplift of circumferential younger granites—or by some combination of the two processes. This interpretation is strengthened by the fact that the tectonics follow the pattern of equal-intensity aeromagnetic lines (Andreasen and Petty, 1974).

Farther north and 38 km southeast of Al Wajd, black schists are exposed for 1 km along the track (von Gaertner and Schurenburg, 1954). The carbonaceous schist extends northward at least as far past Al Wajh as the southeast border of Jabal Libān at lat 26°30′ N., where the older metamorphosed flows and sediments produce a bluish hue on enhanced satellite imagery (Blodget and Brown, 1982). These beds, as mapped by the Japanese Geological Mission (1965), include meta-

gabbro, metabasalt, metadiabase, cherty slate, and limestone (marble). Serpentinite is exposed along an overthrust fault at the eastern edge of the Wajd segment but may not represent the ultramafic base of a possible Wajd ophiolitic suite (Japanese Geological Mission, 1965), although it is in a structural position similar to that of the ophiolite fragments along sutures displaced from the southeast by Najd transverse faulting.

Other ophiolitic suites, generally incomplete as ophiolite was defined at the Penrose Conference (Anonymous, 1972) as a classical stratigraphic section of ocean floor above mantle rocks, occur in fault zones at junctions considered to be plate or island-arc boundaries within the shield. The most complete but fragmented ophiolite (fig. 4) is at Jabal Ess (Al-Shanti and Roobal, 1982) (lat 26°22′ N., long 37°38′ E.); the largest exposures are around Jabal Rayyan (Wask) within the Al 'Ays region northwest of Yanbu' at lat 25° N., long 37°30′–38°10′ E. The longest outcrop of ultramafic and related rocks of probable ophiolitic origin follows the Nabitah fault zone from the Yemen border northward to the Najd fault zone at lat 21° N., where it is offset 120 km left laterally along the Najd fault zone to the northwest (in various fragments), the northwesternmost outcrop being the Tuluhah tectonic belt north of lat 25°30′ N. (Frisch and Al-Shanti, 1977). The easternmost ophiolitic zone is along the front of the Al Amar-Idsas fault near the east edge of the shield. Other than the ophiolite in the Al 'Ays region, the ages of other ultramafic and serpentinized suites are not known to us.

If these rocks are dismembered ophiolites, they should be structurally, not stratigraphically, related to—and of different ages from—adjoining rocks. If the island-arc accretion model is accepted, the ophiolite rocks might be expected to become progressively younger eastward; they should be somewhat older than the island-arc rocks with which they are structurally associated.

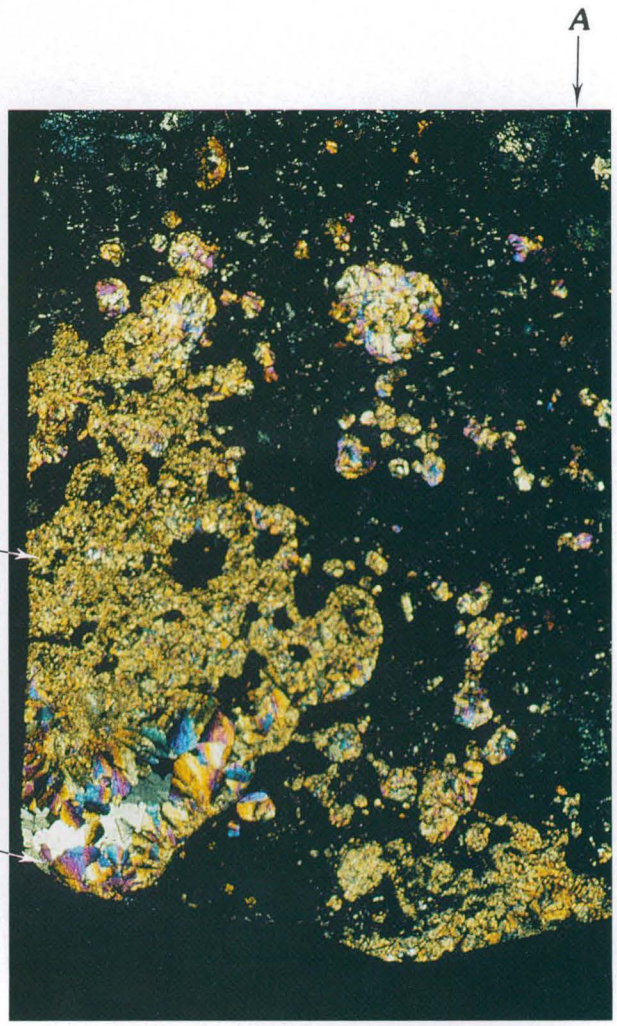

FIGURE 4.—Photomicrograph of amygdaloidal metabasalt at the Jabal Ess ophiolite complex at lat 26°22′ N., long 37°38′ E. The groundmass is equigranular, completely chloritized clinopyroxene(?) and calcic feldspar (*A*) with two generations of amygdules, the oldest fine grained and filled with secondary calcite (bent twinning planes), quartz, chlorite, and prehnite. The multimineral vesicle filling (*B*) was later transected by coarse-grained calcite (*C*). Described by Salman Bloch. Magnification ×10.

BAISH-BAHAH GROUPS

The presumed lowermost and oldest rocks originally described in the Arabian Shield were metadiorite, metagabbro, and amphibolite formerly named the Lith Complex and occupying a 1° square at Al Līth. A 55-km-wide belt of metamorphosed lavas and sedimentary rocks along the banks of Wādī Ḥalī and Wādī Tayyah at lat 18°30′–18°44′ N. were named the "Hali Schist." These rocks consist of two units: (1) basalt and andesitic basalt containing local pillow structure, with interbedded marine volcaniclastic and sedimentary wacke, and (2) carbonaceous and graphitic schists, and minor marble and chert, all metamorphosed to the greenschist facies and generally retrograded from the amphibolite facies. Both of these units were originally shown on the geologic map of the Arabian Peninsula (USGS-ARAMCO, 1963). The Hali Schist was later redefined (Schmidt and others, 1973) as a result of more detailed mapping and was described as quartz-biotite-garnet schist interbedded with marble, stretched-pebble conglomerate, and metamorphosed volcanic rocks, including the older, more metamorphosed "Lith Complex." The name "Lith Complex," shown on the 1963

A *B*

FIGURE 5.—Baish-Bahah Group. *A*, Metasedimentary schists in the Jabal 'Aya quadrangle formerly believed to be of Baish-Bahah age but now believed to belong in the younger Jiddah Group, having been overthrust from the east. View south along the top of the An Nimas escarpment. The beds dip east. *B*, Glaucophane schist near Ad Darb in Bahah Group indicating high pressure in the low-glaucophane schist facies beneath overthrusts from the east. The pocket knife is 9 cm long.

map as the basal rock unit of the shield, was abandoned because it included diverse rock types that were later mapped as separate units.

The Baish Greenstone was first described from exposures in cliffs along Wādī Baysh, at lat 17°40′ N. (Brown and Jackson, 1959, 1960), where spilitic pillow lava crops out (fig. 5) as massive greenstone or sericite-chlorite schist derived from mafic igneous rocks. Also included in the unit were metadiorite, metagabbo, and amphibolite with subordinate siliceous slate. The thickness as originally measured along the western limb of a syncline was 12,000 m, but more recent work suggests a synclinal structure with 6,700 m of tholeiitic basalt on one limb (George Simmons, USGS, oral commun., 1979). The unit was originally thought to overlie the Hali schists downstream in the Baysh Canyon, but the structure is complicated by tight folds and faults and the relationships are still not clear.

Schmidt and others (1973) redefined and raised the Baish Greenstone to group rank and placed it immediately above the Hali Group. The upper schistose part was split off from the marine sediments containing metabasalt cobbles above a disconformity (Greenwood, 1975c) to form the Bahah Group, although the lithologic description remained much the same. Baish and Bahah Groups form the "metabasalt graywacke-chert assemblage" of Greenwood (1975c) or the "basaltic assemblage" of Fleck and others (1980).

The two groups have as common components pillow metabasalt, marble, chert, carbonaceous or graphitic schist, and some meta-andesite, but the components are volumetrically in widely different proportions, hence their separate names. The two groups are quite distinct from the overlying andesitic lavas and volcanogenic sedimentary rocks of the Jiddah and younger groups (Schmidt and others, 1973; Hadley 1975a, 1975c; Greenwood and others, 1976).

The Bahah Group, named from the village of Al Bāḥah in the Jabal Ibrāhīm quadrangle (Schmidt and others, 1973; Greenwood, 1975c), includes formations considered in this report to be structurally below the Baish Group but stratigraphically above or synchronous with the Baish. The marine Bahah Group includes paraschists of clastic or tuffaceous origin with distinct ferruginous quartzite, metachert, and carbonaceous and arkosic members. Marble, stretched-pebble conglomerate, and metabasalt make up less conspicuous beds. Carbonaceous beds common in both the Baish and Bahah Groups appear to owe the carbon to algal growth in water within the photic zone, probably less than 250 m depth (Jackaman, 1972; Kiilsgaard and others, 1978). A similar assemblage of rocks including metabasalt, carbonaceous or graphitic schists, and jasper or chert extending intermittently on promontories of the crystalline shield as far north as Al Wajh at lat 26°16′ N. has been questionably remapped as part of a younger epoch. At Wādī Fāṭimah, paraschist, jasper, and keratophyre (including minor marble, and epidosite) are intruded by "pyroxene granite" (Richter-Bernburg and Schott, 1954) and were contact-metamorphosed to amphibolite facies. Northwest of Yanbu' at lat 24°20′ N., gneiss comprising amphibolite, quartzite,

and leptite is intruded by the Wadi Kamal Complex of norite, orthoamphibolite, anorthosite, and ultramafic (serpentinized) rocks which were tentatively referred to the Hali by Baubron and others (1976).

Three samples of metabasalt near Al Līth at Wādī al Fagh, lat 20°23′ N., gave an age of 1,165±110 m.y. from a whole-rock Rb-Sr isochron (Fleck and others, 1980, p. 31), in contrast to more recent work in another laboratory which resulted in Rb-Sr dates of 836±60 m.y. and 830±9 m.y. for metabasalt in Wādī Sa'dīyah in the western part of the Al Līth area, presumably from rocks considered Baish ("Lith") age (Reischmann, 1981). Minimum ages for the layered rocks based on whole-rock Rb-Sr isochrons of intrusive quartz diorite near Biljurshī' (lat 19°52′ N.) and Al Līth are about 850 and 890 m.y., respectively (Fleck and others, 1980, p. 19); farther north, Aldrich (Aldrich and others, 1978) measured a single K-Ar age of 1,190 m.y. for hornblende in amphibolite at the northwestern corner of Jabal Shār, lat 27°20′ N. (sample 11, table 6). Still farther north, carbonaceous slate containing fossil blue-green algae in southeastern Sinai yielded a Rb-Sr isochron date of 934±80 m.y. (Shimron and Horowitz, 1972; Shimron and Brookins, 1974). However, the Sinai date has been questioned (Halpern, 1980).

JIDDAH GROUP

First shown on the peninsular geologic map (USGS–ARAMCO, 1963) as the Jiddah Greenstone, the meta-andesite in the foothills east of Jiddah, where it is intruded by the Mecca Granodiorite, was described as andesite and andesite porphyry metamorphosed to the greenschist facies. In many places it is schistose, but it includes some diabase, gray slate, conglomerate, dacite, and marble. The first radiometric dates determined for the Mecca Granodiorite range from 965 to 1,025 m.y. for Rb-Sr ages and from 720 to 760 m.y. for K-Ar ages as determined by Aldrich (*in* Brown, Jackson, Bogue, and MacLean, 1963; Aldrich and others, 1978; samples 114 and 124, table 6), using the decay rates adopted by the 25th International Geological Congress (1976). For this reason the Jiddah Greenstone was considered to be among the oldest rocks of the shield and was placed beneath the Baish Greenstone and above the Silasia iron formation of northwestern Arabia, as described by Bogue.

Bhutta (1970) recognized two units within the Jiddah Greenstone: a lower series of metamorphosed flows and pyroclastic rocks (andesite, diabase, andesite porphyry, rhyolite, and greenstone) and an upper, younger sequence of slate, metaconglomerate, tuff, quartzite, and marble (figs. 6*A*, 6*B*). The unit was further defined and named the "Jiddah group" (Schmidt and others,

A

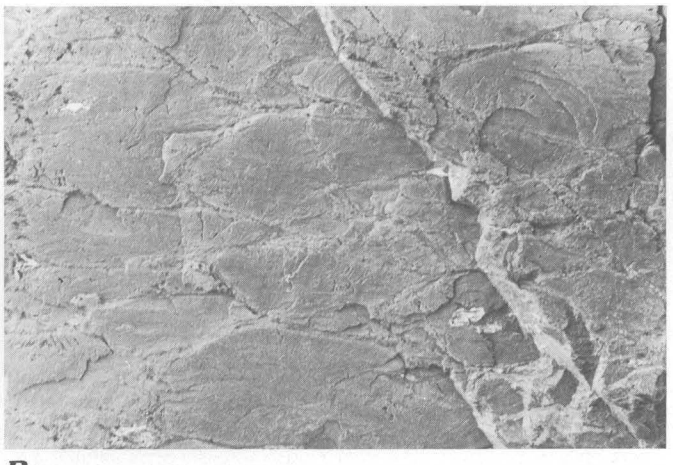

B

FIGURE 6.—*A*, Hornblendite interbedded with pink marble of the Jiddah (Samran) Group in Wādī Fāṭimah. Two periods of folding are apparent. *B*, Pillow lava in basalt, Hilwa area, on north wall of Wādī Baysh gorge, formerly believed to be in the Baish Group but now believed to belong to the Jiddah Group. Lower pillow is about 1 m long.

1973) following more intensive fieldwork and an extended field conference that covered eleven 30′ quadrangles in the southern part of the shield. The relationship between the Baish-Bahah and Jiddah Groups is not clear, but possibly the Baish-Bahah Group is slightly older in that metamorphosed clasts of the older rocks were reported in the basal units of the Jiddah Group (Greenwood and others, 1976) and in turn were overlain with angular unconformity by the Ablah Group. This is the stratigraphic position we had earlier assigned to the meta-andesitic and related rocks exposed within the Southern Hejaz quadrangle (Brown, Jackson, Bogue, and MacLean, 1963).

The Jiddah Group consists of a lower volcanic formation, the Qirshah Andesite, and an upper clastic, predominately immature arkosic and volcaniclastic wacke, the Khutnah Formation (Greenwood, 1975b). The Qirshah Andesite, named for Wādī Kirshah, a tributary to Wādī Ranyah at lat 20°10′ N., consists predominantly of andesitic pyroclastic and flow rocks and includes dacite breccia, ignimbrite, marble, and some pillow basalt, suggesting a marginal marine origin similar to the calc-alkaline suite of island-arc volcanics in contrast to the more mafic (calcic) volcanic rocks and deeper marine beds of the Baish-Bahah Groups. Much of the sedimentary and volcaniclastic schist of the Jiddah Group is graphitic and includes beds of chert and minor basalt, thus resembling the upper Bahah Group. Within the 'Aqīq quadrangle and west of the Ablah graben, the Jiddah Group includes spilitic mafic flows, tan and brown marble, andesite with blobs of serpentine, and fine-grained pyroxenite(?), the ultramafic suite of G. Eijkelboom (oral commun.).

More recent work extending northward along the coast indicates that metabasalt, meta-andesite, and graphitic schists that were mapped as Jiddah Greenstone as far north as Al Wajh lithologically resemble the Baish-Bahah (Blodget and Brown, 1982) and are the same beds named "Samran" by Charles Smith and Vicktor Kahr (unpub. data), later adopted by several authors, and finally defined by Skiba (1980). Some metavolcanic and metasedimentary rocks in the southeastern part of the shield that were considered Jiddah group by Schmidt and others (1973) and by Greenwood and others (1980) also resemble the Baish-Bahah Groups, so that on the basis of chemical analyses, as well as on the basis of structural relations and metamorphism, these rocks are shown to be similar to the Hali schist as it was originally mapped (Brown and Jackson, 1959). The most striking evidence of the Bahah–Hali (now Bahah) affinity is the cherty and carbonaceous or graphitic schists that crop out on both flanks of the Khamis Mushayt gneiss complex in the 'Asīr highlands. In contrast, the Jiddah Greenstone as originally mapped was mostly meta-andesite in greenschist facies. The more extensively mapped Jiddah Group, however, does contain cherty and carbonaceous facies, and, in fact, any island-arc terrane, regardless of age, might be expected to contain this facies; the facies is not group diagnostic. The Jiddah Group as shown on plate 1 also includes andesitic rocks mapped as the Samran series in the area of Jabal Samrān (Nebert, 1969).

A tentative reported age for the volcanic rocks of the Jiddah Group comes from a roof pendant on the An Nimas batholith, where Fleck and others (1980) found an apparent age of 912±76 m.y. from a whole-rock Rb-Sr isochron. The rocks were considered part of the lower Jiddah Qirshah meta-andesite by Greenwood (1979).

Concurrent with and subsequent to the accumulation of the Jiddah Group, calcic and calc-alkalic plutonic rocks of a comagmatic suite ranging from gabbro through quartz diorite to trondhjemite and granodiorite, but mostly diorite and quartz diorite, were synkinematically intruded into the Baish-Bahah and Jiddah Groups during the period 890±67 to 848±28 m.y., according to Rb/Sr isotopic ratios (Fleck and others, 1980). Some of these plutonic rocks were locally reactivated during the period 797±15 to 763±4 m.y. (Cooper and others, 1979) into orthogneiss domes ranging in composition from tonalite to granodiorite; thus they define a minimum Jiddah age. The intrusions and the concomitant orogenies have raised locally the metamorphic rank of the older lithostratigraphic assemblages to amphibolite facies.

Recent, more detailed study of the granitoid intrusives in the Jiddah–Makkah area at the type locality of the Jiddah Group gives ages of 763±159 m.y. from whole-rock isochrons (Fleck, 1985) of samples including quartz diorite and granodiorite gneiss intruded into the calc-alkaline meta-andesite of the Jiddah Group. If correct, this value establishes a younger minimum age for the group than determined by Aldrich and corresponds in general to the K-Ar ages of biotite, 720 and 760 m.y., and of muscovite, 800 m.y., obtained by Aldrich for the same samples yielding Rb-Sr biotite ages of 965 and 1,025 m.y. (table 6). Thus it appears that the major gneiss doming of the subsequent Ablah orogeny at about 763 m.y. reset the intrusive dates, and the relative ages of the Jiddah (Samran) and Baish-Bahah Groups remain uncertain.

ABLAH GROUP

The name "Ablah" was first used for the Ablah Formation (fig. 7) and applied to a belt of sedimentary rocks exposed in a graben extending south-southwest

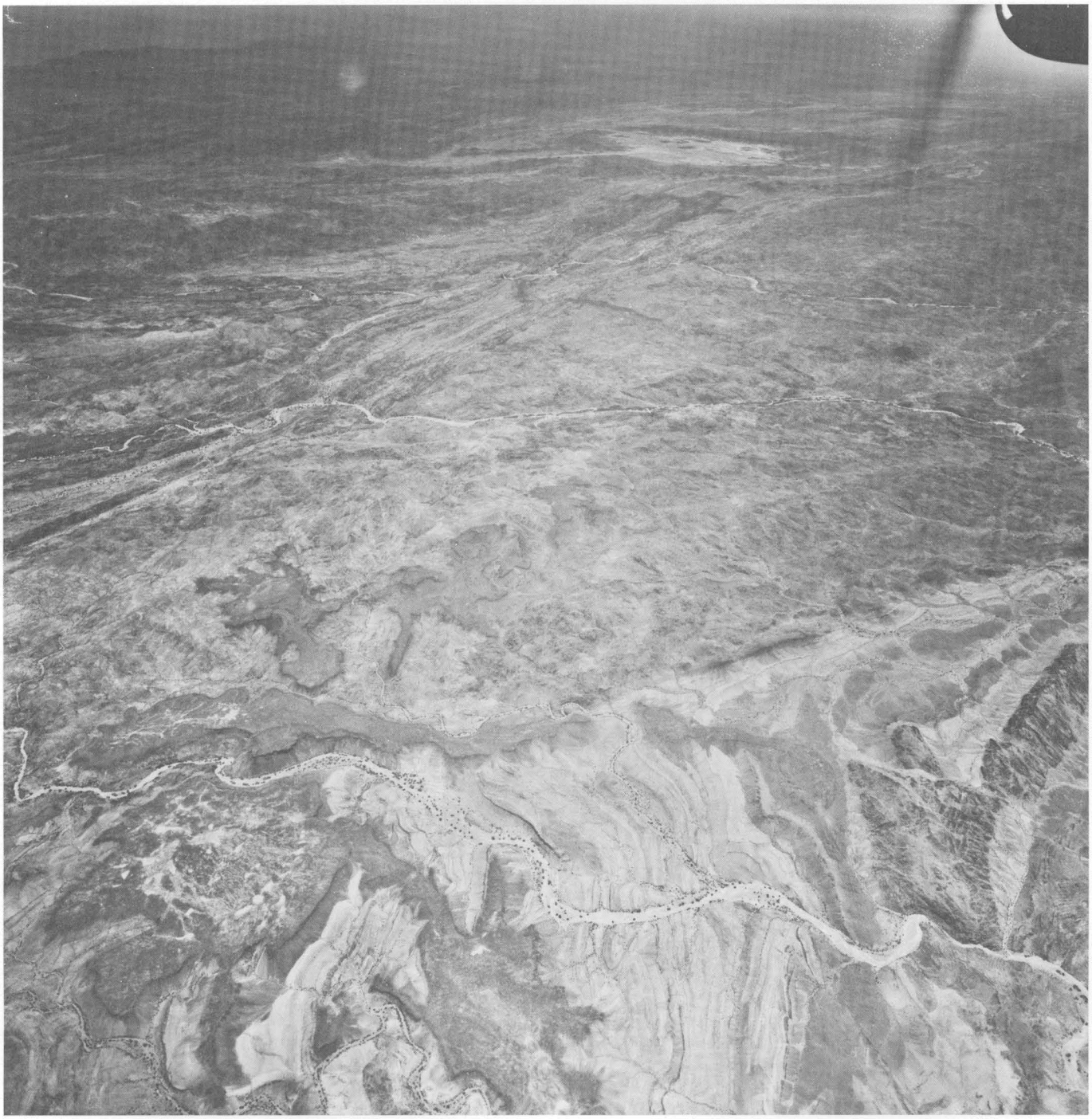

FIGURE 7.—Oblique aerial view to the northwest across the Ablah and Jiddah Groups. The boundary between the groups is the fault line in the lower third of the scene at the edge of the folded Ablah sediments. Wādī Ranyah flows northeast in the foreground, bisecting Tertiary, probably Pliocene, flood-basalt outliers, and the folded and faulted Ablah Group. Wādī Kirshah in the middle distance and Wādī Thurat beyond flow across andesitic metavolcanic rocks of the Jiddah Group. Older dioritic rocks intrude the volcanogenic rocks in a belt east of the oasis of 'Aqīq, the small light-colored plain in the distance.

from Jabal Rafā' (lat 22°30′ N., long 42° E.) past a fluorspar pipe at 'Ablah that was mined during the time of the Abbasid Caliphate (Brown and Jackson, 1960). The basal polymict conglomerate, quartzitic wacke, red sandstone, stromatolitic limestone, arkose, and purple shale rest nonconformably on Jiddah Group metavolcanic and plutonic rocks. They are folded into a series of asymmetric anticlines and dip predominantly to the east. Theobald and Thompson (1966), in a detailed study in the vicinity of a native copper occurrence at Jabal "Namar" (Rumur) in the southeastern part of the 'Aqīq quadrangle, described a sequence of red laminated siltstone and gray crossbedded sandstone containing some conglomerate lenses on disconformities within the sediments which grade upward into ferruginous wacke and andesitic breccia. Andesite flows and feeder dikes are present in the midsection. Some of the coarser grained sedimentary rocks contain fluorite, seemingly epigenetic and coeval with the Ablah fluorite pipe. The copper is stratabound, possibly syngenetic, and is structurally related to the contemporaneous andesite flows and dikes.

The Ablah rocks extend southward discontinuously from the Ablah mine area in a narrow faulted belt in which the rocks are found as roof pendants in, or as grabens between, the diorite-trondhjemite-granodiorite batholiths of the 'Asīr and Tihāmat ash Shām (Bayley, 1972; Greenwood, 1975a, 1975b; Hadley, 1975c; Anderson, 1979). Thin beds of stromatolitic marble thicken southward from two horizons in the Ablah beds at 'Ablah (calcite and siderite cement are common at several horizons). The beds become metamorphosed progressively southward to a greenschist facies in the northern part of the Wādī Yiba quadrangle and to almandine-amphibolite and sillimanite facies at lat 19° N. (Bayley, 1972; Hadley, 1975c) in the Wādī Ḥalī quadrangle. At the north end of the infolded graben at 'Ablah, Greenwood (1975a) divided the Ablah Group into three formations: a basal polymict conglomerate-wacke-marble series metamorphosed to greenschist, his Rafa Formation; a middle unit composed essentially of calc-alkaline flows but including rhyolite, quartz latite, some basaltic extrusives with pillow structure, marble, and pyroclastic rocks, his Jerub Formation; and the younger beds making up the original Ablah Formation, his Thurat Formation. Greenwood (1975a) gives a thickness of the Thurat as 1,100–1,300 m, but the lower units and their southward extension in the Ablah graben are so folded and faulted as to make thickness estimates unreliable. The Ablah Group appears to extend southward to and across the Yemen border at lat 17°30′ N., mostly as paraschist, marble, conglomerate, and quartzite or slate beds (Anderson, 1979). The basal polymict conglomerate is discontinuously exposed from 'Ablah to Jallat al Mawt on the Yemen border, where the pebbles and cobbles are gray gneissic quartz diorite or trondhjemite, quartzite, and chloritic hornfels.

Hadley (1975c) divided the Ablah Group in the Wādī Ḥalī quadrangle into two formations, because the correlation with the three formations defined by Greenwood (1975a) in the 'Aqīq quadrangle is tenuous on the basis of depositional and metamorphic facies changes. Hadley's two formations are the Sarban, mostly paraschist and marble metamorphosed to the amphibolite facies, and the overlying Hadab, likewise amphibolite schist but retrogressively metamorphosed and including gneiss (Hadley, 1975d). However, the Ablah Group comprises a definite sequence of shallow-water and nonmarine beds (fig. 8) overlain by calc-alkalic lavas and stromatolitic limestone and marble above a widespread nonconformity. The basal conglomerates contain boulders of the Jiddah trachytoidal and amygdaloidal andesites and related rocks as well as some rocks from the older Baish-Bahah Groups.

FATIMAH GROUP

The Fatimah Group (fig. 9) exposed in the hills north of Wādī Fāṭimah as originally described by Karpoff (1955, 1957a) is remarkably similar to the Ablah Group. It rests nonconformably on the granodiorite of Mecca and includes red and green immature clastics, stromatolitic limestone, tuffaceous sediments, andesite and basalt flows (Goldsmith, 1966; Nebert and others, 1974). However, the uppermost flows come from feeder dikes which transect the lower sediments and are younger than the sedimentary rocks. The thickness as measured by Goldsmith is about 1,000 m and is comparable to the Thurat Formation at 'Ablah. The age of the Ablah-Fatimah Groups may fall somewhere within the timespan between 816±3 m.y. (Kemp and others, 1982) for the Mahd adh Dhahab area and 763±55 m.y. for the Bagarah gneiss dome of the Ablah belt (Fleck and others, 1980).

Both the Fatimah and the Ablah are intruded by postorogenic magma; an andesite sill and a basalt flow at the top of the exposed section of sedimentary rocks in Wādī Fāṭimah are dated at 592±23 and 576±28 m.y., respectively, by K-Ar whole-rock analyses (table 6); however, both the andesite and the basalt are hydrothermally altered and the ages could be reset. At 'Ablah an intrusive basalt plug that pierces the upper Ablah-Thurat sedimentary rock is dated at 585±39 m.y. (sample 136, table 8). However, stromatolites described by Karpoff are *Collenia* and *Corophyton*, which together in general appearance led him to consider the Fatimah Upper Precambrian in accordance with the age assignment in Africa. More recently, a sample of one stromalolite collected by D.L. Schmidt was examined by

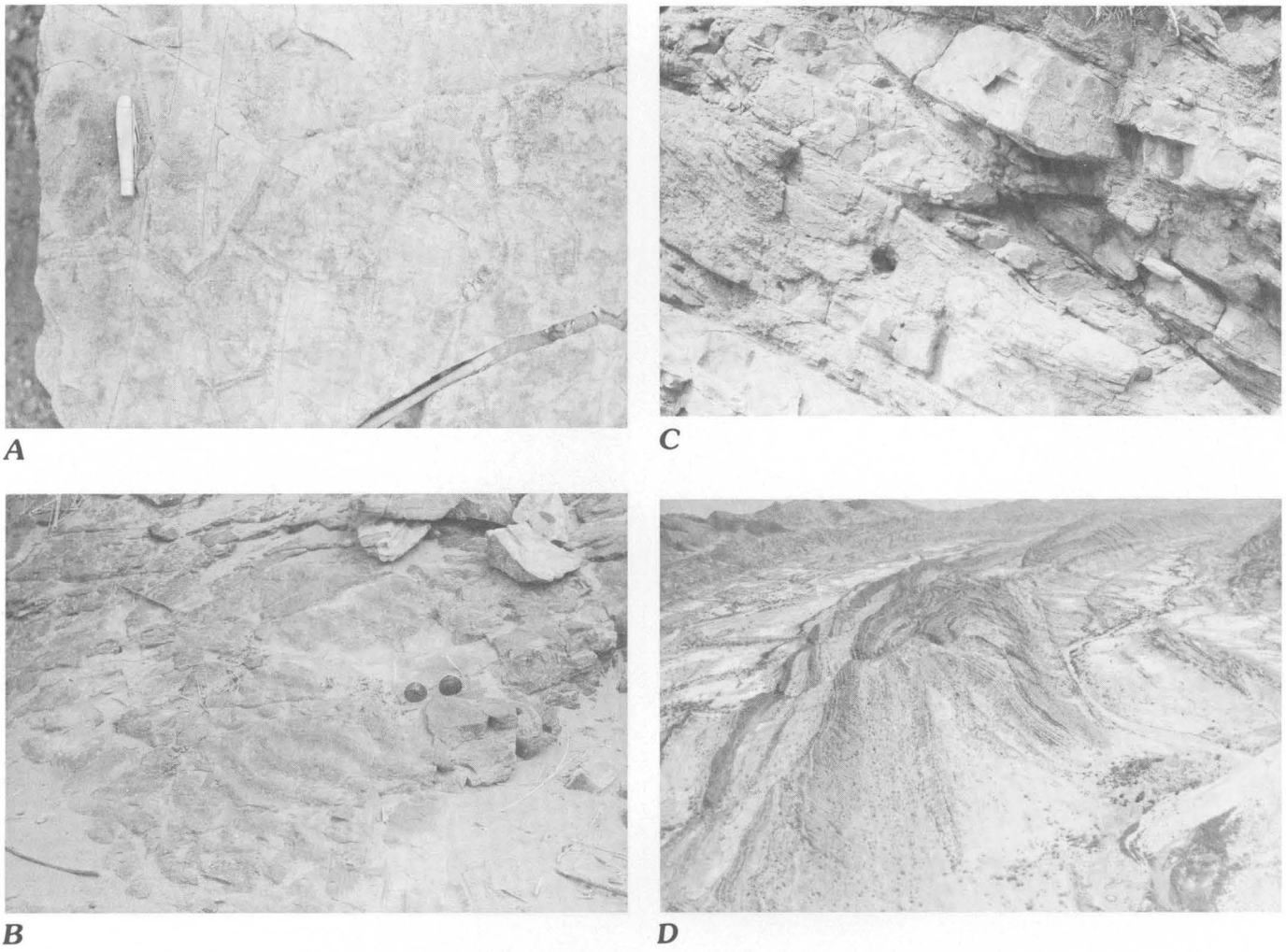

FIGURE 8.—Views of the Ablah Group. *A*, Infilled desiccation cracks in gray siltstone, and *B*, symmetrical ripple marks in associated red siltstone, at type locality of Ablah Group, 7.5 km upstream from the junction in Wādī Kirshah, Al 'Aqīq quadrangle. *C*, Small thrust fault in Ablah Group at the type locality. Siltstone at lower left underlies red faulted sandstone. Thrust is from the east at the junction of Wādī Kirshah and Wādī Ranyah, Al 'Aqīq quadrangle. *D*, Parasediments of the Ablah Group intensely folded into a plunging syncline at Wādī Yiba. View northwest.

Preston Cloud (USGS) and S.M. Awramik (written commun., 1978), who consider the form to be close to the morphology of *Kussiella*, a characteristically lower Riphean form of 1,350 to 1,650 m.y. (glauconite age). However, they report at least one record of *Kussiella* from the upper Riphean or within the timespan 675–950 m.y. (glauconite). Thus, it appears that the Fatimah sedimentary rocks could be coeval with the Ablah. These sedimentary rocks constitute a typical molasse assemblage, in contrast to the underlying Jiddah, Baish, and Bahah Groups, which are predominantly island-arc assemblages.

AL AYS GROUP

The term "Al Ays Group" has been applied in the western part of plate 1 north of lat 24° N. for extensive sedimentary and volcanic rocks that are similar to the Ablah Group rocks in the southwestern shield. Many of the predominantly metavolcanic rocks in an eastern belt had been mapped as Halaban andesite, and many of the predominantly sedimentary rocks of volcanic derivation in a western belt had been mapped as sericite and chlorite schist by Brown, Jackson, Bogue, and Elbert (1963). Hadley, mapping in the northern part of these two belts, had assigned both the sedimentary and volcanic rocks to the Halaban Group on the basis of lithology and limited age relationships. On the basis of more extensive mapping, rock description, and more recent age determinations by Kemp (1981), Pellaton (1979), and Kemp and others (1980), we have tentatively correlated the Al Ays Group with the Ablah Group of the southern shield (pl. 1).

The Al Ays Group is well defined by Kemp (1981) in the Wādī al 'Ays quadrangle (lat 25° N., long 38° E.), where it is divided into a western facies of predominant-

FIGURE 9.—Fatimah Group, north Wādī Fāṭimah. Folds in stromatolitic and clastic sedimentary rocks.

ly metasedimentary rocks and an eastern facies of predominantly metavolcanic rocks. The base of the group consists of conglomerate, minor marble, basalt flows, the minor silicic volcanic rocks overlain by thick deep-water graywacke containing some silicic tuffs. Several regressions and transgressions higher in the section resulted in more conglomerate, stromatolitic marble, and shallow-water graywacke containing silicic welded tuffs and basaltic andesite flows. The volcanic eastern facies is bimodal, containing basaltic andesite and silicic tuffs with minor sedimentary rocks (Kemp, 1981).

The age of the Al Ays Group is not well defined, but the group is underlain by volcanic and plutonic rocks that are probably older than 800 m.y. and is overlain by the Hadiyah Formation of the Murdama Group. Two silicic tuffs within the Al Ays Group have Rb-Sr ages of 743±12 (initial strontium ratio 0.7027) and 725±16 m.y. (initial strontium ratio 0.7046), and the Jabal Salajah tonalite intruding the Al Ays Group has a U-Pb zircon age of 725±12 m.y.

SILASIA FORMATION

Farther north, near lat 28° N., the iron-bearing Silasia Formation is associated with spilitic and diabasic greenstone. The formation was named by Richard Bogue (1953) and was described as consisting of mostly shale, locally sandy, calcareous, or conglomeratic, and enclosing thin-bedded limestone and thin alternate beds of jasper and hematite in the upper part with a thickness of not less than 1,400 m (fig. 10). The typical iron-formation-banded jaspilite-hematite layers, best seen in Wādī Sawāwīn at lat 27°55′ N., are exposed in pods interbedded with slate, limestone, tuffs, agglomerate, and conglomerate, all of which are intruded by fine-grained diabasic diorite and intensely deformed. Bogue believed that the spilitic greenstone, which he named

FIGURE 10.—Silasia Formation showing siliceous hematite outcrops intruded by diorite at Wādī Sawāwīn.

the "Shawaq Greenstone" from the ancient town and wadi 80 km southeast of Wādī Sawāwīn, overlay the iron formation, but he further stated that the iron-bearing beds are highly folded and in places are overturned. Later, Johnson and Trent (1967) believed that the greenstone underlay the Silasia clastics. The Japanese Geological Mission in 1967 correlated the beds with the Hali schist, and Liddicoat (1975) measured a thickness of 919 m for the upper sedimentary section. The Silasia and Shawaq Formations remain enigmatic to this day; on plate 1 the Shawaq Greenstone is mapped as part of the Jiddah Group and the Silasia Formation is retained as a younger volcanogenic metasedimentary unit equivalent to the Ablah type, following the concept that many of the beds formerly named "Hali Schist" are of Ablah age.

HALABAN GROUP

In the eastern part of the Arabian Shield, Bogue (1953) briefly described "a variety of both intrusive and extrusive rocks . . . mostly andesite and fine-grained diorite, but gabbro, basalt, and basalt porphyry are not uncommon"—igneous rocks he considered possibly equivalent to the Shawaq volcanics of northwestern Arabia. Our subsequent mapping suggested that the calc-alkaline volcanic rocks and associated plutonic and hypabyssal intrusives in the eastern regions were most likely somewhat younger than the Shawaq volcanics, although both are regionally metamorphosed, the Shawaq to a somewhat higher grade. Accordingly, we proposed the name "Halaban Andesite," choosing a regional name for the area where Bogue described widespread outcrops in the region around Ḥalabān Pass and the water well near the southern end of the

FIGURE 11.—View north along the strike of stratabound gossan at Wādī Wassāṭ in Halaban Group volcaniclastic sediments cut by late Halaban quartz diorite in foreground. The quartz diorite is locally gneissic from upward movement during the culminant orogeny.

50-km northwest-trending ridge, Samrā' Ḥalabān, and where Sha'īb Ḥalabān, a tributary to Wādī as Sirrah, affords an east-west caravan route. As we could not designate a type section for a formation, it was necessary to use a rock name in accordance with the rules of nomenclature, choosing what Bogue considered the dominant rock in his description (Bogue, 1953). The formation (fig. 11) as mapped includes, besides andesite, agglomerate, quartzite, graywacke, interbedded marble and rhyolite, and a somewhat younger series of epidiorite, diorite, diabase, gabbro, and serpentinite (Brown and Jackson, 1960; Jackson, Bogue, Brown, and Gierhart, 1963). Most of the rocks are metamorphosed to the lower and middle greenschist facies, but higher grades of metamorphism are found locally.

Later, Bureau des Recherches Geologiques et Minieres (BRGM) (Eijkelboom, 1966; Vincent, 1968) mapped

the Ḥalabān region in considerable detail and began to elucidate the lithologic units where we had shown all as Halaban Formation (Jackson and others, 1963). Although BRGM did not assign relative ages and specifically avoided describing a sequence of events, designating only lithologic units, the sequence shown on their maps includes ultramafic rocks, mostly pyroxenite and harzburgite much serpentinized, at the base. As part of an ophiolitic suite, these ultramafic rocks are generally older than the andesite-dioritic basement that they structurally overlie. The calc-alkalic Halaban rocks are variously metamorphosed, mostly in the greenschist facies (chlorite-epidote-zoisite-albite), and are overlain by metamorphic tuffs and sedimentary rock. Some subvolcanic fine-grained diorite intrudes the uppermost metavolcanics and metasedimentary rocks. The structure is complex; in places a melange is present within the section and complicates the stratigraphy, so the suggested sequence might be changed with further study. Vincent raised the Halaban to group status. Eijkelboom separated the volcanic and subvolcanic rocks east of the Al Amar-Idsas fault—the easternmost exposed segment of the Arabian Shield—from those to the west because the flow rocks, namely andesite and dacite, including rhyolite, tuff, agglomerate, volcaniclastic conglomerate, breccia, albitophyre, keratophyre, and some marble and graywacke, are different from the volcanic and subvolcanic rocks west in the vicinity of Ḥalabān.

BRGM later divided the Halaban into four units, including basal ophiolitic melange (BRGM, 1966; Eijkelboom, 1969). Bois (1971) separated the rocks exposed along the northeast edge of Ḥalabān Ridge into ultramafic and gabbroic rocks of an ophiolitic suite, and an overlying unit, the Ar Ridaniyah Formation, consisting of volcaniclastic rocks, chert, and marble beds metamorphosed to the amphibolite facies. Later, the upper units were collectively called the "Pyroclastic Halaban," in contrast to the underlying "Andesitic Halaban" (Bounny, 1973). Still later, the Halaban rocks were formally named the "Afna" and "Nuqrah" Formations (Delfour, 1975) and assigned to the Hulayfah Group, named for Wādī Hulayfah and the town on the wadi where both formations are exposed; the type locality (lat 26° N.) is midway between Al Madīnah and Ḥā'il. The younger Nuqrah Formation was named for the ancient mining site on the Al Madīnah-Al Qaṣīm road 75 km southeast of Ḥulayfah, where it has been studied extensively.

More recently, Delfour (1979a) has recompiled the earlier BRGM mapping of the Ḥalabān quadrangle and, with additional fieldwork in 1975 and 1977, reinterpreted the geology. He separates the Halaban as mapped earlier into four units: three groups above an older basement composed of granite, orthogneiss, and diorite. The groups, in ascending order, are as follows: Ajal, composed of biotite schist, gneiss, and amphibolite; Urd, consisting of two formations, a lower ophiolitic complex and upper Abt Schist; and Hulayfah, here consisting of only the upper formation of the group, the Nuqrah. The Nuqrah is composed of silicic volcanics and volcaniclastic sediments as well as andesite, marble, and jasper, the rocks first described by Eijkelboom as the Al Amar-Idsas Formation.

Also more recently, BRGM has recompiled the 'Afīf quadrangle (Letalenet, 1979), extending the detailed mapping west from the Ḥalabān region. There the formations originally shown as Halaban are divided into five formations grouped into three units besides intrusive diorite, gabbro, ultramafic rocks, and serpentinite. The oldest unit, mostly of sedimentary origin, of schist, gneiss, amphibolite, quartzite, metarhyolite, and meta-andesite, is shown only along the western edge of the quadrangle and has been dated in xenoliths in diorite at 825 m.y. (Baubron and others, 1976; Letalenet, 1979). The remaining formations above these older rocks are calc-alkalic to silicic flows and volcaniclastic sedimentary rocks in general becoming more alkalic and silicic in the uppermost beds, which seem to be similar to the Hulayfah Group of the Nuqrah quadrangle (Delfour, 1977).

Hadley (1973) followed the BRGM classification but omitted the lower ophiolitic complex, and assigned formation names within the Sahl al Maṭrān quadrangle in northwestern Arabia (lat 26°00′–26°30′ N., long 38°00′ E.) as follows: the lowermost 2,550 m of metaclastic rocks and marble he named the "Thaa Formation" from exposures on Wādī Thaa in the southeastern part of the quadrangle; the middle 3,950 m of metabasalt, meta-andesite, and pyroclastics exposed in the hills around the central Matran plain are the Matran Formation; and the upper 3,900 m of lavas, mostly alkalic, and associated pyroclastic rocks are the Jizl Formation, named from the exposures on the flanks of the Wādī al Jizl in the southeastern part of the quadrangle.

Subsequently, the ophiolitic suite, the Ar Ridaniyah Formation, and the overlying Abt Schist were taken together to form the Urd Group, named for Jabal al 'Urḍ at lat 24°05′ N., long 44°50′ E. (Delfour, 1977). Most of the Jabal al 'Urḍ region is underlain by the Abt Schist, which we now believe to be clastic deposits of the Murdama Group metamorphosed to paraschists by underthrusting along the Al Amar-Idsas fault and by later granitic intrusions. We suggest abandoning the group name.

The southern extension of the Halaban rocks includes two formations in the Bi'r Juqjuq quadrangle at

lat 21°00′–21°30′ N., long 43°30′–44°00′ E. (Hadley, 1976): a lower volcanic formation composed of andesite, basalt, and conglomerate, the Juqjuq Formation (from Wādī Juqjuq, a tributary to Wādī ad Dawāsir), and an upper formation, the Arfan, from Jabal Arfan north of Wādī Juqjuq in the northwestern part of the quadrangle. The Juqjuq Formation is more than 13,100 m thick at the type locality, and the Arfan Formation was estimated to be more than 7,600 m thick (Hadley, 1976; Schmidt and others, 1979). Subsequently, it has been suggested by C.R. Ramsey and N.J. Jackson (oral commun., 1980) that some of the rocks of the Arfan Formation belong to the Murdama Group.

Delfour (1977), in describing the rocks of the Hulayfah Group in the Nuqrah quadrangle, reported 6,500 m of the Afna Formation in two units, a lower 2,500 m of conglomerate, marble, tuffs, and siltstone and an upper 4,000 m of predominantly andesite and basalt but including diabase sills and some rhyolitic tuffs and flows at lat 25°–26° N., long 40°30′–42° E. The Nuqrah Formation at the type locality is 4,000 m thick and is composed of three members—a lower rhyolitic tuff and rhyolite with less abundant andesite, a middle unit of marble, graphitic tuff, and sulphide mineralized breccia, cherty tuffite, bedded chert, jasper, rhyolite, and subordinate andesite, and an upper unit of conglomerate, ignimbrite, rhyolite, and tuffite.

The Halaban Group (Brown and Jackson, 1979) covers large areas in the eastern and northern parts of the shield and was considered a possible supergroup (Brown and Jackson, 1979), but this is deferred, needing further elucidation. The outcrops extend in folded and faulted belts for at least 800 km in a north or northwesterly direction and extend laterally as much as 40 km in the type region. The early mapping limited the outcrops almost entirely to the region north and east of the southernmost Najd fault. Geochronologic dates range from about 785 and 775 m.y. for volcanic rocks (Rb-Sr) to 729 (zircon) and 724 m.y. (Rb-Sr) for tonalite intrusive into the volcanic rocks (Aldrich and others, 1978; Cooper and others, 1979; Fleck and others, 1980). Thus, the predominantly calc-alkalic rocks and uppermost beds include a stratigraphic unit that contains rhyolitic flows, ignimbrite, and tuffaceous sedimentary rocks—in all, a typical island-arc assemblage. This assemblage makes up the Halaban Group (Brown, Delfour, and Coleman, 1972; Brown and Jackson, 1979), here comprising the Hulayfah Group, of the northeastern shield, and the Halaban, as widely mapped in recent years in the southeastern shield.

The granite Delfour includes in the older basement extends into and appears to be part of the large granite batholith that extends through the Dawādimī area. It is about 1,400 km^2 in area and, according to Al-Shanti (1976), is composed mostly of two major types, a syntectonic monzogranite in the western part and a late tectonic, evenly grained monzogranite containing xenoliths of the syntectonic granite in the eastern part. A minor part is posttectonic monzogranite and alkalic granite in small stocks and dikes. These phases appear to have one calc-alkaline magmatic source, with granite intrusion beginning during the tectonic phase and continuing after tectonism ceased. As the batholith and related stocks are intruded into the Abt Schist and the invasion culminated at about 570 m.y. according to numerous K-Ar dates (tables 6, 8), consideration of interpreting the Abt Schist coeval with the Murdama Group seems plausible even though regionally metamorphosed in front of the Al Amar-Idsas overthrust fault.

MURDAMA GROUP

The Murdama Formation was named after Jabal al Murdamah 30 km southeast of 'Afīf, a type locality (fig. 12) suggested by Bogue (1954) after his reconnaissance of the eastern shield area. Slate, phyllite, quartzite, graywacke, and conglomerate were seen in a traverse across the north end of the mountain. The contact with the underlying metavolcanic rocks seemed to be conformable at the northwest corner of the mountain (Brown and Jackson, 1960). Later, when the peninsular map was compiled, it became known from additional information that at least some paraschists cropping out along the Najd faults are of Murdama age. The Hadiyah slate was tentatively correlated by Brown, Jackson, Bogue, and Elberg (1963) with the type section of the Murdama Formation, even though the sandstone-siltstone of the Hadiyah slate was first seen 500 km northwest of Jabal al Murdamah at the Hadiyah station on the Hejaz Railroad. The correlation was made on the basis of lithologic similarity, thickness, degree of metamorphism, and an apparent stratigraphic position above rocks considered to be Halaban. Subsequently, the original Murdama Formation was measured in detail by J. Letalenet (1974) on the western flank of Jabal al Murdamah, where he found a polygenetic conglomerate resting on andesite of the Halaban and extending 2,700 m upward as graywacke, siltstone, and sandstone to a reddish-brown rhyolite porphyry overlying a polymict conglomerate. Letalenet (1974) considered the rhyolite to be part of the Murdama because the conglomerate beneath the rhyolite did not contain clasts of the underlying clastics of the Murdama. Earlier we had dated the rhyolite by K-Ar whole-rock methods at 561±25 and 560±20 m.y. (samples 141a, 141b, table 8; Aldrich and others, 1978). The samples are rhyolite crystal tuff and rhyolite porphyry which are deuterically altered (Salman Block, written commun., 1974). More

FIGURE 12A.—Type locality of Murdama Group, view to the southeast. The sediments of the Murdama Group lie in a syncline plunging to the southeast in the middle distance. The syncline rests disconformably on the meta-andesite and metarhyolitic tuffaceous volcanics of the Halaban (Hulayfah) Group exposed in the foreground.

recently, samples from the same locality averaged 544 m.y., using conventional interpretations of K-Ar corrected to the Sydney decay constants (Baubron and others, 1976). Flows southwest of Al Madīnah near the top of a similar thick clastic section gave an age of 633±15 m.y. by Rb-Sr whole-rock isochron (samples 94, 106, table 7). These ages are concordant with those reported by Baubron and others (1976) for the Hibshi

FIGURE 12*B*.—Slate and shale of the Hadiyah Group beneath the flaggy Cambrian Siq Sandstone, which in turn underlies the pinnacled Ram-Umm Sahm Sandstone. North edge of the Arabian Shield.

Formation. Baubron and others (1976) considered the younger ages that they obtained for the Murdama to result from rehomogenization of the argon. We are inclined to consider the rhyolite at the center of Jabal al Murdamah disconformable above the Murdama and belonging to the younger Shammar Group, which is dominantly alkalic flows. The Murdama Formation was raised to group rank by Delfour (1977) to include basal conglomerate and flows (Hibshi Formation), limestone and marble (Farida Formation), and the upper sandstone-siltstone facies (Hadiyah Formation).

East of Jabal al Murdamah in Jibāl al 'Alam, the Murdama includes 500–800 m of fine-grained andesite at the core (top) of the Maslum syncline. The syncline is bisected by a posttectonic calc-alkalic granite which, although not isotopically dated, is similar to granites throughout the northeast shield, with K-Ar dates of about 600 m.y. The Murdama has schistosity indicating two episodes of folding, an earlier episode resulting in low-grade greenschist facies and a later compression during the Najd faulting at about 570 m.y. A third, possibly older, tectonic epoch involves the Abt paraschists which conformably overlie the Ar Ridaniyah calcareous unit in the Ad Dawādimī district at the eastern edge of the shield (Al-Shanti, 1976). The Abt paraschists and the Ar Ridaniyah unit are combined on the geologic map (pl. 1) as the Abt Schist. The lower part of the Ar Ridaniyah is gneissic and quartz-feldspathic schist which can be correlated with the Hibshi Formation, at least in part, whereas the upper calcareous metasedimentary rocks are most likely the extension of the Farida marble underneath the Al Amar-Idsas fault. These beds all dip east except where invaded by posttectonic quartz monzonite and granite or where local folds reverse the dip. The Farida marble in outcrop has been squeezed out of a stratigraphic position above basal conglomerate and graywacke, in places transgressing tectonically over the older Halaban crystalline rocks to overlap the Hibshi conglomerate.

Chitinozoan-like microfossils from dolomite at Jabal Rukhām tentatively correlated with the Murdama Group are similar to forms in the upper Riphean of Greenland and suggest that the span 638–600 m.y. for the Murdama Group from K/Ar ratios is reasonable (Vidal, 1979; Binda and Bokhari, 1980).

SHAMMAR GROUP

The alkalic and peralkalic volcanic rocks of the Shammar Rhyolite and associated gently folded sedimentary beds were considered (Brown and Jackson, 1960) to be the youngest Precambrian rocks in the shield (fig. 13*A*). The sialic, essentially unmetamorphosed volcanic rocks, including flows and tuffs, which are increasingly younger toward the northern edge of the shield, have been divided into two formations (Delfour, 1967). In the northwest Hejaz area, Brown, Jackson, Bogue, and Elberg (1963) later recognized sedimentary rocks interbedded with and above the Shammar, as well as rhyolite and fine-grained granite in dikes and stocks that intrude the Shammar. The younger sedimentary beds, including some flow rocks, were later separated and assigned to the Jubaylah Group by Delfour (1967, 1970), who found the outcrops restricted to long, narrow shear zones or grabens of the northwest-trending Najd fault system.

The radiometric timespan was not closely defined by our early work (Brown and Jackson, 1960). If the age 633±15 m.y. obtained by Hedge (samples 94, 106, table 7) is considered the end of the Murdama epoch, the Shammar could represent volcanism from that time until about 555±25 m.y., the date obtained for the Shammar by Baubron and others (1976, fig. 5) using Rb/Sr data. The rhyolite (561±25 and 560±20 m.y. whole-rock K-Ar; samples 141a, 141b, table 8) at the center of the Jabal al Murdamah syncline is most likely post-Murdama and a later phase of the Shammar rhyolitic volcanism, but hydrothermal alteration in one sample may have caused argon loss and a deceptively young age. The interval 633 to about 555 m.y. was also a period of widespread felsic plutonic activity. Older components are calc-alkalic monzogranitic batholiths; younger components include transgressive plugs and stocks that increase in alkalinity to peraluminous and peralkalic intrusives, including ring dikes. A comagmatic series has been found to range in age from about 620

A

B

C

FIGURE 13.—Shammar and Jubaylah Groups. *A*, Shammar Group. Jabal Garra'ah (lat 27°15′ N., long 36°49′ E.) is composed of lithic tuff and andesite (in foreground); rhyolite dike in background. Jubaylah Group sediments and thin flows overlie these beds on the left (northern) flank. *B*, Jubaylah Group at Jabal Na'adhah, Sahl al Maṭrān quadrangle, at lat 26°25′ N., long 38°13′ E.; view southeast. Rhyolite on lower slope, in the Jubaylah, yielded a K-Ar cooling date of 528±20 m.y. from biotite (sample 40, table 8), whereas the rhyolite on the right below the Jubaylah layered rocks yielded an average age of 574±6.7 m.y. from biotite for the underlying Shammar volcanics (Fleck and others, 1976). *C*, The Jubaylah Group at Jabal Antāq near the north end of Ḥalabān ridge and near the east edge of the shield at lat 24° N. A pebble conglomerate at the base underlies sandstone, siltstone, and shale, here dipping east. Andesite interbedded at the type locality 380 km northwest is dated at 558±6 m.y. ($^{40}Ar/^{39}Ar$), the end of the Precambrian. Geochronology by J.F. Sutter.

to about 550 m.y. (Fleck and others, 1976; Aldrich and others, 1978; Schmidt and others, 1979). This activity appears to have culminated about 570 m.y.

In the region southwest of Ḥā'il in the Nuqrah quadrangle, Delfour (1977) found two formations in the Shammar—the basal Kuara Formation with a basal conglomerate, upper clastic, rhyolite and andesite; and the upper Malha Formation, mostly rhyolite flows and ignimbrites. The oldest reported age, 621±25 m.y., came from the Malha Formation from six Rb-Sr measurements (Baubron and others, 1976; Delfour, 1977), thus indicating that the Murdama Group and the older portions of the Shammar Group are essentially the same age, eruptions of Shammar volcanics continuing at least to the end of the Precambrian.

JUBAYLAH GROUP

Sedimentary beds and flows originally mapped above and interbedded with the upper Shammar rhyolite (Brown, Jackson, Bogue, and Elberg, 1963) were later separated and recognized as a distinct unit above an unconformity (Delfour, 1967). They are the youngest rocks involved in the diastrophism of the Arabian Shield (figs. 13*A*–13*C*)

Outcrops are along and on top of the three principal Najd fault zones in the northern part of the shield, where underlying schistose rocks have been eroded to form troughs or faulted to form grabens. Subsequent horizontal movement and some vertical movement has folded the Jubaylah beds into taphrogeosynclinoria, in which steeper limbs on the northeast flanks reflect the sinistral movement of the Najd faults (Delfour, 1970; Hadley, 1974). The thicknesses of exposures vary, owing in part to subsequent erosion; they range from 155 m at Wādī Murdan (lat 27°40′ N.) near the northwest corner of the shield, where the group dips under the Siq Sandstone, to 750–850 m at the Mashhad area (Hadley, 1974) (fig. 13*B*), and to 2,300 m at Qal'at aṣ Ṣawrah (Hadley, 1975b) west of Ḥarrat Khaybar. Such great thickness could also be explained by irregular, fault-controlled deposition and the proximity to

eruptive centers. At the type locality east of Ḥarrat Khaybar, the thickness of two formations of the Jubaylah Group is more than 3,300 m (Delfour, 1977). The group extends discontinuously southeast to Jabal Antāq on the west flank of Samrā' Ḥalabān at lat 23°50′ N., long 44°10′ E. Along the northeast Najd shear zone and at lat 22°40′ N., long 44° E., along the middle Najd zone, the thickness is about 320 m.

The Jubaylah Group was divided informally by Delfour (1967) at the type locality east of Ḥarrat Khaybar into three units—a basal conglomerate; andesite, basalt, and welded silicic tuff; and a cherty limestone containing stromatolitic structures. Later he named two units, the basal Umm al Aisah and the upper Jifn Formation, but, recognizing that flows and ejecta occurred at various horizons in the section, he did not assign a formal name to the volcanic part (Delfour, 1977). West of Ḥarrat Khaybar, Hadley (1973) found a similar sequence which he named, from base upward, the Rubtayn (conglomerate and fine clastics), Badayi (andesite), and Muraykhah (limestone and shale). West of the Mashhad area described by Hadley (1974) the Jubaylah crops out near Al 'Ulā in small areas along Wādī al Jizl and in Wādī Falqah 32 km west. The wadi follows a Najd fault zone where the following section is exposed: about 100 m of polymict conglomerate; andesitic tuff and agglomerate; siliceous beds with calcareous concretions and lithographic limestone; intraformational conglomerate containing clasts of the limestone; and an uppermost tuffaceous green shale. Fifty kilometers farther northwest, in Wādī al Jizl west of Ḥarrat al 'Uwayriḍ, 85 m of the lower part of the Jubaylah crops out beneath a rhyolite agglomerate thrust block. The beds are red sandstone and polymict conglomerate. Fifteen kilometers east of the above exposure, the basal conglomerate and sandstone are 64 m thick below 118 m of thin-bedded and fetid limestone, paper shale, siltstone, and chert. Ripple and rain-splatter marks in the upper beds suggest a shallow-water and beach environment of deposition.

One hundred fifty kilometers farther northwest, at Wādī Murdan and beyond in Ash Shifā', the beds are polymict conglomerate and trachytoidal andesite porphyry. Along the southwestern flank of Wādī as Sirr in the middle zone of the Najd fault system near where it intersects the Red Sea at lat 27° N., thick red and green shale and fine-grained sandstone overlie a thick polymict conglomerate wherein are clasts from all the older rocks. Originally mapped as Shammar (Brown, Jackson, Bogue, and Elberg 1963), the strata are probably of Jubaylah age, even though schistosity in some zones approaches that of the underlying Murdama Group.

Toward the southeast end of Jubaylah outcrops, near the eastern edge of the shield at Jabal Antāq (900 km southeast of Ash Shifā'), wacke, shale, and siltstone dip 25°–30° E. above gray and red ripple-marked sandstone and a basal conglomerate of white quartz pebbles (fig. 13*C*).

The lava flows throughout the exposures of the Jubaylah are petrographically different from older outpourings and are of interest for possible radiometric dating of the Jubaylah Group. They are composed of andesite, dacite, alkalic basalt (mugearite), and rhyolite or lithic tuffs (minor), are generally porphyritic, often with large (2 cm) plagioclase phenocrysts (An_{40-60}), and are amygdaloidal. Amygdule minerals include quartz (cristobalite?) and calcite, with lesser amounts of barite, celestite, and nepheline (Delfour, 1970). Hadley (1974) described devitrified glass and chlorite, chlorophoenicite, epidote, and calcite; opaque iron-rich minerals are common in all sections except the crystal tuffs. Chlorite, epidote, and zeolites are products of hydrothermal alteration in one rock (see sample 67, an altered andesite, tables 3, 4, 8).

Two samples (samples 67, 69, table 8) from Delfour's type locality gave whole-rock K-Ar ages of 299±11 m.y. for the lower, hydrothermally altered flow containing deuteric calcite (R. Marvin, written commun., 1972) and 548±18 m.y. for the dacite or alkalic andesite flow. The younger apparent age is most certainly unreliable, probably owing to hydrothermal alteration. To check the possible validity of the 548±18 m.y. apparent age for the fresh dacite (sample 69, table 8), John Sutter (written commun., 1982) kindly made an $^{40}Ar/^{39}Ar$ age-spectrum analysis of the dacite (fig. 14) and comments as follows:

> $^{40}Ar/^{39}Ar$ age spectrum plateau age=558±6.6 m.y. where the 6.6 Ma error is reported at the 2 sigma level of confidence (95 percent). The $^{40}Ar/^{39}Ar$ total gas age is 534 Ma which should be essentially equivalent to the conventional K/Ar age for this sample.
>
> The age spectrum indicates loss of ^{40}Ar from the sample by volume diffusion from potassium-bearing mineral phases. I suggest that the major potassium-bearing phase is a feldspar and if so the apparent age of the first two temperature steps on the age spectrum (350–425 °C), about 465 Ma, represents the last time the sample cooled through 100–150 °C, the temperature range below which feldspars tend to retain most of their radiogenic argon.

A modal analysis of the dacite by one of us (A.C.H.) gave 16 percent potash feldspar.

A whole-rock K-Ar age of 515±17 m.y. (sample 22b, table 8) from a potassium-rich mafic flow could be reliable but could also be low owing to argon loss. The chemical analysis (table 4) shows that the rock is oxidized mugearite (oligoclase-andesine basalt), according to George Phair (USGS, written commun., 1976). At the Mashhad area, Fleck and others (1976) determined K-Ar ages of 567±6 and 581±7 m.y. for biotite in rhyolite of the Shammar Group ostensibly underlying the Jubaylah Group, although a fault separates the

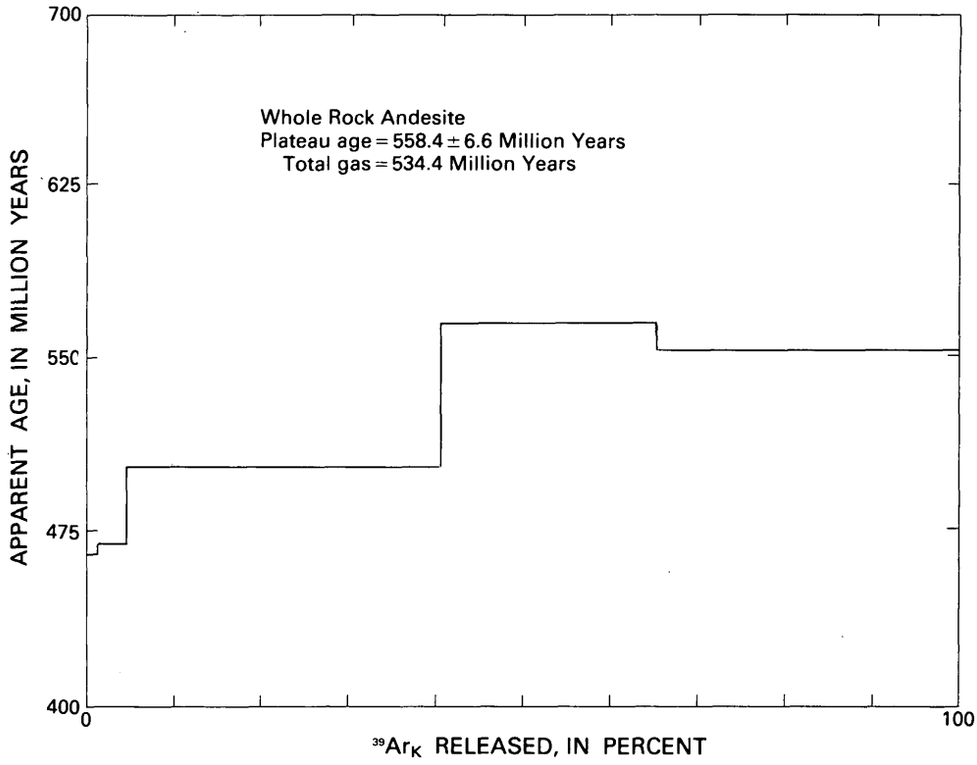

AGE OF SPECTRUM DATA

TEMP	$\frac{^{40}Ar}{^{39}Ar}$	$\frac{^{37}Ar}{^{39}Ar}$	$\frac{^{36}Ar}{^{39}Ar}$	^{39}Ar % of TOTAL	$^{40}Ar^*$ %	^{39}Ar (mole)	APPARENT K/Ca $\frac{mole}{mole}$	APPARENT AGE MILLION YEARS
350	278.124	5.184E-01	8.234E-01	1.2	12.5	1.34E-13	1.00E+00	464.90 ± 98.90
425	66.237	3.015E-01	1.048E-01	3.4	53.3	3.67E-13	1.72E+00	469.89 ± 8.64
500	45.951	3.477E-01	2.669E-02	35.9	82.9	3.90E-12	1.50E+00	502.55 ± 3.14
850	45.840	4.055E-01	7.577E-03	24.7	95.2	2.69E-12	1.28E+00	565.27 ± 3.25
FUSE	48.075	1.355E+00	1.898E-02	34.7	88.5	3.77E-12	3.84E-01	553.44 ± 3.31

SAMPLE WT. = .2383g

TOTAL GAS 534.43
PLATEAU AGE 558.37 ± 3.28

FIGURE 14.—Incremental $^{39}Ar_K$ of the Jubaylah andesite at the type locality of the Jubaylah Group. Analysis by J.F. Sutter (written commun., 1983).

beds (Hadley, 1973). A sample of biotite from andesite, presumably a flow in the Jubaylah, at the Mashhad area gave a K-Ar age of 528±20 m.y., but the stratigraphic position is not certain. Also, a K-Ar age of 532±15 m.y. was determined for a whole-rock sample from a basalt dike 41 km east of the Mashhad area where the dike crops out beneath the unconformity below the Siq Sandstone of probable Late Cambrian age. Baubron, Delfour, and Vialette (1976) measured whole-rock K-Ar ages of 502 and 512 m.y. for flows from the Jubaylah; Delfour suggests that these dates are too young and reflect heating and argon loss during subsequent eruptions. Certainly almost all the samples we have examined show some hydrothermal alteration, but the question of whether this alteration was penecontemporaneous with the eruptions or was related to some later episode remains unanswered, even though much of the evidence points to early hydrothermal metamorphism. The alteration of the lavas studied raises questions about the geological accuracy of the radiometric ages.

The Jubaylah Group as now exposed appears to be of local derivation, even though the sequence in general is similar from basin to basin. Deposition began with

A *B*

FIGURE 15.—*A*, Aerial view to the southeast of Jabal Huassan (lat 24°01′ N., long 45°08′ E.) at the east edge of the shield. The arcuate antiformal ridge is composed of Halaban metasediments graded through epidote schist to amphibolite around the Al Mizil orthogneiss (tonalite-trondhjemite) which underlies the central plain. The dome probably represents anatectonic reactivation of Halaban crust at about 600 m.y. ago or possibly later (Fleck and Hadley, 1985). *B*, Jabal Shāyi' layered gabbro pluton in the southeastern shield near the village of Khaybar at lat 18°47′ N., long 42°53′ E. This carefully studied and drilled pluton yielded an age of 616 m.y. from $^{40}Ar/^{39}Ar$ in hornblende, with a heating event at about 510 m.y. (Coleman, Ghent, and others, 1977).

coarse fluvial clastics, probably fanglomerate, ended with stromatolitic shallow-water marine beds, and was interrupted at various levels by flows of basalt, andesite, and rhyolite or by lithic tuffs. Some mafic small and hypabyssal crystalline intrusives may be of Jubaylah age.

Stromatolitic mats in chert from the Jubaylah Group at Jabal Umm al 'Aisah were studied and found to contain filaments of the blue-green algae *Obruchevella parva*, Reitlinger, a conical stromatolite, *Conophyton*, and unicells of uncertain affinity (Cloud and others, 1979). The paucity of fauna suggests that the Jubaylah Group is near the lower boundary of the Phanerozoic or latest Precambrian (Vendian). The disconformable stratigraphic position below the Siq Sandstone, which in turn is subjacent to or part of fossiliferous sandstone considered Upper Cambrian by Seilacher (1970), allows room for the radiometric dates to be true time of deposition and volcanic eruption, but the Ediacarian fauna in the cherty upper beds of the group, together with the hydrothermal alteration and possible argon loss in the volcanic samples, argue for an earlier, possibly earliest Cambrian or latest Precambrian, age. Subsequent to the above-reported age estimates, Pier Binda and C.R. Ramsay (1980) point out from BRGM work (Baubron and others, 1976) that the Jubaylah is disconformable above the granite of Jabal ar Rahadah, which is dated at 577±15 m.y. by a seven-point Rb-Sr whole-rock isochron (corrected to the Sydney constants). The granite is intruded into the Murdama Group. Binda (1981) concludes that the Jubaylah Group is probably uppermost Vendian (600–570 m.y.). A minimum age younger than 570 m.y. does not invalidate Cloud's and Binda's conclusions, and the spectral age of 558±6.6 m.y. of Sutter (fig. 15) seems most logical from all the evidence.

PRECAMBRIAN PLUTONIC ROCKS OF THE ARABIAN SHIELD

The plutonic rocks of the Saudi Arabian Shield are divided into an older, pretectonic dioritic suite (fig. 15*A*) and a younger, syntectonic and posttectonic, mostly granitic suite which includes an early layered gabbroic phase (fig. 15*B*). Greenwood and Brown (1973, p. 6) estimated that the percentage of granitic to granitic-plus-dioritic rocks, that is, granitic rocks to total plutonic rocks, is 32, 38, and 13, respectively, in the northeast, central, and southwest regions of the shield as mapped on the 1:2,000,000-scale geologic map (USGS–ARAMCO, 1963).

The percentage of granitic rocks relative to dioritic rocks exposed in different parts of the shield is a function of orogenic intensity and depth of erosion. Greater tectonism and less erosion complement each other in producing and preserving, respectively, more granitic rocks in the northeastern part of the shield. Late major tectonism associated with granite emplacement was most intense in the eastern and northeastern parts of the shield relative to the western and southwestern parts and resulted in a greater abundance of granitic plutons in the northeast. The depth of erosion

is shallower in the northeastern part of the shield than in other parts (Brown and Jackson, 1960). This is indicated by abundant exposures of the latest Proterozoic rhyolitic Shammar Group; in places, as at Jabal Aja', granitic intrusive rocks are still preserved in direct, subvolcanic contact with the Shammar volcanic rocks (Stoeser and Elliott, 1980). In the central part of the shield, in a belt about 200 km wide and including the major Najd fault zones, late orogeny was intense and the erosion level is moderately shallow in that many late granitic plutons are exposed with few cogenetic rhyolitic rocks of the Shammar Group. The southern part of the shield is deeply eroded and was less deformed during the late major orogeny, so that this region has the smallest area of granitic plutons and only rare exposures of Shammar-type volcanic rocks.

In addition to the granitic and dioritic suites, a mafic-ultramafic suite of plutonic rocks is present and is characterized by serpentinite in association with ultramafic, gabbroic, basaltic, and diabasic rocks. The mafic-ultramafic suite is confined mostly to narrow belts in large fault zones, is independent of the dioritic-suite rocks, and makes up less than 1 percent of the Precambrian plutonic rocks of the shield. The mafic-ultramafic suite is ophiolite that rarely is complete at any one locality and that probably represents tectonic remnants of oceanic crust of different ages in different places (Bakor and others, 1976; Frisch and Al-Shanti, 1977; Delfour, 1979b; Al-Rehaili and Warden, 1980).

In general, the plutonic rocks of the dioritic and granitic suites are petrographically easily classified into standard rock types. In this report, "granitic" refers to leucocratic plutonic rocks containing more than 5 percent modal potassium feldspar and more than 20 percent modal quartz, thus avoiding the broader term "granitoid." Rock names in this report are those of the classification of plutonic rocks of the International Union of Geological Sciences, Subcommission on the Systematics of Igneous Rocks (Streckeisen, 1973, 1976).

The plutonic rocks are further classified as pretectonic, syntectonic, and posttectonic in reference to a culminant orogeny (dated at about 650±25 m.y.), during which most of the rocks of the early (primary) crust were intensely tectonized during the cratonization of the shield (dated at about 675 to 560 m.y.). This tectonic classification in reference to the culminant orogeny is used in spite of the fact that most of the rocks of the primary crust had been variously deformed and metamorphosed prior to the culminant orogeny.

DIORITIC SUITE

The dioritic suite consists, in order of decreasing abundance, of diorite, quartz diorite, tonalite, trondhjemite, and gabbro. These rocks were emplaced between about 1,000 and 700 m.y. ago (Greenwood and others, 1976; Fleck and others, 1980) and, together with their equivalent volcanic rocks of the andesite assemblage, constitute the primary crust that represents most of the early (precratonization) crust of the shield. Rocks of the dioritic suite are pretectonic in reference to the culminant orogeny.

The plutonic rocks of the dioritic suite are commonly medium grained and hypidiomorphic granular. The diorite contains hornblende with or without varying amounts of biotite and quartz. The quartz diorite and tonalite are quartz-biotite rocks with or without hornblende, and the trondhjemite is a quartz-biotite rock. The gabbro commonly contains clinopyroxene, partly altered to hornblende, and hornblende, partly altered to biotite. In many places, all these plutonic rocks have finer and coarser grained phases and their overall heterogeneous character suggests a shallow level of intrusion. In particular, the diorite commonly has mineral compositions and textures that are variable and heterogeneous even at outcrop and hand-specimen scale, which suggests that some of the diorite was hypabyssal and subvolcanic to overlying andesitic volcanic rocks. Locally, the trondhjemite is graphic or granophyric and contains euhedral quartz phenocysts, which suggests that some trondhjemite is hypabyssal and subvolcanic to overlying dacitic volcanic rocks.

These early rocks were mostly well tectonized, pervasively sheared to a commonly north-trending foliation, and metamorphosed to the greenschist facies before the culminant orogeny and cratonization, when they were tectonically mixed with their volcanic equivalents, the andesitic assemblage, and abundantly intruded by rocks of the granitic suite.

Many of the low-density, more silicic rocks of the dioritic suite, such as the trondhjemites and some tonalites, are found in large gneiss domes, or antiforms, where they had been metamorphosed to amphibolite facies, conspicuously shear foliated, and converted to orthogneisses. These gneiss domes rose gravitationally in response to heating and tectonic thickening during the culminant orogeny. The orthogneisses are tectonically associated with migmatitic and plutonic rocks of the granitic suite.

During past mapping, many granitic gneisses and orthogneissic rock units have been variously depicted as basement rocks older than rocks of the adjoining dioritic suite in any given area. However, none of the isotopic ages of these gneisses has proven to be older than the associated dioritic suite and andestic assemblage rocks. Where well dated, all yield dates related to orogenies that are younger than the dioritic suite in their respective regions. The orthogneisses are in gneiss domes or large fault structures, and most were tectonized and mobilized during the culminant orogeny.

GRANITIC SUITE

The granitic suite consists, in order of decreasing abundance, of granodiorite, granite, alkali-feldspar granite, and peraluminous-peralkalic granite, as well as gabbro. The rocks of the granitic suite are exposed throughout the Precambrian shield and are most abundant in the northeastern half of the shield. Alkali-feldspar granite and peralkalic granite have not been found in the southwestern part of the shield (Stoeser and Elliott, 1980); however, several plutons of syenite and shonkinite intrude this part of the shield. Most of these rocks were emplaced during cratonization after about 675 m.y. ago. Many granitic rocks are slightly to extensively tectonized and partly metamorphosed through pervasive cataclastic shear and are classified as syntectonic; these were intruded during the culminant orogeny. Other granitic rocks were intruded in a posttectonic setting from after the culminant orogeny to about the end of the Precambrian. They commonly produce contact metamorphic aureoles in the adjacent wall rock. A relatively few granitic rocks in the western half of the shield were intruded earlier than the culminant orogeny, during more spatially restricted orogenies, for example, about the time of deposition of the Ablah group of rocks.

The syntectonic granitic rocks commonly form large batholiths of predominantly biotite granodioritic composition and are commonly associated with the large gneiss domes of tonalitic and trondhjemitic orthogneiss. The batholithic granodiorite is mostly conspicuously flow foliated as well as cataclastically sheared in response to late orogenic processes.

Early in the posttectonic setting, biotite granite (monzogranite and syenogranite) was intruded as large, irregularly shaped plutons. Presumably with increasing depth of erosion and the resultant ease of brittle fracture at shallow crustal levels, circular plutons of biotite-perthite granite, a few kilometers to as much as 10 km is diameter, were emplaced somewhat later, about 600 m.y. Many of these are ring structured where they intruded a preexisting structure, or perhaps where some late orogenic forces controlled their emplacement. Some of these circular and elliptical plutons are composed of biotite-perthite alkali-feldspar granite and sodic amphibole peralkalic granite. Some are peraluminous granites. Not all the late, small granitic plutons are circular or layered, but circular layered masses are conspicuous in most parts of the shield.

The posttectonic granitic magmas were bimodal. Some layered granite plutons contain partial concentric layers or irregular intrusive bodies of synchronously intruded basaltic, diabasic, or moderately mafic hybrid rocks. In addition, circular layered plutons of gabbro, commonly leucocratic and from a few kilometers to 10 km in diameter, are conspicuous throughout the shield (fig. 15*B*). These gabbroic rocks are late and nonmetamorphosed, and in a few places they can be seen to cut late granite plutons. That the late gabbro and the diabasic intrusions are intricately and synchronously associated with the circular granitic intrusions indicates that immiscible gabbroic magma was associated with granitic magma deep in the crust during cratonization.

The latest and shallowest granitic rocks of the Precambrian shield are granite to alkali-feldspar granite in small plutons or stocks in or adjacent to the Najd fault zone. Those in the Najd fault zone are readily dated as (1) being slightly younger than most Najd faulting where they cut the strongly sheared rocks of the fault zone and commonly form small circular stocks less than several kilometers in diameter, or (2) having been intruded during Najd faulting where the small plutons are greatly elongated (some elongation ratios to about 1:10) in the fault zone and where the granitic rock is highly flow foliated and sheared. These latter, synkinematic rocks are conspicuous granitic gneisses that often in the past were mapped as granitic orthogneisses of an old basement.

Many dikes of diabase and fewer dikes of rhyolite fill conjugate and secondary fractures complementary to the Najd faults in large areas between the Najd faults (Moore, 1979). Large swarms of diabasic dikes are most common in the large granitic batholiths. For example, granodioritic batholiths were systematically fractured, in contrast to the dioritic plutons, in which strains were relieved by ductal yield along preexisting structural grain. A few diabasic, gabbroic, and syenitic plugs less than 1 km in diameter intruded the Najd fault zones after fault movement had ceased.

CHEMISTRY OF THE PRECAMBRIAN CRYSTALLINE ROCKS

INTRODUCTION

The petrography and classification of 199 Precambrian volcanic and plutonic rocks that form the Saudi Arabian Shield and for which chemical analyses have been made are listed in numerical order in table 3. The analyzed rock samples were collected during reconnaissance geologic mapping, mostly prior to the more detailed 1:100,000-scale mapping, and are from localities (pl. 1) well distributed over the entire shield. The last two samples, numbers 501 and 502, are of Precambrian crystalline rocks from the bottom of two deep drill holes through the Phanerozoic sedimentary rocks in the Eastern province of Saudi Arabia about 400 km east of the eastern edge of the shield; they are not shown on plate 1. Chemical and normative analyses of the 199 Precambrian rocks are given in table 4.

Text continues on p. 65.

TABLE 3.—*Description and classification of crystalline rocks of the Arabian Shield for which chemical analyses are given in table 4*

Sample (loc. given on pl. 1)	Field no.	Location[1] (lat/long)	Rock-unit symbol on pl. 1[2]	Petrography									Remarks[11]	Classification			
				Color	Grain size[3]	Normative color index[4]	Mafic content (percent)[5]	Plagioclase composition[6]	Normative anorthite (percent)[7]	Potassium-feldspar type[8]	Rock texture-structure[9]	Rock name (field or petrography)[10]		Igneous type[12]	Rock name from chemistry[13]	Age[14]	Region[15]
1	8712 (ALD1)	28/35NW.	mgd	Gray	–	16	3,Bi	Olig	30	Or,Pth	Catacl, mr	Granodio	–	Plutonic	Granodio	C,S?+	N
3	B1813	28/35NW.	[gr](ju)	–	–	53	–	–	58	–	–	Amphibo	Jabal Maglah; contact metamorphic, volcanic	Metamor (volcanic)	Amphibo (basalt)	H	N
4a	ALD3	28/35NW.	gr	–	mg	2	2,Bi, Hb	Olig	11	Or,Pth	Minor catacl	Granite	Near Jabal al Lawz; rock similar to sample 4b	Plutonic	Granite	M+	N
4b	B1815	28/35NW.	gr	–	–	2	2,Bi	Olig	11	Or,Pth	Minor catacl	Granite	Near Jabal al Lawz; rock similar to sample 4a	Plutonic	Granite	M	N
8	B1016 (ALD7)	27/35NE.	gp	–	–	2	1,Hb	–	0	Pth,Mc, Or	–	Granite	Jabal Ḥarb; 0.5 km inside west border of pluton	Plutonic	Peralkalic granite	S,N?+	N
9	B1011	27/35NE.	[jd](gp)	Red	mg	7	5,Mt	–	0	Pth	–	Granite	Small satellitic plug related to pluton of sample 13	Plutonic	Peralkalic granite	S,N?	NN
12a	B1009A	27/35SE.	ns	–	–	3	–	–	3	–	–	Syenite	Circular pluton in Najd fault zone	Plutonic	Alkalic quartz syenite	N	NN
12b	B1009B	27/35SE.	ns	–	–	1	–	–	0	–	–	Syenite	Same pluton as sample 12a	Plutonic	Peralkalic quartz syenite	N	NN
13	B1022	27/35NE.	gp	Gray	fg–mg	6	20,Hb, Bi,Mt	–	0	Pth	Graphic mr	Granite	Center of large pluton in Najd fault zone, Jabal Shār	Plutonic	Peralkalic granite	S,N?	NN
14a	B1008C	27/35NE.	gp	Red	–	7	–	–	0	–	–	Granite	Near contact, same pluton as sample 13, Jabal Shār	Plutonic	Peralkalic granite	S,N?	NN
14b	B1008	27/35NE.	gp	–	fg–mg	3	3,Bi, Hb,Mt	–	0	Pth,Mc	Mr	Granite	Same pluton as sample 13, Jabal Shār	Plutonic	Peralkalic granite	S,N?	NN
15	B1023	27/35NE.	gp	–	fg	2	2,Mt	–	0	Mc,Pth	Microgr	Granite	Jabal Shār; large sill or laccolith on Najd fault	Hypabys	Peralkalic granite	S,N?	NN
17	B1007	27/35NE.	gp	Red	mg	1	1,Hm	–	0	Mc,Pth, Or	Microgr	Granite	Jabal Shār; same pluton as sample 13	Plutonic	Peralkalic granite	S,N?	NN
18	B1044	27/36NW.	rt	Red	fg	3	–	–	4	–	Porphyr	Rhyolite porph	Intrudes greenstone; intruded by diabase dikes	Hypabys	Rhyolite	S	N
19	B1046	27/36NW.	nj	–	–	23	–	–	37	–	Trachyt	Andesite	Associated with Najd fault; basaltic andesite?	Volcanic	Alkalic basalt	K	N
20	B1052	27/36NW.	nj	–	–	7	–	–	32	–	Welded tuff	Rhyolite	Clast in basal conglomerate on Najd fault	Volcanic	K-rhyolite?	S	N
21	B1047	27/36NW.	gp	Dark red	mg	5	Hm	–	3	Or,Pth	–	Granite	Appears disconformable below Jubaylah Group	Plutonic	Alk-feld granite	S	N
22a	B1062B	27/36SE.	nj	–	–	2	Oxidized Rieb?	–	6	–	Lithic fragmental	Rhyolite tuff	Flow, 1 m thick, in Jubaylah Group	Volcanic	Na-rhyolite?	K	NN
22b	B1062C	27/36SE.	nj	Dark grn	Cryp-to-cryst	18	26,Px (alt'd.)	Olig-And	21	Or	Porphyr amygd	Basalt	Flow in Jubaylah Group; oxidized mugearite?	Volcanic	Alkalic basalt	K+	NN
23	B1059	26/36NW.	gb	Gray	–	10	14,Hb, Bi	–	3	–	–	Leucogab	Small pluton in Najd fault zone	Plutonic	Trondh	H,N?	WN

Footnotes at end of table.

TABLE 3.—*Description and classification of crystalline rocks of the Arabian Shield for which chemical analyses are given in table 4*—Continued

Sample (loc. given on pl. 1)	Field no.	Location[1] (lat/long)	Rock-unit symbol on pl. 1[2]	Petrography: Color	Grain size[3]	Normative color index[4]	Mafic content (percent)[5]	Plagioclase composition[6]	Normative anorthite (percent)[7]	Potassium-feldspar type[8]	Rock texture-structure[9]	Rock name (field or petrography)[10]	Remarks[11]	Classification: Igneous type[12]	Rock name from chemistry[13]	Age[14]	Region[15]
24	B1037	26/36NW.	ga	Red	mg	3	6,Bi, Mt	–	8	Pth,Mc	–	Granite	Jabal Libān; large granite pluton; 1% modal fluorite	Plutonic	Alk-feld granite	S+	WN
25a	B1823	26/37NW.	gr	–	–	6	5,Hb, Bi	Olig	21	Or	–	Granodio	10-×20-km elliptical pluton	Plutonic	Granodio	S	NN
25b	B1823A	26/37NW.	*[gr](nj)	–	vfg	19	?,Hb	–	53	–	–	Andesite	Small plug or dike in Najd fault zone, similar to sample 28a	Hypabys	Quartz andesite	K?	NN
27	B1824	26/37NW.	sr	–	–	3	–	–	3	–	–	Rhyolite	Shammar? structurally above Jubaylah in Najd fault	Volcanic	Alk-feld rhyolite	S	NN
28a	B1822	26/37NW.	*[mh](di)	–	vfg	22	Cpx,Hb	And	41	–	–	Microdio	Contact zone of satellite near sample 25b	Hypabys	Diorite	K?	NN
28b	B1822A	26/37NW.	*[mh](gm)	–	–	7	10,Hb, Bi	Olig	24	Pth	–	Adam	Small pluton, 2.5 km across, satellitic to pluton at sample 25a	Plutonic	Granodio	S	NN
29	B1825	26/37NW.	*[ay](gp)	Red	fg	2	?,Hm	–	4	Pth,Mc	Microgr	Granite	Granite on Najd fault	Plutonic	Alk-feld granite	S,N?	NN
30	B1831	26/37SW.	npg	–	–	2	1,Bi	–	9	Mc,Or, Pth	Hypidiomorph	Granite	In Najd fault zone	Plutonic	Granite	S	WN
31	B1826	26/37SW.	mog	–	–	3	?,Bi	–	11	–	Flaser gneiss	Granite	Jabal Ghalāl, in Najd fault zone	Gneiss	Trondh	C	WN
32	B1829	26/37SW.	*[ngn](gm)	–	fg-mg	3	?,Bi	–	16	–	Hypidiomorph	Adam	Jabal Ghalāl, in Najd fault zone	Plutonic	Granite	C	WN
33	B1827	26/37SW.	*[npg](gm)	–	cg	2	3,Bi, Hb	Olig	8	Pth,Mc	Hypidiomorph	Granite	Jabal Ghalāl, in Najd fault zone	Plutonic	Alk-feld granite	S	WN
36	B1126	26/37SE.	sr	Dark red	fg	10	?,Hm	–	17	–	Microgr	Felsite	Related to subvolcanic intrusion, Shammar age	Dike	Dacite	S	NN
37	B1125	26/37SE.	*[jq](mgd)	–	–	6	10,Bi,Hb	Olig	22	Or	Mod catacl	Adam	In quartz diorite-diorite body	Plutonic	Granodio	C,S?	NN
38	B1805	26/37SE.	nj	–	–	2	?,Bi	–	19	Or	Welded tuff	Rhyolite	In Jubaylah sedimentary section	Volcanic	K-rhyolite	K	NN
39	B1806	26/37SE.	nj	–	–	3	–	–	12	–	Pyroclastic	–	Highly calcic tuff or calcarenite	Sediment	Calcic tuff	K	NN
41	B1109	26/38SE.	*[ay](gm)	–	–	5	–	–	4	–	Minor catacl	Granite	Qal'at aş Şawrah quadrangle, unit includes granophyre	Plutonic	Alk-feld granite	S	NN
42	B1107	26/38SE.	*[ay](agr)	–	–	7	?,Bi, Hm	–	18	Micropth	–	Granite	Qal'at aş Şawrah quadrangle, weathered	Plutonic	Granite	A	NN
43	B1804	26/38SE.	gr	Red	cg	2	1,Bi	Olig	10	–	–	Adam	Qal'at aş Şawrah quadrangle	Plutonic	Granite	S	NN
45	B1106	26/38SE.	*[agr](agb)	–	–	34	Hb,Bi	–	41	–	–	Diorite	Part of Jabal Abu Safiyah complex	Plutonic	Quartz diorite	A	NN
46	B3906A	26/38SE.	agd	–	–	2	1,Bi	Ab-Olig	2	Mc	Catacl	Gran gn	Qal'at aş Şawrah quadrangle	Gneiss	Alk-feld granite	A?	NN
47	B1104	26/38SE.	agr	Red	fg	1	Bi	And	3	–	Porphyr	Granite	Qal'at aş Şawrah quadrangle, highly altered	Plutonic	Alk-feld granite	S,N?	NN

Footnotes at end of table.

TABLE 3.—*Description and classification of crystalline rocks of the Arabian Shield for which chemical analyses are given in table 4*—Continued

Sample (loc. given on pl. 1)	Field no.	Location[1] (lat/long)	Rock-unit symbol on pl. 1[2]	Petrography: Color	Grain size[3]	Normative color index[4]	Mafic content (percent)[5]	Plagioclase composition[6]	Normative anorthite (percent)[7]	Potassium-feldspar type[8]	Rock texture-structure[9]	Rock name (field or petrography)[10]	Remarks[11]	Classification: Igneous type[12]	Rock name from chemistry[13]	Age[14]	Region[15]
48	B1840	25/37NW.	gr	–	–	2	2,Bi	Olig	9	Pth,Mc	Hypidiomorph	Adam	Cavernous weathering; in Najd fault zone	Plutonic	Alk-feld granite	S	WN
49	B1845	25/37NW.	gr	–	mg	2	2,Bi	Olig	0	Mc,Pth	Hypidiomorph	Adam	–	Plutonic	Granite	S	WN
50	B1839	25/37NW.	gr	–	mg	1	1,Bi	Olig	2	Pth,Mc	Hypidiomorph	Adam	Cavernous weathering	Plutonic	Granite	S	WN
51	B1838	25/37NW.	*[agd]	Black	–	27	50,Hb	–	65	–	Diabasic	Diabase	Wādī al Ḥamḍ	Dike	Leuco diabase	N	WN
52	B1835	25/37NE.	nog	–	fg	2	4,Bi	–	20	–	Gneissic	Trondh	Basement in Najd fault	Gneiss	Trondh	J(N?)	WN
54	S1GFB	25/38NW.	ngn	–	fg-mg	4	7,Bi	–	20	Or	Gneissic	Granite	Wādī al Jizl, in Najd fault zone	Gneiss	Granodio	C? (N?)+	NN
55	B1123	25/38NE.	agb	–	–	52	–	–	55	–	–	Gabbro	Part of Jabal Abu Safiyah complex	Plutonic	Gabbro	A	NN
56	B1843B	25/37SW.	jgb	–	–	7	?,Bi	–	27	–	–	Qtz dio	–	Plutonic	Trondh	J	WN
57	B1630	24/38SW.	jt	–	–	14	20,Hb, Px,Bi	An_{30}	46	–	Gneissic	Qtz dio	Yanbu'	Plutonic	Tonalite	J	WC
58	B1312	27/41NW.	gp	Gray	fg	8	5,Bi, Hb	–	0	Pth	Microgr	Granite	Jabal Aja', gr-gp batholith	Plutonic, gneiss	Peralkalic granite	S	NE
61a	B1310	27/41SW.	*[gm] (gp)	Red	–	1	–	–	10	–	–	Granite	Jabal Aja', layered, layer adjacent to sample 61b; altered	Plutonic	Granite	S	NE
61b	B1311	27/41SW.	*[gm] (gp)	Red	mg	1	Hm,Na-Amph?	–	6	Pth	Hypidiomorph	Granite	Jabal Aja', layer adjacent to sample 61a	Plutonic	Alk-feld granite	S	NE
62	B1308	26/41NE.	gp	–	–	7	Hb (Na-Amph?)	–	3	Pth	Catacl	Granite	Jibāl ar Rummān, gp batholith	Plutonic, gneiss	Alk-feld granite	S	NE
63	B1103	26/39SW.	ay	–	–	1	–	–	?73	–	Agglom?	Rhyolite?	Jabal as Safran, not evaluated	Altered?	–	S?	NN
64	B1325	26/41SE.	*[mgd] (gr)	Red	fg	1	Mt	–	6	–	–	Monz	–	Hypabys	Granite	S	NE
65	17,827	25/39NW.	*[ay] (jq)	Gray	–	17	14,Hb, Bi	Olig	36	Or	–	Qtz dio	Old basement	Plutonic	Tonalite	J	NN
66	B1154	25/40NE.	*[mgd] hv	–	–	26	Bi	–	47	–	–	Phonolite	Nuqrah quadrangle, under Jubaylah cgl	Volcanic	Andesitic basalt	H,K?	HN
67	B1155	25/40NE.	nj	–	vfg	30	14	Ab-Olig	31	–	Amygd	Andesite	Nuqrah quadrangle, flow above Jubaylah cgl	Volcanic	Basaltic andesite	K+	HN
68a	JD1714	25/40NE.	hc	–	–	8	–	–	12	–	–	Rhyolite	Nuqrah quadrangle, from drill core	Volcanic	Na-dacite	H+	HN
68b	JD1713	25/40NE.	hc	–	–	6	–	–	3	–	–	Rhyolite	Nuqrah quadrangle, from drill core, Nuqrah formation	Volcanic	Na-rhyolite	H	HN
69	B1157	25/40NE.	nj	Red-brn	fg	18	35,Hm, Epi	And	30	–	–	Andesite	Nuqrah quadrangle, flow	Volcanic	Andesite?	K+	HN
70	B1145	25/40NE.	hc	–	–	9	12,Mt	Olig	12	–	Porphyr	Rhyolite	Nuqrah quadrangle, flow in pyroclastic section	Volcanic	Na-dacite	H	HN
71	JD1711	25/41NW.	hc	–	Micro-cryst	7	Mt?	Olig	6	Or	Porphyr	Rhyolite	Nuqrah quadrangle, from drill core	Volcanic	Na-rhyolite	H+	TN

Footnotes at end of table.

TABLE 3.—*Description and classification of crystalline rocks of the Arabian Shield for which chemical analyses are given in table 4*—Continued

Sample (loc. given on pl. 1)	Field no.	Location[1] (lat/long)	Rock-unit symbol on pl. 1[2]	Petrography									Classification			
				Color	Grain size[3]	Normative color index[4]	Mafic content (percent)[5]	Plagioclase composition[6]	Normative anorthite (percent)[7]	Potassium-feldspar type[8]	Rock texture-structure[9]	Rock name (field or petrography)[10]	Remarks[11]	Igneous type[12]	Rock name from chemistry[13]	Age[14]	Region[15]
73 —	B207B	24/40NE.	mh(sr?)	–	–	3	–	–	25	–	Breccia	Felsite	Jabal Shidā'	Volcanic	K-rhyolite	S	HC
74 —	B1137	24/40NE.	*[nj](ns)	–	–	35	Px,Opx	Lab	51	–	–	Gabbro	Intrusive into Jubaylah with granophyre	Plutonic	Gabbro	K	HC
75 —	B1138	24/40NE.	nj	–	–	19	–	–	39	–	–	Mug	Al Ḥanākīyah	Volcanic	Andesite	K	HC
76 —	S2GFB	24/39SW.	gm	–	mg	2	3,Bi	Olig	13	Pth,Mc	Catacl	Granite	SW. of Al Madīnah, batholith cut by Najd faults	Plutonic	Granite	M	WC
77 —	S3GFB	24/39SE.	*[gm](ga)	Red	mg	3	3,Mt,Bi	Olig	3	Pth,Mc	Minor catacl	Granite	Al Madīnah, from quarry, small granite body	Plutonic	Alk-feld granite	M+	HC (NN)
78a —	ALD9	27/42SW.	gr	Gray	mg	1	2,Bi	Olig?	6	Pth,Mc	Hypidiomorph	Granite	Jabal Salmá, near sample 78b	Plutonic	Alk-feld granite	S+	NE
78b —	B1316	27/42SW.	gr	Red	–	2	–	–	7	–	–	Granite	Jabal Salmá, near sample 78a	Plutonic	Alk-feld granite	S	NE
79 —	B1333	26/42SW.	gm	Gray	–	12	–	–	27	–	–	Granite	Granitoid, possibly intrudes Hibshi Formation	Plutonic	Quartz monzodiorite	M	NE
80 —	B1339	26/42SW.	*[gm](hq)	Gray	–	29	–	Olig?	36	–	Gneissic	Qtz dio	Gneiss below Hibshi cgl	Gneiss	Quartz diorite	H	NE
81a —	B1338A	26/42SW.	*[mi](gr)	Gray	cg	3	Bi	Olig	19	–	Hypidiomorph	Adam	Jabal Ḥibshī, granite boulder from Hibshi cgl	Plutonic	Granite	M	NE
81b —	B1338B	26/42SW.	*[mi](gr)	Red	fg	1	–	–	11	–	–	Granite	Jabal Ḥibshī, granite boulder from Hibshi cgl	Plutonic	K-granite	M	NE
82a —	ALD10	26/42SW.	gd	Red	–	15	12,Hb,Bi	Olig	26	Or	Hypidiomorph	Monz	Jabal Tīn	Plutonic	Granodio	C+	NE
82b —	B1330	26/42SW.	gd	–	–	13	–	–	29	–	–	Granite	Jabal Tīn	Plutonic	Granodio	C	NE
83b —	B1334	26/42SW.	mi	–	–	5	–	–	15	–	–	Dacite	Flow in upper Hibshi Formation	Volcanic	Dacite	S	NE
84 —	B1301	25/42NW.	ga	White	–	2	Na-Amph?	Olig	8	Pth,Or	–	Qtz monz	Jabal Qutn, 15-km circular pluton in Murdama	Plutonic	Alk-feld granite	M=S	NE
85 —	B1302	25/42NW.	gd	Gray	mg	5	Bi	–	29	Pth,Mc	–	Qtz monz	East of Qutn, 5-km circular pluton in Murdama	Plutonic	Granodio	M=S	NE
86 —	B1317	25/42NW.	gd	Gray	–	6	–	–	29	–	–	Hornbl monz	East of Qutn, 4-km circular pluton in Murdama	Plutonic	Granodio	M=S	NE
87 —	B1318	25/42NE.	gd	Gray	mg	9	–	–	30	–	–	Hornbl qtz dio	East of Qutn, 3-km circular pluton in Murdama	Plutonic	Granodio	M=S	NE
88 —	B1340	25/43SE.	*[as](mgd)	–	–	9	7,Bi	–	34	–	–	Adam	Intrudes Murdama Formation	Plutonic	Granodio	S	NE
89 —	B1341	25/43SE.	mgd	–	–	10	19,Bi, Hb	And	32	Mc,Or	–	Adam	Intrudes Murdama Formation	Plutonic	Granodio	S+	NE
90a —	ALD12	24/43NE.	mgd	–	–	11	11,Bi, Hb	And	28	Or	Catacl	Granite	Intrudes Murdama and Abt Formations	Plutonic	Granodio	S+	NE

Footnotes at end of table.

TABLE 3.—*Description and classification of crystalline rocks of the Arabian Shield for which chemical analyses are given in table 4*—Continued

Sample (loc. given on pl. 1)	Field no.	Location[1] (lat/long)	Rock-unit symbol on pl. 1[2]	Petrography									Remarks[11]	Classification			
				Color	Grain size[3]	Normative color index[4]	Mafic content (percent)[5]	Plagioclase composition[6]	Normative anorthite (percent)[7]	Potassium-feldspar type[8]	Rock texture-structure[9]	Rock name (field or petrography)[10]		Igneous type[12]	Rock name from chemistry[13]	Age[14]	Region[15]
90b	B1342A	24/43NE.	mgd	–	–	3	–	–	25	–	–	Granite	Intrudes Murdama and Abt Formations, similar to sample 90a	Plutonic	Granodio	S	NE
91a	ALD13	24/43NE.	gr	–	–	1	3,Bi (Fl)	Ab-Olig	11	Pth,Mc	Minor catacl	Granite	Circular pluton 7-km diameter, intrudes Abt Formation	Plutonic	Granite	S+	NE
91b	B1345	24/43NE.	gr	–	–	2	–	–	14	–	–	Granite	Circular pluton 7-km diameter, intrudes Abt Formation	Plutonic	Granite	S	NE
93a	Q13064	24/44SW.	gb	–	–	47	–	–	58	–	–	Gabbro	Jabal al Jilani, elliptical gabbro; intruded by Dawadimi batholith, samples 88–90	Plutonic	Gabbro	E?	NE
93b	Q11464M	24/44SW.	gb	–	–	39	–	–	59	–	–	Gabbro	Jabal al Jilani, elliptical gabbro	Plutonic	Gabbro	E?	NE
93c	Q22A64	24/44SW.	gb	–	–	34	–	–	61	–	–	Gabbro	Jabal al Jilani, elliptical gabbro	Plutonic	Gabbro	E?	NE
93d	Q22645	24/44SW.	gb	–	–	37	–	–	59	–	–	Gabbro	Jabal al Jilani, elliptical gabbro	Plutonic	Gabbro	E?	NE
94	B1163	23/39NE.	ju (fa)	–	vfg	13	Bi	Olig	0	Or	–	Rhyolite	Small intrusive into conglomerate of Fatimah formation, see sample 106	Hypabys	Na-rhyolite?	S,F+	WC
98	JD1712	23/40NE.	hc	–	vfg	9	–	And	76	–	Flow banded	Rhyolite	Jabal Sayid, near Najd fault and gp pluton; K metasom	Volcanic	K-dacite?	H+	HC
102	B215	23/41NW.	hc	–	vfg-glassy	11	Hm	And	16	Or?	Porphyr	Dacite	Associated with rhyolite, dacite, red andesite flows	Volcanic	Na-dacite?	H+	HC
103	B216	23/41NW.	*[gr]	–	fg	44	27,Hb, Cpx, Opq	Lab	46	–	–	Diabase	Near Najd fault, Najd? age	Dike	Diabase	N+	HC
104	B1497 (ALD15)	23/41NE.	gb	Dark	–	41	–	–	76	–	Mod gneissic	Diorite	Jabal al Ḥamāmah, Halaban or Jiddah basement	Plutonic	Gabbro	H+	HC
105	B1498	23/41NE.	ht	Light	fg	3	10?, Bi,Hb?	Olig?	21	Or?	Catacl	Granodio	5 km SE. of Jabal al Ḥamāmah	Plutonic	Granodio	C?	HC
106	B1165	23/39SE.	fa	–	fg	3	–	Olig	11	Or?	Porphyr	Latite	Flow or sill at top of Fatimah section, see sample 94	Volcanic	Na-rhyolite	F+	WC
111	B1611	21/39NW.	jq	Gray	mg	6	Hb,Bi	–	25	–	–	Granodio	Dahabān, syntectonic intrusion	Plutonic	Granodio	A?	WS
113	B1610	21/39NW.	gr	Gray	fg	2	–	–	0	–	Granophyr	Granite	North of Jiddah, subvolcanic to Fatimah silicic volcanic	Plutonic	Alk-feld granite	F	WS
114a	B1600 (ALD18)	21/39NW.	*[jd] (gr)	Gray	mg	2	1,Bi, Mu	Olig	13	Pth,Or	Gneissic	Granite	Quarry east of Jiddah airport	Plutonic, gneiss	Granite	A+	WS
114b	B1600A	21/39NW.	*[jd] (agd)	Gray	fg-mg	14	6,Bi, Hb,Mu	Olig	25	Or	Mod catacl	Granite	Quarry east of Jiddah airport	Gneiss	Granodio	A	WS
114c	B1600B	21/39NW.	*[jd] (agd)	Gray	–	5	9,Epi, Chl	Olig-And	21	Or	Catacl	Granite	Quarry east of Jiddah airport	Gneiss	Granodio	A	WS

Footnotes at end of table.

TABLE 3.—*Description and classification of crystalline rocks of the Arabian Shield for which chemical analyses are given in table 4*—Continued

Sample (loc. given on pl. 1)	Field no.	Location[1] (lat/long)	Rock-unit symbol on pl. 1[2]	Petrography: Color	Grain size[3]	Normative color index[4]	Mafic content (percent)[5]	Plagioclase composition[6]	Normative anorthite (percent)[7]	Potassium-feldspar type[8]	Rock texture-structure[9]	Rock name (field or petrography)[10]	Remarks[11]	Classification: Igneous type[12]	Rock name from chemistry[13]	Age[14]	Region[15]
115 —	B1601	21/39NW.	*[jd] (agd)	–	–	4	–	–	29	–	Cataclastic	Granite	East of Jiddah airport	Gneiss	Granodiorite	A	WS
116 —	B1606A	21/39NW.	*[jt]	Dark	fg	24	–	–	57	–	–	Diabase	North of Jiddah, dike in metadiorite	Dike	Quartz diabase	F?N?	WS
117a –	B900	21/39NE.	fa	Dark	–	42	Ol?,Px?, Opq	And-Ab?	3	–	Porphyr	Basalt	Jabal Mukassar, 2-m sill, 10 m below top, upper fa	Sill	Na-andesite?	F=S?+	WS
117b –	B901	21/39NE.	fa	Dark	vfg	18	Bi,Hm	Olig?-And	20	–	Porphyr	Dacite	Jabal Sidr, 30-m sill on top, intrudes limestone	Sill	Na-andesite?	F=S?+	WS
122 —	B1629	21/39SW.	*[jd] (ju)	Dark grn	–	6	–	–	18	–	–	Dacite	Greenstone quarry south of Jiddah	Volcanic	Na-dacite	J	WS
123 —	B1625	21/39SW.	*[agd] (agr)	Red	–	3	–	–	7	–	–	Granite	Small pluton east of Jiddah, north of Makkah road	Plutonic	Na-granite	F	WS
124a –	ALD19	21/39SE.	jq	Gray	–	10	18,Bi, Hb	And	39	–	Cataclastic	Trondhjemite	Fresh rock from pipeline ditch, east of Makkah	Gneiss	Tonalite	J+	WS
124b –	B1603	21/39SE.	jq	–	–	4	–	–	27	–	–	Trondhjemite	Similar to sample 124a	Gneiss	Trondhjemite	J	WS
125 —	ALD21	21/40SW.	agm	–	–	3	–	–	14	–	–	Granite	Aṭ Ṭā'if, small gr pluton, from quarry	Plutonic	Granite	S+	B
126 —	ALD23	20/41NW.	jt	–	–	10	–	–	39	–	–	Qtz diorite	Wādī Shuqub quadrangle, small outlier to large batholith	Plutonic	Tonalite	J+	B
127a –	ALD22	20/41NW.	gp	Pink	cg	2	–	–	6	–	–	Granite	Jabal Qunah pluton, outer ring granite	Plutonic	Alk-feld granite	S+	B
127b –	9B	20/41NW.	gp	–	–	2	–	–	8	–	–	Granite	Similar to sample 127a	Plutonic	Alk-feld granite	S	B
133 —	B1702	20/41SE.	jd	–	–	16	–	–	64	–	–	Diorite	'Aqīq quadrangle, complex diorite batholith	Plutonic	Quartz diorite	J	B
134 —	B1703	20/41SE.	ab	–	–	9	–	–	1	–	–	Rhyolite	'Aqīq quadrangle, Ablah belt, flow near base	Volcanic	Na-rhyolite	A	J
138 —	B1725	20/41SE.	ab	–	–	24	–	–	28	–	–	Andesite	'Aqīq quadrangle, Ablah belt, sill near gr stock	Sill	Andesite	A	J
139 —	B1726	20/41SE.	*(ab)[jc]	–	–	2	–	–	7	–	–	Rhyolite	'Aqīq quadrangle, Ablah belt, 10-m-thick sill	Sill	Alk-feld rhyolite	S	J
141a –	B230A	23/43NW.	mu	Dark	ultra-fg	13	Bi,Cpx	And	23	–	Flow, porphyr	Dacite	Jabal al Murdamah; flows above upper cgl, =Shammar	Volcanic	Dacite-andesite?	S-M+	TN
141b –	B230	23/43NW.	mu	Red-brn	–	3	Cpx,Hb	Olig	14	Or, Micropth	Flow, porphyr	Rhyolite	Jabal al Murdamah; flows above upper cgl, =Shammar	Volcanic	Rhyolite	S-M+	TN
141c–	B229	23/43NW.	mu	Red-brn	ultra-vfg	3	Hb?,Bi	Olig	18	Or	Flow, porphyr	Rhyolite	Jabal al Murdamah; flows above upper cgl, =Shammar	Volcanic	Na-dacite?	S-M	TN
141d –	B1368B	23/43NW.	mu	Red-brn	–	3	–	–	5	–	Flow, porphyr	Rhyolite	Jabal al Murdamah; flows above upper cgl, =Shammar	Volcanic	Rhyolite	S-M	TN
142 —	B233A	23/43NE.	mu	–	vfg	10	–	–	29	–	–	Dacite	'Afīf quadrangle, flow above Murdama, =Shammar	Volcanic	Dacite	S-M	TN

Footnotes at end of table.

TABLE 3.—*Description and classification of crystalline rocks of the Arabian Shield for which chemical analyses are given in table 4*—Continued

Sample (loc. given on pl. 1)	Field no.	Location[1] (lat/long)	Rock-unit symbol on pl. 1[2]	Petrography: Color	Grain size[3]	Normative color index[4]	Mafic content (percent)[5]	Plagioclase composition[6]	Normative anorthite (percent)[7]	Potassium-feldspar type[8]	Rock texture-structure[9]	Rock name (field or petrography)[10]	Remarks[11]	Classification: Igneous type[12]	Rock name from chemistry[13]	Age[14]	Region[15]
143	B247	23/43NE.	hu	–	–	15	–	–	31	–	–	Microdio	'Afif quadrangle, greenstone under Farida marble	Volcanic	Dacitic andesite	H?	TN
144a	ALD14	23/44NE.	ga	–	–	2	Bi	–	10	Pth	–	Granite	Jabal Za'abah, ring-structured, intrudes Abt Formation	Plutonic	Alk-feld granite	S-N?+	NE
144b	B1362	23/44NE.	ga	–	–	6	13,Bi,Hb	Olig	20	Pth,Mc	Hypidiomorph	Granite	Jabal Za'abah, ring-structured, intrudes Abt Formation	Plutonic	Granite	S-N?	NE
145	B1432	23/44SE.	um	–	–	31	–	–	65	–	–	Gabbro	Fault associated, pre-Halaban ophiolite?	Plutonic	Gabbro	pre-H	NE
146	B1512	22/42NE.	[hu](mu)	–	–	1	–	–	4	–	–	Rhyolite	Rhyolite boulder from Murdama cgl (mapped as hu), 146 rhy similar to sample 147a gm=Shammar	Volcanic	Alk-feld rhyolite	M=S?	TC
147a	B1513A	22/42NE.	*[gm](mog)	Gray	–	1	–	–	6	–	–	Granite	Foliated granite, intrudes Halaban? of sample 147b	Plutonic	Alk-feld granite	M?	TC
147b	B1513B	22/42NE.	*[gm](hu)	–	–	29	Px	–	60	–	Flow	Basalt	Flow in Halaban?, intruded by sample 147a	Volcanic	Quartz basalt	H	TC
149a	ALD17	22/44NE.	gm	–	mg	2	2,Bi	Olig	10	Pth	Porphyr	Granite	Jabal Zan, near contact with Halaban? (Ar Ridaniyah Formation)	Plutonic	Granite	S+	TN
149b	B1346	22/44NE.	ngr	–	–	4	–	–	16	–	–	Granite	Similar to sample 149a	Plutonic	Granite	S	TN
150	B1481	22/42SW.	[hu](mog)	–	–	29	Hb	–	53	–	Lineated	Tonalite	Basement gneiss in Najd fault zone	Gneissic	Tonalite	H-N	TC
152	B1493	22/42SE.	[hu](mog)	Gray	–	18	–	–	45	–	Lineated	Tonalite	Basement gneiss in Najd fault zone	Gneissic	Tonalite	H-N	TC
154	B1457	22/44SW.	gr	–	cg	2	Bi	Olig	12	Mc,Pth	–	Granite	Young granite	Plutonic	Granite	S	TC
155	B1492	21/42NE.	gr	–	–	2	Hb	–	3	–	–	Granite	Circular, ring-structured granite cut by Najd fault	Plutonic	Alk-feld granite	S-N?	TC
156	B1347A	21/42NE.	*[hu](ns)	–	–	21	–	–	38	–	–	Diabase	Ain Umm Wizir, 1-km plug of diabase in Najd fault	Hypabys	Diorite	K+	TN
157	B1469	21/43NW.	*[Qu](gp)	–	fg	1	Hb	–	4	–	Lineated	Granite	'Uruq Subay', syntectonic intrusion in Najd fault	Plutonic	Na-alk-feld granite	N	TC
158	B1461	21/44NW.	gm	–	–	1	Hb,Bi	–	6	–	–	Granite	Subvolcanic Shammar? intrusion	Plutonic	Alk-feld granite	S	TC
159a	B1460	21/44NW.	ga	–	fg	3	Hb,Bi	–	15	–	–	Granite	?Ring dike of Shammar ga, adjacent to Najd fault zone	Hypabys	Quartz syenite	S-N?	TC
159b	B1460A	21/44NW.	ga	–	–	2	–	–	4	–	–	Granite	In contact with sample 159a, circular ga intrusion?	Plutonic	Alk-feld granite	S	TC
160	B1459	21/44NW.	ga	–	–	6	–	–	0	–	–	Granite	0.5-km-wide dike of syenitic ga; similar to sample 159a?	Hypabys	Alk-feld quartz syenite	S-N?	TC

Footnotes at end of table.

TABLE 3.—*Description and classification of crystalline rocks of the Arabian Shield for which chemical analyses are given in table 4*—Continued

Sample (loc. given on pl. 1)	Field no.	Location[1] (lat/long)	Rock-unit symbol on pl. 1[2]	Petrography: Color	Grain size[3]	Normative color index[4]	Mafic content (percent)[5]	Plagioclase composition[6]	Normative anorthite (percent)[7]	Potassium-feldspar type[8]	Rock texture-structure[9]	Rock name (field or petrography)[10]	Remarks[11]	Classification: Igneous type[12]	Rock name from chemistry[13]	Age[14]	Region[15]
161	B1458	21/44NW.	mgd	–	–	3	Hb,Bi	–	22	Or	Gneissic	Granite	Late syntectonic batholith	Plutonic	Granodio	C	TC
162	B1487	21/42SE.	gp	–	–	5	–	–	2	–	–	Granite	North of Ranyah, large north-trending red gr batholith	Plutonic	Alk-feld granite	S	HS
163	B1488	21/42SE.	gm	–	–	4	–	–	3	–	–	Granite	Similar to sample 162, near contact with orthogneiss	Plutonic	Alk-feld granite	S	HS
164	B1489	21/43SW.	mgd	–	–	23	Hb	–	32	–	Migmatitic	Gneiss	Migmatized basement, reoriented in Najd fault zone	Gneissic	Quartz monzo-diorite	H	HS (C?, N?)
166	B1462	21/44SW.	ga	Red	–	3	–	–	8	–	–	Granite	10 km east of Jabal Khidā, large pluton	Plutonic	Alk-feld granite	S	TC
167a	B1463	21/44SE.	an	Gray	–	27	–	–	67	–	–	Anortho	Jabal Mahail, 11×30 km, intrusive vs. tectonic?	Plutonic	Leuco-gabbro-norite	E?,C?	TC
167b-h.	11666-11670, 11679	21/44SE.	an	Gray	–	3 to 10	Bi,Hb, Px?	Lab	51 to 65	–	Some cataci	Anortho	7 analyses on same anorthosite body as sample 167a	Plutonic	Anorthosite	E?,C?	TC
170a	B1463A	21/44SE.	gm	Red	–	3	7,Bi	Olig	22	Mc,Or	Hypidio-morph	Granite	Intrusive into anorthosite body sample 167, near contact	Plutonic	Granite	M	TC
171	ALD25	20/42SW.	[jd](agd)	Gray	mg	4	Bi	–	15	–	Lineated	Granodio	Thaniyah quadrangle, An Nimas batholith complex	Plutonic	Na-grano-diorite	A,C?+	J
172	1724	20/42SW.	[jd](agd)	Gray	mg	3	Bi	–	24	–	Gneissic	Granodio	Thaniyah quadrangle, An Nimas batholith complex	Plutonic	Na-grano-diorite	A,C?	J
174	B1700	20/42SW.	[jd](agd)	–	–	7	–	–	20	–	–	Qtz dio	Thaniyah quadrangle, An Nimas batholith complex	Gneissic	Na-grano-diorite	A,C?	J
175	B528	20/42SW.	gb	Dark	mg	43	37,Cpx, 01,Opx	Lab(And)	36	–	–	Gabbro	Thaniyah quadrangle, 5-km diameter, layered intrusion	Plutonic	Olivine gabbro	J?,S?	J
177	B-DS1	20/42SE.	*[mu]	Red-brn	vfg	2	Px, Amph	–	3	Or	Spherul	Rhyolite	Rhyolite from mixed rhyolite-diabase, in Murdama	Dike	Rhyolite	S?,N?	HS
178	B-DS8	20/42SE.	gb	Black	mg	33	–	–	75	–	–	Gabbro	Jabal Sidun, 4×10 km, elliptical, layered gabbro	Plutonic	Leuco-olivine norite	S	HS
182	B1439	24/44SE.	gm	–	–	22	–	–	37	–	–	Granodio	Jabal al Hasraj, small gr pluton, intrudes Abt Formation	Plutonic	Quartz monzo-diorite	S	NE
186	B1456 (ALD16)	23/45SW.	*[hu](hj)	Gray	–	5	5,Bi	And	34	Or	Catacl	Granite	Old basement from east of Al Amar-Idsas fault	Gneissic	Trondh	E+	E
194	B19	19/41NE.	jt	Dark grn	–	30	24,Hb, Cpx, Opq	Lab	50	–	Hypidio-morph	Gabbro	Diorite basement, augitehypersthene quartz diorite	Plutonic	Quartz leuco-gabbro-norite	J+	J
195	B15	19/41NE.	jt	Gray	–	9	–	–	47	–	Lineated	Tonalite	Biljurshī' quadrangle, late diorite basement rock	Gneissic	Trondh	J	J
196	B17	19/41NE.	jt	Gray	–	5	Hb,Bi	–	27	–	–	Qtz dio	Biljurshī' quadrangle, part of An Nimas batholith	Plutonic	Trondh	A	J

Footnotes at end of table.

TABLE 3.—*Description and classification of crystalline rocks of the Arabian Shield for which chemical analyses are given in table 4*—Continued

Sample (loc. given on pl. 1)	Field no.	Location[1] (lat/long)	Rock-unit symbol on pl. 1[2]	Petrography: Color	Grain size[3]	Normative color index[4]	Mafic content (percent)[5]	Plagioclase composition[6]	Normative anorthite (percent)[7]	Potassium-feldspar type[8]	Rock texture-structure[9]	Rock name (field or petrography)[10]	Remarks[11]	Classification: Igneous type[12]	Rock name from chemistry[13]	Age[14]	Region[15]
197	B10	19/41SE.	agd	Pink	mg	2	Bi	–	8	Mc	Some foliation	Granite	Jabal Tharbān, intrudes Bagarah gneiss (763 Ma)	Plutonic	Alk-feld granite	S	J
198	B33	19/41SE.	sy	Dark	–	7	–	–	10	–	–	Syenite	Jabal Tawi (Lakathah), outer circular pluton, 10-km diameter	Plutonic	Syenite	S,A?	J
199	B950	19/41SE.	gb	Black	–	40	Ol	–	59	–	–	Gabbro	Jabal Tawi (Lakathah), core of circular pluton, 6-km diameter	Plutonic	Leuco-gabbro	S,A?	J
200	Birk-2	18/41NE.	*[ab] (ba)	–	–	40	–	–	73	–	–	Amphibo	–	Metamor	Olivine norite?	B	B
201a	B1705	19/42NW.	jt	Gray	–	18	Bi,Hb	And	42	–	Gneissic	Qtz dio	Wādī Tarj quadrangle, An Nimas batholith	Gneissic	Tonalite	A, early	J
201b	B1706	19/42NW.	jt	Light gray	mg	2	Bi	Olig	24	–	Gneissic	Trondh	Wādī Tarj quadrangle, An Nimas batholith	Gneissic	Trondh	A, early	J
202	B1704	19/42NW.	*[aog] (gb)	Dark gray	mg	39	Cpx,Ol, Hb	Lab	62	–	Subophitic	Gabbro	Jabal Uthaynat, 1-km-diameter layered gabbro, outer layer	Plutonic	Olivine norite	S,A?, late	J
203a	B1708	19/43NW.	hd	Gray	fg	2	Bi(Ga)	Olig	29	Mc,Or	Catacl	Granodio	Part of large gneiss dome complex, orthogneiss	Gneissic	Trondh	H(C)	HS
203b	B1709	19/43NW.	[hd] (mgd)	Gray	fg	3	–	–	14	–	Catacl	Granodio	Same locality as sample 203a, migmatitic gneiss	Gneissic	Granodio	C	HS
204	B1722	19/43NW.	[gd](ga)	Red	fg	1	Bi	–	7	Mc	Hypidio-morph	Granite	Center, Jabal al Ḥaṣīr elliptical layered pluton	Plutonic	Alk-feld granite	S	HS
205	B1723	19/43NW.	ga	Red	cg	1	Bi	Olig	5	Pth,Mc	Hypidio-morph	Granite	Outer ring, Jabal al Ḥaṣīr elliptical layered pluton	Plutonic	Alk-feld granite	S	HS
206	B1710	19/43NW.	mog	–	–	3	–	–	26	–	Catacl	Granodio	Part of large gneiss dome complex, orthogneiss	Gneissic	Trondh	H(C)	HS
207	B1716	19/43NE.	mgd	–	–	4	–	–	26	–	Lineated	Granodio	Large syntectonic batholith, complex	Gneissic	Granodio	C	TS
208	B1713	19/43NE.	hd	–	–	28	–	–	47	–	–	Qtz dio	Diorite basement of Halaban age	Plutonic	Quartz diorite	H	TS
209	B1721	19/43SW.	ga	Red	cg	4	Hb,Bi	–	7	Mc,Pth	Hypidio-morph	Granite	Outer ring, Jabal al Ḥaṣīr elliptical layered pluton	Plutonic	Alk-feld granite	S	HS
210	B34	19/41SE.	*[jc] (gr)	–	–	2	–	–	11	–	–	Granite	Granite, west of Lakathah, Wādī Yiba quadrangle	Plutonic	Granite	A,S?	J
212	B1719	19/43SE.	gb	–	–	48	–	–	68	–	–	Gabbro	Jibāl al 'Ashsha, SW. end, elliptical layered gb complex	Plutonic	Olivine gabbro	S	TS
214	B1720	19/43SE.	[gb] (um)	–	–	94	Ol	–	90	–	–	Serpen	Jibāl al 'Ashsha, center, elliptical layered gb complex	Plutonic	Hartzburgite	S	TS
215	B1718	19/43SE.	*[Oєw] (hq)	–	–	10	–	–	38	–	–	Qtz dio	Basement rock outlier in Wajid sandstone	Plutonic	Quartz diorite	H	TS
217	BWP1	18/42NW.	jv	–	–	43	–	–	56	–	–	Basalt	On Wādī Tayyah road	Volcanic	Quartz basalt	J	J
218	BWP1	18/42NW.	jc	–	–	46	–	–	62	–	–	Schist	On Wādī Tayyah road	Volcanic	Basalt	J	J
223a	B1707E	18/43NE.	[gb] (mog)	–	mg	8	Hyp,Hb	And	39	Or	–	Enderbite	Granulite-facies rock along Najd fault zone	Metamor	Trondh?	H(N)	TS

Footnotes at end of table.

TABLE 3.—*Description and classification of crystalline rocks of the Arabian Shield for which chemical analyses are given in table 4*—Continued

Sample (loc. given on pl. 1)	Field no.	Location[1] (lat/long)	Rock-unit symbol on pl. 1[2]	Petrography									Remarks[11]	Classification			
				Color	Grain size[3]	Normative color index[4]	Mafic content (percent)[5]	Plagioclase composition[6]	Normative anorthite (percent)[7]	Potassium-feldspar type[8]	Rock texture-structure[9]	Rock name (field or petrography)[10]		Igneous type[12]	Rock name from chemistry[13]	Age[14]	Region[15]
223b	B1707W	18/43NE.	[gb] (mog)	–	–	64	–	–	70	–	–	Charnock	Granulite-facies rock along Najd fault zone	Metamor	Metabasalt?	H(N)	TS
223c	BSW402	18/43NE.	[gb] (mog)	–	–	4	–	–	19	–	–	Charnock	Granulite-facies rock along Najd fault zone	Metamor	Metagranite?	H(N)	TS
224	GFB151	18/42SW.	gm	–	–	1	1,Bi	Olig	16	Mc	Foliated	Granite	Young, large granite pluton	Plutonic	Granite	C-A?+	J
227	B140	18/42SE.	mog	Dark grn	mg	34	Hb,Bi	–	37	–	–	Diorite	On Abhā-Khamīs Mushayṭ road, basement diorite	Plutonic	Quartz diorite	H	HS
237	B125	17/42NE.	mgd	Gray	–	6	Bi	–	29	–	Some gneissic	Granite	Elliptical pluton, east of Wādī Baysh	Plutonic	Granodio	C-A?	HS
241	B120	17/43SW.	aog	Gray	mg	7	–	–	30	–	Gneissic	Granite	Jabal al Harīsī, syntectonic granitoid complex	Gneissic	Granodio	C-A?	HS
501[16]	–	?	?	–	–	–	–	–	–	–	–	Gray?	Eastern Province, Shagar #1, drill core, top of Pє	Sediment?	Basaltic andesite?	?	EE
502[16]	–	?	?	–	–	–	–	–	–	–	–	Gray?	Eastern Province, Shamasiyah #1, drill core, top of Pє	Sediment?	–	?	EE

[1]Location by 30′ quadrangle; latitude and longitude are for southwest corner of 1° quadrangles that are further subdivided into 30′ quadrants, i.e., NW., NE., SW., SE.

[2]Asterisk indicates that map-unit outcrop represented by the analyzed sample is too small to show at map scale on plate 1. The rock-unit symbol shown on the map is in brackets; the most probable correct rock-unit symbol for the sample is in parentheses.

[3]Grain sizes are standard for plutonic and volcanic rocks: crypto-cryst, crypto-crystalline; microcryst, microcrystalline; vfg, very fine grained; fg, fine grained; mg, medium grained; cg, coarse grained.

[4]Normative color index (Irvine and Baragar, 1971, p. 527) is sum of normative mafic minerals (molar data).

[5]Mafic minerals (modal data) percent where known, listed in order of decreasing abundance: Bi, biotite; Hb, hornblende; Rieb, riebeckite; Amph, amphibolite; Na-Amph, sodic amphibolite; Px, pyroxene; Cpx, clinopyroxene; Opx, orthopyroxene; Hyp, hypersthene; Ol, olivine; Mt, magnetite; Hm, hematite; Opq, opaque minerals; Mu, muscovite; Ga, garnet; Fl, fluorite; Chl, chlorite; Epi, epidote.

[6]Petrographic determination of plagioclase: Ab, albite; Olig, oligoclase; And, andesine; Lab, labradorite.

[7]Normative plagioclase composition (Irvine and Baragar, 1971, p. 527) is 100An/(An+Ab+5/3Ne) (molar data).

[8]Potassium-feldspar minerals, listed in order of decreasing abundance: Or, orthoclase; Pth, perthite; Micropth, microperthite; Mc, microcline.

[9]Mr, myrmekitic; cataci, cataclastic; mod, moderately; hypidiomorph, hypidiomorphic; microgr, micrographic; porphyr, porphyritic; trachyt, trachytoidal; amygd, amygdaloidal; agglom, agglomeratic; granophyr, granophyric; spherul, spherulitic.

[10]Granodio, granodiorite; amphibo, amphibolite; porph, porphyry; leucogab, leucogabbro; microdio, microdiorite; adam, adamellite; gran, granite; gn, gneiss; trondh, trondhjemite; qtz, quartz; dio, diorite; monz, monzonite; mug, mugearite; hornbl, hornblende; anortho, anorthosite; amphibo, amphibolite; serpen, serpentinite; charnock, charnockite; gray, graywacke.

[11]Gr, granite; gp, alkalic granite; K metasom, potassisum metasomatism; fa, map unit—Fatimah Group; cgl, conglomerate; rhy, rhyolite; gm, monzogranite; ga, alkalic granite; gb, gabbro; Pє, Precambrian.

[12]Several nonigneous rocks are listed as sedimentary. Metamor, metamorphic; hypabys, hypabyssal; sediment, sedimentary.

[13]Names where possible are according to Streckeisen (1976, 1979). Granodio, granodiorite; amphibo, amphibolite; alk-feld, alkalic-feldspar; leuco, leucocratic, trondh, trondhjemite.

[14]Age symbols represent stratigraphic and tectonic intervals: B, Baish-Bahah, and J, Jiddah (950–800 Ma); A, Ablah (about 765 Ma); F, Fatimah (Ablah or Shammar age?); H, Halaban (800–650 Ma); C, culminant (collisional?) orogeny (650–625 Ma); M, Murdama (650–580? Ma); S, Shammar (600–580? Ma); N, Najd faulting event (Najd orogeny) (580–560? Ma); K, Jubaylah (about 570 Ma). "E" indicates crustal rocks that may be older than 1,000 m.y. Age in parentheses gives metamorphic age (age of gneiss doming). Plus symbol, +, indicates a geochronological determination on sample; see tables 6, 7, and 8.

[15]Regional subdivision; see figure 16 for symbols. Subdivisions were made in an attempt to observe chemical variations and trends across the shield.

[16]Not on plate 1; location in Eastern province (see text).

TABLE 4.—*Chemical and normative analyses of crystalline rocks of the Arabian Shield*

[In percent]

Analysis number	W165508	W179441	W179456	W165509	W180162	—	D167710	D167711	—	—	—	—
Laboratory[1]	A	A	A	A	A	[D]	C	C	[D]	[D]	[D]	[D]
Sample (location given on pl. 1)	1	3	4a	4b	8	9	12a	12b	13	14a	14b	15
Oxides (wt. percent)[2]:												
SiO_2	64.00	48.40	72.20	75.00	76.40	70.00	65.00	68.00	75.50	76.00	80.00	77.00
Al_2O_3	15.40	15.50	14.70	13.40	11.60	7.60	17.70	15.90	9.45	9.83	7.18	8.50
Fe_2O_3	1.60	1.60	0.69	0.74	1.30	3.33	3.34	2.68	0.78	2.43	1.41	2.38
FeO	2.90	9.20	0.56	0.60	1.00	3.10	—	—	1.80	1.90	1.20	0.36
MgO	3.10	7.40	0.21	0.20	—	0.06	0.11	0.03	0.08	0.43	0.09	0.04
CaO	4.20	11.00	1.00	0.95	0.04	0.55	0.46	0.04	0.66	0.92	0.29	0.97
Na_2O	4.00	2.40	4.00	3.80	4.20	11.32	6.36	6.90	7.00	5.80	5.90	6.70
K_2O	2.90	0.40	5.20	4.20	4.60	4.55	5.38	4.60	3.81	3.61	4.09	3.54
TiO_2	0.81	1.10	0.15	0.21	0.12	0.33	0.15	0.05	0.17	0.44	0.18	0.17
P_2O_5	0.26	0.11	0.02	0.04	0.03	—	0.11	0.06	—	0.07	—	—
MnO	0.07	0.21	0.02	0.04	0.03	0.05	—	—	0.03	0.02	0.01	0.01
CO_2	0.05	0.05	0.08	0.05	0.02	—	—	—	—	—	—	—
$^3H_2O^+$	0.70	1.30	0.42	0.65	0.46	0.19	—	—	0.31	0.16	0.26	1.06
H_2O^-	0.11	0.08	0.12	0.10	0.03	—	—	—	—	—	—	—
Total	100.62	99.58	99.73	100.46	100.13	101.08	98.61	98.26	99.59	101.61	100.61	100.73
Normative minerals[4]:												
Q	15.446	—	27.056	34.909	34.508	26.669	6.671	10.913	35.586	33.086	47.437	39.365
C	—	—	0.917	1.096	—	—	0.853	—	—	—	—	—
Or	17.259	2.428	31.092	25.012	27.363	26.650	32.240	27.664	22.678	21.028	24.085	20.988
Ab	34.089	20.857	34.248	32.404	34.283	13.639	54.575	57.169	27.595	30.029	14.112	24.092
An	15.611	31.158	4.376	4.168	—	—	1.585	—	—	—	—	—
Ac	—	—	—	—	1.315	9.549	—	1.983	2.273	6.930	4.065	6.908
Ns	—	—	—	—	—	16.400	—	—	6.863	2.440	7.221	5.806
Wo	1.397	9.948	—	—	—	1.129	—	—	1.377	1.690	0.599	2.016
En	7.776	13.127	0.529	0.502	—	0.148	0.278	0.076	0.201	1.056	0.223	0.100
Fs	2.816	10.076	0.251	0.220	0.940	5.194	—	—	3.103	2.760	1.918	0.400
Fo	—	4.065	—	—	—	—	—	—	—	—	—	—
Fa	—	3.439	—	—	—	—	—	—	—	—	—	—
Mt	2.336	2.383	1.012	1.081	1.239	—	—	—	—	—	—	—
Hm	—	—	—	—	—	—	3.387	2.042	—	—	—	—
Il	1.549	2.146	0.288	0.402	0.229	0.621	—	—	0.325	0.824	0.341	0.324
Tn	—	—	—	—	—	—	—	—	—	—	—	—
Ru	—	—	—	—	—	—	0.152	0.051	—	—	—	—
Ap	0.620	0.268	0.048	0.095		0.072	—	0.264	0.073	—	0.163	—
Cc	0.115	0.117	0.184	0.115	0.001	—	—	—	—	—	—	—
Sd	—	—	—	—	0.052	—	—	—	—	—	—	—
Total	100.014	100.009	100.001	100.003	100.002	100.001	100.006	99.971	100.000	100.004	100.000	100.000

Footnotes at end of table.

TABLE 4.—*Chemical and normative analyses of crystalline rocks of the Arabian Shield*—Continued

[In percent]

Analysis number	—	W180420	W180027	—	—	—	W180029	—	W180023	W179460	W179461	W179462
Laboratory[1]	[D]	A	B	D	[D]	D	B	D	B	A	A	A
Sample (location given on pl. 1)	17	18	19	20	21	22a	22b	23	24	25a	25b	27
Oxides (wt. percent)[2]:												
SiO_2	80.00	70.70	48.40	77.00	73.50	82.40	48.00	74.00	76.90	66.20	59.40	70.40
Al_2O_3	8.58	15.30	17.00	7.18	10.25	8.50	15.40	12.00	12.20	17.10	16.70	12.60
Fe_2O_3	2.27	2.10	10.50	6.22	3.08	1.70	13.50	1.18	0.70	0.40	2.10	3.60
FeO	0.40	0.12	1.50	0.72	0.68	0.80	0.84	1.60	1.00	2.00	4.70	0.08
MgO	0.05	0.38	4.20	0.36	0.17	0.09	2.50	0.60	0.15	1.00	3.60	0.15
CaO	0.28	0.70	6.00	0.53	0.82	0.42	4.00	2.00	0.70	2.70	6.00	1.60
Na_2O	3.20	4.90	4.00	0.50	2.90	3.83	4.80	6.20	4.10	4.60	2.80	3.80
K_2O	3.91	3.80	2.40	4.58	4.82	0.34	3.10	1.01	4.00	3.90	0.66	4.70
TiO_2	0.16	0.35	3.10	0.47	0.47	0.10	3.10	0.42	0.10	0.51	0.96	0.25
P_2O_5	—	0.17	0.38	0.08	0.06	—	0.74	0.04	—	0.22	0.19	0.01
MnO	0.02	—	0.13	0.18	0.11	—	0.20	0.06	—	0.05	0.16	0.06
CO_2	—	0.06	—	—	—	—	—	—	—	0.11	0.02	1.10
$^3H_2O^+$	0.52	0.78	2.55	1.42	2.06	0.57	3.81	0.69	0.39	0.64	1.10	0.39
H_2O^-	—	0.36	—	—	—	—	—	—	—	0.16	0.34	0.24
Total	99.39	100.53	100.16	99.24	98.92	98.75	99.99	99.80	100.24	100.12	99.71	99.45
Normative minerals[4]:												
Q	47.668	26.611	—	56.346	38.183	58.858	—	30.315	35.663	17.191	20.970	30.188
C	—	2.434	—	0.642	—	1.087	—	—	—	1.198	0.999	0.940
Or	23.369	22.779	14.530	27.668	29.406	2.046	19.046	6.022	23.673	23.328	4.009	28.240
Ab	22.620	42.060	34.676	4.325	25.334	33.009	42.229	52.934	34.745	39.401	24.353	32.694
An	—	2.011	21.866	2.154	0.739	2.122	11.768	1.947	3.076	11.400	29.189	0.934
Ac	4.199	—	—	—	—	—	—	—	—	—	—	—
Wo	0.587	—	0.626	—	1.276	—	—	3.257	0.168	—	—	—
En	0.126	0.960	7.933	0.917	0.437	0.228	2.319	1.508	0.374	2.521	9.216	0.380
Fs	—	—	—	—	—	—	—	1.394	1.095		2.625	5.764
Fo	—	—	1.951	—	—	—	2.911	—	—	—	—	—
Mt	0.901	—	—	1.580	1.227	2.331	—	1.726	1.016	0.587	3.130	—
Hm	0.223	2.130	10.757	5.269	2.334	0.124	14.036	—	—	—	—	3.660
Il	0.307	0.257	3.531	0.913	0.922	0.193	2.289	0.805	0.190	0.980	1.874	0.302
Tn	—	—	3.232	—	—	—	2.704	—	—	—	—	—
Ru	—	0.220	—	—	—	—	0.916	—	—	—	—	0.095
Ap	—	0.408	0.922	0.194	0.147	—	1.822	0.096	—	0.527	0.463	0.024
Cc	—	0.138	—	—	—	—	—	—	—	0.253	0.047	2.544
Total	100.000	100.009	100.022	100.007	100.005	100.000	100.042	100.003	100.000	100.012	100.012	100.001

Footnotes at end of table.

TABLE 4.—*Chemical and normative analyses of crystalline rocks of the Arabian Shield*—Continued

[In percent]

Analysis number	W179458	W179459	W179463	W179451	W179448	W179450	W179449	W180037	W180036	W179439	W179440	W180034
Laboratory[1]	A	A	A	A	A	A	A	B	B	A	A	B
Sample (location given on pl. 1)	28a	28b	29	30	31	32	33	36	37	38	39[5]	41
Oxides (wt. percent)[2]:												
SiO_2	52.60	67.30	74.80	73.60	75.40	72.00	75.30	65.20	68.00	76.10	36.20	68.60
Al_2O_3	17.70	15.80	12.30	14.10	12.70	14.90	13.50	15.40	14.60	13.50	3.80	13.50
Fe_2O_3	2.10	1.10	1.40	0.48	1.40	0.20	0.70	2.20	1.40	1.20	0.49	4.70
FeO	3.80	2.00	0.08	0.48	1.00	1.30	0.96	1.60	1.00	0.08	0.24	0.76
MgO	4.00	1.10	0.05	0.20	0.25	0.45	0.05	2.30	1.30	0.46	0.86	0.05
CaO	10.40	2.60	1.10	0.90	1.20	1.50	0.80	2.10	2.40	1.60	30.70	1.10
Na_2O	4.30	4.20	4.80	4.30	4.80	3.80	4.30	4.90	4.40	1.00	0.50	4.70
K_2O	0.56	3.60	3.50	4.30	1.00	4.10	4.60	2.70	2.90	3.10	1.00	4.80
TiO_2	0.63	0.50	0.10	0.09	0.16	0.19	0.09	0.69	0.42	0.12	0.06	0.26
P_2O_5	0.52	0.13	—	0.01	0.01	0.05	—	0.17	0.15	0.01	0.09	—
MnO	0.11	0.04	—	0.02	0.06	0.02	0.02	0.07	—	0.02	—	0.07
CO_2	2.50	0.05	0.32	0.06	0.02	0.06	0.08	—	—	0.91	23.90	—
$^3H_2O^+$	0.97	0.56	0.32	0.35	0.53	0.65	0.33	2.37	1.85	1.80	1.20	1.26
H_2O^-	0.64	0.13	0.10	0.13	0.15	0.14	0.13	—	—	1.10	0.74	—
Total	102.02	99.56	99.16	99.35	99.14	99.88	101.18	99.70	98.42	103.14	101.22	99.80
Normative minerals[4]:												
Q	4.611	21.814	32.816	30.371	41.380	30.172	30.504	19.384	25.527	57.919	28.527	21.618
C	—	0.705	—	0.912	1.643	1.768	0.177	1.033	0.226	7.872	1.701	—
Or	3.335	21.615	21.008	25.786	6.030	24.580	27.074	16.393	17.746	18.674	6.040	28.785
Ab	36.671	36.110	41.256	36.925	41.445	32.621	36.240	42.600	38.554	8.626	4.324	40.359
An	27.555	11.922	1.705	4.080	5.879	6.833	3.449	9.563	11.315	2.161	0.644	1.586
Wo	2.126	—	0.728	—	—	—	—	—	—	—	—	1.650
En	10.040	2.784	0.126	0.505	0.635	1.137	0.124	5.885	3.353	1.168	2.189	0.126
Fs	4.442	2.045	—	0.379	0.538	1.974	1.069	0.114	—	—	—	—
Mt	3.069	1.620	—	0.706	2.071	0.294	1.011	3.277	2.077	—	0.613	1.953
Hm	—	—	1.422	—	—	—	—	—	0.017	1.223	0.078	3.423
Il	1.206	0.965	0.172	0.173	0.310	0.366	0.170	1.346	0.826	0.216	0.116	0.501
Tn	—	—	0.028	—	—	—	—	—	—	—	—	—
Ru	—	—	—	—	—	—	—	—	—	0.009	—	—
Ap	1.241	0.313	—	0.024	0.024	0.120	—	0.414	0.368	0.024	0.218	—
Cc	5.730	0.116	0.739	0.138	0.046	0.138	0.181	—	—	2.110	55.554	—
Total	100.028	100.007	100.000	100.001	100.001	100.003	100.000	100.010	100.008	100.001	100.005	100.001

Footnotes at end of table.

TABLE 4.—*Chemical and normative analyses of crystalline rocks of the Arabian Shield*—Continued

[In percent]

Analysis number	W180033	W179458	W180032	W179437	W180031	W179442	W179445	W179455	W179454	W179453	W165083	W180035
Laboratory[1]	B	A	B	A	B	A	A	A	A	A	A	B
Sample (location given on pl. 1)	42	43	45	46	47	48	49	50	51	52	54	55
Oxides (wt. percent)[2]:												
SiO_2	73.80	75.10	55.20	73.70	77.60	73.20	73.30	72.40	49.20	77.90	70.11	45.30
Al_2O_3	9.30	14.00	15.70	13.70	12.50	14.50	14.10	14.80	19.20	12.00	15.57	14.30
Fe_2O_3	7.80	0.71	0.21	2.00	0.78	0.69	0.22	0.34	5.50	0.73	0.89	5.10
FeO	0.48	0.20	7.00	—	0.16	0.56	0.80	0.40	4.60	0.52	1.20	10.10
MgO	0.08	0.29	4.60	0.20	0.10	0.22	0.24	0.18	4.80	0.23	0.66	6.20
CaO	0.70	0.82	7.40	0.25	0.20	1.00	1.70	1.00	9.20	2.00	2.64	9.20
Na_2O	1.80	3.60	3.70	4.30	4.10	4.80	4.00	4.60	2.30	4.20	4.67	2.40
K_2O	3.30	4.70	1.10	4.70	3.90	4.40	3.60	4.40	1.00	0.66	3.17	0.80
TiO_2	0.26	0.09	1.60	0.19	0.15	0.14	0.10	0.03	0.55	0.14	0.39	4.70
P_2O_5	—	0.01	0.30	0.02	—	0.02	0.02	—	0.24	0.01	0.29	0.22
MnO	0.04	0.01	0.13	0.27	—	0.04	0.04	0.02	0.17	0.02	0.04	0.58
CO_2	—	0.04	—	0.02	—	0.06	0.56	0.08	0.06	0.06	0.14	—
$^3H_2O^+$	1.01	0.49	1.57	0.54	0.52	0.37	0.64	0.49	1.40	0.29	0.39	1.08
H_2O^-	—	0.31	—	0.28	—	0.07	0.12	0.24	0.32	0.11	0.08	—
Total	98.57	100.96	98.51	100.76	100.01	100.35	99.93	99.50	99.67	99.15	100.55	99.98
Normative minerals[4]:												
Q	50.310	34.269	5.634	30.175	38.445	26.151	33.742	26.882	5.628	47.158	25.023	0.421
C	1.532	1.623	—	1.186	1.176	0.211	1.903	0.852	—	0.917	0.677	—
Or	19.988	27.894	6.705	27.955	23.164	26.097	21.558	26.464	6.103	3.961	18.776	4.780
Ab	15.612	30.594	32.297	36.623	34.871	40.767	34.300	39.617	20.101	36.091	39.607	20.534
An	3.560	3.766	23.707	0.990	0.997	4.468	4.827	4.535	40.396	9.625	10.341	26.171
Wo	—	—	5.069	—	—	—	—	—	1.976	—	—	7.735
En	0.204	0.725	11.818	0.501	0.250	0.550	0.606	0.456	12.347	0.582	1.648	15.613
Fs	—	—	10.605	—	—	0.303	1.213	0.449	3.420	0.160	0.901	7.736
Mt	0.947	0.418	0.314	0.333	0.081	1.004	0.323	0.502	8.236	1.075	1.293	7.477
Hm	7.342	0.425	—	1.784	0.728	—	—	—	—	—	—	—
Il	0.506	0.172	3.135	0.363	0.286	0.267	0.192	0.058	1.079	0.270	0.742	9.026
Ap	—	0.024	0.733	0.048	—	0.048	0.048	—	0.587	0.024	0.688	0.527
Cc	—	0.091	—	0.046	—	0.137	1.291	0.185	0.141	0.139	0.319	—
Total	100.001	100.001	100.018	100.005	100.000	100.002	100.002	100.000	100.015	100.001	100.016	100.019

Footnotes at end of table.

TABLE 4.—*Chemical and normative analyses of crystalline rocks of the Arabian Shield*—Continued

[In percent]

Analysis number	W179444	W180109	—	W180053	W180054	W180052	W180030	W180060	W165086	W180040	—	W180049
Laboratory[1]	A	B	D	B	B	B	B	B	A	B	D	B
Sample (location given on pl. 1)	56	57	58	61a	61b	62	63	64	65	66	67	68a
Oxides (wt. percent)[2]:												
SiO_2	69.90	62.70	71.50	77.30	76.70	73.10	80.20	75.30	64.43	46.20	48.50	70.60
Al_2O_3	14.60	16.20	12.20	12.20	12.20	12.20	11.90	13.80	15.51	17.00	14.93	12.90
Fe_2O_3	1.70	2.40	2.04	0.42	1.40	1.30	0.52	0.39	1.73	13.10	12.04	2.50
FeO	2.60	3.40	1.40	0.32	0.16	3.00	0.20	0.24	3.12	0.88	1.20	2.70
MgO	0.74	2.60	0.48	0.20	0.04	0.05	0.15	0.15	3.27	3.10	4.73	0.85
CaO	3.30	5.30	1.44	0.50	0.43	0.50	0.90	0.55	4.98	8.10	6.02	1.30
Na_2O	4.60	3.30	4.45	2.40	3.70	4.30	0.18	4.30	4.02	3.40	4.23	5.00
K_2O	0.55	1.40	4.72	4.50	4.50	4.40	1.90	4.10	1.29	1.30	1.54	2.30
TiO_2	0.43	0.58	0.24	0.07	0.07	0.45	0.10	0.09	0.68	2.40	2.50	0.52
P_2O_5	0.09	0.10	—	—	—	—	0.01	0.04	0.25	0.38	0.53	0.06
MnO	0.12	0.05	0.05	—	—	0.09	—	0.01	0.09	0.07	0.17	—
CO_2	0.02	—	—	—	—	—	—	—	0.02	—	—	—
BaO	—	—	—	—	—	—	—	—	0.05	—	—	—
$^3H_2O^+$	0.66	1.30	0.86	1.84	0.73	0.20	2.93	0.90	0.91	3.74	2.94	1.40
H_2O^-	0.10	—	—	—	—	—	—	—	0.14	—	—	—
Total	99.89	99.33	99.38	99.75	99.93	99.59	98.99	99.87	101.16	99.67	99.33	100.13
Normative minerals[4]:												
Q	32.296	22.170	25.543	45.646	37.274	28.844	72.619	33.655	20.432	2.911	1.592	28.285
C	0.709	—	—	2.525	0.464	—	8.260	1.399	—	—	—	—
Or	3.295	8.439	28.311	27.159	26.806	26.160	11.688	24.480	7.666	8.008	9.441	13.766
Ab	39.457	28.485	37.023	20.742	31.561	36.609	1.586	36.764	34.208	29.990	37.134	42.853
An	15.871	25.763	—	2.533	2.150	0.999	4.580	2.493	20.581	28.442	17.846	6.039
Ac	—	—	1.055	—	—	—	—	—	—	—	—	—
Wo	—	0.164	3.028	—	—	0.625	—	—	1.080	2.499	2.516	0.040
En	1.868	6.605	1.213	0.509	0.100	0.125	0.389	0.377	8.190	8.048	12.221	2.144
Fs	2.923	3.464	0.892	0.128	—	3.883	—	—	3.363	—	—	2.060
Mt	2.499	3.550	2.474	0.622	0.315	1.896	0.369	0.551	2.522	—	—	3.671
Hm	—	—	—	—	1.194	—	0.287	0.014	—	13.656	12.491	—
Il	0.828	1.124	0.463	0.136	0.134	0.860	0.198	0.173	1.299	2.094	3.007	1.000
Tn	—	—	—	—	—	—	—	—	—	3.434	2.480	—
Ap	0.216	0.242	—	—	—	—	0.025	0.096	0.595	0.938	1.302	0.144
Cc	0.046	—	—	—	—	—	—	—	0.046	—	—	—
Total	100.006	100.006	100.001	100.000	100.000	100.001	100.001	100.002	99.982	100.021	100.031	100.003

Footnotes at end of table.

TABLE 4.—*Chemical and normative analyses of crystalline rocks of the Arabian Shield*—Continued

[In percent]

Analysis number	W180048	W180042	W180044	W180046	W167118	—	W180039	W165085	W165084	W165310	W180059	—
Laboratory[1]	B	B	B	B	A	D	B	A	A	A	B	D
Sample (location given on pl.1)	68b	69	70	71	73	74	75	76	77	78a	78b	79
Oxides (wt. percent)[2]:												
SiO_2	71.30	54.40	65.80	75.60	76.10	47.50	53.50	72.80	69.20	74.20	73.90	62.40
Al_2O_3	13.10	14.00	13.90	11.90	11.80	17.19	15.50	14.11	14.47	13.80	13.70	17.53
Fe_2O_3	3.30	12.60	4.00	0.40	2.10	4.54	10.90	0.95	1.29	0.44	1.10	1.64
FeO	2.50	1.50	2.30	1.30	0.24	5.80	1.50	0.82	1.25	0.60	0.56	2.30
MgO	0.32	1.00	1.00	1.70	0.38	4.31	1.20	0.21	0.01	0.10	0.23	1.91
CaO	0.23	5.60	1.80	0.65	0.72	9.09	7.80	1.43	1.77	0.63	0.50	4.20
Na_2O	3.60	3.90	5.60	5.30	1.00	3.12	3.70	4.18	4.60	4.80	3.90	4.74
K_2O	1.70	2.00	1.90	0.21	5.60	1.45	1.40	4.44	4.41	4.50	5.10	3.60
TiO_2	0.38	2.40	0.76	0.16	0.25	2.60	3.00	0.27	0.48	0.07	0.22	0.50
P_2O_5	0.04	1.10	0.11	—	0.04	0.47	1.00	0.20	0.20	0.02	—	0.24
MnO	—	0.10	0.11	0.02	0.04	0.11	0.08	0.03	0.05	0.06	—	0.04
CO_2	—	—	—	—	0.05	—	—	0.04	0.98	0.05	—	—
$^3H_2O^+$	—	0.92	1.32	1.41	0.80	2.25	1.07	0.35	0.83	0.47	0.86	0.58
H_2O^-	—	—	—	—	0.14	—	—	0.06	0.13	0.10	—	—
Total	96.47	99.52	98.60	98.65	99.86	98.43	100.65	100.15	100.28	100.21	100.07	99.68
Normative minerals[4]:												
Q	43.987	15.141	21.733	40.321	47.796	0.876	13.288	28.790	25.081	27.620	30.525	9.728
C	5.199	—	—	1.822	3.047	—	—	0.402	1.682	0.052	0.862	—
Or	10.413	11.986	11.542	1.276	33.657	8.909	8.308	26.374	26.400	26.787	30.377	21.467
Ab	31.577	33.469	48.711	46.120	8.606	27.449	31.440	35.555	39.433	40.915	33.263	40.473
An	0.912	14.997	7.380	3.316	3.046	29.754	21.641	5.564	1.296	2.698	2.500	16.068
Wo	—	1.546	0.443	—	—	5.821	2.637	—	—	—	—	1.409
En	0.826	2.526	2.560	4.354	0.963	11.160	3.001	0.526	0.025	0.251	0.577	4.800
Fs	1.282	—	—	1.882	—	2.923	—	0.333	0.537	0.740	—	2.137
Mt	4.960	—	5.725	0.596	0.183	6.844	—	1.385	1.895	0.643	1.176	2.399
Hm	—	12.779	0.164	—	2.010	—	10.946	—	—	—	0.297	—
Il	0.748	3.430	1.484	0.312	0.483	5.134	3.353	0.515	0.924	0.134	0.421	0.958
Tn	—	1.541	—	—	—	—	3.060	—	—	—	—	—
Ap	0.098	2.642	0.268	—	0.096	1.157	2.379	0.476	0.480	0.048	—	0.574
Cc	—	—	—	—	0.116	—	—	0.091	2.258	0.115	—	—
Total	100.002	100.059	100.007	100.000	100.003	100.027	100.053	100.011	100.011	100.002	100.000	100.013

Footnotes at end of table.

TABLE 4.—*Chemical and normative analyses of crystalline rocks of the Arabian Shield*—Continued

[In percent]

Analysis number	—	W180064	W180065	W165311	W180061	W180063	W180050	—	—	W180059	W180067	W180068
Laboratory[1]	D	B	B	A	B	B	B	D	D	B	B	B
Sample (location given on pl. 1)	80	81a	81b	82a	82b	83	84	85	86	87	88	89
Oxides (wt. percent)[2]:												
SiO_2	58.80	68.80	75.20	65.30	65.60	69.00	76.40	70.70	70.30	66.30	68.90	66.00
Al_2O_3	16.25	16.20	13.40	15.40	15.80	14.90	12.50	15.68	16.60	16.60	15.80	15.70
Fe_2O_3	1.37	1.10	0.37	1.10	1.00	3.40	0.10	1.92	1.75	0.60	0.30	1.10
FeO	3.80	0.68	0.40	2.60	2.60	0.64	0.92	0.60	1.30	2.40	3.00	1.90
MgO	3.24	0.63	0.15	2.80	2.60	0.59	0.05	0.93	1.19	1.70	1.50	2.10
CaO	7.69	2.00	0.53	3.90	3.90	1.70	0.60	2.25	2.85	3.50	3.20	4.10
Na_2O	4.18	4.30	2.30	4.40	4.20	4.80	3.70	2.99	3.67	4.10	3.30	3.90
K_2O	1.43	4.60	6.90	2.80	2.90	3.70	4.60	3.30	2.82	3.10	2.20	2.90
TiO_2	0.64	0.25	0.08	0.62	0.52	0.52	0.06	0.30	0.30	0.48	0.39	0.67
P_2O_5	0.13	0.11	0.03	0.28	0.24	0.10	—	0.07	0.11	0.19	0.13	0.36
MnO	0.05	—	—	0.08	0.03	0.02	—	—	0.01	0.05	0.03	0.01
CO_2	—	—	—	0.05	—	—	—	—	—	—	—	—
$^3H_2O^+$	1.38	1.20	0.50	0.45	0.59	0.58	0.71	0.72	0.82	0.75	0.73	0.56
H_2O^-	—	—	—	0.07	—	—	—	—	—	—	—	—
Total	98.96	99.87	99.86	100.18	99.98	99.95	99.64	99.46	101.72	99.77	99.48	99.30
Normative minerals[4]:												
Q	9.524	21.557	34.225	16.830	17.642	22.824	35.609	35.112	30.108	19.822	30.817	21.168
C	—	0.785	1.264	—	—	0.148	0.347	3.308	2.569	0.597	2.515	—
Or	8.660	27.549	41.037	16.658	17.242	22.003	27.477	19.749	16.516	18.500	13.165	17.356
Ab	36.247	36.876	19.587	37.483	35.757	40.874	31.647	25.623	30.778	35.036	28.277	33.422
An	21.883	9.327	2.449	14.095		15.791	7.830	3.009	10.842	13.300	16.282	15.216
Wo	6.824	—	—	1.346	0.876	—	—	—	—	—	—	0.516
En	8.269	1.590	0.376	7.020	6.515	1.479	0.126	2.346	2.937	4.276	3.783	5.297
Fs	5.003	—	0.299	3.011	3.165	—	1.524	—	0.460	3.244	4.732	1.512
Mt	2.036	1.487	0.540	1.606	1.459	0.625	0.147	1.078	2.515	0.879	0.440	1.615
Hm	—	0.089	—	—	—	2.991	—	1.201	—	—	—	—
Il	1.246	0.481	0.153	1.185	0.994	0.994	0.115	0.577	0.565	0.921	0.750	1.289
Tn	—	—	—	—	—	—	—	—	—	—	—	—
Ap	0.316	0.264	0.072	0.668	0.572	0.238	—	0.168	0.258	0.454	0.312	0.864
Cc	—	—	—	0.114	—	—	—	—	—	—	—	—
Total	100.008	100.006	100.002	100.016	100.013	100.005	100.000	100.004	100.006	100.011	100.007	100.019

Footnotes at end of table.

TABLE 4.—*Chemical and normative analyses of crystalline rocks of the Arabian Shield*—Continued

[In percent]

Analysis number	W165512	W180070	W165313	W180071	W163663	W163062	W163661	W163660	—	W180047	W167119
Laboratory[1]	A	B	A	B	A	A	A	A	D	B	A
Sample (location given on pl. 1)	90a	90b	91a	91b	93a	93b	93c	93d	94	98	102
Oxides (wt. percent)[2]:											
SiO_2	66.20	71.80	76.20	75.20	53.20	50.80	50.20	48.30	74.00	73.20	62.10
Al_2O_3	15.60	15.40	13.00	13.60	16.70	18.20	20.10	18.40	6.23	12.40	14.00
Fe_2O_3	0.87	0.40	0.23	1.17	1.40	2.50	0.60	2.30	2.35	—	5.20
FeO	2.30	1.00	0.70	0.84	5.30	5.30	6.00	6.80	1.30	2.00	2.30
MgO	2.20	0.54	0.10	0.15	8.20	7.40	8.30	8.70	0.76	1.90	1.50
CaO	3.80	2.40	0.85	1.30	10.80	9.80	9.80	9.40	2.00	3.10	4.10
Na_2O	4.30	3.90	3.50	3.80	2.70	2.80	2.90	2.80	5.55	0.55	5.40
K_2O	2.80	3.00	4.60	4.80	0.14	0.22	0.27	0.34	0.78	2.60	0.97
TiO_2	0.74	0.23	0.08	0.06	0.42	0.70	0.67	1.40	0.01	0.08	1.40
P_2O_5	0.34	0.01	0.02	0.03	0.06	0.11	0.09	0.52	0.01	—	0.59
MnO	0.10	—	0.03	—	0.11	0.13	0.07	0.13	—	0.03	0.15
CO_2	0.05	—	0.05	—	0.08	0.09	0.11	0.08	—	—	1.20
$^3H_2O^+$	0.63	0.79	0.55	0.53	0.44	1.50	0.73	0.60	6.44	3.07	1.40
H_2O^-	0.07	—	0.03	—	0.17	0.32	0.14	0.16	—	—	0.18
Total	100.44	99.47	100.29	101.48	100.15	101.06	100.54	100.44	99.43	98.93	101.48
Normative minerals[4]:											
Q	19.444	31.619	36.228	31.369	2.565	1.503	—	—	45.996	51.052	21.129
C	—	1.416	0.887	—	—	—	—	—	—	3.176	0.814
Or	16.663	17.965	27.358	28.098	0.835	1.326	1.610	2.026	4.957	16.028	5.795
Ab	36.642	33.442	29.807	31.852	23.052	24.164	24.759	23.891	29.791	4.855	46.197
An	15.101	11.999	3.794	5.820	33.331	37.167	41.398	36.940	—	16.043	8.998
Ac	—	—	—	—	—	—	—	—	7.311	—	—
Ns	—	—	—	—	—	—	—	—	2.889	—	—
Wo	0.555	—	—	0.156	8.277	4.637	2.656	2.567	4.426	—	—
En	5.518	1.363	0.251	0.370	20.606	18.796	12.114	13.356	2.035	4.936	3.777
Fs	2.486	1.141	1.026	0.472	8.159	6.887	5.594	5.250	2.549	3.752	—
Fo	—	—	—	—	—	—	6.127	5.951	—	—	—
Fa	—	—	—	—	—	—	3.118	2.578	—	—	—
Mt	1.270	0.588	0.336	1.680	2.048	3.697	0.878	3.363	—	—	3.887
Hm	—	—	—	—	—	—	—	—	—	—	2.576
Il	1.415	0.443	0.153	0.113	0.805	1.356	1.284	2.681	0.020	0.158	2.688
Ap	0.811	0.024	0.048	0.070	0.143	0.266	0.215	1.242	0.025	—	1.413
Cc	0.115	—	0.114	—	0.184	0.209	0.252	0.183	—	—	2.759
Total	100.019	100.001	100.001	100.002	100.005	100.007	100.006	100.029	100.001	100.000	100.033

Footnotes at end of table.

TABLE 4.—*Chemical and normative analyses of crystalline rocks of the Arabian Shield*—Continued

[In percent]

Analysis number	W167120	W180094	W180095	W180045	W180106	W180105	W165316	—	—	W180101	W180104	W174515
Laboratory[1]	A	B	B	B	B	B	A	D	D	B	B	A
Sample (location given on pl. 1)	103	104	105	106	111	113	114a	114b	114c	115	116	117a
Oxides (wt. percent)[2]:												
SiO_2	52.50	46.70	72.60	75.40	70.50	75.50	75.20	66.50	69.50	73.30	52.20	50.70
Al_2O_3	15.30	20.70	14.90	13.70	14.10	12.90	13.70	13.87	14.00	13.80	18.70	16.40
Fe_2O_3	2.60	1.70	1.00	0.70	1.30	1.30	0.43	0.59	0.75	1.30	3.40	1.90
FeO	6.80	5.90	1.20	0.52	1.80	0.36	0.70	1.80	0.76	1.00	5.70	8.30
MgO	5.80	9.40	0.42	0.32	1.00	0.08	0.40	0.72	0.30	0.73	4.10	9.40
CaO	9.50	12.60	1.80	1.50	2.20	0.08	1.20	7.56	7.63	2.40	8.00	1.20
Na_2O	3.40	1.70	3.60	6.10	3.60	4.40	4.10	4.32	4.40	3.50	3.00	2.10
K_2O	0.27	0.20	4.10	1.10	3.50	3.60	3.10	1.80	2.64	2.80	0.55	1.40
TiO_2	1.50	0.16	0.22	0.11	0.55	0.14	0.19	0.28	0.13	0.24	1.10	1.60
P_2O_5	0.24	0.14	0.05	—	0.03	0.28	0.04	0.01	0.09	0.06	0.24	0.19
MnO	0.09	0.10	0.01	0.03	0.01	—	0.05	0.04	—	—	0.10	0.03
CO_2	0.06	—	—	—	—	—	0.05	—	—	—	—	0.64
$^3H_2O^+$	1.70	0.89	0.78	1.50	0.66	0.66	0.73	0.83	0.61	0.59	1.48	5.99
H_2O^-	0.13	—	—	—	—	—	0.04	—	—	—	—	—
Total	101.01	100.19	100.68	100.98	99.25	99.30	100.39	98.32	100.81	99.72	98.57	99.85
Normative minerals[4]:												
Q	4.163	—	31.189	32.220	29.856	36.507	36.554	21.931	22.707	36.314	8.029	14.682
C	—	—	1.388	—	0.468	1.789	1.643	—	—	0.799	—	11.918
Or	1.627	1.190	24.252	6.534	20.978	21.567	18.474	10.911	15.569	16.691	3.348	8.814
Ab	29.339	14.486	30.493	51.886	30.898	37.745	34.987	37.496	37.157	29.876	26.146	18.932
An	26.196	48.600	8.612	6.787	10.872	—	5.421	13.476	10.632	11.615	37.011	0.710
Wo	8.301	5.607	—	0.290	—	—	—	10.408	11.089	—	0.940	—
En	14.731	8.224	1.047	0.801	2.526	0.202	1.005	1.839	0.746	1.834	10.517	24.942
Fs	8.188	3.285	1.034	0.252	1.361	—	0.715	2.493	0.560	0.369	6.208	11.811
Fo	—	10.758	—	—	—	—	—	—	—	—	—	—
Fa	—	4.736	—	—	—	—	—	—	—	—	—	—
Mt	3.844	2.482	1.451	1.020	1.912	0.765	0.629	0.877	1.085	1.901	5.077	2.935
Hm	—	—	—	—	—	0.790	—	—	—	—	—	—
Il	2.905	0.306	0.418	0.210	1.060	0.270	0.364	0.545	0.246	0.460	2.152	3.238
Ap	0.580	0.334	0.119	—	0.072	0.146	0.096	0.024	0.213	0.143	0.585	0.479
Cc	0.139	—	—	—	—	—	0.115	—	—	—	—	1.551
Total	100.014	100.009	100.003	100.000	100.002	99.781	100.003	100.001	100.005	100.003	100.014	100.011

Footnotes at end of table.

TABLE 4.—*Chemical and normative analyses of crystalline rocks of the Arabian Shield*—Continued

[In percent]

Analysis number	W174516	W180108	W180107	W165317	W180102	W165318	W165320	W165319	W165977	W180170	W180171	W180157
Laboratory[1]	A	B	B	A	B	A	A	A	A	A	A	A
Sample (location given on pl. 1)	117b	122	123	124a	124b	125	126	127a	127b	133	134	138
Oxides (wt. percent)[2]:												
SiO_2	59.90	67.80	73.40	63.40	72.40	73.40	66.70	74.30	75.20	60.40	65.70	54.20
Al_2O_3	15.60	14.90	13.30	17.40	15.70	14.50	16.20	13.50	13.00	17.50	15.30	14.30
Fe_2O_3	2.80	3.30	1.70	1.20	0.30	0.53	0.92	0.17	0.90	2.80	3.80	3.80
FeO	5.50	1.70	0.76	3.90	1.60	0.70	2.80	0.60	0.82	4.10	1.40	7.30
MgO	2.90	0.55	0.31	1.00	0.60	0.50	2.10	0.10	0.13	2.90	1.60	3.50
CaO	3.20	2.30	0.83	5.20	3.20	1.20	4.60	0.65	0.77	6.60	0.86	3.80
Na_2O	5.20	5.60	4.80	4.00	4.50	3.70	3.80	4.30	4.00	2.00	6.60	4.10
K_2O	0.57	1.40	2.30	1.20	0.76	4.20	1.30	5.10	4.30	0.58	1.10	2.00
TiO_2	1.20	0.44	0.21	0.50	0.13	0.19	0.42	0.09	0.16	0.42	0.81	2.10
P_2O_5	0.42	0.04	0.13	0.36	0.13	0.06	0.10	—	0.03	0.14	0.23	0.58
MnO	0.13	0.07	0.05	0.20	0.02	0.03	0.10	0.06	0.06	0.17	0.09	0.21
CO_2	0.20	—	—	0.05	—	0.05	0.05	0.05	0.05	0.02	0.30	0.08
$^3H_2O^+$	2.19	1.23	1.59	1.00	0.50	0.46	0.72	0.24	0.45	2.30	1.20	2.80
H_2O^-	—	—	—	0.05	—	0.05	0.26	0.05	0.02	0.05	0.10	0.27
Total	99.81	99.33	99.38	100.09	99.84	99.89	100.75	99.40	100.17	101.36	99.89	100.93
Normative minerals[4]:												
Q	15.642	24.703	35.591	21.804	35.019	32.835	25.521	28.345	33.773	26.967	20.801	8.252
C	2.130	0.088	1.755	1.061	1.981	1.963	0.538	—	0.556	2.011	3.000	0.058
Or	3.450	8.433	13.898	7.206	4.521	25.054	7.753	30.466	25.558	3.511	6.647	12.315
Ab	45.074	48.303	41.534	34.394	38.331	31.605	32.450	36.783	34.044	17.334	57.109	36.150
An	12.156	11.365	3.342	23.503	15.126	5.295	22.052	2.499	3.327	32.471	0.887	15.168
Wo	—	—	—	—	—	—	—	0.184	—	—	—	—
En	7.399	1.396	0.790	2.531	1.504	1.257	5.278	0.252	0.326	7.398	4.075	9.083
Fs	6.194	—	—	5.809	2.529	0.595	3.910	0.934	0.613	4.956	—	7.490
Mt	4.159	4.518	2.049	1.768	0.438	0.776	1.346	0.249	1.313	4.158	2.514	5.741
Hm	—	0.248	0.325	—	—	—	—	—	—	—	2.152	—
Il	2.335	0.852	0.408	0.965	0.249	0.364	0.805	0.173	0.306	0.817	1.573	4.156
Ap	1.019	0.097	0.315	0.866	0.310	0.143	0.239	—	0.071	0.340	0.557	1.431
Cc	0.466	—	—	0.116	—	0.115	0.115	0.115	0.114	0.047	0.698	0.190
Total	100.024	100.003	100.007	100.021	100.007	100.003	100.006	100.001	100.002	100.010	100.013	100.034

Footnotes at end of table.

TABLE 4.—*Chemical and normative analyses of crystalline rocks of the Arabian Shield*—Continued

[In percent]

Analysis number	W180158	W167124	W167122	W167121	W180074	W167123	W167125	W165314	W180073	W180075	W180096	W180097
Laboratory[1]	A	A	A	A	B	A	A	A	B	B	B	B
Sample (location given on pl. 1)	139	141a	141b	141c	141d	142	143	144a	144b	145	146	147a
Oxides (wt. percent)[2]:												
SiO_2	76.10	57.70	73.20	75.70	71.00	66.00	63.70	74.70	70.00	49.70	76.10	75.80
Al_2O_3	11.90	17.50	13.60	12.30	14.25	15.00	15.50	13.30	14.50	21.30	12.70	13.80
Fe_2O_3	1.50	4.90	1.80	1.70	1.82	2.90	2.20	0.21	0.41	0.50	1.40	0.52
FeO	0.60	1.20	0.36	0.20	0.52	1.10	2.40	0.90	2.60	3.80	0.20	0.36
MgO	0.05	1.90	0.54	0.58	0.53	2.40	2.20	0.10	0.55	10.20	0.06	0.02
CaO	1.00	4.80	1.40	2.00	0.60	3.00	4.70	0.78	2.00	9.80	0.36	0.55
Na_2O	4.60	5.30	3.80	3.80	4.61	3.60	4.00	3.60	3.80	2.70	4.20	4.60
K_2O	2.90	3.20	3.20	1.50	4.14	3.60	2.90	5.20	3.80	0.12	4.30	4.20
TiO_2	0.10	0.89	0.33	0.15	0.32	0.44	0.63	0.11	0.38	0.22	0.16	1.00
P_2O_5	0.01	0.32	0.16	0.04	0.10	0.12	0.31	—	0.19	0.04	0.04	0.03
MnO	0.02	0.11	0.10	0.04	0.04	0.06	0.12	0.04	0.01	0.02	—	0.11
CO_2	0.08	0.66	0.05	0.34	—	0.15	0.05	0.05	—	—	—	—
$^3H_2O^+$	0.89	1.30	0.57	0.66	0.29	1.00	1.10	0.57	0.31	0.21	0.80	0.69
H_2O^-	0.11	0.13	0.13	0.07	—	0.08	0.07	0.05	—	—	—	—
Total	100.49	100.79	99.70	99.53	98.22	100.11	100.59	99.99	98.55	98.61	100.32	101.68
Normative minerals[4]:												
Q	36.940	4.945	36.162	44.481	27.110	22.391	17.539	31.873	27.527	—	34.633	31.535
C	—	—	1.866	1.700	1.362	0.368	—	0.452	0.971	—	0.581	0.751
Or	17.335	19.202	19.190	9.013	24.982	21.626	17.361	31.042	22.858	0.721	25.532	24.576
Ab	39.373	45.539	32.631	32.694	39.833	30.967	34.289	30.773	32.731	23.218	35.711	38.542
An	3.295	14.733	5.667	7.637	2.372	13.369	15.980	3.590	8.836	46.387	1.532	2.508
Wo	0.478	1.289	—	—	—	—	2.200	—	—	1.151	—	—
En	0.126	4.805	1.365	1.469	1.348	6.076	5.551	0.252	1.394	12.053	0.150	0.049
Fs	—	—	—	—	—	—	1.796	1.386	3.895	2.960	—	—
Fo	—	—	—	—	—	—	—	—	—	9.645	—	—
Fa	—	—	—	—	—	—	—	—	—	2.610	—	—
Mt	1.729	1.673	0.538	0.346	0.898	2.507	3.231	0.308	0.605	0.737	0.182	—
Hm	0.325	3.822	1.456	1.490	1.239	1.219	—	—	—	—	1.281	0.515
Il	0.192	1.716	0.636	0.290	0.621	0.850	1.212	0.211	0.735	0.425	0.305	0.986
Ru	—	—	—	—	—	—	—	—	—	—	—	0.471
Ap	0.024	0.770	0.385	0.096	0.242	0.289	0.744	—	0.458	0.096	0.095	
Cc	0.184	1.524	0.115	0.786	—	0.347	0.115	0.115	—	—	—	—
Total	100.001	100.018	100.010	100.003	100.006	100.007	100.018	100.000	100.010	100.002	100.002	100.003

Footnotes at end of table.

TABLE 4.—*Chemical and normative analyses of crystalline rocks of the Arabian Shield*—Continued

[In percent]

Analysis number	W180098	W165315	W180072	W180087	W180092	W180078	W180091	W179446	W180086	W180082	W180081	W180081a
Laboratory[1]	B	A	B	B	B	B	B	A	B	B	B	B
Sample (location given on pl. 1)	147b	149a	149b	150	152	154	155	156	157	158	159a	159b
Oxides (wt. percent)[2]:												
SiO_2	52.20	75.50	74.70	57.00	65.40	74.90	76.30	56.80	74.80	76.50	66.00	73.00
Al_2O_3	18.30	13.50	13.20	16.10	15.00	13.70	12.50	15.70	13.20	12.80	17.70	14.40
Fe_2O_3	6.50	0.29	0.30	3.08	2.40	0.80	1.10	2.10	0.25	0.39	0.94	1.10
FeO	3.60	1.00	1.10	6.40	4.00	0.44	0.60	6.70	0.24	0.40	1.40	0.80
MgO	5.10	0.20	0.39	3.80	2.50	0.23	0.10	3.00	0.06	0.04	0.32	0.04
CaO	9.60	0.78	1.60	7.40	5.80	1.10	0.76	5.10	1.20	0.50	1.90	0.63
Na_2O	2.80	3.20	3.50	2.80	3.10	3.90	4.10	3.50	5.60	4.10	5.30	4.70
K_2O	0.12	4.60	4.80	1.10	1.30	4.40	4.30	2.70	2.90	4.30	5.10	4.70
TiO_2	0.08	0.12	0.20	0.44	0.60	0.31	0.12	1.80	0.09	0.06	0.69	0.15
P_2O_5	0.34	0.02	0.08	0.15	0.18	0.09	0.38	0.74	0.02	0.01	0.16	0.24
MnO	0.03	0.04	—	0.20	0.09	—	—	0.12	—	—	0.07	0.02
CO_2	—	0.10	—	—	—	—	—	0.02	—	—	—	—
$^3H_2O^+$	0.50	0.51	0.22	—	0.71	0.20	0.68	0.49	—	0.05	0.30	—
H_2O^-	—	0.07	—	—	—	—	—	0.15	—	—	—	—
Total	99.17	100.30	100.09	98.47	101.08	100.07	100.94	99.35	98.36	99.15	99.88	99.78
Normative minerals[4]:												
Q	9.652	37.214	31.851	13.222	25.540	32.974	35.199	9.714	29.730	35.268	11.247	26.843
C	—	2.132	—	—	—	0.738	0.627	—	—	0.521	0.391	1.012
Or	0.719	27.360	28.401	6.601	7.654	26.035	25.344	16.234	17.423	25.641	30.264	27.835
Ab	24.012	27.255	29.655	24.061	26.135	33.044	34.603	30.134	48.176	35.008	45.036	39.858
An	37.509	3.127	6.139	28.550	23.089	4.875	1.284	19.489	2.354	2.437	8.416	1.561
Wo	3.552	—	0.537	3.230	1.840	—	—	0.504	1.489	—	—	—
En	12.873	0.501	0.973	9.611	6.203	0.574	0.248	7.602	0.152	0.101	0.800	0.100
Fs	1.180	1.483	1.444	8.991	4.522	—	—	7.956	0.087	0.316	0.788	0.351
Mt	9.551	0.423	0.436	4.535	3.467	0.520	1.582	3.098	0.369	0.571	1.369	1.598
Hm	—	—	—	—	—	0.442	0.006	—	—	—	—	—
Il	0.154	0.229	0.380	0.849	1.135	0.590	0.227	3.478	0.174	0.115	1.316	0.286
Ap	0.816	0.048	0.190	0.361	0.425	0.213	0.898	1.783	0.048	0.024	0.381	0.570
Cc	—	0.229	—	—	—	—	—	0.046	—	—	—	—
Total	100.018	100.002	100.004	100.010	100.010	100.005	100.020	100.040	100.001	100.000	100.009	100.013

Footnotes at end of table.

TABLE 4.—*Chemical and normative analyses of crystalline rocks of the Arabian Shield*—Continued

[In percent]

Analysis number	—	W180079	W180088	W180089	W180090	W180083	W180084	—	—	—	—	—
Laboratory[1]	[D]	B	B	B	B	B	B	E	E	E	E	E
Sample (location given on pl. 1)	160	161	162	163	164	166	167a	167b	167c	167d	167e	167f
Oxides (wt. percent)[2]:												
SiO_2	65.50	71.40	73.70	74.30	62.60	73.30	51.70	48.00	50.00	49.10	42.50	48.80
Al_2O_3	15.11	15.20	13.20	13.10	15.70	12.90	21.00	28.30	28.40	29.44	17.00	28.20
Fe_2O_3	4.19	0.76	1.80	1.94	1.60	1.60	0.94	5.04	2.12	2.20	9.34	3.23
FeO	0.36	0.76	1.00	1.40	3.10	0.92	5.90	—	—	—	—	—
MgO	0.35	0.55	0.33	0.06	4.10	0.23	4.40	3.32	0.49	1.16	12.82	2.82
CaO	0.70	2.30	1.20	0.60	4.90	0.83	10.40	10.35	11.47	12.03	10.98	11.94
Na_2O	4.42	4.20	4.70	4.50	3.80	4.30	2.50	3.60	4.70	4.40	1.04	3.76
K_2O	7.20	3.40	4.70	4.90	3.30	4.20	0.35	0.61	0.54	0.47	0.11	0.33
TiO_2	0.37	0.30	0.24	0.20	0.61	0.25	0.56	—	—	—	—	—
P_2O_5	0.07	0.12	—	0.03	0.02	0.03	0.04	—	—	—	—	—
MnO	—	—	0.02	—	0.06	0.03	0.06	—	—	—	—	—
$^3H_2O^+$	0.15	0.04	—	0.55	1.24	0.55	0.89	1.40	1.90	1.80	3.60	1.40
H_2O^-	—	—	—	—	—	—	—	—	—	—	—	—
Total	98.42	99.03	100.89	101.58	101.03	99.14	98.74	100.62	99.62	100.60	97.39	100.48
Normative minerals[4]:												
Q	11.231	28.715	26.141	27.874	11.513	30.699	4.329	—	—	—	—	—
C	—	0.723	—	—	—	—	—	2.922	—	—	—	—
Or	43.296	20.297	27.529	28.660	19.542	25.174	2.114	3.633	3.265	2.811	0.693	1.968
Ab	38.059	35.902	39.419	37.690	32.222	36.906	21.619	30.702	31.495	26.902	9.383	27.695
An	0.127	10.735	1.030	1.063	16.069	3.543	46.034	51.750	56.078	59.910	44.134	59.643
Ne	—	—	—	—	—	—	—	—	4.986	5.841	—	2.393
Wo	1.228	—	2.034	0.705	3.407	0.181	2.683	—	0.899	0.207	5.823	0.059
En	0.887	1.384	0.815	0.148	10.233	0.581	11.199	0.246	0.777	0.179	20.565	0.051
Fs	—	0.275	—	0.631	3.482	0.011	9.448	—	—	—	—	—
Fo	—	—	—	—	—	—	—	5.668	0.331	1.924	9.444	4.931
Mt	0.089	1.113	2.570	2.784	2.325	2.353	1.393	—	—	—	—	—
Hm	4.202	—	0.012	—	—	—	—	5.080	2.169	2.227	9.958	3.260
Il	0.715	0.576	0.452	0.376	1.161	0.482	1.087	—	—	—	—	—
Ap	0.169	0.287	—	0.070	0.047	0.072	0.097	—	—	—	—	—
Total	100.004	100.006	100.000	100.002	100.002	100.002	100.003	100.000	100.000	100.000	100.000	100.000

Footnotes at end of table.

TABLE 4.—*Chemical and normative analyses of crystalline rocks of the Arabian Shield*—Continued

[In percent]

Analysis number	—	—	W180085	W165321	W180156	W180169	W180010	W180150	W180151	W180076	W180077	W165976
Laboratory[1]	E	E	B	A	A	A	B	A	A	B	B	A
Sample (location given on pl. 1)	167g	167h	170a	171	172	174	175	177	178	182	186	194
Oxides (wt. percent)[2]:												
SiO_2	49.50	48.80	73.70	72.20	73.40	71.10	47.70	75.20	44.80	62.20	69.90	54.60
Al_2O_3	30.80	31.40	14.20	14.60	14.50	13.60	16.30	13.00	22.10	16.00	15.80	17.00
Fe_2O_3	2.24	3.23	0.20	1.30	1.00	1.80	3.20	0.49	1.90	1.00	1.20	3.00
FeO	—	—	1.00	1.00	0.72	2.50	7.30	1.20	2.80	3.80	1.60	5.40
MgO	0.76	0.65	0.43	0.80	0.38	0.92	7.40	0.12	12.40	4.20	0.85	4.80
CaO	9.54	11.75	1.80	1.80	2.90	2.20	8.90	0.36	9.80	5.80	3.80	8.50
Na_2O	5.03	3.49	3.40	5.00	4.40	4.50	4.20	3.80	1.80	4.10	4.00	3.40
K_2O	1.01	0.28	4.10	1.70	1.40	1.40	1.50	4.60	0.08	1.30	1.20	0.31
TiO_2	—	—	0.18	0.41	0.14	0.49	2.40	0.14	0.12	0.51	0.25	1.10
P_2O_5	—	—	0.06	0.12	0.06	0.13	0.59	0.03	0.04	0.27	0.08	0.43
MnO	—	—	—	0.14	0.04	0.14	0.14	0.03	0.07	0.05	0.06	0.08
CO_2	—	—	—	0.05	0.23	0.01	—	0.08	0.07	—	—	0.05
$^3H_2O^+$	1.40	0.30	—	0.47	0.65	0.85	—	0.77	3.60	0.67	0.60	1.30
H_2O^-	—	—	—	0.22	—	0.06	—	0.02	0.31	—	—	0.02
Total	100.28	99.90	99.07	100.30	100.20	100.25	99.63	100.31	102.29	99.90	99.34	100.76
Normative minerals[4]:												
Q	—	1.286	33.591	32.162	36.615	33.113	—	34.434	—	14.308	32.517	9.019
C	4.133	4.008	1.050	1.680	1.160	1.029	—	1.386	1.555	—	1.219	—
Or	6.036	1.661	24.455	10.135	8.342	8.374	8.897	27.443	0.493	7.742	7.182	1.857
Ab	32.822	29.650	29.040	42.684	37.543	38.544	24.861	32.463	15.869	34.962	34.279	29.158
An	47.864	58.526	8.618	7.899	12.646	10.124	21.272	1.095		49.921	21.580	18.563
Ne	5.538	—	—	—	—	—	5.856	—	—	—	—	—
Wo	—	—	—	—	—	—	8.007	—	—	2.355	—	3.738
En	—	1.625	1.081	2.010	0.954	2.319	5.358	0.302	10.541	10.541	2.144	12.116
Fs	—	—	1.387	0.349	0.342	2.586	2.052	1.639	1.196	5.445	1.666	5.848
Fo	1.341	—	—	—	—	—	9.208	—	15.161	—	—	—
Fa	—	—	—	—	—	—	3.887	—	1.896	—	—	—
Mt	—	—	0.293	1.902	1.462	2.642	4.657	0.717	2.870	1.461	1.762	4.408
Hm	2.265	3.243	—	—	—	—	—	—	—	—	—	—
Il	—	—	0.345	0.786	0.268	0.942	4.575	0.268	0.237	0.976	0.481	2.117
Ap	—	—	0.143	0.287	0.143	0.312	1.403	0.072	0.099	0.644	0.192	1.032
Cc	—	—	—	0.115	0.527	0.023	—	0.184	0.166	—	—	0.115
Total	100.000	100.000	100.003	100.008	100.004	100.009	100.032	100.002	100.003	100.015	100.005	100.024

Footnotes at end of table.

TABLE 4.—*Chemical and normative analyses of crystalline rocks of the Arabian Shield*—Continued

[In percent]

Analysis number	W165973	W165974	W165975	W165972	W180148	W180144	W180173	W180174	W180172	W180161	W180163	W180159
Laboratory[1]	A	A	A	A	A	A	A	A	A	A	A	A
Sample (location given on pl. 1)	195	196	197	198	199	200	201a	201b	202	203a	203b	204
Oxides (wt percent)[2]:												
SiO_2	71.20	71.70	72.90	62.70	41.20	45.60	59.80	71.40	47.20	73.40	70.40	75.20
Al_2O_3	13.80	14.60	13.20	18.20	17.20	19.30	16.50	16.50	18.70	15.80	16.10	13.60
Fe_2O_3	1.60	1.50	1.30	1.40	5.30	1.60	2.40	1.10	1.20	0.68	0.64	0.53
FeO	2.90	1.20	0.42	1.90	6.80	7.40	3.70	0.36	7.10	0.56	0.96	0.44
MgO	1.30	1.00	0.22	1.00	5.30	13.00	3.30	0.13	12.20	0.24	0.54	0.04
CaO	4.50	3.20	1.80	1.90	12.80	9.40	5.80	3.20	9.00	3.40	1.70	0.62
Na_2O	2.80	4.60	4.90	6.70	2.60	1.80	3.80	5.30	2.60	4.40	5.00	4.00
K_2O	0.35	1.00	3.50	4.40	0.36	0.12	1.10	0.49	0.16	0.40	3.40	4.80
TiO_2	0.25	0.30	0.24	0.94	3.70	0.26	0.82	0.10	0.64	0.10	0.36	0.08
P_2O_5	0.02	0.05	0.02	0.25	1.90	0.06	0.24	0.08	0.08	0.06	0.12	0.02
MnO	0.12	0.08	0.09	0.13	0.15	0.12	0.08	0.02	0.12	0.04	0.02	0.01
CO_2	0.05	0.05	0.76	0.05	0.03	0.08	0.04	0.03	0.07	0.06	0.01	0.04
$^3H_2O^+$	1.00	0.64	0.41	0.42	2.10	1.10	1.50	0.53	0.74	0.74	0.58	0.62
H_2O^-	0.06	0.05	0.04	0.05	0.08	0.12	0.13	0.06	0.10	0.02	0.05	0.07
Total	100.59	100.39	100.08	100.33	100.82	100.72	100.21	99.67	100.44	100.35	100.27	100.50
Normative minerals[4]:												
Q	40.904	33.003	29.207	1.904	—	—	16.158	32.371	—	39.131	24.096	32.426
C	0.806	0.370	—	—	—	—	—	1.716	—	2.249	1.425	0.843
Or	2.091	5.952	20.818	26.113	2.185	0.718	6.661	2.933	0.954	2.384	20.243	28.541
Ab	23.959	39.206	41.734	56.938	22.602	15.425	32.952	45.433	22.207	37.555	42.628	34.058
An	22.123	15.343	3.710	6.619	35.132	44.792	25.329	15.361	39.246	16.236	7.644	2.709
Wo	—	—	0.130	0.371	7.164	0.638	0.957	—	2.024	—	—	—
En	3.274	2.509	0.551	2.501	5.622	7.402	8.423	0.328	5.234	0.603	1.355	0.100
Fs	3.857	0.622	—	1.026	0.970	2.757	3.696	—	1.932	0.379	0.682	0.258
Fo	—	—	—	—	5.563	17.791	—	—	17.824	—	—	—
Fa	—	—	—	—	1.058	7.304	—	—	7.249	—	—	—
Mt	2.346	2.191	0.958	2.039	7.894	2.349	3.566	0.948	1.756	0.994	0.935	0.773
Hm	—	—	0.648	—	—	—	—	0.461	—	—	—	—
Il	0.480	0.574	0.459	1.793	7.219	0.500	1.596	0.192	1.227	0.192	0.689	0.153
Ap	0.048	0.119	0.048	0.595	4.623	0.144	0.583	0.192	0.191	0.143	0.286	0.048
Cc	0.115	0.115	1.740	0.114	0.070	0.184	0.093	0.069	0.161	0.138	0.023	0.092
Total	100.003	100.004	100.002	100.015	100.103	100.005	100.014	100.004	100.006	100.004	100.006	100.001

Footnotes at end of table.

TABLE 4.—*Chemical and normative analyses of crystalline rocks of the Arabian Shield*—Continued

[In percent]

Analysis number	W180160	W180164	W180166	W180165	W180155	W180168	W180154	W180167	W180152	W180153	W180175	W180176
Laboratory[1]	A	A	A	A	A	A	A	A	A	A	A	A
Sample (location given on pl. 1)	205	206	207	208	209	212	214	215	217	218	223a	223b
Oxides (wt percent)[2]:												
SiO_2	75.50	70.80	70.80	58.70	72.90	49.00	35.30	63.30	51.40	46.70	68.00	49.40
Al_2O_3	13.10	16.60	14.70	15.20	12.60	18.40	1.40	17.70	15.20	15.20	14.50	13.70
Fe_2O_3	1.00	0.75	0.88	3.10	1.70	1.00	11.70	0.67	3.00	1.70	3.60	2.70
FeO	0.40	0.68	1.20	4.20	1.80	5.20	2.80	3.30	6.80	9.00	2.40	8.70
MgO	—	0.44	0.77	4.60	0.17	10.70	33.20	1.70	7.50	10.30	0.88	9.80
CaO	0.48	3.20	3.30	6.90	0.62	12.00	1.40	5.60	8.20	7.40	4.40	11.50
Na_2O	4.10	4.90	3.80	3.00	3.80	2.10	0.02	4.50	2.40	2.00	3.30	1.40
K_2O	4.30	1.00	2.30	1.40	5.00	0.16	0.12	1.00	1.10	0.92	0.28	0.24
TiO_2	0.10	0.12	0.31	0.54	0.32	0.37	0.08	0.67	0.90	1.10	0.38	0.37
P_2O_5	—	0.08	0.14	0.27	0.04	0.05	0.08	0.39	0.22	0.26	0.13	0.08
MnO	0.01	—	0.02	0.16	0.09	0.10	0.17	0.08	0.18	0.20	0.06	0.21
CO_2	0.04	0.01	0.56	0.07	0.07	0.07	0.76	0.04	0.05	0.08	0.30	0.07
$^3H_2O^+$	0.55	0.49	0.82	1.40	0.64	0.82	9.99	0.77	2.40	3.80	0.82	1.30
H_2O^-	0.04	0.02	0.06	0.08	0.07	0.05	0.86	0.10	0.06	0.23	0.07	0.10
Total	99.98	99.39	100.20	100.51	100.26	100.55	106.64	100.37	100.86	101.32	99.67	100.42
Normative minerals[4]:												
Q	34.612	31.462	33.553	15.170	29.950	—	—	18.093	3.798	—	38.442	0.912
C	0.930	1.880	1.612	—	0.068	—	0.740	0.060	—	—	1.807	—
Or	25.659	5.994	13.759	8.430	29.812	0.954	0.815	5.972	6.705	5.731	1.684	1.445
Ab	35.033	42.060	32.552	25.866	32.443	17.922	0.194	38.482	20.947	17.840	28.427	12.067
An	2.149	15.510	12.064	24.326	2.393	40.653	1.860	25.246	28.317	31.394	19.426	30.955
Wo	—	—	—	3.468	—	7.772	—	—	4.942	2.081	—	10.930
En	—	1.112	1.941	11.674	0.427	13.387	35.645	4.279	19.267	17.220	2.231	24.862
Fs	—	0.437	1.014	4.644	1.554	4.168	—	4.597	9.136	9.181	0.934	13.777
Fo	—	—	—	—	—	9.453	41.599	—	—	6.883	—	—
Fa	—	—	—	—	—	3.244	—	—	—	4.045	—	—
Mt	1.042	1.103	1.292	4.580	2.487	1.462	10.739	0.982	4.487	2.598	5.314	3.988
Hm	0.291	—	—	—	—	—	6.037	—	—	—	—	—
Il	0.192	0.231	0.596	1.045	0.613	0.709	0.175	1.286	1.763	2.202	0.735	0.716
Ap	—	0.192	0.336	0.652	0.096	0.119	0.218	0.934	0.537	0.649	0.313	0.193
Cc	0.092	0.023	1.289	0.162	0.161	0.161	1.986	0.092	0.117	0.192	0.695	0.162
Total	100.000	100.004	100.008	100.016	100.003	100.004	100.007	100.021	100.014	100.017	100.008	100.007

Footnotes at end of table.

TABLE 4.—*Chemical and normative analyses of crystalline rocks of the Arabian Shield*—Continued
[In percent]

Analysis number	W180419	W167131	W167130	W167129	W167128	D167712	D167713
Laboratory[1]	A	A	A	A	A	C	C
Sample (location given on pl. 1)	223c	224	227	237	241	501[5]	502[5]
Oxides (wt percent)[2]:							
SiO_2	69.70	74.90	55.70	69.20	65.30	51.60	38.70
Al_2O_3	15.30	14.40	15.10	15.70	17.30	21.30	17.80
Fe_2O_3	0.84	0.29	1.50	1.00	1.00	9.86	19.10
FeO	1.80	0.32	5.10	1.60	1.80	—	—
MgO	0.41	0.17	5.40	0.96	1.20	3.10	7.55
CaO	2.00	1.50	7.70	3.50	3.90	7.02	0.62
Na_2O	4.10	4.00	3.90	4.40	4.40	4.76	0.08
K_2O	4.70	3.00	1.20	2.20	2.80	1.25	4.04
TiO_2	0.50	0.07	1.70	0.41	0.66	0.50	3.50
P_2O_5	0.15	0.05	0.58	0.11	0.36	0.26	0.73
MnO	—	0.05	0.10	0.04	0.07	—	—
CO_2	0.07	0.05	0.24	0.05	0.05	—	—
$^3H_2O^+$	0.49	0.41	0.92	0.77	0.60	—	7.50
H_2O^-	0.05	0.11	0.08	0.10	0.06	—	—
Total	100.44	99.67	99.83	100.59	99.91	99.65	99.62
Normative minerals[4]:							
Q	22.868	37.262	6.527	26.234	19.533	0.215	12.506
C	0.355	2.106	—	0.097	0.929	—	14.433
Or	27.894	17.943	7.220	13.109	16.740	7.413	25.916
Ab	34.843	34.258	33.599	37.543	37.669	40.419	0.735
An	8.536	6.881	20.517	16.465	16.876	33.177	—
Wo	—	—	5.417	—	—	—	—
En	1.026	0.429	13.693	2.411	3.024	7.748	20.412
Fs	1.793	0.329	5.605	1.522	1.537	—	—
Mt	1.223	0.426	2.214	1.462	1.467	—	—
Hm	—	—	—	—	—	9.895	20.734
Il	0.954	0.135	3.287	0.785	1.268	—	—
Tn	—	—	—	—	—	0.047	—
Ru	—	—	—	—	—	0.482	3.799
Ap	0.357	0.120	1.399	0.263	0.863	0.618	1.210
Cc	0.160	0.115	0.556	0.115	0.115	—	—
Total	100.008	100.003	100.032	100.006	100.020	100.013	99.745

[1]Laboratory and analytical method: A—USGS, Washington, D.C., rapid rock analysis, single-solution method (Shapiro, 1967). Analysts: Paul Elmore, Sam Botts, and Lowell Artis (Nov. 1964); S.M. Berthold (July 1965); Paul Elmore, Sam Botts, Lowell Artis, H. Smith, John Glenn, G. Chloe, and D. Taylor (Dec. 1965, Jan. 1966, Aug. 1966); Lowell Artis (June 1973); and Paul Elmore (Sept. 1973). B—USGS, Washington, D.C., rapid rock analysis, single-solution method (Shapiro, 1967). Analysts: Herbert Kirshenbaum (Oct. 1973), and Sam Botts and John Glenn (May 1973); CO_2 not determined, H_2O from DGMR-USGS laboratory, Jiddah. C—USGS, Denver, Colo., colorimetric and atomic absorption analyses, Claude Huffman, Jr., supervisor. Analysts: G.T. Burrow and Wayne Mountjoy (July 1974). D—DGMR-USGS, Jiddah, atomic absorption, volumetric, and gravimetric methods, W.L. Campbell, technical advisor. Analysts: Ibrahim Baraja, Souhar Al Farouki, Adel Hakeem, Mahoud Ashy, Abdulaziz Masoud, and others (July 1972). FeO, TiO_2, P_2O_5, MnO, USGS laboratory, Washington, D.C. Analysts: Sam Botts and John Glenn (May 1973). Of the 21 "D" analyses, 8 in brackets, [D], were not used in the chemical synthesis and plot figures of this report. E—DGMR-USGS, Jiddah, atomic absorption, volumetric, and gravimetric methods, W.L. Campbell, technical advisor. Analysts: Ibrahim Baradja and Souhar Al Farouki (Oct. 1971).

[2]The chemical analyses of samples 9, 13, 14a, 14b, 15, 17, 20, 21, 22a, 63, 223a, 223b, and 223c are nondefinitive as standard igneous rocks, presumably because of metamorphism, alteration, or analytical problems, and have not been used on the chemical plots.

[3]Where only one value for H_2O is given, the amount is for total water as loss on ignition.

[4]Normative minerals: Q, quartz; C, corundum; Or, orthoclase; Ab, albite; An, anorthosite; Ne, nepheline; Ac, acmite; Ns, sodium metasilicate; Wo, wollastonite; En, enstatite; Fs, ferrosilite; Fo, forsterite; Fa, fayalite; Mt, magnetite; Hm, hematite; Il, ilmenite; Tn, titanite; Ru, rutile; Ap, apatite; Cc, calcite; Sd, siderite.

[5]Not on plate 1; location in Eastern province (see text). Samples 39, 501, and 502 are sedimentary(?) and have not been used on the chemical plots.

Most of the analyses were made in the U.S. Geological Survey laboratory, Washington, D.C., under the direction of F.J. Flanagan and Leonard Shapiro, using the single-solution, rapid-rock method of analysis (Shapiro, 1967). A very few of the analyses reported in table 4 were made by other methods in Jiddah at the Saudi Arabia Directorate General of Mineral Resources–USGS laboratory.

The normative analyses were calculated on the USGS Multex System (Honeywell 6880 computer) using a graphic normative analysis program (Bowen, 1971) as modified by Stuckless and VanTrump (1979). The computer liaison was done by George VanTrump, Jr. The analyses were not corrected for the effects of hydration, oxidation, and introduction of CO_2 (Irvine and Baragar, 1971). For most samples for which CO_2 and H_2O are given, these effects can be discounted without significantly affecting the results.

In table 3, petrographic data are given and each sample is classified by igneous type, name, age, and tectonic region in order to compare the chemistry of the various categories of rocks. The rock names given in the classification part of the table are those recommended by the International Union of Geological Sciences (IUGS) Subcommission on the Systematics of Igneous Rocks (Streckeisen, 1973, 1976, 1979). Each rock name is a consensus or a best compromise of the available petrography and of the normative mineralogy, but for consistency the naming strongly emphasizes the classification schemes of the IUGS subcommission and of Irvine and Baragar (1971). Where naming proved difficult, a further check was made by using weight-percent chemical data directly, in the classification of Church (1975).

The samples used for whole-rock analyses are biased toward granitic rocks, which are represented by 96 analyses, compared with 53 analyses of dioritic and gabbroic rocks, 42 analyses of volcanic rocks, and 8 analyses of dike rocks. Most of the rocks have calc-alkalic compositions that fit normal distributions in any of the three classification schemes used. A majority of the rocks were classified preliminarily on the Q-Or-(An+Ab) ternary diagram using the IUGS classification. On this diagram, compositions of granite and granodiorite generally separate well. The subdivision of the rocks of granite composition constitutes a major problem (the feldspar problem of normative analyses; Irvine and Baragar, 1971; Le Maitre, 1976) in determining the amount of normative Ab-molecule to allocate to normative anorthite and potassium feldspar.

Peralkalic granite is defined by molar data where the $(Na_2O+K_2O)/Al_2O_3$ ratio is greater than 1; the norm of these granites contains acmite and (or) sodium silicate. The separation of alkali-feldspar granite and granite on the basis of chemical data is not defined in any of the classifications named above; the allocation of albite in the normative analysis makes it impossible to classify on either the Q-Or-(An+Ab) or the Q-(Or+Ab)-An ternary diagram. For this report, alkali-feldspar granite is arbitrarily separated from granite on the basis of molar data in which the $(Na_2O+K_2O)/Al_2O_3$ ratio is greater than 0.850. This separation of alkali-feldspar granite is well demonstrated on the ternary diagram Al_2O_3-CaO-(Na_2O+K_2O), which also separates the peralkalic and peraluminous rocks. The granitic compositions are well separated on the Q-OrT-AnT diagram, where T equals (Or+Ab+An)/(Or+An) (Le Maitre, 1976), and on the Q-Or-An diagram, but statistical boundaries for naming the granitic rocks on these diagrams are not available.

For purposes of synthesizing the chemistry of the 199 rock analyses from widely scattered localities here first published, all the rocks, including those reported elsewhere, were divided into the categories of region, igneous rock type, and age (table 3). Throughout the chemical examination, a fourth category, quality of the chemical analysis (listed in table 3), was constantly considered. The regional divisions are tectonic provinces shown in figure 16. Because the rocks were collected with a shieldwide distribution, it is reasonable to look for regional chemical differences in rocks of the same type and age.

All the rocks were classified as either plutonic or volcanic. A few are of other types (table 3), but after examination of field descriptions, petrography, and chemistry, they were studied as part of either the plutonic or the volcanic category. Nine rocks from dikes and sills were best examined under the volcanic category, and nine rocks from hypabyssal intrusive bodies were examined under the plutonic category. The 23 samples of gneiss appear to be orthogneiss and migmatite and were classified as plutonic. Five highly metamorphic rocks were classified as either plutonic or volcanic depending on the available data. Three sedimentary rocks were not included in the chemical study.

All the rocks were further classified according to an assigned age category (table 3). Each age category is a stratigraphic interval with the exception of age categories that correspond to the culminant orogeny and the Najd faulting event. From oldest to youngest, the age categories are Baish-Bahah, Jiddah, Ablah, Fatimah, Halaban, culminant orogeny, Murdama, Shammar, Najd faulting event, and Jubaylah. These age categories relate to stratigraphy discussed earlier in this report and in various reports summarizing the stratigraphy, plutonism, tectonism, and cratonization of the Arabian Shield (for example, Schmidt and others, 1973;

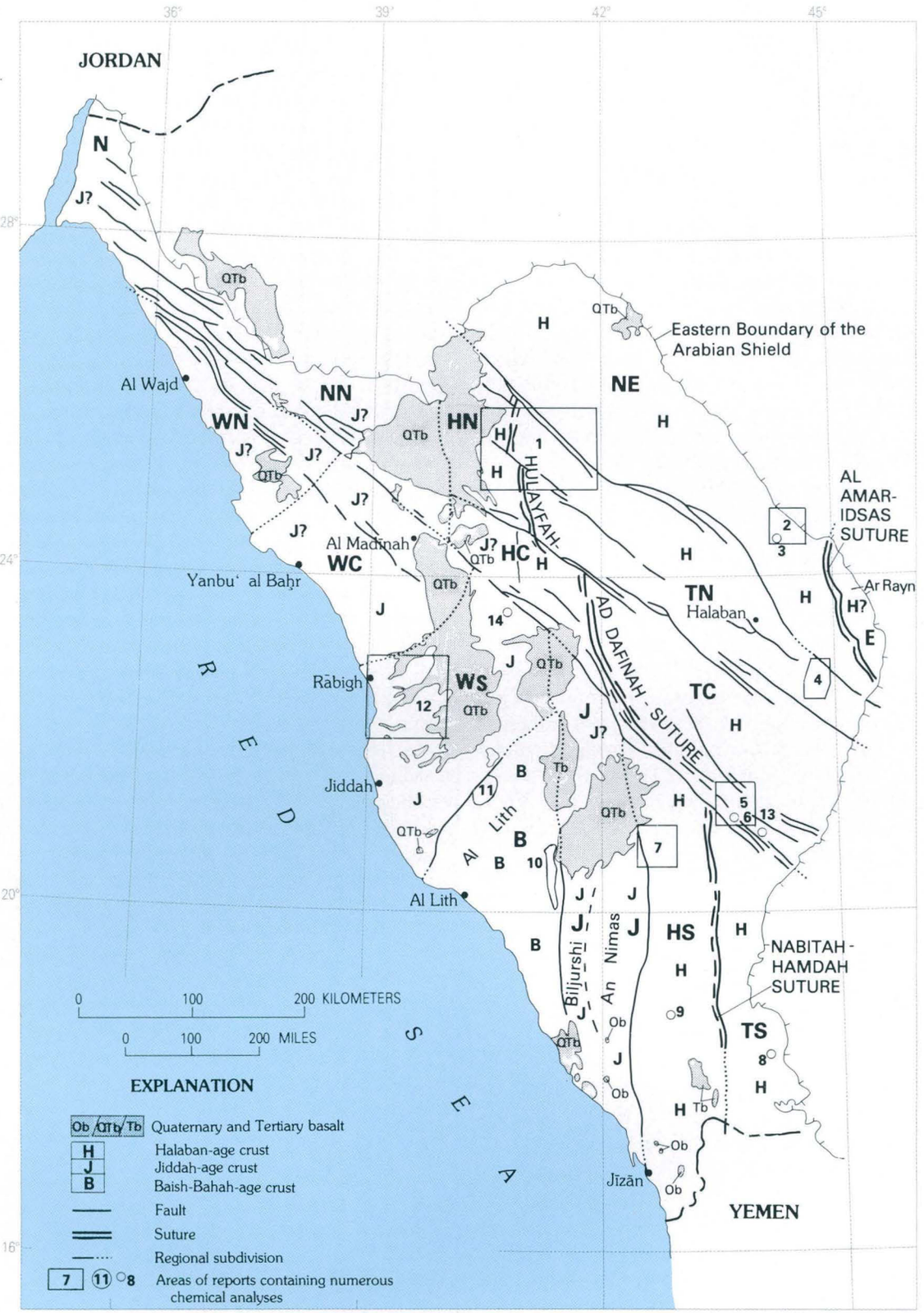
36°
39°
42°
45°
28°
24°
20°
16°
JORDAN
N
J?
QTb
Al Wajd
NN
WN
HN
H
1
HULAYFAH
Eastern Boundary of the Arabian Shield
NE
AL AMAR-IDSAS SUTURE
2
3
Al Madīnah
WC
HC
Yanbu' al Baḥr
TN
Halaban
Ar Rayn
H?
E
AD DAFINAH - SUTURE
4
Rābigh
WS
12
14
TC
Jiddah
11
Tb
Lith
Al
B
10
5
6
13
7
Al Lith
HS
NABITAH - HAMDAH SUTURE
Biljurshi
An Nimas
9
TS
8
Ob
Jīzān
YEMEN
RED SEA
0 100 200 KILOMETERS
0 100 200 MILES
EXPLANATION
Ob QTb Tb Quaternary and Tertiary basalt
H Halaban-age crust
J Jiddah-age crust
B Baish-Bahah-age crust
Fault
Suture
Regional subdivision
7 11 8 Areas of reports containing numerous chemical analyses

Schmidt and others, 1979; Greenwood and others, 1980) and, with some changes in terminology and nomenclature, to the summary report of Delfour (1979b).

The Baish-Bahah age category includes primitive volcanic rocks from the Wādī Bidah region (region B, fig. 16) as defined by Schmidt and others (1973) and modified by Greenwood and others (1980); Baish-Bahah Groups have been defined in the Wādī Bidah-Bahah area by Greenwood (1975c) even though the name "Baish" is from Wādī Baysh in the southwestern part of the shield, where the "Baish" rocks of Wādī Baysh have been subsequently mapped as Jiddah rocks (pl. 1). The Jiddah age category includes volcanic and plutonic rocks of the andesite assemblage and dioritic suite from the Biljurshī'-An Nimās region (region J, fig. 16). Jiddah rocks were originally named by Brown (USGS–ARAMCO, 1963) for rocks in the vicinity of the city of Jiddah, but the rocks of the Jiddah Group have been described subsequently in more detail in the Biljurshī'-'Aqīq area east of Wādī Bidah by Greenwood (1975b, 1975c), and the Jiddah-age rocks (region J, fig. 16) are defined herein in the Biljurshī' and 'Aqīq quadrangles. The Ablah age category includes rocks of the Bidah and Biljurshī'-An Nimās regions (regions B and J, fig. 16) that are younger than the Jiddah-age rocks but are older than the culminant orogeny. The Halaban age category includes andesitic-assemblage rocks and dioritic-suite rocks from the Nuqrah quadrangle (Delfour, 1977) (area 1, fig. 16) and the Bi'r Juqjuq quadrangle (Hadley, 1976; Dodge and others, 1979) (area 5, fig. 16) from the eastern half of the shield.

The culminant-orogeny age category includes the gneiss domal and batholithic granodiorite rocks of the Jabal al Qarah and Junaynah quadrangles (Schmidt 1981a, 1985) (Bishah area). These syntectonic rocks are well represented throughout the eastern half of the shield and are younger than Halaban rocks but are synchronous with early Murdama and Shammar rocks. Many large gneiss domes (antiforms) formed during the culminant orogeny, but these orthogneisses are tectonized older plutonic rocks, and for chemical comparison they are classified according to their intrusive age rather than the age of tectonism (their tectonic age is generally shown in parentheses after their plutonic age in table 3). In contrast, these orthogneisses are mapped on plate 1 according to their tectonic age.

The Murdama-Shammar age category includes post-tectonic plutonic, hypabyssal, and volcanic rocks that intruded at least some Murdama rocks or are stratigraphically within the Murdama and Shammar Groups. The Murdama-Shammar rocks are designated as either Murdama age or Shammar age depending on local stratigraphy; in general, rocks classified as Shammar age are slightly younger than those classified as Murdama age. The Jubaylah-Najd age category includes volcanic, dike, and hypabyssal rocks stratigraphically within or intrusive into the Jubaylah Group in the Najd fault system and intrusive rocks associated with or slightly postdating the Najd faulting event.

Because the 199 chemically analyzed rocks of this report are widely distributed (diluted in space) and are divisible into many age categories (diluted in time), it is desirable to control or compare the chemistry of rocks of this report with the published chemistry of rocks from local areas where stratigraphy and age relations are well known. Fourteen such control areas are shown in figure 16. About 300 control analyses have been examined using the same computed normative program and plots as were used for the 199 analyses reported herein.

CHEMICAL VARIATION OF VOLCANIC AND PLUTONIC ROCKS

VOLCANIC ROCKS

The Na_2O-CaO-K_2O (NCK) ternary diagram shows the spread or chemical separation of the analyzed rocks as well as or better than many of the other ternary diagrams examined. For the normative data, the nearly comparable Ab-An-Or diagram does almost as well. Figure 17 shows the distribution of the metavolcanic rocks of the shield used for control. Figure 17*A* shows the distribution of the low-K_2O, mafic volcanic rocks of Baish-Bahah age from Wādī Bidah (area 10, fig. 16). The consistently low K_2O rocks of wide compositional range, from basalt to dacite and sodic rhyolite (at least some quartz keratophyre), of the Samran Group from the Rābigh area (area 12) have been mapped on plate 1 as Jiddah-age rocks. Figure 17*B* shows the distribution

FIGURE 16.—Tectonic belts and regions used to define regional variations and trends in the chemical data examined for this report. Broad tectonostratigraphic belts (small capital letters) are defined by the age of the underlying crust (from pl. 1). The Al Lith belt and the Biljurshi and An Nimas subbelts are located. Large boldface capital letters identify regions used to areally subdivide the chemical data of this report (see table 3). Numbers indicate quadrangles and areas from which published chemical analyses were used for control of the chemical synthesis of this report: 1, Nuqrah quadrangle (Delfour, 1977); 2 and 3, Ad Dawādimī district (Al-Shanti, 1974, 1976); 4, Jabal al Ḥawshah (Kanaan, 1979); 5, Bi'r Juqjuq quadrangle (Dodge and others, 1979); 6, Bi'r Juqjuq area (Kroner and others, 1979); 7, Wādī al Miyah (Schmidt, 1980, unpub. data); 8, Wādī Wassāṭ (Jackaman, 1972); 9, Jabal Shāyi' (Coleman, Ghent, and others, 1977); 10, Wādī Bidah (Jackaman, 1972); 11, Aṭ Ṭā'if (Nasseef and Gass, 1977); 12, Khulayṣ quadrangle (W.J. Skiba and C.F. Gilboy, written commun., 1975; Skiba, 1980); 13, Jabal Yafikh (Schmidt, 1981b); 14, Mahd adh Dhahab district (R.J. Roberts, written commun., 1980).

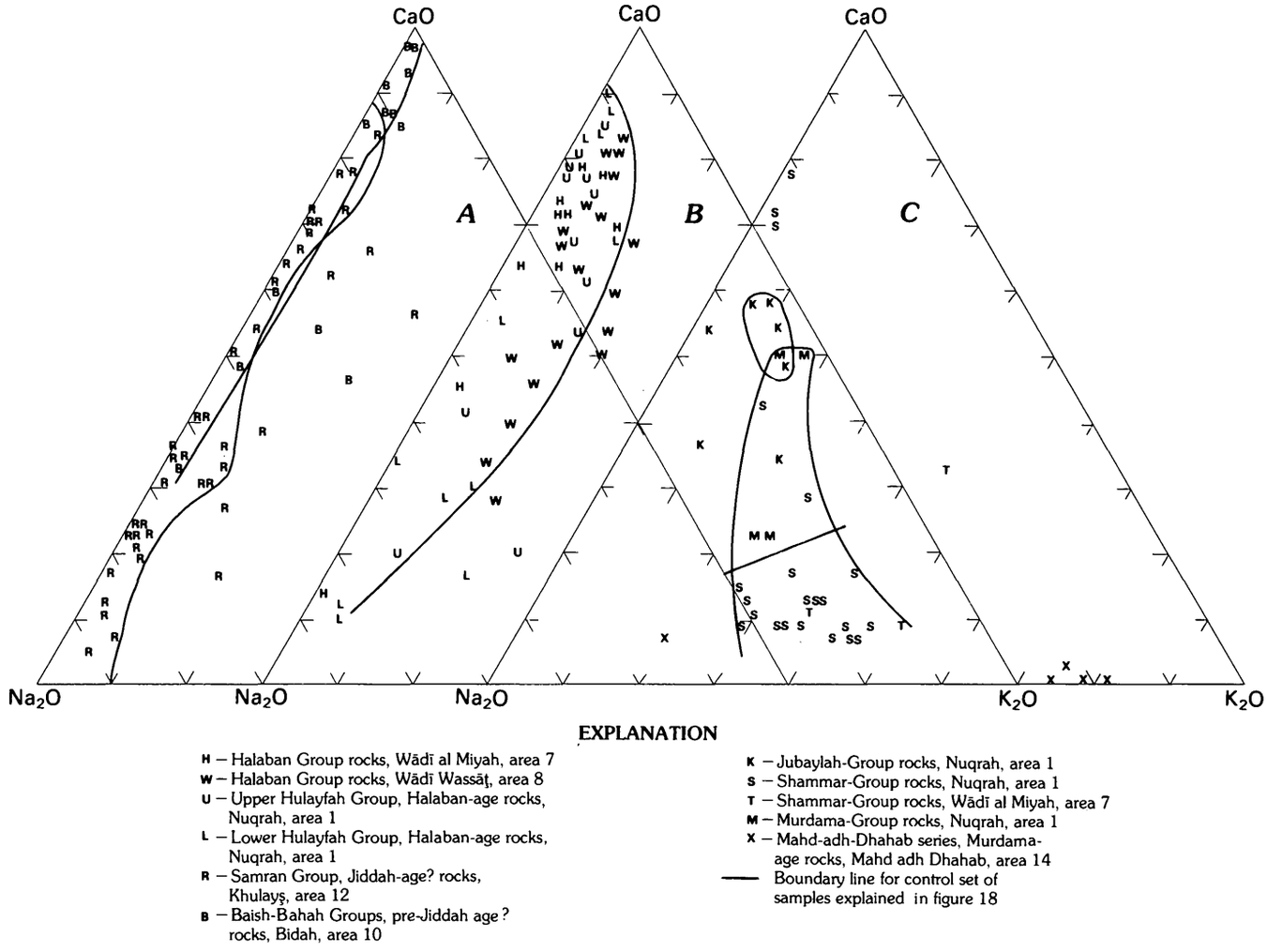

FIGURE 17.—Na_2O-CaO-K_2O diagrams showing the chemical distribution (molar data) of control samples of metavolcanic rocks from the following groups of rocks: Baish-Bahah, Jiddah, Halaban, Murdama, Shammar, and Jubaylah. The samples are from local areas where these stratigraphic units have been described and chemically analyzed (see fig. 16). The chemistry of rocks of the Baish-Bahah and Jiddah (Samran) Groups is shown in *A*; of the Halaban Group, *B*; and of the Murdama, Shammar, and Jubaylah Groups, *C*.

of Halaban rocks. Many Halaban rocks are low in K_2O, but overall they differ from the Baish-Bahah and Jiddah rocks of figure 17*A* in that many Halaban rocks range to higher K_2O. These Halaban control samples are from the Nuqrah quadrangle, (area 1), the Wādī al Miyah quadrangle (area 7), and Wadi Wassāṭ (area 8).

Figure 17*C* shows the distinctly high-K_2O, low-CaO, dacitic to rhyolitic rocks of the Murdama and Shammar Groups as well as the less potassic, more mafic rocks of the Jubaylah Group, from the Nuqrah quadrangle (area 1) or the Wādī al Miyah quadrangle (area 7). In figure 17*C* Murdama, Shammar, and Jubaylah rocks separate with little compositional overlap.

Figure 18 shows the metavolcanic rocks analyzed for this report along with the rock-group boundary lines drawn from the control samples of figure 17. In figure 18, the Shammar and Murdama volcanic rocks are clearly separated by their high K_2O content from the older volcanic rocks. The Jubaylah volcanic rocks form a cluster that extends toward a composition that is more calcic than the control set, but this is emphasized partly by three diabasic dike rocks (symbol N, fig. 18) of Najd age. The 10 Halaban-age rocks shown scatter widely between the CaO and Na_2O corners and have varying K_2O content within the range of the Halaban control rocks (fig. 17*B*). Three Jiddah-age rocks are as potassic as the most potassic of the Jiddah control group (fig. 17*A*).

Three analyses of Fatimah rocks from the Jiddah-Rābigh region (region WS, fig. 16) are on the potassic

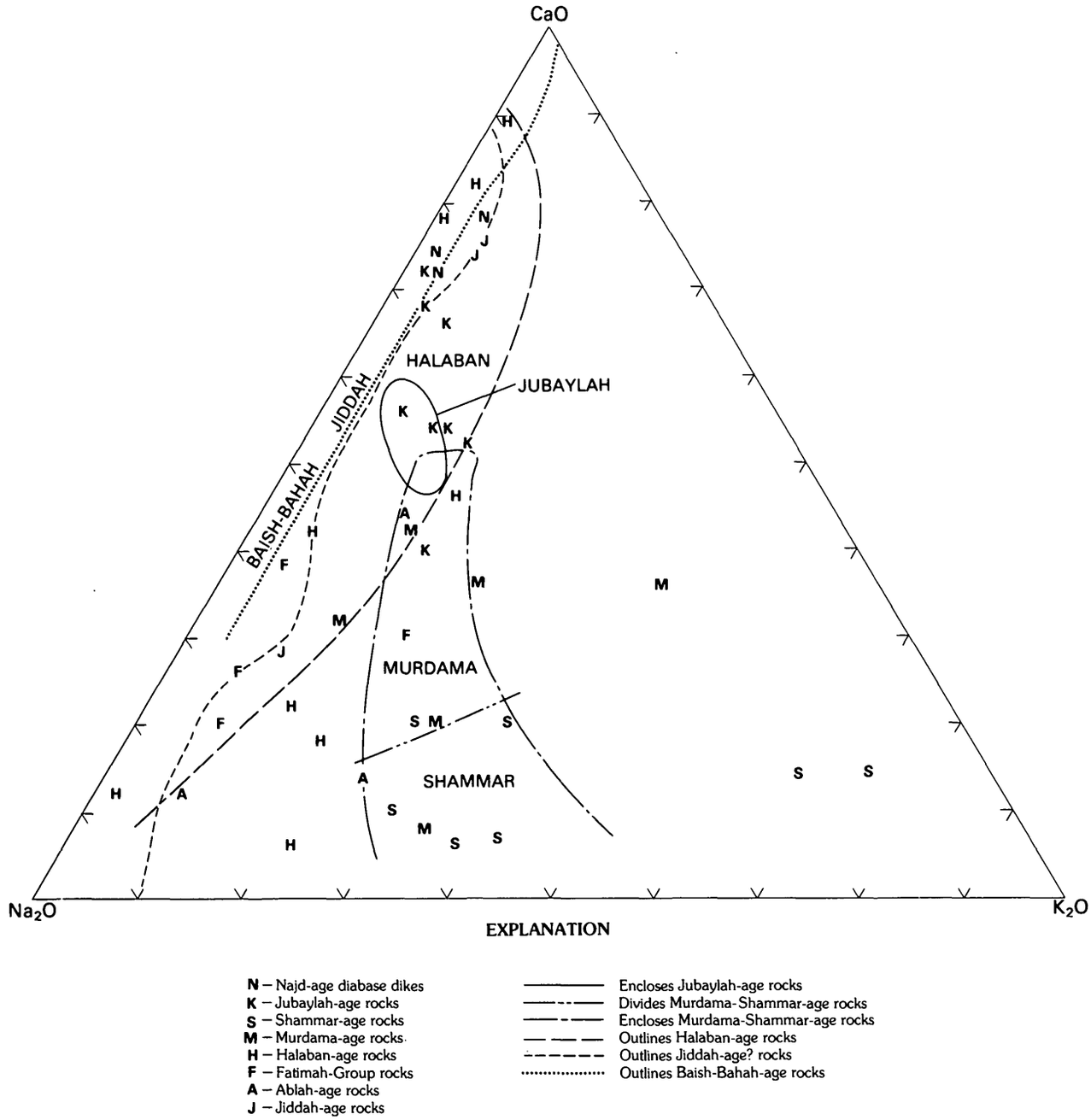

FIGURE 18.—Na_2O-CaO-K_2O diagram showing chemical distribution (molar data) of metavolcanic rocks and a few dike rocks reported in this report in tables 3 and 4. Boundary lines are those drawn in figure 17 for control set of samples.

side of the Jiddah control rocks from the Rābigh area (area 12), whereas one is as potassic as the Shammar rocks. The Fatimah rocks rest unconformably on rocks of the Samran (Jiddah?) Group of the Rābigh area and are distinctly younger (Skiba, 1980). Three Ablah-age rocks have highly varying potassic contents and plot on the sodic side of the diagram (fig. 18). These few samples of Fatimah and Ablah rocks distinctly suggest rock chemistry that is more mature than that of the calc-alkalic rocks of the Jiddah and Halaban Groups. The scant chemistry does not distinguish between Fatimah and Ablah but does strongly suggest that neither is correlative with either the Murdama or the Shammar rocks.

The consistently low K_2O content of the Baish-Bahah rocks (Wādī Bidah area, area 10) and the Samran rocks

(Jiddah Group?, Rābigh area, area 12) in figure 17*A* suggests an origin in an intraoceanic (ensimatic) island-arc environment. The Halaban Group rocks in figure 17*B* are presumably of similar origin, but the Halaban rocks in this report are restricted to the eastern half of the shield, a part of the shield that was intruded by late granitic plutons much more abundantly than the western half as represented by control samples of the Rābigh area (area 12) and the Wādī Bidah area (area 10). The inference made here is that many more Halaban rocks have been altered by late granitic plutonism and, hence, the Halaban rocks show a much larger spread toward K_2O enrichment.

A second factor suggests that late potassic hydrothermal metasomatism has altered many of the Halaban rocks because many of the samples, especially the control samples, were collected in mineralized districts, for example, the Nuqrah and Wādī Wassāṭ districts. This argument is less forceful, however, because hydrothermal alteration may also be prevalent in parts of the Wādī Bidah and Rābigh areas. In this regard, six analyses of samples (R.J. Roberts, written commun., 1980) from the Mahd adh Dhahab mineralized district (area 14) are plotted in figure 17*C*. Two analyses are of pyroclastic rocks from near the Mahd adh Dhahab mine workings and are probably of Murdama (or Shammar) age, and two are from a rhyolitic plug within the mine workings. These four are highly hydrothermally metasomatized, especially in silica and potassium, as indicated by petrography as well as by the chemistry in figure 17*C*. A fifth sample from a rhyolite dike 2.5 km northeast of the mine is little altered, has a quartz trachyte composition, and is probably a subvolcanic intrusive of Murdama age. A sixth sample is highly sodic. These Mahd adh Dhahab analyses are presented as an extreme case of known potassium hydrothermal metasomatism of one set of igneous rocks.

A third factor suggests that more samples of siliceous and potassic volcanic rocks are represented in the Halaban samples than in the Baish-Bahah and Jiddah samples because the Halaban Group is younger and less deformed and therefore is less eroded than the Baish-Bahah and Jiddah Groups.

PLUTONIC ROCKS

The plutonic rocks from the Arabian Shield, both the control samples (fig. 19) and the samples analyzed for this report (fig. 20), are well separated on the Na_2O-CaO-K_2O diagram. Figure 19 shows the chemistry of the control samples from the control areas shown in figure 16. In this sampling, analyses of the pretectonic rocks of the dioritic suite, especially of rocks of diorite composition, are sparse. Five analyses of amphibolite gneiss from the Aṭ Ṭā'if area (area 11) (Nasseef and Gass, 1977) are gabbroic and of very similar composition and may be orthogabbros; they are classified herein as Baish-Bahah age. Three analyses of the ophiolitic suite from the Nuqrah quadrangle (area 1) are given. The Halaban-age trondhjemite from area 6 (Kroner and others, 1979) forms a tight cluster in figure 19 despite its conversion to orthogneiss during Najd faulting. Two samples (symbols HN and N, fig. 19) of this set are from migmatitic layers in the trondhjemite orthogneiss; one (HN) is a mixture of trondhjemite (Halaban age) and granite (Najd age), and the other (N) is probably entirely granite of Najd age.

The mostly granodioritic rocks of large batholiths from areas 1, 4, 7, and 11 (fig. 19) are syntectonic rocks classified in this report as having been intruded during the culminant orogeny. The rocks of granite composition and posttectonic age are classified as Murdama or Shammar age, according to the geologists working in the areas from which the samples were reported. As a generalization, regardless of area, the granitic rocks assigned a Murdama age by different geologists are distinctly more calcic in composition than the Shammar-age rocks, even though a distinction between Murdama-age and Shammar-age plutonic rocks is difficult during mapping. The chemical difference between Murdama-age granite and Shammar-age granite is likely that of an early, less evolved granite in contrast to a late, more evolved one. The elliptical layered gabbroic pluton of Jabal al Jilani in the Ad Dawādimī district (area 3) (Al-Shanti, 1974) is herein considered to be Shammar (or Murdama) age and to be comagnetic with Shammar (or Murdama) granitic rocks.

Figure 20 shows the chemistry of samples analyzed for this report. The distribution of the samples according to age is similar to that in figure 19. Many more primary rocks of the Halaban crust and a few of the Jiddah crust are represented in figure 20, in contrast to the few in figure 19. These pretectonic, primary, crustal rocks of trondhjemitic, tonalitic, and gabbroic composition are consistently low in K_2O and lie between the Na_2O and CaO corners of the diagram. Seven analyses (samples 167b–h, table 3) form a tight cluster of anorthositic rocks from Jabal Mahail, an anorthosite body about 10 km wide by 30 km long located about 90 km north of Wādī ad Dawāsir. These rocks are associated with crustal rocks of Halaban age on plate 1, but they are coded "E" in figure 20 as they may represent an older suite of rocks such as the rocks from the crustal block east of the Al Amar-Idsas fault (region E, fig. 16).

Syntectonic, granodioritic rocks of the culminant orogeny are well represented in figure 20, as in figure 19. However, granodioritic rocks classified as Ablah age form a scatter of points that is distinctly more sodic than rocks associated with the culminant orogeny.

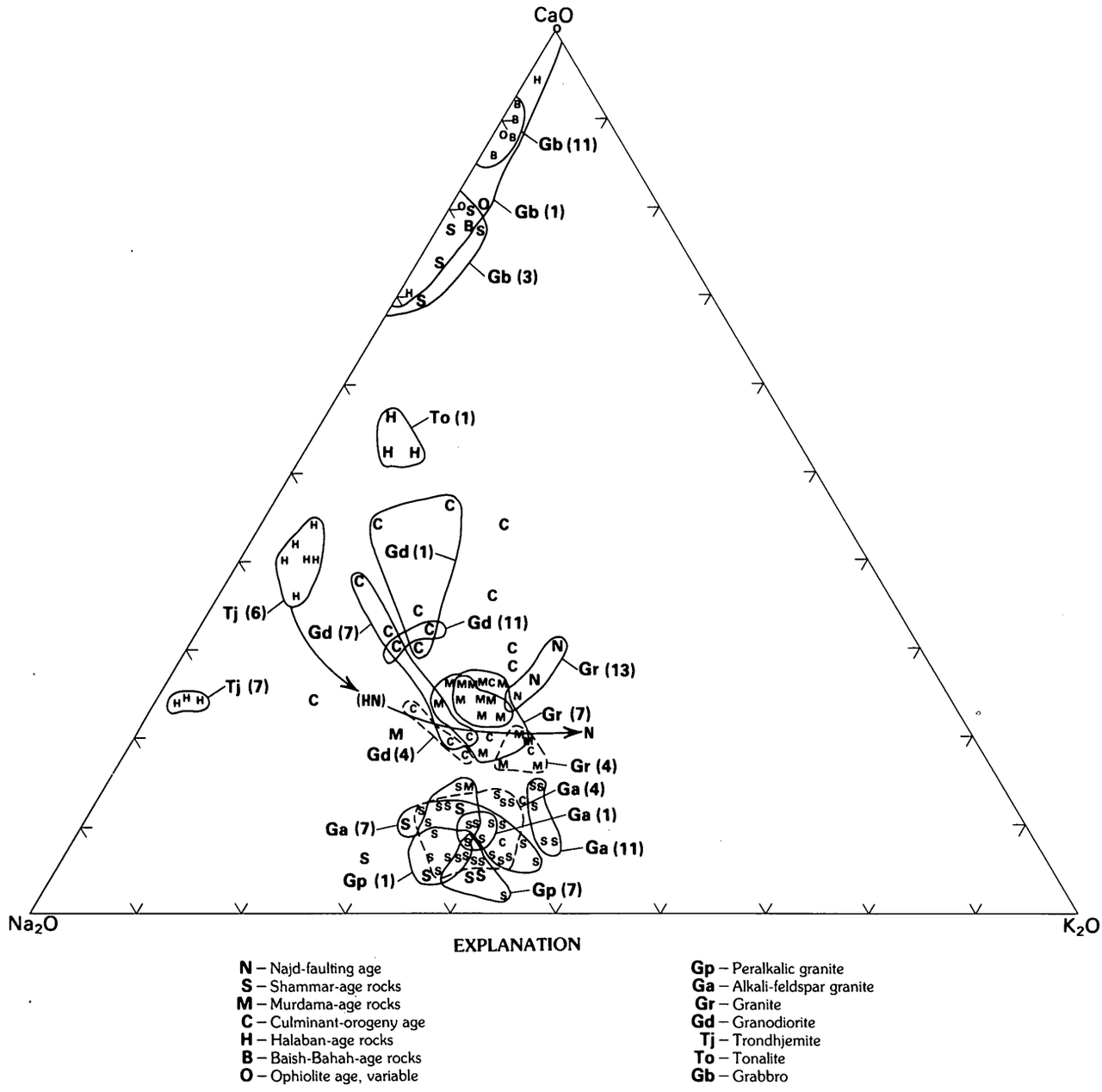

FIGURE 19.—Na_2O-CaO-K_2O diagram showing plutonic-rock chemistry (molar data) of control samples classified by age. Lines enclose representative samples of rocks of different composition and age from specific areas (areas, identified by numbers in parentheses, correspond to areas shown in fig. 16). The cluster of trondhjemite of Halaban age from area 6 (Tj(6)) consists of orthogneiss containing migmatitic layers (HN) of mixed Halaban-age and Najd-age rock and granitic layers (N) of Najd age. Samples HN and N are joined by arrowed tie lines showing compositional trend of migmatization.

These granodiorites are presumably associated with a post-Jiddah-age orogeny of about Ablah age (Ablah-age orogeny). The lower K_2O content of both the volcanic and plutonic rocks of Ablah age suggests an earlier orogeny in a crust slightly more primitive, thinner, and less cratonized than the crust at the time of the culminant orogeny.

The posttectonic plutonic granites of Murdama and Shammar age show a distribution similar to that of the control samples. The greater overlapping distribution of rocks of Murdama and Shammar age in figure 20 may result from greater subjectivity in the age classification of the rocks analyzed for this report compared with the control set. Only one Najd-age granitic rock is

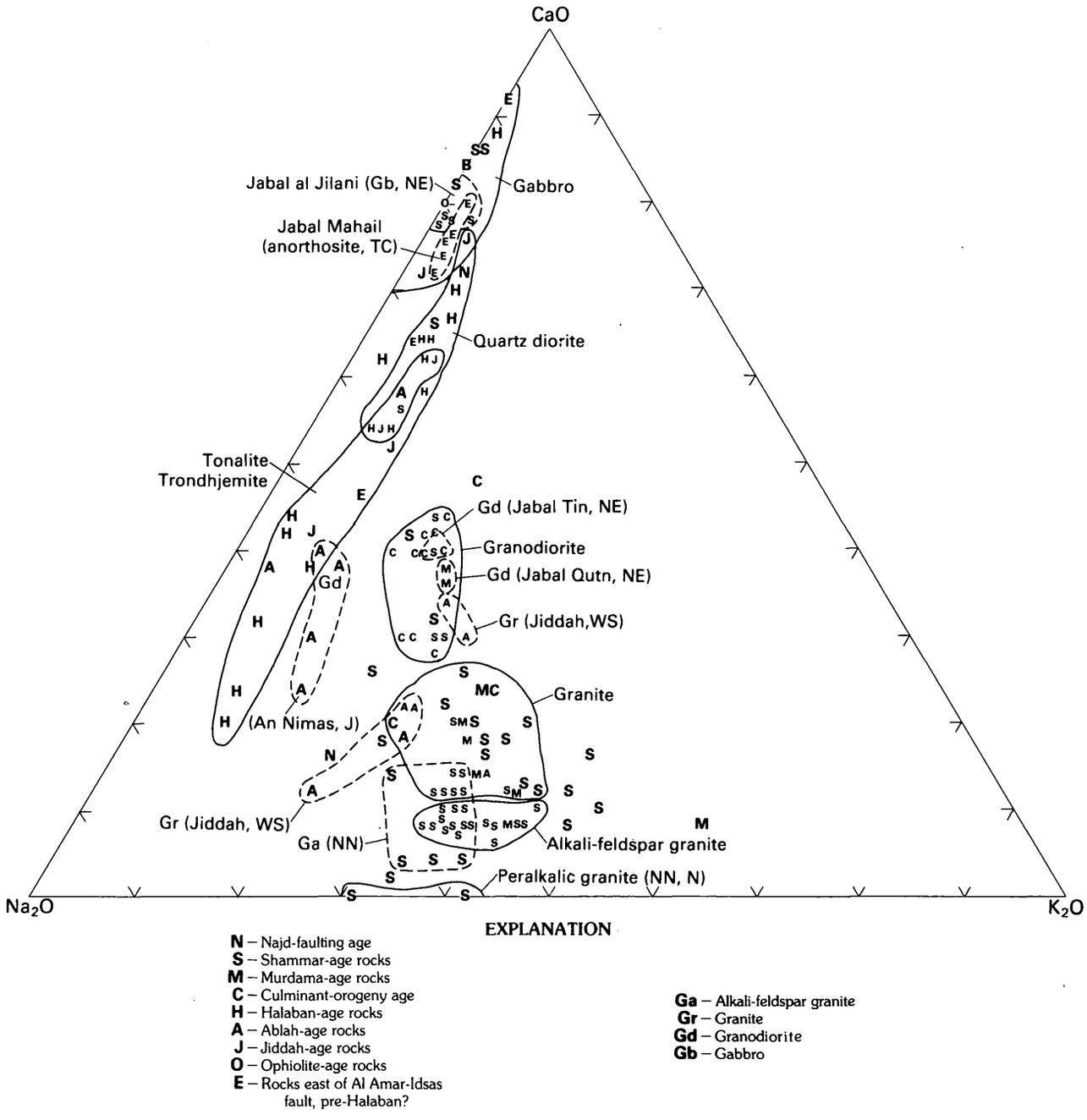

FIGURE 20.—Na_2O-CaO-K_2O diagram showing plutonic-rock chemistry (molar data) of samples reported in this report in tables 3 and 4 and classified by age. Lines enclose representative samples of rocks of different types. Samples from several specific localities (for region code, see fig. 16) are enclosed by dashed lines.

shown in figure 20 in spite of the fact that other granitic rocks are suggested in table 3 to be of possible Najd age. Field criteria are not available to adequately classify these youngest Precambrian rocks, and on this diagram preference is given to a Shammar age.

Granodioritic batholithic rocks (samples 88, 89, 90a, and 90b, table 3) from the Ad Dawādimī area are classified as youngest Shammar age because they intrude the schist of the Abt Formation as well as rocks of the Murdama Group. Large volumes of granodioritic rocks as young as Shammar age are unusual in the shield where batholithic granodioritic rocks are associated consistently with the culminant orogeny. We infer that youthful granodioritic as well as granitic pluton-

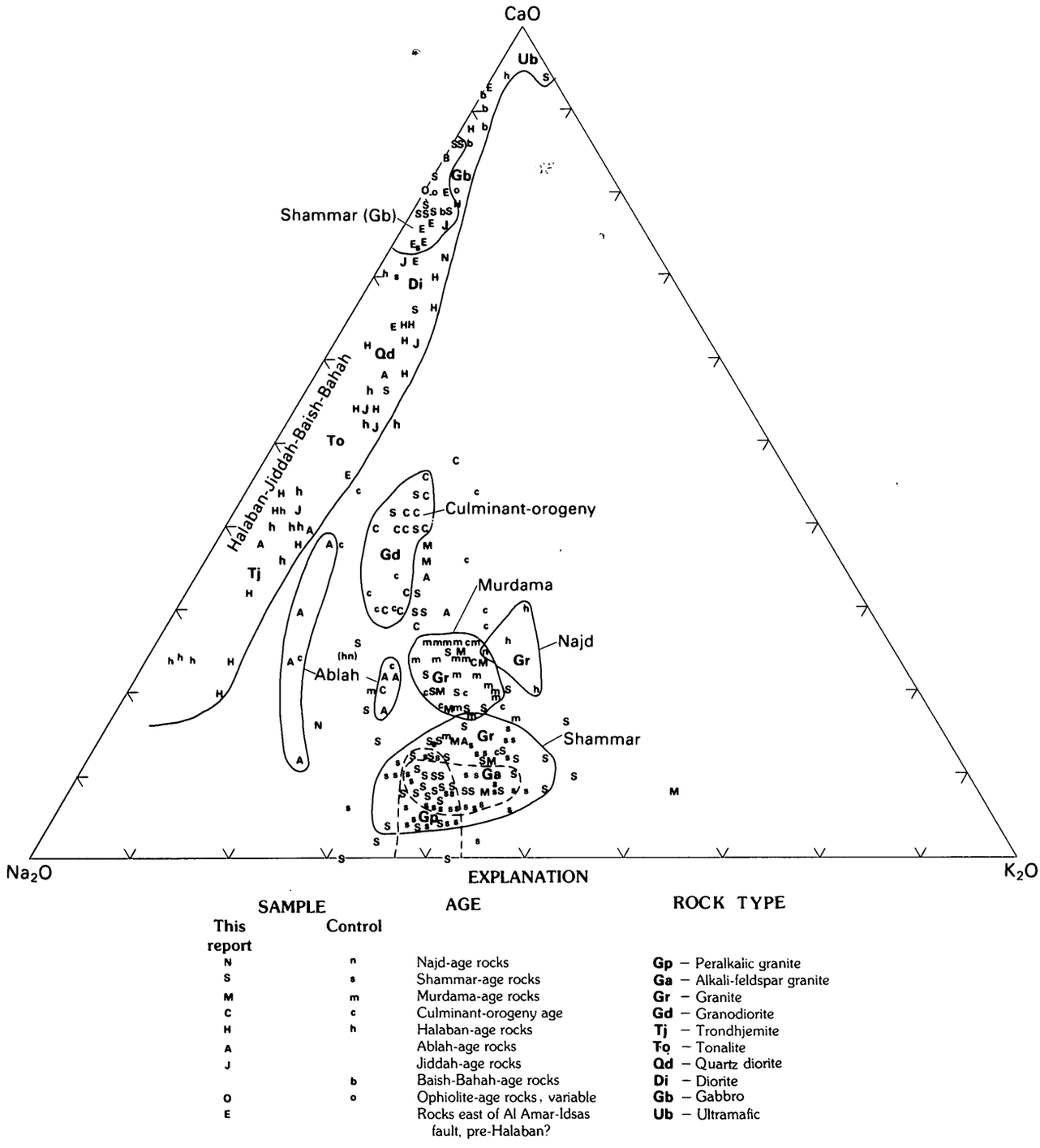

FIGURE 21.—Na_2O-CaO-K_2O diagram summarizing all the plutonic-rock chemistry (molar data) examined for this report (combination of figs. 19 and 20). Each sample is classified according to an assigned age. Solid lines enclose clusters of rocks of different age. Dashed lines enclose tight clusters of plutonic rocks of alkali-feldspar granite (Ga) and peralkalic granite (Gp) compositions within the sample cluster of rocks of Shammar age.

ism in the large area west of the Al Amar-Idsas fault is an exception in an area of especially intensive and perhaps longer lasting tectonism.

Figure 21 summarizes the distribution of all plutonic-rock analyses classified by age on the Na_2O-CaO-K_2O diagram. Consistently, the pretectonic, dioritic-suite

plutonic rocks of the primary crusts of Baish-Bahah, Jiddah, and Halaban ages have low K_2O compositions that range from gabbro to trondhjemite. They have a similar distribution in figure 21, as do the volcanic rocks of the same ages in figures 17 and 18. These plutonic and volcanic rocks together constitute the primary crusts of Baish-Bahah, Jiddah, and Halaban ages. In general, the syntectonic, granodioritic batholithic rocks of the granitic suite and of culminant-orogeny age form a distinct cluster that signifies the first abundance of K_2O in plutonic rocks of the shield. Equivalent volcanic rocks of culminant-orogeny age are sparse or nonexistent (fig. 17*C*). An exception to this generalization, that culminant-orogeny rocks are the first to contain abundant potassium, is that the less abundant granodioritic rocks of Ablah age, of course, contain moderate amounts of potassium and are older than the culminant orogeny. The Ablah granodiorites represent an earlier, more restricted orogeny.

The youthful, posttectonic, granitic-suite plutonic rocks form distinct clusters of Murdama and Shammar age. A comparable distribution of volcanic rocks of the same age is seen in figures 17*C* and 18. The alkali-feldspar granites form a tight cluster exclusively within the Shammar-age field. The peralkalic granites form a similarly tight cluster that overlaps the alkali-feldspar granite cluster within the Shammar-age field. These peralkalic granite rocks from control areas 1 and 7 (fig. 16) are representative of a broad belt of peralkalic granite plutons that parallels the Hulayfah-Ad Dafinah-Nabitah-Hamdah serpentinite-bearing fault zone. Many of the alkalic and peralkalic granite plutons of the shield (Stoeser and Elliott, 1980) are associated with this zone of tectonic ophiolite (Frisch and Al-Shanti, 1977; Delfour, 1979b; Schmidt and others, 1979).

The Shammar-age magmatism was bimodal, and a distinct cluster of Shammar-age gabbro occurs in the gabbroic field of the diagram (fig. 21). These Shammar gabbros are from concentrically layered plutons that are associated in age with the widespread circular granitic plutons of the shield. The few analyses of Najd-age granite form a distinctive high-K_2O cluster in figure 21.

THOLEIITIC, CALC-ALKALIC, AND ALKALIC COMPOSITIONS

GENERAL STATEMENT

The (Na_2O+K_2O)-FeO*-MgO (AFM; FeO* is total iron as FeO) ternary diagram (Irvine and Baragar, 1971; Miyashiro, 1974) and the (Na_2O+K_2O)-SiO_2 (alkali-silica) linear diagram (Kuno, 1966; Irvine and Baragar, 1971) have been widely used to distinguish between volcanic rocks of tholeiitic, calc-alkalic, and alkalic composition as related to genesis in oceanic or continental environments. Both types of diagrams have been used in the literature on the Arabian Shield to show the chemical distribution of rocks from some of the local areas listed in figure 16. The reports for these local areas indicate that the bulk of the shield rocks (andesite assemblages and plutonic rocks of Greenwood and others, 1980; dioritic-suite and most granitic-suite rocks of this report) are of calc-alkalic composition, for example, Delfour (1977, Nuqrah quadrangle, area 1, fig. 16) and Dodge and others (1979, Bi'r Juqjuq quadrangle, area 5). A small proportion of the shield rocks, the mafic metavolcanic rocks (basalt assemblage, Greenwood and others, 1980), are in part tholeiitic, as are some rocks of the Baish-Bahah Group (Jackaman, 1972, Wādī Bidah area, area 10). The widespread, but overall small-volume, ophiolitic rocks (Delfour, 1979b, Nuqrah quadrangle, area 1) are entirely tholeiitic. A few of the latest Precambrian rocks of the shield, rocks of Shammar age and Najd age, are alkalic and peralkalic (Stoeser and Elliott, 1980).

A composite of the published analyses of rocks from the shield (herein the control set of about 300 analyses) and the analyses of this report (about 200 analyses) affirm that the shieldwide, bulk composition is calc-alkalic and that only small volumes of the shield rocks are tholeiitic and alkalic (figs. 22 through 29). During the current study, all the analyses were examined on other diagrams used in genetic classifications of volcanic rocks, but for an overview of shieldwide rocks, little additional information is gained by doing so and the results are not reported here. In particular, these other diagrams include those of SiO_2, FeO*, and TiO_2 versus FeO*/MgO (Miyashiro, 1974), as used, respectively, by Delfour (1977, Nuqrah quadrangle, area 1) and by Greenwood and others (1980, Wādī Bidah area, area 10, and Wādī Wassāṭ area, area 8).

VOLCANIC ROCKS

The metavolcanic rocks of the Baish-Bahah, Jiddah (Samran of control area 12), and Halaban (Hulayfah) Groups for the control data on the AFM diagram are shown in figure 22. The chemical distribution scatters widely within the calc-alkalic field (Irvine and Baragar, 1971) but is confined within the outer bounds of the composition of the calc-alkalic rocks of the Cascade Mountains (USA; outer dotted line, fig. 22). These metavolcanic rocks of the andesitic and basaltic assemblages completely overlap in distribution, and all range well into the tholeiitic field on the basalt side of the diagram. The only within-group stratigraphic data available are for the Halaban rocks, referred to as the "Hulayfah" by Delfour (1977), where chemistry for

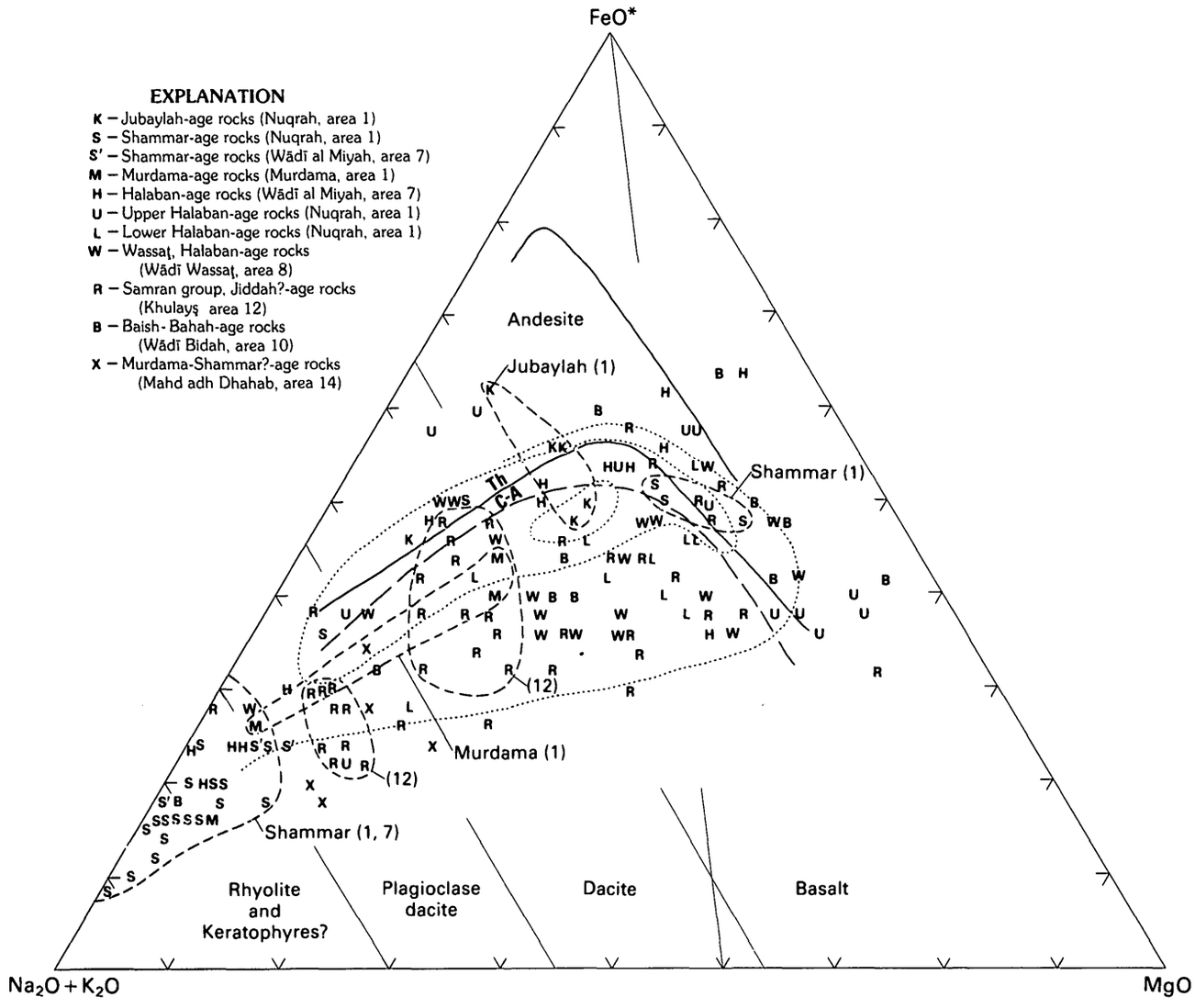

FIGURE 22.—AFM diagram showing metavolcanic-rock chemistry (weight percent data) of control samples classified by age. Samples are from local control areas shown in figure 16. Lower solid line separates tholeiitic compositions (above line) and calc-alkalic compositions (below line) according to Irvine and Baragar (1971, p. 528); upper solid line is the Skaergaard liquid trend. Two inner dotted lines are approximate contours drawn on plotted data of calc-alkalic volcanic rocks from the Aleutians (Irvine and Baragar, 1971, p. 528). Outer dotted line encloses calc-alkalic volcanic rocks from the Cascade Mountains in northwestern North America (Irvine and Baragar, 1971, p. 528). Long-dashed line separates upper Hulayfah Group rocks (upper Halaban; above line) from lower Halayfah Group rocks (lower Halaban; below line) from the Nuqrah quadrangle (area 1). Short-dashed lines enclose some specific age-area sets, as labeled (numbers in parentheses correspond to numbered areas in fig. 16). Rock-type classification (approximate) is shown by diagonal lines intersecting the sides of the diagram.

upper and lower units are reported (Delfour, 1977). However, the upper Hulayfah rocks consistently straddle the tholeiitic–calc-alkalic line, whereas the lower rocks consistently lie below the line on the calc-alkalic side. This is opposite of what would be expected, and we wonder, because of structural complications, whether these rocks can be mapped stratigraphically in the field.

The alkali-silica diagrams, figures 26*A* and 26*B*, show a similar wide distribution for the metavolcanic rocks of the control set. On these two diagrams, the rocks of the Baish-Bahah and Jiddah (Samran) Groups are distinctly more tholeiitic than the rocks of the Halaban Group, but overlap of some rocks of each group provides a nearly complete intermixing of the data. The rocks of the Halaban (Hulayfah) Group range from tholeiitic to

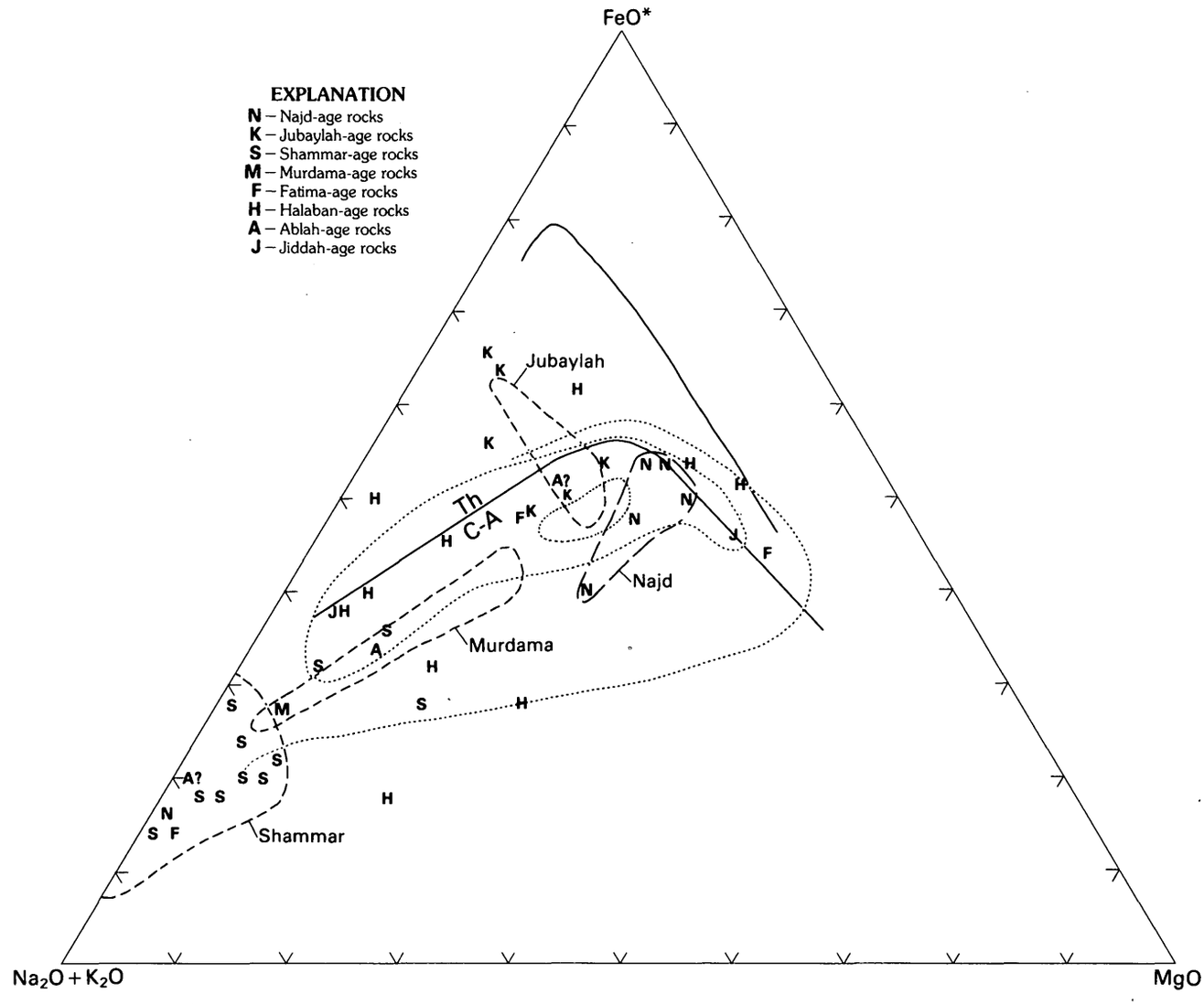

FIGURE 23.—AFM diagram showing chemical (weight percent data) distribution of metavolcanic rocks and a few dike rocks given in tables 3 and 4. Solid and dotted lines are as in figure 22. Short-dashed lines enclose specific age-area sets of control samples (from fig. 22). Long-dashed line encloses andesitic and diabasic rocks in dikes and small plug intrusions associated with Najd faulting. Lower solid line separates tholeiitic (Th) and calc-alkalic (C-A) compositions according to Irvine and Baragar (1971), p. 528.

alkalic by the classification of Kuno (1966). The Wādī Wassāṭ (Halaban) rocks in particular tend to be more alkalic. Rocks of all three groups tend to separate into more tholeiitic clusters and more alkalic clusters for rocks of andesitic and basaltic compositions.

The Jiddah and Halaban metavolcanic rocks analyzed for this report are shown in figures 23 and 27*B*. The data show a wide distribution in the calc-alkalic field on the AFM diagram, figure 23; the wide distribution is similar to that of the control-set data in figure 22, even with the small number of data points available. On the alkali-silica diagram, figure 27*B*, the Jiddah and Halaban rocks mostly form a linear array of calc-alkalic composition. These metavolcanic rocks of the basaltic and andesitic assemblages have an overall average calc-alkalic composition that extends into the tholeiitic field.

The younger volcanic rocks are distinctly segregated on the AFM and alkali-silica diagrams (figs. 22, 23, 27*A*, 27*B*). The volcanic rocks of the Shammar Group, both the control set and those analyzed for this report, are well segregated as rhyolites. The Shammar volcanics of the control set are distinctly alkalic, by the classification of Kuno (1966), in figure 27*A*. A few mafic volcanic rocks of the Shammar Group from the Nuqrah quadrangle (area 1) make a calc-alkalic cluster that trends into the tholeiitic field (figs. 22, 27*A*). The samples of

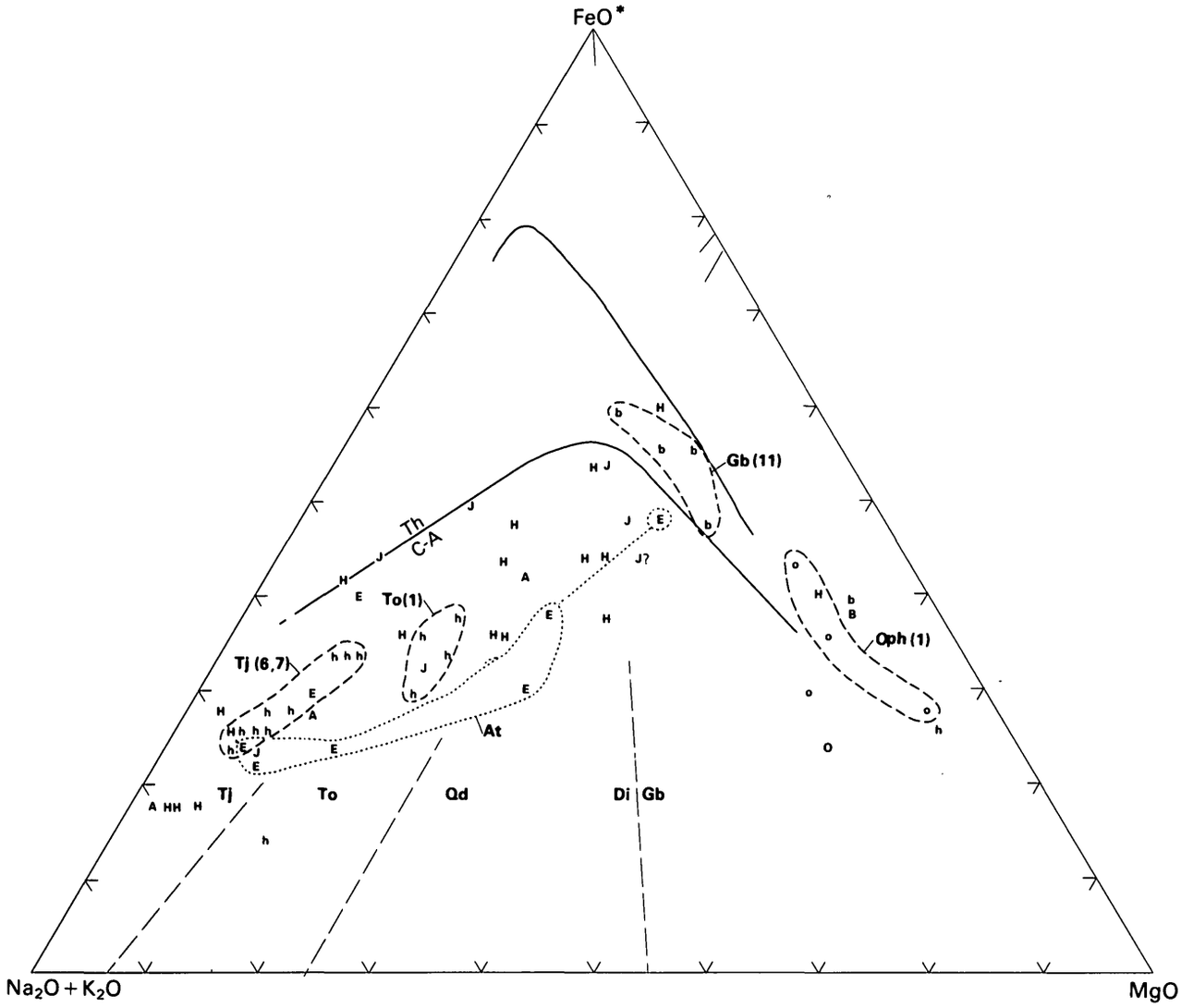

EXPLANATION

SAMPLE		AGE	ROCK TYPE
This report	Control		
H	h	Halaban-age rocks	**Tj** – Trondhjemite
A		Ablah-age rocks	**To** – Tonalite
J		Jiddah-age rocks	**Qd** – Quartz diorite
B	b	Baish-Bahah-age rocks	**Di** – Diorite
O	o	Ophiolite-age rocks (variable)	**Gb** – Gabbro
E		Rocks east of Al Amar-Idsas fault, pre-Halaban-age rocks	**At** – Anorthosite
			Oph – Ophiolite

FIGURE 24.—AFM diagram showing chemical (weight percent data) distribution of rocks of the dioritic suite from the Saudi Arabian Shield. Analyses are classified by age; single lower case letters represent control analyses; single upper case letters represent analyses of this report. Lower solid line separates tholeiitic (Th) and calc-alkalic (C-A) compositions according to Irvine and Baragar (1971, p. 528); upper solid line is the Skaergaard liquid trend. Short-dashed lines enclose specific control samples; rock type and source area (number in parentheses; see fig. 16) are given. Dotted line encloses anorthositic rocks (sample 167, table 3). Long-dashed lines approximately divide diagram into principal rock types of the dioritic suite.

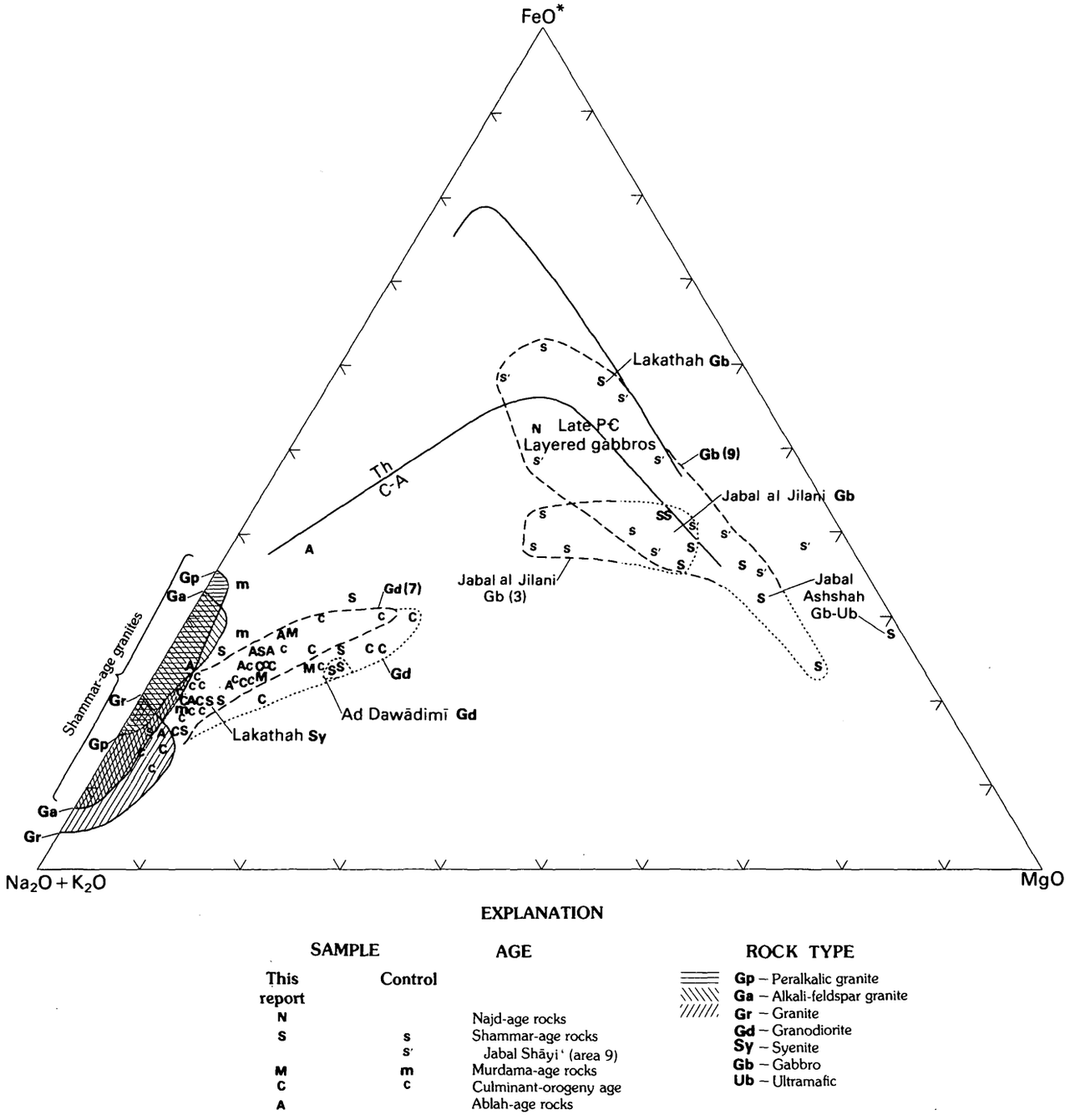

FIGURE 25.—AFM diagram showing chemical (weight percent data) distribution of rocks of the granitic suite from the Saudi Arabian Shield. Analyses are classified by age; single lower case letters represent control analyses; single upper case letters represent analyses of this report. Solid lines are as in figure 24. Short-dashed lines enclose specific sets of control samples; rock type and source area (number in parentheses; see fig. 16) are given. Dotted lines enclose specific sample sets of this report.

the Murdama Group available (figs. 22, 23, 27*A*, 27*B*) are mostly calc-alkalic dacites but are too few to satisfactorily define the trend suggested in figures 22 and 27*A*. Rocks of the Jubaylah Group of both the control set and the set of this report make a distinctive cluster that straddles the tholeiitic and calc-alkalic line for mafic to intermediate compositions (figs. 22, 23, 27*A*, 27*B*). Diabasic dike rocks of Najd age form a cluster mostly close to the tholeiitic line but range to calc-alkalic compositions (fig. 23).

Limited data for metavolcanic rocks of the Ablah and Fatimah Groups are available only for analyses of this report (figs. 23, 27*B*). In figure 27*B*, the few Fatimah rocks form a distinct calc-alkalic trend ranging from andesitic to rhyolite composition and the few Ablah rocks follow a similar trend.

The effects of alteration, such as spilitization, nonisochemical metamorphism, and late hydrothermal alteration, are little known for the metavolcanic rocks herein studied. Increase in NaO_2 caused by spilitization may be expected, particularly for the rocks of the Baish-Bahah Group (basaltic assemblage), and mobility of NaO_2 may be expected during the widespread greenschist metamorphism. Such alteration of the alkali content in the rocks of the basaltic and andesitic assemblages may account for some of the spread of the analyses across the alkalic-to-tholeiitic fields on the AFM and alkali-silica diagrams (figs. 22, 23, 26*A*, 26*B*). As described above, alkalic alteration may be expected to be more intense in the Halaban metavolcanic rocks because late granitic intrusion and late hydrothermal alteration were more intense in the northeastern half of the shield. Therefore, on the AFM and alkali-silica diagrams, as well as on the NCK diagram, the Halaban-rock chemistry does have an alkali range that is wider than that of the Baish-Bahah and Jiddah rocks of the southwestern half of the shield.

Late hydrothermal alteration is widespread in the shield, and many of the analyzed samples, particularly samples from the control set, came from mineralized districts where more detailed studies have been concentrated. It must be assumed, however, that the samples were collected as representive of the least altered rocks. An extreme example of the effects of hydrothermal alteration is shown by five samples from the Madh adh Dhahab district (area 14, fig. 16; R.J. Roberts, written commun., 1980) in figures 22 and 27*A*. These volcanic and dike samples of possibly Murdama or Shammar(?) age were collected in the vicinity of the Madh adh Dhahab gold-quartz-vein deposit, and petrographic study and chemical analyses (R.J. Roberts, oral commun., 1980) document well that hydrothermal alteration was intense in all but one sample; figure 27*A* suggests an extreme increase in SiO_2 with variable change in alkalies, whereas figure 22 suggests a large increase in alkalies relative to total iron as FeO (FeO*).

PLUTONIC ROCKS

The plutonic rocks of the dioritic suite follow a well-defined calc-alkalic trend on the AFM diagram (fig. 24); most samples are quartz diorite, tonalite, and trondhjemite of Halaban age. Few diorite and gabbro samples are represented. The mafic rocks of ophiolitic association, several Baish-Bahah rocks, and two Halaban rocks are tholeiitic. As might be expected, none of the rocks suggest a trend toward iron enrichment of the Skaergaard trend.

On the alkali-silica diagram (fig. 28), the dioritic-suite plutonic rocks systematically increase in alkalies with increased silica to SiO_2 contents of about 70 percent; as silica increases further, alkali content decreases. This trend of the plutonic rocks (fig. 28) is similar to that of the volcanic rocks (figs. 26*A*, 26*B*) and suggests a comagmatic relationship between the volcanic rocks of the andesitic and basaltic assemblages and the plutonic rocks of the dioritic suites. Specific classification of these plutonic rocks as calc-alkalic or tholeiitic is not possible because the compositional boundaries of Kuno (1966) are defined for volcanic rocks. However, in figure 28 the dioritic-suite rocks of Jiddah age tend to be less alkalic than equivalent rocks of Halaban age, although most samples overlap on the diagram. The anorthositic rocks of sample 167 (tables 3, 4; fig. 28) distinctly lie outside the plutonic rock trend of the dioritic suite. The ophiolitic rocks of the Nuqrah quadrangle (area 1; fig. 28) are tholeiitic and lie within the general dioritic-suite trend but are restricted to the mafic end of the trend. As expected, on the AFM diagram (fig. 24) the ophiolitic rocks form a distinct cluster of high-MgO, tholeiitic composition.

The plutonic rocks of the granitic suite are distinctly bimodal in composition in figures 25, 29*A*, and 29*B*. The gabbroic rocks, characteristic of the small, circular, layered plutons of youthful Precambrian (Shammar) age, tend toward distinct iron enrichment but much less so than on the Skaergaard trend. On the alkali-silica diagrams (figs. 29*A*, 29*B*) the Shammar gabbros spread across the alkalic to tholeiitic fields of the volcanic classifications of Kuno (1966) and Irvine and Barager (1971). The granodiorite and granite rocks of culminant-orogeny age and Shammar age follow a broken calc-alkalic trend that is considerably enriched in total alkalies (figs. 25, 29*A*, 29*B*) relative to the trend of the dioritic-suite rocks on similar diagrams (figs. 24, 28). The late alkali-feldspar granite and peralkalic granite samples follow a distinctly different trend of total iron enrichment (fig. 25) and of alkali enrichment (figs. 29*A*, 29*B*).

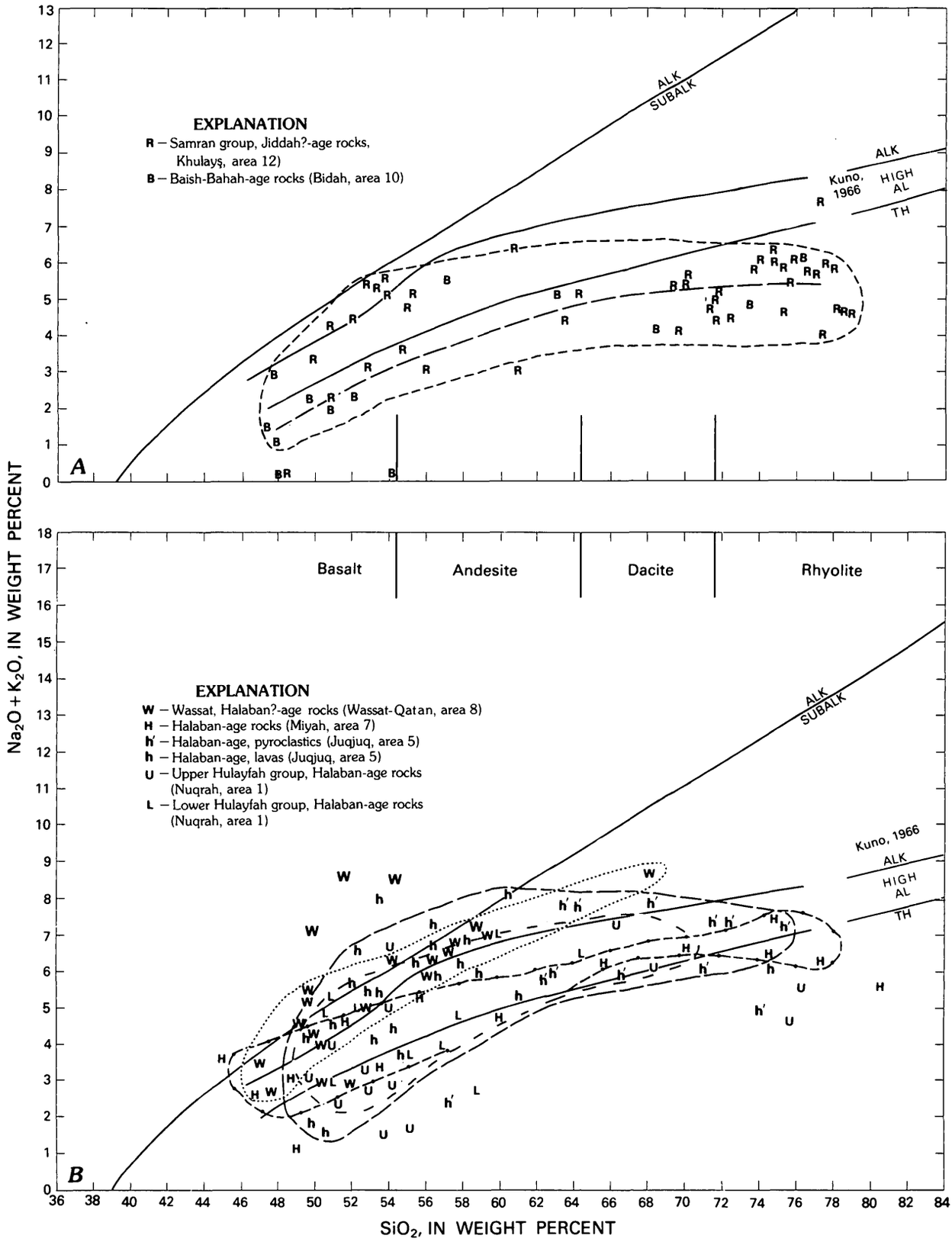
EXPLANATION
R – Samran group, Jiddah?-age rocks, Khulays, area 12)
B – Baish-Bahah-age rocks (Bidah, area 10)
ALK
SUBALK
Kuno, 1966
HIGH AL
TH
A
Basalt
Andesite
Dacite
Rhyolite
EXPLANATION
W – Wassat, Halaban?-age rocks (Wassat-Qatan, area 8)
H – Halaban-age rocks (Miyah, area 7)
h' – Halaban-age, pyroclastics (Juqjuq, area 5)
h – Halaban-age, lavas (Juqjuq, area 5)
U – Upper Hulayfah group, Halaban-age rocks (Nuqrah, area 1)
L – Lower Hulayfah group, Halaban-age rocks (Nuqrah, area 1)
B
Na2O + K2O, IN WEIGHT PERCENT
SiO2, IN WEIGHT PERCENT

The few analyses of Ablah plutonic rocks, mostly granodiorite and granite, follow the calc-alkalic trend of rocks of culminant-orogeny age on the AFM diagram (fig. 25) but are distinctly less alkalic than rocks of culminant-orogeny age on the alkali-silica diagram (fig. 29*B*). The low total-alkalic content of the Ablah rocks is caused by a low K_2O content that is much lower than in younger granodiorite and granite rocks from elsewhere in the shield. In general, this is characteristic of the early, precratonization granitic rocks of the western part of the shield. This is more strikingly so if the control set of granodioritic gneisses from the Aṭ Ṭā'if area (area 11, fig. 16) of the western shield in figure 29*A* is considered to be Ablah age rather than culminant-orogeny age. We have no age data that dispute such a reclassification of these rocks. The distinctive alkalic cluster of syenitic and quartz monzonitic rocks in figures 29*A* and 29*B* are common, but not abundant, for rocks of Shammar age from widely separated parts of the shield. They suggest a trimodal distribution for plutonic rocks of Shammar age.

DISCUSSION OF CHEMISTRY

The chemical variation of the volcanic and plutonic rocks of the Saudi Arabian Shield has been examined regionally by Greenwood and Brown (1973), Greenwood and others (1976), Greenwood and others (1980), and Delfour (1979b) and locally by Jackaman (1972), Delfour (1977), Al-Shanti (1974, 1976), Kanaan (1979), Dodge and others (1979), Nasseef and Gass (1977), Skiba (1980), and others. This report contributes the fact that the chemical evolution of these rocks is systematic with age in any given region and is similar for different regions throughout the shield regardless of age. The chemical data presented above, as well as this discussion of the chemistry, have been summarized in a review paper by Schmidt and Brown (1984).

The major-element chemistry is readily divisible into major categories of age (stratigraphy) that are related directly to the chemical evolution and systematic genesis of the shield. Chemical evolutionary trends are summarized on NCK diagrams—metavolcanic rocks in figure 18 and plutonic rocks in figure 21. The evolutionary trend fits especially well two major categories of crustal development: (1) a primary crust of early, multiple, intraoceanic island arcs broadly categorized agewise (stratigraphically) as Baish-Bahah, Jiddah, and Halaban, and (2) late cratonization crust categorized agewise (stratigraphically and structurally) as the culminant orogeny, Murdama-Shammar, and Jubaylah-Najd. The chemistry of the early crustal rocks of different ages (Baish-Bahah, Jiddah, and Halaban) is similar regardless of age and is not distinctly subdivided within itself. The chemistry of the late cratonization rocks is more distinctly and more readily subdivided within itself.

The primary crust (that is, the first or early crust) of the shield is composed of calc-alkalic metavolcanic rocks and equivalent calc-alkalic plutonic rocks. Most of the metavolcanic rocks are classified as an andesitic assemblage that ranges in composition from basalt to sodic dacite but whose calc-alkalic composition varies little areally or agewise across the shield. The abundant plutonic rocks are classified in a dioritic suite that ranges in composition from gabbro to trondhjemite and, again, whose calc-alkalic composition varies little with area or age across the shield. Calc-alkalic volcanic and plutonic rocks of such large volume as is found in the Arabian Shield are characteristic of volcanic-magmatic arcs and might be expected to have more mafic and tholeiitic compositions in their early, immature stages of development and more silicic and calc-alkalic compositions in their later, more mature stages of development (Miyashiro, 1974). This is suggested in the chemical data of the major elements (figs. 26*A*, 26*B*, 28, 22, 24). However, the Arabian Shield is tectonically complex and deeply eroded, and to date, distinctively immature and mature parts of individual volcanic-magmatic arcs have only been proposed and suggested; more detailed mapping, chemistry, and dating are needed. The sparse age data allow divisions into large regions of primary crustal rocks that have been designated Baish-Bahah, Jiddah, and Halaban ages, but these large regions are in themselves far too large and complex to encompass single volcanic-magmatic arcs. It is likely that each age group actually encompasses several independent arcs that have been collisionally combined at different stages of shield development.

The metavolcanic rocks of the Baish-Bahah, Jiddah, and Halaban Groups do contain some tholeiitic rocks (figs. 26*A*, 26*B*, 27*B*). A slight chemical discrimination

FIGURE 26.—Alkali-silica diagram showing metavolcanic-rock chemistry (weight percent data) of control samples of the Baish-Bahah and Jiddah Groups (*A*) and of the Halaban Group (*B*). Rocks are classified by age. Upper solid line divides alkaline and subalkaline fields for Hawaiian data (Irvine and Baragar, 1971), and two lower solid lines divide tholeiite (TH), high-alumina basalt (HIGH AL), and alkali-olivine basalt according to Kuno (1966). Approximate rock-type divisions are based on SiO_2 content. In *A*, long-dashed line shows trend of Baish-Bahah rocks and short-dashed line encloses total distribution of Baish-Bahah and Jiddah rocks. In *B*, long-dashed line encloses most Halaban rocks of the Bi'r Juqjuq quadrangle (area 5, fig. 16), short-dashed line encloses most Halaban rocks of the Nuqrah quadrangle (area 1), dash-dot line encloses most Halaban rocks of the Wādī al Miyah area (area 7), and dotted line encloses most Halaban rocks of the Wādī Wassāṭ area (area 8).

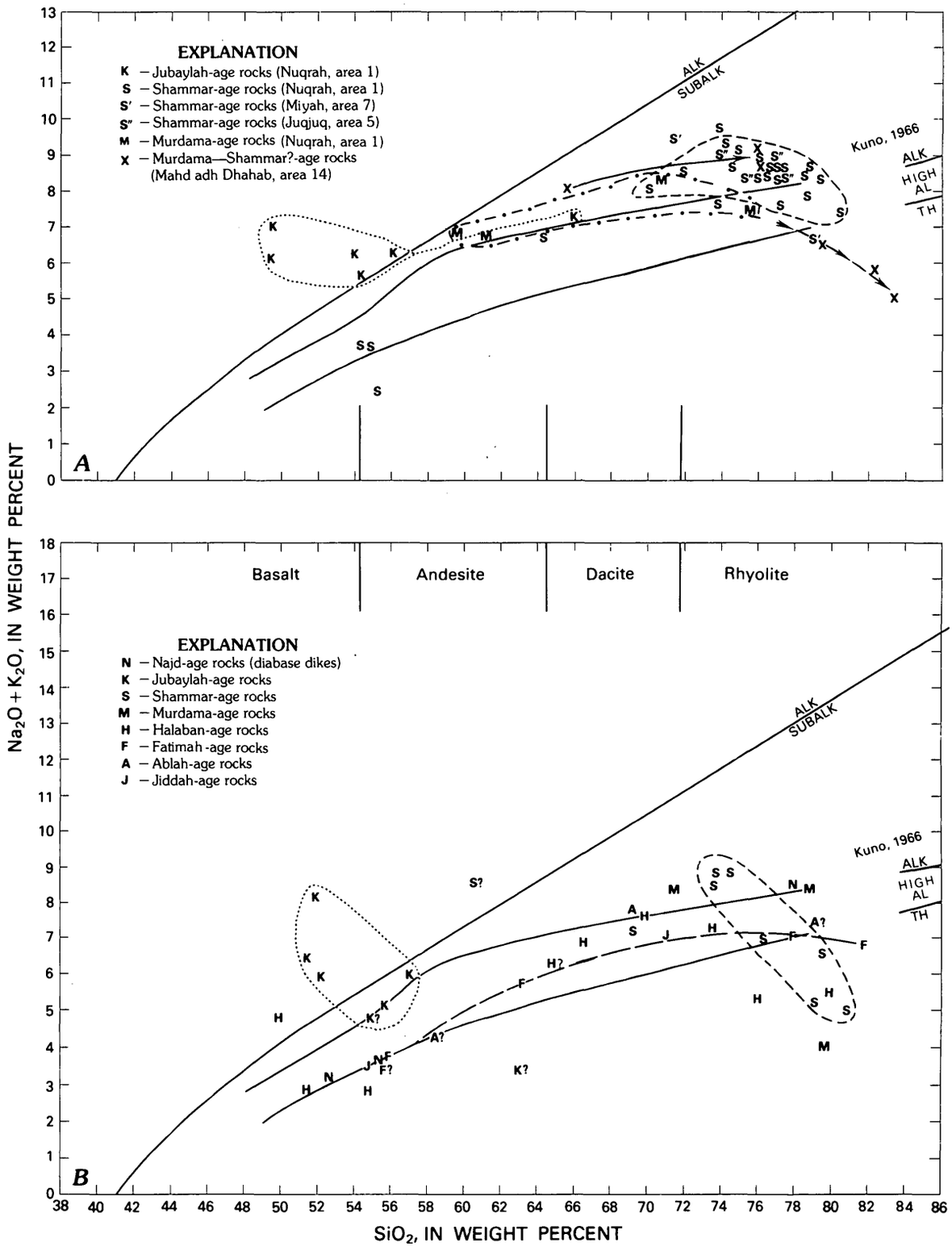
EXPLANATION
K – Jubaylah-age rocks (Nuqrah, area 1)
S – Shammar-age rocks (Nuqrah, area 1)
S′ – Shammar-age rocks (Miyah, area 7)
S″ – Shammar-age rocks (Juqjuq, area 5)
M – Murdama-age rocks (Nuqrah, area 1)
X – Murdama—Shammar?-age rocks (Mahd adh Dhahab, area 14)
ALK
SUBALK
Kuno, 1966
ALK
HIGH AL
TH
A
Basalt
Andesite
Dacite
Rhyolite
EXPLANATION
N – Najd-age rocks (diabase dikes)
K – Jubaylah-age rocks
S – Shammar-age rocks
M – Murdama-age rocks
H – Halaban-age rocks
F – Fatimah-age rocks
A – Ablah-age rocks
J – Jiddah-age rocks
B
$Na_2O + K_2O$, IN WEIGHT PERCENT
SiO_2, IN WEIGHT PERCENT

toward a more tholeiitic composition for the metavolcanic rocks of the Baish-Bahah Group compared with the Jiddah Group can be seen in figure 26*A*, and a slight discrimination toward a less calc-alkalic composition can be seen for the Baish-Bahah and Jiddah Groups compared with the Halaban Group (figs. 26*A*, 26*B*). However, sampling is localized and limited in amount, considering the tectonic complexity of the shield, and the older age and deeper erosion of the Baish-Bahah and Jiddah rocks may simply mean that more rocks of an immature, lower part of the Baish-Bahah and Jiddah have been sampled in comparison with the Halaban. Also, the Halaban rocks of the eastern part of the shield have been much more intruded by young granitic rocks and may have been subjected to more alteration subsequent to their emplacement.

Syntectonic plutonic rocks of the granitic suite of culminant-orogeny age mostly form large granodioritic batholiths of calc-alkalic composition (figs. 25, 29*A*, 29*B*). Within their calc-alkalic composition, these rocks are distinctly more alkalic than are plutonic rocks of similar SiO_2 content of the dioritic suite (figs. 24, 28). Volcanic equivalents of these syntectonic plutonic rocks have not been recognized in the field, although the few analyses of volcanic rocks of the Murdama Group are chemically similar to the granodiorite of culminant-orogeny age. In general, the Murdama-age volcanic rocks in their association with molassic sedimentary rocks are classified as posttectonic and early Shammar equivalents, but a sharp distinction between late syntectonic and posttectonic ages of molassic sedimentary rocks cannot be made, especially because this age boundary probably varies slightly from region to region across the shield.

The plutonic rocks of culminant-orogeny age are deep-seated rocks commonly spatially associated with the orthogneisses of large gneiss domes (antiforms), and it seems likely that little magma was erupted at the paleosurface at that time. This syntectonic granodiorite formed during tectonic thickening of the shield when the shield in many places was hot enough and thick enough for some old trondhjemitic and tonalitic masses to rise gravitationally as gneiss domes. The thickened crust seems definitely related to this first appearance of large volumes of potassic magma within the shield.

The potassic magmatism continued in a posttectonic cratonic environment, as represented by the plutonic, granitic-suite rocks of Shammar age and their volcanic equivalents of the Shammar Group. These plutonic and volcanic rocks have a distinctive major-element chemistry that is bimodal in granite-rhyolite and gabbro-basalt (figs. 22, 25, 27*A*, 27*B*). Their chemistry is distinctly more potassic than that of the plutonic and volcanic rocks of the dioritic suite and the andesite assemblage. The Shammar rocks formed from calc-alkalic magmas that in part evolved to alkalic magmas (figs. 27, 29*A*).

Synorogenic potassic volcanic and plutonic rocks that are older than the culminant orogeny are those of the Ablah and Fatimah Groups from the southwestern shield regions (regions J, B, and WS, fig. 16). These rocks are distinctly much less potassic than the later culminant-orogeny rocks and are exemplified by the An Nimas batholith and the batholithic rocks of the Jiddah-Makkah area. The Ablah rocks seem related to an earlier orogeny in a restricted part of the shield that had a thinner, less mature crust than that associated with the later, shieldwide culminant orogeny. On the basis of chemistry, the Fatimah rocks of the Jiddah-Makkah area (region WS, fig. 16) are similar to the Ablah rocks and formed in a similar crustal environment, but on a different crustal block and perhaps at a different time.

The Jubaylah Group volcanic rocks form a distinctive assemblage of mafic to intermediate rocks that range from calc-alkalic to alkalic in composition (figs. 27*A*, 27*B*). They are the youngest rocks of the Arabian Shield, and their composition is suggestive of the magmatism of a continental rift system. However, no characteristic rift existed at Najd faulting time. The Jubaylah volcanic rocks erupted during the compressional, transcurrent faulting of Najd age (Moore, 1979), but they erupted only in restricted, tensional parts of the large-displacement, sinuous faults in the complex Najd fault system.

Granite of Najd age together with minor gabbro and syenite in plugs and sills is penecontemporaneous and bimodal with Jubaylah volcanic rocks (fig. 29*A*). The Najd-age granite is exposed in the Najd fault zones at different places than the Jubaylah volcanic rocks. The chemical analyses of the Najd granite are too few for satisfactory comparison, but the composition seems

FIGURE 27.—Alkali-silica diagram showing metavolcanic-rock chemistry (weight percent data) of control samples of the Murdama, Shammar, and Jubaylah Groups (*A*) and of the metavolcanic rocks analyzed for this report (*B*). Rocks are classified by age. Solid lines are published alkalic and subalkalic divisions of volcanic rocks, as in figure 26. Approximate rock-type divisions are based on SiO_2 content. In *A*, short-dashed line encloses most rocks of the Shammar Group, dash-dot line encloses rocks of the Murdama Group, and dotted line encloses rocks of the Jubaylah Group. Solid arrow suggests direction of intense hydrothermal alteration of "rhyolite porphyry" in dikes and a plug in the Madh adh Dhahab district (area 14, fig. 16), and dashed arrow, for pyroclastic rocks in the same area. In *B*, short-dashed line encloses rocks of the Shammar Group, long-dashed line shows trend of rocks of the Fatimah Group, and dotted line encloses rocks of the Jubaylah Group.

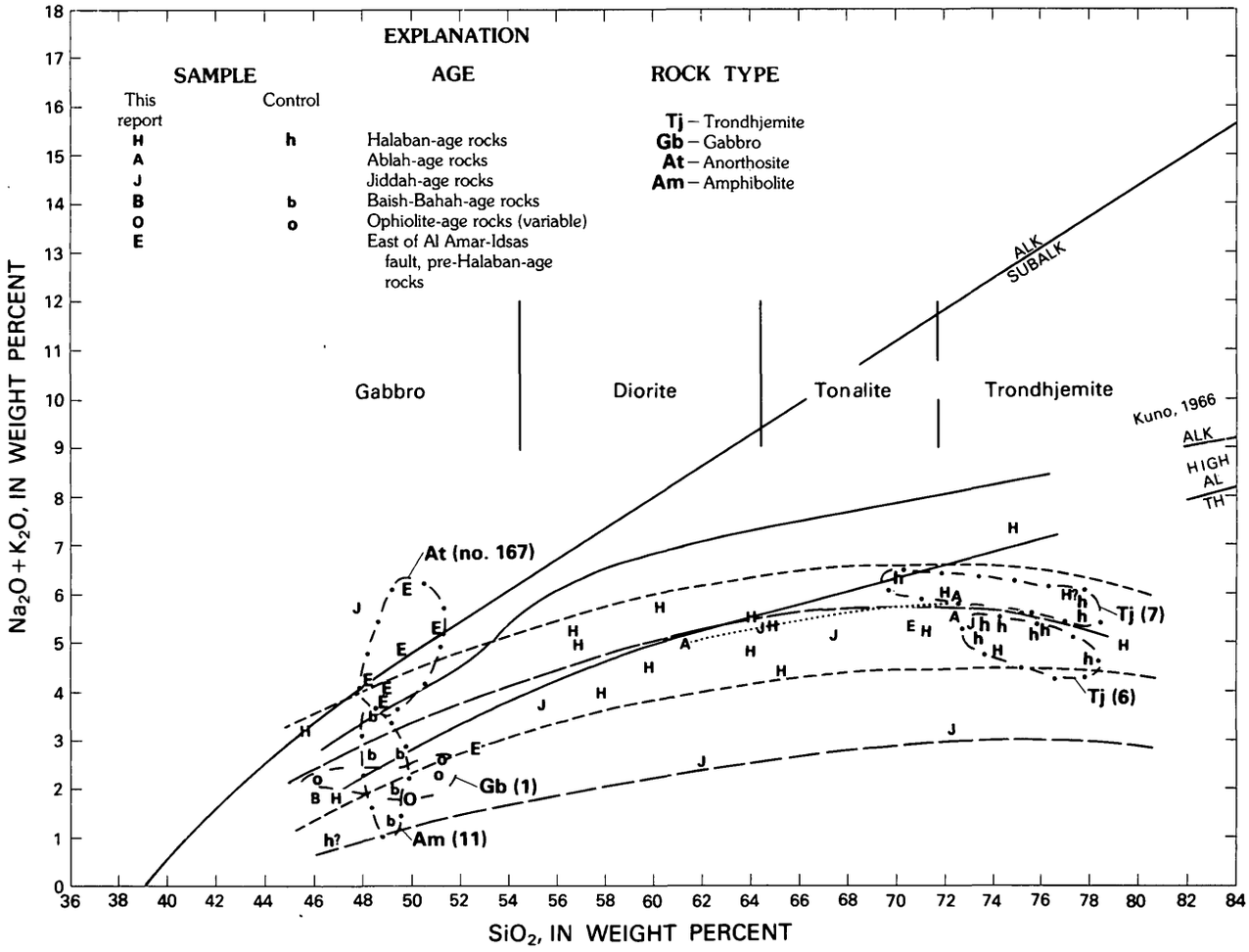

FIGURE 28.—Alkali-silica diagram showing plutonic-rock chemistry (weight percent data) of dioritic suite for samples of this report and of control set. Rocks are classified by age. Solid lines are alkalic-subalkalic divisions of volcanic rocks from the literature, as in figure 26. Approximate rock-type divisions are based on SiO_2 content. Long-dashed lines enclose Baish-Bahah-age and Jiddah-age rocks, short-dashed lines enclose Halaban-age rocks, dotted line connects rocks of Ablah age from the An Nimas batholith, and dash-dot lines enclose sample sets from specific area (numbers in parentheses correspond to numbered areas in fig. 16; no. 167 from table 3).

distinctly alkalic and probably in part overlaps that of the Shammar field.

GEOCHRONOLOGIC DATA FOR THE ARABIAN SHIELD

FIRST RADIOMETRIC AGE DETERMINATIONS

By L.T. Aldrich

The radiometric ages reported below were determined during the period 1957–63. The rock samples were provided and examined petrographically by Glen F. Brown and his associates at the U.S. Geological Survey. The 25 Rb-Sr ages of biotites and feldspars and the 25 K-Ar ages of biotites, hornblendes, and total-rock samples constituted the initial suite of ages for the Arabian Shield. Zircons in the quantity required for analysis were not found in any of the rocks examined. The sample locations are distributed over the entire Arabian Shield; the locations, the sample numbers, and the rock types as determined by petrographic examination of thin sections are given in table 6. Of the 50 dates, 31 have been published without supporting chemical data on U.S. Geological Survey geologic maps I–200A, I–204A, I–206A, I–210A, and I–211A (Bramkamp, Brown, and others, 1963; Bramkamp, Ramirez, and others, 1963; Brown, Jackson, Bogue, and Elberg, 1963; Brown, Jackson, Bogue, and MacLean, 1963; Jackson, Bogue, Brown, and Gierhart, 1963). Table 5

TABLE 5.—*Isotopic chemistry of mineral samples used to determine K-Ar and Rb-Sr ages (table 6) of Precambrian rocks from Saudi Arabia*

[ppm, parts per million; * indicates radiogenic ion. Analyses by L.T. Aldrich]

Sample	Mineral	^{87}Rb (ppm)	$^{87}Sr^*$ (ppm)	$^{87}Sr/^{88}Sr$	$^{87}Sr^*/^{87}Rb$	K (percent)	^{40}K (ppm)	$^{40}Ar^*$ (ppm)	$^{40}Ar^*/^{40}Ar$ (total)	$^{40}Ar^*/^{40}K$
1	Hornblende	–	0.590	–	–	0.956	1.14	0.0363	0.74	0.0318
2	Feldspar	44.8	0.131	0.0901	0.0131	11.0	–	–	–	–
3	Biotite	221	0.482	0.219	0.00616	5.35	–	–	–	–
4	Hornblende	–	–	–	–	0.409	0.487	0.0213	0.72	0.0437
5	Hornblende	–	–	–	–	0.465	0.555	0.0155	0.38	0.0279
6	Feldspar	125.3	1.157	0.253	0.00923	13.2	–	–	–	–
7	Hornblende	–	–	–	–	0.937	1.118	0.0430	0.84	0.0384
8	Hornblende	–	–	–	–	0.398	0.485	0.0464	0.58	0.0977
9	Biotite	320	2.63	0.335	0.00822	5.61	6.69	0.272	0.67	0.0406
	Feldspar	84.9	0.623	0.0992	0.0072±.0005	7.99	–	–	–	–
10	Biotite	40.9	0.356	0.0976	0.0087±.0005	3.16	3.77	0.170	0.70	0.0451
11	Biotite	57.5	0.275	0.0904	0.0048±.0005	5.84	6.97	0.229	0.90	0.0329
12	Biotite	95.9	0.718	0.1161	0.00748	6.34	7.56	0.303	0.85	0.0401
	Feldspar	123	1.01	0.1274	0.00822	9.59	–	–	–	–
13	Biotite	230	1.930	0.2104	0.00839	5.09	6.07	0.2388	0.89	0.0393
14	Biotite	301	2.36	0.434	0.00784	6.09	7.27	0.2650	0.97	0.0365
	Feldspar	101	0.926	0.1226	0.00932	7.52	–	–	–	–
15	Hornblende	–	–	–	–	0.544	0.649	0.0448	0.90	0.0690
	Biotite	88.5	0.845	0.1152	0.00952	4.87	5.81	0.304	0.94	0.0523
16	Biotite	53.5	0.765	0.1181	0.0145	6.30	7.52	0.287	0.95	0.0382
17	Biotite	235	1.80	0.1304	0.00766	4.88	5.82	0.218	0.95	0.0375
18	Biotite	116	1.70	0.1403	0.0147	5.44	6.49	0.333	0.85	0.0513
19	Biotite	50.7	0.699	0.1100	0.0138	7.40	8.83	0.484	0.92	0.0548
20	Muscovite	99.4	1.177	1.301	0.0118	8.88	10.50	0.617	0.86	0.0588
21	Biotite	116.4	0.874	0.1004	0.0075±.0005	3.93	4.69	0.1703	0.75	0.0393
22	Biotite	130	0.950	0.1432	0.00735	4.54	5.42	0.1413	0.72	0.0261
	Feldspar	66.5	0.603	0.1256	0.00908	9.42	–	–	–	–
23	Biotite	30.5	0.342	0.1092	0.0112±.0005	5.06	6.04	0.256	0.77	0.0424
24	Biotite	763	6.25	3.97	0.00819	7.82	9.33	0.360	0.84	0.0386
	Feldspar	319	2.57	0.401	0.00808	10.53	–	–	–	–
25	Biotite	85.7	0.881	0.1420	0.0103	7.05	8.41	0.449	0.94	0.0534
26	Total rock	–	–	–	–	2.20	2.62	0.0686	0.93	0.0261
27	Total rock	–	–	–	–	1.54	1.84	0.0647	0.92	0.0352

includes the minerals analyzed and the analytical data obtained. The sample numbers correspond to those in table 6. All the analyses were made using stable isotope dilution procedures described (Aldrich, 1956; Aldrich and others, 1956). The precision of the ratios $^{87}Sr^*/^{87}Rb$ is better than 5 percent for all samples having a ratio $^{87}Sr/^{88}Sr>0.11$. For cases in which $0.085<^{87}Sr/^{88}Sr<0.11$, the error in the ratio $^{87}Sr^*/^{87}Rb$ is indicated. The precision of the ratio $^{87}Sr/^{88}Sr$ is 0.3 percent or less and is independent of the assumption of the ratio 86/88 to the first order. The absolute ratio $^{87}Sr/^{88}Sr$ may be in error as much as 0.5 percent owing to processes in thermal ionization and to errors in thermal calibrations which have not yet been discovered.

The precision of the argon determinations is better than 1.0 percent. This upper limit is set by the variations in the ratios $^{36}Ar/^{40}Ar$ in atmospheric argon observed over the years during which it has been measured at the Carnegie Institution of Washington. The ^{40}K determination has an error of 3.0 percent or less based on reproducibility of results on the same rock sample and the results of mixing standard potassium solutions of different isotopic composition. The errors in the ratios $^{40}Ar/^{40}K$ are less than 4 percent.

Table 6 gives the ages derived from the analytical measurements of table 5 based on the assumptions as to the isotopic abundances and decay constants stated.

Figure 29*C* is a histogram of the distribution of ages found by the different methods applied to hornblende, biotite, and feldspar-muscovite. The first result of these measurements is the indication that the last event affecting the ages occurred over most of the Arabian Shield about 500 m.y. ago. Secondly, remnants of minerals as old as 1,100 m.y. have been found in several places on the shield. The Rb-Sr ages of potassium feldspars and muscovites have been found to be consistently resistant to alteration by metamorphic events which do affect the biotite ages (Aldrich and others, 1965). The six feldspars and the muscovite (see table 5) do not give a pattern basically different from

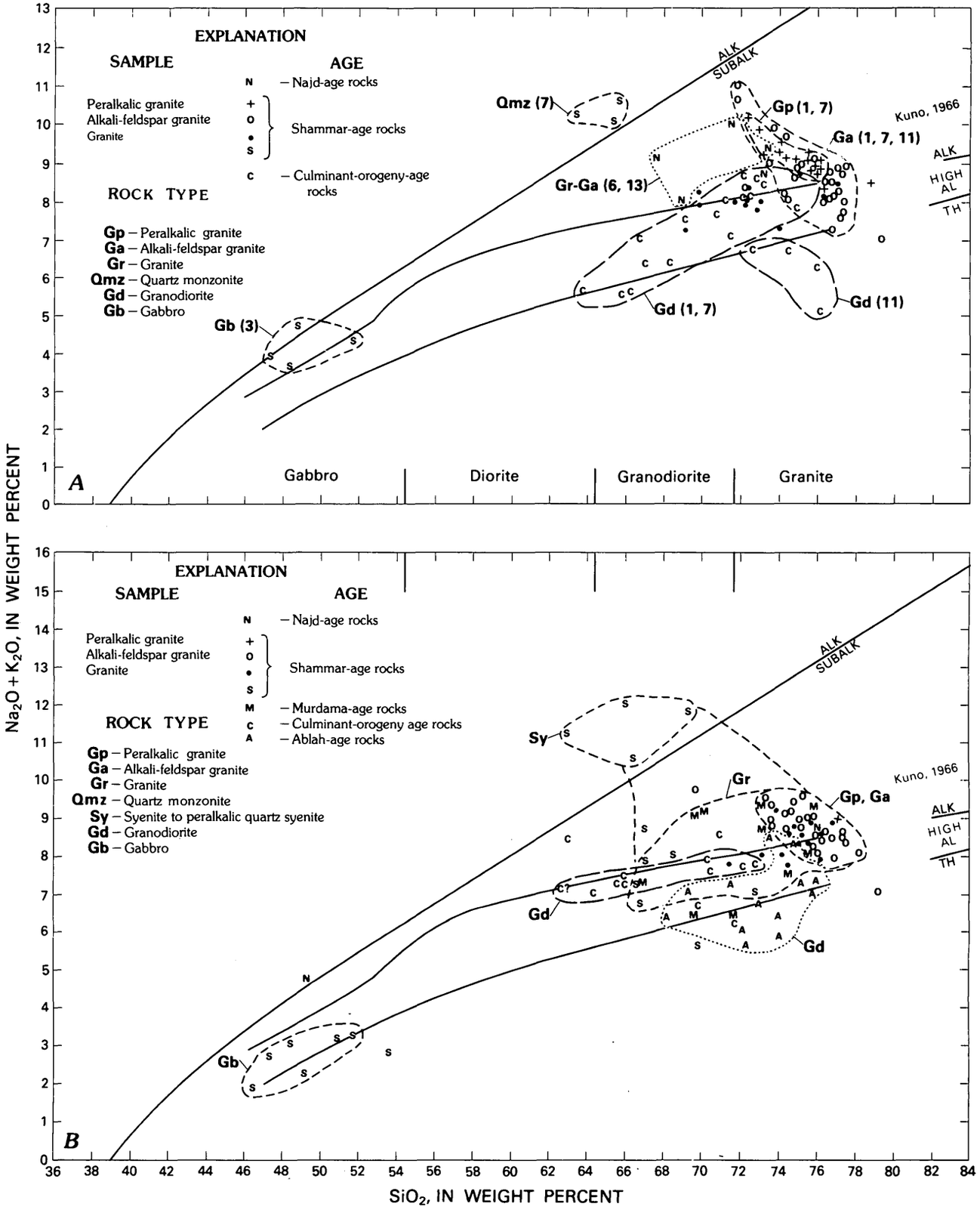
EXPLANATION
SAMPLE
AGE
N – Najd-age rocks
Peralkalic granite
Alkali-feldspar granite
Granite
+ O • S
Shammar-age rocks
C – Culminant-orogeny-age rocks
ROCK TYPE
Gp – Peralkalic granite
Ga – Alkali-feldspar granite
Gr – Granite
Qmz – Quartz monzonite
Gd – Granodiorite
Gb – Gabbro
Qmz (7)
Gp (1, 7)
Ga (1, 7, 11)
Gr-Ga (6, 13)
Gb (3)
Gd (1, 7)
Gd (11)
ALK
SUBALK
Kuno, 1966
ALK
HIGH AL
TH
A
Gabbro
Diorite
Granodiorite
Granite
M – Murdama-age rocks
A – Ablah-age rocks
Sy – Syenite to peralkalic quartz syenite
Gr
Gp, Ga
Gd
B
Na2O + K2O, IN WEIGHT PERCENT
SiO2, IN WEIGHT PERCENT

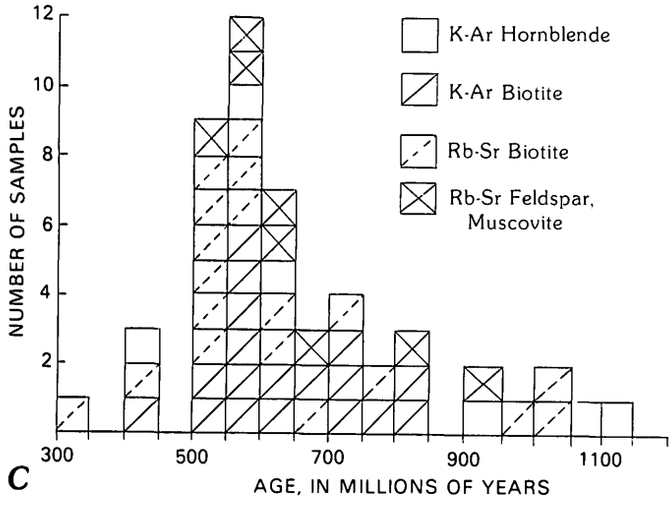

FIGURE 29*C*.—Histogram showing distribution of K-Ar and Rb-Sr ages for several minerals.

that of the biotites by themselves or from that seen in all of the Rb-Sr ages measured. The pattern of hornblende K-Ar ages is also similar to that obtained for the other minerals. The simplest generalized picture of the Arabian Shield from these data is that of a large area about 1,000–1,200 m.y. old on which has been superposed an event culminating about 550 m.y. ago. A particular sequence of samples with geographic proximity is that starting at Jiddah with sample 18 and continuing southeast about 300 km. Samples 18, 19, 20, 23, and 25 (table 6) have an age pattern similar to that observed for Precambrian rocks in the Appalachians—generally discordant and ranging down from 1,050 m.y. Samples 21, 22, and 24 are relatively concordant and may represent younger rocks associated with the event that lowered the age of the other rocks.

These data should be compared with the K-Ar ages obtained in eastern Egypt in the area between long 33° and 35° E. as published by Higazy and El-Ramly (1960).

FIGURE 29.—Alkali-silica diagrams showing plutonic-rock chemistry (weight percent data) of granitic suite: *A*, Samples of control set; *B*, Samples of this report. Rock are classified by age. Solid lines are alkalic-subalkalic divisions of volcanic rocks from the literature, as in figure 26. Approximate rock-type divisions are based on SiO_2 content. In *A*, lines enclose control samples from specific areas (numbers in parentheses correspond to numbered areas in fig. 16): long-dashed lines enclose two sets of granodiorite of culminant-orogeny age, short-dashed lines enclose Shammar-age rocks of different compositions, and dotted line encloses Najd-age granitic rocks. In *B*, lines enclose samples of this report of different composition and age: long-dashed line encloses rocks of culminant-orogeny age, short-dashed lines enclose rocks of Shammar age of various compositions, and dotted line encloses rocks of Ablah age.

The total-rock argon ages of samples 26 and 27 from the 'Asīr are presented not as a measure of their true age or even an approximation of the time of any "event" in this area, but rather as an indication of the minimum age that may be ascribed to these rocks. It must be pointed out that these samples could be older than those in the northern part of the shield and still have this young apparent age, owing to argon leakage from the potassium feldspars.

EARLY TABULATION OF RB-SR AND K-AR AGES

By G.F. Brown, Carl Hedge, and Richard Marvin

During the course of initial geologic fieldwork by the U.S. Geological Survey in the Arabian Shield, 101 radiometric ages were determined from rocks in the Precambrian-Cambrian basement. These ages were determined between 1963 and 1970 after the pioneering work of L.T. Aldrich (see preceding section) but before the extensive dating of the rocks of the Precambrian Shield after 1972. A tabulation of these Rb-Sr and K-Ar ages is presented recognizing the limitations of Rb-Sr and K-Ar ages.

Thirty samples were analyzed, using the Rb-Sr method, by Carl Hedge (table 7) in the Denver laboratory, U.S. Geological Survey. Eight of the 80 K-Ar ages listed in table 8 were determined by Richard Marvin, Harald Mehnert, and Violet Merritt in the Denver laboratory. Thirty-one K-Ar ages were determined by Geochron Laboratories, Kruger Enterprises, Inc., Cambridge, Mass., and 41 K-Ar ages by Teledyne Isotopes, Westwood, N.J.

Of the 30 Rb-Sr age determinations by Hedge (table 7), 19 were used to plot seven isochron diagrams. The samples used for the plots range from gneissic quartz monzonite to aegirine granite and porphyritic felsite. Rb-Sr isochron ages range downward from 731 m.y. for the gneissic quartz monzonite to 572 m.y. for the porphyritic felsite. Samples from the aegirine granite gave an isochron age of 590 m.y. Where they could be precisely determined, the initial $^{87}Sr/^{86}Sr$ ratios were relatively low—0.703–0.705. An initial ratio of 0.704 was therefore used to calculate the individual ages reported in table 7. Rhyolite sills or flows in the upper beds of the Murdama Group gave an age of 633 m.y., whereas rhyolite near the top of the underlying and older Hulayfah (Halaban) Group gave a minimum age of 658 m.y. (sample 68, table 7). The latter is especially significant as the rhyolite samples came from drill cores in stratabound ore deposits syngenetically deposited above the middle Hulayfah (Halaban) andesite and in the lower part of the uppermost rhyolite of the Halaban Group.

TABLE 6.—*Locations, rock types, and ages of mineral samples from Precambrian rocks of Saudi Arabia*
[Analyses by L.T. Aldrich]

Sample (location given on pl.1)	Aldrich sample no. (see table 5)	Locality (J.=Jabal; W.=Wādī)	Latitude (North)	Longitude (East)	Rock type	Mineral	Rb-Sr age[1] (m.y.)	K-Ar age[2] (m.y.)
1	1	W. 'Ifāl (Afal)	28°51′40″	35°09′17″	Granodiorite	Hornblende	—	480
2	2	W. Moss	28°35′08″	35°04′18″	Biotite granite	Feldspar	920±200	—
4	3	J. al Lawz	28°33′28″	35°24′35″	Biotite perthite quartz monzonite	Biotite	430	—
5	4	Sha'īb as Siq	28°02′10″	35°44′47″	Diorite	Hornblende	—	630
6	5	Sha'īb as Siq	28°02′26″	35°47′05″	Amphibolite schist	Hornblende	—	425
7	6	J. Harb	27°55′24″	35°36′08″	Microcline granite	Feldspar	645	—
8	7	J. Harb	27°55′20″	35°37′14″	Quartz syenite	Hornblende	—	565
[3]11	8	J. Shār (near)	27°42′42″	35°42′31″	Amphibolite	Hornblende	—	1,190
78	9	J. Salmá	27°08′33″	42°07′22″	Perthite biotite granite	Biotite	575	590
						Feldspar	505±50	—
82	10	J. Tīn	26°16′09″	42°19′24″	Orthoclase granite	Biotite	610±40	645
53	11	J. al Aswad	25°33′32″	38°13′35″	Albite biotite granite	Biotite	340±70	490
90	12	J. Umm ad Dībān	24°57′25″	43°51′54″	Biotite granodiorite	Biotite	525	585
						Feldspar	575	—
91	13	J. Jabalah	24°50′00″	43°55′12″	Biotite granite	Biotite	590	575
144	14	J. Za'ābah	23°47′42″	44°48′24″	Biotite perthite granite	Biotite	550	540
						Feldspar	655	—
104	15	J. Ḥamām	23°41′12″	41°38′06″	Granodiorite gneiss	Hornblende	—	915
						Biotite	665	730
186	16	J. Qusās (Idsas)	23°18′06″	45°14′31″	Granite gneiss	Biotite	1,010	560
149	17	J. Zan (E. Batholith)	22°36′16″	44°55′30″	Biotite granite	Biotite	540	550
114	18	Jiddah	21°30′49″	39°16′06″	Two-mica granite	Biotite	1,025	720
124	19	Makkah	21°30′00″	39°57′12″	Trondhjemite (quartz diorite)	Biotite	965	760
	20	Makkah	21°32′11″	40°01′52″	Pegmatite	Muscovite	825	800
125	21	Aṭ Ṭā'if	21°13′54″	40°27′06″	Biotite quartz monzonite	Biotite	525	535
127	22	SE. J. Qunah	20°51′49″	41°16′26″	Microcline biotite granite	Biotite	515	400
						Feldspar	635	—
126	23	W. Turabah	20°43′24″	41°14′33″	Quartz diorite	Biotite	785	615
140	24	J. Rafā'	20°27′30″	41°57′30″	Peralkaline granite	Biotite	575	565
						Feldspar	565	—
171	25	W. Ranyah	20°21′00″	42°01′36″	Calcalkalic granite gneiss	Biotite	720	740
238	26	W. Wahrugh (D-34)	17°42′13″	43°07′25″	Biotite granite	Total rock	—	400
239	27	W. Qa'ah (D-24)	17°42′30″	43°17′30″	Orthoclase granite	Total rock	—	525

[1]Ages based on ^{87}Rb properties: 0.283 g $^{87}Rb/g$ ^{87}Rb, $\lambda\beta(^{87}Rb)=1.42\times10^{-11}$ yr^{-1}.
[2]Ages based on ^{40}K properties: 119.3 μg $^{40}K/g$ K, $\lambda e(^{40}K)=0.581\times10^{-10}$ yr^{-1}. $\lambda\beta(^{40}K)=4.962\times10^{-10}$ yr^{-1}.
[3]This sample was collected by V. Kahr from near a fault contact with gray syntectonic granodiorite and Jabal Shar alkali granite which has since been dated at ±570 Ma.

TABLE 7.—*Rb-Sr ages of Precambrian crystalline rocks of Saudi Arabia*
[ppm, parts per million. Analyses by Carl Hedge]

Sample (location shown on pl. 1)	Age[1] (m.y.)	Rb (ppm)	Sr (ppm)	$^{87}Rb/^{86}Sr$[2]	$^{87}Sr/^{86}Sr$	Material analyzed	Rock	Collected by	Location	
									Lat N.	Long E.
59a	492±15	229	16.4	41.60	0.9968	Whole rock	Granite	Petty	27°42′	41°25′
59b	580±18	169	19.6	25.65	0.9173	do.	do.	do.	27°42′	41°25′
68	658±40*	29.9	58.1	1.491	0.7174	do.	Rhyolite	Delfour	25°45′	40°45′
71	658±40*	5.3	157	0.098	0.7052	do.	do.	do.	25°36′	41°26′
98	658±40*	45.8	61.3	2.167	0.7245	do.	do.	do.	23°51′	40°56′
77	673±60	119	128	2.701	0.7289	do.	Granite	Brown	24°30′	39°30′
94	633±15*	124	82.6	4.364	0.7440	do.	Rhyolite	do.	23°42′	39°40′
106	633±15*	44.7	107	1.211	0.7149	do.	Latite	do.	23°23′	39°44′
95	520±15	821	53.2	44.61	1.0202	Biotite	Granite	Goldsmith	23°36′	40°32′
96	572±35*	10.0	111	0.263	0.7068	Whole rock	Porphyritic felsite	do.	23°30′	40°50′
97	572±35*	85.3	141	1.753	0.7184	do.	do.	do.	23°32′	40°54′
99	731±15	13.7	924	0.53	0.7046	do.	Gneissic qtz. monzonite	do.	23°26′	40°59′
100a	692±15*	72.1	5.5	38.38	1.077	do.	Granite	do.	23°32′	41°06′
100b	692±15*	123	5.1	69.25	1.383	K-feldspar	do.	do.	23°32′	41°06′
100c	692±15*	72.5	13.2	15.90	0.8682	Whole rock	do.	do.	23°32′	41°06′
101a	590±10*	382	21.9	22.05	0.8821	do.	do.	do.	23°32′	41°10′
101b	590±10*	659	86.5	50.60	1.1390	do.	do.	do.	23°32′	41°10′
101c	590±10*	320	1.9	494.9	4.857	do.	do.	do.	23°32′	41°10′
108	555±15	535	43.5	35.62	0.9699	Biotite	Granite	do.	23°27′	41°21′
135a	617±10*	98.5	48.2	5.94	0.7587	Whole rock	Granodiorite	Brown	20°02′	41°51′
135b	617±10*	88.9	24.2	10.73	0.7980	do.	do.	do.	20°02′	41°51′
137	582±20	64.5	20.5	9.32	0.7827	do.	Qtz. monzonite	do.	20°11′	41°52′
169	530±20	496	140	10.33	0.7807	K-feldspar	Granite gneiss	do.	20°58′	43°49′
176	576±25	188	78.8	6.896	0.7603	Whole rock	Granite	Whitlow	20°55′	44°23′
193	583±15	184	49.5	10.77	0.7930	do.	do.	Trent	19°33′	41°44′
224	549±30	212	131	4.625	0.7421	do.	do.	Brown	17°57′	42°11′
233	586±35	148	118	3.629	0.7361	do.	Rhyolite	Overstreet	18°20′	44°15′
234	585±10	387	9.3	121.0	1.755	Microcline	Pegmatite	do.	18°07′	44°14′
235	550±20	122	29.2	12.06	0.8040	Whole rock	Granite porphyry	do.	18°08′	44°15′
240	694±30	129	60.6	6.185	0.7653	do.	Gneissic granite	Brown	17°26′	42°54′

[1]Asterisk indicates isochron age.

[2]Decay constant for ^{87}Rb: $\lambda=1.42\times10^{-11}$/yr.

The K-Ar ages range from 299 to 932 m.y. (table 8). The ages younger than about 500 m.y. undoubtedly reflect some severe resetting caused by late Precambrian hydrothermal alteration and some resetting caused by uplift and deep erosion. In places, some resetting may have been caused by heating by Tertiary volcanism associated with the formation of the Red Sea rift. Hornblende ages, which are least susceptible to resetting (argon loss), cluster around 550 and 570 m.y. and from 590 to 660 m.y. These ages represent events in the Pan African orogeny. Older hornblende ages, 710–778 m.y., are from calc-alkaline syngenetic, generally gneissic, quartz monozonite, granodiorite, and granite bodies which are usually exposed in domes. Ages in the span 805–932 m.y. were obtained mostly from diorite, quartz diorite, and granodiorite plutons exposed in the scarps and foothills east of the Red Sea and in the southern part of the Arabian Shield.

Following the earlier geochronological work (tables 6, 7, 8), an intensive study was begun in 1972, with geochronologists working in the field parties. Early analyses of the intensive program were limited to K-Ar determinations (Fleck and others, 1976), but when analytical work became more accurate for low rubidium values, attention was directed to Rb-Sr determinations (Fleck and others, 1980). It became apparent that many K-Ar analyses—especially of the biotite and feldspar fractions—gave ages that coincided with dates when magmas cooled below the point at which the daughter argon was retained in the rock. Thus, many K-Ar dates at about 550 m.y. in schist belts of the Najd fault zones suggest that an important period of fault movement occurred at or near the end of cratonization. A later cooling event, possibly representing erosion of cover rocks and upper crust of the shield during Middle to Late Cambrian, was recorded at 520–535 m.y. ago (Fleck and others, 1976). This event was further verified by a "fission track" age on four grains of sphene from a diorite in southwestern Arabia (C.W. Naeser, written commun., 1969), which gave an average of 510±52 m.y. as a cooling date, that is, the date when the tracks stopped annealing. The K-Ar age of the hornblende from the diorite was 615±12 m.y.

Later work using zircon and measuring daughter leads from uranium and thorium decay in zircons has helped define the two earlier major orogenies when the

TABLE 8.—*K-Ar ages of Precambrian crystalline rocks of Saudi Arabia*

Sample (location given on pl. 1)	Age (m.y.)	K (percent)	$^{40}Ar \times 10^{-10}$ (moles/g)	^{40}Ar (percent)	$^{40}Ar/^{40}K$	Analyzed by	Material analyzed	Rock	Collected by	Location	
										Lat N.	Long E.
12b	487±17	5.06	40.71	97	0.0318	USGS	Whole rock	Syenite	Brown	27°28′	35°07′
22b	515±17	2.63 2.67	27.33	94	0.0346	USGS[1]	do.	Oxidized[2] mugearite	do.	27°45′	36°10′
26	591±18	6.29 6.34	75.81 77.31	96 89	0.0406	Geochron[3]	Biotite	Granite	Trent	26°47′	37°05′
34	605±18	6.68 6.72	82.07 85.07	98 96	0.0418	do.	do.	do.	do.	26°13′	37°30′
40	528±20	6.53 6.43	68.91	99	0.0356	USGS	do.	Rhyolite	Brown	26°28′	38°13′
44	532±15	1.895 1.872	20.19 20.24	63 91	0.0360	Geochron	Whole rock	Andesite	do.	26°20′	38°37′
54	567±16	6.52 6.36	74.06 74.81	97 98	0.0387	do.	Biotite	Gneiss(?)	do.	25°48′	38°22′
65	827±40	0.385 0.401	7.061 7.231	75 81	0.0609	do.	Hornblende	Quartz diorite	do.	25°48′	39°13′
67	299±11	1.30 1.32	7.393	83	0.0189	USGS	Whole rock	Andesite (some alteration)	do.	25°33′	40°43′
69	548±18	1.70 1.71	18.95	95	0.0372	do.	do.	Andesite	do.	25°33′	40°45′
72	525±16	1.532 1.500	16.11 15.91	81 82	0.0354	Geochron	do.	do.	do.	24°52′	39°11′
89	577±15	7.27 7.29	89.07 82.57	98 97	0.0395	do.	Biotite	Granite	Mytton	25°01′	43°48′
92	595±12	6.12 6.10	75.31 74.06	95 97	0.0409	do.	do.	do.	do.	24°30′	43°19′
102	566±30	1.095 1.126	13.24 12.38	30 80	0.0386	do.	Whole rock	Dacite	Brown	23°29′	41°23′
103	506±15	2.180 2.198	22.19 22.17	83 92	0.0339	do.	do.	Diabase dike	do.	23°50′	41°25′
112	585±12	0.50 0.49	5.959 5.915	86 86	0.0402	Isotopes[4]	Hornblende	Schist	Hanford	22°24′	39°24′
117a	592±23	1.247 1.222	15.11 14.91	88 82	0.0407	Geochron	Whole rock	Altered basalt	Brown	21°35′	39°38′
117b	576±28	0.550 0.518	6.280 6.280	69 68	0.0394	do.	do.	Andesite	do.	21°35′	39°38′
119	549±20	6.65 6.48	71.56 74.81	74 91	0.0373	do.	Biotite	Grantite	Goldsmith	21°43′	40°27′
120	577±18	7.10 7.03	82.32 84.32	84 96	0.0395	do.	do.	Quartz monzonite	do.	21°41′	40°40′
121	570±17	7.15 7.22	83.82 83.32	97 98	0.0390	do.	do.	Granite	do.	21°41′	40°41′
128	827±16	0.32 0.33	5.829 5.995	82 73	0.0609	Isotopes	Hornblende with 5% impurities	Diorite	Brown	20°32′	41°25′
129a	932±46	0.489 0.440	9.858 9.808	82 86	0.0709	Geochron	Hornblende	do.	do.	20°32′	41°31′
	821±16	0.49 0.50	8.865 8.994	95 95	0.0604	Isotopes	Hornblende with 5% impurities	do.	do.	20°32′	41°31′
129b	912±18	0.44 0.45	9.240 9.070	91 90	0.0689	do.	do.	Quartz diorite	do.	20°32′	41°31′

Footnotes at end of table.

TABLE 8.—*K-Ar ages of Precambrian crystalline rocks of Saudi Arabia*—Continued

Sample (location given on pl. 1)	Age (m.y.)	K (percent)	$^{40}Ar \times 10^{-10}$ (moles/g)	^{40}Ar (percent)	$^{40}Ar/^{40}K$	Analyzed by	Material analyzed	Rock	Collected by	Location	
										Lat N.	Long E.
130	805±16	0.25	4.301	90	0.0590	do.	Amphibole with 15% impurities	Quartz diorite	do.	20°26′	40°26′
		0.24	4.323	92							
131	595±12	3.72	44.86	90	0.0410	do.	Muscovite	Paraschist	do.	20°26′	40°49′
		3.52	43.75	97							
132	717±18	0.42	6.312	90	0.0512	do.	Hornblende	Gneiss	do.	20°28′	40°56′
		0.42	6.517	94							
136	585±39	0.43	5.150	87	0.0401	USGS	Whole rock	Basalt plug	do.	20°10′	41°52′
		0.43									
141a	561±25	3.646	42.78	97	0.0382	Geochron	do.	Andesite	do.	23°39′	43°08′
		3.635	40.28	98							
141b	560±20	2.162	24.92	94	0.0382	do.	do.	Dacite(?)	do.	23°39′	43°08′
		2.277	25.67	94							
148	574±12	5.32	62.58	98	0.0393	Isotopes	Biotite (+60 mesh)	Granite	do.	22°53′	44°56′
		5.24	62.62	99							
	585±12	5.10	60.08	99	0.0401	do.	biotite (–60 mesh)	do.	do.	22°53′	44°56′
		4.98	60.66	99							
151	644±23	6.44	86.65	95	0.0450	USGS	Biotite	Gabbro	Hanford	22°19′	42°24′
		6.47									
153	496±12	0.48	4.721	76	0.0331	Isotopes	Plagioclase and quartz	Granite	Brown	22°25′	43°48′
		0.49	4.876	26							
156	513±17	2.66	22.73	95	0.0345	USGS	Whole rock	Gabbro chilled rim	do.	22°28′	44°34′
156b	458±15	5.87	44.09	93	0.0303	do.	Biotite	Gabbro	do.	22°28′	44°34′
165	596±12	0.69	8.485	77	0.0410	do.	Hornblende with 20% impurities	Quartz monzonite	do.	21°15′	43°57′
		0.71	8.664	87							
168a	778±16	0.090	1.530	72	0.0565	do.	Whole rock	Troctolite	do.	20°32′	42°32′
		0.092	1.538	72							
168b	710±16	0.092	1.418	63	0.0506	do.	Whole rock	Syenite	do.	20°32′	42°32′
		0.096	1.421	70							
169	539±20	0.38	4.034	29	0.0365	do.	Plagioclase and quartz	Gneiss	do.	20°58′	43°49′
		0.36	4.022	31							
173	826±16	4.18	74.99	98	0.0608	do.	Biotite with 10% impurities	Diorite?	do.	20°17′	42°08′
		4.21	77.31	97							
173a	711±30	0.39	5.762	27	0.0506	do.	Hornblende	do.	do.	20°17′	42°08′
		0.36	5.564	24							
175	484±10	0.12	1.119	78	0.0323	do.	Whole rock	Leucogabbro	do.	20°16′	42°28′
		0.11	1.097	79							
180a	598±12	5.11	63.07	99	0.0412	do.	Biotite	Granite	do.	23°58′	45°01′
		5.03	61.51	99							
180b	584±12	6.48	77.00	99	0.0401	do.	Biotite	do.	do.	23°58′	45°01′
		6.40	77.17	99							
181	597±12	6.49	80.17	99	0.0411	do.	Biotite	Granodiorite	do.	23°58′	45°05′
		6.54	79.67	99							
183	597±12	7.75	94.63	99	0.0411	do.	Biotite	do.	do.	23°41′	45°08′
		7.81	96.41	99							

Footnotes at end of table.

TABLE 8.—*K-Ar ages of Precambrian crystalline rocks of Saudi Arabia*—Continued

Sample (location given on pl. 1)	Age (m.y.)	K (percent)	$^{40}Ar \times 10^{-10}$ (moles/g)	^{40}Ar (percent)	$^{40}Ar/^{40}K$	Analyzed by	Material analyzed	Rock	Collected by	Location	
										Lat N.	Long E.
184	583±12	6.51	77.71	98	0.0400	do.	Impure biotite	do.	do.	23°53′	45°07′
		6.51	77.62	98							
	546±5	0.50	5.580	89	0.0370	do.	Hornblende	Granite	do.	23°53′	45°07′
		0.51	5.580	89							
187	589±12	7.88	95.88	99	0.0405	do.	Biotite	do.	do.	23°01′	45°29′
		7.97	95.57	99							
188	619±12	5.27	68.69	99	0.0429	do.	Biotite	do.	do.	23°01′	45°33′
		5.40	67.94	99							
	629±12	1.38	18.04	95	0.0437	do.	Hornblende	do.	do.	23°01′	45°33′
		1.40	18.23	98							
189	632±12	4.96	63.87	97	0.0440	do.	Biotite with minor hornblende	Quartz diorite	do.	22°36′	45°07′
		4.92	65.79	99							
	611±12	0.75	9.418	92	0.0422	do.	Hornblende	do.	do.	22°36′	45°07′
		0.74	9.373	92							
190	759±20	7.41	123.1	98	0.0548	Geochron	Biotite	Granite	Trent	19°55′	41°33′
		7.55	121.6	98							
191a	646±12	0.86	11.62	89	0.0451	Isotopes	Hornblende with 10% impurities	Granite gneiss	Brown	19°53′	41°37′
		0.87	11.69	80							
191b	759±31	0.931	15.71	91	0.0548	Geochron	Hornblende	do.	do.	19°53′	41°37′
		0.978	15.54	93							
	694±14	1.03	15.09	98	0.0492	Istopes	Hornblende with 20% impurities	do.	do.	19°53′	41°37′
		1.01	14.88	97							
192	607±12	0.88	10.88	96	0.0419	do.	Hornblende	Gneiss	do.	19°52′	41°43′
		0.88	11.15	97							
194	676±28	0.408	5.830	84	0.0476	Geochron	Plagioclase	Quartz diorite	do.	19°35′	41°53′
		0.398	5.630	82							
213a	578±12	0.10	1.214	82	0.0396	Isotopes	Whole rock	Gabbro	do.	19°09′	43°48′
		0.10	1.148	60							
213b	516±10	0.084	0.8735	77	0.0347	do.	do.	do.	do.	19°09′	43°48′
		0.083	0.8548	77							
219a	656±14	0.090	1.319	87	0.0460	do.	do.	Norite	do.	18°45′	42°53′
		0.102	1.318	79							
219b	484±10	0.15	1.443	86	0.0323	do.	do.	do.	do.	18°45′	42°53′
		0.15	1.448	83							
221a	494±12	0.073	0.7258	88	0.0330	do.	do.	do.	do.	18°56′	43°02′
		0.070	0.6820	57							
221b	422±8	0.12	0.9806	92	0.0276	do.	do.	do.	do.	18°56′	43°02′
		0.12	0.9967	92							
225a	655±12	7.14	95.38	99	0.0458	do.	Biotite	Diorite	do.	18°13′	42°32′
		6.98	97.80	98							
	615±12	0.98	12.73	91	0.0425	do.	Hornblende	do.	do.	18°13′	42°32′
		1.02	12.67	92							
225b	686±14	4.86	68.34	98	0.0485	do.	Biotite with 20% impurities	do.	do.	18°13′	43°32′
		4.70	70.03	98							
228a	649±23	6.72	90.83	97	0.0453	USGS	Biotite	Gabbro	do.	18°24′	42°42′
		6.70									
228b	615±12	8.50	106.9	93	0.0426	Isotopes	Muscovite	Pegmatite	do.	18°24′	42°42′
		8.49	109.2	94							
229a	588±17	1.970	24.17	95	0.0404	Geochron	Whole rock	(Drill core)	do.	18°08′	44°07′
		2.008	23.82	95							

Footnotes at end of table.

TABLE 8.—*K-Ar ages of Precambrian crystalline rocks of Saudi Arabia*—Continued

Sample (location given on pl. 1)	Age (m.y.)	K (percent)	$^{40}Ar \times 10^{-10}$ (moles/g)	^{40}Ar (percent)	$^{40}Ar/^{40}K$	Analyzed by	Material analyzed	Rock	Collected by	Location	
										Lat N.	Long E.
229b	577±16	2.17	25.40	94	0.0395	do.	do.	Andesite (drill core)	do.	18°08′	44°07′
		2.13	25.27	90							
229c	572±15	2.15	24.37	94	0.0391	do.	do.	do.	do.	18°08′	44°07′
		2.07	24.92	94							
229d	571±15	2.61	30.80	94	0.0390	do.	do.	do.	do.	18°08′	44°07′
		2.63	30.25	93							
229e	595±18	2.179	26.87	76	0.0409	do.	do.	do.	do.	18°08′	44°07′
		2.194	26.57	83							
230	544±15	3.282	36.18	90	0.0369	do.	do.	Andesite	Overstreet	18°24′	44°11′
		3.192	35.18	85							
231a	519±15	3.608	36.65	93	0.0350	do.	do.	do.	do.	18°22′	44°14′
		3.503	37.56	93							
231b	579±22	0.485	5.454	68	0.0396	do.	do.	do.	do.	18°22′	44°14′
		0.450	5.604	67							
232	575±15	2.232	25.57	83	0.0393	do.	do.	do.	do.	18°20′	44°15′
		2.204	26.52	87							
234	600±24	1.087	13.09	83	0.0414	do.	do.	Diorite	do.	18°06′	44°15′
		1.015	12.86	83							
236	565±16	3.624	42.48	96	0.0385	do.	do.	Felsite dike	do.	18°07′	44°15′
		3.701	41.73	95							

Constants, $^{40}K\lambda\epsilon = 0.581 \times 10^{-10}$/yr. $\lambda\beta = 4.962 \times 10^{-10}$/yr. Atomic abundance, $^{40}K = 1.167 \times 10^{-4}$.

[1] USGS analysts R.F. Marvin, H.H. Mehnert, and Violet Merritt.
[2] Identified by George Phair.
[3] Geochron Laboratories, Inc., Cambridge, Mass.
[4] Isotopes, Inc., later Teledyne Isotopes, Westwood, N.J.

zircons were palingenetically new—the Ablah and culminant orogenies at 797–763 m.y. and 660–666 m.y. (Cooper and others, 1979). Also, in recent years the French (BRGM) have made numerous analyses (more than 360 samples) in their laboratory at Orleans (Baubron and others, 1976). Likewise, analyses have been reported from the University of Leeds (Kroner and others, 1979) and at the Department of Geology, Nottingham, and the Institute of Geological Sciences, London (Duyverman and others, 1982).

CRUSTAL HISTORY OF THE PRECAMBRIAN SHIELD

GENERAL STATEMENT

The evolutionary history of the Precambrian Arabian Shield must be evaluated across a structural width of more than 1,000 km, or a total of more than 1,500 km if the Nubian Shield of Egypt and Sudan is included. Across these widths, the crustal rocks of the Arabian Shield and the Nubian Shield are grossly similar in petrology, chemistry, structure, and age. Across both shields, the crustal rocks were made and cratonized in about 450 m.y., from about 1,000 m.y. to about 550 m.y.

No continental crust older than about 1 Ga has been reported in the Arabian Shield despite a concerted effort to find "old" continental crustal rocks. In the easternmost part of the shield, a 2,100-m.y.-old continental crust may be nearby, as recent lead-isotope studies indicate that some of the youthful Precambrian granitoid rocks there contain old leads (Stacey and others, 1981). It is not resolved whether the crustal block of the Ar Rayn region east of the Al Amar-Idsas fault (region E, fig. 16) is actually part of this old crust or whether the old crust is still farther east beneath the Phanerozoic sedimentary rocks.[5]

The shield has been subdivided (fig. 16) on the basis of the early crustal stratigraphic groups, the Baish-Bahah, Jiddah, and Halaban. The actual rock boundaries between these groups are not easily mapped because the overall lithologies of each group are similar. The boundaries in figure 16 are drawn largely along major north-trending structures that bound early crustal volcanic and plutonic rocks of similar age. The north-trending stratigraphic belts are strongly offset by the Najd faults of youngest Precambrian or oldest Cambrian age. The volcanic and plutonic rocks of the late cratonization history are superimposed on the early crustal rocks and, hence, do not affect the subdivisions in figure 16.

The Wādī Bidah region (region B, fig. 16) contains the type reference area of the Baish-Bahah Groups (basaltic assemblage). In the Biljurshī' region (region J, fig. 16), early crustal rocks of the Jiddah Group (andesitic assemblage) are described and dated at between 900 and about 850 m.y. This region also

[5]Since this was written, evidence for original emplacement in early Proterozoic time has been established at about 1,630 m.y. ago, with subsequent metamorphism or remobilization at about 660 Ma (see Stacey and Hedge, 1984). We consider the anorthosite at Jabal Mahail east of Jabal Khidā' to be original crust surviving later orogeny.

contains the type locality of a younger group, the Ablah Group, that is dated at between 800? and about 750 m.y. The type area for the Halaban Group is centered around Ḩalabān in region TN (fig. 16). Correlatives of the Halaban rocks are well described as the Hulayfah Group in region HN in the Nuqrah quadrangle (Delfour, 1977) and as the Halaban Group in region TC in the Bi'r Juqjuq quadrangle. The Tathlīth regions, TN, TC, and TS, and the northeast region, NE, are largely underlain by crust of Halaban age about 800 to 725 m.y. old, and their western boundary is the long serpentinite fault zone of Hulayfah-Ad Dafinah-Nabitah-Hamdah. Regions HS, HC, and HN form a western belt that at least in large part, perhaps entirely, consists of Halaban crustal rocks.

The early crustal rocks in the western and northern regions have not been named consistently in the literature or well dated. The initial type area of the Jiddah Group is in the vicinity of the townsite of Jiddah, and the available dates suggest that regions WS, WC. and perhaps WN may be underlain by crustal rocks of Jiddah age. A Jiddah age is not denied by the available dates from the Eastern Desert of Egypt (Hashad, 1980), which was an integral part of the Arabian Shield. Region NN is highly faulted by the convergence of the Najd fault system, and, for the time being, the early crust of this northern Najd fault region (NN) and of the northern region (N) is also considered Jiddah age. Region E, east of the Al Amar-Idsas fault, has been most commonly mapped as consisting of Halaban rocks, but it may be older, as suggested earlier in this chapter.

The primary crustal rocks of the shield, that is, the first formed rocks or initial crustal rock at any given locality in the shield, consist of metavolcanic and metasedimentary rocks of a basaltic assemblage and an andesitic assemblage and of plutonic rocks of a dioritic suite; in addition, subordinate tectonic remnants of ophiolitic rocks are scattered in linear belts throughout much of the shield. These rock groupings are based on petrology, petrography, and chemistry (Greenwood and others, 1976; Delfour, 1979b; Dodge and others, 1979) and on Rb-Sr and Pb isotopic studies (Baubron and others, 1976; Fleck and others, 1980; Stacey and others, 1981). Most of the rocks are of the andesitic assemblage and dioritic suite that formed in intraoceanic island arcs as volcanic-magmatic arcs. The basaltic assemblage of the Baish-Bahah Group as sampled in the Wādī Bidah area has a distinctly more tholeiitic composition than the andesitic-assemblage rocks and may have an oceanic crust affinity. More likely the Baish-Bahah rocks are simply an early and basal, more tholeiitic part of the Jiddah andesitic assemblage and of Jiddah age because the basaltic assemblage rocks across regions J and B (fig. 16) are interspersed with andesitic-assemblage rock of the Jiddah Group and dioritic-suite rock that consistently date between 900 and 800 m.y.

The problem of the age and origin of the Baish-Bahah rock clearly points out the fact that the study of the Arabian Shield has barely begun to decipher individual volcanic-magmatic arcs as well as other specific constructional blocks that form the composite early crust as it is known today. Each of the early stratigraphic groups is broadly bounded by a meaningful age range, but each likely consists of more than a single constructional block within that age range.

The following early and late crustal history of the shield outlines one possible sequence of events that in each event might be expected to be much more complex than described. This crustal history has been summarized in a review paper by Schmidt and Brown (1982).

EARLY CRUSTAL HISTORY

The early, primary crust of the Saudi Arabian Shield is a composite of several intraoceanic island arcs and subordinate remnants of oceanic crust (ophiolite). These primary constructional blocks have been combined at different times in different places during several subduction and collisional events from after 900 to about 650 m.y. Especially the older constructional blocks have been tectonized, and the combined crust has been tectonically and magmatically thickened during these collisional events. Throughout most parts of the shield, compressional structures are consistently north-trending, and it is presumed that the original island arcs trended generally northward and that subduction may have been both westward and eastward under different arcs at different times. Deep erosion during the late crustal history, discussed below, means that, for the most part, we see today the deep magmatic parts of the volcanic-magmatic arcs. Most of the metavolcanic and metasedimentary rocks exposed adjacent to these deeply eroded magmatic arcs were originally deposited marginally to the volcanic-magmatic arcs. Therefore, the early layered rocks exposed throughout the shield contain a large proportion of pyroclastic and immature clastic metasedimentary rocks derived from the island-arc volcanic rocks. The original andesitic volcanic piles in the upper part of the magmatic arcs are less commonly preserved, except where they have been thrust into adjacent basins prior to the deep erosion of the volcanic arc.

The early, primary crust consists predominantly of an andesitic assemblage of metavolcanic and metasedimentary rocks and comagmatic plutonic equivalents of the dioritic suite. These primary crustal rocks have been well dated in the southern part of the shield at

between about 900 and 700 m.y. (Fleck and others, 1980). In a broad western belt about 250 km wide between Al Līth and Qal'at Bīshah (regions B and J, fig. 16), rocks of the dioritic suite as well as those of the andesitic assemblage are between 900 and 800 Ma and are mapped mostly as Jiddah Group as characterized in the Biljurshī' quadrangle (Greenwood, 1975b). Rocks of similar composition are dated at between 800 and 700 m.y. in a broad eastern belt, about 200 km wide, between Qal'at Bīshah and the eastern edge of the exposed shield (regions HS and TS, fig 16) and are mapped mostly as Halaban rocks as characterized in the Bi'r Juqjuq quadrangle (Hadley, 1976). Both of these belts, one of early primary crust of Jiddah age and the other of late primary crust of Halaban age, are tectonically complex, and undoubtedly each is composed of more than one constructional block of intraoceanic, island-arc materials.

The Jiddah-age crust in regions B and J can be further subdivided by age along the 42d meridian. To the east of the 42d meridian, dioritic-suite rocks of the An Nimas batholith (fig. 30) are dated at between 850 and 800 m.y. The An Nimas batholithic complex (Anderson, 1977) consists of plutons of diorite, quartz diorite, tonalite, and trondhjemite as well as subordinate gabbro and small screens of metavolcanic rocks. The complex is about 70 km wide and extends 150 km from lat 19°00′ northward to 20°30′ to where it is covered by the Tertiary flood basalt Ḥarrat al Buqūm. The An Nimas batholithic complex is probably the deeply eroded core of a volcanic-magmatic arc and is just one integral constructional block within the Jiddah-age crust. At one locality within the batholithic complex, meta-andesitic and metadacitic rocks are dated at 912±76 m.y. (initial $^{87}Sr/^{86}Sr=0.7024$, Fleck and others, 1980), which is about 60 to 100 m.y. older than the age of the comparable quartz dioritic and trondhjemitic rocks; the 912 m.y. date may be too old and must be substantiated by further study.

To the west of the 42d meridian for about 200 km, the plutonic rocks of the dioritic suite are dated consistently at between 900 and 850 m.y. and are interspersed with andesitic-assemblage rocks mapped as Jiddah Group as represented in the Biljurshī' quadrangle (Greenwood, 1975b) and with basaltic-assemblage rocks mapped as Baish-Bahah Group as represented in the Jabal Ibrāhīm quadrangle (Greenwood, 1976c). The basaltic-assemblage rocks of the Baish-Bahah Group are possibly a more tholeiitic, basal, and immature part of the predominantly calc-alkalic andesitic assemblage of the Jiddah Group rather than remnants of oceanic crust, as has been suggested in the literature. The rocks are folded, faulted, and probably thrust faulted as well. On the west side near Al Līth, metabasalts mapped as Baish Group have been dated at 1,165±110 m.y. (initial $^{87}Sr/^{86}Sr=0.7029$, Hadley and Fleck, 1980a), yet they are intruded by quartz dioritic rocks dated at 895±173 m.y. (initial $^{87}Sr/^{86}Sr=0.7025$). Again, as in the An Nimas batholithic complex, the metavolcanic rocks seem to date too old for the presumably comparable plutonic rocks. An alternative, less likely, explanation is that the volcanic rocks of an older constructional block are tectonically mixed with the Jiddah-age crustal rocks.

The andesitic-assemblage rocks in the vicinity of Jiddah townsite, the original type area for the Jiddah Greenstone, are possibly Jiddah age (as defined in the Biljurshī' quadrangle) on the basis of some dated plutonic rocks (table 6). Fifty to 100 km north of Jiddah and east of Rābigh (region WS, fig. 16), andesitic-assemblage rocks of the Samran Group of Skiba (1980) are calc-alkalic and trend toward a tholeiitic composition (fig. 26*A*). These rocks may be correlated tentatively with those at Jiddah, but ages have not been determined. Still farther northwestward, along the western edge of the shield, ages of early crustal rocks also have not been determined. Support for early crustal rocks of Jiddah age can be extrapolated from dates on the dioritic-suite rocks from the southern part of the Eastern Desert of Egypt where six Rb-Sr whole-rock ages range from 987 to 830 m.y. (Hashad, 1980, p. 41). The areal distribution of these rocks in Egypt extrapolates to Saudi Arabia from south of Yanbu' al Baḥr to north of Al Wajh.

The Halaban-age crust in regions HS and TS (fig. 16) are subdivided structurally by the serpentinite belt of Hulayfah-Ad Dafinah-Nabitah-Hamdah into at least two constructional blocks. The belt of Halaban crust west of the serpentinite belt, region HS, contains andesitic-assemblage rocks that are dated at between 786±96 m.y. (initial $^{87}Sr/^{86}Sr=0.7025$) and 746±16 m.y. (initial $^{87}Sr/^{86}Sr=0.7021$) and quartz diorite to tonalite plutonic rocks of the dioritic suite that are dated at 723±107 (initial $^{87}Sr/^{86}Sr=0.7025$) and 724±93 m.y. (initial $^{87}Sr/^{86}Sr=0.7027$) (Fleck and others, 1980). The belt of Halaban east of the serpentinite belt (region TS) contains Halaban andesitic-assemblage and dioritic-suite rocks that have not been satisfactorily dated but suggest ages of between 800 and 700 m.y. These two belts of Halaban-age crust can be extended, using the serpentinite belt, northward across the shield through the type area of the Hulayfah Group (Halaban equivalent; Delfour, 1977) and through the Halaban type area in the vicinity of Ḥalabān Ridge.

In summary, the early, primary crust of the shield is a combination of several constructional blocks, of which each is an intraoceanic island arc consisting of an andesitic assemblage of metavolcanic rocks and a

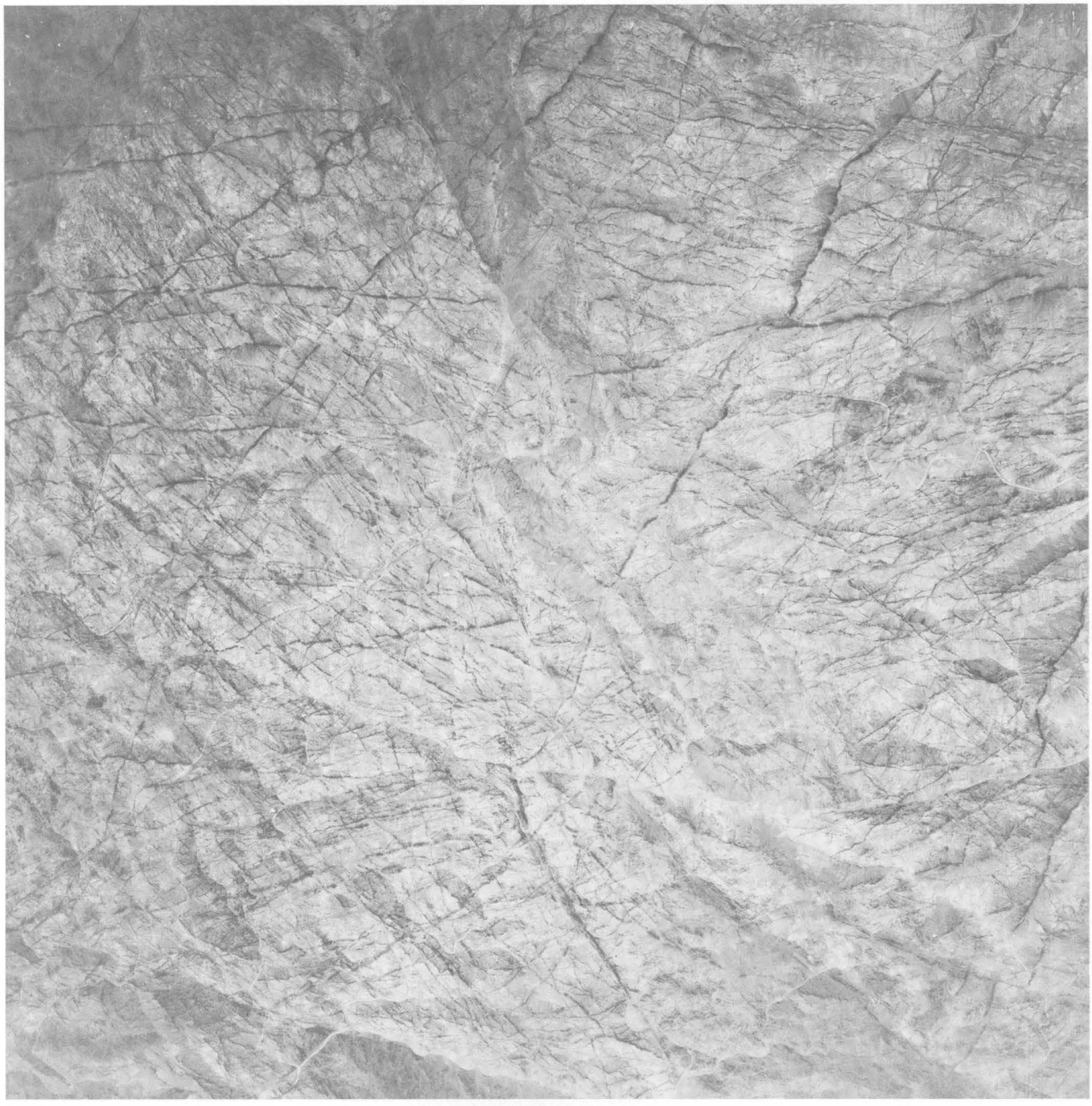

FIGURE 30.—Vertical aerial photograph of the northern portion of the An Nimas batholith, representative parts of which are dated at 816±4 m.y. (Cooper and others, 1979) and 837±50 m.y. (Fleck and others, 1980). The syntectonic batholith ranges in composition from diorite to tonalite, with much interlayered quartz diorite. The darker areas represent diorite or mixed rocks. The terrain is crisscrossed with metabasalt and meta-andesite dikes following lineations—faults and joints from at least two and possibly three orogenic episodes. At least some conjugate dikes were formed during the Najd orogeny. (Geology after Green, 1983.)

dioritic suite of plutonic rocks. For the convenience of discussion, these rocks are lumped into a primary crust of Jiddah age (900 to 800 m.y.) and a primary crust of Halaban age (800 to 700 m.y.).

EARLY COLLISIONAL OROGENY

In the southern part of the shield, several widely spaced gneiss domes of tonalitic-trondhjemitic ortho-

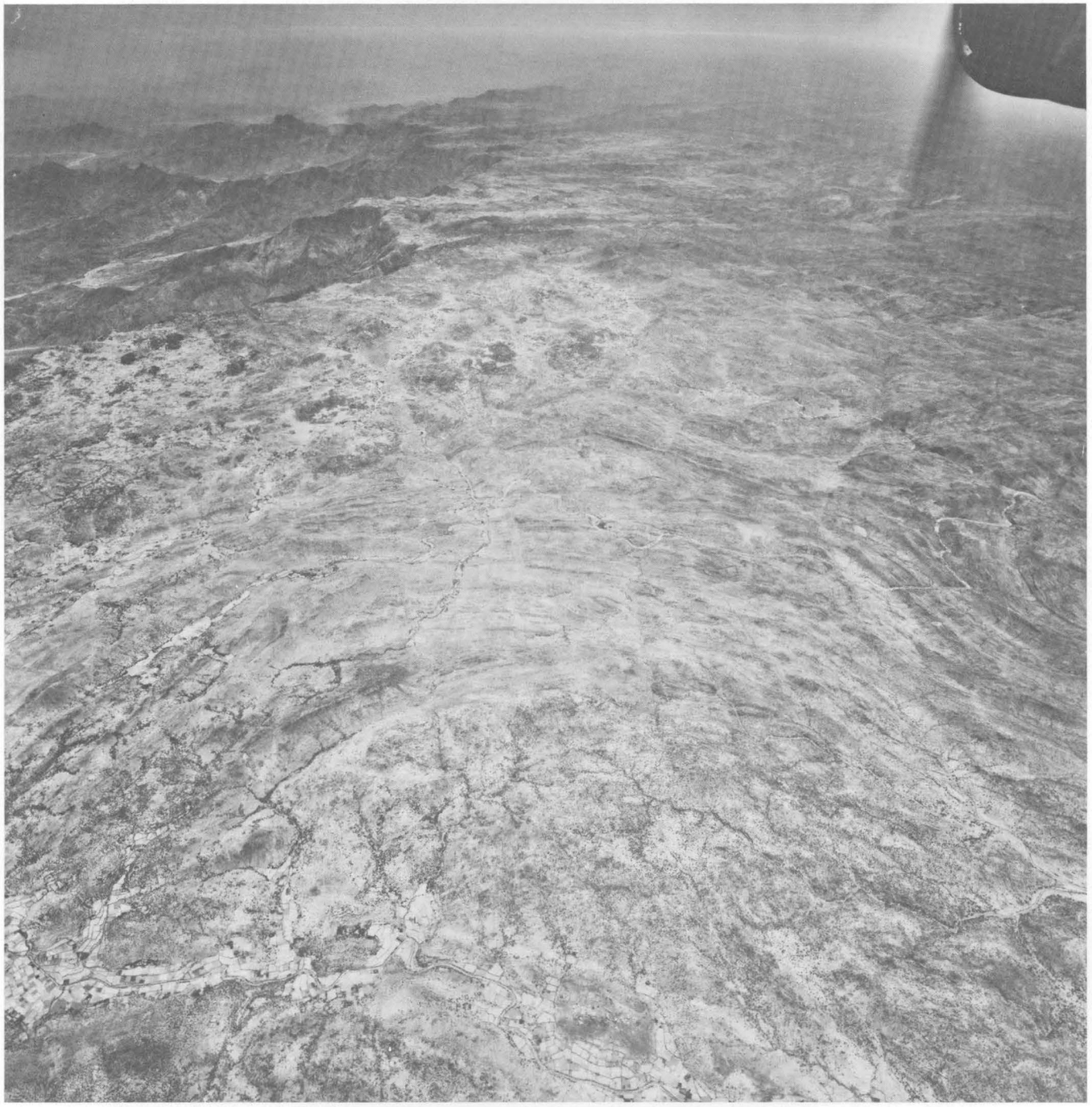

FIGURE 31.—Oblique aerial view to the northwest of orthogneiss dome containing enfolded amygdaloidal metabasalt flows of the Baish Group. K-Ar age of hornblende in the gneiss yielded a K-Ar age estimate of 759±31 m.y. (table 8, sample 191b), which compares to a total fusion, $^{40}Ar/^{39}Ar$ age of 782±35 m.y. (Fleck and others, 1976.) The town of Biljurshī' rests on the northwestern flank of the arch, which includes quartz diorite (K-Ar age of 759±20 m.y.; table 8, sample 190) and overlooks the 'Asīr escarpment. The Biljurshī' intrusive yielded Rb/Sr isochron ages of 848±282 m.y. and 890±87 m.y. (Fleck and others, 1980, p. 19). Thus the dome represents rejuvenation of quartz diorite estimated to have first solidified at 890±67 Ma. (Geology after Greenwood, 1975b.)

gneisses are indicative of crustal heating, tectonism, metamorphism, and the gravitational rise of less dense plutonic parts of the primary crust of Jiddah age (fig. 31). Syntectonic intrusion of granodioritic batholiths accompanied the rise of orthogneisses and represents the first large volumes of potassic plutonic rocks in the

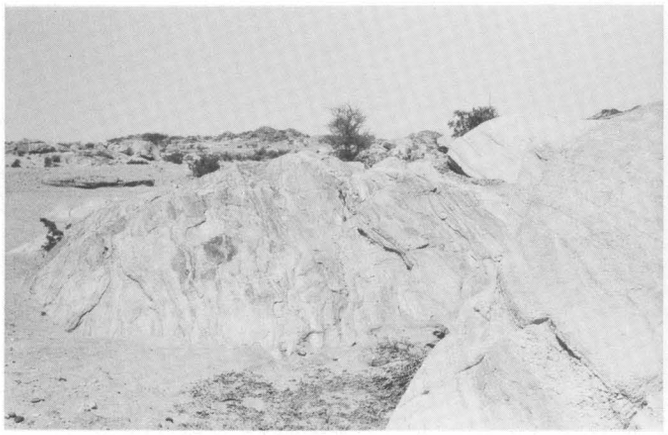

A

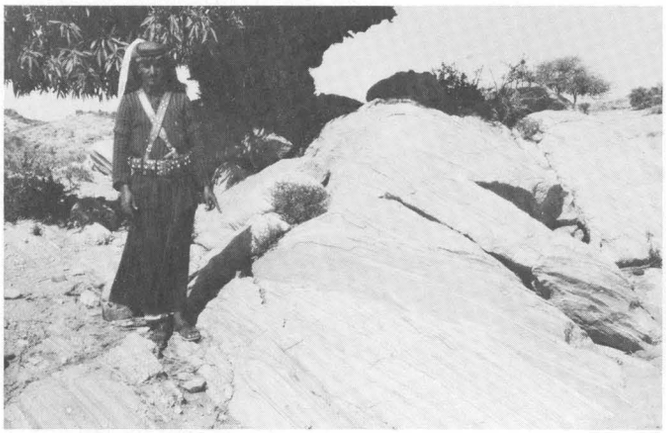

B

C

FIGURE 32.—Schistose gneiss at Wādī Dhuqiyah 65 km southeast of Aṭ Ṭā'if. The lineation dips east. *A*, Biotite albite xenolithic fragment above pegmatite stringers; *B*, Detailed drag folds in the gneissose limestone, N. 20° E. sinistral movement; *C*, Gneiss considered to have been formed by the doming at the end of the Ablah cycle (near ±760 m.y. ago), the crenulation later during Najd time (about ±570 m.y. ago).

early crust at any locality. The best documented example is the Baqarah gneiss dome in the southern end of the An Nimas batholith, where tonalitic and trondhjemitic orthogneisses are accompanied by synkinematic granodioritic gneissic batholithic rocks that are dated at 763±53 m.y. (initial $^{87}Sr/^{86}Sr=0.7032$; Fleck and others, 1980) and 763±4 m.y. by the U-Pb zircon method (Cooper and others, 1979). A similar gneiss domal complex at the northern end of the An Nimas batholith gives less reliable K-Ar dates of between 740 and 711 m.y. (sample 171, table 6; sample 173, table 8). Interpretation suggests that while the early, primary, Halaban-age crust was forming somewhere to the east, the older Jiddah-age crust was subjected to combining and consolidation by early collisional tectonism involving tectonic and magmatic crustal thickening, gneiss doming, and granodiorite intrusion.

The orogenic mountains were eroded and resulted in deposition of molassic sedimentary rocks that along the west side of the An Nimas batholith are mapped as the metasedimentary rocks of the Ablah Group. These voluminous graywacke deposits of the Ablah Group are commonly quartz bearing and even contain some quartz sandstones, indicating derivation from large volumes of quartz diorite, tonalite, and trondhjemite in the Jiddah crust. These quartzose sedimentary rocks, together with thick marble deposits, indicate deposition from a deeply eroded crust and in a semistable basin, and this is indicative of a nearly continental environment. However, the generally low-K_2O, calc-alkalic volcanism associated with the Ablah rocks indicates that the continental crust had not uniformly established full thickness.

Other gneiss domes and molassic metasedimentary rocks superposed elsewhere on Jiddah-age crust in the western shield may be related to the same early collisional orogeny and may be correlatives of the Baqarah orthogneiss and Ablah Group rocks or may represent other early collisional orogenies of slightly different age and place. Another example is the metasedimentary rocks mapped as Ablah Group west of a large gneiss domal complex in the adjoining quadrangle of Jabal 'Afaf (Hadley and Fleck, 1980b) and Jabal Ibrāhīm (Greenwood 1975c) (fig. 32). The Fatimah Group and abundant adjacent orthogneisses and intrusive granodiorites, dated at the Jiddah airport at 763±159 m.y. (initial $^{87}Sr/^{86}Sr=0.7026$; Fleck and others, 1980), are of Ablah age and may represent the same or perhaps a different early collisional orogeny.

LATE CRUSTAL HISTORY

CULMINANT OROGENY AND POSTTECTONIC GRANITES

The late crustal history of the Arabian Shield began sometime after 700 m.y. ago and involved the final

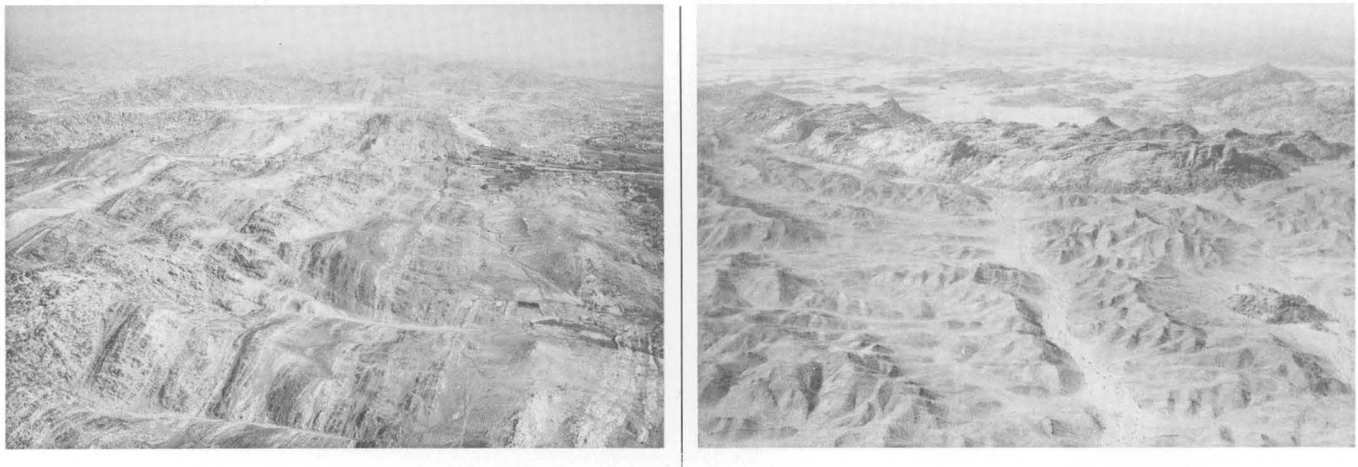

A *B*

FIGURE 33.—*A*, Aerial view south of the eastern edge of the Khamis Mushayt gneiss dome flanked by paragneiss which in turn has subsequently been intruded by the monzogranite at Tindahah. The Khamis Mushayt gneiss dome of 664±9 m.y. (Rb-Sr age) has metamorphosed volcaniclastic sediment of Halaban age (785–665 m.y.) or possibly of Jiddah age (850–780 m.y.). Subsequent to the doming, the Tindahah monzogranite batholith was posttectonically intruded on the eastern flank (K-Ar cooling age about 563 m.y.) (Fleck and others, 1976; Fleck and others, 1980). The village of Tindahah is in middle distance on right. *B*. Jabal al Hidab at lat 19°40′ N., long 42°45′ E. Alkalic red granite forming hills in the middle distance is intruded into paragneiss and amphibolite gneiss dome composed of Halaban rocks in a syntectonic dome formed during culminant orogeny. The alkalic granite is posttectonic, with a biotite K-Ar age of 595±9 m.y. (Fleck and others, 1976).

combining, consolidation, and cratonization of the shield as a whole. The major orogeny associated with this late crustal history is rightly called the culminant orogeny; it was the ultimate orogeny involved in the cratonization of the entire shield. The late crustal history is characterized by many gneiss domes (gneiss antiforms), granodioritic batholiths, and granite plutons that in general became progressively more potassic with decreasing age (fig. 33). The syntectonic and posttectonic granodioritic and granitic rocks constitute about 50 percent of the eastern part of the shield and diminish in abundance westward across the western shield.

The culminant orogeny probably began slightly before 650 m.y. and extended to about 620 m.y. The histograms of rock ages in figure 34 show a distinct secondary mode between 650 and 620 m.y. ago. One late, syntectonic granodiorite batholith associated with the large gneiss dome east of Qal'at Bīshah in the Jabal al Qarah quadrangle (Schmidt, 1981a) gives a high-quality Rb-Sr isochron age of 623±18 m.y. (initial $^{87}Sr/^{86}Sr=0.7033$; Fleck and others, 1980).

During the culminant orogeny, widespread crustal heating caused amphibolite-facies metamorphism in the primary crustal rocks at intermediate crustal depths. Under these conditions, large, low-density bodies of trondhjemite and tonalite became gravitationally unstable adjacent to denser diorites and meta-andesitic–assemblage rocks, and the trondhjemites and some tonalites rose as orthogneisses in elongated gneiss domes along north-trending axes. Rb-Sr dating of these massive orthogneisses at amphibolite facies indicates that many of them retained their original plutonic age (Halaban or Jiddah age). Large volumes of granodioritic magma with associated granodioritic migmatite accompanied or shortly followed the rise of the orthogneiss and was emplaced at about the same crustal level as the gneiss domes. The granodioritic magma, however, originated presumably from a crustal source that was deeper than the crustal level from which the trondhjemite orthogneiss rose because the orthogneisses rarely show but the slightest evidence of having been partially melted. The granodiorite magma represents partial melting of deep, lower crustal rocks of Halaban and Jiddah age, because the initial strontium ratios (for example, 0.7033) of the granodiorite would be expected from primitive crustal rocks whose ^{87}Rb had evolved over 100 m.y. ago or at most less than several hundred million years.

The very widespread, culminant orogeny is believed to have been caused by collision between the Halaban crust and an older continental crust at the east edge of—or somewhat farther east of—the exposed shield. Such collisional orogeny resulted in the final combining of the various constructional blocks of the primary crust (of Jiddah and Halaban age) and in the final

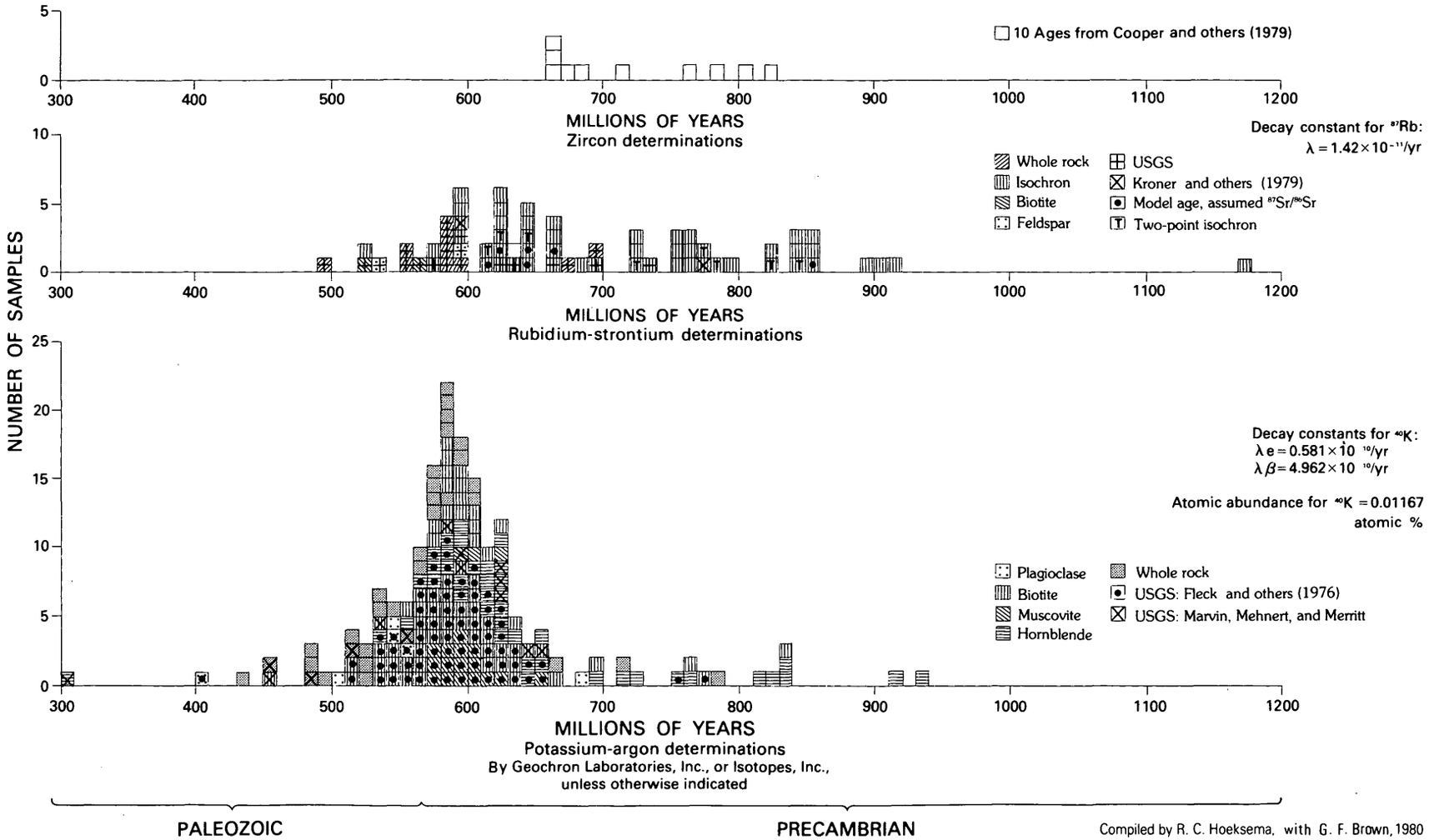

FIGURE 34.—Histograms showing results of geochronologic analyses of Paleozoic and Precambrian rocks.

tectonic thickening of the combined crust, such that potassic granitic magma was produced in the lower crust and was intruded at shallow crustal levels in both syntectonic and posttectonic settings.

Production of granitic magma was greatest near the collisional zone in the eastern shield and along other older structures where tectonic thickening was concentrated during the culminant orogeny. Examples are along the Hulayfah-Ad Dafinah-Nabitah-Hamdah serpentinite belt and also, perhaps, in the Egyptian crust where late granitic intrusives are particularly abundant.

The large volume of posttectonic granite was intruded mostly in circular or, more commonly, elliptical plutons oriented northward parallel to the old structural grain. A major mode for Rb-Sr ages of shield rocks suggests maximum emplacement of posttectonic granites at about 600 m.y. (fig. 34). The potassic magma of about 600 m.y. was intruded commonly as ring-structured plutons near the paleosurface and was voluminously erupted at the surface as rhyolitic rocks of the Shammar Group. Much of this granitic rock is alkalic and has a peralkalic or peraluminous composition. It was most abundantly intruded in the northernmost part of the shield, as at Jabal Aja' and Jabal Salmá, and in a zone about 100 km wide to the west of the Hulayfah-Ad Dafinah-Nabitah-Hamdah serpentinite belt (Stoeser and Elliott, 1980), where prior tectonic thickening of the crust during the culminant orogeny may have been particularly significant. In contrast, only small volumes of alkalic granite are found dispersed elsewhere across the shield.

The posttectonic granitic magma was bimodal with associated gabbroic magma deep in the crust. Gabbro, commonly fractionated and leucocratic, was intruded at high crustal levels as circular, layered plutons that are conspicuous but not abundant in the eastern half of the shield. Some circular, ring-structured granite plutons (the deep roots of calderas) contain partial layers and pods of gabbro and diabase (Schmidt, 1980), well indicative of bimodal magmatism.

The posttectonic granites seem to be partial melts of primitive lower crustal rocks (Dodge, 1979; Stoeser and Elliott, 1980) that fractionated in time with increased K_2O content. The bimodal gabbroic magmas, originating in the mantle, likewise fractionated within the crust and were a major contributor of heat to the crust during the late crustal history of the shield. The two magmas did not mix, except subordinately where they mutually produced a few intrusive breccias of mixed rhyolite-diabase and a few intrusive hybrid rocks of metasomatized rhyolite or diabase (Schmidt, 1981b).

The major mountain building of the culminant orogeny resulted in extensive erosion and deposition of molassic deposits of the Murdama Group. The basal Murdama at any given locality contains granitic boulders and cobbles, indicating that everywhere Murdama deposition followed some early granite plutonism. Some granite plutons also intrude the Murdama. The Murdama sedimentary deposits in many places contain a few silicic volcanic units, many of which may have been ignimbrites that flowed considerable distances from late, eruptive granite plutons.

The Murdama molassic deposits filled basins between orogenic mountains, and as the mountains were eroded the Murdama sediments transgressed across them. The thickest and most extensive deposits are in the eastern part of the shield. Extensive but generally thinner deposits are in the western shield. Only remnants of the youngest transgressive basal Murdama appear in the wide zone along the Hulayfah-Ad Dafinah-Nabitah-Hamdah serpentinite belt. This emphasizes that the highest orogenic mountains, along zones of most intensive orogeny, were adjacent to this serpentinite belt and adjacent to the Al Amar-Idsas fault zone. Gneiss domes, which are the roots of the orogenic mountains, are particularly abundant on either side of the serpentinite belt. Along the margins of the domes, only small, thin, remnant, conglomeratic deposits of Murdama are found. These deposits are commonly younger than the youngest granite plutons in the area; Murdama deposits within the orogenic mountains were scant and late. Thick marble deposits are found in thick sections of the Murdama Group that accumulated in basins adjacent to the orogenic mountains, and are indicative of an already stabilized continental crust.

The quartz-feldspar-biotite and quartz-sericite-chlorite schists of the Abt Formation (and the Ar Ridaniyah Formation) are most probably of Murdama age and constitute a thick, fine-grained, eastern facies of the Murdama Group. The Abt sedimentary rocks were subjected to especially intense late tectonism in the vicinity of the Al Amar-Idsas fault. Alternatively, the Abt Schist may be a continental-marginal sedimentary rock that was associated with the crustal block east of the Al Amar-Idsas fault (region E, fig. 16) and was tectonically emplaced during the collision between this east block and the Halaban crust (fig. 35).

The large batholithic complex in the Ad Dawādimī area is composed largely of granodioritic and subordinate granitic rocks that intrude the Abt deposits (Al-Shanti, 1976). It has been suggested that the highly tectonized and metamorphosed Abt Schist (and the Ar Ridaniyah Formation, as well) is older than Murdama and the culminant orogeny. However, 100 km northeast, similar syntectonic granodioritic batholithic rocks intrude Murdama deposits. It seems likely that either the Murdama and Abt metasedimentary rocks of this

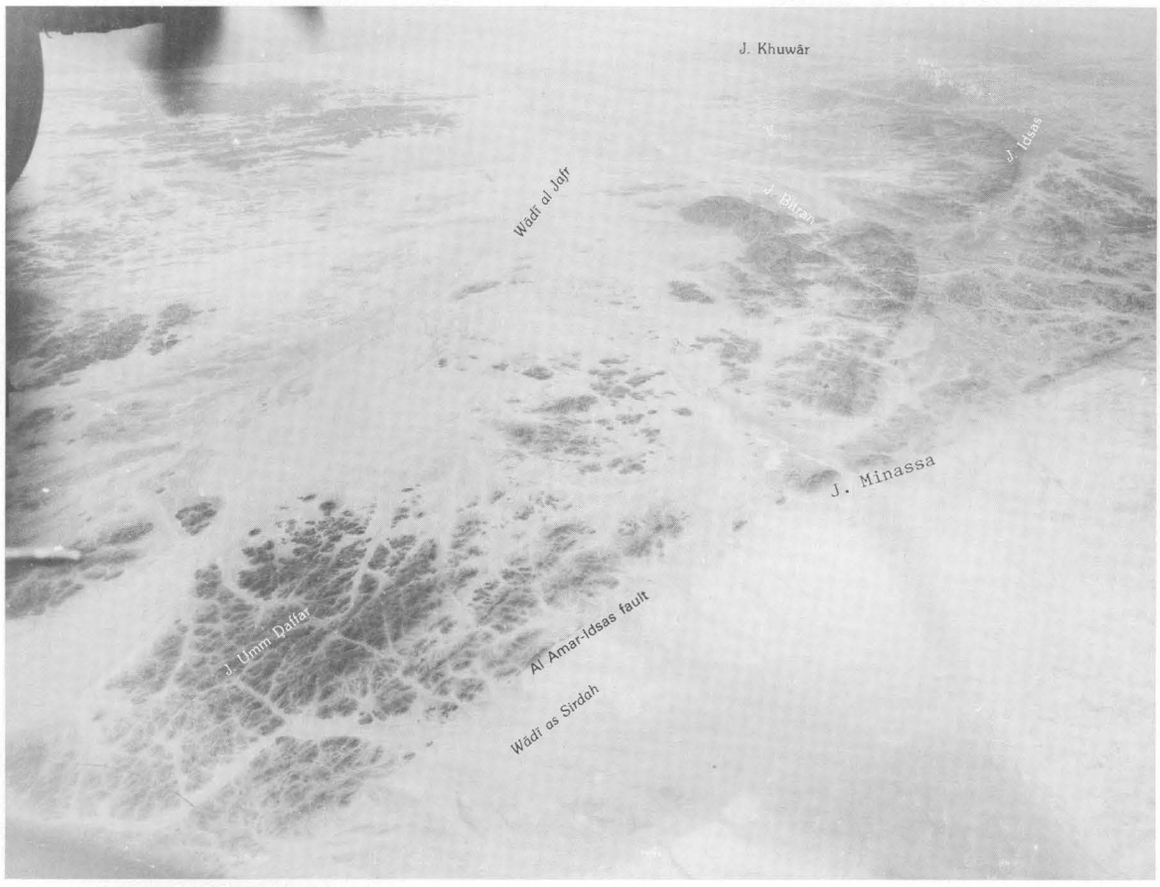

FIGURE 35.—Oblique aerial photograph of view to the southeast from lat 23°05′ N., long 45°05′ E. near the east edge of the shield. The Al Amar-Idsas fault bounds the east side of the Wādī as Sirdah plain, which is underlain by the Abt Schist (pl .1). The lobate overthrust fault front is apparent along the southeastern extension. An ophiolite melange marks the fault zone, including a southern bifurcation south of Jabal Minassa. The outcrops east of the fault zone make up the Ar Rayn granitoid province of figure 16 (Al-Shanti and Gass, 1983) and include volcanic facies in Jabal Umm Ḍaffar in left foreground and west of calc-alkaline to alkalic plutonic rocks.

area are of early culminant-orogeny age or the broad area west of the Al Amar-Idsas fault was orogenically active later, possibly as late as 600 m.y. ago or even just prior to the Najd faulting. If the tectonism of the culminant orogeny did persist in some areas to 600 m.y. or slightly later, then the large volumes of granodiorite in the Ad Dawādimī area were unusually late in comparison to the rest of the shield, where posttectonic, high-K_2O granites were being intruded at that time. We cannot determine the time variability of the culminant orogeny because Murdama deposition was not everywhere the same age but was within a timespan of about 50 m.y.

Tectonic remnants of ultramafic rocks and serpentinite, gabbro, sheeted dike complexes, tholeiitic metabasaltic rocks, and ocean-floor metasedimentary rocks occur in varying combinations in many places in the shield. Many of these have been described as tectonized and deeply eroded ophiolites of either oceanic or back-arc crustal origin (Bakor and others, 1976; Frisch and Al-Shanti, 1977; Delfour, 1979b; Al-Rehaili and Warden, 1980).

Remnants of ophiolites are to be expected, considering that most or all of the shield is a composite of many primary constructional blocks originally separated by oceanic crust. Further, it is likely that the different dismembered ophiolites in different parts of the shield are of different ages because different constructional blocks were combined at different times and involved different oceanic crusts and (or) back-arc basinal crusts.

Most of the exposed ophiolites of the shield are small remnants because erosion has been deep and only those remnants that had been structurally placed deep in the crust by tectonism have been preserved. All ophiolites should be associated with specific sutures between different constructional blocks, but the direct relationship is obscured in many places.

The Hulayfah-Ad Dafinah-Nabitah-Hamdah serpentinite belt is a highly tectonized zone that was especially orogenically active during the culminant orogeny. This deeply eroded belt is most likely a suture zone in which in most places mobile serpentine is the only remaining component of the former oceanic crust (Frisch and Al-Shanti, 1977; Schmidt and others, 1979). The much better preserved dismembered ophiolite at Bi'r Umq west of the serpentinite belt in the central shield may be an ophiolite that was obducted (Al-Rehaili and Warden, 1980) before the suture closed during the collisional, culminant orogeny. The broad zone of major faults containing much tectonized serpentinite in the vicinity of—and within—the Al Amar-Idsas fault zone is also very likely a major tectonized suture zone (Al-Shanti and Mitchell, 1976; Schmidt and others, 1979).

NAJD FAULTING EVENT

The Najd faulting event or Najd orogeny of Brown (1972) was the final tectonism and final cratonization event of the Arabian Shield. East-west compressional forces acted one last time and the by-then noncompressible, thick, cratonized shield was fractured along a few great shears (fig. 36) rather than by more penetrative internal compression as before. A northwest-trending, left-lateral, transcurrent fault system (Brown and Jackson, 1960; Moore, 1979) prevailed over the conjugate northeast-trending, right-lateral, transcurrent fracturing.

The shield was displaced left laterally more than 250 km (Brown, 1972), mostly along three major northwest-trending fault zones, each 5 to 10 km wide. This major, large fault movement on the Najd fault system is in a region 300 km wide by 1,100 km long, but the effects of the Najd stresses can be found throughout the shield. At least some, and possibly most, of the northeast-trending structures between Jiddah and Wādī Suwass in the Qal'at aş Şawrah quadrangle (regions B, WS, and WC, fig. 16) may be as young as Najd age. Within this large strained region, many older faults were activated and some were rotated toward and into a northwestern direction. These reactivated and rotated older faults give the unwarranted impression that the age of the Najd faulting event began long before 600 m.y., but we cannot agree with this interpretation.

Each of the three major northwest-trending fault zones is in part sinuous, braided, en echelon, and branching, and the whole movement system is convergent to the northwestern part of the shield and into the area of the ancestral Gulf of Suez. The sinuous and branching geometry of the fault zones resulted in a few localized extensional segments consisting of grabens filled with taphrogeosynclinal sedimentary and volcanic rocks of the Jubaylah Group and a few ultracompressional segments in which elongated gneiss antiforms (domes) rose (fig. 37).

The andesitic basalt volcanism of the Jubaylah Group in the taphrograben structures (Delfour, 1970; Hadley, 1974) trends from calc-alkalic to strongly alkalic in composition (figs. 23, 27*B*), similar to some of the volcanism associated with large continental rifts. For the Najd system, however, these are small, localized continental pseudorifts. The Najd "grabens" formed in a crust that was fully continental and along newly formed, deep-crustal shear structures that tapped magma generated in the mantle.

The gneiss antiforms in the few ultracompressional segments of the Najd fault system are exemplified in the Jabal Yafikh quadrangle (Schmidt, 1981b) where trondhjemitic orthogneiss, 3 km wide by more than 60 km long, rose within the fault zone at almandine-amphibolite–facies temperatures. The initial plutonic trondhjemite was part of the primary crust of Halaban age (dated 766±26 m.y., initial $^{87}Sr/^{86}Sr$=0.7030; Kroner and others, 1979; area 6, fig. 16). The trondhjemite of the Halaban crust within the fault zone was heated by an increment of frictional heat within the highly sheared fault zone and was additionally heated in part by mantle-derived magma. The magmatic heat is implied by small synkinematic plutons of alkalic granite that intruded along the margins of the gneiss antiform well within the fault zone. Mantle magmatism is implied by the very abundant (hence, voluminous) diabasic dikes of Najd age that intruded large areas between the major faults, by the mafic volcanism in the Jubaylah Group, and by strong magnetic anomalies over most Najd fault zones. The anomalies may imply the presence of gabbroic intrusions at depth. The Najd-age magmatism was bimodal.

A few dated gabbro plugs and granite plutons within the Najd fault zones and a few dated andesitic basalt flows in the Jubaylah Group average about 530±20 m.y. by the K-Ar whole-rock method. Such a date for the Najd faulting event is too young and may represent crustal cooling after uplift and erosion. A high-quality, whole-rock Rb-Sr isochron of 577±15 m.y. (Baubron and others, 1976, p. 58) on granite is probably only slightly older than the Jubaylah Group, because the granite intrudes the Murdama Group and disconformably underlies the basal Jubaylah conglomerate. The granite date agrees with the suggestion that algal fossils in limestone of the Jubaylah Group are about the age of

FIGURE 36.—Aerial view, looking northwest, of the Najd fault zone southwest of 'Afīf. The infolded beds at near right are believed to be of Jubaylah and Shammar age; Murdama Group clastics at near left are infolded within metaclastic rocks of Halaban age (Letalenet, 1979).

FIGURE 37.—Jabal Adhqān al 'Aṭshān (lat 22°41′ N., long 44°06′ E.). A structure in the northeast flank of a gneiss dome of Najd age. Granite intruded into the Halaban Group, at the southwestern base of the mountain, later sheared in the Najd fault zone near the end of shield cratonization. Aerial view to the northwest.

the Precambrian-Cambrian boundary (about 570 m.y.; Cloud and others, 1979; Binda and Ramsay, 1980). The Jubaylah was folded into asymmetric synclines during the final Najd fault movement, and K-Ar biotite dates averaging about 550 m.y. (table 8) may represent this last spasmodic movement of the cratonization. Minor plugs and sills of gabbro and syenite may be subsequent to last synclinal folding of the Jubaylah, as evidenced by the K-Ar biotite dates. A gabbro plug intruded into the Najd fault zone at Wādī ar Rikā' (lat 28°28′ N., long 44°34′ E.) gave a whole-rock K-Ar age of 513±17 m.y. for the chilled edge of the plug (sample 156a, table 8) and 458±15 m.y. for the deuterically altered core (sample 156b, table 8). Likewise, gabbro and diorite interpreted as a dike or sill at Khashm Qa'in (lat 24°46′ N., long 40°40′ E.) has a possible age of 502–512 m.y. (Delfour, 1981). In the northwestern extension of the Najd fault zone, a quartz syenite plug on the Red Sea coast (lat 27°28′ N., long 35°07′ E.) yielded a whole-rock K-Ar age of 487±17 m.y. (sample 12b, pl. 1, table 8). This is considered a minimum age by the analyst, Richard Marvin (oral commun., 1974). These younger dates are comparable to the youngest K-Ar ages in southwest Jordan (Lenz and others, 1972) and are to be compared with fission track ages from sphene in diorite in southwest Arabia which range from 450 to 576 m.y. and average 510±52 m.y. as analyzed by C.W. Naeser (written commun. to R.G. Coleman, 1969). Taken with Sutter's age estimate of 465 m.y. as the last time the Jubaylah quartz andesite or dacite passed through 100–150 °C, it would appear that the shield went through an epeirogenic epoch toward the end of the Cambrian and early during the Ordovician. At least the northwestern part of the Najd fault system was covered by stable continental quartz sandstones by Late Cambrian time. Nearby in Jordan, trilobites in limestone within the stable sandstones are dated as early Middle Cambrian (Bender, 1975, p. 16).

AGE AND STRONTIUM EVOLUTION

An overview of the evolution of the Arabian Shield in terms of Rb-Sr whole-rock geochronology is succinctly shown in figure 38 (adapted from Fleck and others, 1980). In figure 38, the primary crusts of the several volcanic-magmatic arcs of Baish-Bahah, Jiddah, and Halaban ages are well represented by low initial strontium ratios for the volcanic and plutonic rocks between 900 and 680 m.y. The partial cratonization of Ablah age (early restricted collisional orogeny) is represented by granodioritic rocks between about 775 and 740 m.y. These rocks have initial strontium ratios greater than those of the primary crusts. The final cratonization of the entire shield is represented by granodioritic and granitic rocks between 660 and 580 m.y. These abundant rocks again have initial strontium ratios greater than those of the primary crust.

The granitic rocks of the craton are products of melts of the primary crust in which isotopic strontium decayed within this crust during only 100 to 300 m.y. and resulted in low initial strontium ratios (0.703 to 0.704) in the granitic melts. These low ratios are distinctly crustal (by Arabian Shield standards), but they also indicate that old (greater than 1 Ga) continental basement may not be found in the Arabian Shield, except possibly in the easternmost part.

PALEOZOIC SEDIMENTARY COVER ROCKS AT EDGE OF THE ARABIAN SHIELD

SIQ SANDSTONE

The landward edge of the Arabian Shield is covered by sandstone beds of Cambro-Ordovician age, except for a gap of 130 km along the eastern end of the northern flank, which is occupied by the Great Nefud, and 420 km along the eastern rim, where the Khuff Limestone Formation of Permian age overlaps the shield. Of the rim rocks, the Siq Sandstone in northwest Arabia is probably the oldest. It is a reddish-brown massive and arkosic arenite exposed immediately above the crystalline rocks at Sha'īb as Siq, lat 28°04′ N., long 35°40′ E., where Leopold Kober first saw it in 1910 (Kober, 1919). There the Siq Sandstone is exposed in a 65-m vertical cliff below a thinner section of reddish-brown, somewhat more stratified, flaggy sandstone on

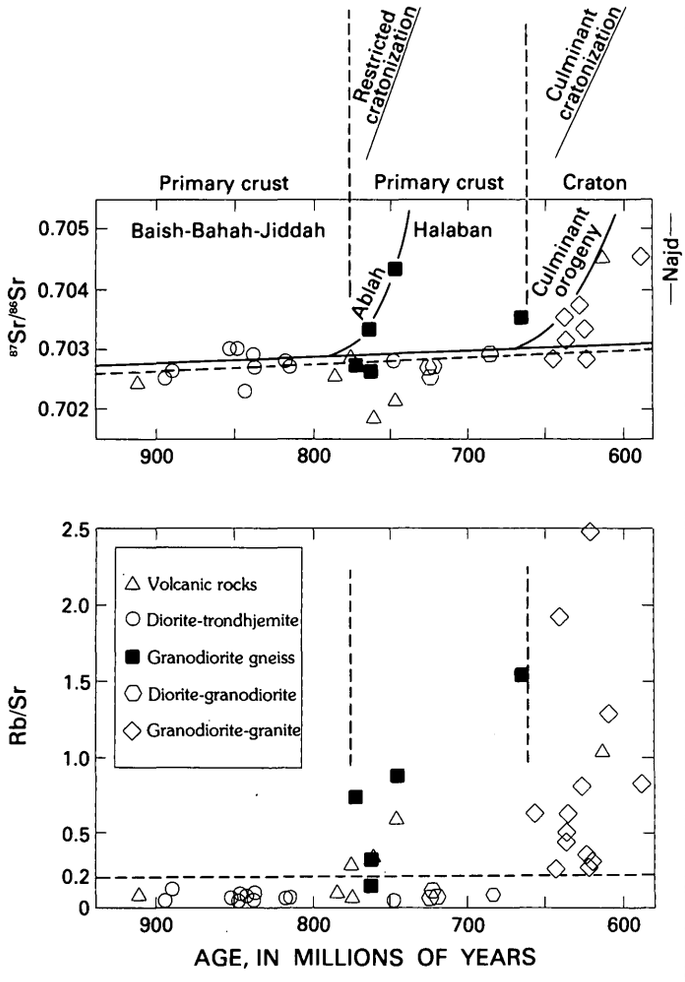

FIGURE 38.—Diagrams showing variations in initial $^{87}Sr/^{86}Sr$ (upper) and Rb/Sr (lower) ratios with age (adapted from Fleck and others, 1980, fig. 26). Events and rocks on upper diagram added for this report. Vertical dashed lines show major changes in strontium-isotope composition and Rb/Sr ratio of magmas corresponding to an earlier, regionally restricted orogenic event of partial cratonization of Ablah age and to a later, shieldwide culminant orogeny and cratonization. Strontium-evolution line (solid line; Faure and Powell, 1972) representing single-stage evolution from meteorite to average modern island arc is compared with least squares fit (upper dashed line) for Arabian Shield data having Rb/Sr ratios less than 0.2 (lower dashed line).

the plain above (figs. 39*A*–39*C*). From here the Siq extends eastward beneath the upland surface of the Ḥismā Plateau to the isolated stacks and pinnacles on mesas of the stratigraphically higher white and buff exposures of the Ram-Umm Sahm Sandstone.

The basal few meters are gritty arkosic sandstone and conglomerate containing pebbles from the underlying crystalline rocks, but the more massive vertical walls of the Siq are composed of fine- to medium-grained, occasionally coarse-grained, quartz sandstone, channel crossbedded with most foresets dipping from northwest to northeast. The beds extend northward into Jordan, where Bender (1974a) considered them to be nonmarine and Lower Cambrian, the Quweira Sandstone of Quennell (1951). The flaggy upper member, which forms distinctive plains and benches, contains lenses and layers of silt and clay and some manganiferous and hydrated iron-oxide concretions which on weathering leave a cavernous surface (figs. 39*A*–39*C*). Irregular calcareous cement also causes a cavernous weathering similar to that of the oxides.

The reddish-brown-weathering Siq Sandstone thickens to 115 m above Wādī Ḥujīl 50 km to the southeast, and to 223 m 10 km farther at Wādī Amadan, where it overlies the Jubaylah Group across a basement graben. There the top of a massive middle section forms a bench 135 m above the shield rocks, and a second flagstone unit of the upper section extends above to the base of the younger cliff-forming and massively crossbedded Ram-Umm Sahm Sandstone (figs. 12, 39*B*). The sandstone thins southeastward and becomes more thin bedded; 275 km distant (lat 26°24′ N., long 38°42′ E.), in the Qal'at aṣ Ṣawrah quadrangle, the Siq is about 90 m thick at a 50-m cliff 7 km north of the northern rim of the shield near Jabal Abadiyah. The lower section there is massive, red and tan, tabular, and trough-crossbedded sandstone under a 5-m-thick slab of finer grained silty sandstone whereon are trace fossils.

The Siq Sandstone questionably extends eastward along the northern edge of the shield from the Qal'at aṣ Ṣawrah area as far as long 40°25′ E., where outliers of flat-surfaced sandstone cap mesas in the easternmost of three basement grabens extending southeastward into the shield along the structural direction of the Najd fault system. West of long 40°25′ E., other outliers extend southward intermittently to the latitude of Al Madīnah (lat 24°30′ N.). Most are small except in the vicinity of Bi'r Suwaydarah, east of Al Madīnah, where about 250 km^2 of sandstone underlies the plain along a major Najd fault zone. The sandstone doubtless extends northwest under Ḥarrat Khaybar (Bigot and Chapelain, 1973; Delfour, 1977). The lithology is that of the Siq Sandstone farther northwest, and we have shown it as such although no fossils were found except at Qal'at aṣ Ṣawrah which were identified and considered by A. Seilacher to be of Late Cambrian age (written commun., 1978). The fossils are *Cruziana* sp. (not *Cruziana* aff. *C. furcifera* d'Orbigny nor *Cruziana huberi* (Meunier)) and what appear to be radula marks of a large grazing gastropod, possibly *Climactichnites* sp. (fig. 39*C*), which is found elsewhere in the Potsdam Sandstone of Late Cambrian age. At Sha'īb as Siq the flaggy sandstone a few meters above the basement crystalline rocks contains limonite and psi-

A

B

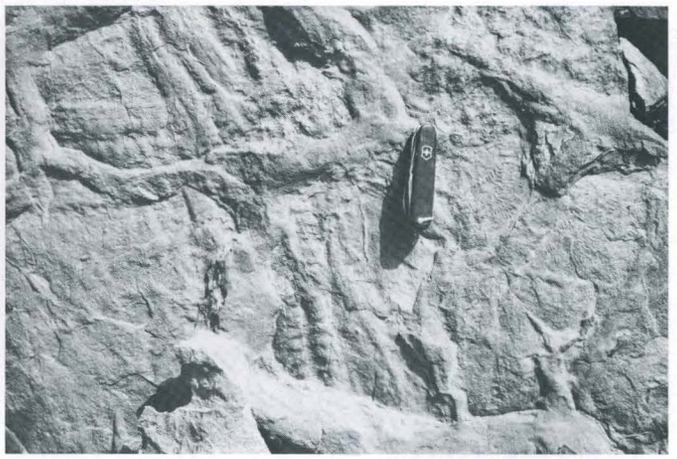

C

FIGURE 39.—The Siq Sandstone. *A*, Ferric and manganiferous concretions is lenses and seams within the basal beds of the Siq Sandstone at the upper rim at Sha'ib as Siq, the type locality. *B*, Siq Sandstone resting horizontally on Precambrian Hadiyah sedimentary rocks and beneath pinnacled Ram-Umm Sahm Sandstone. Headwaters of Wādī Shawāq. *C*, *Cruziana* sp. track in Siq Sandstone. Markings to the right of the knife appear to be grazing marks of a gastropod, probably *Climactichnites*(?) sp., of Late Cambrian(?) age. Near Jabal Abadiyah (lat 26°24′ N., long 38°42′ E.).

lomelane as well as calcareous concretions (fig. 39*A*) reminiscent of the manganiferous and cupiferous sediments in the upper part of the Middle Cambrian Burj Limestone Group in southwest Jordan (Bender, 1965, 1974a). If this correlation is valid and if the *Cruziana* sp. and *Climactichnites*(?) beds 275 km southeast are Upper Cambrian (Potsdamian), the sandstone becomes progressively younger toward the southeast and represents an onlapping shallow marine tongue.

SAQ SANDSTONE AND RAM-UMM SAHM SANDSTONE

The Saq Sandstone of Arenigian Age (uppermost Lower Ordovician) occupies the northeast flank of the shield, where it is stratigraphically below the Hanadir Shale of Llanvirhian Age (Bender, 1963) (lowermost Middle Ordovician) and above the crystalline rocks. There it represents a younging of the sandstone on the overlap along the north edge of the shield, probably the eastern extension of the Ram-Umm Sahm Sandstone. Farther south the sandstone crops out between the crystalline rocks and the Permian Khuff Limestone, which overlaps the Hanadir Shale as well. The large-scale, planar-crossbedded, white, tan, and gray Saq Sandstone resembles and is stratigraphically equivalent to the Ram-Umm Sahm Sandstone of northwest Arabia and southwest Jordan in that it is a mature arenite, in many places lacking arkosic beds. In places it rests on basement rocks without a basal conglomerate, although commonly there are lenses of grit and the basal few meters are reddish with iron cement. Cement in the basal beds may also be gypsiferous as well as calcareous, but the nonferrous cement is generally somewhat above the basal beds. Rare well-rounded pebbles, mostly quartz, some citrine, form local lenses in large-scale planar crossbedding of finer sand (N. Layne, written commun., 1959–60; Powers and others, 1966).

The only evidence of age reported heretofore is trace fossils collected from near the southern end of the outcrop near the top of the sandstone at Jabal Ḥaqil, 37 km northeast of Ad Dawādimī. These were identified by P.E. Cloud, Jr., as *Cruziana* aff. *C. furcifera* d'Orbigny and *C. huberi* (Meunier), which belong to the *Cruziana rugosa* group of Seilacher (1970). The *C. rugosa* traces are found in shale lenses in northwest Arabia and in Jordan in the upper part of the Ram-Umm Sahm Sandstone, where they are considered to be of Arenigian Age (uppermost Lower Ordovician) (Bender, 1975).

WAJID SANDSTONE

The southeast edge of the shield is covered by the Wajid Sandstone, which crops out beneath the Permian Khuff Formation at Wādī ad Dawāsir, 420 km south of the southernmost exposure of the Saq Sandstone. Flat-lying or gently arched, unmetamorphosed, and broken only by late Tertiary and Quaternary high-angle tension faults, and earlier considered devoid of fossils, it could heretofore be assigned only a pre-Permian and post-shield age.

The type locality is Jabal al Wajid at lat 19°06′ N., long 44°27′ E., where a thickness of 950 m was calculated (Powers and others, 1966). More recently, the sandstone has been drilled downdip to the east of the northern end of the outcrop, where a thickness of 500 m was measured beneath a disconformity, a thickness comparable to an estimate of 600 m by Alabouvette and Villemur (1973). Shaly beds above the disconformity contain three chitinozoan species of Silurian age, *Conochitina latifrons*, *C. micracantha* subsp. *robusta*, and *Ancyrochitina nodosa* (D. Hemer, oral commun., 1969). In addition, a recent study of the outcrop belt has yielded *Scolithus* (*Tigillites*), arthropod trails (*Cruziana* sp.?), and conical or circular structures at the base of the Wajid Sandstone (Alabouvette and Villemur, 1973), forms that are similar to those in the upper Saq Sandstone and, farther north, in the Ram-Umm Sahm Sandstone. Thus the Wajid in Jabal al Wajid appears to be uppermost Lower Ordovician or possibly somewhat younger, as the *Tigillites* trace fossils are most abundant in the Tabuk Formation of Lower Ordovician to Lower Devonian age exposed farther north in Arabia (Powers and others, 1966).

A Cambrian-Ordovician age for the Wajid Sandstone was first suggested by Darwin O. Hemer, who found algal forms in well cuttings similar to those described from the lower Paleozoic in the Russian Baltic region (Hemer, 1968).

The lithology of the Wajid Sandstone also tends to make such an age reasonable. The bulk of the sandstone is composed of mature grains and pebbles of quartz and displays large-scale planar crossbedding. Indeed, the disconformity reported by Alabouvette and Villemur (1973) may be equivalent to the top of the Saq Sandstone and the bottom of the Tabuk on the northern flanks of the shield, although the basal Tabuk Hanadir Shale with the *Didymograptus* index graptolite (Powers and others, 1966) is missing. Intermittent exposures and subcrop in the Al ʻĀriḑ region east of Jabal al Wajid, including sandstone, boulder beds, and fossiliferous shale ranging in age up to Lower or Middle Permian, have recently been included in the Wajid Sandstone (McClure, 1980). More recently, an Ordovician age was strengthened by the discovery of the Ordovician Hydrozoan *Disophyllum* cf. *peltatum* associated with glaciogene sediments in Tigray, northern Ethiopia (Saxena and Assefa, 1983), beds that were correlated with the Wajid Sandstone (Dow and others, 1971; Beyth, 1973). Also, if a glacial origin is accepted for the exposures in uppermost Ordovician or lowermost Silurian in north-central Arabia, they would be coeval with glacial rocks in Algeria and Mali (Dow and others, 1971; McClure, 1978). However, the dropstones at Khashm Khaṭmah and Jabal Umm Ghīrān, easternmost outcrops of what have been considered Wajid Sandstone, are now known from flora in nearby drill holes to be uppermost Carboniferous or lowermost Permian (McClure, 1980). This flora correlates with the flora in the glaciogene Haushi Group in Oman (Hudson, 1958) and the tillites in Yemen (Roland, 1978; Kruck and Thiele, 1983). Thus it appears that there was widespread glaciation during youngest Ordovician, and possibly oldest Silurian, in northern Arabia and north Africa, extending as far south as northern Ethiopia, and a late Paleozoic widespread glaciation (Gondwana Ice Age) extending into southern and southeastern areas of the Arabian Peninsula.

Occasional outliers of basement igneous and metamorphic rocks are kopjes or bornhardts, as at Bi'r Idima, where the bornhardt serves as a ground-water dam. Exposures of gabbro and metamorphosed mafic rocks in knobs as much as 50 m wide lie in disturbed lower Wajid Sandstone at Hijmah (lat 19°07′ N., long 44°05′ E.; Stoeser, oral commun., 1976), indicating movement during Wajid time and possibly disturbance during the Late Cambrian or Early Ordovician epeirogeny, suggested by the radiometric dates described above.

The descriptions of Alabouvette and Villemur (1973) show no organic forms in the south such as occur farther north near Wādī ad Dawāsir (Jackson and others, 1963). Furthermore, the calcareous cement and trough crossbedding resemble features described in the Siq Sandstone (Hadley, 1973), but by no means prove correlation.

A few widely scattered outliers of sandstone are deep within the shield. A small sandstone crest at Jabal Tīn, lat 22° N., near Khurmah, 600 km south of the northern rim of the shield and 260 km northwest of the nearest outcrops of the Wajid, resembles the Wajid. The crest is composed of 16 m of white, fine-grained, massive sandstone, flat lying above basement gneiss. Similarly, a prominent outlier capping Jabal Ṭamīyah, 425 m above the desert floor at lat 25°36′ N., long 42° E., and 80 km west of the Saq Sandstone, at the eastern edge of the shield, is 82 m thick, flat lying, and crossbedded. The base of the Saq Sandstone near Ḥā'il also lacks a

basal conglomerate. A Saq age at Jabal Ṭamīyah and a Wajid age at Jabal Tīn fits the concept of the younging of the lower Paleozoic fringe sandstones toward the southeast.

KHUFF FORMATION

The eastern edge of the shield between outcrops of the Saq Sandstone and the Wajid Sandstone is nonconformably overlain by the Permian Khuff Formation. Outcrops directly overlying the basement and overlapping the Saq Sandstone are mostly in the area east of the Al Amar-Idsas fault, extending from lat 22°40′ N. to lat 24°28′ N. Farther south, the Khuff probably rests on the basement, but the exposures are poor and may be those of an older Paleozoic paleosol.

The Khuff ranges in thickness to as much as 320 m, but only 171.4 m was measured at the reference section between Wādī ar Rayn and Jabal ath Thuwayr (Powers, 1968). The base is a lateritic duricrust only a few meters thick at most, resulting from Paleozoic weathering beneath the basal conglomerate and sandstone of the Khuff. The bulk of the formation above the paleosol is neritic dolomite, shale or claystone, and limestone that dip gently eastward. These beds were deposited during a widespread marine transgression at the end of the Paleozoic. The Khuff Formation has been divided into five informal members on the basis of lithofacies changes both vertically and along the strike (Delfour and others, 1982).

MESOZOIC SEDIMENTARY ROCKS

KHUMS FORMATION

DEFINITION

The Khums Formation takes its name from Wādī Khums, where it was first mapped in the foothills east of the Tihāmat al Yemen (coastal plain) near the Yemen border (lat 16°50′ N., long 43°01′ E.) (Brown and Jackson, 1959). At the type locality, crossbedded and graded grit of the Khums nonconformably overlies Precambrian crystalline rocks where the contact is not a fault. Elsewhere it overlies the Wajid Sandstone of Cambro-Ordovician age. The uppermost quartzitic sandstone of the formation underlies Upper Jurassic limestone, apparently comformably (fig. 40).

OCCURRENCE AND THICKNESS

The Khums Formation crops out in a belt 3 km or less wide and extends for 35 km parallel to the Red Sea rift zone to the north and south of Wādī Khums. A similar belt lies 10 km southeast and extends into the Yemen.

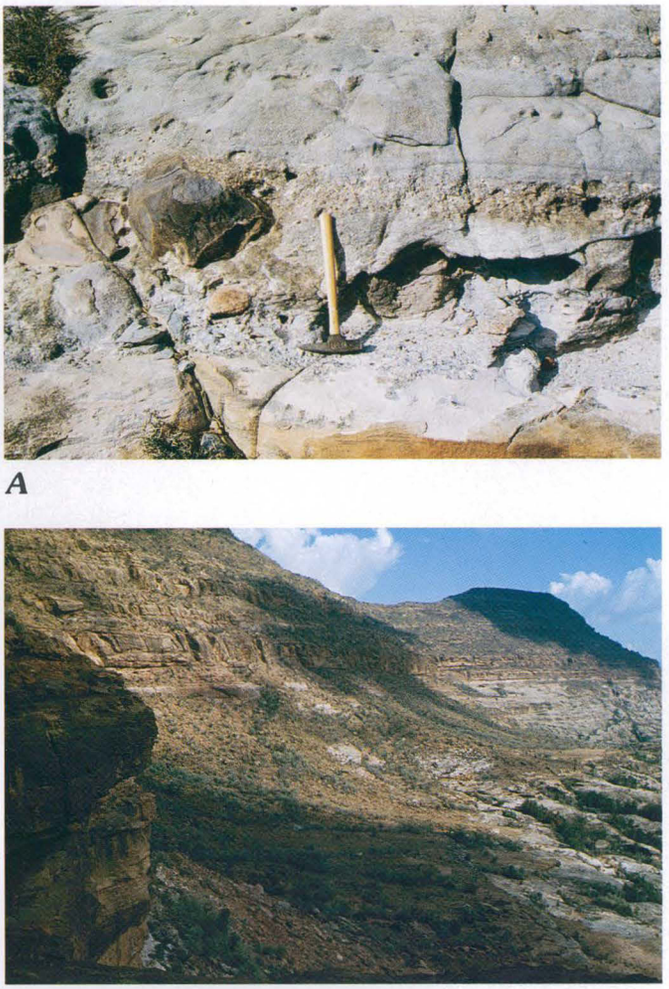

FIGURE 40.—The Triassic Khums Sandstone. *A*, Contact at base of Khums Sandstone marked by grit. Hammer rests on top of Wajid Sandstone. *B*, View of the south slope of Jabal Abū Ḥasan showing contact between the Cambro-Ordovician white Wajid Sandstone below and the tan Triassic Khums Sandstone above.

Both belts are partly bound by faults. Outliers occur on the crest of the scarp mountains to the east. The formation is of variable thickness, and because it is highly block faulted in places along the flank of the Red Sea rift, the thickness is somewhat difficult to estimate. Gillmann (1968) measured a maximum of 880 m of sandstone in the faulted section of the Wādī Khums belt where we suggest that 400 m is Khums Sandstone, underlain by 480 m of Wajid Sandstone and overlain by the Jurassic Amran Formation. The Khums narrows to 10 m at the north end of the belt on the banks of Wādī Jīzān, but its top is a fault. Thirty kilometers north of Wādī Jīzān, an

isolated outcrop of the Khums Formation measures 100 m in thickness. About 145 km northwest of the Wādī Khums locality and 15 km northwest of Ad Darb, tectonized and quartzitic sandstone is associated with calcareous and kaolinitic beds that contain rare molluscan steinkerns common to the Amran Series, a unit of the Jurassic marine beds of Yemen (Geukens, 1960). However, the bulk of the small outcrop northwest of Ad Darb could be the lower Paleozoic Wajid Sandstone, which caps the mountains to the east; a sliver of upper Khums containing Amran-type fossils may overlie the Wajid in this downdropped, shattered block. On the crest of the scarp mountains east of the Tihāmat, the Khums clastic deposits overlie the Wajid Sandstone on the mesa crest of Jabal Abū Ḥasan (al Qahar) 75 km north of Wādī Khums (figs. 40*A*, 40*B*). At Jabal Abū Ḥasan, between altitudes of 1,541 to 1,861 m, we measured 320 m where the beds are relatively undisturbed. Subsequently, D.G. Hadley and D.L. Schmidt (written commun., 1974) measured a thickness of 160 m at nearby Jabal al Qahar on the south side of Jabal Abū Ḥasan. R.E. Anderson measured another outlier of the Khums Formation near Alb Pass 40 km east of Jabal Abū Ḥasan on the high plateau of Al Yemen in Saudi Arabia near the Yemen border. There he found a thickness of 125 m (Anderson, 1979, p. 20), the same as the thickness of clastic rocks (Khohlan Series) above the basement and below the Upper Jurassic Amran Series measured by Geukens (1966, p. 8) 90 km southeast near Sa'dah in Yemen.

Altitude (meters)	*Thickness*	
		Amran Formation
		Khums Formation
1,861		Upper member.
	189	Alternate massive and bedded tan sandstone, considerable large-scale crossbedding.
	48	Tan massive sandstone; lower 10 m has a reddish cast.
		Basal and middle member.
1,623		Top of bench composed of dark-red, sandy, clay shale and silty sandstone; some concretionary sandstone, locally calcareous; algal markings and questionable echinoid fragments; upper silty beds cavernous. Boundary between clastic and calcareous sediments transitional, increasingly calcareous upward.
	83	White and purple coarse sandstone and conglomerate; minor shale lenses, poorly sorted pebbles and grains, mostly well rounded, white quartz although some grains are fragments of phyllite, andesite, and quartzite. Calcareous cement but no recognizable organic remains in the samples collected.
Total	320	Thickness of 320 m may be excessive owing to minor block faults.
1,541	160+	Wajid Sandstone. Massive white and tan medium- to coarse-grained sand and grit. Joints form caves and vertical cliffs.

LITHOLOGIC CHARACTER

The Khums Formation in the rift zone is mostly a hard quartzitic sandstone containing minor beds of siltstone and occasional pebbles and boulders of quartzite. Granitoid and metamorphosed basement rocks are well rounded in the basal grits. The siltstone is gray green or gray and reddish brown and contains pebbles. The beds are highly disturbed and intruded by Tertiary basalt dike swarms that have contact-metamorphosed the sediments. Michel Gillmann (1968) examined the Khums outcrops along the foothills and divided the formation into three members: a lower crossbedded and coarse sandstone (480 m); a middle member of fine-grained phosphatic sandstone, conglomerate, and ferruginous shale (violet colored) with some tuffaceous beds (110 m); and an upper member of fine-grained siliceous sandstone (290 m). We suggest, however, that the lower sandstone probably is Wajid Sandstone. Our section on Jabal Abū Ḥasan, where the bedding is approximately horizontal, was measured in 1965 and is as follows:

Anderson (1979) divided the Khums Formation near 'Alb Pass into a lower 35 m of alternating sandstone and pebbly ferruginous shale, a middle 80 m of massive buff and crossbedded buff sandstone and gritstone, and an upper 10 m of grayish-red, red-purple, and pale-yellow sandstone with ferruginous beds.

Lithology considerably dissimilar to the Khums Formation but cropping out in Yemen between basement rocks or the Wajid Sandstone and the Amran Series was described by P. Lamare (1930b) as 215 m thick near Amran, 280 m thick at Jabal Ashmur 20 km to the west (quoting C. Rathjens), and 700 m thick near At Tur, 40 km still farther west, and near the western edge of the scarp mountains. This gives an increase in thickness toward the Red Sea graben similar to that in Saudi Arabia. The beds change from alternating sandy marl and sandstone and lignitic beds in the upper part near Amran to increasingly arenaceous outcrops westward toward the Red Sea. These rocks in the Yemen are called the Khohlan Series (Geukens, 1960).[6]

[6]Since this paper was written, a Carboniferous section of glaciogene sedimentary rocks was mapped above the basement or Wajid Sandstone and below the Khohlan Sandstone (Kruck and Thiele, 1983).

PALEONTOLOGY AND AGE

The Khums Formation has only plant fossils, rare in outcrop, and the trace fossil *Arthrophycus* (Anderson, 1979, p. 20). This trace fossil, a trail made by arthropods or worms, is generally considered Ordovician-Silurian, although similar furrows are reported from Cretaceous and upper Tertiary beds (Hantzschel, 1975, p. W38, W39). The beds containing questionable algal impressions and echinoid spines at Jabal Abū Ḥasan may belong in the overlying marine Amran Formation. In Yemen, Geukens (1960) found worm borings, possibly *Arthrophycus*, in the uppermost beds at the same stratigraphic position as that described by Anderson near 'Alb Pass. P. Lamare and C.A. Carpentier (1932) reported a flora in lignitic lenses in the Yemen that they considered to be Lower Jurassic (Lias) or possibly uppermost Triassic (Rhaetian), which could be coeval with the Khums Formation. However, 115 km southeast of the Khums locality, carbonaceous beds occur in marl and sandstone near the village of Amran, where the lithology is considerably different.

The Khums Formation can be any age from Cambro-Ordovician to Early Jurassic on the basis of adjacent formations. However, the bulk of the evidence suggests that the Khums is paraconformable on the Cambro-Ordovician sandstone (Anderson, 1979) and possibly equivalent to part or all of the nonmarine Late Triassic Minjur Sandstone of central Arabia (Powers and others, 1966). The Minjur contains lignite beds in the subsurface at Riyadh, and this is similar to the lithology at the Amran locality. Samples from below 1,110 m in a test water well at Riyadh contained three new species of the conifer *Brachyphyllum* that were considered possibly to be middle Liassic, entirely on the basis that the overlying Marrat Formation is upper Liassic (Toarcian) (Boureau, 1956). Owing to the fragmentary nature and absence of stomata in the descriptions of the only conifer identified from the Yemen, *Pagiophyllum peregrinum* Sch., Boureau (1956) could not compare it with the Minjur fossils. However, in central Arabia the Minjur is truncated by a regional unconformity (Dubay, 1969), and Cameron (1974), in a more recent study of palynomorphs from the Minjur Sandstone, has proven it to be of Late Triassic age. Thus, the Khums Formation is here regarded as Upper Triassic (Rhaetian) or Lower Jurassic.

AMRAN FORMATION

DEFINITION

A blue-gray lithographic limestone (figs. 41, 42), silicified and brecciated in places, crops out above the Khums Formation in the foothills at the east edge of the coastal plain south of Wādī Khums. It was mapped in 1951 (Brown and Jackson, 1959) and named for the Hanifa Formation of Late Jurassic age in central Arabia on the basis of the similarity of its fossils to those of the Hanifa (R.A. Bramkamp, written commun., 1951). Subsequent work has established that the fauna of this limestone represents a greater timespan than that of the Hanifa, as the Hanifa has later been more precisely defined, and that the rocks are homologous to the Amran Series of Yemen (Lamare, 1930b).

A

B

FIGURE 41.—Limestone of the Amran Formation. *A*, The Amran Limestone above Khums Sandstone on the top of Jabal Abū Ḥasan. *B*, Toe of 'Asīr Mountains east of Jīzān with the Jurassic Amran Limestone dipping west beneath the coastal plain and overlying the Khums Sandstone, which crops out in foothills on the left. The sediments have been downfaulted to the west. At Wādī Khums, east of Jīzān.

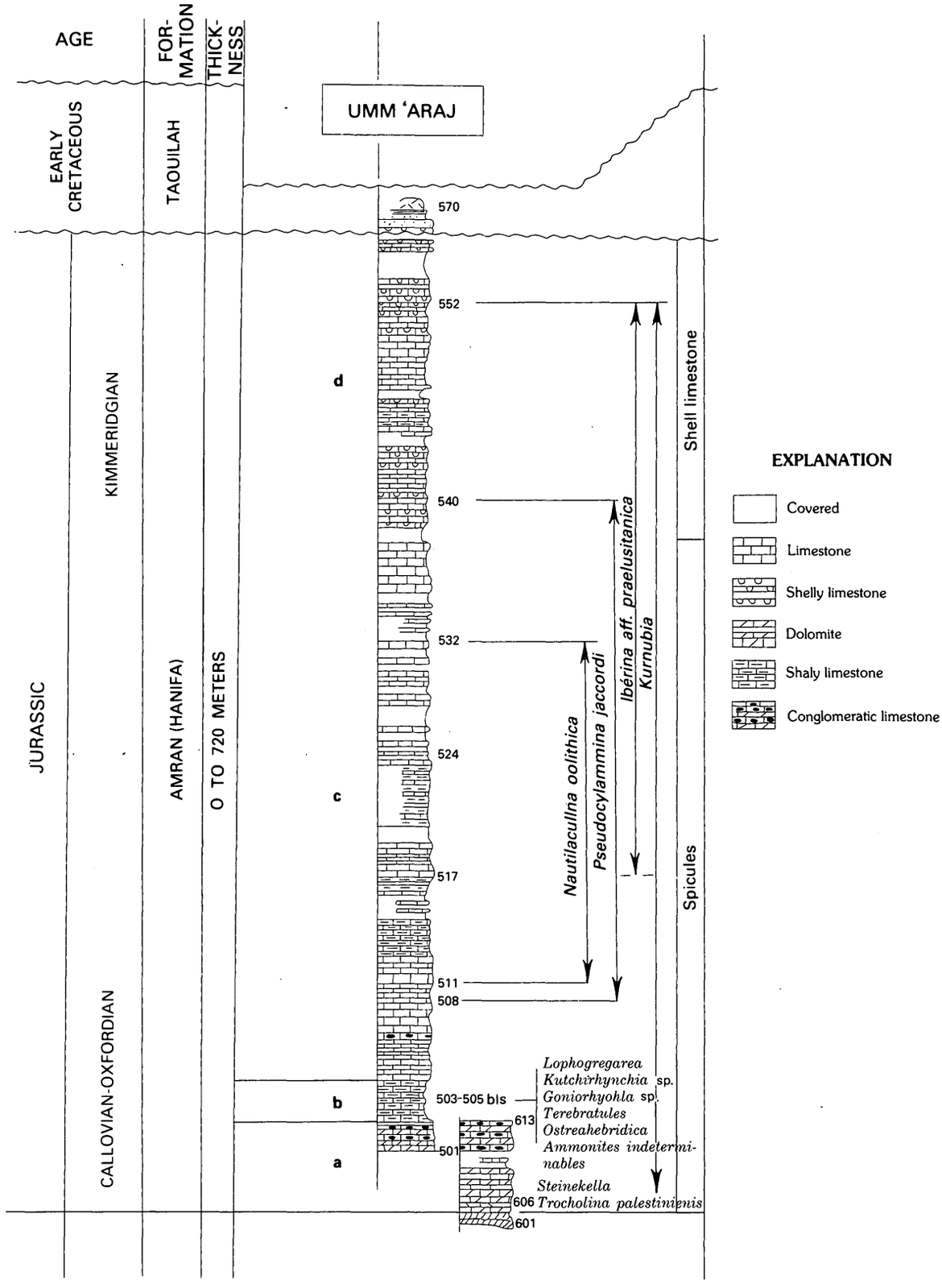

FIGURE 42.—Type section of the Amran Formation at Umm 'Araj. (Modified from Gillmann, 1968.)

OCCURRENCE AND THICKNESS

The Amran Formation shown as the Hanifa Formation on the geologic maps of the 'Asīr quadrangle (Brown and Jackson, 1959) and of the Arabian Peninsula (USGS–ARAMCO, 1963) crops out at Wādī Fija, 3 km north of Wādī Khums, and in faulted blocks about 10 km southeast of Wādī Khums near Umm 'Araj (lat 16°46′ N., long 43°06′ E.). Ten kilometers farther southeast, a more extensive outcrop extends 20 km along the Yemen boundary and into Yemen. Smaller outliers are present on Jabal Abū Ḥasan (al Qahar) and near 'Alb Pass, where calcareous beds apparently disconformably overlie the Khums Formation. The Amran Formation is extensively exposed in northern Yemen, where the name is taken from outcrops near the town of Amran, 45 km northwest of Ṣan'ā' (Lamare, 1930b; Geukens, 1960, 1966; Grolier and Overstreet, 1978). Near Umm 'Araj, Gillmann (1968) divided the formation, there 720 m thick, into two major divisions, a lower unit (500 m) composed of three members and an upper unit (220 m) of phosphatic limestone.

Farther east on the crest of the 'Asīr escarpment, 82 m of sandstone and interbedded limestone and sandy limestone contain marine fossils.

Section of Amran Formation on the southern slope of Jabal Abū Ḥasan (al Qahar) (elev. 1,861 to 1,942 m), top of mesa

	Thickness (meters)
Limestone, fossiliferous, tan, sandy, echinoid spines, small gastropods and pelecypods	1
Sandstone, massive, tan	29
Sandstone, moderately massive and bedded, medium-grained	37
Sandstone, alternating brown, calcareous, and white, medium-grained	7
Limestone, thin-bedded, tan, sandy, in three benches: indeterminate small pelecypods and oyster fragments; *Topha* sp., *Turritella* sp.; Naticid indet.	8
Total thickness	82
Khums Formation at base of section	

At the small mesa near 'Alb Pass, Anderson (1979) found 20 m of calcareous sandstone and thin interbedded strata of sandy fossiliferous limestone which he compared to the Amran Series that crops out 30 km southeast in Yemen.

The Amran Series of Yemen crops out extensively in northwest Yemen, where the thickness is given as 100–265 m (Basse and others, 1954), thickening to 550 m to the southwest (Geukens, 1960) but thinning northward toward the isolated outcrops in Saudi Arabia (Geukens, 1960). Geukens measured 105 m near Sa'dah, 90 km southeast of the easternmost outcrop in Saudi Arabia.

LITHOLOGIC CHARACTER

In the only extensive outcrop in Saudi Arabia near the Yemen border at the southeast corner of the Jizan coastal plain, most of the Amran is crystalline blue-gray limestone and dolomite. Minor beds of shale and tuff are near the top. The rocks have been dropped down in the Red Sea graben and intruded by Tertiary dikes and sills of basalt, gabbro, and related igneous rocks of the early oceanic coastal rock of the Red Sea.

Gillmann (1968, p. 195) described the lower 500 m of sponge-spicule limestone as follows: "It includes 70 m at the base of dark-gray crystalline or sublithographic limestone and dark-gray dense dolomite with chert nodules at the top. In the middle, 30 m of gray, argillaceous, very fossiliferous limestone. Last, 400 m of dark-blue sublithographic limestone in thick massive layers with some intercalated beds of brown shelly limestone."

The upper shelly limestone is "formed of 220 m of violaceous fragmental limestone, gray-blue lithographic limestone, and marl and shale (with chlorite)" (Gillmann, 1968, p. 195).

In Yemen the limestone grades into a sandy facies, which farther east grades to interbedded gypsum and, in the eastern extension of Wādī Jauf, to salt beds that crop out in diapiric structures at the throat of Wādī Hadramaut (Brown, 1972).

NATURE OF CONTACT

The Amran Formation rests parallel to the bedding of the underlying Khums Formation, but as the Amran contains Upper Jurassic fossils and the Khums Formation is most likely Upper Triassic (Rhaetian) or lower to middle Liassic (lowermost Jurassic), there appears to be a substantial hiatus or a period of extremely slow deposition prior to deposition of the marine Amran. Geukens (1960) considered this an epeirogenic period.

The only occurrence of overlying beds of Mesozoic age in Saudi Arabia is reported by Gillmann (1968, p. 195), who described 10 m of "coarse sandstone, breccia with limestone fragments, and brown shale" which could be compared to the sandstone in the Lower Cretaceous Tawilah Group in Yemen. However, the Early Cretaceous age may be open to question, as the Tawilah Group of sandstone beds cannot be separated with certainty from the overlying, lithologically similar Medj-zir Series, which contain Paleocene or Eocene fossils (Geukens, 1960; Grolier and Overstreet, 1978).

PALEONTOLOGY AND AGE

On the 'Asīr 1:500,000-scale geologic map (Brown and Jackson, 1959), the Amran Formation was named the

"Hanifa Formation" on the basis of the similarity of the megafossils and lithology to the Hanifa Formation in central Arabia. These fossils, as identified by R.A. Bramkamp (written commun., 1951), are as follows:

Basal fauna north and south of Wādī Khums, east of the Red Sea coastal plain:
Somalirhynchia (two species)
Gryphaea balli Stefanini
Lopha aff. *solitaria* Sowerby
Parallelodon sp.
Lower part of limestone, north bank of Wādī Khums:
Terebratula sp.
Rhynchonella sp.
Middle portion of the limestone section:
Cidaroid sp.
Ostrea sp.

Bramkamp at that time considered this fauna to be Hanifa, which was then questionably correlated with the Oxfordian stage of the European Jurassic, but he had reservations that it might be in part somewhat younger and of Jubaila (Upper Jurassic) Limestone equivalency (lower Kimmeridgian) of eastern Arabia (Steineke and others, 1958). Later, the limestone of the Amran Formation was studied more intensively by Michel Gillmann (1968, p. 195), who identified the following foraminifera and pelecypods:

Lower 70 m of limestone and dolomite:
Steinekella (Redmond)
Trocholina palestiniensis (Henson)
Kurnubia aff. *jurassica-wellengsi*
Pseydocyclammina sp.
Next 30 m of argillaceous limestone:
Lopha gregarea Sowerby
Kutchirhynchia sp.
Goniorhynchia sp.
Terebratulas
Ostrea hibridica Sowerby
Third unit of 400 m of limestone:
Pseudocyclammina jaccardi
Iberina spirocyclina sp. Henson
Nauticulina oolithica
Upper 220 m of limestone, marl, and shale:
Iberina aff. *praelusitanica* (Maync)

These fossils range in age from Bathonian (upper Middle Jurassic) to Kimmeridgian (Upper Jurassic) (Gillmann, 1968). The Amran Series in Yemen has been identified from at least four collections as Malm, the epoch that includes the Upper Jurassic stages, Oxfordian, Kimmeridgian, and Portlandian, whereas the Amran Formation at Umm 'Araj in Saudi Arabia seemingly does not include the younger Portlandian fossils but extends downward into the Middle Jurassic. As the Hanifa Formation has more recently been restricted to the lower Kimmeridgian (Powers, 1968), it seems desirable to apply the formational name from Yemen to the outcrops along the border in Saudi Arabia.

KHURMA FORMATION

The Khurma Formation consists of a quartzitic sandstone, locally including conglomerate and red shale, that is exposed on the Rakbah plain 150 km northeast of Aṭ Ṭā'if and northwest of Al Khurmah, where it rests on Precambrian shield rocks and underlies early Tertiary lakebeds and early Miocene basalt (Brown, Jackson, Bogue, and MacLean, 1963). The sandstone contains numerous *Tigillites* borings associated with small pelecypod casts. Although the outcrops are poorly exposed and mostly bound by faults, the sandstone is at least 50 m thick. Similar sandstone, tentatively correlated with the Khurma Formation (Madden and others, 1980), crops out beneath the Paleocene Umm Himar Formation 100 km east of Aṭ Ṭā'if and 75 km southeast of the widespread outcrops northwest of Al Khurmah. There the clastic rocks include a basal quartz-pebble conglomerate resting on the crystalline basement. The sandstone is crossbedded with foresets indicating a northerly transport direction at the time of deposition. It is generally friable and is locally cemented by secondary silica and iron oxides (Baghanem, 1972). Similar small outcrops of sandstone containing vertical borings are exposed at the edge of the crystalline shield on the coastal plain 70 km south of Jiddah. However, nearby sediments of Oligocene age suggest that these beds are younger than those exposed at Jabal Umm Himar. Likewise, sandstone beneath the Paleocene(?) Usfan Formation northeast of Jiddah should probably be identified with the Khurma Formation.

A precise age for the mature Khurma Formation is not possible to determine with the information available to us. The age could range from early Paleozoic to Tertiary, as the *Sabellarifex dufrenoyi* (*Tigillites dufrenoyi* Rouault) occurs in Ordovician sandstone in Jordan (which should be named *Tigillites* because it differs from *Sabellarifex* by its distinct annulation (Hantzschel, 1975, p. W38–39)). *Tigillites*(?) borings occur in all the lower Paleozoic sandstones fringing the shield in Saudi Arabia, though many are not annulated as are the borings in the Khurma Formation. The lower Paleozoic sandstone extends south onto the shield in numerous small, isolated outliers as far south as the latitude of Al Madīnah (lat 24°30′ N.), 270 km northwest of the Khurma Formation, as well as in a single outcrop at Jabal Tīn northeast of Aṭ Ṭā'if. However, these sandstones are massive, evenly bedded, and

devoid of *Tigillites* vertical boreholes. Certainly the Khurma clastics are pre- or early Paleocene, as they are disconformable below the Paleocene Umm Himar Formation (Madden and others, 1980). General evidence, including lithology and stratigraphic position, suggests a Cretaceous age similar to the fluviatile (Nubian-type) clastics widespread in east Africa, Yemen, and Jordan.

These beds were first observed by Richter-Bernburg and Schott (1954, p. 44, 45), who described silicified limestone with red sandy shale, greenish-gray, marly, somewhat silicified shale, coarse-grained sandstone, and purple and green variegated shale over a distance of about 21 km beginning 13 km west of Al Khurmah, to which they gave the name "Khurma Series." Most of these lithologies can be assigned to the Umm Himar Formation. As these beds strike N. 30°–80° E. and are underlain by greenschist and granitic gneiss striking N. 30°–60° E., Richter-Bernburg and Schott (1954) considered them younger than the basement. The only vertical non-Precambrian beds we have seen in this area are marginal to feeder necks and hypabyssal intrusions of basalt. In a western belt, gastropod molds, undoubtedly from the overlying lakebeds, are associated with the Umm Himar deposits. Because of the vertical dips, it is problematic that those writers saw the quartzitic sandstone underlying the Paleocene. This sandstone we have tentatively identified with the Lower Cretaceous Nubian Sandstone of Egypt and the Sudan. An alternative explanation would require tectonism in the Al Khurmah area during late Mesozoic or early Tertiary, for which we have seen no evidence elsewhere on the upland plateau of the shield, although there is normal faulting of the sandstone.

MESOZOIC-CENOZOIC SEDIMENTARY ROCKS

USFAN FORMATION

DEFINITION

Tertiary fossiliferous sediments in western Saudi Arabia were first shown on a map prepared as part of a search for a water supply for Jiddah (Steineke and others, 1944). Cropping out in the low hills east and north of Jiddah, the continental and marine clastics contain bivalve and gastropod fossils that were identified as of Eocene age (R.A. Bramkamp, oral commun., 1944).

Subsequently, Karpoff (1956) published a description of the sediments. He divided them into two units: the Usfan Series, a red continental series of clastic rocks including a light-colored lacustrine limestone with rare leaf imprints as exposed at 'Usfān Pass (lat 21°54.8′ N., long 39°21.2′ E.) 50 km northeast of Jiddah, and the "Shumaysi Sandstone," a light-colored quartz-pebble sandstone, locally iron-stained and calcareous with a silicious limestone at the top, seen 45 km east of Jiddah on the Makkah road. A year later, Karpoff (1957b) published a more comprehensive account following identification of a marine fauna considered to be of Maestrichtian (Late Cretaceous) age from 'Usfān Pass which led him to assign that series to a Maestrichtian-Eocene(?) span. The overlying red clastics of continental origin, the "Shumazi (Shumadi) Series," he thought might be Oligocene-Miocene, based on resemblance to the Tertiary of north Africa (Karpoff, 1956).

On the 1963 geologic map of the Southern Hejaz quadrangle (Brown, Jackson, Bogue, and Elberg, 1963), the Usfan Formation is shown in grabens trending more or less en echelon, parallel to the Red Sea rift, the Tertiary sediments flanked by Precambrian rock and overlain by Pliocene basalt. The nonmarine upper beds were split off and assigned to the Shumaysi Formation, following Karpoff.

OCCURRENCE AND THICKNESS

The Usfan Formation crops out in steeply dipping beds for an exposed thickness of 75 to 100 m across the Al Madīnah-Makkah road at 'Ufān Pass. Additional exposures rim the basalt northwest of the pass for 20 km, and marine or littoral sediments 170 m thick, which may be an extension, crop out in a secondary graben at Ḥaddat ash Shām, 45 km southeast of 'Usfān and 60 km northeast of Jiddah. Intermittent exposures extend north and south of Ḥaddat ash Shām for 32 km and locally contain some marine fossils, but the sediments are almost entirely sandstone and were shown on the 1963 geologic map as part of the overlying Shumaysi. They were mapped by AUXERAP (1967) as an extension of the Usfan Formation, perhaps on the basis of marine foraminifera, but if the lower part of the Shumaysi is Eocene, these outcrops should not be assigned to the Usfan.

LITHOLOGIC CHARACTER

The Usfan at the type locality (fig. 43) at 'Usfān Pass 4 km northwest of the village of 'Usfān is mostly fine-grained sandstone, cemented by iron in some layers. It has a fossiliferous and nodular gray limestone near the base and some glauconitic fine sandstone near the top. The uppermost bed is 6 m of bedded phosphatic chert that is weathered; elsewhere it is lateritic (fig. 43). Poorly exposed sandstone beneath the lower fossiliferous limestone may be lowermost Usfan, but the beds have tubular borings across the bedding and contain plant fossils and ferruginous layers which may be

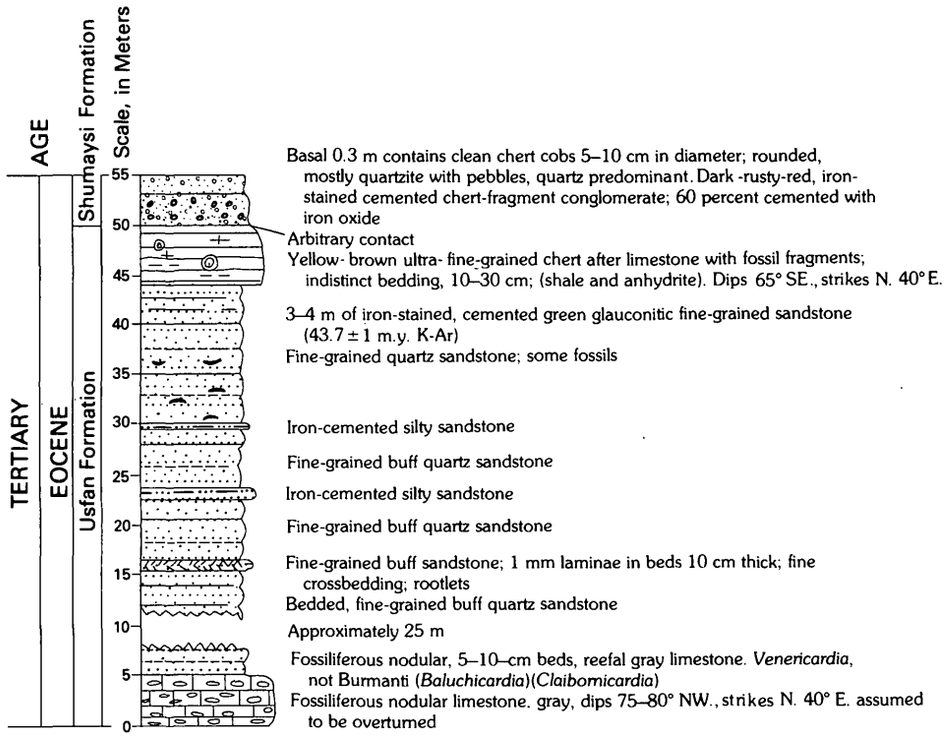

FIGURE 43.—Type section of the Usfan Formation at 'Usfān Pass.

either younger or older than the marine beds that are designated Usfan. The structure is obscure.

NATURE OF CONTACT

The Usfan Formation rests nonconformably on Precambrian crystalline rocks where the nonfaulted basal surface can be observed. It has been dropped down in a narrow graben, so sandstone or conglomerate adjacent to the crystalline rocks may be part of the overlying Shumaysi or, more likely, equivalent to the older Khurma Formation. The nonmarine Shumaysi disconformably rests on the Usfan; the basal sediment is a ferrous, iron-cemented, fragmental conglomerate composed of clasts of Usfan chert, limestone, shale, and pebbles and boulders of basement rocks.

PALEONTOLOGY AND AGE

The bivalves determined by D. Mongin on which Karpoff (1957b) based his Maestrichtian age are as follows:

Cardita (Venericardia) ameliae Peron
Cardita (V.) ameliae var. *orfellensis* Rossi-Ronchetti
Corbula striatuloides Forbes
Lucina cf. *L. desioli* Ch-Rispoli

This fauna came from about 10 m above the base of a dark-gray limestone 3 km north of the village of 'Usfān (Karpoff, 1957b). Because the Maestrichtian age did not agree with the earlier determination by Bramkamp, we visited the outcrops and collected both bivalves and gastropods.

From two localities: the type outcrop, 3 km north of 'Usfān, and another exposure 9 km to the northwest:

Venericardia sp. large and small (possibly two species)
Phacoides (*Miltha*?)
Mesalia sp.
Turritella sp.

These were studied by F.S. MacNeil (USGS, written commun., 1954), who reported as follows:

If these fossils were from North America, I would say that a Paleocene or lower Eocene age is indicated. The large *Venericardia* recalls *V. wilcoxensis* Dall, *V. smithi* Aldrich, and *V. bulla* Dall, species from the Paleocene of the Gulf Coast. The later is related to *"Cardita" beaumonti* from the Paleocene of India. The Arabian species looks to me more like these Paleocene species than it does the middle and upper Eocene species, *V. alticostata* (Courad). Even these likenesses might not be significant, however, considering that Arabia is nearly half way around the world.

Large *Mesalia* of the type found in the Arabian material are also characteristic of the Paleocene and lower Eocene of the Gulf Coast. The Arabian *Mesalia* is very similar to *M. mavericki* Gardner from the Paleocene of Texas and to *M. wilcoxiana* (Aldrich) from the

Paleocene of Alabama. A smaller species with more spirals, *M. alabamiensis* (Whitfield), occurs in the lower Eocene (Wilcox) of Alabama.

The *Turritella* also appears to be close to an Alabama Midway species, *T. alabamensis* Whitfield.

The *Phacoides* is also similar to one described from the Paleocene of Texas by Gardner as *Phacoides (Miltha?) albaripa.*

In spite of these similarities with the Gulf Coast Paleocene, I would not trust it entirely until comparison with faunas from Egypt, India, and east Africa has been made. It is certainly true that some species groups and some generic assemblages which characterize the lower Tertiary of North America, are found in much younger beds, and even Recent, in the Indo-Pacific region."

Subsequently, MacNeil commented further:

Finlay and Marwick [New Zealand Geological Survey Paleontology Bulletin 15, 1937] figures a gastropod as *Kaitangata hendersoni* which may be close to the *Mesalia* in the Arabian material. The New Zealand fossil is from the Wangaloan beds, dated as Danian (supposed to be between our Paleocene and our Upper Cretaceous).

[L.R.] Cox (Annals and Mag., ser. 11, v. 1, 1938) described a species as *Venericardia daviesi.* This, as he says, is related to *"Cardita" beaumonti.* It comes from the Hangu shale of northwestern India which he assigns to the "Lower Eocene, Montian?. The Montian is the lower part of the Paleocene of Belgium."

Dr. Ralph Stewart examined the same collection and agreed with MacNeil's evaluation of Paleocene or early Eocene age. However, because of the long distances from North American fossils, he suggested that L.R. Cox of the British Museum could offer a valuable opinion. Cox's study, in which he concentrated on the gastropods, led him to comment as follows:

Turritella delettrei Coquand. A single broken *Turritella* is referred to this species, originally described [Coquand, 1862, Geology and paleontology of the southern region of the Province of Constantine, p. 266, pl. 30, figs. 1 and 2] from beds considered to be Lower Eocene (Suessonian) in age. The species is characterized by the presence of a single prominent, rounded cord adjoining the adapical suture of each whorl. The growth lines form a sinus just below the cord. The surface of the last whorl is quite flat between the latter and the abapical suture.

Calyptraea cf. *aperta* (Solander). A single eroded cast of a *Calyptraea* does not seem distinguishable from Solander's species. The European range of *C. aperta* is from Ypresian to Priabonian, and in Egypt it occurs in the Upper Libyan and Mokattam stages of the Eocene. No species of *Calyptraea* has been reported either from the *Venericardia beaumonti* beds or from the Eocene of India and Pakistan. The genus occurs in the Midway group of Texas. Its identification in Upper Cretaceous beds in England and elsewhere is doubtfully correct. (Locality A). Locality A is the type locality for the Usfan."

Phacoides sp. indet. A crushed, orbicular *Phacoides* of medium size is not clearly identifiable with any species described from the Eocene of the Middle East or Mediterranean area (Locality A).

Commenting on the age of the fauna, L.R. Cox (written commun., 1957) states:

There is insufficient evidence for arriving at a definite conclusion as to the stage of the Eocene represented. Of the species definitely identified, *Mesalia fasciata* is long ranging, and the evidence of *Turritella delettrei* rests upon the Suessonian (Lower Eocene) age assigned (on unknown grounds) to the formation in which it was originally found. The smaller *Venericardia* has been referred, with qualification, to *Venericardia sindensis* Cox, authentic modern records of which are from the Middle Eocene (Lutetian), although it may possibly also occur in the Lower Eocene (Ypresian), the stage to which the Laki beds belong. It is probable that the *Calyptraea* is not earlier than Ypresian. As the large *Venericardia* is a new species, it throws no light on geological age.

I am inclined to dismiss the suggestion that the formation is as old as Paleocene. The presence of *Turritella delettrei,* if this species is correctly stated to have been found in the Lower Eocene in northern Africa, rather suggests that the age of the formation is lower Eocene (Ypresian).

More recently, Dr. Druid Wilson (written commun., 1979) examined specimens from the 5-m bed of gray limestone near the base of the exposure at 'Usfān and identified the larger bivalve as *Venericardia (claibornicardia)* sp., which is known with certainty only from the middle Eocene of Eastern North America and the Paris basin, but he feels that this occurrence in Saudi Arabia should not be used as a basis for a firm age determination.

In connection with the paleontological age of the Usfan, an ostracod fauna has been described at a depth of 1,637–1,638.7 m from an exploration well drilled on Maghersum Island off the coast of Sudan 220 km southwest of 'Usfān (Masoli, 1969). The ostracods include uppermost Cretaceous and Paleocene species according to Masoli, who also identified three foraminifera. Of the foraminifera, one, *Cibicides* sp., was found in the Haddat ash Sham graben southeast of 'Usfān and was also identified by Ruth Todd (USGS, written commun., 1959). She stated that no age determination could be made as the form occurs in both Cretaceous and Tertiary beds. Furthermore, the external shells seem to have been replaced, suggesting redeposition.

Thus, it appears from the available fossil evidence that the Usfan Formation can be either middle or lower Eocene or Paleocene but most likely is not Maestrichtian. This view is further strengthened by two K-Ar ages, 43.7±1.0 and 56.4±1.2 m.y., obtained from glauconite near the top of the exposure at 'Usfān Pass (samples 34a and 34b, table 10; pl. 2). These ages are middle Eocene and latest Paleocene; as argon can be lost from the mica by sufficient burial, the Paleocene age seems more reasonable, but the 56.4±1.2 m.y. age may represent a Paleocene detrital component in a middle Eocene deposit (Dalrymple and Lanphere, 1969, p. 172, 173). The percentage of potassium is between 3.02 and 3.60, values that are lower than ideal for K-Ar ages (Hunziker, 1979, p. 60–62).

CENOZOIC ROCKS

UMM HIMAR FORMATION (PALEOCENE)

DEFINITION

Lakebeds questionably assigned to the Miocene on the 1963 geologic map (Brown, Jackson, Bogue, and MacLean, 1963), on the basis of freshwater gastropods,

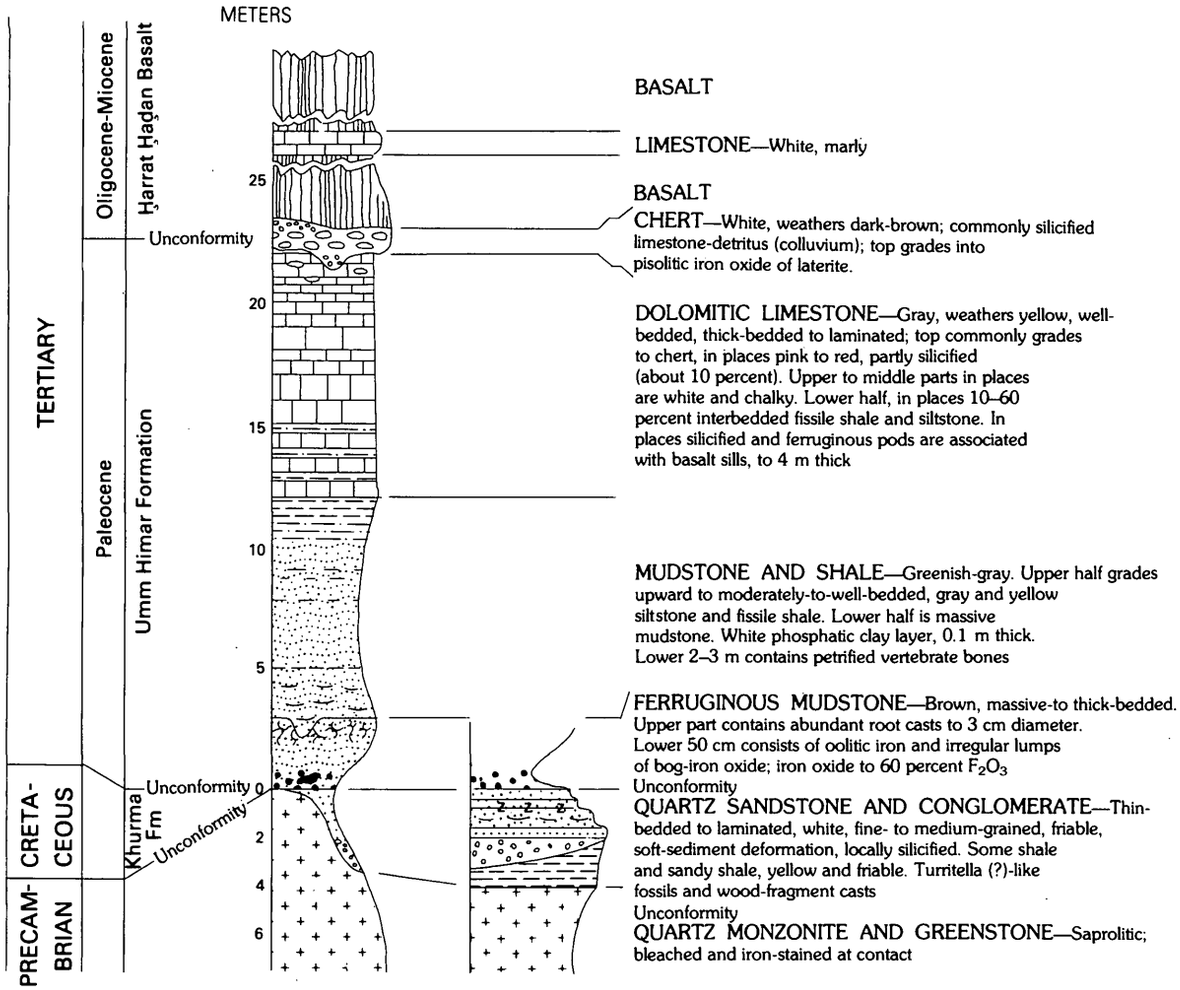

FIGURE 44.—Composite columnar section of the Umm Himar Formation and overlying and underlying rocks in the Jabal Umm Himar area. (From Madden and others, 1980.)

have since been studied and more extensively mapped (Baghanem, 1972; Baghanem and Mickelson, 1972; Gonzales, 1973). The lowermost beds now constitute the Umm Himar Formation as exposed on the eastern flank of Jabal Umm Himar, 100 km east of Aṭ Ṭa'if (Madden and others, 1980). Madden and others divided the Umm Himar into three members: a basal ferruginous mudstone; a middle greenish-gray and yellow siltstone and shale containing fossil vertebrate bones; and an upper dolomitic limestone (fig. 44). The middle member contains numerous vertebrate fossils including sharks, rays, fish, turtles, primitive crocodiles, and a primitive lung fish, a fauna considered mid-Paleocene and indicative of a coastal marine or estuarine environment (Madden and others, 1980).

OCCURRENCE AND THICKNESS

The lacustrine (and estuarine) beds are exposed intermittently within an elliptical ring enclosing an area 145 km north-south by 60 km east-west within a wide, shallow basin on the Rakbah plain east of Aṭ Ṭa'if and surrounding the Ḥarrat Ḥaḍan lava fields. The basalt beds rest on the older estuarine beds and are interbedded with younger sediments. Most of the older (Umm Himar) beds are exposed in an area of about 200 km^2 along the southern and southeastern edge of the lava fields west and north of Turabah, but sporadic small outcrops lie within the lava fields or along wadi banks within the Ḥarrat Ḥaḍan and on the plains in low hills throughout the outer ring. The formation's average thickness is 22 m.

LITHOLOGIC CHARACTER

The lowermost 3 m of ferruginous mudstone contains abundant root casts and oolitic and bog-iron ore. The middle 9 m includes vertebrate fossils in the lower 2 to 3 m of mudstone and grades upward into bedded gray and yellow siltstone and fissile shale. The upper 10 m is

A

B

FIGURE 45.—Laterite under As Sarāt lavas. *A*, Laterite (white saprolite zone) weathered from underlying basement rocks and beneath As Sarāt lava (black); view to northeast near southwest end of lava plateau. Laterite is early Tertiary in age. *B*, Calcareous feldspathoidal syenite plug in the midst of the As Sarāt lava plateau at Al Wārah. The syenite, with an early Miocene age of 22 m.y., transects the laterite and the lower beds of the As Sarāt basalt. (See table 10, samples 67, 68, 69; pl. 2.)

dolomitic limestone and includes some interbedded shale and siltstone in the lower part; it grades into cherty limestone at the top.

NATURE OF CONTACTS

The Umm Himar unconformably overlies either deeply weathered quartz monzonite, andesitic greenstone, or the Khurma Formation, all beveled by the Hejaz pediplain to topography conducive to low coastal marshes and lacustrine sedimentation. The beds overlying the Umm Himar are likewise iron-rich soils corresponding to the widespread pre-Miocene saprolite and laterite found in the Sudan, Ethiopia, and the southwestern uplands of the Arabian Peninsula. Latest Oligocene or earliest Miocene latite and phonolite (22.2±3.5 m.y., sample 40, table 10; pl. 2) intrude the Umm Himar Formation, and late Oligocene lower basalt flows (27.8±1.4, 26.6±1.3 m.y., Arno and others, 1980b) overlie the Umm Himar, whereas younger, probably earliest Miocene, lakebeds are interlayered with the lavas.

LATERITE AND SAPROLITE

A deeply weathered saprolitic and lateritic profile representing a post-Mesozoic erosion interval underlies the As Sirat basalt on the crest of the 'Asir Mountains in southwest Arabia (fig. 45) (Overstreet and others, 1973, 1977). Of varying thicknesses ranging from a few centimeters to more than 50 m, but mostly 20 to 30 m, it is missing in places where the plateau basalt rests on the Wajid Sandstone and is thickest over Precambrian crystalline rocks rich in feldspar. The profiles are typical of those developed under tropical conditions, and they have a surface zone of pisolitic material, here goethite or kaolinite, grading downward to bleached clays, above a zone of enrichment in silica (silcrete); the lower section customarily is a saprolite (Overstreet and others, 1977, p. 5). The most important clay minerals belong to the kaolinite group, with montmorillonite minor. Minor amounts of alunite were also discovered by Overstreet (1973). Hydrated ferrous minerals have concentrated in the upper lateritic zones where the underlying rocks contain ferromagnesian minerals or have been transported.

The age of the weathered zone is somewhat problematic. A minimum age is that for the base of the basalt, on the plateau of As Sirāt, 30.1±1.0 m.y. (sample 69, table 10; pl. 2), using K-Ar decay rates established in 1976 by the International Union of Geological Sciences. A similar situation exists on the northern Ethiopian plateau, where an age of 37.1±1.2 m.y. (table 10) was obtained on a dike at Asmara, Ethiopia, which appeared to be intrusive into the lateritic red soils there underlying the plateau basalts. A recent analysis for a basal flow at Adigrat 130 km south of Asmara in northern Ethiopia, using the new decay constants, gave 30.0±0.7 m.y. (Jones and Rex, 1974). In that area the laterite has been described as the upper part of the Amba Aradam Formation of Cretaceous age (Arkin and others, 1971, quoting M.M. Shumburo, 1968). Likewise, the Trap Series in Yemen (plateau basalts) have recently yielded ages of 29 to 20 m.y., and volcanic rock overlying the Medj-zir Series (Eocene) northwest of Ṣan'ā' and in south-central Yemen have been dated at about 25 m.y.

(Civetta and others, 1978). However, the lateritic profile is not shown in those areas, as it is limited to the basalt outliers northwest of the Jawf graben in extreme northwestern Yemen. Thus, it would appear that the As Sirat laterite could range in age from Cretaceous to mid-Oligocene (to about 30 m.y.). If the saprolite laterite in the Ḥarrat Ḥaḍan area represents the same epoch as the As Sirat, the age span would be reduced to Paleocene–mid-Oligocene.

SHUMAYSI FORMATION

DEFINITION

The Shumaysi Formation was named by Karpoff (1956, 1957a) for clastic sediments, mostly sandstone of continental and lacustrine origin, exposed along the western flank of Wādī Shumaysi, a southern distributary of Wādī Fāṭimah 50 km east of Jiddah. On the southern Hijaz geologic map (Brown, Jackson, Bogue, and MacLean, 1963), the Shumaysi Formation is shown extending intermittently beneath the Tertiary basalt flows in the Usfan graben from Wādī Khulays south to lat 21° N. mostly as outliers on the crystalline basement. It is exposed farther east in the Haddat ash Sham graben and questionably includes sediments beneath basalt in the Tihāmat foothills as far north as lat 22° N. The type section at Wādī Shumaysi was divided by Al-Shanti (1966) into three members, a lower unit of mostly sandstone and conglomerate, a middle member including two oolitic iron-ore beds, and an upper member dominantly composed of shale and siltstone. A reference section has been designated on the west flank of Wādī al Fajj 20 km northwest of Wādī Shumaysi and north of Wādī Fāṭimah, where the lithology is similar, where underlying crystalline basement and overlying basalt flows are likewise exposed, and where the identified fossils have been found.

OCCURRENCE AND THICKNESS

The widely scattered and separated outcrops of the Shumaysi beds range in thickness from 77 to 191 m and are 148 m thick at the type locality (fig. 46), as measured by Al-Shanti (1966). They are faulted, ramped, and skewed in a clockwise direction, the dips mostly to the northeast within the Usfan graben and to a lesser degree in the Haddat ash Sham graben, where nearly 200 m of sandstone crops out above a thin sandy shale containing ferrous oolites, *Tigillites* borings, and marine fossils, possibly reworked. Below the fossiliferous beds, which are 170 m thick, a coarse crossbedded sandstone may be either part of the Usfan Formation or sandstone of the Khurma Formation (AUXERAP, 1967).

LITHOLOGIC CHARACTER

The three members of the Shumaysi have been described and mapped in detail by A.M.S. Al-Shanti (1966) and M.A. Yamani (1968). The lower beds are clastics ranging from pebbly to conglomeratic and from siltstone to fine-grained sandstone. Considerable brown, thinly laminated shale is also present, especially in the outcrops north of Wādī Fāṭimah. The middle member includes two beds of oolitic iron ore interbedded in shale and siltstone. Yamani (1968) has shown that the iron-ore beds, which range in thickness from a thin layer to 5 m, are best developed in the vicinity of the Precambrian Fatimah Group, which crops out in the hills along the north side of Wādī Fāṭimah. His measurements of foresets and ripple marks in the Shumaysi Formation indicate that current directions for the water-laid clastics radiate from the outcrops of the Fatimah Group, which he considers to be the source of the iron. However, the immediate source is laterization of a paleosol. In addition to the clastic material, the upper beds include volcanic ash, which crops out about 40 m below the top of the formation, and calcareous sediments. The beds above the volcanic ash are especially fossiliferous.

NATURE OF CONTACTS

In most outcrops where the basal sandstone of the Shumaysi Formation is exposed, it rests unconformably on Precambrian crystalline rocks, except where the Usfan Formation can be identified below. Where both formations can be seen, a lateritic breccia containing numerous vertical borings above glauconitic and phosphatic beds of the Usfan may represent a time break—a diastem—or a longer disconformity between the Usfan and Shumaysi Formations. Similar lateritic and siliceous beds overlie the Umm Himar Formation of Paleocene age 175 km east of Wādī Shumaysi. The overlying beds above the Shumaysi Formation are basaltic and andesitic lava flows of late Oligocene age, based on K-Ar age determinations.

PALEONTOLOGY AND AGE

The Shumaysi Formation contains terrestrial, lacustrine, and marine fossils. Most of the pelecypods and gastropods are steinkerns. However, L.R. Cox (written commun., 1957) was able to identify a marine gastropod, *Turritella* (*Protoma*) *cathedralis* Brongniart, var. *suprainflata* Sacco of Oligocene-Miocene age in sandstone, near the top of the Shumaysi a few meters below a basalt flow dated at 32.6±2 m.y. (K-Ar whole-rock; sample 35, table 10; pl. 2). Samples submitted by Al-

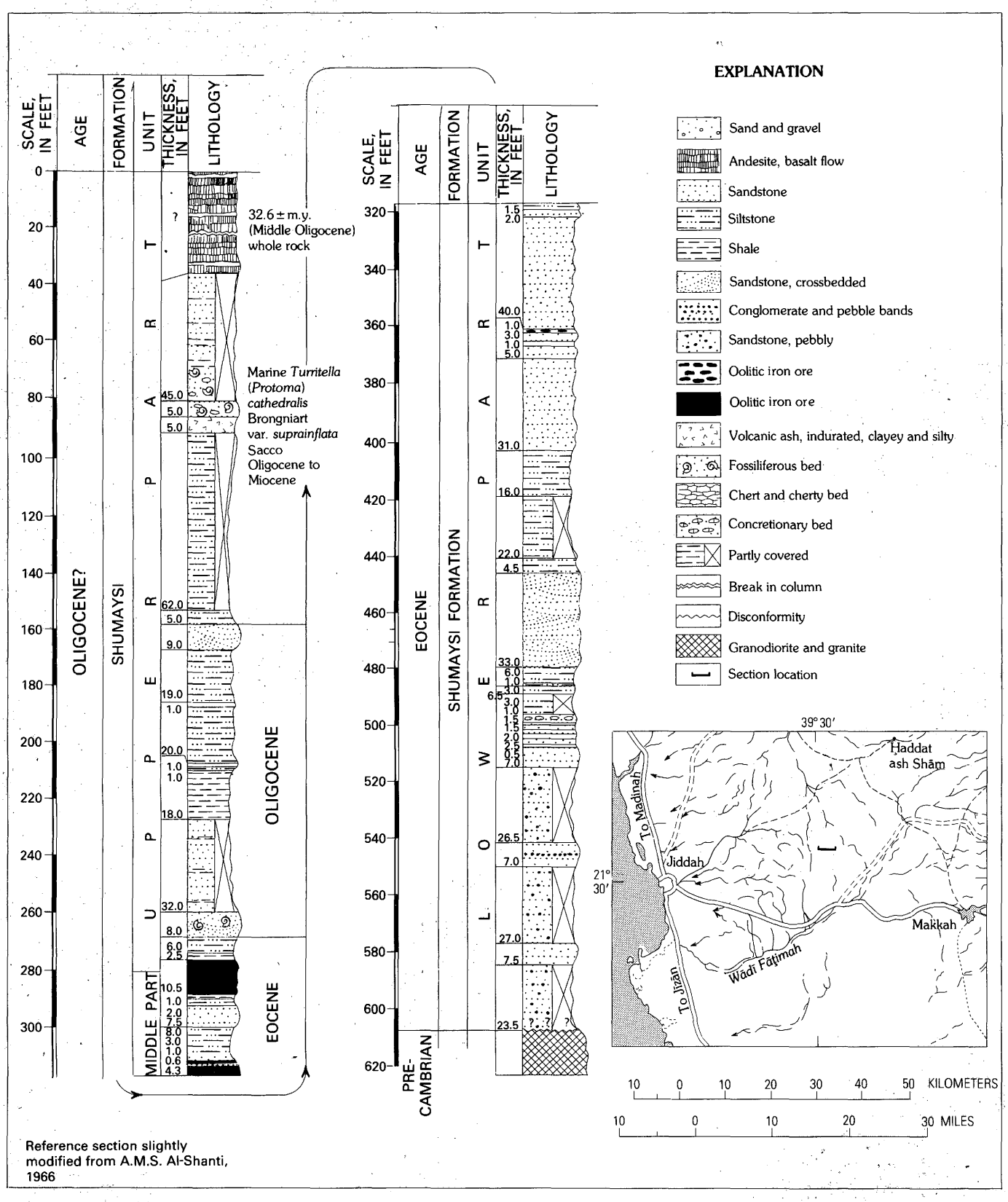

FIGURE 46.—Type referenced section slightly modified from locality of the measured Shumaysi Formation. (From Al-Shanti, 1966.)

Shanti and identified by Cox as *Lanistes*, late Eocene-Holocene age in northeastern Africa, Cox considered "differing slightly from the upper Eocene *L. antiqus*, but on the other hand not identical with any described form of later date." Cox also identified freshwater gastropods *Melanoides* (*Tarebia*) aff. *M. barjacensis* (Fontannes) as of Oligocene age and *Ischurestoma* sp. as of Eocene to Oligocene age.

Fossils from the Haddat ash Sham graben, including *Haplophragmoides* sp. and *Cibicides* sp., could not be assigned an age (Ruth Todd, USGS, written commun., 1960). Todd stated that "the *Cibicides* seemed to have been replaced, and the *Haplophragmoides* was laterally compressed and probably filled. The rarity of the specimens together with their replaced and filled conditions suggest they may be redeposited fossils." Likewise I.G. Sohn (USGS, written commun., 1960) reported that no age assignment could be made from very poorly preserved ostracodes from the outcrops in the Ḥaddat ash Shām area. However, the foraminifera *Operculina alpina multseptata* Silvestri reported in the sedimentary section at Ar Rawdah on the north bank of Wādī Fāṭimah in the Haddat ash Sham graben (AUXERAP, 1967) was originally assigned to the lower Eocene of Libya (Silvestri, 1937). In Arabia it may represent uppermost Usfan or may have been redeposited in the Shumaysi Formation during late Eocene or Oligocene. More recent work includes identification of pollen grains considered of early Eocene age (Moltzer and Binda, 1981). Fossiliferous and arenaceous beds 8 m above the upper oolitic iron stratum are possibly the base of the Oligocene beds which carry Oligocene gastropods higher in the section. These fossiliferous beds in turn are capped by basalt of late Oligocene age (32.6–25.8 m.y., K-Ar).

BAID FORMATION

DEFINITION

The continental Baid Formation was named after exposures seen along Wādī Bayd (lat 17°37′ N., long 42°22′ E.) while mapping the Tihāmat 'Asīr in 1951 (Brown and Jackson, 1959). Later it was also found farther north on the Tihāmat ash Shām (Brown and Jackson, 1958). Most of the exposures of the siliceous nonmarine and volcaniclastic sedimentary beds and associated eruptive rocks are exposed along the banks of the lower courses of wadis flowing toward the Red Sea on the coastal plain, and at the eastern edge of the coastal lowlands in more-or-less continuous belts between wadis. Following our reconnaissance survey, the formation was studied in much more detail by AUXERAP (1967). As the discovery exposure represents only a fraction (40 m) of the distinctive Baid lithology, a better stratotype was designated 15 km northwest of Wādī Bayd near Ad Darb along the south side of Wādī 'Itwad, where dissection of the coastal alluvium has exposed 1,200 m of the underlying Baid (fig. 47) (Gillmann, 1968). The Baid Formation has since been studied in detail from 10 km south of Wādī Qununah to north of Wādī ad Duqah, the northernmost 75 km of outcrop (Greenwood, 1975d; Hadley, 1975a, 1979).

OCCURRENCE, THICKNESS, AND LITHOLOGY

Intermittent exposures of the Baid Formation extend from south of Wādī Jīzān at lat 16°50′ N. northwestward to lat 19°48′ N., a distance of 370 km along the strike parallel to the coast. The exposures are in belts as much as 10 km wide and dip generally 30° toward the Red Sea underneath surficial alluvial and coralline deposits. The exposure on Wādī Jīzān was first, and correctly in our opinion, interpreted as septa within hypabyssal dikes and interbedded flows of dacite, diabase, and obsidian (Gillmann, 1968). More recently, the siliceous argillite (silicite) of the Baid Formation has been described as resting discomformably on a dike swarm of the igneous Miocene Tihamat-Asir Complex, which is considered part of an ophiolitic suite (Coleman and others, 1979). Certainly the siliceous and volcaniclastic rocks are discomformable above the Khums Formation and are intruded by diabase dikes that are part of a Miocene igneous complex (fig. 48).

At Wādī Bayd, 40 m of the Baid Formation is exposed, striking N. 30° W. and dipping 14° southwest, 2 km downstream from agglomerate and metamorphosed mafic igneous rocks, all intruded by diabase. The Baid Formation is here cut by normal faults which also shear the diabase dikes (fig. 48). At Wadi 'Itwad near Ad Darb, the most complete section of the Baid Formation is exposed between 5 and 8 km west of the Precambrian rock on the coastal plain. According to Gillmann (1968), it is "1,200 m of chiefly gray, buff, red, or green silicite with fish fossils and intercalated green or violaceous shale (chlorite, illite and montmorillonite), volcanic tuffs, and diabase sills" (fig. 47).

Crystalline schists of the basement extend to the coast north of Ad Darb, where they are nearly covered with Quaternary basalt and ash of the Al Birk lava fields. The Baid is faulted off, apparently as a result of sinistral movement on a Red Sea transform fault at Ad Darb (Coleman and others, 1979), but another coastal plain reentrant, the Tihāmat ash Shām, extends north of the Al Birk harrat and the Baid Formation appears again along the eastern edge of the coastal plain. At Wādī Ḥalī, about 60 m of argillite, silicite, conglomer-

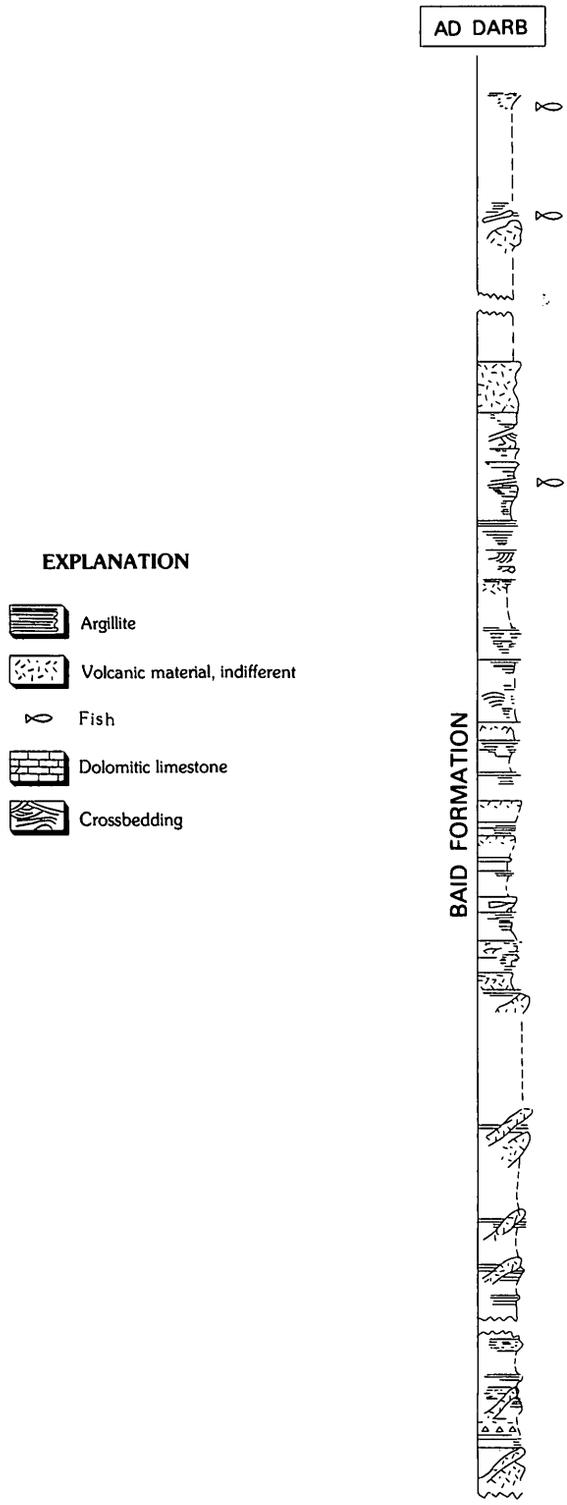

FIGURE 47.—Stratotype section of the Baid Formation, near Ad Darb. (Modified from Gillmann, 1968.)

ate, and related volcaniclastic rocks are exposed in low hills on the coastal plain north of the wadi. The Baid Formation is also exposed along the southern flank of Wādī Yiba, 20 km farther north, where the beds are more calcareous, especially in the upper part. Still farther north, on the south flank of Wādī Qununah, the exposed lower 20 m of the Baid Formation is a polymict conglomerate with a thin bed of limestone near the top; it is in fault contact with Precambrian quartz diorite. The upper 17 m is argillite, the remainder, except 2 m of sandstone at the base, being covered with scree (Hadley, 1975a). The volcaniclastic rocks continue northward across Wādī Lumah, Wādī Ahsibah, and Wādī ad Duqah (Brown and Jackson, 1958). The lower part of the northernmost exposure 15 km north of Wādī ad Duqah is composed of tuff below tuffaceous siltstone and limestone (Hadley, 1979). Although a total thickness cannot be measured because of the alluvial cover and the faulting of the formation, the northern extension may be as much as 3,000 m thick, of which 275 m in the midportion consists of basalt flows and diabase dikes and sills.

The rock, mostly volcaniclastic, ranges from coarse conglomerate, in places agglomeratic, through graywacke sandstone to silt and clay, the last in many places being indurated to shale and argillite, which make up the majority of the exposures. Considerable tuff, both lithic and vitric, and chert are present, and most sediments are siliceous, the silica probably derived ultimately from ash. The southernmost outcrops in the Jizan coastal plain include flows and dikes of diabase, dacite, and obsidian (Gillmann, 1968).

The Baid Formation rests disconformably on the Jurassic Khums Formation at Wādī Jīzān, according to Gillmann (1968). Everywhere it is intruded by the Tihamat-Asir dike swarm, indicating that dikes represent a younger hypabyssal intrusive episode. The Baid is disconformably overlain by alluvial deposits, mostly outwash from the 'Asīr scarp mountains.

PALEONTOLOGY AND AGE

The Baid Formation contains few fossils, Gillmann reporting only ostracods and fish impressions difficult to identify. Fish remains from the outcrops near Ad Darb were examined by D.H. Dunkle, U.S. National Museum (written commun., February 10, 1953), who commented as follows:

> Included among this suite of specimens are representatives of two families of freshwater fishes of widespread distribution in Asia and Africa today. One of these fishes is a cyprimid or minnow, which falls within the structural range of the recent genus *Barbus*. The other is of a cichlid, close, if not identical to, the living *Tilapia*. The incompleteness of the present specimens makes specific comparisons unfeasible. The past history, although very incompletely known, suggests a middle Tertiary age for this occurrence—late Oligocene or Miocene (Brown, 1970).

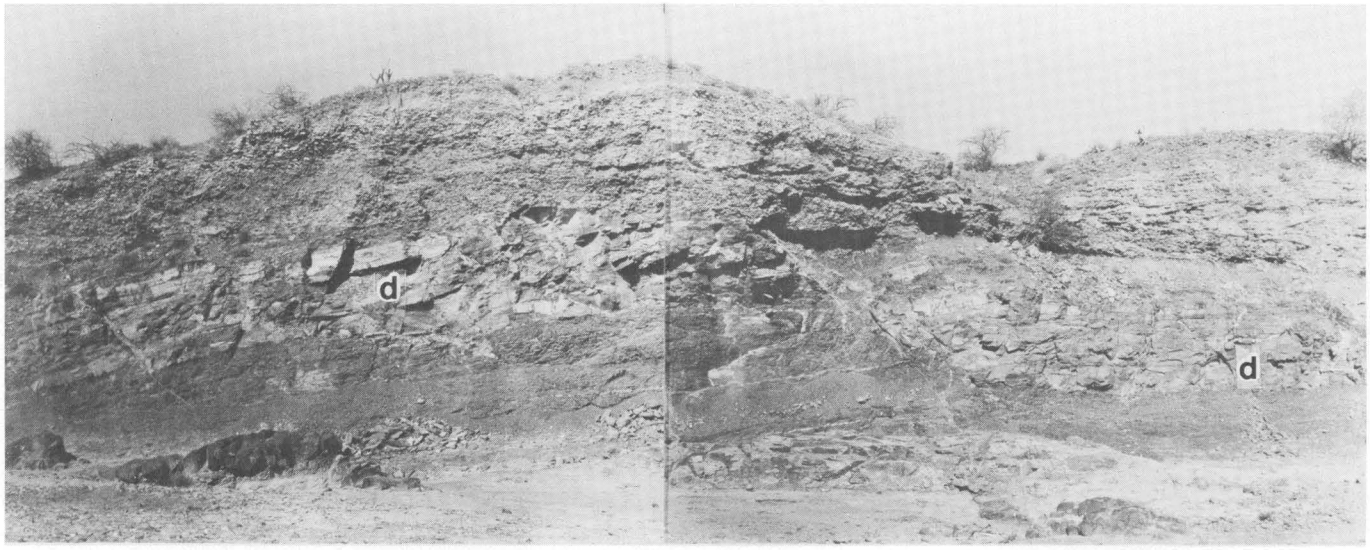

FIGURE 48.—Baid Formation at Wādī Bayd. About 40 m of tuffaceous sandstone and concoidal fracturing, siliceous, red, green, and gray shale containing calcareous concretions is exposed over an older agglomerate. Section is cut by a diabase sill (d) of the Tihamat-Asir Complex.

A K-Ar age of 19±0.6 m.y. (sample 54, table 10, fig. 49) for the diabase sill in the middle Baid of the Tihamat ash Sham coastal plain agrees within instrumental error with three other ages of these sills reported by Coleman and others (1979), that is, an early Miocene age.

JIZAN GROUP

Recently, the middle Tertiary stratigraphy of the southern Red Sea coastal plain has been clarified and revised (Schmidt and others, 1983). The siliceous nonmarine and volcaniclastic sedimentary rocks and associated eruptive rocks exposed along the coastal plain between Jiddah and the Yemen border are assembled into the Jizan Group. Named for the Jīzān coastal-plain region, the Jizan Group is divided into five formations, of which one is the Baid Formation, now redefined and restricted to rocks of a siliceous lakebed facies.

The five formations of the Jizan Group are as follows: a thin, local, basal sandstone formation; a thick formation of mafic volcanic rocks; a silicic, commonly welded tuff, volcanic formation; the widely recognized lakebeds of the Baid Formation; and an upper, thick, mafic to felsic volcanic, largely pyroclastic formation. The upper volcanic formation is everywhere covered across an angular unconformity by younger coastal-plain sediments. The redefined Baid Formation is buff to light-reddish-brown, thin-bedded to laminated, siliceous, tuffaceous siltstone and claystone constituting a freshwater lakebed facies of the predominantly volcanic Jizan Group. The Baid rocks form a contiguous unit and in part interdigitate with the volcanic rocks of the overlying and underlying formations of the Jizan Group.

The 1:1,000,000 scale of the geologic map (pl. 1) is appropriate only to show the Jizan Group, but where the Baid Formation is predominant, as in the Al Qunfudhah region, the group is represented on the map by the Baid Formation. Where the volcanic formations either above or below the Baid are predominant, as in

FIGURE 49.—Exposure of the Bathan boulder conglomerate in the foreground overlying the Miocene Jizan Group in the middle distance. The Jizan Group here is altered siliceous and limonitic tuff of the Baid Formation. View downstream toward the Red Sea and along Wādī ad Duqah in the Jabal Shada quadrangle.

the Jīzān region, the group is shown as a volcanic formation.

The Jizan Group variably overlies the Wajid Sandstone, Khums Formation, and Amran Formation in the Jīzān region. It overlies the Precambrian shield rocks in the Al Qunfudhah region and overlies rocks as young as the Shumaysi Formation at Jabal Sitā', south of Jiddah. The Jizan rocks are everywhere intruded by the mafic rocks of the Tihamat-Asir Complex. Accordingly, the Jizan Group is of late Oligocene to early Miocene age (about 30 to 20 m.y.; Schmidt and others, 1983).

BATHAN FORMATION (MIOCENE)

DEFINITION

The Bathan Formation at its type locality is named for Wādī Baṯḥān, a tributary of Wādī Līth, 15 km northeast of Al Līth (Hadley and Fleck, 1980a). The exposure adjacent to Wādī Baṯḥān was first described, though not named, by Brown, Jackson, Bogue, and MacLean (1963) as "dissected and not obviously related to present drainages." They believed that this boulder conglomerate may be much older than Quaternary. Brown mapped similar deposits east and northeast of Jiddah (Brown, Jackson, Bogue, and Maclean, 1963), and Nebert and others (1974) described one of these deposits north of Wādī Fāṭimah.

LITHOLOGY AND THICKNESS

The Bathan is a terrigenous, polymictic clastic deposit consisting of boulder, cobble, and pebble conglomerate, sparse beds of coarse-grained sandstone, and rare, thin beds of red siltstone. Clasts consist of many types of Precambrian rocks; especially conspicuous are Precambrian granite and clasts of silicic tuffs and flows of the Baid Formation. The conglomerate is poorly sorted and commonly chaotically immature; some thick, massive beds contain boulders as much as 2 m across. Many clasts are angular to subrounded. The thickness of the Bathan at its type locality probably well exceeds 700 m.

OCCURRENCE AND NATURE OF CONTACTS

The Bathan, where mapped, underlies the Red Sea coastal plain or the adjacent low foothills. In most places it is poorly exposed; in fact, it is mostly identified by a flat surface of residual lag of coarse, resistant boulders (fig. 49). Its upper surface everywhere is an erosional surface and its base, where rarely exposed, rests on a compound erosion surface that cuts across the Baid Formation, early Tertiary laterite, and Precambrian basement as at Wādī Baṯḥān. At Ḥarrat Tuffil (Shamā), the Bathan rests on rhyolitic volcanic deposits associated with the Baid Formation (Pallister, 1983). Where bedding is visible, the beds dip gently as much as 15° either southwest or northeast in block-fault structures.

PALEONTOLOGY AND AGE

No fossils have been found in the Bathan. It is younger than the stratigraphically underlying early Miocene Baid Formation and tholeiitic dikes of the Tihamat-Asir Complex. The Bathan Formation is probably of about middle Miocene age, as it is the erosional product of rapid uplift of the Red Sea Escarpment (Hadley and Fleck, 1980a) during the middle Miocene (Schmidt and others, 1983). During future mapping the Bathan probably will be identified between Jiddah and the Gulf of Aqaba, and it will probably be found to lie beneath the Raghama Formation.

RAGHAMA FORMATION (MIOCENE)

DEFINITION

The Raghama Formation was mapped on three USGS Miscellaneous Geologic Investigations Maps: Geology of Wādī as Sirḥān (I-200A, Bramkamp, Brown, and others, 1963), Geology of the Northwestern Hijaz (I-204A, Brown, Jackson, Bogue, and Elberg, 1963), and Geology of the Arabian Peninsula (I-270A, USGS–ARAMCO, 1963). The type locality was chosen for the area where the most complete exposure of Miocene reef limestone, gypsum, and related clastics was found during the reconnaissance mapping.

Jabal ar Raghamah forms the western flank of the lower alluvial plain of Wādī 'Ifāl in the Ash Shifā' region east of the Gulf of Aqaba at lat 28°20′ N. The Raghama Formation is exposed from lat 28°10′ N. to 28°35′ N. and extends westward from the alluvial plain of Wādī 'Ifāl to the coast of the Gulf of Aqaba, the Maqnā-Al Bad' area (Bramkamp, Brown, and others, 1963).

These sediments were first described in 1952 by Mustafa Sadek, who investigated the occurrence of native sulphur earlier reported by Burton (1878). The outcrops were revisited the following year by H.J. Philby and R.G. Bogue (Bogue, 1953) to further study the occurrence of the sulphur in the gypsiferous beds. Bogue described the area as basal coarse grit and conglomerate overlain by "sandstone, siltstone, and shale with interbeds of limestone and shale which often contains some volcanic tuff." Sulphur was identified with gypsiferous sandstone in the upper beds. The next year W. Schott of the German Geological Survey

described the following section (Richter-Bernburg and Schott, 1954, p. 32):

Sedimentary section near "Al Bad'"
- Sandy reef rocks
- Sandstone, partly with boulders
- Sandy claystone to clayey sandstone without microfossils, about 25 m thick
- Gypsum, light- to whitish-gray, partly compact, partly unclean, at least 300 m thick
- Clayey marlstone, probably partly missing, about 15 m thick
- Sandy reef rocks to coarse porous limestone, 100–150 m thick
- Coarse-grained sandstone, crossbedded

_____Transgression

- Nubian sandstone (?Paleozoic) sandy horizon, reddish gray with gravels and boulders

_____Transgression

Basement

He questionably assigned a Miocene age to the beds above the Nubian Sandstone, including the gypsum.

In 1966, V.A. Trent and R.F. Johnson briefly investigated the economic possibilities of the area (Trent and Johnson, 1966). A study of the sulphur deposits was made by Bodenlos and Lari (1970), who divided the Raghama Formation into three major units: a basal coarse-grained clastic section; a middle unit of green marl, siltstone, and interbedded gypsum, with dolomite and sandstone in the upper part; and an upper unit of red sandstone containing a few thin beds of gypsum and siltstone.

A more detailed columnar section given by Bigot and Alabouvette, French Bureau des Recherches Geologiques et Minieres, of the outcrops in the Maqnā-Al Bad' area could be considered a reference section (Bigot and Alabouvette, 1976, fig. 6). However, they state that the Miocene in the Jabal ar Raghamah region (Maqnā-Al Bad' area) cannot be correlated with the Miocene detrital rocks of the "Jabal Dhaylan Series," exposed on the coastal plain 350 km southeast of Jabal ar Raghamah. At Jabal Dhaylān, the Tertiary beds have been studied in connection with mineralization at the base of the middle Miocene. This latest study divides the Raghama Formation, shown as a single formation unit on the 1963 USGS maps, into three units: a lower continental clastic section; a middle section of marine and littoral deposits, including reef limestones, gypsum, marl, and dolomite; and an upper section of clastics, oyster reefs, and gypsum.

OCCURRENCE, THICKNESS, AND LITHOLOGY

The Raghama Formation was shown on the 1963 USGS maps as outcropping intermittently from Yanbu' at lat 24° N. to the Maqnā-Al Bad' area at lat 28°35′ N. The localities at Yanbu', Umm Lajj, Jabal Dhaylān, and north from Al Wajh were considered of Miocene age on the basis of meager formal evidence. Thickness is variable, as might be expected from the marine transgressive reef and lagoonal evaporite type of sedimentation.

The basal conglomerate and sandstone are not present in all the outcrops, and the thickness where the basal conglomerate and sandstone have been measured ranges from less than a meter to more than 100 m (Bodenlos and Lari, 1970; Bigot and Alabouvette, 1976), with the maximum in the northern part of Jabal ar Raghamah near Al Bad'. As much as 1,500 m of partly arkosic sandstone has been reported from Tīrān Island (Goldberg, 1963) in the northern Red Sea, 30 km south of the Raghama outcrop area east of the Gulf of Aqaba.

The middle member section is 400 m thick at the type locality at Jabal ar Raghamah (Bodenlos and Lari, 1970), but it ranges from 25 m to several hundred meters in thickness at various places along the Tihāmat (Bigot and Alabouvette, 1976). On Tīrān Island the middle member is 250–450 m thick. According to Bodenlos and Lari (1970), the upper member of 100–200 m in the lowlands in the southwest corner of the peninsula south of Maqnā is comparable to the 250 m reported at Tīrān Island off the peninsular point.

The section on Tīrān Island resembles the submarine Miocene of the Red Sea, as reported in various drilling records. The submarine section includes a midpart of evaporite more than 1,200 m thick consisting mostly of halite but including anhydrite above and below the salt beds that overlie 1,000 m of middle Miocene marl characterized by *Globigerina*. The sediments above the evaporite section proper are mixed beds of conglomerate, calcareous sandstone, limestone, clay shale, anhydrite, and salt, as would be expected above a dynamic sea floor.

NATURE OF CONTACTS

The Raghama Formation overlaps the crystalline basement in many places (fig. 50). More commonly it rests on sandstone and conglomerate of doubtful age, probably Oligocene, as near Jiddah, but farther north it overlies the possible Eocene or Cretaceous Nubian-type sandstone. At Jabal ar Raghamah, the sandstone beneath the marine beds was questionably considered to be Paleozoic by W. Schott (Richter-Bernburg and Schott, 1954). However, sandstone of Early Cretaceous Senonian age is faulted down in a small graben 5 km east of Aqaba in Jordan (Bender, 1968), and similar beds occupy a similar graben in Arabia 5 km southeast of the graben in Jordan. The beds in Arabia consist of 10 m of conglomerate and coarse arkosic sandstone below 5 m of fine-grained sandstone, variegated in color and crossbedded (Trent and Johnson, 1966). This

FIGURE 50.—The Raghama Formation, along the coast southeast of Ḍubā where Raghama carbonate beds dip southwest about 45° along the northeast side of the coastal plain, reflecting the ramping of Miocene rocks. The underlying Precambrian crystalline rocks of the Ḥismá (Midian) block were rotated and elevated in a counterclockwise direction during the opening of the Red Sea rift.

is very likely composed of the same clastic material described by Bender (1968). These deposits may also be coeval with the basal sandstone at Jabal ar Raghamah, but without fossil evidence such a correlation is tenuous.

The Raghama underlies Quaternary terrace deposits, including Pliocene, Pleistocene, and Holocene coral reefs, in contrast to reefal coral of Miocene age that overlies the volcaniclastic sediments of the Baid Formation east of Al Qunfudhah. Northwest of Yanbu' the Raghama is overlain by Quaternary basalt flows.

PALEONTOLOGY AND AGE

The extensive exposures of Miocene reefs in the Yanbu' basin and northwestward toward Sharm al Khawr contain the coral *Montastrea* sp. cf. *M. pedunculata* (Duncan), previously known from the Miocene Gaj Formation of Pakistan, according to J.W. Wells (written commun., 1953), who identified it. Farther south and 10 km inland from Tuwwal, 80 km north of Jiddah, a dolomitic reef yielded the following foraminifera and algae (collected by B. Steenstra and identified by H.A. McClure):

Foraminifera

Borelis melo (common)
Heterostegina sp.
Taberina? *malabarica*
Peneroplis? *farsensis*
?*Cycloclypeus*

Algae

Halimeda cf. *H. monile* or *incrassata*

McClure (ARAMCO, written commun., 1975) considers the *Borelis melo* a widespread guide fossil for the upper Burdigalian, thus marking the approximate lower boundary of the middle Miocene (about 15 m.y. ago). The Tuwwal reef is correlated tentatively with the Globigerina Marl of the Gulf of Suez region.

Still farther south and east of Al Qunfudhah, 320 km south of Jiddah and 15 km inland near Sūq al Aḥad, a coralline reef yielded the following corals, identified by J.W. Wells (USGS, written commun., 1953):

Favites sp. cf. *F. profunda* (Michelotti)
Montastrea or *Plesiastrea* sp.
Montastrea sp. cf. *M. reussiana* (M.E. & H.) var. *minor* (Zuffardi)

The *Favites* sp. cf. *F. profunda* is known from the Miocene of Italy and Red Sea areas, and the *Montastrea* sp. cf. *M. reussiana* var. *minor* is known from the Miocene of Cyrenaica (Libya) and Red Sea areas, according to Wells.

In addition, from the fossils found at Al Qunfudhah F.S. MacNeill reported "several specimens of *Cerithium* belonging to the group of *C. jonkeri* Martin and *C. poetjanganensis* Altena. *C. jonkeri* has been reported from the upper Miocene to the Pleistocene in the East Indies and the Philippines, the latter possibly only a subspecies of *C. jonkeri* from the Pleistocene of Nias and Java."

The oyster *Ostrea crasissima* Lamarck, which is synonymous with *O. gryphoides*, was found by us north of Umm Lajj. It was also found later near Al Wajd and south of Al Muwaylih by W. Schott, who reported (Richter-Bernburg and Schott, 1954) the opinion of K. Staesche that the source beds were Miocene, based on the associated microfauna. Although a review of post-Miocene Ostreidae by L.R. Cox (1929) indicates that the form extends into the Pliocene in the Indian Ocean affinity, it became extinct in the Mediterranean fauna at the end of the Miocene. The end of the Miocene coincides with the top of the evaporite section in the Raghama. In the sediments of the Red Sea, this datum is marked by an accoustic reflector—now dated at 5 m.y., near the beginning of the Pliocene when the Red Sea opened anew to allow ingress of Indian Ocean fauna.

As these limestone beds at Al Qunfudhah overlie the Baid Formation, which contains a diabase sill (19.1±0.6 m.y., K-Ar; sample 54, table 10, pl. 2), most of the evidence points to a middle to younger Miocene age for the Raghama Formation, with the possibility that some of the upper reefs may be Pliocene.

In this connection, the basalt flow east of Tuwwal, which caps the ridge containing the approximate lower

boundary of the middle Miocene, was dated by K-Ar methods at 4.4±0.4 m.y. (sample 30, table 10, pl. 2). An adjacent flow to the south in an identical physiographic setting was dated at 4.2±0.8 m.y. (sample 32, table 10). Thus, a minimum age is established.

CENOZOIC IGNEOUS ROCKS[7]

Igneous activity in western Saudi Arabia appears to have been dormant from late Proterozoic or earliest Cambrian until mid-Tertiary, when the opening of the Afro-Arabian rift system renewed magmatic upwelling which has continued until the present. The distribution of Tertiary intrusive rocks, represented by various dikes, plugs, stocks, and small plutons, and Cenozoic extrusive rocks, represented by the extensive flood-basalt fields, are shown on plate 2. Chemical and normative analyses (table 9) and K-Ar age determinations (table 10) for these igneous rocks are discussed in the appropriate sections that follow. The time distribution of the K-Ar ages of the Cenozoic igneous rocks of this report as well as of some other Cenozoic rocks from around the Red Sea is shown in the histogram of figure 51. Although some K-Ar radiometric ages greater than about 30 m.y. are reported for the Tertiary igneous rocks that flank the rift system, they are suspect, especially where the magma has penetrated thick Precambrian terrane rich in argon (Megrue and others, 1972). Various plots of the chemical and normative data are given in figures 52–56 and are briefly discussed in the text.

The Cenozoic rocks comprise flood basalt on the Arabian Shield, basaltic to rhyolitic volcanic rocks in a continental rift valley along the proto-Red Sea, tholeiitic dikes and gabbro and granophyre plutons likewise in the rift valley, and continental dikes inland from the rift valley (table 11).

Outpouring of alkali-olivine basalt marked the beginning of mid-Tertiary volcanism in western Saudi Arabia. Well within the craton these late Oligocene-early Miocene flows spread out as large flood-basalt fields upon a lowland of low altitude as well as low relief. The basal eruptions about 30 m.y. old were undersaturated picrite and ankaramite fed mostly from volcanic centers (feeder pipes) to form shield volcanoes. Overlying flows were mostly basanite, including some hawaiite that formed the great composite flood-basalt fields. Late products formed plugs of latite (phonolite), analcime syenite, and rhyolite (comendite) with ages of about 22 m.y.

During the same time interval along the present-day coastal plain of the Red Sea, bimodal volcanics of the Jizan Group were deposited in a continental rift valley along the proto-Red Sea. About 20 m.y. ago, as seafloor spreading began, dike swarms of tholeiitic basalt and diabase intruded the Jizan Group volcanics in the rift valley. At about the same time and place, plutons of tholeiitic gabbro and granophyre were intruded through the thinned continental crust of the rift valley. Slightly inland along the continental margin, long, thick dikes (pl. 2) ranging from gabbro to quartz syenite (fig. 52) intruded the thicker, less extended, less thinned cratonic crust. A second pulse of flood basalt beginning during middle-late Miocene was superposed on the older basalt fields on the craton, but the lavas erupted along the continental margin as well. The flows continued to erupt to Recent time, and again were predominantly alkali olivine basalt that evolved to minor silicic phases, especially in the latest eruptions (fig. 60).

TERTIARY HYPABYSSAL IGNEOUS ROCKS

Intrusive igneous rocks associated with the Tertiary opening of the Red Sea include dikes, pipes or plugs, small stocks, and layered-gabbro plutons (Brown, 1960; Brown and Hase, 1971; Blank, 1977; Coleman, Fleck, and others, 1977). Dikes predominate although they are areally insignificant compared with the coeval harrats (flood-lava fields). The dikes consist of a swarm of hydrothermally altered diabase sheets associated with granophyre and cumulative gabbro plutons which together make up the Tihamat-Asir Complex. The complex extends intermittently 150 km north from the Yemen border as far as lat 17°45′ N., where it is terminated by the Ad Darb Red Sea transform fault.[8] Northward beyond the Ad Darb fault, the individual dikes, which there transect continental rocks in the scarp mountains, are much larger, are separated by Precambrian screens, and are designated continental dikes by Blank and Coleman (Blank, 1977; Coleman and others, 1979). They extend northward 1,375 km to lat 28°30′ N., in Ash Shifā', east of the Gulf of Aqaba, and thence across southern Sinai (pl. 2) (Bartov and others, 1980). Whereas the Tihamat-Asir dike swarm extends inland 50 km, the continental dikes are found as much as 100 km from the Red Sea coast. They are characterized by remarkably linear and predominantly reversely polarized magnetic anomalies (Blank, 1977), range in width from 50 to 300 m, and are mostly gabbro,

[7]For a more complete discussion of the Cenozoic volcanic rocks, the reader is referred to USGS Open-File Report 83–788 by R.G. Coleman, R.T. Gregory, and G.F. Brown (1983), which is based on this report plus later field and laboratory work by Coleman and Gregory.

[8]Since this was written, J.S. Pallister mapped a Tertiary dike swarm at Wādī Ad Damn 100 km southeast of Jiddah having composition and age similar to the Tihamat-Asir Complex (Pallister, 1983).

Text continues on p. 145.

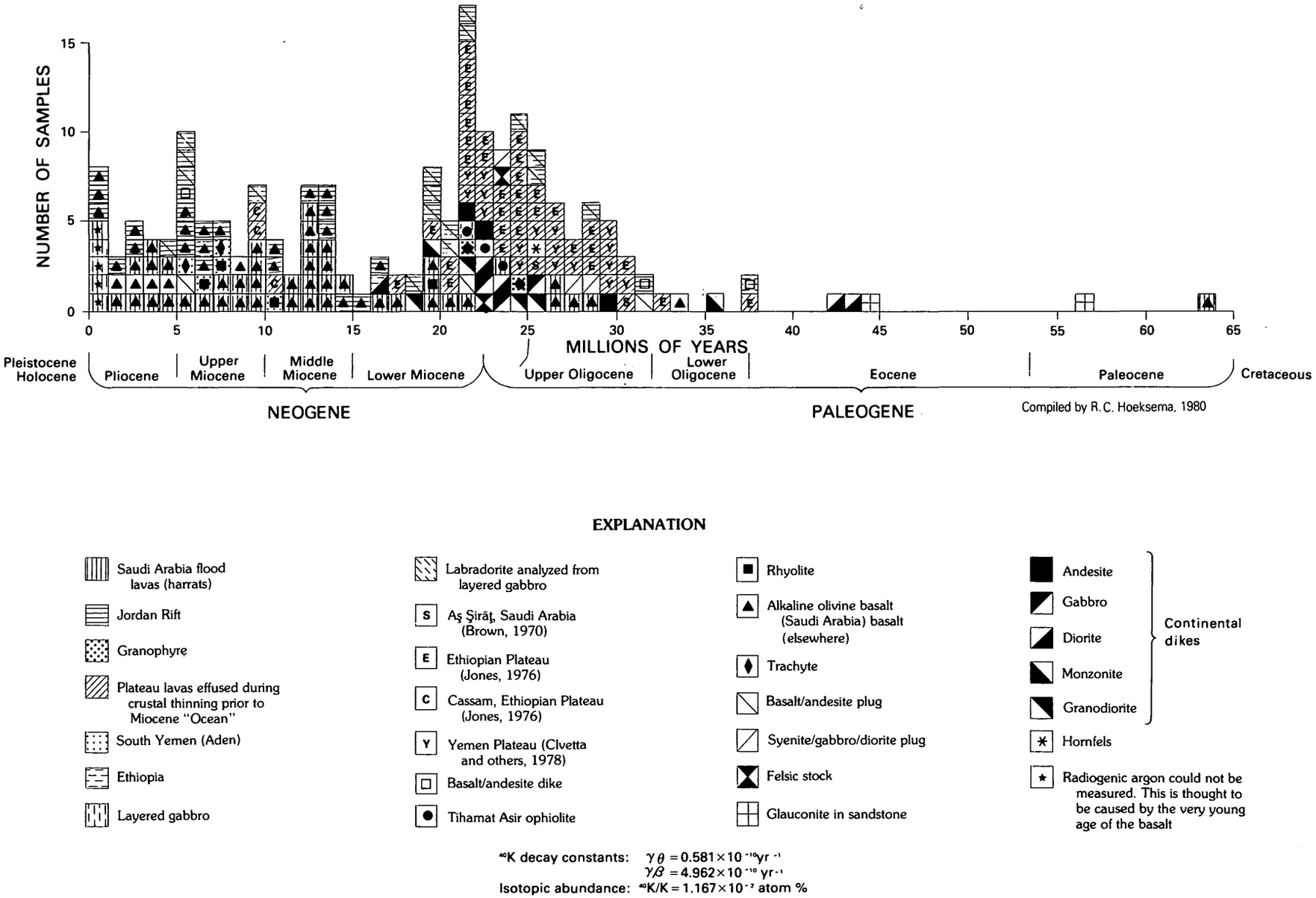

FIGURE 51.—Histogram showing ages of selected Tertiary igneous rocks and glauconite from around the Red Sea. Most ages are from table 10; other sources are referenced in explanation of the figure.

TABLE 9.—*Chemical and normative analyses of Cenozoic igneous rocks from western Saudi Arabia*[1]

Sample (location given on pl. 2)[2]	1	2	3	5	6T	6B	7T	7B	8	9T	9B	10
Field no.[2]	47000	47001	47002	47004	917T	917B	916T	916B	B1818	915T	915B	913
Type of source rock[3]	X	X	X	X	X	X	X	X	O	X	X	X
Unadjusted oxides (wt. percent):												
SiO_2	46.30	46.30	47.40	51.50	46.60	45.70	42.50	43.70	49.30	43.70	46.60	45.70
Al_2O_3	14.60	13.20	15.60	14.60	17.10	16.10	14.00	14.40	15.30	15.00	16.10	16.90
Fe_2O_3	6.40	3.91	3.80	2.59	3.20	4.20	6.70	3.60	1.70	4.00	1.70	3.80
FeO	4.90	7.90	7.40	7.30	8.40	6.40	4.40	7.30	10.20	7.10	10.00	6.80
MgO	8.10	8.87	8.50	6.60	4.50	8.00	9.20	9.50	5.80	8.60	6.90	4.50
CaO	11.20	12.30	10.60	10.40	7.60	10.30	11.80	11.20	9.00	10.00	7.50	10.80
Na_2O	3.70	3.62	3.30	4.53	4.20	2.60	4.40	2.80	2.70	3.70	3.80	4.30
K_2O	0.96	0.78	0.54	0.92	1.40	0.35	0.67	0.80	1.00	1.40	1.20	1.40
H_2O	—	2.40	1.80	0.40	2.70	3.00	1.72	2.50	0.97	1.65	2.58	1.10
TiO_2	1.80	1.60	1.60	2.00	2.60	1.50	2.30	1.90	2.50	2.40	2.10	2.20
P_2O_5	0.27	0.17	0.16	0.23	0.68	0.28	0.58	0.40	0.37	0.50	0.41	0.44
MnO	0.12	0.13	0.12	0.11	0.18	0.15	0.18	0.16	0.18	0.18	0.15	0.15
CO_2	—	—	—	—	0.14	0.46	0.81	0.67	0.02	0.46	0.06	0.84
Total	98.35	101.18	100.82	101.18	99.30	99.04	99.26	98.93	99.04	98.69	99.10	98.93
Adjusted oxides:												
SiO_2	47.08	45.76	47.01	50.90	46.93	46.14	42.82	44.17	49.78	44.28	47.02	46.19
Al_2O_3	14.84	13.05	15.47	14.43	17.22	16.26	14.10	14.56	15.45	15.20	16.25	17.08
Fe_2O_3	6.51	3.86	3.77	2.56	3.22	4.24	6.75	3.64	1.72	4.05	1.72	3.84
FeO	4.98	7.81	7.34	7.21	8.46	6.46	4.43	7.38	10.30	7.19	10.09	6.87
MgO	8.24	8.77	8.43	6.52	4.53	8.08	9.27	9.60	5.86	8.71	6.96	4.55
CaO	11.39	12.16	10.51	10.28	7.65	10.40	11.89	11.32	9.09	10.13	7.57	10.92
Na_2O	3.76	3.58	3.27	4.48	4.23	2.63	4.43	2.83	2.73	3.75	3.83	4.35
K_2O	0.98	0.77	0.54	0.91	1.41	0.35	0.67	0.81	1.01	1.42	1.21	1.42
H_2O	—	2.37	1.79	0.40	2.72	3.03	1.73	2.53	0.98	1.67	2.60	1.11
TiO_2	1.83	1.58	1.59	1.98	2.62	1.51	2.32	1.92	2.52	2.43	2.12	2.22
P_2O_5	0.27	0.17	0.16	0.23	0.68	0.28	0.58	0.40	0.37	0.51	0.41	0.44
MnO	0.12	0.13	0.12	0.11	0.18	0.15	0.18	0.16	0.18	0.18	0.15	0.15
CO_2	—	—	—	—	0.14	0.46	0.82	0.68	0.02	0.47	0.06	0.85

Footnotes at end of table.

TABLE 9.—*Chemical and normative analyses of Cenozoic igneous rocks from western Saudi Arabia*[1]—Continued

Sample (location given on pl. 2)[2]	1	2	3	5	6T	6B	7T	7B	8	9T	9B	10
Field no.[2]	47000	47001	47002	47004	917T	917B	916T	916B	B1818	915T	915B	913
Type of source rock[3]	X	X	X	X	X	X	X	X	O	X	X	X
Normative minerals:												
Quartz	—	—	—	—	—	—	—	—	0.107	—	—	—
Corundum	—	—	—	—	—	—	—	—	—	—	—	—
Orthoclase	5.768	4.555	3.165	5.373	8.331	2.088	3.989	4.779	5.967	8.383	7.156	8.362
Albite	21.225	13.740	24.350	31.008	32.285	22.214	14.712	17.622	23.068	15.739	28.141	22.349
Anorthite	20.736	17.261	25.945	16.590	23.838	31.528	16.594	24.624	26.933	20.454	23.541	22.922
Nepheline	5.747	8.957	1.813	3.725	1.898	—	12.350	3.428	—	8.660	2.333	7.817
Wollastonite	14.182	17.516	10.512	13.744	3.660	6.381	13.949	10.279	6.505	9.837	4.559	9.588
Enstatite	11.828	11.593	7.050	8.620	1.978	14.055	12.055	7.140	14.585	6.986	2.448	5.890
Ferrosilite	0.564	4.658	2.674	4.283	1.557	4.292	—	2.291	13.664	1.991	1.961	3.150
Forsterite	6.085	7.176	9.774	5.344	6.523	4.248	7.728	11.756	—	10.313	10.436	3.811
Fayalite	0.320	3.177	4.086	2.926	5.659	1.430	—	4.157	—	3.239	9.216	2.246
Magnetite	9.435	5.603	5.465	3.711	4.672	6.149	8.163	5.276	2.489	5.877	2.487	5.569
Hematite	—	—	—	—	—	—	1.120	—	—	—	—	—
Ilmenite	3.476	3.003	3.014	3.754	4.973	2.876	4.401	3.648	4.794	4.619	4.025	4.223
Apatite	0.650	0.398	0.376	0.538	1.622	0.670	1.384	0.958	0.885	1.200	0.980	1.053
Calcite	—	—	—	—	0.321	1.056	1.856	1.540	0.046	1.060	0.138	1.931
Total	100.016	97.638	98.224	99.618	97.319	96.987	98.300	97.496	99.042	98.357	97.420	98.913
Sálic	53.476	44.513	55.273	56.697	66.353	55.830	47.644	50.452	56.075	53.235	61.170	61.451
Femic	46.540	53.125	42.951	42.921	30.965	41.157	50.655	47.044	42.968	45.122	36.250	37.462
Diopside[4]	26.574	33.768	20.237	26.647	7.196	12.222	26.004	19.710	12.863	18.814	8.968	18.627
DiWo	14.182	17.516	10.512	13.744	3.660	6.381	13.949	10.279	6.505	9.837	4.559	9.588
DiEn	11.828	11.593	7.050	8.620	1.978	4.475	12.055	7.140	3.282	6.986	2.448	5.890
DiFs	0.564	4.658	2.674	4.283	1.557	1.367	—	2.291	3.075	1.991	1.961	3.150
Hypersthene[5]	—	—	—	—	—	12.506	—	—	21.891	—	—	—
HyEn	—	—	—	—	—	9.580	—	—	11.303	—	—	—
HyFs	—	—	—	—	—	2.926	—	—	10.589	—	—	—
Olivine[6]	6.405	10.353	13.859	8.271	12.182	5.678	7.728	15.912	—	13.552	19.653	6.058
OlFo	6.085	7.176	9.774	5.344	6.523	4.248	7.728	11.756	—	10.313	10.436	3.811
OlFa	0.320	3.177	4.086	2.926	5.659	1.430	—	4.157	—	3.239	9.216	2.246
Wollastonite minus DiWo	—	—	—	—	—	—	—	—	—	—	—	—

Footnotes at end of table.

TABLE 9.—*Chemical and normative analyses of Cenozoic igneous rocks from western Saudi Arabia*—Continued

Sample (location given on pl. 1)[2]	12	13	14	15	16	17	18	19	19a	22	23	24
Field no.[2]	912	1843	919	920	921	911	910	922	1309	907	909	908
Type of source rock[3]	X	O	X	X	X	X	X	X	P	X	X	X
Unadjusted oxides (wt. percent):												
SiO_2	43.40	46.50	46.60	46.20	44.10	47.40	44.80	45.30	39.80	46.70	43.20	45.00
Al_2O_3	15.20	14.90	16.70	16.90	15.20	16.50	16.70	15.80	13.40	16.50	14.60	14.90
Fe_2O_3	3.00	5.00	3.60	2.10	4.10	2.40	3.90	2.30	4.60	1.20	5.30	2.20
FeO	8.40	9.80	8.90	10.30	7.40	9.20	9.70	8.20	8.20	9.10	5.60	9.20
MgO	9.80	4.90	7.20	6.50	9.50	8.00	6.00	9.00	9.90	9.20	9.80	10.50
CaO	9.90	7.60	8.60	8.60	9.50	7.50	7.50	9.90	11.80	10.80	11.70	9.80
Na_2O	2.70	2.90	3.80	3.70	2.70	4.20	3.50	2.50	3.80	2.70	2.80	2.40
K_2O	1.10	1.10	0.89	0.86	0.86	0.74	0.67	0.74	0.90	0.25	0.64	0.67
H_2O	2.58	2.86	0.87	0.46	2.39	1.23	2.86	2.34	2.19	0.75	1.10	1.41
TiO_2	2.40	3.90	2.10	2.40	2.40	2.20	2.60	1.70	2.80	1.50	1.70	1.80
P_2O_5	0.41	0.69	0.57	0.40	0.51	0.38	0.32	0.42	0.94	0.14	0.36	0.17
MnO	0.18	0.17	0.18	0.18	0.15	0.18	0.18	0.15	0.20	0.15	0.15	0.19
CO_2	0.04	0.04	0.08	0.04	0.08	0.04	0.08	0.35	0.06	0.21	2.30	0.26
Total	99.11	100.36	100.09	98.64	98.89	99.97	98.81	98.70	98.59	99.20	99.25	98.50
Adjusted oxides:												
SiO_2	43.79	46.33	46.56	46.84	44.60	47.41	45.34	45.90	40.37	47.08	43.53	45.69
Al_2O_3	15.34	14.85	16.68	17.13	15.37	16.50	16.90	16.01	13.59	16.63	14.71	15.13
Fe_2O_3	3.03	4.98	3.60	2.13	4.15	2.40	3.95	2.33	4.67	1.21	5.34	2.23
FeO	8.48	9.76	8.89	10.44	7.48	9.20	9.82	8.31	8.32	9.17	5.64	9.34
MgO	9.89	4.88	7.19	6.59	9.61	8.00	6.07	9.12	10.04	9.27	9.87	10.66
CaO	9.99	7.57	8.59	8.72	9.61	7.50	7.59	10.03	11.97	10.89	11.79	9.95
Na_2O	2.72	2.89	3.80	3.75	2.73	4.20	3.54	2.53	3.85	2.72	2.82	2.44
K_2O	1.11	1.10	0.89	0.87	0.87	0.74	0.68	0.75	0.91	0.25	0.64	0.68
H_2O	2.60	2.85	0.87	0.47	2.42	1.23	2.89	2.37	2.22	0.76	1.11	1.43
TiO_2	2.42	3.89	2.10	2.43	2.43	2.20	2.63	1.72	2.84	1.51	1.71	1.83
P_2O_5	0.41	0.69	0.57	0.41	0.52	0.38	0.32	0.43	0.95	0.14	0.36	0.17
MnO	0.18	0.17	0.18	0.18	0.15	0.18	0.18	0.15	0.20	0.15	0.15	0.19
CO_2	0.04	0.04	0.08	0.04	0.08	0.04	0.08	0.35	0.06	0.21	2.32	0.26

Footnotes at end of table.

TABLE 9.—*Chemical and normative analyses of Cenozoic igneous rocks from western Saudi Arabia*—Continued

Sample (location given on pl. 1)[2]	12	13	14	15	16	17	18	19	19a	22	23	24
Field no.[2]	912	1843	919	920	921	911	910	922	1309	907	909	908
Type of source rock[3]	X	O	X	X	X	X	X	X	P	X	X	X
Normative minerals:												
Quartz	—	2.203	—	—	—	—	—	—	—	—	—	—
Corundum	—	—	—	—	—	—	—	—	—	—	—	—
Orthoclase	6.559	6.477	5.255	5.152	5.139	4.374	4.007	4.430	5.394	1.489	3.811	4.020
Albite	14.862	24.451	28.088	26.548	22.264	30.692	29.973	21.433	2.974	23.029	23.872	20.492
Anorthite	26.341	24.302	25.858	27.337	27.116	23.991	28.214	30.096	17.089	32.423	25.570	28.329
Nepheline	4.437	—	2.187	2.813	0.455	2.632	—	—	16.057	0.001	—	0.068
Wollastonite	8.458	3.558	5.237	5.432	6.957	4.381	2.845	6.114	14.896	8.070	6.636	7.613
Enstatite	5.664	12.160	3.155	2.868	4.971	2.623	3.268	7.083	10.585	4.813	6.163	4.829
Ferrosilite	2.163	7.714	1.801	2.401	1.369	1.529	2.325	3.359	3.008	2.840	0.853	2.300
Forsterite	13.288	—	10.343	9.491	13.283	12.128	8.307	10.951	10.108	12.813	12.914	15.220
Fayalite	5.591	—	6.507	8.755	4.032	7.791	6.514	5.723	3.165	8.333	1.969	7.991
Magnetite	4.389	7.224	5.215	3.087	6.011	3.481	5.723	3.379	6.765	1.754	7.743	3.238
Hematite	—	—	—	—	—	—	—	—	—	—	—	—
Ilmenite	4.599	7.380	3.985	4.621	4.609	4.180	4.997	3.271	5.394	2.872	3.253	3.471
Apatite	0.980	1.628	1.349	0.960	1.222	0.900	0.767	1.008	2.258	0.334	0.859	0.409
Calcite	0.092	0.091	0.182	0.092	0.184	0.091	0.184	0.806	0.138	0.481	5.270	0.600
Total	97.421	97.188	99.162	99.557	97.612	98.792	97.125	97.653	97.831	99.253	98.912	98.580
Salic	52.198	57.433	61.388	61.849	54.974	61.689	62.193	55.959	41.514	56.942	53.253	52.908
Femic	45.223	39.755	37.774	37.708	42.638	37.103	34.931	41.694	56.316	42.311	45.659	45.672
Diopside[4]	16.285	6.948	10.193	10.701	13.297	8.532	5.576	11.839	28.488	15.724	12.543	14.742
DiWo	8.458	3.558	5.237	5.432	6.957	4.381	2.845	6.114	14.896	8.070	6.636	7.613
DiEn	5.664	2.074	3.155	2.868	4.971	2.623	1.595	3.883	10.585	4.813	5.189	4.829
DiFs	2.163	1.316	1.801	2.401	1.369	1.529	1.135	1.841	3.008	2.840	0.718	2.300
Hypersthene[5]	—	16.483	—	—	—	—	2.863	4.717	—	—	1.109	—
HyEn	—	10.086	—	—	—	—	1.673	3.200	—	—	0.974	—
HyFs	—	6.398	—	—	—	—	1.190	1.517	—	—	0.135	—
Olivine[6]	18.879	—	16.850	18.246	17.315	19.919	14.821	16.674	13.273	21.146	14.883	23.211
OlFo	13.288	—	10.343	9.491	13.283	12.128	8.307	10.951	10.108	12.813	12.914	15.220
OlFa	5.591	—	6.507	8.755	4.032	7.791	6.514	5.723	3.165	8.333	1.969	7.991
Wollastonite minus DiWo	—	—	—	—	—	—	—	—	—	—	—	—

Footnotes at end of table.

TABLE 9.—*Chemical and normative analyses of Cenozoic igneous rocks from western Saudi Arabia*—Continued

Sample (location given on pl. 1)[2]	25	26	27	28	30	33	36	37	38	40	41
Field no.[2]	1314	923	905	904	GFB1	GFB2	902	47027B	47026	47024	47023
Type of source rock[3]	X	X	X	X	X	X	X	X	P	P	X
Unadjusted oxides (wt. percent):											
SiO_2	44.30	46.60	47.40	47.00	48.50	45.50	44.40	47.30	46.50	61.40	43.70
Al_2O_3	17.38	15.20	16.20	16.60	14.20	14.20	16.40	16.50	13.60	15.30	14.50
Fe_2O_3	4.54	4.00	3.60	1.70	3.03	6.01	5.60	3.40	7.29	6.50	6.20
FeO	6.70	7.40	7.40	9.50	7.90	5.90	5.30	7.60	4.60	0.28	5.60
MgO	7.29	9.50	8.60	8.10	9.12	8.22	6.50	8.10	8.60	0.12	8.50
CaO	11.61	9.80	10.30	10.80	10.10	10.60	12.00	10.60	7.84	1.90	10.50
Na_2O	3.56	2.90	3.10	2.70	4.31	4.18	2.70	3.00	5.05	5.80	3.60
K_2O	0.80	0.60	0.48	0.22	1.13	0.94	0.35	0.65	1.78	4.80	1.20
H_2O	0.63	0.85	0.79	0.56	0.60	2.40	2.13	1.40	0.60	2.14	1.48
TiO_2	1.50	1.60	1.40	1.40	1.50	2.00	1.70	1.60	2.40	0.38	2.40
P_2O_5	0.18	0.32	0.13	0.12	0.18	0.38	0.21	0.31	0.53	0.11	0.63
MnO	0.12	0.18	0.15	0.15	0.14	0.15	0.15	0.14	0.13	0.18	0.20
CO_2	—	0.30	0.12	0.08	—	—	0.16	—	—	0.86	0.95
Total	98.61	99.25	99.67	98.93	100.71	100.48	97.60	100.60	98.92	99.77	99.46
Adjusted oxides:											
SiO_2	44.92	46.95	47.56	47.51	48.16	45.28	45.49	47.02	47.01	61.54	43.94
Al_2O_3	17.62	15.31	16.25	16.78	14.10	14.13	16.80	16.40	13.75	15.34	14.58
Fe_2O_3	4.60	4.03	3.61	1.72	3.01	5.98	5.74	3.38	7.37	6.51	6.23
FeO	6.79	7.46	7.42	9.60	7.84	5.87	5.43	7.55	4.65	0.28	5.63
MgO	7.39	9.57	8.63	8.19	9.06	8.18	6.66	8.05	8.69	0.12	8.55
CaO	11.77	9.87	10.33	10.92	10.03	10.55	12.30	10.54	7.93	1.90	10.56
Na_2O	3.61	2.92	3.11	2.73	4.28	4.16	2.77	2.98	5.11	5.81	3.62
K_2O	0.81	0.60	0.48	0.22	1.12	0.94	0.36	0.65	1.80	4.81	1.21
H_2O	0.64	0.86	0.79	0.57	0.60	2.39	2.18	1.39	0.61	2.14	1.49
TiO_2	1.52	1.61	1.40	1.42	1.49	1.99	1.74	1.59	2.43	0.38	2.41
P_2O_5	0.18	0.32	0.13	0.12	0.18	0.38	0.22	0.31	0.54	0.11	0.63
MnO	0.12	0.18	0.15	0.15	0.14	0.15	0.15	0.14	0.13	0.18	0.20
CO_2	—	0.30	0.12	0.08	—	—	0.16	—	—	0.86	0.96

Footnotes at end of table.

TABLE 9.—*Chemical and normative analyses of Cenozoic igneous rocks from western Saudi Arabia*—Continued

Sample (location given on pl. 1)[2]	25	26	27	28	30	33	36	37	38	40	41
Field no.[2]	1314	923	905	904	GFB1	GFB2	902	47027B	47026	47024	47023
Type of source rock[3]	X	X	X	X	X	X	X	X	P	P	X
Normative minerals:											
Quartz	—	—	—	—	—	—	—	—	—	8.096	—
Corundum	—	—	—	—	—	—	—	—	—	—	—
Orthoclase	4.794	3.572	2.846	1.314	6.630	5.528	2.119	3.818	10.633	28.430	7.130
Albite	13.390	24.724	26.318	23.094	19.951	19.404	23.407	24.692	24.304	49.191	21.270
Anorthite	29.490	26.887	28.966	32.877	15.949	17.125	32.372	29.459	9.284	1.540	19.969
Nepheline	9.295	—	—	—	8.809	8.558	0.001	0.293	10.235	—	5.069
Wollastonite	11.577	7.550	8.638	8.342	13.627	13.670	10.932	8.685	11.079	0.726	9.281
Enstatite	7.916	8.407	5.768	6.431	8.869	10.685	8.427	5.641	9.575	0.300	7.593
Ferrosilite	2.746	2.834	2.311	4.465	3.822	1.485	1.342	2.451	—	—	0.563
Forsterite	7.355	10.814	11.017	9.783	9.589	6.790	5.718	10.099	8.463	—	9.594
Fayalite	2.812	4.018	4.865	7.486	4.554	1.040	1.003	4.836	—	—	0.784
Magnetite	6.675	5.843	5.237	2.491	4.362	8.672	8.319	4.900	8.384	0.390	9.038
Hematite	—	—	—	—	—	—	—	—	1.587	6.246	—
Ilmenite	2.889	3.062	2.668	2.688	2.829	3.780	3.308	3.021	4.608	0.723	4.583
Apatite	0.432	0.764	0.309	0.287	0.423	0.896	0.510	0.730	1.269	0.261	1.500
Calcite	—	0.687	0.274	0.184	—	—	0.373	—	—	1.960	2.172
Total	99.372	99.163	99.216	99.442	99.415	97.633	97.831	98.626	99.423	97.863	98.547
Salic	56.969	55.184	58.130	57.285	51.340	50.614	57.899	58.263	54.457	87.257	53.438
Femic	42.403	43.979	41.086	42.157	48.075	47.019	39.932	40.363	44.966	10.606	45.110
Diopside[4]	22.239	14.493	16.652	16.334	26.318	25.840	20.701	16.777	20.655	0.646	17.437
DiWo	11.577	7.550	8.638	8.342	13.627	13.670	10.932	8.685	11.079	0.347	9.281
DiEn	7.916	5.193	5.721	4.717	8.869	10.685	8.427	5.641	9.575	0.300	7.593
DiFs	2.746	1.751	2.292	3.275	3.822	1.485	1.342	2.451	—	—	0.563
Hypersthene[5]	—	4.297	0.065	2.904	—	—	—	—	—	—	—
HyEn	—	3.214	0.046	1.714	—	—	—	—	—	—	—
HyFs	—	1.084	0.019	1.190	—	—	—	—	—	—	—
Olivine[6]	10.167	14.832	15.882	17.270	14.143	7.830	6.721	14.935	8.463	—	10.379
OlFo	7.355	10.814	11.017	9.783	9.589	6.790	5.718	10.099	8.463	—	9.594
OlFa	2.812	4.018	4.865	7.486	4.554	1.040	1.003	4.836	—	—	0.784
Wollastonite minus DiWo	—	—	—	—	—	—	—	—	—	0.379	—

Footnotes at end of table.

TABLE 9.—*Chemical and normative analyses of Cenozoic igneous rocks from western Saudi Arabia*—Continued

Sample (location given on pl. 1)[2]	42	43	44	45	46a	46b	51a	51b	51c	52a	52b	52c
Field no.[2]	47022	47021	47025	926	927A	927B	623A	623B	623C	928A	928B	928C
Type of source rock[3]	X	X	X	P	P	P	O	O	O	O	O	O
Unadjusted oxides (wt. percent):												
SiO_2	43.20	44.20	44.50	70.30	46.20	46.60	52.50	51.50	51.50	53.80	48.40	61.90
Al_2O_3	14.30	14.50	14.50	14.70	22.10	22.90	17.60	15.02	16.90	18.20	13.40	14.60
Fe_2O_3	6.60	4.20	2.90	2.50	2.90	2.00	3.78	4.45	3.83	5.40	7.00	4.80
FeO	5.10	7.70	8.80	0.20	3.60	3.30	5.50	8.60	7.00	3.80	8.70	2.50
MgO	9.00	9.80	11.00	0.28	3.80	3.40	4.38	3.32	3.98	1.60	4.30	1.50
CaO	11.10	9.20	10.00	1.10	13.30	12.50	8.90	8.95	8.95	6.10	7.00	3.70
Na_2O	3.20	2.90	2.80	4.70	2.60	2.90	3.53	3.57	4.96	4.00	3.10	3.80
K_2O	1.20	1.00	0.81	4.20	0.32	0.38	0.92	0.92	1.41	1.30	1.30	2.30
H_2O	1.55	1.97	0.90	1.84	2.80	3.94	1.50	0.90	1.30	2.61	2.84	3.12
TiO_2	2.30	2.60	2.00	0.18	1.10	0.88	1.20	2.80	1.40	1.60	3.00	1.10
P_2O_5	0.58	0.51	0.33	0.05	0.17	0.19	0.30	0.40	0.34	0.56	0.30	0.31
MnO	0.20	0.20	0.20	0.03	0.11	0.07	0.12	0.16	0.14	0.15	0.22	0.11
CO_2	1.00	0.30	0.98	0.02	0.02	0.02	—	—	—	0.02	0.02	0.02
Total	99.33	99.08	99.72	100.10	99.02	99.08	100.23	100.59	101.71	99.14	99.58	99.76
Adjusted oxides:												
SiO_2	43.49	44.61	44.62	70.23	46.66	47.03	52.38	51.20	50.63	54.27	48.60	62.05
Al_2O_3	14.40	14.63	14.54	14.69	22.32	23.11	17.56	14.93	16.62	18.36	13.46	14.64
Fe_2O_3	6.64	4.24	2.91	2.50	2.93	2.02	3.77	4.42	3.77	5.45	7.03	4.81
FeO	5.13	7.77	8.82	0.20	3.64	3.33	5.49	8.55	6.88	3.83	8.74	2.51
MgO	9.06	9.89	11.03	0.28	3.84	3.43	4.37	3.30	3.91	1.61	4.32	1.50
CaO	11.17	9.29	10.03	1.10	13.43	12.62	8.88	8.90	8.80	6.15	7.03	3.71
Na_2O	3.22	2.93	2.81	4.70	2.63	2.93	3.52	3.55	4.88	4.03	3.11	3.81
K_2O	1.21	1.01	0.81	4.20	0.32	0.38	0.92	0.91	1.39	1.31	1.31	2.31
H_2O	1.56	1.99	0.90	1.84	2.83	3.98	1.50	0.89	1.28	2.63	2.85	3.13
TiO_2	2.32	2.62	2.01	0.18	1.11	0.89	1.20	2.78	1.38	1.61	3.01	1.10
P_2O_5	0.58	0.51	0.33	0.05	0.17	0.19	0.30	0.40	0.33	0.56	0.30	0.31
MnO	0.20	0.20	0.20	0.03	0.11	0.07	0.12	0.16	0.14	0.15	0.22	0.11
CO_2	1.01	0.30	0.98	0.02	0.02	0.02	—	—	—	0.02	0.02	0.02

Footnotes at end of table.

TABLE 9.—*Chemical and normative analyses of Cenozoic igneous rocks from western Saudi Arabia*—Continued

Sample (location given on pl. 1)[2]	42	43	44	45	46a	46b	51a	51b	51c	52a	52b	52c
Field no.[2]	47022	47021	47025	926	927A	927B	623A	623B	623C	928A	928B	928C
Type of source rock[3]	X	X	X	P	P	P	O	O	O	O	O	O
Normative minerals:												
Quartz	—	—	—	24.286	—	—	4.057	4.861	—	11.768	5.323	21.859
Corundum	—	—	—	0.588	—	—	—	—	—	0.513	—	—
Orthoclase	7.139	5.964	4.800	24.794	1.910	2.266	5.424	5.405	8.192	7.749	7.714	13.624
Albite	19.204	22.619	20.315	39.730	22.218	24.767	29.801	30.031	34.309	34.140	26.342	32.232
Anorthite	21.253	23.813	24.673	4.999	48.158	48.794	29.393	22.111	19.354	26.707	18.888	16.026
Nepheline	4.364	1.163	1.866	—	—	—	—	—	3.768	—	—	—
Wollastonite	10.024	7.088	6.974	—	7.193	5.183	5.304	8.113	9.235	—	5.800	0.091
Enstatite	8.522	5.061	4.633	0.697	5.989	3.969	10.883	8.220	5.031	4.019	10.754	3.745
Ferrosilite	0.185	1.399	1.832	—	1.647	1.446	5.206	7.744	3.877	0.155	5.672	—
Forsterite	9.841	13.716	16.005	—	2.501	3.208	—	—	3.304	—	—	—
Fayalite	0.235	4.179	6.975	—	0.758	1.288	—	—	2.806	—	—	—
Magnetite	9.634	6.146	4.217	0.221	4.246	2.927	5.468	6.414	5.460	7.897	10.192	5.241
Hematite	—	—	—	2.345	—	—	—	—	—	—	—	1.197
Ilmenite	4.398	4.984	3.809	0.342	2.110	1.687	2.274	5.287	2.614	3.065	5.722	2.094
Apatite	1.383	1.219	0.784	0.118	0.407	0.454	0.709	0.942	0.792	1.338	0.714	0.736
Calcite	2.290	0.689	2.235	0.045	0.046	0.046	—	—	—	0.046	0.046	0.046
Total	98.472	98.041	99.117	98.165	97.183	96.034	98.520	99.128	98.741	97.398	97.166	96.890
Salic	51.960	53.560	51.654	94.397	72.286	75.827	68.676	62.407	65.623	80.878	58.267	83.741
Femic	46.512	44.481	47.463	3.768	24.897	20.207	29.845	36.720	33.118	16.521	38.899	13.149
Diopside[4]	18.731	13.548	13.439	—	13.748	9.969	10.272	16.045	18.143	—	11.263	0.169
DiWo	10.024	7.088	6.974	—	7.193	5.183	5.304	8.113	9.235	—	5.800	0.091
DiEn	8.522	5.061	4.633	—	5.141	3.508	3.361	4.084	5.031	—	3.577	0.078
DiFs	0.185	1.399	1.832	—	1.414	1.278	1.608	3.848	3.877	—	1.887	—
Hypersthene[5]	—	—	—	0.697	1.081	0.629	11.122	8.032	—	4.174	10.963	3.666
HyEn	—	—	—	0.697	0.848	0.461	7.523	4.136	—	4.019	7.177	3.666
HyFs	—	—	—	—	0.233	0.168	3.599	3.896	—	0.155	3.785	—
Olivine[6]	10.077	17.895	22.980	—	3.259	4.496	—	—	6.110	—	—	—
OlFo	9.841	13.716	16.005	—	2.501	3.208	—	—	3.304	—	—	—
OlFa	0.235	4.179	6.975	—	0.758	1.288	—	—	2.806	—	—	—
Wollastonite minus DiWo	—	—	—	—	—	—	—	—	—	—	—	—

Footnotes at end of table.

TABLE 9.—*Chemical and normative analyses of Cenozoic igneous rocks from western Saudi Arabia*—Continued

Sample (location given on pl. 1)[2]	52d	55a	56a	56b	56c	58a	58b	58c	60	61	62	63
Field no.[2]	928D	930	933A	933B	933C	BRK4A	BRK4B	BRK4C	935	938A	937	936
Type of source rock[3]	O	O	O	O	O	O	O	O	O	X	X	O
Unadjusted oxides (wt. percent):												
SiO_2	63.40	55.00	46.80	47.00	56.50	48.30	51.60	50.20	59.90	45.40	47.90	51.00
Al_2O_3	14.60	17.50	14.90	15.80	18.20	17.40	16.80	16.80	14.60	16.20	16.40	17.40
Fe_2O_3	2.70	2.70	1.40	3.10	2.10	3.00	3.90	3.30	4.20	5.40	3.80	3.80
FeO	4.20	5.60	10.40	9.60	5.20	7.30	6.80	6.80	5.60	6.00	6.80	6.70
MgO	1.50	1.50	5.40	5.00	1.80	3.40	2.30	3.50	1.50	7.40	7.60	3.00
CaO	3.70	6.50	8.50	8.20	6.20	9.20	6.40	7.80	2.60	10.40	8.90	7.00
Na_2O	4.00	4.00	3.50	3.40	4.30	3.10	4.00	3.80	4.40	3.40	3.50	3.60
K_2O	2.60	1.80	0.89	1.20	1.70	0.95	1.30	1.20	2.90	1.00	1.20	1.60
H_2O	2.30	2.81	5.25	2.55	2.59	2.30	4.00	2.37	2.60	1.03	0.85	2.52
TiO_2	0.98	1.30	2.80	3.10	1.20	2.60	1.40	2.20	0.96	2.60	2.00	2.20
P_2O_5	0.29	0.46	0.58	0.58	0.42	0.83	0.77	0.82	0.15	0.50	0.36	0.58
MnO	0.11	0.15	0.18	0.23	0.15	0.21	0.26	0.20	0.15	0.19	0.15	0.19
CO_2	0.02	0.04	0.06	0.06	0.02	0.08	0.08	0.25	0.04	0.36	0.06	0.08
Total	100.40	99.36	100.66	99.82	100.38	98.67	99.61	99.24	99.60	99.88	99.52	99.67
Adjusted oxides:												
SiO_2	63.15	55.35	46.49	47.08	56.29	48.95	51.80	50.58	60.14	45.45	48.13	51.17
Al_2O_3	14.54	17.61	14.80	15.83	18.13	17.63	16.87	16.93	14.66	16.22	16.48	17.46
Fe_2O_3	2.69	2.72	1.39	3.11	2.09	3.04	3.92	3.33	4.22	5.41	3.82	3.81
FeO	4.18	5.64	10.33	9.62	5.18	7.40	6.83	6.85	5.62	6.01	6.83	6.72
MgO	1.49	1.51	5.36	5.01	1.79	3.45	2.31	3.53	1.51	7.41	7.64	3.01
CaO	3.69	6.54	8.44	8.21	6.18	9.32	6.43	7.86	2.61	10.41	8.94	7.02
Na_2O	3.98	4.03	3.48	3.41	4.28	3.14	4.02	3.83	4.42	3.40	3.52	3.61
K_2O	2.59	1.81	0.88	1.20	1.69	0.96	1.31	1.21	2.91	1.00	1.21	1.61
H_2O	2.29	2.83	5.22	2.55	2.58	2.33	4.02	2.39	2.61	1.03	0.85	2.53
TiO_2	0.98	1.31	2.78	3.11	1.20	2.64	1.41	2.22	0.96	2.60	2.01	2.21
P_2O_5	0.29	0.46	0.58	0.58	0.42	0.84	0.77	0.83	0.15	0.50	0.36	0.58
MnO	0.11	0.15	0.18	0.23	0.15	0.21	0.26	0.20	0.15	0.19	0.15	0.19
CO_2	0.02	0.04	0.06	0.06	0.02	0.08	0.08	0.25	0.04	0.36	0.06	0.08

Footnotes at end of table.

TABLE 9.—*Chemical analyses and normatives of Cenozoic igneous rocks from western Saudi Arabia*—Continued

Sample (location given on pl. 1)[2] / Field no.[2] / Type of source rock[3]	52d 928D O	55a 930 O	56a 933A O	56b 933B O	56c 933C O	58a BRK4A O	58b BRK4B O	58c BRK4C O	60 935 O	61 938A X	62 937 X	63 936 O
Normative minerals:												
Quartz	19.422	8.298	—	—	7.991	3.189	5.711	3.041	13.511	—	—	4.485
Corundum	—	—	—	—	—	—	—	—	—	—	—	—
Orthoclase	15.303	10.705	5.225	7.104	10.008	5.689	7.712	7.145	17.206	5.916	7.125	9.486
Albite	33.712	34.065	29.422	28.822	36.248	26.585	33.979	32.401	37.381	24.349	29.044	30.563
Anorthite	14.147	24.637	22.170	24.350	25.242	31.171	24.140	25.432	11.568	26.019	25.617	26.681
Nepheline	—	—	—	—	—	—	—	—	—	2.414	0.387	—
Wollastonite	0.886	1.895	6.505	5.106	1.061	3.790	0.909	2.743	0.060	8.388	6.682	1.608
Enstatite	3.721	3.760	5.387	6.981	4.466	8.582	5.751	8.784	3.751	6.542	4.605	7.496
Ferrosilite	4.052	6.225	5.468	5.817	6.088	7.119	7.466	6.550	5.529	0.929	1.538	5.904
Forsterite	—	—	5.588	3.850	—	—	—	—	—	8.346	10.101	—
Fayalite	—	—	6.251	3.536	—	—	—	—	—	1.306	3.719	—
Magnetite	3.899	3.940	2.017	4.503	3.033	4.408	5.677	4.821	6.114	7.839	5.536	5.528
Hematite	—	—	—	—	—	—	—	—	—	—	—	—
Ilmenite	1.854	2.485	5.283	5.898	2.270	5.005	2.669	4.210	1.831	4.944	3.817	4.192
Apatite	0.684	1.097	1.365	1.376	0.991	1.992	1.831	1.957	0.357	1.186	0.857	1.378
Calcite	0.045	0.092	0.136	0.137	0.045	0.184	0.183	0.573	0.091	0.820	0.137	0.183
Total	97.725	97.198	94.816	97.478	97.443	97.715	96.028	97.657	97.399	98.997	99.166	97.504
Salic	82.584	77.705	56.817	60.275	79.488	66.635	71.543	68.020	79.666	58.698	62.174	71.215
Femic	15.141	19.493	37.999	37.203	17.955	31.080	24.485	29.638	17.733	40.299	36.993	26.289
Diopside[4]	1.761	3.819	12.897	10.056	2.124	7.464	1.817	5.383	0.121	15.859	12.826	3.162
DiWo	0.886	1.895	6.505	5.106	1.061	3.790	0.909	2.743	0.060	8.388	6.682	1.608
DiEn	0.419	0.725	3.172	2.700	0.450	2.008	0.395	1.512	0.025	6.542	4.605	0.869
DiFs	0.456	1.200	3.220	2.250	0.613	1.666	0.513	1.128	0.036	0.929	1.538	0.685
Hypersthene[5]	6.898	8.060	4.463	7.847	9.491	12.027	12.308	12.693	9.219	—	—	11.846
HyEn	3.302	3.035	2.215	4.280	4.016	6.574	5.355	7.271	3.726	—	—	6.627
HyFs	3.596	5.025	2.248	3.567	5.475	5.453	6.953	5.422	5.493	—	—	5.219
Olivine[6]	—	—	11.839	7.386	—	—	—	—	—	9.652	13.820	—
OlFo	—	—	5.588	3.850	—	—	—	—	—	8.346	10.101	—
OlFa	—	—	6.251	3.536	—	—	—	—	—	1.306	3.719	—
Wollastonite minus DiWo	—	—	—	—	—	—	—	—	—	—	—	—

Footnotes at end of table.

TABLE 9.—*Chemical and normative analyses of Cenozoic igneous rocks from western Saudi Arabia*—Continued

Sample (location given on pl. 1)[2]	64	65	66	67	73
Field no.[2]	939	941	940	520	514-5
Type of source rock[3]	O	X	X	X	T
Unadjusted oxides (wt. percent)					
SiO_2	51.50	47.00	47.00	52.50	47.70
Al_2O_3	18.60	15.50	17.10	11.80	15.70
Fe_2O_3	2.90	3.20	3.90	4.75	4.90
FeO	5.80	8.90	7.60	7.20	7.20
MgO	2.40	9.20	5.60	4.64	7.10
CaO	7.00	8.90	8.70	7.00	10.30
Na_2O	4.40	3.30	4.00	6.00	2.90
K_2O	1.40	0.96	1.10	0.10	0.37
H_2O	2.82	0.69	0.89	0.80	2.06
TiO_2	1.60	1.90	2.40	2.80	1.40
P_2O_5	0.76	0.32	0.41	0.62	0.21
MnO	0.15	0.18	0.18	0.13	0.21
CO_2	0.08	0.04	0.06	—	0.05
Total	99.41	100.09	98.94	98.34	100.10
Adjusted oxides:					
SiO_2	51.81	46.96	47.50	53.39	47.65
Al_2O_3	18.71	15.49	17.28	12.00	15.68
Fe_2O_3	2.92	3.20	3.94	4.83	4.90
FeO	5.83	8.89	7.68	7.32	7.19
MgO	2.41	9.19	5.66	4.72	7.09
CaO	7.04	8.89	8.79	7.12	10.29
Na_2O	4.43	3.30	4.04	6.10	2.90
K_2O	1.41	0.96	1.11	0.10	0.37
H_2O	2.84	0.69	0.90	0.81	2.06
TiO_2	1.61	1.90	2.43	2.85	1.40
P_2O_5	0.76	0.32	0.41	0.63	0.21
MnO	0.15	0.18	0.18	0.13	0.21
CO_2	0.08	0.04	0.06	—	0.05

Footnotes at end of table.

TABLE 9.—*Chemical and normative analyses of Cenozoic igneous rocks from western Saudi Arabia*—Continued

Sample (location given on pl. 1)[2]	64	65	66	67	73
Field no.[2]	939	941	940	520	514-5
Type of source rock[3]	O	X	X	X	T
Normative minerals:					
Quartz	2.181	—	—	0.371	—
Corundum	—	—	—	—	—
Orthoclase	8.322	5.668	6.570	0.601	2.184
Albite	37.453	24.820	29.781	51.627	24.514
Anorthite	27.026	24.623	25.728	5.053	28.700
Nepheline	—	1.668	2.399	—	—
Wollastonite	1.004	7.160	6.182	10.915	8.627
Enstatite	6.013	4.544	3.850	11.751	14.242
Ferrosilite	5.927	2.161	1.961	4.998	5.841
Forsterite	—	12.858	7.180	—	2.399
Fayalite	—	6.739	4.032	—	1.084
Magnetite	4.230	4.636	5.715	7.003	7.097
Hematite	—	—	—	—	—
Ilmenite	3.057	3.605	4.607	5.408	2.656
Apatite	1.811	0.757	0.982	1.493	0.497
Calcite	0.183	0.091	0.138	—	0.114
Total	97.205	99.329	99.124	99.221	97.956
Salic	74.981	56.778	64.478	57.652	55.399
Femic	22.223	42.551	34.646	41.569	42.557
Diopside[4]	1.988	13.865	11.993	21.073	16.640
DiWo	1.004	7.160	6.182	10.915	8.627
DiEn	0.496	4.544	3.850	7.127	5.682
DiFs	0.489	2.161	1.961	3.031	2.330
Hypersthene[5]	10.955	—	—	6.592	12.070
HyEn	5.517	—	—	4.624	8.560
HyFs	5.438	—	—	1.967	3.511
Olivine[6]	—	19.597	11.212	—	3.483
OlFo	—	12.858	7.180	—	2.399
OlFa	—	6.739	4.032	—	1.084
Wollastonite minus DiWo	—	—	—	—	—

[1]Most analyses at USGS, Washington, D.C., using rapid-rock, single-solution method (Shapiro, 1967); Analysts: Lowell Artis (Oct. 1970), Herbert Kirschenbaum (Oct. 1983), and Paul Elmore (Sept. 1973). Samples 2, 5, 25, 30, 33, 38, 51a, 51b, 51c, and 67 analyzed at DGMR-USGS, Jiddah, using atomic-absorption, volumetric, and gravimeter methods; W.L. Campbell, technical advisor; Analysts: Ibrahim Baraja, Souhail El Farouki, Adel Hakeem, Mahmoud Ashy, Abdulaziz Masoud, and others (July 1972). FeO, TiO_2, P_2O_5, and MnO analyzed at USGS, Washington; Analysts: Sam Botts and John Glenn (May 1973).

[2]T and B indicate top and bottom flow, respectively, of thick section of many flows at same sample locality; a, b, c, and d indicate multiple samples from same locality.

[3]X, lava flow; O, hypabyssal dike; P, plug; T, Jabal at Tirf gabbro.

[4]DiWo, wollastonite content of diopside; DiEn, enstatite content of diopside; DiFs, ferrosilite content of diopside.

[5]HyEn, enstatite content of hypersthene; HyFs, ferrosilite content of hypersthene.

[6]OlFo, forsterite content of olivine; OlFa, fayalite content of olivine.

TABLE 10.—*K-Ar ages for Cenozoic igneous rocks collected from western Saudia Arabia*

[All material analyzed was whole rock except samples 34a and 34b, which were glauconite, and sample 70, which was labradorite. Decay constants: $\lambda\beta=4.963\times10^{-10}$/yr; $\lambda\zeta=0.581\times10^{-10}$/yr; κ–40/K=1.167×10^{-4} atomic percent]

Sample (location given on pl. 2)[1]	Field no.	Age (m.y.)	Potassium (percent)	$^{40}Ar\times10^{-10}$ (moles/g)	^{40}Ar (percent)	$^{*40}Ar/^{40}K$	Analyzed by	Rock	Collected by	Location Lat N.	Location Long E.
1	47000	12.0±0.4	0.88	0.1891	41	0.00070	Isotopes[2]	Basalt	Flanigan	30°48′	38°06′
			0.90	0.1824	40						
2	47001	11.4±0.4	0.50	0.0982	31	0.00066	do.	do.	do.	30°54′	38°08′
			0.50	0.1003	34						
3	47002	13.4±0.4	0.49	0.1144	36	0.00078	do.	do.	do.	30°54′	38°10′
			0.49	0.1140	39						
4	47003	12.0±0.4	0.73	0.1508	38	0.00070	do.	do.	do.	30°54′	38°11′
			0.70	0.1477	39						
5	47004	12.9±0.6	0.58	0.1310	35	0.00075	do.	do.	do.	30°54′	38°12′
			0.56	0.1248	50						
6T	917T	10.9±1.1	1.054	0.2102	26	0.00064	Geochron[3]	do.	Brown	27°30′	36°46′
			1.053	0.1902	31						
6B	917B	9.4±2.5	0.388	0.0701	15	0.00055	do.	do.	do.	27°30′	36°46′
			0.349	0.0500	8						
7T	916T	7.4±1.5	0.630	0.0976	8	0.00043	do.	do.	do.	27°05′	37°18′
			0.597	0.0600	8						
7B	916B	26.7±2.6	0.689	0.3753	7	0.00156	do.	Basanite	do.	27°05′	37°18′
			0.670	0.2577	6						
8(D)	B1818	22.9±1.4	0.845	0.2801	20	0.00131	USGS[4]	Olivine, gabbro-norite	do.	26°49′	36°05′
9T	915T	7.8±1.0	1.208	0.2177	4	0.00045	Geochron	Basalt	do.	26°38′	37°43′
			1.271	0.1176	2						
9B	915B	9.4±1.0	1.081	0.1826	13	0.00055	do.	do.	do.	26°38′	37°43′
			1.138	0.1801	14						
10	913	7.5±0.8	1.270	0.2052	4	0.00044	do.	do.	do.	26°05′	38°42′
			1.286	0.1301	2						
12	912	11.5±2.3	1.015	0.2477	11	0.00067	do.	do.	do.	25°28′	38°54′
			1.006	0.1576	8						
14	919	([5])	0.796	---	---	---	do.	do.	do.	25°09′	37°26′
			0.767	---	---	---					
15	920	6.2±0.8	0.775	0.0901	20	0.00036	do.	do.	do.	25°09′	37°28′
			0.764	0.0751	17						
16	921	---	0.823	---	---	---	do.	do.	do.	24°44′	37°40′
			0.823	---	---	---					
17	911	21.2±2.1	0.713	0.2902	18	0.00124	do.	do.	do.	24°50′	38°42′
			0.729	0.2427	18						
18	910	28.3±2.9	0.606	0.3628	13	0.00166	do.	do.	do.	24°48′	38°48′
			0.593	0.2302	18						
19	922	([5])	0.611	---	---	---	do.	do.	do.	24°25′	37°45′
			0.627	---	---	---					
20	3729Br	9.3±0.7	0.315	0.0525	10	0.00054	do.	do.	do.	24°40′	39°16′
			0.301	0.0475	8						
22	907	1.1±1.0	0.269	0.008	1	0.00006	do.	do.	do.	25°02′	40°14′
			0.254	0.002	0.1						
23	909	62.6±4.3	0.554	0.6855	10	0.00370	do.	do.	do.	24°41′	39°20′
			0.539	0.5179	7						
				0.6080	6						
24	908	20.0±2.0	0.665	0.2152	8	0.00117	do.	do.	do.	24°36′	40°13′
			0.641	0.2277	10						
				0.2402	8						
26	923	([5])	0.592	---	---	---	do.	do.	do.	23°03′	39°08′
			0.606	---	---	---					
27	905	12.6±2.5	0.416	0.0926	3	0.00074	do.	do.	do.	23°05′	39°43′
			0.393	0.0851	3						
28	904	13.2±1.5	0.216	0.050	4	0.00077	do.	do.	do.	22°46′	39°46′
			0.196	0.045	4						

Footnotes at end of table

TABLE 10.—*K-Ar ages for Cenozoic igneous rocks collected from western Saudia Arabia*—Continued

[All material analyzed was whole rock except samples 34a and 34b, which were glauconite, and sample 70, which was labradorite. Decay constants: $\lambda\beta=4.963\times10^{-10}$/yr; $\lambda\zeta=0.581\times10^{-10}$/yr; κ-40/K=1.167×10^{-4} atomic percent]

Sample (location given on pl. 2)[1]	Field no.	Age (m.y.)	Potassium (percent)	$^{40}Ar\times10^{-10}$ (moles/g)	^{40}Ar (percent)	$^{*40}Ar/^{40}K$	Analyzed by	Rock	Collected by	Location Lat N.	Location Long E.
29	4702B	2.4±0.8	1.184	0.0375	2	0.00014	do.	do.	Flanigan	22°40′	41°24′
			1.207	0.0826	5						
				0.0275	1						
30	GFB1	4.4±0.4	0.35	0.0270	12	0.00026	Isotopes	do.	Brown	22°14′	39°27′
			0.37	0.0283	10						
32	GFB3	4.2±0.8	0.45	0.0353	16	0.00024	do.	do.	do.	21°56′	39°15′
			0.44	0.0295	14						
33	GFB2	19.1±0.6	0.61	0.2019	48	0.00112	do.	do.	do.	21°58′	39°18′
			0.61	0.2056	59						
34a	USFAN	43.7±1.0	3.60	2.758	53	0.00257	do.	Sandstone (glauconite)	do.	21°58′	39°21′
			3.56	2.738	44						
34b	USFAN	56.4±1.2	3.02	2.961	60	0.00333	do.	do.	do.	21°58′	39°21′
			3.04	3.059	66						
35	Well 4	32.6±2	0.594	0.3403	47	0.00191	Geochron	Basalt	do.	21°34′	39°32′
			0.589	0.3353	46						
36	902	25.8±5.0	0.381	0.1776	3	0.00151	do.	do.	do.	21°50′	39°42′
			0.351	0.1526	2						
37	47027B	8.7±2.0	0.493	0.0450	2	0.00050	do.	do.	Flanigan	21°51′	40°44′
			0.494	0.0851	7						
				0.0926	2						
38	47026	8.0±0.5	1.121	0.1676	9	0.00047	do.	do.	do.	21°40′	40°58′
			1.150	0.1501	8						
39	Well 3	25.9±3.0	0.395	0.1826	21	0.00152	do.	do.	Brown	21°24′	39°39′
			0.385	0.1701	22						
40(P)	47024	22.2±3.5	4.187	1.596	14	0.00130	do.	Hornblende, latite-phonolite	Flanigan	21°18′	41°10′
			4.166	1.841	14						
				1.409	11						
41	47023	16.6±1.5	0.854	0.2477	18	0.00097	do.	Basalt	do.	21°21′	41°20′
			0.861	0.2477	19						
42	47022	3.4±0.5	0.912	0.0550	1	0.00020	do.	do.	do.	21°20′	41°20′
			0.876	0.0500	1						
43	47021	16.2±1.8	0.796	0.2702	24	0.00095	do.	do.	do.	21°20′	41°25′
			0.774	0.1927	21						
				0.2027	31						
44	47025	([5])	0.599	---	---	---	do.	Basalt	do.	21°05′	41°35′
			0.595	---	---	---					
45(P)	926	19.3±0.9	3.785	1.284	28	0.00113	do.	Rhyolite	Brown	20°56′	39°31′
			3.843	1.286	33						
46a(P)	927A	26.8±4.5	0.272	0.1351	6	0.00157	do.	Gabbro	do.	20°58′	39°35′
			0.263	0.1151	4						
46b(P)	927B	27.9±5.5	0.282	0.1576	6	0.00164	do.	do.	do.	20°58′	39°35′
			0.266	0.1101	4						
47	6MX68	7.0±4.3	0.17	0.0295	1	0.00041	Isotopes	Basalt	do.	20°56′	39°36′
			0.19	0.01415	1						
48(P)	66	21.3±2.1	3.40	1.101	7	0.00125	Geochron	Trachyte	Gaskill	20°53′	39°38′
			3.37	1.376	9						
				1.301	8						
49	5MX68	2.9±0.2	1.00	0.0516	22	0.00017	Isotopes	Basalt	Brown	20°44′	39°40′
			0.96	0.0480	24						
50	HT	2.8±0.1	1.33	0.0652	32	0.00016	do.	do.	do.	20°42′	39°42′
			1.31	0.0623	35						

Footnotes at end of table

TABLE 10.—*K-Ar ages for Cenozoic igneous rocks collected from western Saudia Arabia*—Continued

[All material analyzed was whole rock except samples 34a and 34b, which were glauconite, and sample 70, which was labradorite. Decay constants: $\lambda\beta=4.963\times10^{-10}$/yr; $\lambda\xi=0.581\times10^{-10}$/yr; κ–40/K=1.167×10^{-4} atomic percent]

Sample (location given on pl. 2)[1]	Field no.	Age (m.y.)	Potassium (percent)	$^{40}Ar\times10^{-10}$ (moles/g)	^{40}Ar (percent)	$^{40}Ar/^{40}K$	Analyzed by	Rock	Collected by	Location Lat N.	Location Long E.
51a(D)	623A	177.±13	0.50	1.632	53	0.0108	USGS	Gabbro	do.	20°26′	40°13′
			0.51								
51b(D)	623B	21.5±2.3	0.91	0.3397	26	0.00126	do.	do.	do.	20°26′	40°13′
			0.90								
51c(D)	623C	273.±20	0.54	2.731	41	0.0171	do.	do.	do.	20°26′	40°13′
			0.53								
52a(D)	928A	18.0±1.3	1.364	0.4153	17	0.00105	Geochron	Monzonite	do.	20°22′	40°21′
			1.317	0.4253	16						
52b(D)	928B	25.3±1.8	1.008	0.4504	26	0.00148	do.	do.	do.	20°22′	40°21′
			1.022	0.4479	26						
52c(D)	928C	23.6±1.3	2.221	0.9107	24	0.00137	do.	do.	do.	20°22′	40°21′
			2.210	0.9032	24						
52d(D)	928D	20.8±1.2	2.246	0.7981	10	0.00121	do.	do.	do.	20°22′	40°21′
			2.307	0.8532	11						
53	601	1.8±1.2	0.68	0.0204	14	0.00010	USGS	Basalt	do.	20°51′	42°17′
			0.66								
54(D)	Qun	19.1±0.6	0.49	0.1615	39	0.00112	Isotopes	Diabase	do.	19°15′	41°19′
			0.48	0.1617	28						
55a(D)	930	22.4±1.4	1.723	0.6855	14	0.00131	Geochron	Diorite	do.	18°45′	41°32′
			1.705	0.6530	14						
55b	931	12.4±1.2	0.917	0.1977	1	0.00072	do.	Basalt	do.	18°45′	41°32′
			0.923	0.1977	4						
56a(D)	933A	43.1±3.0	0.880	0.6180	31	0.00253	do.	Diorite	do.	18°32′	41°38′
			0.855	0.6931	33						
56b(D)	933B	41.7±2.8	0.847	0.6105	23	0.00245	do.	do.	do.	18°32′	41°38′
			0.836	0.6205							
56c(D)	933C	34.7±2.1	1.245	0.7731	34	0.00203	do.	Grano-diorite	do.	18°32′	41°38′
			1.280	0.7606	33						
57a	932	2.1±1.0	0.691	0.025	3	0.000121	do.	Basalt	do.	18°28′	41°31′
			0.694	0.025	4						
57b	932	2.8±1.5	0.669	0.0450	6	0.00016	do.	do.	do.	18°28′	41°31′
			0.685	0.0200	3						
59	934	12.4±3	0.549	0.0926	3	0.00072	do.	do.	do.	18°08′	41°34′
			0.509	0.135	4						
60(D)	935	19.2±1.1	2.753	0.9458	42	0.00112	do.	Grano-diorite	do.	18°09′	41°40′
			2.696	0.8807	42						
61	938A	12.1±1.5	0.798	0.160	9	0.00070	do.	Basalt	do.	18°07′	41°44′
			0.799	0.175	9						
62	937	4.3±0.6	1.090	0.0901	8	0.00025	do.	do.	do.	18°04′	41°45′
			1.084	0.0726	8						
63(D)	936	23.0±1.5	1.375	0.5755	26	0.00135	do.	Diorite	do.	18°04′	41°46′
			1.367	0.5254	25						
64(D)	939	25.3±1.7	1.298	0.5680	35	0.00148	do.	Gabbro	do.	18°02′	41°53′
			1.313	0.5855	28						
65	941	5.1±1.5	0.881	0.0776	7	0.00029	do.	Basalt	do.	18°30′	42°02′
			0.885	0.0776	7						
66	940	5.1±1.5	1.049	0.0776	7	0.00030	do.	do.	do.	18°01′	42°05′
			1.082	0.113	8						
67	520	25.3±0.5	1.34	0.5901	92	0.00148	Isotopes	do.	do.	18°10′	43°10′
			1.32	0.5865	93						
68	519B	22.5±0.7	3.865 avg.	1.262	84	0.00129	USGS	Syenite	do.	18°05′	43°11′
69	518	30.1±1.0	0.52	0.2773	36	0.00176	Isotopes	do.	do.	17°57′	43°12′
			0.54	0.2799	32						
70(L)	103B	21.8±1.4	0.23	0.0830	14	0.00128	do.	Diorite	do.	17°26′	42°36′
			0.20	0.0808	20						
72a(L)	516C	20.5±2	0.093	0.0290	13	0.00119	do.	Gabbro	do.	17°03′	42°55′
			0.080	0.0327	18						

Footnotes at end of table

TABLE 10.—*K-Ar ages for Cenozoic igneous rocks collected from western Saudia Arabia*—Continued

[All material analyzed was whole rock except samples 34a and 34b, which were glauconite, and sample 70, which was labradorite. Decay constants: $\lambda\beta=4.963\times10^{-10}$/yr; $\lambda\xi=0.581\times10^{-10}$/yr; κ-40/K=1.167×10^{-4} atomic percent]

Sample (location given on pl. 2)[1]	Field no.	Age (m.y.)	Potassium (percent)	$^{40}Ar\times10^{-10}$ (moles/g)	^{40}Ar (percent)	$^{*40}Ar/^{40}K$	Analyzed by	Rock	Collected by	Location Lat N.	Location Long E.
72b(H)	517C	24.9±1.0	3.12	1.351	26	0.00145	do.	Hornfels	do.	16°57′	42°57′
			3.15	1.371	27						
73(L)	514-5	23.4±2	0.14	0.0051	19	0.00137	do.	Gabbro	do.	16°58′	42°57′
			0.14	0.0595	15						
74a(G)	515A	21.1±0.6	3.17	1.171	43	0.00123	do.	Grano-phyre	do.	16°56′	42°58′
			3.13	1.143	43						
74b(G)	515B	23.9±1.0	1.71	0.7209	26	0.00140	do.	do.	do.	16°56′	42°58′
			1.70	0.7048	29						
Yemen (G)	ROJ1	23.3±0.9	1.26	0.4247	61	0.00136	do.	Granite	Jackson	13°30′	44°02′
Ethiopia (D)	Asmara	37.1±1.2	0.29	0.1884	32	0.00218	Isotopes	Basalt	Brown	15°17′	38°56′
				0.1826	32						

NOTE—$^{*40}Ar$ is radiogenic argon.

[1]T and B indicate top and bottom flows, respectively, of thick section of many flows at same sample locality. (D) indicates dike; (P), plug; (L), layered gabbro; (H), hornfels; (G), granophyre; absence of letter in parentheses indicates lava flow. Lowercase letters (a, b, c, d) indicate multiple samples from same locality.

[2]Isotopes, Inc., later Teledyne Isotope, Westwood, N.J.

[3]Geochron Laboratories, Inc., Cambridge, Mass.

[4]USGS analysts, R.F. Marvin, H.H. Mehnert, and Violet Merritt.

[5]Radiogenic argon could not be measured, owing, it is believed, to the very young age of the basalts.

anorthosite, and diorite or quartz monzogabbro, although a few are as alkaline as quartz syenite (fig. 52).

The chemical composition of the sheeted dikes, cumulative gabbro, granophyre, and associated rocks of the Tihamat-Asir Complex resemble the ophiolites of Cyprus, Oman, and Newfoundland and are considered to be ophiolitic in the Tihamat-Asir by Coleman and others (1979). These writers found that a plot of FeO* (total iron as FeO), SiO_2, and TiO_2 against FeO/MgO places the gabbro, granophyre, and sheeted dikes as well as the continental dikes of the complex within the tholeiitic series rather than the calc-alkalic series. The continental dikes between Jiddah and Ad Darb range in K-Ar age from 273±20 to 18.0±1.3 m.y. (table 10, pl. 2). The older ages undoubtedly represent additional argon derived from the invaded Precambrian terrane, a situation similar to that in Liberia, where tholeiitic dikes parallel to the Atlantic coastline gave anomalously old ages in the Precambrian but concordant and younger ages in the Paleozoic sedimentary rocks (Dalrymple and others, 1975). One dike 175 km southeast of Jiddah, near Al Līth (sample 51, table 10, pl. 2), gave ages of 177±13 and 273±20 m.y. (K-Ar whole-rock, normalized to the Sydney decay rate) from the midzone, but an age of 21.5±2.3 m.y. from the chilled edge, most likely near the age of emplacement. Nine whole-rock samples from five other dikes range in age from 18.0±1.3 to 25.3±1.7 m.y. (table 10), with an arithmetic mean of 22.1 m.y. A gabbroic body (normative anorthosite) in a small outcrop 70 km south of Jiddah at Jabal Sitā' gave ages of 26.8±4.5 and 27.9±5.5 m.y. (sample 46, table 10, pl. 2); it is probably to be correlated with the continental dikes. If so, this marks the northern end of the southern continental dikes, there being a distinct break in the continental dike set about the latitude of Jiddah (pl. 2). A linear magnetic low in the eastern Red Sea west of Jiddah strikes S. 63° E. and passes near the leucocratic gabbro (normative anorthosite) outcrop (Kabbani, 1970). The magnetic anomalies associated with the southern continental dikes reappear 80 km to the northeast of Makkah, suggesting either a transverse fault with horizontal movement, possibly a transform zone, or a major en echelon offset in the northwest-trending fracture pattern, as suggested by Blank (1977). The only age determination on the northern continental dikes is of an olivine gabbronorite northwest of Al Wajd, which gave an age of 22.9±1.4 m.y. (sample 8, table 10). This age is concordant with the ages of the southern continental dikes, but the dike lacks a magnetic signature. The ages of five whole-rock samples from the layered gabbro and granophyre plutons that are part of the Tihamat-Asir ophiolite at Jabal at Tirf range from 20.5±2 to 24.9±1 m.y. (samples 72–74, table 10) with a mean of 22.7±2 m.y. A comparable age of 21.8±1.4 m.y. (sample 70, table 10) for labradorite is from a layered diorite at Wādī Baysh 60 km northwest of Jabal at Tirf.

The Tihamat-Asir Complex intrudes the Precambrian basement, the overlying Paleozoic and Mesozoic sedimentary rocks, and the early Miocene Jizan Group, including the freshwater Baid Formation. Diabase sills intruded into the Baid Formation at lat 19°15′ N. gave a K-Ar age of 19.1±0.6 m.y. (sample 54, table 10, pl. 2), concordant with the ages measured by Fleck (Coleman and others, 1979), and this confirms that the tholeiitic rocks are younger than the Baid Formation.

TABLE 11.—*Locations and rock types for Cenozoic igneous rocks for which chemical analyses are given in table 9 and isotopic ages in table 10*

[Petrographic names are based on CIPW normative calculations, after Irvine and Baragar; modal names are based on petrographic studies by Salman Bloch, Robert Coleman, and Richard Blank. m, meters]

Sample (location given on pl. 2)[1]	Field no.	Rock type and location	Remarks
1	47000	Alkaline basalt. Al Harrah (Ḥarrat ash Shama).	Near basal outcrop 186 m above lowermost buried flow. Zeolitic.
2	47001	do.	Do.
3	47002	do.	Do.
4	47003	do.	Do.
5	47004	Hawaiite.	Do.
6T	917T	Hawaiite. Uppermost flow, Ḥarrat ar Raḥāh, west edge.	—
6B	917B	Alkaline basalt. Basal flow, Ḥarrat ar Raḥāh, west edge.	—
7T	916T	Hawaiite. Uppermost flow of crater rim in Ḥarrat 'Uwayriḍ, near west edge.	—
7B	916B	Alkaline basalt. Basal flow, Ḥarrat 'Uwayriḍ.	—
8(D)	B1818	Olivine-gabbro norite. Nonmagnetic dike, Wādī Marrā.	—
9T	915T	Hawaiite. Uppermost flow, Ḥarrat 'Uwayriḍ, south tip.	—
9B	915B	Hawaiite. Basal flow, Ḥarrat 'Uwayriḍ, south tip.	—
10	913	Hawaiite. Upper of four flows, northwest outlier of Ḥarrat Khaybar.	—
12	912	Alkaline basalt. Lowermost flow, west side Ḥarrat al Kūrá. Vesicular.	—
13D	7843	Gabbro, altered, minor interstitial quartz. Dike Wādī Umm Natash. Questionable Tertiary.	—
14	919	Hawaiite. Lower 6-m flow in Ḥarrat Lunayyir.	—
15	920	Hawaiite. Recent black aa; uppermost Ḥarrat Lunayyir.	—
16	921	Basanite. Recent flow, 10 m thick. Jabal Salajah.	—
17	911	Hawaiite. Uppermost 15-m flow, Ḥarrat I'shara.	—
18	910	Alkaline basalt. Lowermost of 12 or more flows resting on early Tertiary silt, Ḥarrat al Jarf.	—
19	922	Basanite. Base of Holocene or Pleistocene 10-m flow, Ḥarrat an Nabah, on coastal plain.	—
19a(P)	1309	Hawaiite. Plug intruded into Aja' Granite, Jabal Shammar.	—
20	3729B	Basanite. Basal flow at Khaybar, Ḥarrat Khaybar.	—
21	906	Rhyolitic crystal tuff. Abyad wa Ubayyid. Holocene eruption, east side Ḥarrat Khaybar.	—
22	907	Alkaline basalt. Jabal al Khuraym.	—
23	909	Alkaline basalt. Jabal Abū Widah; oldest lava in Wādī al Ḥamḍ trough.	—
24	908	Alkaline basalt. North upper edge, Ḥarrat Kuramā'.	—
25	B1314	Alkaline basalt. Ḥarrat al Hutaymah. 12-m flow containing basaltic hornblende.	—
26	923	Alkaline basalt. Uppermost Holocene flow, Ḥarrat Raḥaṭ.	—
27	905	Alkaline basalt. Western overflow from Ḥarrat Raḥaṭ.	—
28	904	Alkaline basalt. Western edge, Ḥarrat Raḥaṭ, lowermost flow in Wādī Thamrah.	—
29	4702B	Alkaline basalt. Southeast edge of Ḥarrat al Kishb.	—
30	GFB1	Hawaiite. Basalt remnant at Wādī Khulayṣ.	—
32	GFB3	Alkaline basalt. Eroded lava stream north of Al Kurā'.	—
33	GFB2	Hawaiite. Older basalt above Eocene in graben at 'Usfān.	—
34a	USFAN	Sandstone. Glauconite bearing.	—
34b	USFAN	Sandstone. Glauconite bearing.	—
35	Well 4,	Andesite. Overlies or intrudes Lower Eocene Shumaysi Formation. Area 1 (Al-Shanti, 1966).	—
36	902	Alkaline basalt. On graben of Ḥaddat ash Shām.	—
37	47027B	Alkaline basalt. Ḥarrat Biss.	—
38	47026	Hawaiite. Jabal al Barz. Isolated outlier on Sahl Rakbah.	—
39	Well 3,	Basalt-andesite. Overlies or intrudes Lower Eocene Shumaysi Formation. Area 2A (Al-Shanti, 1966).	—
40(P)	47024	Trachyte-phonolite plug. Jabal 'Ān.	—
41	47023	Hawaiite. West side of Ḥarrat Ḥaḍan, lowermost exposure.	—
42	47022	Hawaiite. West side of Ḥarrat Ḥaḍan, top flow.	—
43	47021	Alkali basalt. West side of Ḥarrat Ḥaḍan.	—

Footnote at end of table

TABLE 11.—*Locations and rock types for Cenozoic igneous rocks for which chemical analyses are given in table 9 and isotopic ages in table 10* —Continued

[Petrographic names are based on CIPW normative calculations, after Irvine and Baragar; modal names are based on petrographic studies by Salman Bloch, Robert Coleman, and Richard Blank. m, meters]

Sample (location given on pl. 2)[1]	Field no.	Rock type and location	Remarks
44	47025	Basanite. West side of Ḥarrat Nawāṣif, Wādī al Jarah.	—
45(P)	926	Rhyolite. Subalkaline. Shama rhyolite of Pallister (1983).	—
46a(P)	927A	Olivine gabbro. Jabal Sitā', intrusive, darker phase.	—
46b(P)	927B	Olivine gabbro. Serpentinized. Jabal Sitā', intrusive, lighter phase.	—
47	6MX68	Alkali basalt. Outlier of Ḥarrat ad Damm.	—
48(P)	66	Trachyte plug. Probably part of Sita formation of Pallister (1983).	—
49	5MX68	Alkali basalt. Upper flow, Ḥarrat Tuffil (Shamā).	—
50	HT	Alkali basalt. Lowermost southeast edge Ḥarrat Tuffil (Shamā).	—
51a(D)	623A	Diabase. Chilled southwest border of dike.	300 m wide, in Wādī Ghālah.
51b(D)	623B	Olivine gabbro. Glomeroporphyritic.	Do.
51c(D)	623C	Diabase. Chilled northeast edge of dike.	Do.
52a(D)	928A	Quartz monzonite. Dike.	—
52b(D)	928B	Felsite(?). Chilled north border of dike.	400 m wide, in Wādī al Fagh.
52c(D)	928C	Quartz diorite. Altered micrographic; in wall of dike.	Do.
52d(D)	928D	Schist. Quartz albite chlorite, wall rock of dike.	Do.
53	601	Alkali-olivine basalt. Basal flow at Wādī Ranyah, Ḥarrat al Buqūm.	—
54(D)	Qun	Diabase. Sill in Miocene Baid Formation, Wādī Qununah.	—
55a(D)	930	Diorite. Dike, north edge of Ḥarrat al Birk in Wādī Ḥalī.	—
55b	931	Alkali-olivine basalt. Base of Ḥarrat al Birk at Wādī Ḥalī.	—
56a(D)	933A	Meladiorite or gabbro. 40-m dike (southwestern of two dikes).	Wādī Majm'ah, east edge of Ḥarrat al Birk.
56b(D)	933B	Meladiorite or gabbro. 40-m dike (northwestern of two dikes).	Do.
56c(D)	933C	Quartz monzodiorite. Dike southwest of sample 56a.	Do.
57a	932	Alkali-olivine basalt. Top of lava flow.	In Wādī 'Amq.
57b	932	Alkali-olivine basalt. Middle and upper flows.	Do.
58a	BRK4A	Gabbro. Dike, chilled northeast edge.	Wādī Dhahabān, east side of Ḥarrat al Birk.
58b	BRK4B	Gabbro. Dike, middle, coarse-grained.	Do.
58c	BRK4C	Gabbro. Dike, chilled southwest edge.	Do.
59	934	Cinder. Cone on island offshore from Wādī Dhahabān.	—
60(D)	935	Quartz monzonite. Dike, diabasic texture, Wādī Dhahabān.	—
61	938A	Hawaiite basalt. Upper layer of lower flows, Ḥarrat al Birk.	—
62	937	Hawaiite. Basal flow, zoned olivine, interstitial calcite, Ḥarrat al Birk.	—
63(D)	936	Quartz monzodiorite or quartz monzogabbro. Large dike in swarm.	—
64D	939	Diorite or epigabbro. 20-m dike crosses Jabal Umm as Sawdah and Jabal Ghumās.	—
65	941	Basanite. Lowermost flow in Wādī Ḥalī gorge below Jabal al Haylah.	—
66	940	Hawaiite. Upper part of lower flow beneath Jabal Baqarah.	—
67	520	Mugearite. Uppermost flow of As Sirāt volcanic plateau.	—
68	519B	Syenite plug.	—
69	518	Picrite-ankaramite basalt. Basal flow of As Sirāt volcanic plateau.	—
70	103B	Olivine meladiorite. Tertiary intrusive, northern end, Tihamat Asir dike swarm.	—
71	B94	Gabbro. In Tihamat Asir dike swarm, north bank, Wādī Jīzān.	—
72a	516C	Gabbro. In layers at Jabal at Tirf.	—
72b	517C	Hornfels. Jabal at Tirf, intrusive.	—
73	514-5	Gabbro. Jabal at Tirf, intrusive.	—
74a	515A	Granophyre. Jabal at Tirf, intrusive.	—
74b	515B	Granophyre. Jabal at Tirf, intrusive.	—
Yemen	ROJ1	Granite. Jabal Sabir.	—
Ethiopia(D)	Asmara	Basalt. Asmara dike.	—

[1]T and B indicate top and bottom flows, respectively, of thick section of many flows at same sample locality. (D) indicates dike; (P), plug. Lowercase letters (a, b, c, d) indicate multiple samples from same locality.

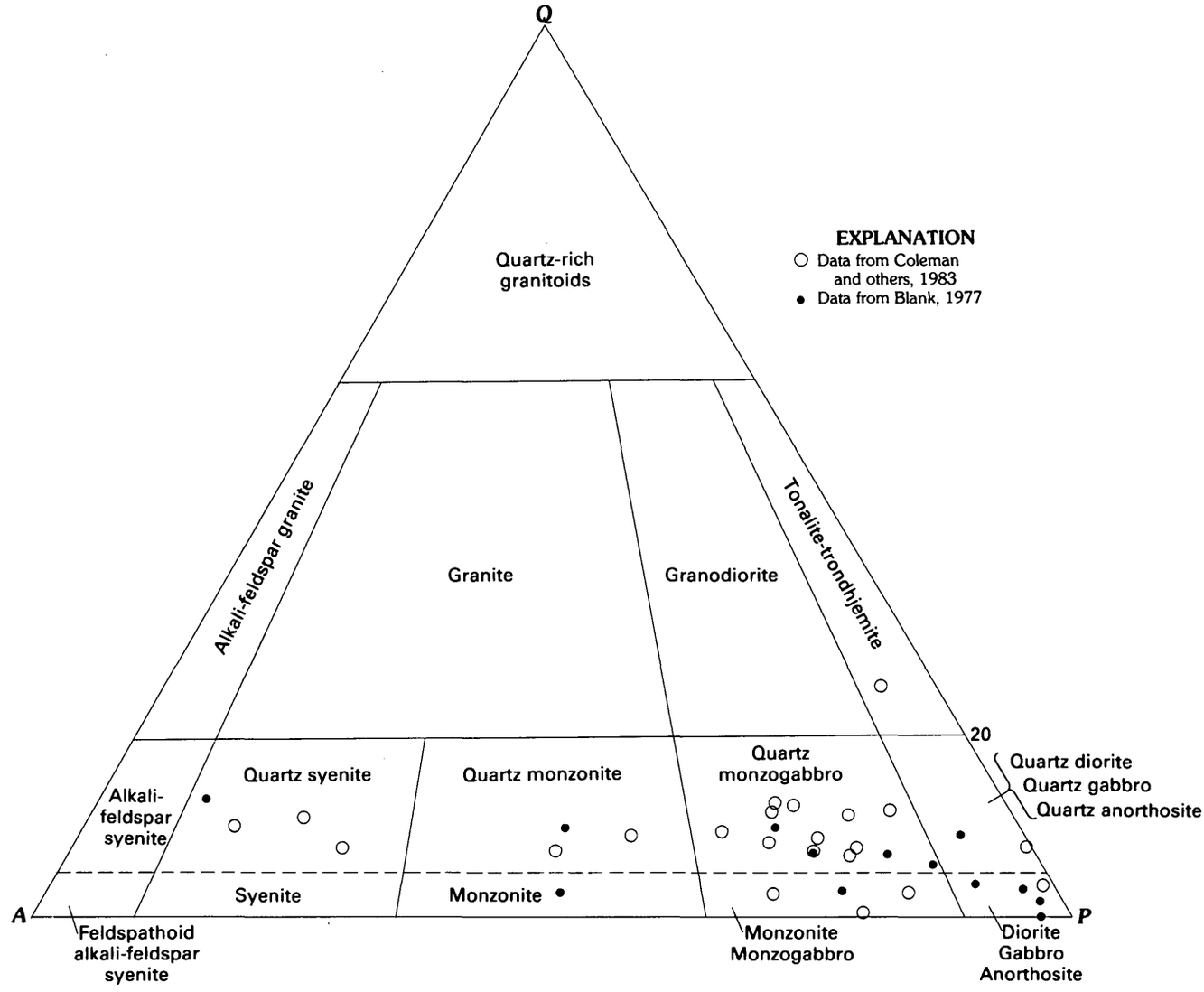

FIGURE 52.—Modal analyses of Tertiary continental dikes plotted on quartz (Q)-alkali feldspar (A)-plagioclase (P) diagram (Streckeisen, 1976).

In addition to the continental dikes, numerous isolated plugs and feeder pipes are exposed 100–500 km inland on the crystalline shield (Brown, 1972). Most of these can be identified, both chemically and by isotopic ages, with nearby plateau flood-basalts, especially in the As Sarāt region where the Jabal as Sarāt basalts have been eroded and where 26 feeder pipes are exposed (pl. 2; Coleman, Fleck, and others, 1977) in an area extending as far as 70 km northwest of the flows. Similar pipes exposed east of Aṭ Ṭā'if at lat 21° N. are either associated with the Ḥarrat Ḥaḍan flood basalts or are isolated intrusions; from lat 26°15′ to 26°35′ N., outlying pipes may be associated with the growth of Ḥarrat al Ithnayn (Hutaym) and Ḥarrat Khaybar; and at lat 26°45′ to 27°20′ N., in a belt extending northeastward across the northeastern corner of the shield in the Jabal Shammar region, similar pipes probably were associated with an entirely eroded harrat, perhaps similar to the accumulation of local basalt flows and ash centers east of Jabal Salmá at lat 27° N., long 42°25′ E., the Ḥarrat al Hutaymah.

The As Sarāt feeder pipes are alkaline, either nepheline basalt or basanite (Coleman, Fleck, and others, 1977), as are pipes at or near other lava fields farther north. One isolated volcanic neck forming a spine in the Jabal Shammar belt, within the southern part of the granite batholith of Jabal Aja' at the north edge of the shield, is normative nepheline basanite (sample 19a, table 9). The basanite pipes near As Sirāt are 24.7±2 and 25.4±2.7 m.y. old, based on K-Ar ages (Coleman, Fleck, and others, 1977).

Coeval felsic intrusives form stocks as much as 2 km in diameter. One stock in Jabal as Sarāt near the Yemen border at Al Wārah (sample 68, pl. 2) is analcite-

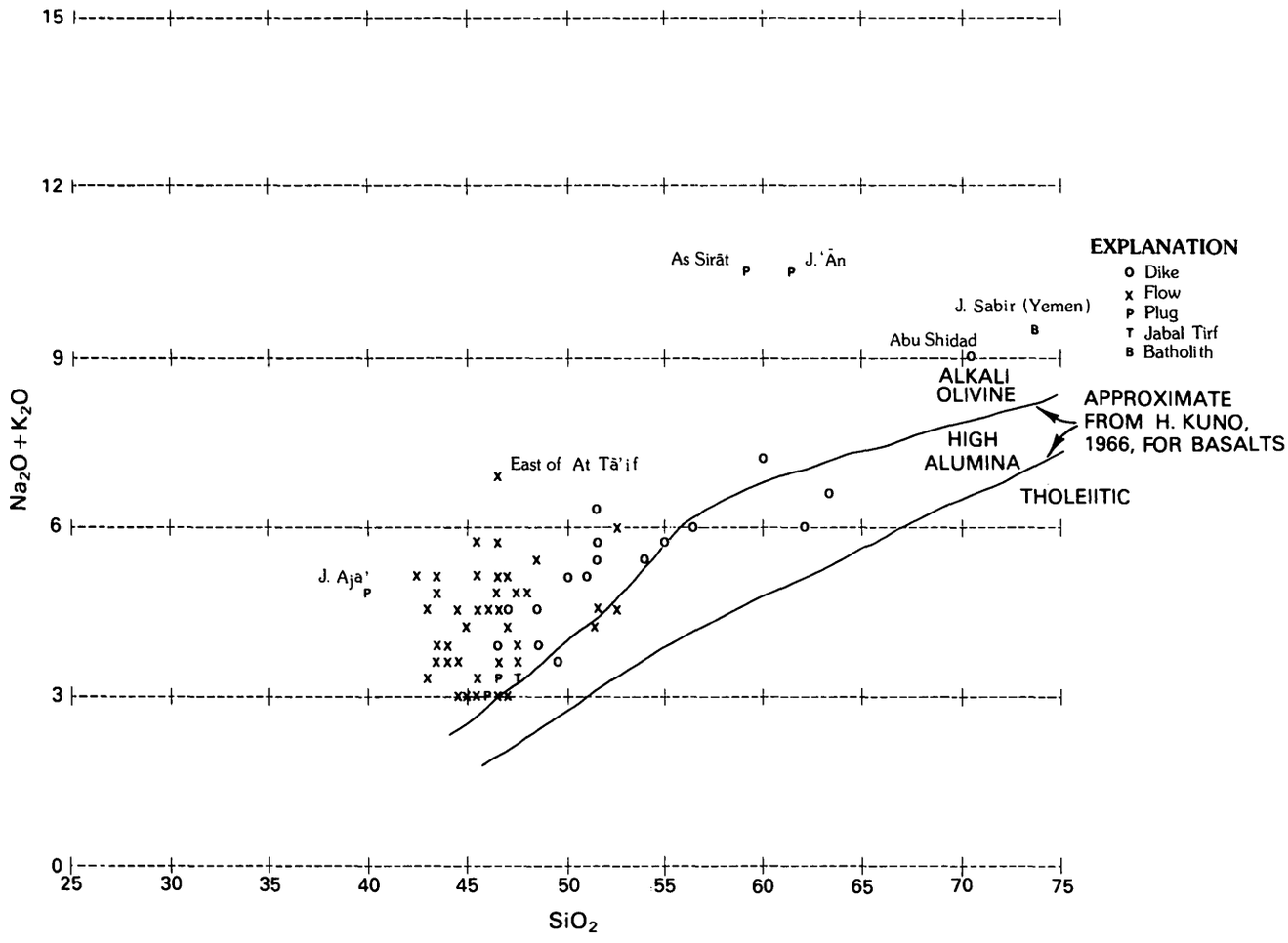

FIGURE 53.—Harker diagram showing alkalies plotted against silica for Tertiary igneous rocks.

bearing syenite surrounded by an analcite-trachyte rim, whereas a contemporary plug at Jabal 'Ān 410 km northwest and adjacent to Ḩarrat Ḩaḍan has a core of trachyte or hornblende latite with a rim of phonolite (sample 40, table 10) (Richter-Bernburg and Schott, 1954; Gonzales, 1973). The As Sarāt stock is 81 percent orthoclase, 5 percent augite, 7 percent opaque minerals, 2 percent calcite, and 5 percent analcite (Salman Bloch, written commun., 1976), whereas the chilled edge is 71 percent albite and anorthoclase, 15.5 percent aegirine-augite, 7.5 percent opaque, and 6 percent analcite. The Jabal 'Ān stock, one of four in the neighborhood, is 45 percent potassium feldspar, 35 percent plagioclase, 15 percent hornblende, and 5 percent magnetite (Gonzales, 1973) and is dated at 22.2±3.5 m.y. (K-Ar whole-rock), compared with 22.5±0.7 m.y. for the As Sarāt stock (sample 68, table 10, pl. 2). A coeval age of 23.3±0.9 m.y. (Yemen, table 10) from the granite of Jabal Sabir at lat 13°30′ N. near Ta'izz is one of many Tertiary alkalic granite and diorite plugs, stocks, and plutons continuing southward in the Yemen Arab Republic, many of which are concentrated along the rift scarp (Grolier and Overstreet, 1978).

CENOZOIC BASALTIC LAVA FLOWS

Lava fields (harrats) are scattered along the eastern seaboard of the Red Sea and on the western Arabian highlands. They extend intermittently northward from the Yemen Volcanics ("Trap Series"), which cover as much as 35,000 km^2 of the southwestern Yemen Highlands to the Haurān of Jabal ed Drouz of comparable size in Syria. From there the lavas extend across eastern Jordan and into Saudi Arabia, where they are known as Al Ḩarrah, or Ḩarrat ash Shama. Within Saudi Arabia the larger harrats, in order of size, are as follows (pl. 2):

Harrat	*Approximate area (km^2)*
Khaybar-al Ithnayn (Hutaym)-al Kurā'	21,400
Rahaṭ	18,100
Al Ḩarraḥ (ash Shama)	15,200

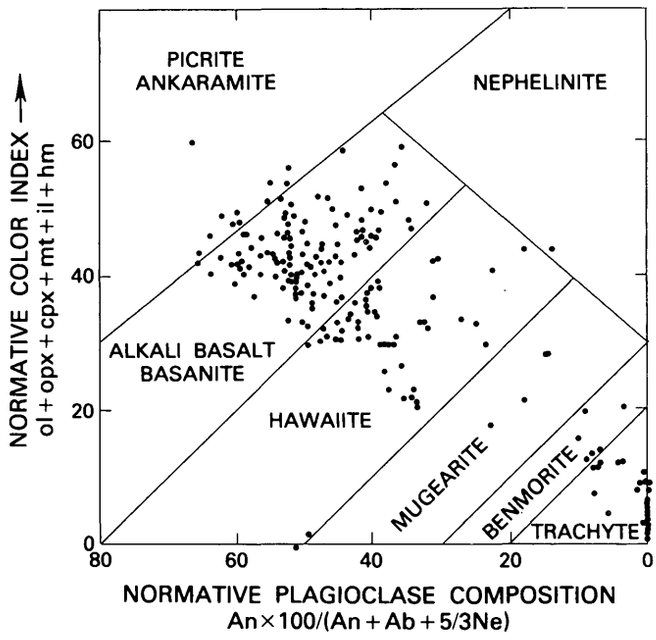

FIGURE 54.—Irvine and Baragar (1971) classification diagram. Normative color index versus normative plagioclase for analyzed samples from the harrats of Saudi Arabia. Values for minerals derived from CIPW normative calculation. (From Coleman and others, 1983.)

Harrat	*Approximate area (km²)*
Nawāṣīf-al Buqūm	10,800
Ar Raḥāh-'Uwayriḍ	7,150
Al Kishb	6,700
Ḥaḍan	3,700
Al Birk	1,800
I'shara-Khirsāt	< 1,800
Luna'yir	1,750
Harairah	< 1,530
Kuramā' (Hirmah)	1,100
Al Hutaymah	900
As Sirāt	750
Jibāl al Khaṭībah	320
Malaki	115

Besides the above, there are numerous spatter or cinder cones and small flows or ash fields. K-Ar dates on the lavas range from 62.6±4.3 m.y. to historical times. Most dates fall between 29 and 18 m.y. and between 14 and <1 m.y. (fig. 51, table 10; Gregory and others, 1982; Coleman and others, 1983). The most widespread lower flows of the lava fields between Makkah and Al Madīnah are 12–13 m.y. old (middle Miocene), the same age span as the lower flows in the Al Ḥarrah of Wādī as Sirḥān and the basalt flows of the Hebron Formation in the Jordan Valley. These

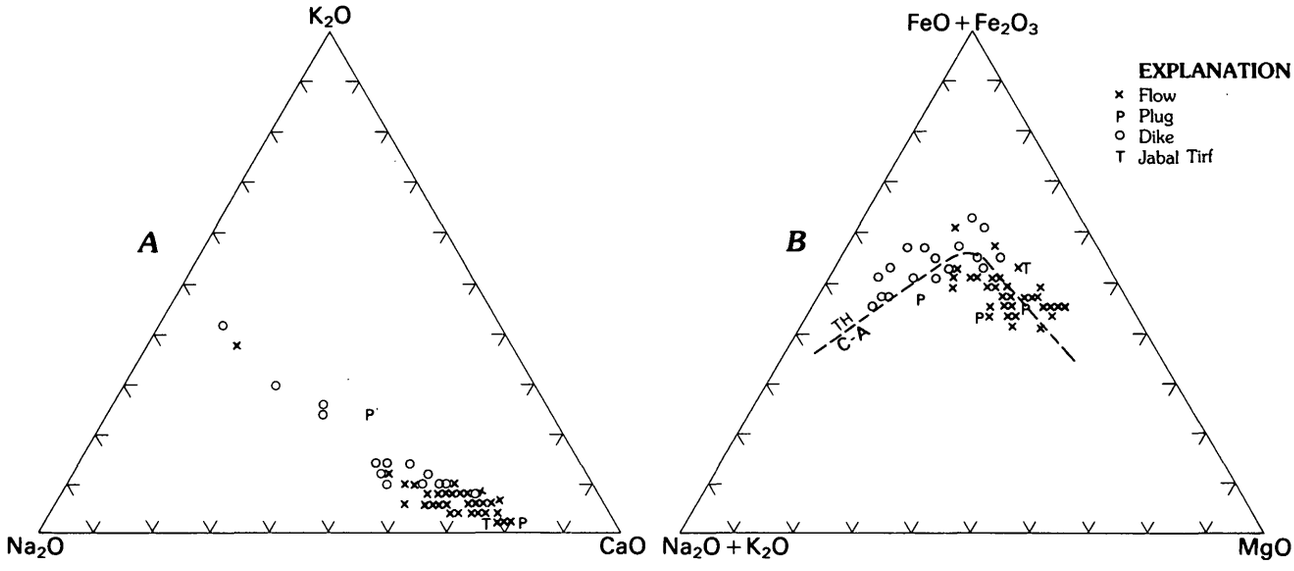

FIGURE 55.—Ternary diagrams showing distribution of Tertiary igneous rocks from western Saudi Arabia. *A*, Na_2O-K_2O-CaO ternary diagram. *B*, AFM diagram. Dashed line separates tholeiitic (above) and calc-alkalic (below) compositions according to Irvine and Baragar (1971).

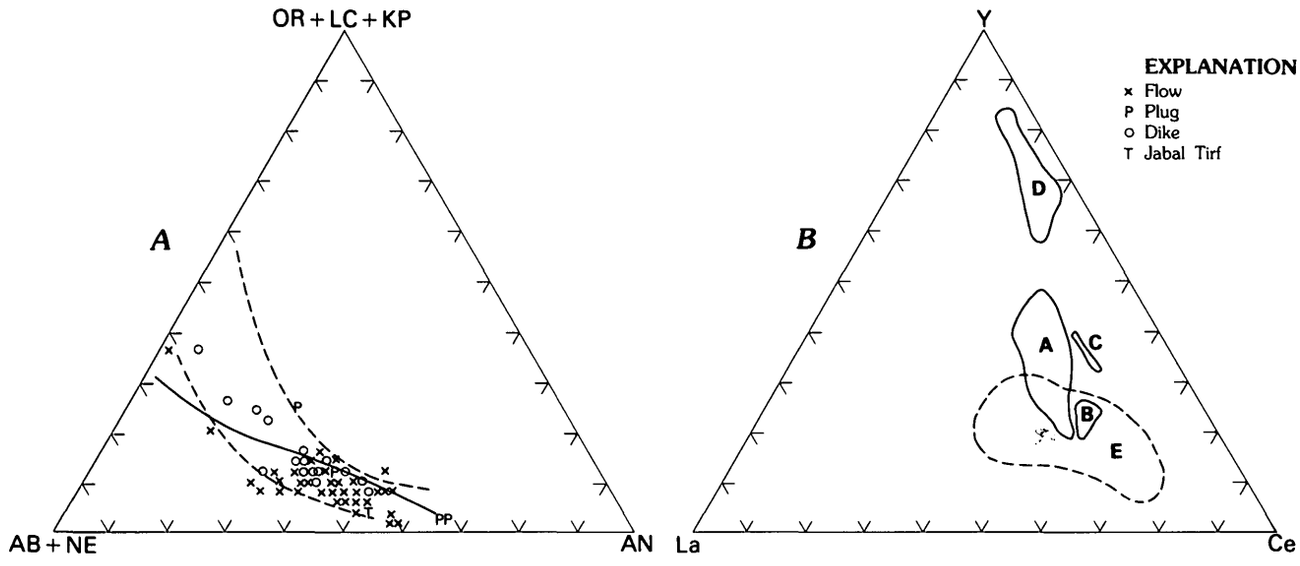

FIGURE 56.—Ternary diagrams showing distribution of Tertiary igneous rocks from western Saudi Arabia. *A*, Normative albite+nepheline-orthoclase-anorthite diagram. Subdivisions are according to Irvine and Baragar (1971); solid line separates potassic (above) from sodic (below) rocks of alkali olivine basalt series, and dashed lines separate K-poor (below) and K-rich variants from "average" subalkaline rocks. *B*, Y-La-Ce ternary diagram. A, field of calc-alkaline andesites and basaltic andesites; B, field of ocean island alkali basalts; C, field of ocean island tholeiitic basalts; D, field of ocean-floor basalts and island-arc tholeiites; E, Tertiary igneous rocks of Saudi Arabia. (Fields except Arabian Tertiary igneous rocks from R.S. Thorpe, 1972.)

lower flows are interbedded with lacustrine marls. Where the lava has ascended via narrow vents through basement rocks, the apparent ages determined from K/Ar ratios tend to be older, because of argon enrichment, than physiographic evidence and degree of weathering would indicate. The larger flows seem to have escaped much of this contamination. The early flows erupted from fissures parallel to the Red Sea, are composed of picrite-ankaramite, and commonly are interbedded with shallow-water sediments (Gregory and others, 1982; figs. 53, 54, this report). Younger, more widespread flows are alkali-olivine basalts (pl. 2, table 11) containing sparse peridotitic inclusions. The most recent become bimodal, with hawaiite devoid of mantle inclusion and intermingled, sparse silicic flows and ash. The composition of only the most silicic may reflect minor melting of the sialic Arabian plate (Coleman and others, 1983, p. 68).

THE HARRATS

AL ḤARRAḤ

The northernmost harrat, Al Ḥarraḥ, or Ḥarrat ash Shama, extends south from Jabal ed Drouz in Syria, where it is known as the Haurān, thence across Jordan and along the northeastern flank of Wādī as Sirḥān into Arabia. Al Ḥarraḥ covers 15,200 km^2 in Saudi Arabia, which is one-third of the total area of the combined lava fields of Jabal ed Drouz and Al Ḥarraḥ. In Saudi Arabia, the basalt flows extend southeastward 210 km in a belt averaging 75 km wide with a maximum relief of 300 m and reaching altitudes of as much as 1,128 m in Jabal Liss. Al Ḥarraḥ is characterized by numerous flows and many craters, calderas, and cones. In Jordan, six major emissions culminated with outpourings of basaltic tuffs and fissure eruptions (dikes) parallel to the Red Sea rift (Bender, 1974b). Of these, the lower three are known only in drill cores.

The surface rocks of Al Ḥarraḥ in Jordan are considered to range in age from Miocene to Pleistocene and have been divided into four units, the lower three of which are separated by lacustrine sediments (Bender, 1974b). In Arabia the lower flows are interbedded with calcareous lacustrine sediments. These lower flows were sampled in outcrops along the north side of the Sabkhat Ḥaẓawẓā' (lat 30°50′ N., long 38°10′ E.) and were found to range in K-Ar age from 13.4±0.4 to 11.4±0.4 m.y. (samples 1–5, table 10, fig. 51). Test drilling to depths of 319 m beneath the sabkhah near the sample localities disclosed seven basalt flows interbedded in the lacustrine sediments, the lowermost 186 m of flow rocks being below the dated flows on the surface (C.L. Smith, 1980). The K-Ar ages of the outcrops on the north side of Sabkhat Ḥaẓawẓā' fall within the upper middle Miocene. The sampled rocks

are comparable in age and stratigraphic position to the "lower basalts" on the shores of Lake Tiberias in Jordan 360 km to the northwest. At Lake Tiberias, basalt flows interbedded in the Hebron (Horodus) Formation of fluviolacustine origin (Michelson, 1978) have K-Ar ages of 15.6±1.6 to 10.3±2.0 m.y., whereas an upper interbedded flow elsewhere in the Hebron Formation has a K-Ar age of 4.9±1.3 m.y. (Steinitz and others, 1978). This timespan extends from middle Miocene to Pliocene and includes at least four periods of weathering and soil development, as well as lacustrine sedimentation. The presence of northwest-trending faults in the lower lava, as mapped by Gettings (1979) in the Sabkhat Ḥaẓawẓā' area, strengthens the concept that the lower lavas in Saudi Arabia predate the last period of epeirogeny of the Red Sea-Jordan rift, that is, they are more than 5 m.y. old.

The unnamed lacustrine beds at Sabkhat Ḥaẓawẓā' were shown to be 150 m thick in a test well drilled by the Arabian-American Oil Company near the axis of the trough occupied by the sabkhah. These lacustrine beds disconformably overlie the Paleocene-Eocene Hibr Formation (Meissner and Ankary, 1972).

Following the older series of interbedded flows in Jordan, a younger flow exhibits late Pleistocene erosion followed by the accumulation of tuff and cinder cones. Final eruptions from basaltic cones along fissures parallel to the Red Sea have continued in Jordan to historic times (Bender, 1975). In Saudi Arabia, the southeasternmost lava fields in Al Ḥarraḥ are considered to be Pleistocene to Holocene, but the possibility is recognized that some of the lowermost flows may be Pliocene. Numerous craters, some eroded, mark the landscape, although dikes along the fault flank of the Khawr Umm Wu'āl graben at the southeast edge of the harrat suggest fissure eruptions. A total of 527 plugs or necks, cones, craters, dikes, and tholoids or domes have been mapped, of which 286 are plugs or necks (Donald Holm, ARAMCO, written commun., 1960).

Most flows are a few meters thick; the maximum total measured is 100 m at the southeastern extension in Khwar Umm Wu'āl. In places, flows are scoriaceous and vesicular and include pyroclastic lenses and thin leucocratic dikes. Lava surfaces are blocky and weather into large boulders, for the most part making traversing difficult (Donald Holm, ARAMCO, written commun., 1960).

The chemical analyses of the dated samples are those of typical alkalic continental flood basalts (samples 1–5, table 9; fig. 54) and are very similar to the average for similar flows in Jordan (Bender, 1974b). The predominant mineral is andesine-labradorite; titaniferous augite and olivine are major components, and calcite and opaque oxides are minor constituents. The samples from Sabkhat Ḥaẓawẓā' are amygdaloidal and contain secondary zeolite fillings.

ḤARRAT AR RAḤĀH-'UWAYRIḌ

Ḥarrat ar Raḥāh-'Uwayriḍ forms the crest of the northwestern scarp mountains, extending from lat 28°05′ N. in Al Ḥismá southeastward to lat 26°30′ N., a distance of 225 km. The two harrats are continuous; however, Ḥarrat ar Raḥāh has been nearly split by erosion, leaving only a narrow divide occupied by a number of isolated volcanic plugs. Ar Raḥāh is widest (35 km) at the western front, narrowing to less than a kilometer at the Matar divide. The terrain is nearly flat, standing 150–300 m above Al Ḥismá, and is composed of as many as 20 flows, increasing to as much as 25 flows for a total thickness of 515 m to the southwest. This thickness includes many weathering zones. Within the northwestern segment of the southern lobe where flows are most numerous, the lava shield rises 550 m above the plain. The flows were extruded from pipes (or perhaps from fissures that are no longer discernible). One such volcanic throat, Al Batra, stands on the sandstone plain west of the northern lobe of the lava field. The flows are of three distinct ages. The lower flows, of Miocene age (K-Ar determination), form the cliffs facing the Red Sea and rise above the Cambrian Siq Sandstone. The upper flows are Pleistocene and Holocene. Both the sandstone and the harrat are deeply dissected along the southern and southwestern fronts. Most of the younger lava flowed in a northeasterly direction, some along wadi channels no longer extant, suggesting eruption following regional tilting. The lava-filled channels now form interstream divides. More recent drainage dissects the flows or is parallel to them. An explosion crater at the source of the longest of these flows north of the harrat attests to continuing volcanic activity in the recent past.

The lava shield southeastward rises to a maximum altitude of 1,950 m, compared with 1,750 m for the northwestern block (fig. 57).

The southeastern extension of Ḥarrat ar Raḥāh, Ḥarrat 'Uwayriḍ, is comparable in extent to Ḥarrat ar Raḥāh, rises to a reported height of 1,920 m (fig. 58), and is somewhat more deeply eroded. However, the region of Al Jaww, a depression partly separating the harrat, was the site of the most recent eruption in the lava plateau. A dome in the Tabuk Formation at the northwestern corner of this belt appears to be a volcanic diapir of Tertiary age that failed to reach the surface (Brown, Jackson, Bogue, and Elberg, 1963). Even though wind scour from sandblasting through the gap has cut lineations trending N. 45° E., the flows and cinder cones are little eroded. Indeed, an eruption at

FIGURE 57.—The ruptured crater at the crest of Ḥarrat al 'Uwayriḍ at an elevation of about 1,900 m above the Red Sea. A sample of hawaiite from the steeply westward dipping tuff gave an age of 7.4 m.y. (K-Ar whole rock). As the tuff came from a Holocene eruption at the eastern edge of the harrat, the sample may be an inclusion from a lower and older flow through which the explosion passed. View to the northwest.

FIGURE 58.—Basalt erosional front of Ḥarrat ar Raḥāh on the right above the Ram-Umm Sahm Sandstone bench. View from the base of Ḥaarrat al 'Uwayriḍ where the lower basalt flow of picrite-ankaramite gave a late Miocene age of 9.4±2.5 m.y. (K-Ar whole rock). A Holocene eruption formed silicic domes and necks on the skyline (Coleman and others, 1983). Boulders in the foreground compose one of the discontinous earlier Tertiary clastic outliers. The Ordovician Ram-Umm Sahm Sandstone forms white pinnacles in the middleground; the darker reddish Siq Sandstone below is probably Upper Cambrian age. View to the northwest.

Hallat al Badr on Jabal Thadra in Al Jaww was reported to have destroyed bedouin and their flocks in historic time (Musil, 1926). Likewise, the name "Ḥarrat an Nar" (the fire harrat) of ancient geographers was considered by Musil (1926) to be Ḥarrat ar Raḥāh-'Uwayriḍ, although the ancient reference may have been to Jibal al Abyaḍ in Ḥarrat Khaybar or to Jabal Ithnayn in Ḥarrat al Ithnayn, which likewise are surmounted by fresh cinder-ash cones of Holocene age.

Samples of basalt gave K-Ar whole-rock ages ranging from 26.7 to 7.4 m.y. (samples 7B and 7T, table 10, pl. 2), the oldest from 5 m above the base of Ḥarrat 'Uwayriḍ, above the bed of Wādī al Jizl. However, basal samples from northern Al 'Uwayriḍ and the southern tip gave ages of 9.4±2.5 (sample 6B) and 9.4±1.0 m.y. (sample 9B), respectively, a more likely age for the inception of volcanism. Samples taken from the highest flows gave ages of 7.8±1.0, 7.4±1.5, and 10.9±1.1 m.y. (samples 9T, 7T, and 6T, respectively). The last sample, however, came from lava out of a Holocene crater, and the age is obviously too great when analysis of a sample from the basal flow nearby yielded 9.4±2.5 m.y. (sample 6B). The deeply eroded lower flows are possibly late Miocene, ranging in age from 9.4 to 7.5 m.y. (table 10). The younger flows (not dated) in Ḥarrat ar Raḥāh came from eruptions after the present drainage system was established, altering the older incised meanders to form more recent flood channels, suggesting a middle to late Pleistocene age. Thus the latest eruptions are undoubtedly Holocene.

Estimation of age from the erosion rate of the basalt is difficult because of climatic change, and also because of the erosive differences of sandblasting by wind and erosion by water, especially where there is a wide range of rock-fragment size in bed load. Doughty (1888, p. 419, v. 1) described conditions in Ḥarrat 'Uwayriḍ thus:

> Viewing the great thickness of lava floods, we can image the very old beginning of the Harra—those streams upon streams of basalt, which appear in the walls of some wady-breaches of the desolate Aueyrid. Seeing the hillian are no greater, we may suppose that many of them (as the Averine Monte Nuovo) are the slags and the powder cast up in one strong eruption. The earlier over-streaming lavas are older than the configuration which is now of the land: – We are in an amazement, in a rainless country, to see the lava-basalt pan of the Harra, cleft and opened to a depth of a hundred fathoms to some valley-grounds as Thirba. Every mass is worn in grooves in the infirmer parts by aught that moves upon it; but what is this great outwearing of "stones of iron," indomitable and almost indestructible matter. We see in the cliff-inscriptions at Medain, that the thickness of your nail is not wasted from a face of soft sandstone, under this climate, in nearly 2,000 years.

Doughty's observations are accurate where the inscriptions on the sandstone tomb at Madā' in Ṣāliḥ are a few meters above land surface, but where the facades bearing dated Nabatean inscriptions are exposed to the wind near land surface, sandblasting and spalling has undercut as much as a meter into the lower 1 or 2 m of

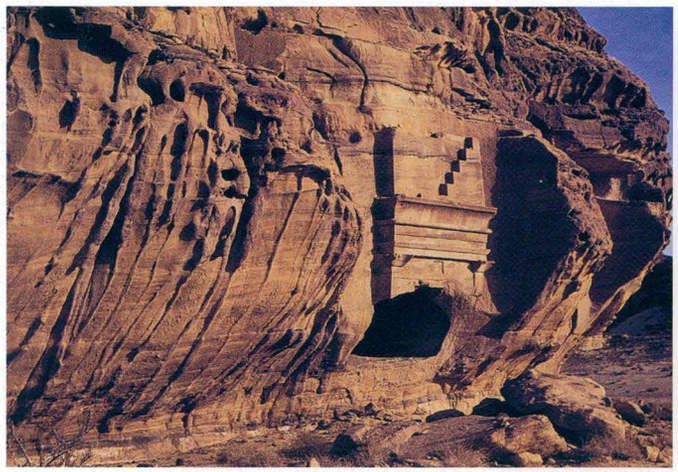

FIGURE 59.—Eolian undercutting of Ram-Umm Sahm Sandstone at a Nabatean tomb (65 A.D.) at Madā'in Ṣālih showing 1 m of wind-sand scour and spalling during two millennia.

FIGURE 60.—The Holocene crater of white rhyolite tuff and lapilli of Abyaḍ wa Ubayyid in Ḥarrat Khaybar. The crater is 1.6 km wide, and the cone of rhyolite and pumice breccia in the center is 300×500 m across.

the face during the last 2,000 years (fig. 59) (Brown, 1960). This amounts to 500 m/m.y. As sandstone underlies the lavas all along the western front of Ḥarrat ar Raḥāh-'Uwayriḍ, a timespan of 9 m.y. (the K-Ar age of the earliest volcanic eruption) would allow a scarp retreat of 4.5 km under present climatic conditions. If this process functioned alone, the lava cliffs should stand directly above the sandstone face, spalling off as the sandstone face retreated. Instead, we see the lava removed ahead of the sandstone, all indented by a dendritic drainage pattern among isolated sandstone buttes, then sandstone buttes capped with basalt, and finally, in the headwaters, the basalt front along the toe of the mountain face above a sandstone bench (fig. 58). Evidently insolation and the wide diurnal temperature range cause the lava to fracture so that most exposures are great piles of boulders often faceted into windkanter from sandblast. The boulders and cobbles are removed down the slopes by gravity, especially during the occasional desert rainstorms, to form the present terrain. Isolated lava-capped buttes suggest that the harrat scarp has receded as much as 5 km during the desert erosion cycle. As this rate must be more rapid than that of the present-day desert cycle, a late Miocene age for the oldest flows would be maximum.

The lavas we sampled from the base and top of the volcanic pile of Ḥarrat 'Uwayriḍ are alkali-olivine basalts falling within the hawaiite field on the plagioclase-color index normative diagram (fig. 54); they contain phenocrysts of forsteritic olivine, some zoned toward fayalite rims, clinopyroxene, and opaque oxides, as well as some interstitial calcite and chlorite (Salman Bloch, written commun., 1976). Sample 7B (table 10) is unusually rich in olivine phenocrysts, as is the youngest flow at the crater crest near the center of the harrat where the olivine is glomeroporphyritic and zoned; some phenocrysts of fayalite are rimmed with iron oxides, and rare picotite is rimmed with opaque ore minerals. Amygdules contain calcite and stilbite.

ḤARRAT KHAYBAR

Ḥarrat Khaybar, the adjoining Ḥarrat al Ithnayn (Hutaym) on the northeast, and the southwestern extension, known locally as Ḥarrat al Kurā', together form the largest plateau-basalt field in Saudi Arabia, although it is only slightly larger than Ḥarrat Rahaṭ between Al Madīnah and Makkah. Ḥarrat Khaybar extends from long 38°30' E. to long 40°46' E. and from near Al Madīnah at lat 24°39' N. to lat 26°11' N. The Ḥarrat al Ithnayn segment extends an additional 75 km north and as much as 85 km farther east. The basalt plateau rises from an altitude of 475 m at the crystalline basement along Wādī al Ḥamḍ to 2,015 m in Jabal al Abyaḍ in the center of the pile 115 km to the east. Boreholes have proven basalt thicknesses of more than 500 m (Delfour and Dhellemmes, 1980).

The older flows cover the western part, extending at least as far as the Al Madīnah–Khaybar road; K-Ar ages normalized to the Sydney constants range from 11.5±2.3 to 7.5±0.8 m.y. (samples 12 and 10, table 10, pl. 2) for the part of the harrat called Al Kurā'. The age of the base of a flow at the south edge of the Khaybar oasis is 9.3±0.7 m.y. (sample 20, table 10). Thus the timespan for the Ḥarrat al Kurā' flows is similar to that for the lower flows of the Ḥarrat 'Uwayriḍ. The degree of erosion appears similar, and there is some evidence that the lavas flowed westward prior to the

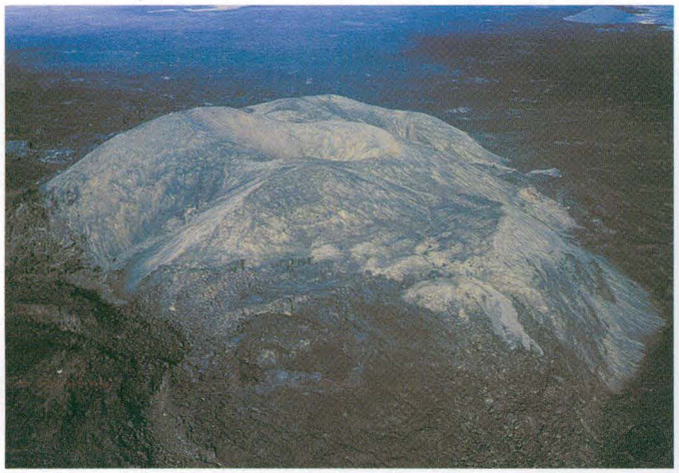

FIGURE 61.—The tholoid of Jabal Ithnayn, Ḥarrat al Ithnayn.

FIGURE 62.—The crater of Jabal Hibran, Ḥarrat al Ithnayn.

elevation and tilting of the Red Sea flank. The basalt outlier west of the elbow of capture of Wādī al Jizl at the junction with Wādī al Ḥamḍ suggests, but does not prove, that the lava streamed down the ancestral Wādī al Jizl valley to the northwest. All more recent flows constituting the eastern half of Khaybar and Ḥarrat al Ithnayn (Hutaym) flowed radially from volcanic centers, but the general trend during the Quaternary is southeastward down wadis into the Wādī ar Rimah drainage (alkali basalt, 1.1±1.0 m.y., Jabal al Khuraym, sample 22, table 10, pl. 2), most recent volcanic activity being within historical time.

The older lavas are alkali-olivine basalt, where sampled. Sample 12 (table 10, 11.5±2.3 m.y., K-Ar) at the western base may be considered a basanite from the normative analysis which disclosed an exceptionally low content of silica (table 9). Sample 10, from an outlier northwest of Ḥarrat Khaybar in the Qal'at aṣ Ṣawrah quadrangle, falls within the basanite or hawaiite field. Similar lavas in the lower part of Ḥarrat Khaybar and around and near Abyaḍ wa Ubayyid (fig. 60) are reported to be largely hawaiite but also to include such minor rock types as nephelinite, trachybasalt, trachyandesite, phonolite, trachyte, and rhyolite (Baker and others, 1973). The more alkalic flows are generally the youngest, and at Abyaḍ wa Ubayyid (the "white mountain") peralkaline rhyolite and rhyolitic crystal tuff is concurrent with or slightly older than the youngest alkali basalts. The peralkaline rocks of Abyaḍ wa Ubayyid are unique among the great bulk of the Tertiary and Quaternary alkaline basaltic volcanic rocks on and near the Arabian Shield in Saudi Arabia, although the latest eruptions in all the harrats are ash cinder cones, generally indicating a more silicious termination. Recently, the chemical variation from basanite to peralkaline rhyolite has been confirmed (Delfour and Dhellemmes, 1980)

Ḥarrat al Ithnayn (Hutaym), the northeast extension of Ḥarrat Khaybar, is made up of rocks similar to the volcanic deposits around Abyaḍ wa Ubayyid. The largest volcanic cone, Jabal Ithnayn (fig. 61), on the meridian of the north-south line of cones through Abyaḍ wa Ubayyid and 22 km north, is a gray, dome-shaped cinder cone or tholoid surmounting a black Holocene basalt flow at an altitude of 1,416 m. Recent volcanic activity was suggested to Doughty (1888) in 1883 by bedouin who described a warm, smoking vapor around the crest after winter rains. Numerous other cones of cinder, ash, and agglomeratic and scoriacious flows trend northwesterly parallel to Al Ḥarrah at Wādī as Sirḥān and to a northwesterly extension of the Najd fault system (Brown, 1972). Jabal Hibran, the largest crater in Ḥarrat al Ithnayn, is composed of layered ash, scoria, and bombs of welded trachyte or rhyolite (fig. 62).

ḤARRAT LUNAYYIR

Ḥarrat Lunayyir (lat 25° N.), on the lower slopes of the scarp mountains north of Yanbu' al Baḥr, was formed during two principal volcanic episodes during Pleistocene, including possibly late Pliocene and Holocene, time and has been mapped by Kemp (1981) and Pellaton (1982). Recent seismic studies in the Yanbu' region yielded microseismicity with epicenters clustered in the Ḥarrat Lunayyir area (Merghelani and Irvine, 1981). The lava fields lie mostly at 1,000 m above the Red Sea, but flows spread down wadi channels in

every direction, reaching the Red Sea at two places. Although parts are covered with alluvium on the coastal plain, the coastal lava overlies Pleistocene terraces, and individual flows are both younger and older than coralline benches on the coast (Bigot, 1975). The more than 50 vents whence came the flows lie as much as 60 or more kilometers inland where the harrat overlies Precambrian crystalline rocks. The K-Ar age of 6.2±0.8 m.y. determined for sample 15 (table 10) is undoubtedly too old, as the sample came from the most recent flow, a black lava of the younger volcanic episodes. Samples 14 and 16 (table 10), also from the most recent eruptions, contain insufficient radiogenic argon to measure, which indicates a young age in keeping with the physiographic evidence. Kemp (1981) has divided the younger volcanic episode into five eruptions; the last possibly took place in the 10th century or earlier (von Wissman, 1963). Sample 16 comes from a small isolated eruption at Jabal Salajah (pl. 2) which terminated with an only slightly eroded cinder ash cone 20 km south of Ḥarrat Lunayyir. The same volcanism continued intermittently farther south to near Yanbu' al Baḥr and is also too young to measure by K-Ar methods (sample 19, table 10).

A series of small, very recent, perhaps historical, flows and cinder cones are widely scattered from Ḥarrat Lunayyir (lat 25° N.) to Ḥarrat al Birk (lat 18° N.) along the coastal plain and in the foothills and are apparently contemporaneous or penecontemporaneous with the scores of cinder and ash cones above the source fissures of the larger flood-basalt harrats. The young flows are black and scoriaceous, in contrast to the reddish-brown and gray weathered older flows. Chemically, the Holocene flows are all alkali-olivine basalts where sampled (sample 14, tables 9, 10, 11, approaches hawaiite from the normative andesine). Some of the scoriaceous and vesicular flows contain secondary calcite; ophitic to subophitic textures are formed by phenocrysts of olivine and labradorite in a groundmass of clinopyroxene, labradorite, olivine, and opaque iron-bearing minerals. Inclusions of the underlying crystalline shield rocks and ultramafic xenoliths are fairly common.

ḤARRAT I'SHARA-KHIRSĀT AND ḤARRAT HARAIRAH

Remnants of older flows cap ridges along the flanks of Wādī al Ḥamḍ and Wādī al Jizl northwest of Al Madīnah. The mesas and buttes range in thickness from 5 m to more than 400 m, and K-Ar ages range from 21.2±2.1 and 62.6±4.3 m.y. (samples 17, 18, and 23, table 10). These ages contrast with 7.7±0.7 and 11.1±0.8 m.y. (Baubron and others, 1976, reported in Pellaton, 1979), the latter being coeval with the oldest flows of Ḥarrat Raḥaṭ, which extends south of Al Madīnah. The oldest sample came from the uppermost of three flows west of Jabal al Bayḍa', 35 km northwest of Al Madīnah, where olivine basalt contains zoned xenocrysts of forsterite rimmed by fayalite in a groundmass of plagioclase (An_{60}), clinopyroxene, and accessory opaques. The content of calcite is high in amygdules and in the groundmass (Salman Bloch, written commun., 1976). The normative values of sample 23 are similar to those of the lower flows of Ḥarrat Khaybar in being especially low in silica (43.2 percent). As the generally accepted K-Ar age for the oldest flows of the shield is about 30 m.y., the 62.6-m.y. age seems excessive, especially in light of the fact that the lavas forming butte tops at Al Jarf 50 km northwest gave ages of 21.2±2.1 and 28.3±2.9 m.y. (samples 17 and 18, table 10) and are comparable in age to lavas at Ḥarrat Ḥaḍan and Jabal as Sirāt farther south. The 28.3-m.y. age is from the basal flow of hydrothermally altered basalt containing olivine that is partially altered to bowlingite, and the clinopyroxene is partially changed to chlorite and calcite; the labradorite is unaltered (Salman Bloch, written commun., 1976). The 21.2-m.y. age is from the topmost 15 m flow, which is 12 or more flows above the lower sample; it is typical alkali-olivine basalt. The deeply eroded basalt pile at Ḥarrat I'shara-Khirsāt is 820 m thick (some of this thickness may be attributed to fault repetition) and rests locally on flat-lying varvelike silt and fine sand of lacustrine or deltaic origin. Farther northwest at Ḥarrat Harairah, a conglomerate bed above the basement and below the lowermost flow contains chert boulders with casts of Eocene fossils (Brown, 1970). However, the fossiliferous boulders were not seen at the northernmost outcrop of the harrat at the head of Wādī Tharīb (ash Schism). There, a small mesa rises above 1,500 m at the crest of the peninsular divide where 12 flows aggregate about 200 m of amygdaloidal and olivine-rich basalt. Two beds of gravel are interbedded in the flows above the basal gravel, which overlies Precambrian basement.

The occurrence of post-Eocene gravel and conglomerate (similar to that shown in fig. 49), the retilting flow direction, and the extensive erosion suggest that Ḥarrat I'shara-Khirsāt and Ḥarrat Harairah are at least as old as Ḥarrat 'Uwayriḍ northward and possibly are coeval with Ḥarrat Ḥaḍan and As Sirāt southward (Coleman and others, 1983). Indeed, the general sequence of picrite-ankaramite below peridotite-nodule-bearing olivine basalt and overlying diktytaxitic alkali-olivine basalt is common to widespread outcrops (Coleman and others, 1983), suggesting a general correlation for the older volcanism. Most evidence points to two general eruptive episodes, late Oligocene-early Miocene (29–20 m.y.) and middle to late Miocene (10–7 m.y. timespans).

ḤARRAT KURAMĀ'

This relatively small harrat, which lies directly south of Ḥarrat Khaybar and due east of the north end of Ḥarrat Rahaṭ at Al Madīnah, is also known as Ḥarrat Hirmah (Pellaton, 1981). The area drains west through Wādī Shaqrah and its tributaries, terminating at the Qā' Ḥazawẓā', which is a sabkhah formed by the lava dam of Ḥarrat Rahaṭ. The wadi nearly divides the harrat into two lobes, the westernmost part apparently the older and the only part sampled. An eroded and cratered cone rises 90 m above the harrat surface near the northwestern edge of the lobe and is the source of the surrounding flows. The scoriaceous and subophitic olivine basalt (sample 24, table 9) contains amygdules of calcite; the olivine is not zoned, in contrast to other samples, but some grains are altered to iddingsite (Salman Bloch, written commun., 1976). The K-Ar analysis yielded an early Miocene age of 20.0±2.0 m.y. (sample 24, table 10), which may be excessive. However, the weathering of the basalt and the well-developed drainage on a general southwesterly sloping surface suggests preramping flowage into the ancestral Wādī al Ḥamḍ valley and an eruptive epoch older than that of adjoining, much larger olivine-basalt floods.

The harrat lobe east of Wādī Shaqrah is marked by hummocks forming irregular lineaments similar to those in the southern portion of Al Ḥarrah near the Jordan frontier. They were evidently formed by younger, very fluid flows. The eruption came from a crest of 960 m in the central part of the harrat, the highest part surrounding the collapsed Hirma crater in the west-central part. The crater is 6x4 km in area and has vertical walls at least 25 m in height. Although the crater floor is a saline silt plain and the lower walls are sandstone, similar to the Siq Sandstone exposed southeast of the harrat, the entire thickness of the basalt flows is exposed.

ḤARRAT RAHAṬ

Ḥarrat Rahaṭ extends from Al Madīnah at lat 24°30' N. to Wādī Fāṭimah north of Makkah (lat 21°40' N.), a distance of 310 km. Ḥarrat Rahaṭ has an average width of 60 km. The basalt has filled the upper valley of Wādī al Ḥamḍ, whose ancestral thalweg probably extended from the headwaters of Wādī Fāṭimah northward to Al Madīnah, thence beyond to Wādī al Jizl where the present channel sought a more direct course to the Red Sea through a narrow gap in the foothills at lat 26° N. The harrat surface rises southward from 650 m above the Red Sea at Al Madīnah to a maximum altitude of 1,640 m at lat 23° N., decreasing somewhat in the southern part, where the crest is 1,570 m. The high points are linear clusters of cinder and ash cones (many breached) or Holocene domes and represent four centers of late volcanicity, so Ḥarrat Rahaṭ is actually four coalescing harrats: Ḥarrat Madīnah, which is essentially contiguous with Ḥarrat abu Rashid to the south; Ḥarrat Bani Abdullah still farther south; Ḥarrat Turrah, which includes the crest; and Ḥarrat ar Rukhā', the southernmost. The cone and dome eruptions occur as segments of the north-south volcanic central linear ridge that continues northward en echelon across Ḥarrat Khaybar and probably represent fissure (fault) control (Brown, Jackson, Bogue, and MacLean, 1963). The youngest peaks are near Al Madīnah, where the latest flow erupted in A.D. 1256 (Doughty, 1888, v. 1, p. 593). Numerous cones in the segment some 75 km south, Ḥarrat abu Rashid, likewise have young black flows, mostly aa-type and similar to Ḥarrat Madīnah flows, with somewhat scattered eruptive centers trending N. 20° W. compared with a trend of N. 10° W. for Ḥarrat Bani Abdullah. Many of the black scoriaceous flows erupted after a late period of more siliceous cinder and ash eruptions, a sequence similar to that at Abyaḍ wa Ubayyid in the Ḥarrat Khaybar (Pellaton, 1981). Another segment of medial cones and craters was erupted on the older flows of Ḥarrat Turrah, with the eruptive centers trending N. 08° W., very similar to the trend of Ḥarrat ar Rukhā'. The weathering and fracturing of the blocky basalt and the accumulation of ventifacts developed an extremely rough terrain. Lava flowed centrifugally from each center, abutted flows from adjoining centers, and then flowed either east or west onto the flanks of the ancestral Ḥamḍ valley. On the west, numerous lavas from the three southernmost harrats flowed through passes in the scarp mountains and down the broad wadis draining the westward front of the Hejaz Scarp. The fluid basalt streams then flowed out onto the coastal plain; most of the flows lie on a pediplain that was about 75 m above the present surface (Brown, Jackson, Bogue, and MacLean, 1963). Ḥarrat Rahaṭ has been drilled at numerous places for water supply, notably south of Al Madīnah and along its northeast border. A thickness of 70 m was drilled at Dhumariyah, 85 km southeast of Al Madīnah near the north edge of Ḥarrat abu Rashid, where three lower flows are separated by white marl (Durozoy, 1972). Most flows are only a few meters thick. The decrease of maximum altitude toward the southern edge of the harrat suggests that the younger flows total at least 170 m in thickness, assuming that the ancestral Wādī al Ḥamḍ valley slopes uniformly northward.

The drilling at Dhumariyah (Durozoy, 1972) penetrated a carbonaceous marl overlying basement rocks. Red marl, sand, and gravel overlie the basal marl and underlie the basal lava. The carbonaceous marl contains a microflora of probable Oligocene age which may, however, correlate with the uppermost nonmarine and carbonaceous sediments of the Shumaysi Formation

west of Makkah. There, basalt flows or sills overlying the Shumaysi are dated at 25.9±3.0 and 32.6±2 m.y. from bore samples (samples 35 and 39, table 10) and 20.1±0.7 m.y. from a basalt outcrop (Coleman and others, 1979). The Shumaysi Formation contains freshwater fossils of Eocene and Oligocene age, the middle and lower carbonaceous beds containing Eocene spores below an upper and meager Oligocene fauna (Al-Shanti, 1966; Moltzer and Binda, 1981). Another surface sample from Ḥaddat ash Shām, west of the southern Ḥarrat Raḥaṭ, gave an age of 25.8±5.0 m.y. (sample 36, table 10). This basalt overlies sediments containing early Tertiary, apparently Eocene, marine foraminifera. The sediments are locally capped by a laterite zone under the basalt. Thus, it appears that the earliest lavas adjacent to and possibly underlying westernmost Ḥarrat Raḥaṭ lavas are near Oligocene in age and belong to the continental rift volcanism prior to uplift. Indeed, two K-Ar whole-rock ages from the lowermost of the upper lava streams overflowing the scarp divide, and thus representing upper flows of Ḥarrat Raḥaṭ, are 12.6±2.5 and 13.2±1.5 m.y. (samples 27 and 28, table 10), or middle Miocene in age. Younger flows at Khulayṣ and at the harrat north of Sharm Abḥur 40 km north of Jiddah (samples 30 and 32, table 10), dated at 4.4±0.4 and 4.2±0.8 m.y., are remnants of tongues that spilled over the rising Hejaz Escarpment from the upper Ḥamḍ valley.

All analyzed lavas are normative alkali basalt, including the sample from locality 37 (table 9) at Ḥarrat Biss ('Ushayrah), which is separated from but near the southeast corner of Ḥarrat ar Rukhā' and which yielded an age of 8.7±2.0 m.y. (table 10). However, flow rock from locality 38, a small lava field at Jabal al Barz, 35 km southeast of 'Ushayrah, gave a coeval age of 8.0±0.5 m.y. (table 10) and an analysis of 6.83 percent K_2O+Na_2O and 10.24 percent normative nepheline (table 9) composition of greatly increased alkali that trends toward the nearby and older Jabal 'Ān compound plug (sample 40, pl. 2), which is hornblende latite-phonolite. Sample 33, from lava overlying the early Tertiary Usfan sediments in the Usfan graben north of Jiddah, contains 5.12 percent K_2O+Na_2O and 8.56 normative nepheline (table 9). The K-Ar age is 19.1±0.6 m.y. (table 10). The youngest flows in Ḥarrat Raḥaṭ are alkali-olivine basalt which erupted soon after a late episode producing sodic lavas ranging from soda mugearite to phonolite (C.L. Smith, 1980; Kemp and others, 1982; J.W. Smith, 1982).

ḤARRAT AL KISHB

Ḥarrat al Kishb lies east of the southern part of Ḥarrat Raḥaṭ. It appears to be Pleistocene and Holocene, but its radiogenic argon content was insufficient to measure age except for sample 29, from a 3-m basal flow at the south edge of the harrat that gave an age of 2.4±0.8 m.y. (table 10). A partial chemical analysis shows it to fall within the basanite field on the alkali-silica diagram, but many of the white lavas in this harrat are tholoids (domes) and doubtless are trachytic or dark rhyolitic. The earlier flows are dark gray, and more recent flows are vitreous. More than 150 cinder and scoriae cones (many breached with small lava flows) and tholoids rise above the lava field (fig. 63). A remarkable phreatic explosion caldera or crater, Al Wahbah, is 2 km wide and 270 m deep midway along the western margin of the harrat (fig. 64).

The walls are Precambrian granitoid, and the crater is rimmed with ash and other ejecta formed by a phreatic explosion. A more recent basalt flows around the ash rim. Ultramafic xenoliths, mostly dunitic, are scattered through the ash. On the harrat the cones and craters (fig. 63) often lie along lines following sublava fissures. The most prominent in the northwestern quadrant of the harrat trends N. 15° W., about parallel to similar lines of cones on Ḥarrat Raḥaṭ.

ḤARRAT AL HUTAYMAH

Craters similar to Al Wahbah are scattered on crystalline rocks east of Jabal Salmá in the Ḥarrat al Hutaymah at the extreme northeast corner of the shield and, like Al Wahbah, expose crystalline basement rocks in the shattered walls of craters rimmed by ejecta and volcanic ash. One at Jabal Humayyan is 1.25 km wide and 110 m deep (Bramkamp, Ramirez, and others, 1963). According to J. Mytton (USGS, written commun., 1964), lava flows are of the pahoehoe type at Al Jubb (Na'ai), a village in a collapsed cone, that lies within the crags of Jabal Salmá. The ash at many craters contains large pyroxene-rich crystals and inclusions from the underlying Precambrian rocks. The chemical analysis of a 12-m-thick flow above 40 m of volcanic ash at Jabal Humayyan is that of an alkaline basalt approaching basanite (sample 25, table 9).

ḤARRAT ḤAḌAN

Ḥarrat Ḥaḍan lies on the plain east of Aṭ Ṭā'if and south of Ḥarrat al Kishb. The alkali-olivine basalt rests on a laterite above the Paleocene sedimentary rocks of the Umm Himar Formation. The Hadan section, gently dipping eastward and about 150 m thick, consists of a lower part of basalt flows, a middle part as much as 17 m thick of white, bedded, tufalike limestone with thin interlayers of basalt (D.G. Hadley, USGS, written commun., 1977), and an upper part of basalt flows. The flows are deeply weathered to saprolite and are deeply

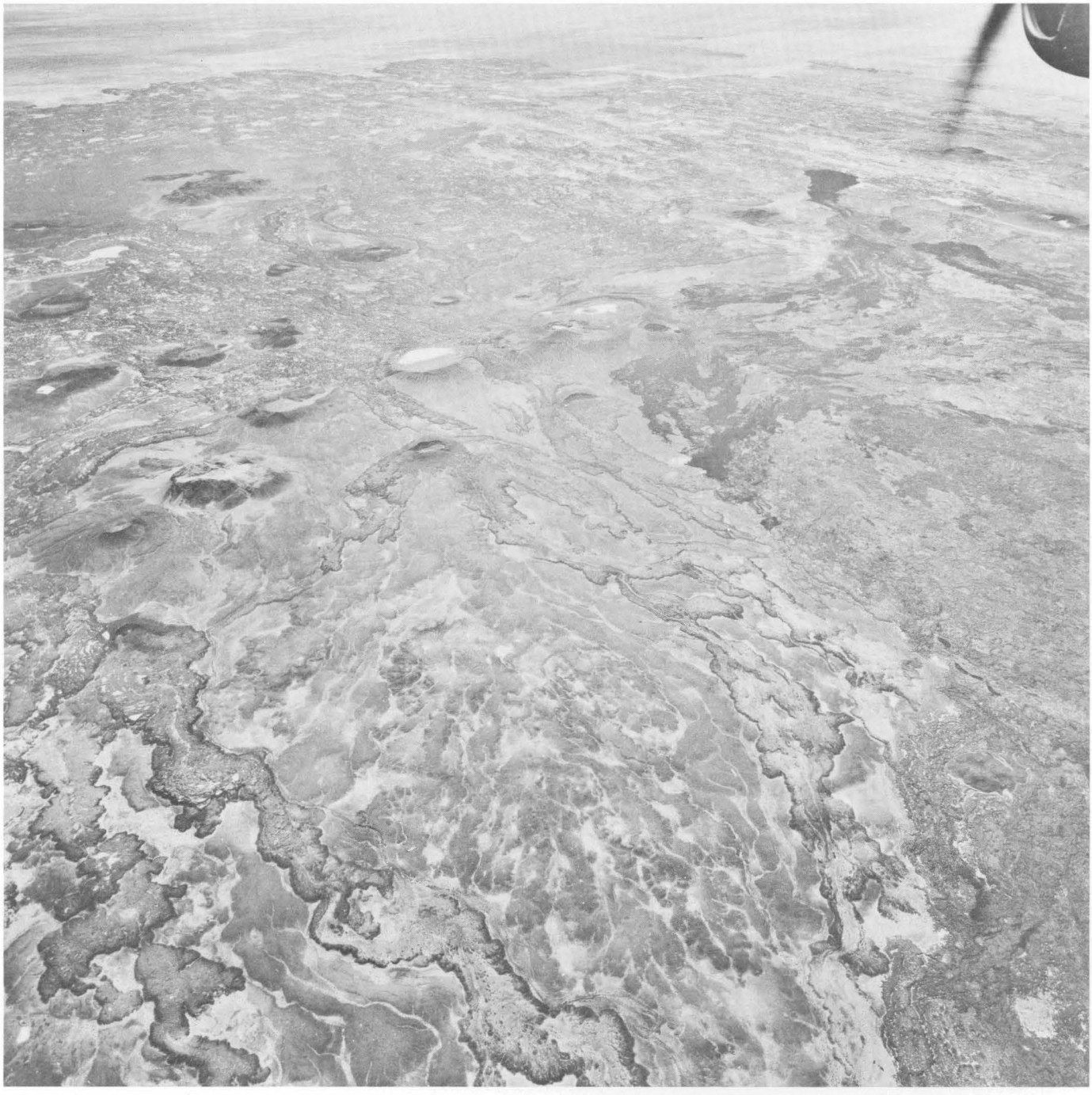

FIGURE 63.—Oblique aerial view east-northeast of Ḥarrat al Kishb. Early flows were toward the basement peneplain to the east and northeast owing to ramping from Red Sea rifting. Jabal ash Sauwahah in middle distance centers Holocene centrifugal lava streams resulting from the buildup of older eruptions, creating slopes opposing the regional ramp. Note meridional linearity of the Holocene craters and tholoids.

eroded. Physiographically, Ḫarrat Ḥaḍan resembles the As Sirāt harrat (Madden and others, 1980), Ḫarrat I'shara-Khirsāt, and Ḫarrat Harairah. It should be of comparable age.

The lava sampled from the upper flows in the southwestern part of the harrat were dated at 16.6±1.5 and 16.2±1.8 m.y. (samples 41 and 43, table 10). Two flows sampled more recently from basal flows of the

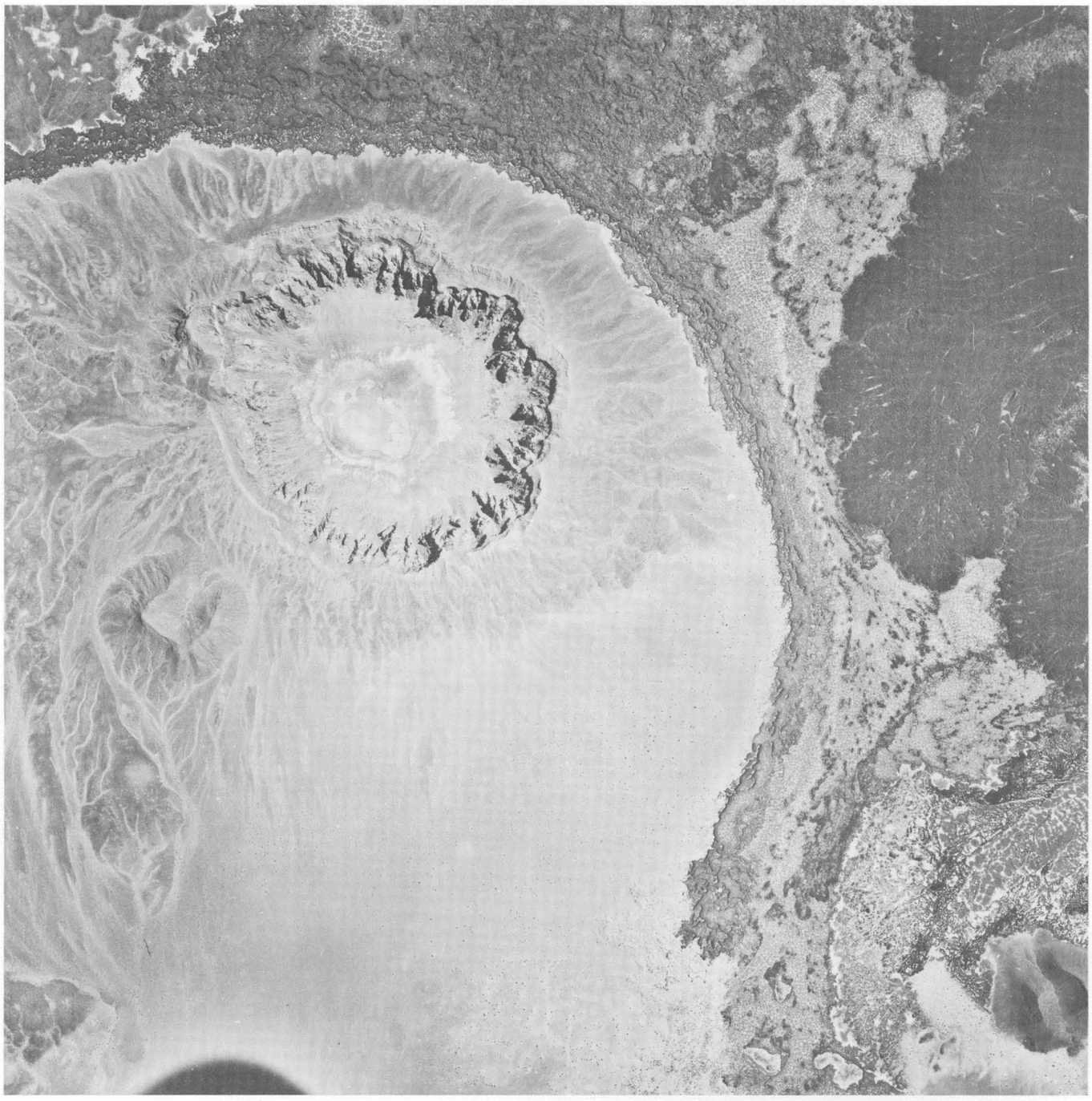

FIGURE 64.—Al Wahbah phreatic crater from a Holocene eruption at the northwestern corner of Ḥarrat al Kishb. The crater is 2 km wide and 270 m deep and is blasted out of basement crystalline rocks. Vertical aerial photograph. North is to the left.

harrat by Arno and others (1980b) gave K-Ar whole-rock ages of 27.8±1.4 and 26.6±1.3 m.y., which are well within the age range of the other late Oligocene-early Miocene harrats of the shield. One uppermost exposed flow gave an age of 3.4±0.5 m.y. (sample 42, table 10) but is probably too young according to the geomorphology. The chemical analyses of the three dated samples of the upper flows are similar and lie within the basanite field on the alkali-silica diagram (Cox and others, 1979).

The flows in part erupted from feeder pipes now exposed as isolated hills on the plain along the western,

southern, and northern edges of the harrat; however, other isolated hills are lava-capped outliers. One of the isolated outlying hills, Jabal 'Ān southwest of Ḥarrat Ḥaḍan, consists of a localized dike set or complex volcanic neck composed of a core of trachyte or hornblende latite and a chilled phonolitic rim (sample 40, table 9) that has a K-Ar whole-rock age of 22.2±3.5 m.y. (sample 40, table 10). By composition and age, the Jabal 'Ān neck is similar to, though somewhat more evolved than, the syenite-trachyte stock of the As Sirāt harrat (sample 75, pl. 2).

ḤARRAT NAWĀṢĪF-AL BUQŪM

The flood basalts of the large Ḥarrat Nawāṣīf-al Buqūm extend in a northeasterly direction southeast of Ḥarrat Ḥaḍan and form the fourth largest lava-covered region in western Saudi Arabia. The combined harrats form a remarkably uniform and youthful-appearing, nearly flat lava dome with tongues of basalt radiating outward from its edges. The relatively higher flattish central part is dotted with many Holocene scoria cones and ash rings that trend N. 20° E. on a belt averaging 20 km wide. One flow tongue 2 to 4 km wide extends 40 km eastward beyond the edge of the harrat down Wādī Ranyah valley to Ranyah. At Ranyah this deeply weathered, mostly saprolitic basalt gave a K-Ar whole-rock age of 3.5±0.3 m.y., whereas a shorter tongue of less weathered basalt 30 km west-northwest of Ranyah gave an age of 1.1±0.3 m.y. (Hotzl and others, 1979). A sample of the lowest exposed basalt in the Wādī Ranyah canyon, 75 km southwest of Ranyah, yielded an age of 1.8±1.2 m.y. (sample 53, table 10). On the west edge of the harrat, a youthful basalt flowed about 65 km down the Wādī Turabah valley, mostly as a tongue only 1 km wide. A sample of this flow contained insufficient argon to measure (sample 44, table 10), whereas about 2 km away Arno and others (1980b) reported a sample probably from the same flow that give a K-Ar age of 2.7±0.4 m.y. A sample of the northernmost tongue is reported by Arno and others (1980) to have an age of 4.4±1.0 m.y.

Thus, the harrat is probably only about 5 m.y. old, although somewhat older flows may underlie its undissected central region. Arno and others (1980) reported three other ages from the harrat. One from a neck in basement in the southwestern part of the harrat gave an old K-Ar whole-rock age, 22.8±1.1 m.y.; either this hypabyssal rock contains excess argon or, more likely, it is an erosional outlying plug of Ḥarrat Ḥaḍan, as the collection site lies only 40 km southeast of Ḥarrat Ḥaḍan. Another sample reported from the neck of a youthful scoria cone in the northeastern part of the harrat gave an age of 15.8±0.8 m.y., which is too old and may be attributable to excess argon. The underlying flow nearby gave an age of 7.3±1.8 m.y., which also is much too old for its morphology.

One chemical analysis (sample 44, table 9) is that of an alkali-olivine basalt; Arno and others (1980b), using many analyses, found that the basalts are basanite and nepheline basanite.

ḤARRAT AD DAMM AND ḤARRAT TUFFIL (SHAMĀ)

From 70 to 105 km south of Jiddah, small lava flows overlie crystalline basement or Tertiary rhyolite on the coastal plain and the foothills of the scarp mountains. Ḥarrat ad Damm, the oldest flow, consists of elongate erosional remnants sloping seaward on the crystalline foothills about 110 m above the modern wadi channels. A sample from the northwesternmost remnant gave an age of 7.0±4.3 m.y. by K-Ar whole-rock analysis (sample 47, table 10), an age comparable to ages from the upper lavas of Ḥarrat 'Uwayriḍ and the erosional remnant west of Ḥarrat Khaybar in the Qal'at as Şawrah quadrangle. Ḥarrat Tuffil (Shamā) flowed out on a younger ancestral coastal pediplain similar to the harrat at Yanbu' al Baḥr and Al Birk. However, the Tuffil lava came from a single vent rising 100 m above the general altitude of the modern coastal plain. The dissected base of the lava lies about 50 m above the modern coastal plain and 15 to 20 km inland from the modern shoreline. Two samples (samples 49 and 50, table 10) gave ages of 2.9±0.2 and 2.8±0.1 m.y. by whole-rock K-Ar methods. This basalt overlies rhyolitic tuff of the Baid Formation along its west edge and Precambrian granite farther east. The sheared and brecciated tuff was considered to be Precambrian on USGS geologic map I–210A (Brown, Jackson, Bogue, and MacLean, 1963), but a sample from Jabal Abū Shidad, 30 km north of the harrat, gave a whole-rock K-Ar age of 19.3±0.9 m.y. (sample 45, table 10). This is an early Miocene age compatible with the age of the Baid Formation elsewhere along the southern coast. The tuff is somewhat younger than the leucocratic gabbro intrusive nearby (sample 46, table 9). Subsequent work has extended the Baid rhyolite south to beneath the western edge of Ḥarrat Tuffil (Laurent, 1976).

ḤARRAT AL BIRK

The lavas of Ḥarrat al Birk, also know as Ḥarrat Hayil or Hubhub al Sheikh, cover the coastal plain from lat 18°45′ to lat 17°45′ N. and separate the Tihāmat ash Shām from the Tihāmat 'Asīr. Volcanic activity appears to be limited to an extensive Quaternary outpouring of alkaline basalt culminating with abundant Holo-

cene cinder cones. Near Al Birk the older, bluish, olivine-rich basalt underlies a coquina bed which is 3 m above the sea; in turn, the coquina is overlain by 15–20 m of reddish-weathering basalt. Throughout Ḥarrat al Birk, four samples representative of lower or older flows (samples 55b, 59, 61, and 62, table 10) gave K-Ar whole-rock ages of between 12.4 and 4.3 m.y., and two samples representative of upper or younger flows (samples 57a and 57b) gave ages of 2.8 and 2.1 m.y., but certainly some of these latter flows are as young as late Quaternary, judging by their geomorphic form. On the basis of comparison with 12 independent samples collected recently from throughout the harrat, which range in age from 1.51±0.39 to 0.25±0.04 m.y. (Coleman and others, 1983), and 4 widely spaced samples, which range in age from 1.9±0.05 m.y. to too young to determine (Arno and others, 1980a), our early determinations seem too old by an order of magnitude.

The Quaternary cinder cones are abundantly dispersed throughout the harrat and represent late feeder pipes. Farther east of the Al Birk lava fields, at Jabal Bā'ā (Hadley, 1975c) and Jabal al Qishr (fig. 65), isolated patches of ash on the mountain slopes around a vent are freshly eroded and appear to represent an eruption during the last century. Elsewhere on the Tihāmat 'Asīr, both east of Ḥarrat al Birk and south on the Jizan coastal plain, separate volcanoes ejected ash as well as alkali-olivine basalt. These volcanoes also appear to be young, especially on the Tihāmat 'Asīr. Lava from the two volcanoes east of Ḥarrat al Birk, Jabal Baqarah and Jabal al Haylah, contain alkali-olivine basalt as well as hawaiite and the basanite variety of alkali-olivine basalt (samples 65 and 66, table 11; Coleman, Fleck, and others, 1977). Samples from the basal flows yielded ages of 5.1±1.5 m.y. (K-Ar whole-rock, samples 65 and 66, table 10), but later analysis of samples from Jabal al Haylah gave ages of 0.18±0.06 and 0.25±0.04 m.y. (Coleman and others, 1983). This is a more reasonable age, especially for the cone, which sits on a surface containing rolled Achulean axes in the valley of Wādī Tayyah (Overstreet, 1973). However, the basal flow that was originally sampled could be appreciably older than the youthful volcanic cone. Youthful volcanoes on the Jizan plain, Jibāl 'Akwatain and Jibāl Umm al Qummatain, have been dated by K-Ar whole-rock analyses at 0.31±0.32 and 0.53±0.08 m.y., and basalt flows in the foothills in Wādī Jīzān gave an age of 0.99±0.23 m.y. (another sample of basalt was too low in argon to yield a radiometric age) (Coleman and others, 1983).

A volcanic eruption occurred at Ḥarrat Gar'atain between Jibāl 'Akwatain and Jibāl Umm al Qummatain on the east side of the Jizan plain near the Yemen border early in the last century, according to Lamare

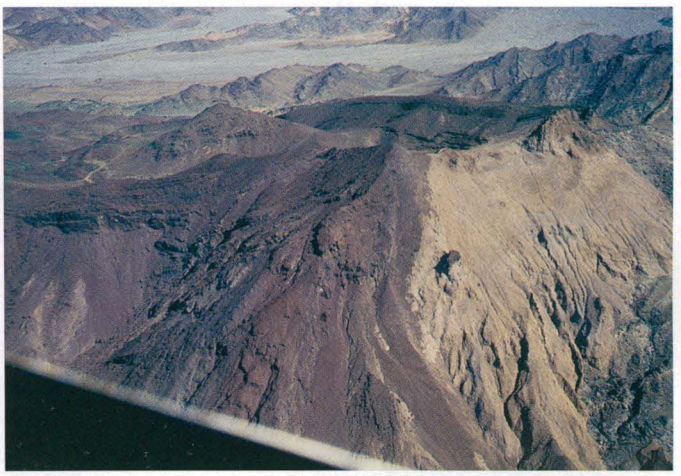

FIGURE 65.—Cinder-ash cone, Jabal al Qishr, an easternmost vent of Ḥarrat al Birk, probably a historical eruption. Lat 18°31′ N., long 41°48′ E.

(Neumann Van Padang, 1963; pl. 2). Much volcanic ash in the rich soils and alluvium of the eastern Jizan coastal plain attest to the accuracy of the report. Further, more tenuous evidence are several nearby extinct and active hot springs. The northern and larger of the Al Waghrah springs discharges 1 km east of the southernmost cinder cones of the harrat. It has a reported temperature of 56.6 °C, whereas an active spring 4 km distant measured 54.2 °C (Fairer, 1982). However, a higher temperature, 78 °C, is reported at 'Ayn Khulab, 30 km southeast near the Yemen border. Both Al Waghrah and 'Ayn Khulab are in or near the faults of the Red Sea rift and associated volcanism, as is 'Ayn al Ḥarrā, 450 km north near Al Līth, which has the highest reported temperature, 86 °C (Lopoukhine and Stieltjes, 1976). Other warm springs, as 'Ayn ad Damad, 40 km northeast of Al Waghrah (43 °C), and 'Ayn al Junah, 31 km southeast of 'Ayn al Ḥarrā (46 °C), may not have direct association with volcanism, the temperatures being somewhat elevated above the mean annual surface temperature because of deep circulation of meteoric water in the fractural Precambrian rocks exposed around the springs (Donald White, written commun., 1971; Lopoukhine and Stieltjes, 1976).

Ultramafic inclusions in the lavas at Al Birk, especially in the ejecta of the Quaternary cinder cones, consist of a mixture of harzburgite, websterite, and gabbro, which is in contrast to the composition of inclusions farther south in the Jizan coastal plain, where only harzburgite was found. The differences are attributed to magmatic penetration through a thick sialic crust in the Al Birk area, whereas the southern lava fields came

from pipes that penetrated a thinner oceanic crust (Gettings, 1977; Ghent and others, 1980). The older K-Ar ages of the Al Birk lavas could be attributed to excess argon derived from the underlying Precambrian crystalline rocks, which are argon-rich, or to the mafic inclusions in the younger ejecta.

JABAL AS SARĀT

The southernmost harrat on the 'Asīr highlands, Jabal as Sarāt, extends to the Yemen border (pl. 2). Jabal as Sarāt appears to be a northern remnant of the lower portion of the Yemen Volcanics (Trap Series), with ages from 30.1±1.0 m.y. in the lowermost flow to 25.3±0.5 m.y. in the uppermost flow (samples 67 and 69, table 10). Ages from the Yemen Trap Series (29.7±0.9 to 20.8±1 m.y) and the Northern Ethiopian Plateau volcanics at Adigrat (30.0±0.7 to 19.4±0.6 m.y.) all range in age from late Oligocene to early Miocene (Jones and Rex, 1974; Jones, 1976; Coleman, Fleck, and others, 1977; Civetta and others, 1978) (fig. 51). In addition to alkali-olivine basalt rocks, the Yemen volcanic rocks include hawaiite, mugearite, ignimbrite (rhyolite), andesite, trachyte porphyry, and tuff, whereas the As Sarat flows are picritic basalt at the base and grade up to alkali-olivine basalts (basanite) and to hawaiite. The 17 to 20 flows of Jabal as Sarāt total 580 m in thickness (Coleman, Fleck, and others, 1977), which is considerably less than half the maximum thickness of the Yemen Volcanics. Isolated feeder pipes of basalt and andesite crop out as far as 20 km east of the Sarāt harrat fields and as far as 70 km to the northwest at Jabal Qarn and Banī Thwar. These were isotopically dated at 24.7±2 and 25.4±2.7 m.y. ago (Coleman, Fleck, and others, 1977), whereas the Al Wārah syenite plug in the midst of the harrat gave an age of 22.5±0.7 m.y. (table 10, sample 68), the same isotopic age as the Jabal 'Ān stock near Ḥarrat Ḥaḍan, 410 km to the northwest.

CENOZOIC HISTORY AND EVOLUTION OF THE RED SEA

EARLY TERTIARY SETTING

Structural elements in the Red Sea area prior to development of the continental rift valley beginning in late Oligocene to early Miocene time are not evident. Early Tertiary events in the Red Sea region were presumably independent of later Red Sea evolution. Slight epeirogenic downwarping during Paleocene time resulted in a shallow marine sea extending from the Mediterranean through Egypt and Jordan south to the vicinity of Jiddah, where about 100 m of limestone and fine-grained sandstone were deposited as the Usfan Formation (Brown, 1970, p. 80, 81), and 200 km to the east in the vicinity of Ḥarrat Ḥaḍan, where more than 22 m of mudstone, shale, and limestone were deposited as the Umm Himar Formation (Madden and others, 1980). The last vestiges of this sea (arms of the dying Tethys Sea) probably lasted through middle Eocene time in northern Saudi Arabia (Kluyver and others, 1981) and are represented in the Jiddah area possibly by part of the Shumaysi Formation (Moltzer and Binda, 1981, p. 70). In North Yemen, more than 200 m of marine sandstone of the Paleocene Medj-zir Series was deposited (Geukens, 1966).

Cratonic stability during early Tertiary time is indicated by the thick lateritic soil (a kaolinite-ferruginous cap, from 1 to 2 m thick, underlain by from 20 to 30 m of saprolite; Overstreet and others, 1977, p. 6) that developed across the low-relief, low-altitude, crystalline rocks of the Precambrian Shield.

CONTINENTAL RIFT-VALLEY STAGE

Continental rifting along the proto-Red Sea began about 30 Ma (fig. 66) as a mantle plume rose beneath the Afar triple junction and fracturing and rifting progressively extended along three axes: the proto-Red Sea, the Gulf of Aden, and the East African Rift. The continental rift valley progressively developed until about 20 m.y. ago. The heat regime at and near the triple junction in Ethiopia, Somalia, and especially Yemen was much greater than farther north along the proto-Red Sea axis. Near the triple junction, abundant silicic and mafic volcanic rocks were deposited in a wide continental rift valley as well as inland from the rift. Farther north along the continental rift valley (the proto-Red Sea axis), the volume of volcanic rocks decreased, the rift narrowed, and silicic volcanism was restricted to within the rift. Silicic volcanism within the rift extended as far north as Jiddah, 1,100 km north-northwest of the triple junction. The distinct northward decrease in the size of the continental rift and in the intensity of volcanic activity seems directly related to a decreasing heat flow away from the triple junction and to the progressive northward development with time of mantle convection along the proto-Red Sea axis. North of Jiddah, volcanic rocks of the continental-rift-valley stage are limited to small remnants of basaltic flows that extended northward in the northwestern reaches of the Shumaysi and Wādī al Ḥamḍ-Jizl troughs. During the approximately 10 m.y. of the continental-rift-valley stage, both the mafic and silicic volcanic rocks seem to have evolved with time, that is, their K_2O content increased with decreasing age, as the heat flow increased beneath the rift valley.

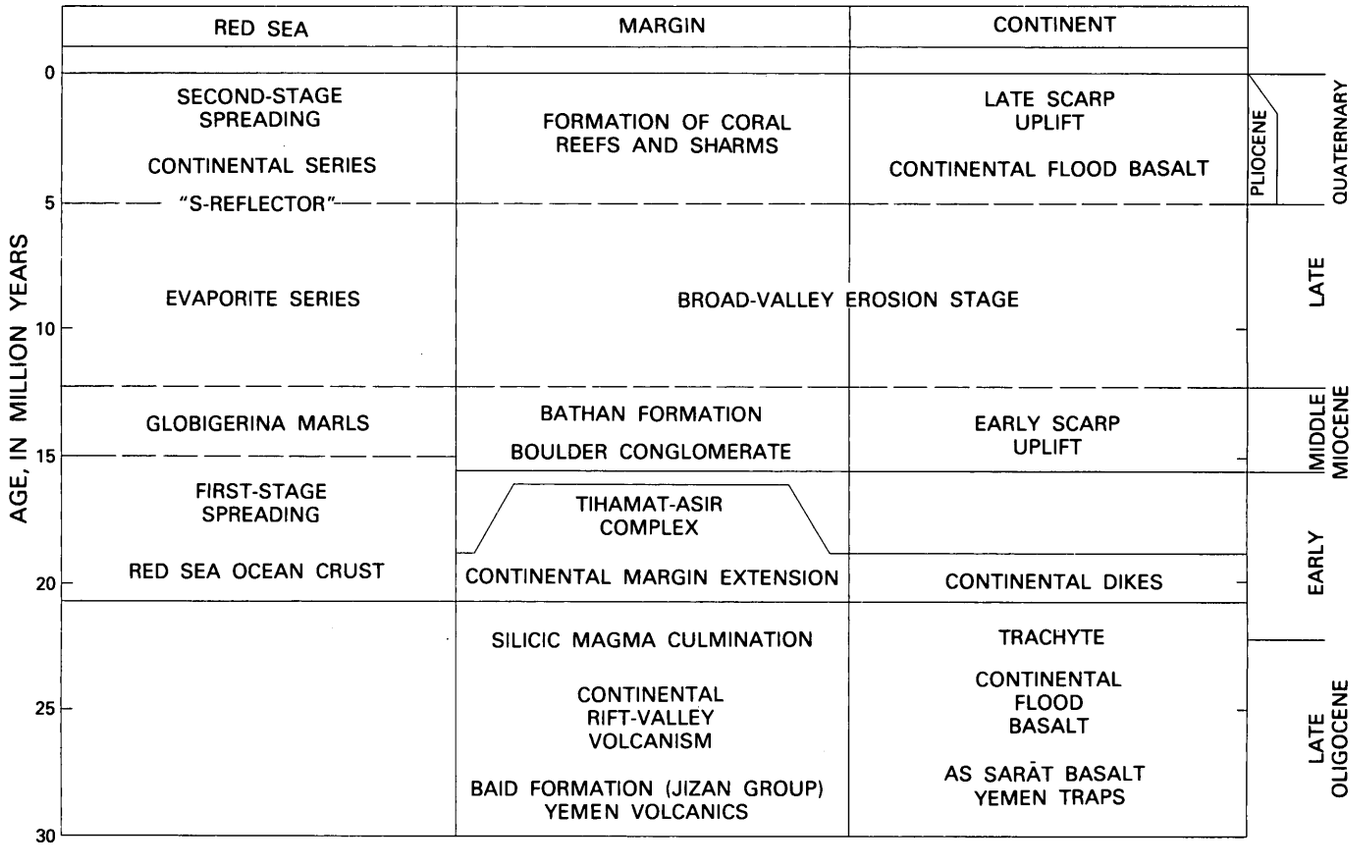

FIGURE 66.—Summary of the geologic history of the southern coastal plain area (continental margin) relative to that of the adjacent Red Sea and the adjacent continental area beginning with the formation of the continental rift valley through the present-day Red Sea. (After Schmidt and others, 1985.)

In southern Arabia, the oldest Tertiary volcanic rocks indicative of an active and rising mantle are dated at about 30 m.y. Inland from the Red Sea area, flows of alkali-olivine basalt are well preserved in the deeply eroded fields of As Sarāt (about 600 m thick, 100 km inland) and Ḥarrat Ḥaḍan (about 150 m thick, 200 km inland). In both places, early Tertiary lateritic deposits are well preserved beneath the basalt flows (Overstreet and others, 1977; Madden and others, 1980). The As Sarāt basalts and underlying laterite extend southward into the Yemen to the latitude of Sa'dah. South of Sa'dah, the volcanic pile, the Yemen Trap Series, is about 1,000 m thick and consists of peralkaline rhyolite (comendite and pantellerite), trachyte, trachyandesite, olivine basalt, and ankaramite (Shukri and Basta, 1955, p. 160). Laterite beneath the volcanic rocks south of Sa'dah has not been recorded, and its absence suggests some slight erosion that is represented by a few thin beds of Nubian-type sandstone reportedly at the base of or intercalated within the volcanic rocks. Some slight upwarping over a broad region may be suggested by the erosion of the laterite beneath the Yemen Volcanics (Trap Series) and by the related thin, intercalated quartz sandstones, but there is no evidence of erosion deeper than the thickness of the saprolite. A topographically high regional dome as implied by Gass (1970) did not exist. A similar large areal distribution of laterite on basement and beneath alkali-olivine basalt extends southward in Eritrea to where the basalt rests directly on sandstone, attesting to a prerift continuity across the Red Sea (Abul-Haggag, 1961).

The distribution of middle Tertiary volcanic rocks clearly indicates increased continental heat flow as the Afar triple junction is approached. North of Sa'dah (about 450 km north of the triple junction), mantle-derived alkali-olivine basalt and subordinate trachyte (Coleman, Fleck, and others, 1977) was extruded through a full continental thickness (Healy and others, 1983). South of Sa'dah, similar basaltic rocks are interlayered in a one-to-one ratio with rhyolitic ignimbrites that were derived from thinned, hot, continental crust beneath the continental rift. The ignimbrites of the Yemen Volcanics (Trap Series) probably originated from abundant explosive volcanoes, now eroded down to their granite roots, in a highly active continental rift that had a half-width of 50 km or more. On eruption,

these ignimbrites traveled more than 100 km east of their rift vents. The conspicuous increase in K_2O with decreasing age (from 30 to 20 m.y.) for both the basaltic and rhyolitic volcanic rocks in the Yemen sequence implies an increase in crustal heat with time within the thinned continental crust beneath the rift valley and within the thicker crust marginal to the rift, for distances of as much as 200 km.

Tertiary granite plutons in the wide continental rift of north Yemen are exposed as far as 350 km north of the triple junction (Grolier and Overstreet, 1978). Silicic volcanic rocks (without exposed granite plutons) within the narrow rift on the southernmost coastal plain of Saudi Arabia, from 450 to 600 km north-northwest of the triple junction, are subordinate to felsic and mafic rocks and imply that silicic magma production in the continental crust in this area was much less than in Yemen. Again, the heat flow from the convecting mantle ridge beneath the continental rift in southern Saudi Arabia was less than to the south.

The Baid Formation is the key and unifying feature in identification of the continental rift valley in Saudi Arabia. Its composition and distribution indicate that explosive volcanism produced siliceous ash throughout the rift to as far north as Jiddah. We have only two age determinations (19.3 and 21.3 m.y.; samples 45 and 48, table 10) on rhyolite and trachyte(?) from the Jabal Sitā' area and the major-element chemistry from the Jabal Shama (Ḥarrat Tuffil) perlite (Laurent, 1976; Schmidt and others, 1982; Pallister, 1983) to suggest that the age and chemistry of silicic magmatism did not change significantly along the continental rift in spite of the apparent northward decrease in heat flow.

FIRST-STAGE SEA-FLOOR SPREADING

About this time the Tihamat-Asir Complex of tholeiitic diabase, basalt dikes, gabbro, and granophyre plutons was intruded into the rift volcanic rocks (Jizan Group) within the continental rift of the coastal plain of Saudi Arabia. The Tihamat-Asir Complex is inferred to be restricted to a narrow zone, probably about 12 km wide, at the thinned continental margin of the Arabian Shield.

The chemistry of the Tihamat-Asir dikes and the layered gabbro of Jabal at Tirf suggest a mantle origin from tholeiitic magma similar to that of modern Red Sea oceanic basalt (Coleman and others, 1979). The origin of the voluminous granophyre of the same age is less certain, and it could in fact be derived from the lower crust. However, the mafic-rock chemistry (including the rare-earth-element contents and Rb/Sr ratios) has been modified considerably, probably by contamination with older continental crust as well as by differentiation at shallow crustal depths (Coleman and others, 1979). Both contamination and shallow differentiation are likely if these rocks intruded a complexly faulted and thinned continental crust in a continental rift, as we propose. A continental-rift environment, involving circulating nonmarine water, also helps to explain the large depletion in ^{18}O values in the Jabal at Tirf layered gabbro (Taylor and Coleman, 1977). As further evidence that at least a thin continental crust underlies the exposed rift belt, xenoliths of metamorphosed Wajid Sandstone and rare Precambrian gneisses are found in the basalts of Quaternary volcanoes located from 2 to 3 km west (seaward) of the Jabal at Tirf layered gabbro.

Once sea-floor spreading began, the Arabian-Nubian Shield parted along the full length of the Red Sea and the formation of oceanic crust was synchronous along this entire length, as predicted by rigid-plate tectonic theory and as shown by the magnetic-stripe anomalies of Hall (1980). In the Jīzān area, Blank and others (1981) showed that the easternmost magnetic-stripe anomalies of the Red Sea (Hall and others, 1977) are produced by the Tihamat-Asir Complex, that is, the oldest magnetic stripe actually is produced by the dikes that intrude continental crust. The easternmost anomaly is positive, and the reversed second anomaly appears on the western edge of the complex.

Modeling of magnetic-stripe anomalies of the Red Sea, exclusive of those of the axial trough, using synthetic anomalies generated from the Tertiary geomagnetic polarity time scale, shows a good match for the interval from 21 to 15 or 14 m.y. (M.E. Gettings, written commun., 1981). This model evidence, though not decisive, agrees with our geologic age assignments.

A brief continental-margin extensional episode accompanied the initiation of sea-floor spreading. Most deformation of the rift volcanic rocks (Jizan Group), the underlying Paleozoic and Mesozoic sedimentary rocks, and the underlying Precambrian crystalline rocks occurred at this time. The continental extension had the character of collapsing toward the new ocean crust. The relative age of this extension is well recorded by the geology. The Jizan Group as a whole was rotated about 30° seaward, and the earlier, most intensely altered Tihamat-Asir dikes were similarly rotated and dip steeply eastward (Kellogg and Blank, 1982), whereas the younger, less altered Tihamat Asir dikes are typically vertical. This episode of initial spreading and crustal extension lasted perhaps 1 to 2 m.y. during the time that the first ocean crust was emplaced, consolidated, and cooled.

The thicker continental crust, from 50 to 100 km inland of the continental rift, was distended on vertical fractures that were filled with magma originating in the deep, underlying convecting mantle. The average

age of these continental dikes is about 20 m.y. (Eyal and others, 1981) or 22 m.y. (Blank, 1977), which at least roughly agrees with the initiation of sea-floor spreading. Hence, the continental crust marginal to the continental rift was distended at the same time the continental rift was extended.

Initially, the continental margin extended and the sea floor spread while the world rigid-plate configuration and dynamics were such that the Arabian plate could rotate away from Africa, that is, the continental margin extended briefly until the linear rate of formation of new lithosphere equaled the rate of plate movement. When these two parameters were balanced, continental-margin extension ceased.

The present-day crustal structure across the extended continental rift at Ad Darb, from the Arabian Shield on the northeast to the oceanic crust at the Farasan Islands (pl. 1), has been determined using a seismic deep-refraction profile (Mooney, 1980; H.R. Blank and M.E. Gettings, written commun., 1981; Healy and others, 1983) and a gravity study in the Jīzān area (Gettings, 1977). The crust of the Arabian Shield is about 40 km thick, and the oceanic crust beneath the Farasan Islands is about 9 km thick. Several kilometers east of the exposed rift belt at Ad Darb, the continental crust thins to about 18 km; hence, across the continental rift itself, a thinned continental crust 10 to 15 km thick is reasonable. The gravity study east of Jīzān suggests an oceanic-continental crust boundary east of Abū 'Arīsh within a steep 150-milligal (Mgal) step (4–5 Mgal/km) in the gravity data. Our field studies indicate that the entire exposed rift belt is underlain by continental crust; hence, the ocean-crust boundary actually lies a few kilometers west of the exposed rift belt but east of Abū 'Arīsh and entirely beneath the Quaternary cover.

SUBSEQUENT EVENTS

The first-stage opening of the Red Sea (Girdler and Styles, 1974) possibly extended from 20 to 15 or 14 Ma, a period of 5 or 6 m.y. This suggests a half-spreading rate of about 2.2 cm/yr. Four to six kilometers of clastic and evaporitic sedimentary rocks were deposited upon the newly formed oceanic crust. These include the middle Miocene Infra-Evaporite Series, the upper Miocene Evaporite Series, and the Continental Series of Gillmann (1968), as recorded in the Mansiyah drill hole (3,931.6 m deep) 40 km north of Jīzān. The Infra-Evaporite Series is correlated with the lower and upper Globigerina Marls of the Gulf of Suez (Tromp, 1950; Said, 1962, p. 19, 180, 313; Souaya, 1966) by way of comparable rocks in the Sudan coastal area (Sestini, 1965; Gillmann, 1968, p. 204; Whiteman, 1971, p. 205–211), as well as with reef limestone in the Jiddah area, where Vindobonian (middle Miocene) foraminifera have been reported (B. Steenstra and H.A. McClure, written commun., 1975). The Infra-Evaporite Series constrains a minimum age of middle Miocene for the end of the first-stage opening of the Red Sea. The top of the Evaporite Series is well dated by the "S" anhydrite reflector throughout the Red Sea and presumably corresponds to the "M" reflector of the Mediterranean Sea at about 5 m.y. (Ross and Schlee, 1977, p. E13).

Gillmann (1968) suggested that the Baid Formation may correlate with his Infra-Evaporite Series, located at a depth of 4,000 m in the Mansiyah drill hole. By our interpretation, the Oligocene-lower Miocene tuffaceous Baid Formation will not be found in any of the Red Sea sedimentary rocks that overlie oceanic crust and also not, as suggested by Gillmann, on top of the Evaporite Series in the Jizan salt dome. The Baid Formation is restricted to the continental margin east of Abū 'Arīsh, and a sequence correlative with the Baid Formation should be found on the Sudan coastal plain in the western half of the continental rift.

One of the enigmas of the Red Sea history is the age of the Red Sea Escarpment. It has been postulated that an early, large dome rose over the mantle plume at the triple junction and above the convecting mantle ridges beneath the triple arms of the Red Sea, Gulf of Aden, and East African Rift (Gass, 1970). No polymictic sands or gravels are found beneath or within the Jizan Group, and no Precambrian detritus is found in the extensive Baid Formation, which contains only volcanic ash and erosional volcanic debris. Additionally, the early Tertiary lateritic paleosol is preserved today only beneath the Jizan volcanic rocks near sea level in the Al Līth and Ad Darb areas and beneath the flood-basalt flows on the inland plateau in the As Sarāt, Ḩarrat Ḩaḍan, and Sa'dah (north Yemen) areas. This implies that the laterite was widespread and erosionally stable through the continental-rifting stage and that it was thoroughly eroded only upon uplift of the Red Sea Escarpment.

The Nubian-type basal sandstone of the Jizan Group and Yemen Volcanics (Trap Series) represents erosion of a thin saprolitic surface of low relief on stable Precambrian crystalline rocks near sea level. In contrast, the chaotic coarse conglomerate of the Bathan Formation is the first clue of the uplift of a Red Sea Escarpment at some time considerably after deposition of the Jizan Group. Possibly correlative terrigenous conglomerates and sandstones in the Infra-Evaporite Series suggest a middle Miocene age for the Bathan.

During a long nontectonic interlude, a broad-valley erosional stage developed on the early escarpment and

the initial rugged relief of the scarp was greatly subdued. Two broad erosional valleys, transecting the escarpment west of Ḥarrat Raha̲ṭ northeast of Jiddah, are preserved beneath upper Miocene basalt flows from Ḥarrat Raha̲ṭ. In contrast, the present-day streams flow in steep canyons incised below the broad-valley level.

In the Biljurshī' area, Greenwood (1975b) suggested a two-stage uplift of the escarpment and identified an ancient elevated erosion surface that cuts across steeply dipping Precambrian structures and that probably represents the broad-valley erosional stage. These highly eroded, relict surfaces are vaguely recognizable in other places, such as south of Khamis al Bahr (40 km north-northeast of Al Birk).

Most significantly, the broad-valley erosional stage (or the nontectonic interlude) is well documented by the late Miocene pause in shear movement on the Dead Sea Rift when Jordanian drainages flowed across the rift to the Mediterranean Sea (Zak and Freund, 1981).

During and since Pliocene time, the Red Sea Escarpment was rejuvenated in a second-stage scarp uplift. This late uplift is likely still in progress, as evidenced by the very rugged and steep topography of the modern scarp, by deeply incised wadis, and by the commonly reversed topographic relief of 100 m or more on latest Miocene basalt flows in the coastal plain north and south of Jiddah.

Approximate timing of the cyclic Red Sea Escarpment uplifts is suggested by the stratigraphy in the Mansiyah drill hole. Gillmann (1968, p. 199, 205) notes "some conglomerate" as a "regressive facies" in the middle Miocene(?) Upper Infra-Evaporite Series, and we suggest that this conglomerate facies correlates with the Bathan Formation. The apparent lack of clastic detritus in the thick upper Miocene Evaporite Series may correspond inland to the broad-valley erosional stage. The thick, post-Miocene Continental Series consists of clastic debris, including "sandstone and conglomerates" and "50 m of graywacke and polygenic conglomerate" (Gillmann, 1968, p. 196) that we suggest may correspond to the rejuvenated, second-stage scarp uplift.

During Pliocene-Pleistocene-Holocene time, that is, the last 5 m.y., a second stage of sea-floor spreading produced the 60-km-wide axial trough of the Red Sea and suggests a spreading half-rate of about 0.6 cm/yr. At the same time and earlier, abundant alkali-olivine basalt flows were extruded on the Red Sea coastal plain (150 km from the Red Sea axis), in the Hejaz Mountains (300 km for the axis), and on the upland plateau of the Najd (400–500 km inland from the axis). Some of these youthful volcanic fields may be as old as middle Miocene.

GEOMORPHOLOGY

CYCLES OF EROSION

To understand the terrain development in western Arabia, one should first visualize the morphology of landforms in a waterless desert, that is, in a true arid cycle (fig. 67). In general, subaerial physiographic features are produced by the degrading and weathering action of water, gravity, ice, winds, and organisms in opposition to the aggrading internal agencies of diastrophism and volcanicity. The action of weathering agents tends to decrease altitude and, although the end product may be a plain or may approach a plain, increase in relief is an early and normal result of the action of any of them. As the action of water and gravity are nearly universal, the so-called normal erosive process is the humid or fluvial cycle. In subfreezing temperatures, ice action is dominant (glacial cycle), and where both ice and water play a subordinate role, the wind produces the characteristic features of the true arid cycle.

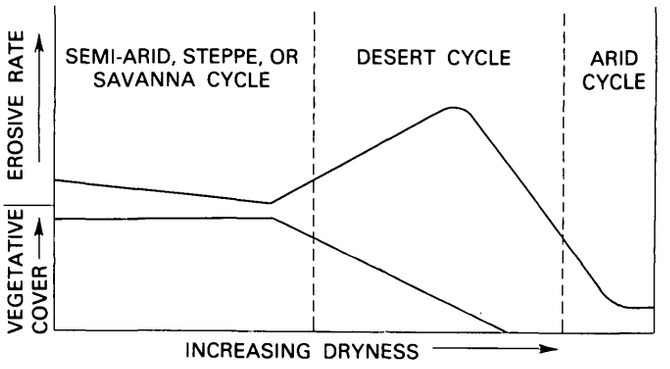

FIGURE 67.—The savanna, desert, and arid cycle.

ARID CYCLE

In an area of diverse rocks exposed only to the action of the wind, gravity, and temperature changes, the regional terrain must of necessity be initially tectonic. The wind readily attacks the softer beds wherever they are exposed; gravity works on the steeper slopes, fragments becoming available through fracturing due to pressure release and to insolation (the breakage of rocks due to surface changes of temperatures, which are great in such waterless areas). There is very little rock decomposition; rather, unstable minerals persist in the weathering products. Thus, sandstone and shale are carved out at a rate that depends on relative hardness

and cementation; grains less than 0.08 mm in diameter are carried away from the region until they reach a place having sufficient moisture to hold them, whereas grains 0.08 to 1 mm in diameter are moved into sand masses, such as dunes, sand sheets, and ergs. The sand scours the bedrock (fig. 68) wherever it is carried over the exposed surfaces and impinges against the rock surfaces, abrading them and slowly releasing more material for transport. As the process continues, the harder beds form ridges of increasing vulnerability to attack by insolation and wind, and they too eventually are reduced until an extensive plain, cutting across all rock types, is formed, without reference to the usual concept of base level. Such a process of beveling must be many times slower than erosion by water or ice, in part because the sand forms a protective cover over an ever-increasing part of the terrain. Indeed, if the wind direction were constant, the sand probably would early form thin sheets or make sand shadows that protect the low areas on the lee side of the rock ridges. Eventually the sand would move out of the region until it reached a place of anchorage by vegetation or was blown into a distant sea. If there should be conflicting winds, and none dominant enough to carry the sand out of the region, the sand would probably form expanding ergs which would grow in depth and area, shifting from place to place, until the region would be covered with sand and the rock floor beneath the dunes would have an undulating pattern, hollows developing where wind erosion had been active longest. Under these conditions, the process might be thought of as operating under inverse control by an ever-moving base level at the surface of the sand.

Apparently no area has been rainless sufficiently long to allow such an eolian-dominated process to develop a plain—at any rate, such a plain has not been recognized. In most desert areas sufficient rain falls, usually of the torrential type, to impose special terrain features that are ultimately more subdued than those described above. The combination of wind and water together with the other less important agents produces distinctive landforms in a process termed the "desert cycle" by E. De Martonne (1926) and by von Engeln (1942).

COMMON DESERT EROSION CYCLE

The distinguishing features of the common desert erosion cycle, developed by infrequent desert torrential rainfall under conditions of meager vegetation, wide temperature fluctuation, and eolian as well as fluvial erosion and transportation, as evolved by earlier authors (Davis, 1905, 1933; Cotton, 1942) may be stated as follows:

1. Rock disintegration predominates over decomposition.
2. The accumulation of sand into dunes, ergs, and sand sheets by the wind is localized by the deposition of wadi alluvium.
3. Basins that do not have surface drainage to the sea may contain playa lakes which exert a base-level control.
4. The local base rises as the basin fills with debris, resulting in a buried rock floor that is convex upward.
5. The centripetal drainage lines into the basins are occupied by intermittent streams that are about the same size or shorter than the slopes of the basin flanks; the spottiness of desert rainfall prevents development of master valleys.
6. Pediments, or carved plains, are formed that rise on slopes of 0.5 to 7 percent from the local or regional base level to the base of desert mountains; they are cut with uniform grade across different structures and rock types.
7. As the region becomes more mature, the spreading basins intersect, resulting in coalescence of base levels and integration of drainage.
8. In maturity, wind action becomes more effective as fluvial power decreases, but if the deserts are in a rain shadow and the erosive processes lower the mountain fringe, rainfall may increase and the cycle shift into a more humid form.

The relative importance of wind and running water in desert regions has been debated at length. As a desert becomes drier, the vegetative cover decreases and the erosive action of the increasingly intermittent storms increases. When the periods between rains are sufficiently long and relative humidity becomes too low for effective dews, the vegetation, if any, is too sparse materially to retard the rate of erosion. This acceleration of erosion by water during increasing desiccation makes the effects of eolian erosion difficult to distinguish, except for the local and rather small-scale effects of corrasion such as polished and fluted rocks, pedestals, and yardangs. It is more difficult to recognize the larger forms of eolian erosion such as those caused chiefly or wholly by deflation. The problem is illustrated qualitatively by figure 67, which shows that as vegetative cover decreases, the erosive rate by water increases, until there is no effective vegetative cover. Thereafter, erosion is largely a function of the concentration of rainfall and the effects of wind abrasion.

Most of the large features of deserts appear to result from water action, although wind-scoured hollows as much as 400 ft deep and 10 or 12 mi across in Mongolia have been described (Berkey and Morris, 1927). Their origin seems to require deflation on soft sands and silts

FIGURE 68.—Landsat image showing effects of wind erosion, north of Wādī ar Rimah and east of Ḥarrat Khaybar and Ḥarrat Ithnayn. Regional wind direction is toward about N. 70° E. Note preponderance of yardang troughs upwind (from S. 70° W.) from southeast-draining wadis, especially where there is a grus plain. There is a paucity of yardangs on the northeast flanks of these streams where the sand has been removed during floods, thus depriving the wind of a scouring tool (see arrow).

(but some are on granites and other crystalline rocks in Arabia), aided by gullying in the short walls on the flanks. According to Berkey and Morris, the basins progress downward, possibly to the water table, then grow laterally at a rate faster than debris is brought in by the centripetal gullies. This vertical removal of debris is at approximate right angles to the removal of bedrock in the arid cycle and requires initiation by water. The concentration of wind action carrying sandblast leads to deeper and deeper cutting down the swales in a desert surface. This downcutting by wind scour is effectively measured by temperature variation past the dewpoint so that moisture trickles down flanking slopes to the bottoms of gullies. Such moisture concentration there leads to chemical decomposition, and subsequent floods or sandblast scour out the loose material. As a result, yardangs and yardang troughs are major features in the older deserts, especially in coarse-grained igneous rocks whose feldspars weather, forming grus (figs. 75, 76).

Not all deserts have interior drainage; about one-third of the world's deserts have drainage to the sea (De Martonne, 1926), either because streams flowing across them have headwaters in more humid regions or because of initial tectonic conditions. Furthermore, most, if not all, deserts, and in particular the Sahara and Arabian deserts, were more humid during episodes of the Pleistocene when the climate was at least semiarid or steppelike. In Arabia during the Pleistocene, Wādī as Shabā' seems to have reached the Arabian Gulf, or nearly so, as did Wādī ar Rimah and possibly Wādī ad Dawāsir, although the last may have debouched into lakes in the Rub al Khali basin.

Davis (1905) has pointed out that the evolution of the desert cycle is largely controlled by the initial relief, which may be of a wide valley and range, as in central Arabia, or of a massive mountain, as in the Hejaz. If the region is one of gently dipping sedimentary rock, as in the Najd, the cycle would begin in a manner similar to the ideal humid cycle operating on an uplifted peneplain formed either by former fluvial or marine planation or on a desert peneplain following a long period of cliff retreat. Without a substantial period of bahada accumulation, the harder beds would form cuestas. The wind would keep pace with the gullying of promontories, and the pediment would extend to near the cliff base by "direct replacement of one already well-planed rock floor by another at a lower level" (Cotton, 1942). The desert cycle in such sedimentary rocks has been described in Australia, Libya, the Kalahari, Mongolia, and the mesa country of Southwestern North America. The beveled surfaces that seem flattest in the drier areas are believed to have suffered greatest desiccation, in contrast to the formation of coalescing alluvial fans and sloping pediments in areas where conditions have approached or entered the semiarid cycle.

TIHĀMAH

The coastal plain (pl. 3) along the eastern shore of the Red Sea, known as the Tihāmah, extends with few interruptions from the Gulf of Aqaba on the north to Bābal Mandab on the south of the Red Sea. The Tihāmat appears to have developed during alternations of desert and savanna cycles, with the Red Sea as a variable base level of erosion. The coastal plain ranges in width from narrow beaches to as much as 40 km. In the southern part, the Tihāmat al Yemen and Tihamat 'Asīr, a 2- to 3-m elevated beach, extends northward as far as Al Wajh. It is marked by low headlands and overhanging scarps ascribed by Guilcher (1952) to chemical weathering (solution) activated by surf and eolian action. Near Jiddah, the surface rises eastward about 1.5 m/km for about 5 km to altitudes of about 10 m. Above 10 m the slopes are steeper, on the order of 10 m/km, until a general altitude of about 100 m is reached at the foot of the coastal mountain belt. Remnants of a 20-m beach underlie a basalt flow north of Jiddah, and surfaces at 6, 10, 22, and 31 m, mostly on coralline rocks, have been measured from Umm Lajj northward to near the Gulf of Aqaba (fig. 69). The surface culminates at an altitude of 525 m on Tīrān Island at the mouth of the gulf (500 m according to Goldberg, 1963), and marine benches extend up to at least 320 m, facing southwest (Schick, 1958). The surfaces appear to be elevated primarily by vertical movement along the old transverse Najd fault system

FIGURE 69.—Terrace benches at 6, 22, and 31 m above the northern Red Sea north of Al Wajh resulting from intermittent ramping of the Ḥismá (Ash Shifā') block of the peninsula during the Quaternary. View to the northwest.

as part of the ramping of the northeast flank of the rift valley (Brown, 1972). However, relative movement of blocks between transform faults that cross the Red Sea in a northeast direction may also account for some of the uplift. The generally accepted two-stage opening of the Red Sea, with two poles of rotation as developed by Girdler and Styles (1974) and by Richardson and Harrison (1976), would cause vertical uplift from compression during the second, Pliocene-Pleistocene-Holocene stage, as the sea floor widened in an easterly direction and the peninsula rotated about 7° counterclockwise.

The seaward, lower part of the Tihāmah is, for the most part, a depositional or coralline surface that gradually merges eastward into an erosional pediment that extends across the rift fault zone of the eastern edge of the Red Sea rift. The coastal-plain surface in many places can be followed continuously from Tertiary sedimentary and igneous rocks eastward onto the pediment beveled across the crystalline rocks of the Precambrian basement. Thus, most of the pediment developed after the last large-scale movement on the easternmost margin and after the inception of a major rift opening at about 22 Ma in the southern Tihāmah, when gabbro and related dike swarms were emplaced (see samples 72 and 73, table 10; Coleman and others, 1979). An ancestral remnant of an old pediment surface is preserved beneath the about 3-m.y.-old basalts, Ḥarrat Tuffil, 100 km south of Jiddah, where the ancestral pediment, beveled on Precambrian rock and protected from erosion by its basalt cover, lies 50 m above the modern coastal plain midway between the coast and the foothills on a 30-km-wide coastal plain.

At intervals along the present shore are small inlets called sharms (locally, khawr or marsa). Some are connected to present drainage debouchment from the coastal mountains (pl. 4); others are not related to present drainage. Typically they are "T" or bottle-shaped, widening out landward from a narrow throat, about 30 m deep, and maintaining a depth of as much as 10 m behind the coralline ridges on the flanks of the throat entrances. The water bays behind the throats are commonly 5 to 9 km long parallel to the coral ridge and extend inland from 2 to 5 km. There is now no active, or only very minor, erosion in the sharms. Also, as floods now rarely reach the Red Sea across the coastal plain except in a few of the largest wadis, there must have been more rainfall when the sharms were formed. The openings in the coralline fringing reefs suggest that less saline, perhaps silt-laden, water from runoff in wadis draining the western slopes of the uplands may have inhibited growth of coral across the throats before the present pediment was elevated 3 m or more. Thus, at first glance it would appear that the sharms are coeval with the time of coral growth now exposed in the flanks of the throats. However, much evidence points to a later breaching of the fossil reef. For instance, the bifurcation and trifurcation of the sharms behind the beach ridge, as noted by Gvirtzman and others (1977), was thought to represent lagoons that existed before the reefs were breached.

The age of the elevated coral reef making up the seaward edge of the sharms is greater than a minimum ^{14}C age of 40,000 yr, as determined by Meyer Rubin (*in* Brown, 1970), for the coral at Jiddah. Goldberg and Yaron (1978) assigned a $^{230}Th/^{234}U$ age of 146,000±16 yr for the reef that is at 11–13 m altitude today on the southeastern coast of Sinai. The elevated reef, commonly beneath a 2–3-m terrace, along the central and southern Red Sea of Saudi Arabia is elevated as high as 50 m on the Jīzān salt dome and is possibly about 135,000 yr old (uranium-series dating of the coral; J.W. Whitney and B. Szabo, USGS, oral commun., 1983). An elevated coralline reef in the Afar rift is 54,000±4,600 yr ($^{230}Th/^{234}U$ dating of the unrecrystallized mollusk *Tridacna*; Bonatti and others, 1971), but the Afar is considerably more active than the Red Sea coast and the age is probably younger than the Red Sea elevated coral. At any rate, the coral is old relative to the assumed youthful erosional age of the sharms, for any estuarine depression behind the coral reef would have been filled long before the formation of the sharms.

The 30-m depth at the throat of some of the sharms suggests a period of downcutting when the Red Sea level was 30 m or more below present sea level. Low base levels existed during the various Quaternary glaciations, when large volumes of the Earth's water were stored in glacial ice. Recently described evidence from many sources indicates that epochs of maximum glaciation were coeval with aridity in the low-latitude deserts, at least during the late Pleistocene, even though the present interglacial epoch is arid (Bowler, 1976; Deuser and others, 1976; Wendorf and others, 1976; Sarnthien, 1978). Therefore, pluvial epochs seem to correspond to the interval between glacial and interglacial, that is, the more or less equivalent intervals of deglaciation on one hand and warming on the other. It is during these pluvial epochs when integrated drainage across the coastal plain to the Red Sea might be expected and when erosional cutting of the sharms probably took place.

Pluvial lakebeds were deposited in Ar Rub 'al Khālī, according to ^{14}C dates, between 36,000 and 17,000 yr B.P., with a cluster of ages from 30,000 to 21,000 yr B.P., and younger lakebeds were deposited from 9,000 to 6,000 yr B.P. (McClure, 1977). The older pluvial epoch was about contemporary with the ^{14}C ages of 20,400±500 to 24,630±500 yr B.P., for the deep artesian

water from widely scattered wells in central and eastern Arabia (Thatcher, Rubin, and Brown, 1961).

Farther afield, Sarnthien (1978) gives wet intervals for the Sahara of from 12,500 to 11,000 yr B.P., from 10,000 to 7,500 yr B.P., and from 6,500 to 5,500–5,000 yr B.P. The oldest interval coincides with an extensive pluvial interval of the Nile (Fairbridge, 1977), although the Nile floods come from a different climatic zone that may not be synchronous with the desert cycle. Sarnthien (1978) states that prior to the moist interval, active sand dunes extended from lat 10° to lat 37° N. in the Sahara about 18,000 yr ago—synchronous with the polar ice maximum (about 20,000 yr B.P.; Peltier, 1980) and with maximum desert aridity. The pluvial chronology is further strengthened by an analysis of oxygen isotope ratios from the planktonic foraminiferal fauna of the Red Sea and the Gulf of Aden (Deuser and others, 1976) which showed that the cold intervals for the Red Sea coincided with intervals of major deglaciation. The last of these cold intervals, recorded in the cores from the Deep Sea Drilling Project (Scripps Institution of Oceanography, University of California), occurred from about 17,000 to 8,000 yr B.P., that is, between the Wurm glacial maximum and the climatic optimum of the Paleolithic.

The pluvials of Arabia and the Sahara seem to be of much shorter duration than the interglacial epochs, so that if glacial expansion corresponds to desert-cycle aridity, interglaical does not entirely correspond to desert-cycle pluvial. Hence, perhaps the interval of change, that is, the interval of rapid ice retreat-rapid deglaciation, should be considered the dynamic climatic control for the pluvial interval. Perhaps the present aridity of Arabia during an interglacial epoch is explained by the correlation of the pluvial only with relatively short transitional time during rapid deglaciation.

The origin of the sharms requires a coincidence of low sea level and pluvial conditions such that the coastal-mountain water flowed to the Red Sea. Streamflow to a sea level lower than the present would allow the erosional breaching of the elevated reef and at the same time allow lateral erosion of some of the soft estuarian sediment fill behind the reef, thus forming the typical "T" pattern of the sharms. The post-Wurm rise in sea level for the Red Sea can be extrapolated from data by Peltier (1980, fig. 8). Accordingly, the sea level rose from about –75 m, 13,000 yr ago, to –30 m, about 9,000 yr ago, and to about the present sea level, 5,000 yr ago.

The sharms can be estimated to have formed about 12,000 to 8,000 yr ago, during the early half of the Sahara-Arabian pluvial and when sea level rose from about –60 m to –20 m. At the maximum low sea level of about –120 m, 18,000 yr ago, climate was too arid, and after about 8,000 yr ago, sea level was too high for the sharms to form. Certainly after about 5,000 yr ago the climate also was too arid. A fossil coralline reef in the Gulf of Aqaba now at intertidal level has been dated at 4,770±140 yr B.P. (Friedman, 1965)—the sharms must have been cut before this time. Similar sharms probably formed earlier during the early part of other interglacial epochs, for example, perhaps between 36,000 and 32,000 yr ago, during the early part of the last Wurm interglacial.

The eastern and higher Tihāmah is in places covered with eolian sand, generally accumulating transversely to the offshore-onshore winds, usually in barchan dunes. In several places where winds shift alternately from northwest to southwest and vice versa, long seif dune ridges accrete approximately perpendicular to the trend of the coastal plain. In general, the sand grains are 3 and 4 mm in diameter, much coarser than the bulk of the sand accumulated in the great interior nafuds. They accumulate in para-ripples. The smaller grains generally are deposited in dunes farthest from the shoreline against the base of the scarp mountains (Guilcher, 1952).

SCARP MOUNTAINS

The ramping of the eastern flank of the Red Sea rift and subsequent faulting has exposed a southwest-facing scarp (fig. 70) against which atmospheric weathering has been active, probably since the middle Miocene. This has formed a mountainous belt 40 to 140 km wide which rises eastward to the rim of the great interior plateau of Najd, the Hejaz-'Asīr highlands area in southern Arabia (pl. 3), and the Ḥismá Plateau in northern Arabia. The crest reaches a maximum 3,000 m in Jabal as Sūdah in the 'Asīr near the Yemen border. The crest line gradually declines northward to a minimum height of about 1,000 m in the mountains northwest of Al Madīnah, where the mountainous belt is widest and where Wādī al Ḥamḍ has been captured and flows more directly to the Red Sea through a precipitous canyon.

Farther north, another block is tilted upward along a series of faults that cut obliquely across the belt, forming the mountains of Ash Shifā', which lie in front of the Ḥismá Plateau and extend into Jordan. The highest point of Ash Shifā' is Jabal al Lawz, 2,400 m above the Gulf of Aqaba, but five peaks making up the Ash Shifā' region as far as 100 km south are 2,000 m or more in altitude. A series of knife ridges and canyons marks the southwestern fronts of each block. These

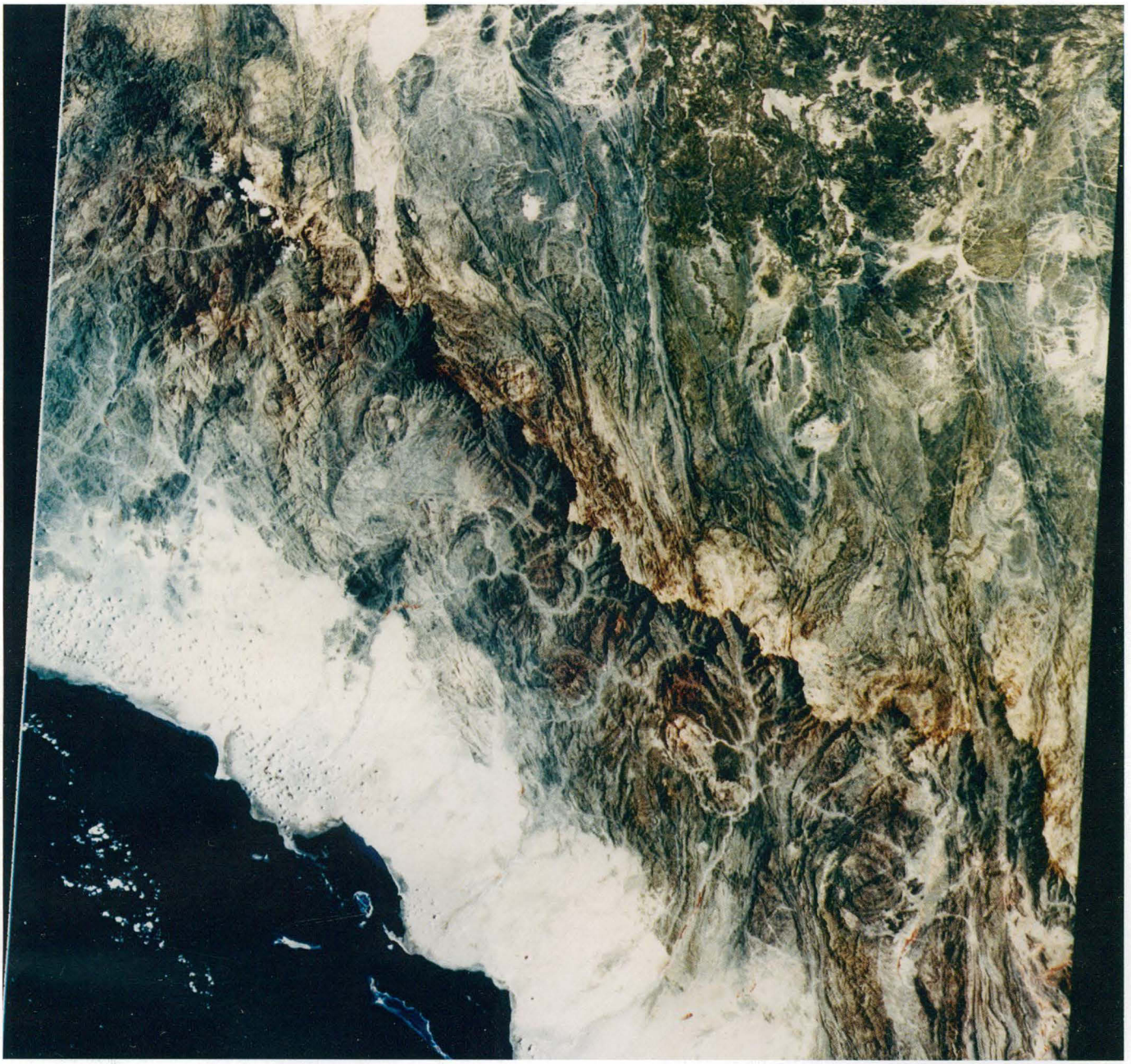

FIGURE 70.—Landsat image of the erosional scarp of 'Asīr at lat 20° N. Red Sea on lower left, bordered by the Tihāmat 'Asīr (coastal plain) and the scarp mountains cut back to the Najd pediplain (upper right). The pediplain here has been ramped up to altitudes of as much as 2,600 m. The southern end of the plateau lavas of Ḥarrat Buqūm occupy the northeast corner of the scene. From Jet Propulsion Lab.

southwest-facing slopes are in places transected by north-trending valleys which permit passage from one canyon to the next. Some north-trending valleys are subsequent erosional valleys carved parallel to the structural grain in basement schist. Narrow valleys trending northwest are underlain by the wide Tertiary mafic dikes that weather more rapidly than the Precambrian crystalline wall rocks. Some of these narrow valleys are flanked by thick walls representing the fine-grained chilled margins of the mafic dikes. Subsequent erosion has developed the north-south tributaries, along which it is possible to cross watersheds at the heads of the subsequent streams without being aware of a reverse in slope, such was the flatness of the pre-uplift pedimentation.

Many lower courses of the larger wadis draining the scarp mountains show stream capture (pl. 3). Wādī al Ḥamḍ is an outstanding example, with an elbow of capture at the junction of Wādī al Jizl. Evidently the wadi prior to the uplift of the Hējāz Mountains flowed out to the coast north of the present mouth at lat 26° N., perhaps as far north as the emergence of the major Najd fault into the Red Sea at lat 28° N. The schists of the shear zones formed valleys on the shield toward the end of cratonization, a natural environment for the development of subsequent streams on the early Tertiary lowland of the northern Red Sea coast (Madden and others, 1980). If so, the ancestral wadi was captured progressively southward as the peninsula rotated counterclockwise and ramped upward in response to the compressional and sinistral stresses toward and along the Jordan (Dead Sea) rift. A subsequent outlet may have been via the Wādī Saluwah-Wādī Damā thalweg, debouching through upper Wādī as Surr, followed by a later capture southward via Wādī Bayda and the lower Wādī as Sirr trough. As the tilting continued along the Najd fault system, Wādī Thalbah and Wādī Azlam captured the lower As Sirr valley and Wādī al Ḥamḍ reached the sea via its present course. Regardless of the precise channelways, the northeast tilting (elevation) of the Hisma block undoubtedly caused the wadi to seek an outlet to the sea in a southerly or westerly direction as the earlier lower course was elevated.

In a similar manner, wadis farther south were captured (pl. 3). Notably, Wādī al Far'ah from the east side of Jabal Raḍwá, near Yanbu' al Baḥr, had a previous channel extending south and debouching through Wādī al Faqir onto the coastal plain 40 km south of the present mouth. This ancestral stream sought a more western outlet as the country south of Wādī al Faqir rose. Test drilling in Wādī al Faqir penetrated alluvium about 100 m thick, whereas the current drainage in Wādī al Far'ah has a shallow bed over granite. Similarly, Wādī as Safra', 30 km farther southeast, drains two meridional valleys—Musayj'īd or Wādī as Safrā (3 km wide) and Tasḥah (1 km wide)—through a 200-m-wide gorge, creating a flood hazard on the Al Madīnah-Jiddah road.

Wādī Fāṭimah between Jiddah and Makkah likewise debouched southward through Wādī Shumaysi, which has a deep alluvial valley in comparison to the nearly bare rock floor of the present lower Wādī Fāṭimah whose debouchment is 30 km northwest of the ancestral valley. Farther south, Wādī Qununah, Wādī Yiba, and Wādī Ḥalī in particular seem to have changed drainage directions. Thus, the wadis draining the scarp mountains have been captured or have reversed flow toward the northwest as the Asir block ramped, tilted, and skewed in a counterclockwise direction under tensional conditions. Wadis on the southwest flank of the Ḥismā block north of the Najd faults, however, moved southwest as the country rose to the northwest under compressional conditions.

Tertiary igneous rocks, both hypabyssal and extrusive, have been emplaced along the original rift zone at or near the toe of the scarp mountains. These rocks commonly give an initially deceptive rugged appearance to the lower foothills of the scarp-mountain terrain when viewed from the Tihāmah, but the prerift pedimentation surface is well developed below the dissected volcanic rocks.

HEJAZ-'ASĪR AND ḤISMĀ PLATEAUS

The Hejaz-'Asīr Plateau forms the uplifted and dissected southwestern corner of the Najd pediplain of western Arabia. Triangular in shape, it extends southward from Aṭ Ṭā'if to and beyond the Yemen border, an area of about 40,000 km^2 above 2,100 m in altitude. Broadening and increasing in altitude southward, it culminates in Jabal as Sūdah at 3,000 m near Abhā, the capital of 'Asīr Province and the most salubrious region in Arabia. As the western lip next to the scarp mountains is approached, more abundant rainfall results from orographic convection over the scarp, especially during the late summer monsoon season. Great rainfall increases the amount of dissection, as do the fracturing and warping of the bedrock caused by ramping in connection with the evolution of the Red Sea rift. Rainfall greater than 20 cm annually is limited to a crest zone 20–30 km wide. Consequently, eastward and northward wadi flow decreases rapidly downstream and deposition is greater than erosion near the eastern edge of the plateau. Berms and strath surfaces indicate

FIGURE 71.—Loessal silt in Wādī Tathlīth above Ḥamḍah. (Photograph by Thomas Smallwood.)

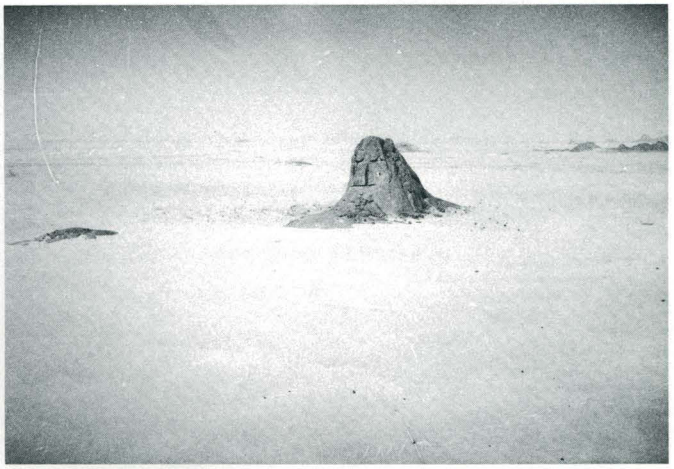

FIGURE 72.—Bornhardt at Jabal Kursh, lat 22°25′ N., long 43°39′ E.

intermittent uplift or climatic change, with at least one relatively static period.

The wadis widen in midcourse where runoff from tributaries coalesce, but many are constricted by narrow throats, particularly where reentering metamorphic terrain from a grus plain underlain by granite rock. Such constrictions have ponded floods and deposited loessal silt (fig. 71) upstream (behind them) during periods of excessive flooding (Brown, 1960). The paucity of grit and gravel suggests low relief and gentle stream gradients at the time of silt deposition. Charcoal from fire hearths on the upper part of the loessal silt have been dated by ^{14}C measurement at 6,350±350 and 5,830±300 yr B.P. (Schmidt and others, 1983), which is in excellent agreement with the age of the Holocene pluvial epoch (9,000 to 6,000 yr B.P.) as determined by ^{14}C dates of lacustrine deposits in Ar Rub' al Khālī (McClure, 1977). The accumulation upstream from constrictions was increased by the higher water table and longer moist periods so that vegetation accumulated, as evidenced by abundant root casts in the silt deposit. The absence of fossil pulmonate gastropod shells seen in present-day loess may be attributed to dissolution of the carbonate by humid acid from the vegetation (Schmidt and others, 1983).

In northwestern Arabia east of the Gulf of Aqaba, the Ḥismā Plateau is an upland comparable to the Hejaz-'Asīr, lying between the scarp mountains of Ash Shifā' on the west and the great northern sandstone plains extending eastward to the Great Nafud. Likewise, the high position of the Ḥismā Plateau results from concomitant ramping in connection with the counterclockwise rotation of Arabia away from Africa. The sandstone plateau rim extends southward from the Jordan border at an altitude of 1,800 m and descends to 1,100 m at lat 28° N., east of the mouth of the Gulf of Aqaba. The surface slopes eastward to the western edge of the Great Nafud basin to an altitude of about 800 m, where the Hejaz Railroad crosses the plain. The southern rim of the Ḥismā is higher south of lat 28° N., where the multiple flows of plateau-flood basalt have built up the surface to 2,000 m in the Ḥarrat ar Raḥāh. Except for the plateau basalts in the Southern Ḥismā, sandstone buttes and mesas dot the plain, increasing in height and numbers toward the rim east of and somewhat below the crests of the crystalline mountains of Ash Shifā'.

NAJD PEDIPLAIN

The crystalline Najd pediplain formed from coalescing pediments begins at the northeastern edge of the Hejaz-'Asīr Plateau, where the ramping of the plateau flattens out toward the northeast. It is a vast reg or serir on which are scattered isolated inselbergs of more resistant igneous and metamorphic rocks, bornhardts and kopjes that are generally granitic, and lava fields present mostly along the western edge (figs. 72, 73, 74).

Where granitoid rocks crop out, most of the terrain is nearly flat and featureless, especially where the crystalline rocks have been tectonized and weathered to clay by periodic hydration of feldspars and where wind

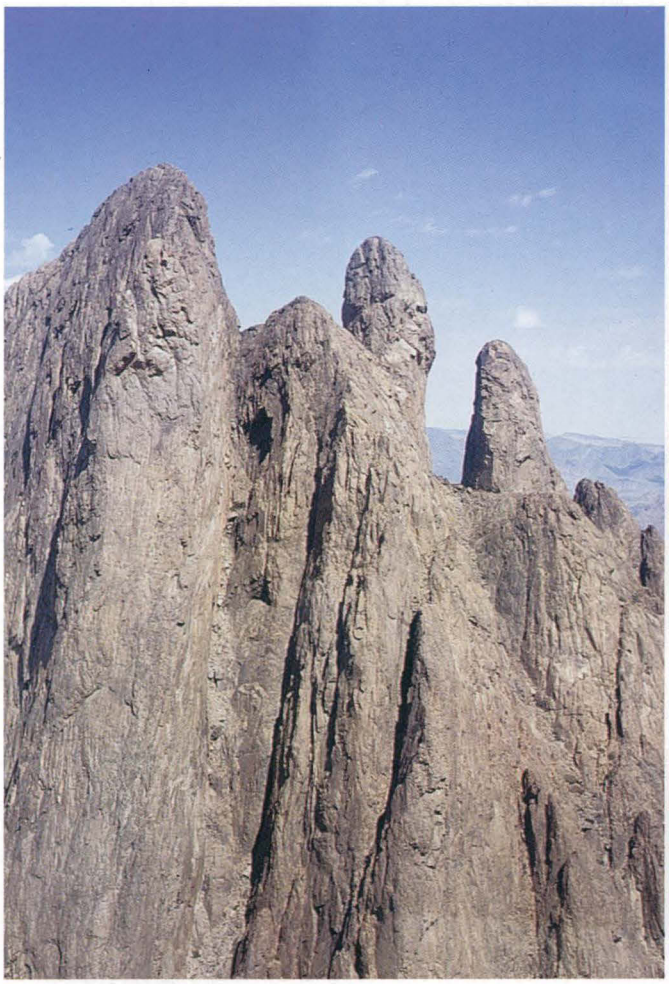

FIGURE 73.—Spines of Jabal Shār rising to an altitude of 1,990 m east of Al Muwayliḥ on the Red Sea coast at lat 27°39′ N. The small batholith is composed almost entirely of posttectonic graphic granite. A U/Pb age of 625±5 m.y. was obtained by Hedge (1984).

FIGURE 74.—Base of the conical inselberg of Jabal al Gharāmīl at lat 21°51′ N., long 42°54′ E. The jabal wall of posttectonic granite rises at an angle of 65° from the horizontal; the lower slope rising at 21° is underlain by contact-metamorphosed sediments of Murdamah age. Nearby the jabal is cut by a Najd fault.

scour has removed the residual grains. The wide temperature range, especially when the cooling falls below the dewpoint and below freezing, hastens the disintegration. The differential rate of expansion and contraction of the polymineralic rocks also hastens the process, even where there has been little or no postemplacement tectonism. Thus, the ridges and higher hills are composed mostly of lavas and metasedimentary rocks, the isolated bornhardts being the exception.

From maximum altitudes of 2,100 m, the plains decline to a minimum of 670 m where Wādī ar Rimah debouches onto the sedimentary Najd at Al Qaṣīm. The desert floor is not a uniform slope but is broken, hinge fashion, along the northwest-trending Najd fault system into four segments or blocks—the southwest, or Asir, block, two central blocks between the three Najd faults, and a northern, or Shammar, block.

The surface of the Asir block slopes evenly from about 1,400 m to 1,000 m in a northeasterly direction to the southernmost Najd fault.

The two central blocks each lie between two flanking Najd faults. Their surfaces are considerably flatter than the Asir block but are tilted somewhat, also to the northeast, and fall from a general altitude of 1,050 m

along the northern edge of the southern Najd fault to a low region of sabkhahs (playas) at about 940 m. Thence, they rise to 1,100 m northeastward toward the middle of the three principal Najd fault zones (USGS–ARAMCO, 1963). The elevation of the southern edge is dramatically shown at Wādī Subay'. Ground water pumped up onto the elevated bank of Wādī Subay' flows by gravity northward (60 km) to Ẓalim and to a sabkhah floor; yet the wadi, entrenched in crystalline rocks, flows east and south, to be lost in the 'Irq Subay' in and along the southern flank of the Najd fault. The central region, which falls between the flanking Najd faults, is the lowest part of the Najd pediplain exclusive of the lower reaches of Wādī ar Rimah. It is nearly devoid of drainage lines and is characterized by numerous small, irregular sabkhahs in desert sinks seemingly scoured by the wind. These sabkhahs are nearly devoid of alluvial debris, and their salt crust directly overlies decomposed bedrock.

The northern, or Shammar, block of the crystalline Najd pediplain falls from 1,100 m along the northernmost Najd fault to 950 m in the extreme northeast corner, where Wādī Ḥā'il flows northeast onto the sedimentary rocks, and to 670 m at Ar Rass, where Wādī ar Rimah flows northeast off the crystalline rocks. Along the western part of this crystalline Najd surface, the larger wadis follow the northwest direction of the Najd fault system where large horizontal movements have created schistose shear zones that are readily deflated or, where above grade, are scoured by floods to create thalwegs. Eastern portions drain northeastward into the well-integrated, dendritic, and slightly entrenched drainage system of Wādī ar Rimah.

The increased rainfall shown by the 10-cm isohyetal lines in the Shammar block (fig. 2) is not easily explained from our limited knowledge of precipitation derived from interpretation of vegetation and from the short timespan of measured rainfall. However, satellite images show a strong wind direction from S. 70° W., parallel to yardang-troughlike grooves in the landscape, a direction confirmed from general sand movement eastward from sand sources on grus plains and wadi floors (figs. 68, 75, 76). The western lava fields have increased in height from repeated eruptions and epeirogenic uplift to general altitudes of 1,300 m in Ḥarrat Rahaṭ between Aṭ Ṭā'if and Al Madīnah and to a maximum elevation of 2,000 m at Abyaḍ wa Ubayyid in the Ḥarrat Khaybar north of Al Madīnah. This barrier, together with the permanent low-pressure area generated from the rising thermal off the black lava fields and the southwest wind direction, causes orographic convection and precipitation. Farther north, away from the extensive lava fields, the rainfall declines to less than 5 cm until still farther north the westerlies of the Mediterranean climate begin to influence precipitation (fig. 2).

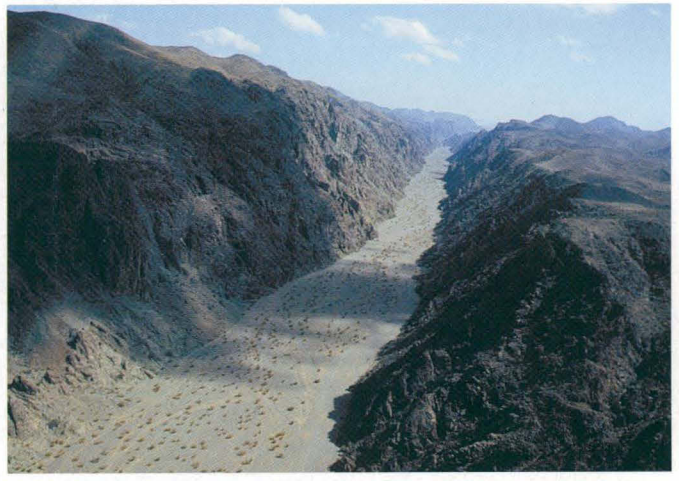

FIGURE 75.—Wādī Tharīb (Ash Schism) yardang valley (lat 26°30′ N., long 37°20′ E.) cut in metavolcanic-metasedimentary greenstone and parallel to a subsidiary Najd fault. View looking N. 85° W.

The Najd pediplain exhibits much evidence of the desert cycle of erosion. Besides accumulations of sand dunes and wind-scoured sinks (sabkhahs), windblown sand, moving along the desert surface, cuts channels parallel to wind direction wherever there is an initial low area such as a schist belt, joint, fault, or other lineation. Once a channel starts, the accumulation of rain, or even dew resulting from the wide diurnal temperature range of the desert, tends to chemically weather the thalweg of the groove or channel. Subsequent sandblast, concentrated in the lowest surfaces of the terrain, removes the chemically or frost-loosened debris, which, together with flash floods, deepens the channel, further concentrating the sandblast and creating streamlined valleys or "yardang troughs" (figs. 68, 76). On the Najd pediplain these features form valleys and ridges that are often at large angles to structural lineations in the basement rocks. Where a transverse wadi deposits coarse flood debris in the main stream, the trough ends because sandblast is missing downwind from the streambed. These yardang troughs are most abundant from lat 24° N. north to the north edge of the shield, particularly east of the wind gaps between Ḥarrat Rahaṭ and Ḥarrat Khaybar and at the north end of Ḥarrat Khaybar, where the yardang troughs are often 10 to 20 m deep, especially in crystalline rocks (fig. 75).

FIGURE 76.—Yardang troughs following one set of joints parallel to the wind direction to N. 70° E. on southern end of Jabal Salmá. Rhyolite dike on the east side (discontinuous ridge on right) which has been dissected by sandblast is downwind from the major yardang troughs. Jabal Salmá is a complex late and posttectonic pluton where two sets of joint systems are apparent. Jabal Shammar region, northeast corner of the Arabian Shield. Vertical aerial photograph; width of aerial view is about 13 km.

REFERENCES CITED

Abul-Haggag, Y., 1961, A contribution to the physiography of northern Ethiopia: London, University of London, Athlone Press, 159 p., 64 figs.

Akaad, M.K., and Noweir, A.M., 1969, Lithostratigraphy of the Hammamat-Um Seleimat district, Eastern Desert, Egypt: Nature, v. 223, no. 5203, p. 284, 285.

_____1978, Geology and lithostratigraphy of the Arabian desert orogenic belt of Egypt between latitudes 25° 35′ and 26° 30′ N. [abs.]: Precambrian Research, v. 6, p. A6.

Alabouvette, B., and Pellaton, C., 1975, Geology and minerals exploration of the Wadi Kamal quadrangle, 24/37D: [France] Bureau des Recherches Geologiques et Minieres Technical Record 75–JED–18, 46 p., 1 fig., 3 maps.

Alabouvette, B., and Villemur, J.R., 1973, Reconnaissance of the Wajid sandstone: [France] Bureau des Recherches Geologiques et Minieres Open-File Report 73–JED–3, 22 p., 17 pls., map, app.

Aldrich, L.T., 1956, Measurement of radioactive ages of rocks: Science, v. 123, p. 871–875.

Aldrich, L.T., Brown, G.F., Hedge, C.E., and Marvin, R.F., 1978, Geochronologic data for the Arabian Shield: U.S. Geological Survey Open-File Report IR (Saudi Arabia)–240, 20 p., 1 fig; *also* USGS Open-File Report 78–75, 22 p.

Aldrich, L.T., Davis, G.L., and James, H.L., 1965, Ages of minerals from metamorphic and igneous rocks near Iron Mountain, Michigan: Journal of Petrology, v. 6, p. 445–472.

Aldrich, L.T., Davis, G.L., Tilton, G.R., and Wetherill, G.W., 1956, Radioactive ages of minerals from the Brown Derby mine and the Quartz Creek granite near Gunnison, Colorado: Journal of Geophysical Research v. 61, p. 215–232.

Al-Rehaili, M.H., and Warden, A.J., 1980, Comparison of the Bir Umq and Hamdah ultrabasic complexes, Saudi Arabia, *in* Cooray, P.G., and Tahoun, S.A., eds., Evolution and mineralization of the Arabian-Nubian Shield: Oxford, Pergamon Press Ltd., Institute for Applied Geology Bulletin 3, v. 4, p. 143–156.

Al-Shanti, A.M.S., 1966, Oolitic iron ore deposits in Wadi Fatima between Jeddah and Mecca, Saudi Arabia: Saudi Arabian Directorate General of Mineral Resources Bulletin 2, 51 p., 13 pls., 33 figs., 8 tables.

_____1974, Al Ji'lani layered basin intrusion, Ad Dawādimī district, Kingdom of Saudi Arabia: Saudi Arabian Directorate General of Mineral Resources Bulletin 12, 45 p., 1 pl., 27 figs., 10 tables.

_____1976, Geology of Ad Dawādimī district, Kingdom of Saudi Arabia: Saudi Arabian Directorate General of Mineral Resources Bulletin 13, scale 1:100,000, 57 p., 33 figs.

Al-Shanti, A.M.S., and Gass, I.G., 1983, The Upper Proterozoic ophiolite melange zones of the easternmost Arabian Shield: Journal of the Geological Society of London, v. 140, p. 867–876, 4 figs., 1 table.

Al-Shanti, A.M.S., and Mitchell, A.H.G., 1976, Late Precambrian subduction and collision in the Al Amar-Idsas region, Arabian Shield, Kingdom of Saudi Arabia: Tectonophysics, v. 30, p. 41–47.

Anderson, R.E., 1977, Geology of Wadi Tarj quadrangle, sheet 19/42A, Kingdom of Saudi Arabia: Saudi Arabian Directorate General of Mineral Resources Geologic Map GM–29, scale 1:100,000, *with* text, 23 p., 7 figs., 1 table.

_____1979, Geology of the Wadi 'Atf and Mayza quadrangles, Kingdom of Saudi Arabia: Saudi Arabian Directorate General of Mineral Resources Bulletin 25, 33 p., 2 maps, scale 1:100,000, 6 illus., 3 tables.

Andreasen, G.E., and Petty, A.J., 1974, Total intensity aeromagnetic map of the northern Hijaz quadrangle and part of the Wadi As Sirhan quadrangle, Kingdom of Saudi Arabia: Saudi Arabian Directorate General of Mineral Resources Geologic Map GM–9, scale 1:500,000.

Andrews, F.W., 1950, 1952, 1956, The flowering plants of the Sudan, v. 1, 2, 3: London, T. Buncle and Co., Ltd., p. 237, 485, 579.

Anonymous, 1972, Ophiolites, Penrose Field Conference: Geotimes, December, p. 24, 25.

Arkin, Y., Beyth, Michael, Dow, D.B., Levitte, D., Haile, Temesgen, and Hailu, Tsegaye, 1971, Geologic map of Mekele sheet, area ND 37–11 Tigre Province: [Addis Ababa] Imperial Ethiopian Government, Ministry of Mines, Geological Survey of Ethiopia Map ND 37–11, scale 1:250,000.

Arno, V., Bakashwin, M.A., Baker, A.Y., Barberi, F., Basahel, A., Dipaola, G.M., Ferrara, G., Gazzaz, M.A., Giuliani, A., Heikel, M., Marinelli, G., Nassief, A.O., Rosi, M., and Santacroce, R., 1980a, Recent basic volcanism along the Red Sea coast: The Al Birk lava field in Saudi Arabia, *in* Zanettin, Bruno, Geodynamic evolution of the Afro-Arabian rift system: Rome, Accademia Nazionale dei Lincei, p. 645–654.

_____1980b, Recent volcanism within the Arabian plate, Preliminary data from Harrats Hadan and Nawasif-Al Buqum, *in* Zanettin, Bruno, Geodynamic evolution of the Afro-Arabian rift system: Rome, Accademia Nazionale dei Lincei, p. 629–643.

Auxiliar Enterprise de Recherches et l'Activities (AUXERAP), 1967: Unpublished report to the Ministry of Petroleum and Mineral Resources, Kingdom of Saudi Arabia, Jiddah.

Baghanem, A.M., 1972, Geology of the lake beds near Turabah, Saudi Arabia: M.S. thesis, South Dakota School of Mines and Technology, Rapid City, S. Dak.

Baghanem, A.M., and Mickelson, J.C., 1972, Geology of the lake beds near Turabah, Saudi Arabia [abs.]: Geological Society of America, Rocky Mountain Section Meeting, Denver, 1972, p. 363.

Baker, P.E., Brosset, R., Gass, I.G., and Neary, C.R., 1973, Jebel al Abyad: A recent alkalic volcanic complex in western Saudi Arabia: Lithos, v. 6, no. 3, p. 291–314.

Bakor, A.R., Gass, I.G., and Neary, C.R., 1976, Jabal al Wask, northwest Saudi Arabia: An Ecocambrian back-arc ophiolite: Earth and Planetary Science Letters, v. 30, no. 1, p. 1–9.

Bartov, Y., Steinitz, G., Eyal, M., and Eyal, Y., 1980, Sinistral movement along the Gulf of Aqaba—Its age and the relation to the opening of the Red Sea: Nature, v. 285, p. 220–222.

Basse, Elaine, Karrenberg, Herbert, Lehman, J.P., Alloiteau, James, and LeFranc, J.P., 1954, Fossiles du jurassique superierur et des "gres de Nubie" de la region de Sanaa (Yemen): Society of the Geology of France Bulletin, ser. 6, v. 4, p. 655–687.

Baubron, J.C., Delfour, J., and Vialette, Y., 1976, Geochronological measurements (Rb/Sr; K/Ar) on rocks of the Arabian Shield, Kingdom of Saudi Arabia: [France] Bureau des Recherches Geologiques et Minieres Open-File Report 76–JED–22, 152 p.

Bayley, R.W., 1972, Geologic map and section of the Wadi Yiba quadrangle, Tihamat ash Sham area [Kingdom of Saudi Arabia]: Saudi Arabian Directorate General of Mineral Resources Geologic Map GM–1, scale 1:100,000.

Bender, Friedrich, 1963, Stratigraphic der "Nubiochen Sandsteine" in Sud-Jordanien: Geologie Jahrb., v. 81, p. 237–276, 11 figs., map.

_____1965, Zur geologie der kupfererzvorkommen am ostrand des Wadi Araba, Jordan: Geologie Jahrb., ser. B, v. 10, p. 16.

_____1968, Geologic map of Jordan-Aqaba Ma'in sheet, Federal Republic of Germany, Bundesanstalt fur Bodenforschung, map, scale 1:250,000.

_____1974a, Explanatory notes on the geological map of the Wadi Araba, Jordan: Geologic Jahrb. ser. B, v. 19, 62 p., 12 figs., 4 pls.

_____1974b, Geology of Jordan: Contributions to the regional geology of the Earth: Berlin, Gebrüder Borntraeger, supp. ed., v. 7, p. 107.

_____1975, Geology of the Arabian Peninsula–Jordan: U.S. Geological Survey Professional Paper 560–I, scale 1:500,000, 36 p.

Berkey, C.P., and Morris, F.K., 1927, Geology of Mongolia: American Museum of Natural History, v. 2, p. 56, 58, 146, 201.

Beyth, Michael, 1973, Correlation of Paleozoic-Mesozoic sediments in northern Yemen and Tigre, northern Ethiopia: Bulletin of the American Association of Petroleum Geologists, v. 57, p. 2440–2443.

Bhutta, M.A., 1970, Geology and economic possibilities of the Wadi Hajir–Wadi al Fara area (23/39 D): Saudi Arabian Directorate General of Mineral Resources Report 363, 123 p. 5 figs. 5 pls.

Bigot, M., 1975, Geology and mineral exploration of the Umm Lajj quadrangle, 25/37C: [France] Bureau des Recherches Geologiques et Minieres Open-File Report 75–JED–7, scale 1:100,000, 47 p., 2 pls.

Bigot, M., and Alabouvette, B., 1976, Geology and mineralization of the Tertiary Red Sea coast of northern Saudi Arabia: [France] Bureau des Recherches Geologiques et Minieres Open-File Report 76–JED–5, 84 p. 7 pls., 11 figs.

Bigot, M., and le Chapelain, J.R., 1973, Geology and mineral exploration of the As Suwaydirah quadrangle, 24/40A: [France] Bureau des Recherches Geologiques et Minieres Open-File Report 73–JED–7, scale 1:100,000, 26 p., 2 pls.

Binda, P.L., 1981, The Precambrian boundary in the Arabian Shield: A review: Jiddah, King Abdul Aziz University, Faculty of Earth Science Bulletin 4, p. 107–120.

Binda, P.L., and Bokhari, M.M., 1980, Chitinozoan-like microfossils in a late Precambrian dolostone from Saudi Arabia: Geology, v. 8, p. 70, 71.

Binda, P.L., and Ramsay, C.R., 1980, Earliest Phanerozoic or latest Proterozoic fossils from the Arabian Shield: Precambrian Research, v. 13, p. 375–377.

Black, R., Morton, W.H., and Rex, D.C., 1975, Block tilting and volcanism within the Afar in the light of recent K/Ar age data, *in* Pilger, A., and Rosler, A., eds., Afar depression of Ethiopia: International Symposium on the Afar Region and Related Rift Problems, Bad Bergzabern, 1974, Proceedings, v. 1: Stuttgart, E. Schweizerbartsche Verlagsbuchhandlung (Nagele u. Obermiller), p. 296–300.

Blank, H.R., Jr., 1977, Aeromagnetic and geologic study of Tertiary dikes and related structures on the Arabian margin of the Red Sea, *in* Hilpert, L.S., ed., Red Sea research 1970–1975: Saudi Arabian Directorate General of Mineral Resources Bulletin 22, p. G1–G18.

Blank, H.R., Jr., and Gettings, M.E., 1985, Geology of the Jizan quadrangle, sheet 16/42B, Kingdom of Saudi Arabia: U.S. Geological Survey Open-File Report 85–0724.

Blank, H.R., Jr., Gettings, M.E., and Kellogg, K.S., 1981, Linear magnetic anomalies onshore and offshore in southwest Saudi Arabia [abs.]: EOS, Transactions of the American Geophysical Union, v. 62, no. 17, p. 407.

Blank, H.R., Jr., Gettings, M.E., Petty, A.J., and Andreasen, G.E., 1980, Total-intensity aeromagnetic map of the Precambrian Arabian Shield, Kingdom of Saudi Arabia: Saudi Arabian Deputy Ministry for Mineral Resources Geoscience map, Technical Record 6, SA–(IR)–344, scale 1:2,000,000. (in color)

Blodget, H.W., and Brown, G.F., 1982, Geological mapping by use of computer-enhanced imagery in western Saudi Arabia: U.S. Geological Survey Professional Paper 1153, 10 p., 2 pls.

Bodenlos, A.J., and Lari, Ahman, 1970, Possibilities of sulphur mineralization in Saudi Arabia: U.S. Geological Survey Open-File Report (IR)SA–113, 29 p., 2 figs.

Bogue, R.G., 1953, Report on geologic reconnaissance in northwestern Saudi Arabia: Saudi Arabian Directorate General of Mineral Resources Open-File Report 27, 30 p.

_____1954, Reconnaissance of mineral deposits in a part of western Saudi Arabia: Saudi Arabian Directorate General of Mineral Resources Open-File Report 31, 66 p.

Bois, J., 1971, Geology and mineral exploration of the northwestern part of the Jabal Damkh quadrangle (sheet 23/44 A): [France] Bureau des Recherches Geologiques et Minieres Open-File Report 71–JED–2, 27 p., 3 app., scale 1:100,000.

Bonatti, Enrico, Emiliani, Cesare, Ostlund, Gote, and others, 1971, Final desiccation of the Afar rift, Ethiopia: Science (AAAS), v. 172, no. 3982, p. 468, 469, sketch map.

Bounny, I., 1975, Geology and mineral exploration of the Wadi Dwayrah area, Kingdom of Saudi Arabia: [France] Bureau des Recherches Geologiques et Minieres Open-File Report 75–JED–25, 72 p., 6 pls., 2 figs.

Boureau, Edourad, 1956, Contribution a l'etude de flores Jurassiques d'Asie, II, Sur des coniferes noveaux d'Arabie Seoudite: Societe Geologique de France Bulletin 6, p. 653–657, 2 figs.

Bowen, R.W., 1971, Graphic normative analysis program: U.S. Geological Survey Computer Contribution 13, 80 p., 2 tables.

Bowler, J.M., 1976, Aridity in Australia: Age, origins, and expressions in aeolian land forms and sediments: Earth-Science Review, v. 12, p. 279–310.

Bramkamp, R.A., Brown, G.F., Holm, D.A., and Layne, N.M., Jr., 1963, Geologic map of the Wadi as Sirhan quadrangle, Kingdom of Saudi Arabia: U.S. Geological Survey Miscellaneous Geologic Investigations Map I–200A, scale 1:500,000 [1964].

Bramkamp, R.A., Gierhart, R.D., Owens, L.D., and Ramirez, L.F., 1963, Geologic map of the western Rub al Khali quadrangle, Kingdom of Saudi Arabia: U.S. Geological Survey Miscellaneous Geologic Investigations Map I–218A, scale 1:500,000 [1964].

Bramkamp, R.A., Ramirez, L.F., Brown, G.F., and Pocock, A.E., 1963, Geologic map of the Wadi ar Rimah quadrangle, Kingdom of Saudi Arabia: U.S. Geological Survey Miscellaneous Geologic Investigations Map I-206A, scale 1:500,000.

Breed, C.S., Fryberger, S.G., Andrews, Sarah, McCanley, Carmilla, Lennartz, Frances, Gebel, Dana, and Horstman, Kevin, 1979, Regional studies of sand seas, using Landsat (ERTS) imagery, *in* McKee, E.D., ed., A study of global sand seas: U.S. Geological Survey Professional Paper 1052, p. 305–397 [1980].

Brown, G.F., 1948, Geology and groundwater of Al Kharj district, Nejd, Saudi Arabia: Ph.D. thesis, Northwestern University, Evanston, Ill., 128 p., 43 pls., 1 fig.

_____1960, Geomorphology of western and central Saudi Arabia: International Geological Congress, 21st, Copenhagen, 1960, Proceedings, pt. 21, p. 150–159.

_____1970, Eastern margin of the Red Sea and the coastal structures in Saudi Arabia: Philosophical Transactions of the Royal Society of London, A–267, p. 75–87.

_____1972, Tectonic map of the Arabian Peninsula: Saudi Arabian Directorate General of Mineral Resources, Arabian Peninsula Map AP–2, scale 1:4,000,000.

Brown, G.F., Delfour, Jacques, and Coleman, R.G., 1972, Geologic formations in the Arabian Shield [summary]: International Geological Congress, 24th, Montreal, 1972, Proceedings, sec. 1, p. 333.

Brown, G.F., and Hase, D.H., 1971, Explanatory note of the tectonics of the Pre-Cambrian Arabian segment of the African Shield: Tectonics of Africa, UNESCO sciences de la terre, v. 6, p. 429, 430.

Brown, G.F., and Jackson, R.O., 1958, Geology of the Tihamat ash Sham quadrangle, Kingdom of Saudi Arabia: U.S. Geological Survey Miscellaneous Geologic Investigations Map I–216A, scale 1:500,000 [1959].

_____1959, Geology of the Asir quadrangle, Kingdom of Saudi Arabia: U.S. Geological Survey Miscellaneous Geologic Investigations Map I-217A, scale 1:500,000.

_____1960, The Arabian Shield: International Geological Congress, 21st, Copenhagen, 1960, Proceedings, pt. 9, p. 69–77.

_____1979, An overview of the geology of western Arabia, *in* Tahoun, S.A., ed., Evolution and mineralization of the Arabian-Nubian Shield: King Abdulaziz University, Institute of Applied Geology Bulletin 3 (Oxford-New York, Pergamon Press Ltd.), v. 1, p. 3–10.

Brown, G.F., Jackson, R.O., Bogue, R.G., and Elberg, E.L., Jr., 1963, Geologic map of the northwestern Hijaz quadrangle, Kingdom of Saudi Arabia: U.S. Geological Survey Miscellaneous Geologic Investigations Map I-204A, scale 1:500,000.

Brown, G.F., Jackson, R.O., Bogue, R.G., and MacLean, W.H., 1963, Geologic map of the southern Hijaz quadrangle, Kingdom of Saudi Arabia: U.S. Geological Survey Miscellaneous Geologic Investigations Map I-210A, scale 1:500,000.

Bureau des Recherches Geologiques et Minieres (BRGM), 1966, Annual report, February 1965 to January 1966: [France] Bureau des Recherches Geologiques et Minieres Open-File Report SG-JED 66-A-7.

Burton, R.F., 1878, The gold mines of Midian and the ruined Midianite cities: London, C. Kegan Paul and Co., 395 p.

Calvez, J.Y., Alsac, C., Delfour, J., Kemp, J., and Pellaton, C., 1983, Geologic evolution of western, central and eastern parts of the northern Precambrian Shield, Kingdom of Saudi Arabia: Saudi Arabian Deputy Ministry for Mineral Resources Open-File Report BRGM-OF-03-17, 57 p., 1 app., geologic sketch map, scale 1:1,000,000.

Cameron, D.K., Jr., 1974, New Triassic palynomorphs from the Arabian Peninsula: Grana, v. 14, p. 4–10, 2 figs., 1 pl.

Chessex, R., Delaloye, M., Muller, J., and Weidmann, M., 1975, Evolution of the volcanic region of Ali Sabieh (T.F.A.I.), in the light of K-Ar age determinations, *in* Pilger, A., and Rosler, A., eds., Afar depression of Ethiopia: International Symposium on the Afar Region and Related Rift Problems, Bad Bergzabern, 1974, Proceedings, v. 1: Stuttgart, E. Schweizerbartsche Verlagsbuchhandlung (Nagele u. Obermiller), p. 221–227.

Church, B.N., 1975, Quantitative classification and chemical comparison of common volcanic rocks: Geological Society of America Bulletin, v. 86, no. 2, p. 257–263.

Civetta, Lucia, La Volpe, Luigi, and Liere, Lucio, 1978, K-Ar ages of the Yemen Plateau: Journal of Volcanology and Geothermal Research, v. 4, p. 307–314.

Cloud, Preston, Awramik, S.M., Morrison, Karen, and Hadley, D.G., 1979, Earliest Phanerozoic or latest Proterozoic fossils from the Arabian Shield: Precambrian Research, v. 10 p. 73–93.

Coleman, R.G., Fleck, R.J., Hedge, C.E., and Ghent, E.D., 1977, The volcanic rocks of southwest Saudi Arabia and the opening of the Red Sea, *in* Hilpert, L.S., ed., Red Sea research, 1970–1975: Saudi Arabian Directorate General of Mineral Resources Bulletin 22, p. D1–D30.

Coleman, R.G., Ghent, E.D., Fleck, R.J., and Griscom, Andrew, 1977, Jabal Shāyi' gabbro in southwest Saudi Arabia: Saudi Arabian Deputy General for Mineral Resources Bulletin 17, 46 p., 1 pl., 32 figs., 16 tables.

Coleman, R.G., Gregory, R.T., and Brown, G.F., 1983, Cenozoic volcanic rocks of Saudi Arabia: U.S. Geological Survey Open-File Report OF-03-93, 86 p., 23 figs., 6 tables.

Coleman, R.G., Hadley, D.G., Fleck, R.G., Hedge, C.T., and Donato, M.M., 1979, The Miocene Tihama Asir ophiolite and its bearing on the opening of the Red Sea, *in* Tahoun, S.A., ed., Evolution and mineralization of the Arabian-Nubian Shield: Institute for Applied Geology Bulletin 3, Oxford, Pergamon Press Ltd., v. 1, p. 173–186.

Cooper, J.A., Stacey, J.S., Stoeser, D.C., and Fleck, R.J., 1979, An evaluation of the zircon method of isotopic dating in the southern Arabian craton: Contributions to Mineralogy and Petrology, v. 68, p. 429–439.

Cotton, C.A., 1942, Climatic accidents in landscape-making: New York, John Wiley and Sons, p. 3–47.

Cox, K.G., Bell, J.D., and Parkhurst, R.J., 1979, The interpretation of igneous rocks: London, George Allen Unwin, p. 14.

Cox, L.R., 1929, Notes on the post-Miocene Ostreidae and Pectinidae of the Red Sea region, with remarks on the geological significance of their distribution: Malacologia, Proceedings, v. 18, p. 165–185.

Dalrymple, G.B., Gromme, C.S., and White, R.W., 1975, Potassium-argon age and paleomagnetism of diabase dikes in Liberia: Initiation of central Atlantic rifting: Geological Society of America Bulletin, v. 86, no. 3, p. 399–411.

Dalrymple, G.B., and Lanphere, M.A., 1969, Potassium-argon dating: San Francisco, W.H. Freeman and Co., p. 172, 173.

Daniel, E.J., 1963, International lexicon of stratigraphy for Jordan: Centre National de la Recherche Scientifique International Geologic Congress, Commission de Stratigraphie, p. 360–369, and addendum, Bender, Friedrich, Litho-stratigraphic and time-stratigraphic subdivision of the Nubian sandstones in S. Jordan, p. 403–419.

Davies, F.B., 1980, Reconnaissance geology of the Duba quadrangle: Saudi Arabian Directorate of Mineral Resources Geologic Map GM-57, scale 1:100,000.

Davis, W.M., 1905, The geographical cycle in an arid climate: Journal of Geology, v. 13, p. 381–407.

_____1933, Geomorphology of mountainous deserts: International Geological Congress, 16th, Washington, D.C., Proceedings, v. 2, p. 703–714.

Delfour, Jacques, 1967, Report on the mineral resources and geology of the Hulayfah-Musayna'ah region (sheet 78, zone 1 north): [France] Bureau des Recherches Geologiques et Minieres Open-File Report JED-66, 138 p., scale 1:100,000.

_____1970, Le groupe de j'balah une nouvelle unite du bouclier Arabe: [France] Bureau des Recherches Geologiques et Minieres Bulletin, ser. 2, sec. 4, no. 4, p. 19–32, 5 figs., 2 tables; *see also* The J'Balah Group, A new unit of the Arabian Shield: [France] Bureau des Recherches Geologiques et Minieres Open-File Report 70-JED-4, 31 p., 5 figs.

_____1975, Vulcanism and mineral deposits of the Arabian-Nubian shield: [France] Bureau des Recherches Geologiques et Minieres Open-File Report 75-JED-24, 35 p., 6 illus., 2 tables.

_____1977, Geology of the Nuqrah quadrangle, sheet 25E, Kingdom of Saudi Arabia: Saudi Arabian Directorate General of Mineral Resources Geologic Map GM-28, scale 1:250,000 *with* text, 32 p., 2 figs.

_____1979a, Geologic map of the Halaban quadrangle, Kingdom of Saudi Arabia: Saudi Arabian Directorate General of Mineral Resources Geologic Map GM-46 A, scale 1:250,000, *with* text, 32 p., 22 figs.

_____1979b, Upper Proterozoic volcanic activity in the northern Arabian Shield, Kingdom of Saudi Arabia, *in* Tahoun, S.A., ed., Evolution and mineralization of the Arabian-Nubian Shield: Institute for Applied Geology Bulletin 3, Oxford, Pergamon Press Ltd., v. 2, p. 59–75.

_____1981, Geologic map of the Al Hissu quadrangle, sheet 24E, Kingdom of Saudi Arabia: Saudi Arabian Directorate General of Mineral Resources Map 58C, scale 1:250,000, *with* text, 47 p., 21 figs.

Delfour, Jacques, and Dhellemmes, R., 1980, Geologic map of the Khaybar quadrangle, sheet 25D, Kingdom of Saudi Arabia: Saudi Arabian Directorate General of Mineral Resources Geologic Map GM–50–A, scale 1:250,000, *with* text, 24 p., 5 figs., 5 tables.

Delfour, Jacques, Dhellemmes, Robert, Elgass, Philippe, Vaslet, Denis, Brosse, Jean-Michel, Le Nindre, Yves-Michel, and Dottin, Olivier, 1982, Geologic map of the ad Dawadimi quadrangle, sheet 24G, Kingdom of Saudi Arabia: Saudi Arabian Deputy Ministry for Mineral Resources Geologic Map GM–60–A, scale 1:250,000, *with* text, 36 p., 21 figs.

De Martonne, E., 1926, Geographie physique, v. 2: Paris, Payot, p. 965–967.

Deuser, W.G., Ross, E.H., and Waterman, L.S., 1976, Glacial and pluvial periods: Their relationship revealed by Pleistocene sediments of the Red Sea and Gulf of Aden: Science, v. 191, p. 1168–1170.

Dodge, F.C.W., 1979, The Uyaijah ring structure, Kingdom of Saudi Arabia: U.S. Geological Survey Professional Paper 774–E, p. E1–E17.

Dodge, F.C.W., Fleck, R.J., Hadley, D.G., and Millard, H.T., Jr., 1979, Geochemistry and $^{87}Sr/^{86}Sr$ ratios of Halaban rocks of the Central Arabian Shield, *in* Tahoun, S.A., ed., Evolution and mineralization of the Arabian-Nubian Shield: Institute for Applied Geology Bulletin 3 (Oxford, Pergamon Press Ltd.), v. 2, p. 153–163.

Doughty, C.M., 1888, Travels in Arabia deserta: (2 v.): Cambridge, Cambridge University Press. Reprinted 1920, 1921, New York, Random House; v. 1, 621 p., v. 2, 690 p., map.

Dow, D.B., Beyth, Michael, and Hailu, Tsegaye, 1971, Paleozoic glacial rocks recently discovered in northern Ethiopia: Geologic Magazine, v. 108, no. 1, p. 53–60.

Dubay, Lavesloo, 1969, Water development surveys, geological investigations: Unpublished report, Italconsult, for Ministry of Agriculture and Water, Kingdom of Saudi Arabia.

Durozoy, G., 1972, Hydrogeologie des basaltes du Harrat Rahat: [France] Bureau des Recherches Geologiques et Minieres Bulletin, ser. 2, sec. 3, no. 2, p. 37–50, 6 figs., 2 tables.

Duyverman, H.J., Harris, N.B.W., and Hawkesworth, C.J., 1982, Crustal accretion in the Pan African: Nd and Sr isotope evidence from the Arabian Shield: Earth and Planetary Science Letters, v. 59, p. 315–326.

Eijkelboom, Garet, 1966, The mineral resources and geology of the Jibal Damkh-Arwah region (sheet 115, zone II): [France] Bureau des Recherches Geologiques et Minieres Open-File Report 66–A–13, 18 p., 1 fig., 9 app., scale 1:100,000.

_____1969, BRGM mineral exploration and geological mapping, *in* Mineral resources research 1967–68: Saudi Arabian Directorate General of Mineral Resources, p. 81–86.

Von Engeln, O.D., 1942, Geomorphology: New York, Macmillan Co., p. 399–438.

Eyal, M., Eyal, Y., Bartov, Yosi, and Steinitz, G., 1981, The tectonic development of the western margin of the Gulf of Elat (Aqaba) Rift: Tectonophysics, v. 80, p. 39–66.

Fairbridge, R.W., 1977, Global climate change during the 13,500 b.p. Gothenburg geomagnetic excursion: Nature, v. 265, February 1977, p. 340, 341, 1 fig.

Fairer, G.M., 1982, Reconnaissance geology of the Sabya quadrangle, sheet 17/42 D, Kingdom of Saudi Arabia: Saudi Arabian Deputy Ministry for Mineral Resources: Geoscience Map GM-68, 26 p., scale 1:100,000, *with* text, 12 p.

_____1982, Reconnaissance geology of the Ad Darb quadrangle, sheet 17/42 A, Kingdom of Saudi Arabia: Saudi Arabian Deputy Ministry for Mineral Resources map series, USGS Open-File Report OF–02–87, scale 1:100,000.

Faure, Gunter, and Powell, J.L., 1972, Strontium isotope geology: Berlin, Springer-Verlag, 188 p.

Finlay, and Marwick, 1937, New Zealand Geological Survey Paleontology Bulletin 15, p. 41, figs. 4, 5, pl. 5.

Fleck, R.J., 1985, Age of diorite-granodiorite gneisses of the Jiddah-Makkah region, Kingdom of Saudi Arabia: Saudi Arabian Deputy Ministry for Mineral Resources Professional Paper PP–2, p. 21–27.

Fleck, R.J., Coleman, R.G., Cornwall, H.R., Greenwood, W.R., Hadley, D.G., Schmidt, D.L., Prinz, W.C., and Ratte, J.C., 1976, Geochronology of the Arabian Shield, western Saudi Arabia, K-Ar results: Geological Society of America Bulletin, v. 87, p. 9–21.

Fleck, R.J., Greenwood, W.R., Hadley, D.G., Anderson, R.E., and Schmidt, D.L., 1980, Rubidium-strontium geochronology and plate-tectonic evolution of the southern part of the Arabian Shield: U.S. Geological Survey Professional Paper 1131, 38 p.

Fleck, R.J., and Hadley, D.G., 1985, Ages and strontium initial ratios of plutonic rock in a transect of the Arabian Shield: U.S. Geological Survey Open-File Report 85–0727, 43 p., 19 figs.

Frakes, L.A., Kemp, E.M., and Crowell, J.C., 1975, Late Paleozoic glaciation: Part 6, Asia: Geological Society of America Bulletin, v. 86, p. 454–464.

Freund, R., Garfunkel, Zri, Zak, I., Goldberg, M., Weissbrod, T., and Derin, B., 1970, The shear along the Dead Sea rift: Philosophical Transactions of the Royal Society of London, v. 267A, p. 107–130.

Friedman, G.M., 1965, A fossil shoreline reef in the Gulf of Elat (Aqaba): Israel Journal of Earth Science, v. 14, p. 86–90.

Frisch, W., and Al-Shanti, A.M.S., 1977, Ophiolite belts and the collision of island arcs in the Arabian Shield: Tectonophysics, v. 43, p. 292–306.

von Gaertner, H.R., and Schurenburg, H., 1954, Final report, Geological research in western Arabia: Hannover, Amt fur Bodenforschung, 103 p.

Gass, I.G., 1970, The evolution of volcanism in the junction area of the Red Sea, Gulf of Aden and Ethiopian rifts: Philosophical Transactions of the Royal Society of London, v. 267A, p. 369–381.

Gettings, M.E., 1977, Delineation of the continental margin in the southern Red Sea region from new gravity evidence, *in* Hilpert, L.S. ed., Red Sea research 1970-1975: Saudi Arabian Directorate General of Mineral Resources Bulletin 22, p. K1–K11.

_____1979, Preliminary results of the Sabkhah Hazawza gravity project, Wadi as Sirhan area, Kingdom of Saudi Arabia: U.S. Geological Survey Open-File Report 79–1660, 12 p., 4 figs.

_____1982, Heat-flow measurements at shot points along the 1978 Saudi Arabia seismic deep-refraction line, Part 2: Discussion and interpretation: U.S. Geological Survey Open-File Report 82–0794, 43 p.

Geukens, F.P.M., 1960, Contribution a la geologie du Yemen: Institut Géologique de L'Université de Louvain, Memoires, v. 21, p. 122–179, 8 pls., geol. map.

_____1966, Geology of the Arabian Peninsula, Yemen: U.S. Geological Survey Professional Paper 560–B., 23 p., 17 figs.

Ghent, E.D., Coleman, R.G., and Hadley, D.G., 1980, Ultramafic inclusions and host alkali olivine basalts of the southern coastal plain of the Red Sea, Saudi Arabia: American Journal of Science, v. 280A, p. 499–527.

Gillmann, Michel, 1968, Primary results of a geological and geophysical reconnaissance of the Jizan coastal plain in Saudi Arabia: American Institute of Mining and Metallurgical Engineers Regional Technical Symposium, 2d, Dhahran, Saudi Arabia, 1968, Report, p. 159–209.

Girdler, R.W., and Styles, P., 1974, Two stage Red Sea floor spreading: Nature, v. 247, p. 7–11.

Goldberg, M., 1963, The geology of Tiran Island: Proceedings of the Israel Geological Society, v. 12, p. 83, 84.

Goldberg, M., and Yaron, F., 1978, The Th^{230}/U^{234} ages of raised Pleistocene marine terraces on the Island of Tiran and the southeastern coast of Sinai with some tectonic implications: International Congress on Sedimentology, 10th, Jerusalem, July 9–14, 1978, Abstracts, v. 1, p. 258, 259.

Goldsmith, Richard, 1966, Section of the Fatimah Formation near Bahrah, Saudi Arabia: Saudi Arabian Directorate General of Mineral Resources–U.S. Geological Survey Open-File Report (IR)SA–65, 6 p., 1 fig.

Gonzales, Louis, 1973, Geologic map and sections of the Jabal 'In quadrangle: Saudi Arabian Directorate General of Mineral Resources Geologic Map GM-2, scale 1:100,000, *with* text, 7 p.

Greene, R.C., 1983, Reconnaissance geology of the Thaniyah quadrangle, sheet 20/42C, Kingdom of Saudi Arabia: U.S. Geological Survey Open-File Report 83–0448, 25 p., scale 1:100,000.

Greenwood, W.R., 1975a, Geology of the Al 'Aqiq quadrangle, sheet 20/41D: Saudi Arabian Directorate General of Mineral Resources Geologic Map GM–23, scale 1:100,000.

_____1975b, Geology of the Biljurshi quadrangle, sheet 19/41B, *with a section on* Geophysical investigations by G.E. Andreasen *and a section on* Geochemical investigations and mineral resources by V.A. Trent and T.H. Kiilsgaard: Saudi Arabian Directorate General of Mineral Resources Geologic Map GM–25, scale 1:100,000.

_____1975c, Geology of the Jabal Ibrahim quadrangle, sheet 20/41C, Kingdom of Saudi Arabia, *with a section on* Economic geology by R.G. Worl and W.R. Greenwood: Saudi Arabian Directorate General of Mineral Resources Geologic Map GM-22 *with* text, 18 p., scale 1:100,000.

_____1975d, Reconnaissance geology of the Jabal Shada quadrangle, sheet 19/41A, Kingdom of Saudi Arabia: Saudi Arabian Directorate General of Mineral Resources Geologic Map GM–20, scale 1:100,000.

_____1979, Geology of the An Nimas quadrangle, sheet 19/42C, Kingdom of Saudi Arabia: Saudi Arabian Directorate General of Mineral Resources Geologic Map GM–37, scale 1:100,000.

Greenwood, W.R., Anderson, R.E., Fleck, R.J., and Roberts, R.J., 1980, Precambrian geologic history and plate tectonic evolution of the Arabian Shield: Saudi Arabian Directorate General of Mineral Resources Bulletin 24, 35 p.

Greenwood, W.R., and Brown, G.F., 1973, Petrology and chemical analyses of selected plutonic rocks from the Arabian Shield, Kingdom of Saudi Arabia: Saudi Arabian Directorate General of Mineral Resources Bulletin 9, 9 p.

Greenwood, W.R., Hadley, D.G., Anderson, R.E., Fleck, R.J., and Schmidt, D.L., 1976, Late Proterozoic cratonization in southwestern Saudi Arabia: Philosophical Transactions of the Royal Society of London, A. v. 280, p. 517–527.

Gregory, R.T., Coleman, R.G., and Brown, G.F., 1982, Cenozoic volcanic rocks of Saudi Arabia: Evidence from the continent for a two-stage opening of the Red Sea: Geological Society of America Abstracts, v. 14, no. 7, p. 502.

Grolier, M.J., and Overstreet, W.C., 1978, Geologic map of the Yemen Arab Republic (Ṣan'ā'): U.S. Geological Survey Miscellaneous Geologic Investigations Map I–1143–B, scale 1:500,000.

Guilcher, Andre, 1952, Formes et processus d'erosion sur les recifs coralliens du nord du bac Farasan (Mer Rouge) [Erosion forms and processes on coral reefs of the northern part of the Farasan bank]: Revue de Geomorphologie Dynamique, An. 3, no. 6, p. 261–274 (French and English summaries).

Gvirtzman, Gdaliahu, Buchbinder, Binyamin, Sneh, Amihai, Nir, Yaacov, and Friedman, G.M., 1977, Morphology of the Red Sea fringing reefs: A result of the erosional pattern of the last-glacial low-stand sea level and the following Holocene recolonization: Memoirs du Bureau des Recherches Geologiques et Minieres (France), no. 89, 12 p.

Hadley, D.G., 1973, Geology of the Sahl al Matran quadrangle, Northwestern Hijaz, Kingdom of Saudi Arabia: Saudi Arabian Directorate General of Mineral Resources Geologic Map GM–6, scale 1:100,000, *with* text, 11 p.

_____1974, The taphrogeosynclinal Jubaylah group in the Mashhad area, Northwestern Hijaz, Kingdom of Saudi Arabia: Saudi Arabian Directorate General of Mineral Resources Bulletin 10, 18 p., 19 figs., 2 tables.

_____1975a, Geology of the Al Qunfudhah quadrangle, sheet 19/41C, Kingdom of Saudi Arabia: Saudi Arabian Directorate General of Mineral Resources Geologic Map GM–19, scale 1:100,000, *with* text, 11 p.

_____1975b, Geology of the Qal'at as Sawrah quadrangle, sheet 26/38D: Kingdom of Saudi Arabia: Saudi Arabian Directorate General of Mineral Resources Geologic Map GM–24, scale 1:100,000, *with* text, 28 p.

_____1975c, Geology of the Wadi Hali quadrangle, sheet 18/41B, Kingdom of Saudi Arabia: Saudi Arabian Directorate General of Mineral Resources Geologic Map GM–21, scale 1:100,000, *with* text, 19 p.

_____1976, Geology of the Bi'r Juqjuq quadrangle, sheet 21/43D, Kingdom of Saudi Arabia: Saudi Arabian Directorate General of Mineral Resources Geologic Map GM–26, scale 1:100,000, *with* text, 30 p.

_____1979, Reconnaissance geology of the Musaylim quadrangle, sheet 19/40B, Kingdom of Saudi Arabia: Saudi Arabian Directorate General of Mineral Resources Geologic Map GM–34, scale 1:100,000, *with* text, 7 p.

_____1982, Reconnaissance geology of the Manjamah quadrangle, sheet 18/41A, Kingdom of Saudi Arabia: U.S. Geological Survey Open-File Report 82–0285, 13 p., scale 1:100,000.

Hadley, D.G., and Fleck, R.J., 1980a, Reconnaissance geologic map of the Al Lith quadrangle, sheet 20/40C, Kingdom of Saudi Arabia: Saudi Arabian Directorate General of Mineral Resources Geologic Map GM–32, scale 1:100,000, *with* text, 10 p.

_____1980b, Reconnaissance geologic map of the Jabal Afaf quadrangle, sheet 20/40D, Kingdom of Saudi Arabia: Saudi Arabian Directorate General of Mineral Resources Geologic Map GM–33, scale 1:100,000, *with* text, 10 p.

Hall, S.A., 1980, A total intensity magnetic anomaly map of the Red Sea and its interpretation: U.S. Geological Survey Open-File Report 80–0131, 271 p.

Hall, S.A., Andreasen, G.E., and Girdler, R.W., 1977, Total-intensity magnetic anomaly map of the Red Sea and adjacent coastal areas: A description and preliminary interpretation, *in* Red Sea research 1970–1975: Saudi Arabian Directorate General of Mineral Resources Bulletin 22, p. F1–F15.

Halpern, M., 1980, Rb-Sr "Pan-African" isochron ages of Sinai/igneous rocks: Geology, v. 8, p. 48–50.

Hantzschel, Walter, 1975, Trace fossils and problematics: Geological Society of America, Treatise on Invertebrate Paleontology, pt. W., misc., supp. 1, p. W38, W39.

Hashad, A.H., 1980, Present status of geochronological data on the Egyptian basement complex, *in* Cooray, P.G., and Tahoun, S.A., eds., Evolution and mineralization of the Arabian-Nubian Shield: Institute for Applied Geology Bulletin 3, Oxford, Pergamon Press Ltd., v. 3, p. 31–46.

Hatcher, R.D., Jr., Zietz, Isidore, Regan, R.D., and Abu-Ajamieh, Muhammad, 1981, Sinistral strike-slip motion on the Dead Sea rift: Confirmation from new magnetic data: Geology, v. 9, p. 458–462.

Healy, J.H., Mooney, W.D., Blank, H.R., Gettings, M.E., Kohler, W.M., Lamson, R.J., and Leone, L.E., 1983, Saudi Arabian

seismic deep-refraction profile: Final project report: Saudi Arabian Deputy Ministry for Mineral Resources Open-File Report USGS-OF-02-37; also U.S. Geological Survey Open-File Report 83-390, 429 p.

Hedge, C.E., 1984, Precambrian geochronology of part of northwestern Saudi Arabia, Kingdom of Saudi Arabia: U.S. Geological Survey Open-File Report 84-381, 12 p.

Hemer, D.O., 1968, Diagnostic palynologic fossils from Arabia: American Institute of Mining Engineers Regional Technical Symposium, 2d, Dhahran, Saudi Arabia, 1968 Report, p. 311-315.

Higazy, K.A., and El-Ramly, M.F., 1960, Potassium-argon ages of some rocks from the eastern desert of Egypt: United Arab Republic Geological Survey and Mining Department Paper 7, 19 p.

Hotzl, H., Lippolt, H.J., Maurin, V., Moser, H., and Rauert, W., 1979, Quaternary studies on the recharge area situated in crystalline rock regions, *in* Al-Sayari, S.S., and Zotl, J.G., eds., Quaternary period in Saudi Arabia: Vienna and New York, Springer-Verlag, p. 230-236.

Huber, Charles, 1891, Journal d'un voyage en Arabie 1883-1884: Paris, Imprimerie Nationale, 778 p. (Illustrated atlas, with list and brief descriptions of Huber's rock collection)

Hudson, R.G.S., 1958, *in* Discussion on King's paper, Basic palaeography of Gondwanaland during the late Paleozoic and Mesozoic eras: Geological Society of London, Proceedings, v. 114, p. 70, 71.

Hunziker, J.C., 1979, Potassium-argon dating: Lectures in isotope geology; New York, Springer-Verlag, p. 58-63.

Irvine, T.N., and Baragar, W.R.A., 1971, A guide to the chemical classification of the common volcanic rocks: Canadian Journal of Earth Sciences, v. 8, no. 5, p. 523-548.

Jackaman, Barry, 1972, Genetic and environmental factors controlling the formation of the massive sulphide deposits of Wadi Bidah and Wadi Wassat, Saudi Arabia: Saudi Arabian Directorate General of Mineral Resources Technical Record TR 1972-1, p. 243.

Jackson, R.O., Bogue, R.G., Brown, G.F., and Gierhart, R.D., 1963, Geologic map of the southern Najd quadrangle, Kingdom of Saudi Arabia: U.S. Geological Survey Miscellaneous Geologic Investigations Map I-211 A, scale 1:500,000.

Japanese Geological Mission [Okuni, Shizuka; Komura, Kojiro; Hatanaka, Takefumi; Iso, Miyoji; and Kuwagata, Hisao], 1965 [rev. 1967 by Hirayama, Ken], Gold deposits in Al Wajh district with data on limestone and water resources: Japanese Geological Survey, Saudi Arabian Mission Open-File Report JGM-A-1, 216 p., 151 illus.

Japanese Geological Mission, 1967, Report on the iron ore deposits in the Wadi Sawawin district: Japanese Geological Survey, Saudi Arabian Mission Report JGM-A-2. (Later revised and published as Ministry of Petroleum and Mineral Resources Technical Record TR-1978-11, 62 p., 15 figs., 8 tables.)

Johnson, R.F., and Trent, V.A., 1967, Mineral reconnaissance of the Wadi as Surr quadrangle, Kingdom of Saudi Arabia: Saudi Arabian Directorate General of Mineral Resources Mineral Investigations Map MI-5, scale 1:100,000.

_____1968, Mineral reconnaissance of the Wadi al 'Ays quadrangle, Kingdom of Saudi Arabia: Saudi Arabian Deputy Ministry of Mineral Resources Open-File Report USGS-(IR)SA-45, map scale 1:100,000, 8 p., 1 fig.

Jones, P.W., 1976, Age of the lower flood basalts of the Ethiopian Plateau: Nature, v. 261, p. 567-569.

Jones, P.W., and Rex, D.C., 1974, New dates from the Ethiopian Plateau volcanics: Nature, v. 252, p. 218, 219, 1 fig.

Jordi, H.A., and Lonfat, F., 1963, Stratigraphic subdivision and problems in Upper Cretaceous-Lower Tertiary deposits in northwestern Libya: Revue l'Institut Francais du Petrole, Revue, v. 18, pt. 2, p. 1428-1436.

Kabbani, F.K., 1970, Geophysical and structural aspects of the central Red Sea rift valley: Philosophical Transactions of the Royal Society of London, v. A-267, p. 89-97.

Kahr, V.P., 1961, Geology north of Yanbu al Bahr: Saudi Arabian Directorate General of Mineral Resources Open-File Report 126, 213 p., 289 figs., 3 pls.

Kanaan, F.M., 1979, The geology, petrology, and geochemistry of the granitic rocks of Jabal al Hawshah and vicinity, Jabal al Hawshah quadrangle, Kingdom of Saudi Arabia: Saudi Arabian Directorate General of Mineral Resources Bulletin 23, 114 p., 1 pl., 18 tables.

Karpoff, Roman, 1955, Observations preliminaries sur le socle Ancien de L'Arabie: Societe de Geologique de France, Comptes rendus, p. 105, 106.

_____1956, Sur quelques series sedimentaires d'Arabie occidentale et centrale: Societe de Geologique de France, Comptes rendu Sommaire des Seances, no. 2, Sea. Jan 23, p. 17, 18.

_____1957a, Esquisse geologique de l'Arabie Seoudite: Geologique Societe de France, 6 ser., v. 7, p. 672-676.

_____1957b, Sur l'existence du Maestrichtien au nord de Djeddah (Arabie Seoudite): Academie des Sciences [Paris], Compter rendu, t. 245, no. 16, p. 1322-1324.

_____1960, L'antecambrian de la peninsula Arabique: International Geologic Congress, 21st, Copenhagen, 1960, pt. 9, p. 80-93.

Kazmin, V., 1971, Precambrian of Ethiopia: Nature, Physical Science, v. 230, no. 16, p. 176, 177, sketch map.

Kellogg, K.S., and Blank, H.R., Jr., 1982, Paleomagnetic evidence bearing on Tertiary tectonics of the Tihamat Asir coastal plain, southwestern Saudi Arabia: U.S. Geological Survey Open-File Report 82-1047, 40 p.

Kemp, John, 1981, Geology of the Wadi Al 'Ays quadrangle, sheet 25C, Kingdom of Saudi Arabia: Saudi Arabian Deputy Ministry for Mineral Resources Geologic Map GM-53-A, scale 1:250,000, *with* text, 39 p.

Kemp, John, Gros, Yves, and Prian, Jean-Pierre, 1982, Geologic map of the Mahd adh Dhahab quadrangle, sheet 23E, Kingdom of Saudi Arabia: Saudi Arabian Deputy Ministry for Mineral Resources Geologic Map GM-64 A, scale 1:250,000, *with* text, 39 p.

Kemp, John, Pelleton, C., and Calvez, J.Y., 1980, Geochronological investigations and geologic history in the Precambrian of northwestern Saudi Arabia: [France] Bureau des Recherches Geologiques et Minieres Open-File Report 01-1, 120 p., 41 figs.

Kiilsgaard, T.H., Greenwood, W.R., Puffett, W.P., Haqvi, Mohammad, Roberts, R.J., Worl, R.G., Merghelani, Habib, Flanigan, V.J., and Gazzaz, A.R., 1978, Mineral exploration in the Wadi Bidah district, 1971-1976, Kingdom of Saudi Arabia: U.S. Geological Survey Open-File Report 78-771, 95 p., 17 figs.

Kingsley, Charles, 1873, Town geology: London, Strahan and Co., p. 224.

Kluyver, H.M., Bege, V.B., Smith, G.H., Ryder, J.M., and Van Eck, M., 1981, Sirhan-Turayf phosphate project: Results of work carried out under the phosphate agreement, 29th Dhual Hijjah 1398-30th Jumad Thani 1401 [29th November 1978-4th May 1981]: Saudi Arabian Deputy Ministry for Mineral Resources Technical Record RF-TR-01-5, 77 p.

Kober, Leopold, 1911, Report on a trip through Hijaz: Academy of Science, Vienna, Anzeiger, v. 48, p. 285, 286.

_____1919, The northern Hejaz: Academy of Natural Science and Mathematics, Vienna, K.L. Denkschiften, v. 96, p. 794-813.

Kroner, A., Roobol, M.J., Ramsay, C.R., and Jackson, N.J., 1979, Pan-African ages of some gneissic rocks in the Saudi Arabian Shield: Journal of the Geological Society, London, v. 136, pt. 4, p. 455-461.

Kruck, Wolfgang, and Thiele, Joachim, 1983, Late Paleozoic glacial deposits in the Yemen Arab Republic: Geol. Jahr. Reihe B. Heft. 46, 32 p., 3 figs., 7 pls.

Ku, T.L., 1969, Uranium series isotopes in sediments from the Red Sea hot-brine area, *in* Degens, E.T., and Ross, D.A., eds., Hot brines and recent heavy metal deposits in the Red Sea: New York, Springer-Verlag, p. 512–524.

Kuno, H., 1966, Lateral variation of basalt magma type across continental margins and island arcs: Volcanologique Bulletin, v. 29, p. 195–222.

Lamare, Pierre, 1923, Sur l'existence do granites alcaline dans le Shammar (Arabie), et sur la constitution geologique de cette region: Societe Geologique de France, Comp. Rend. Som. Seances, no. 16, p. 188–190.

_____1930a, Etudes Geologie en Ethiopie, Somalie, et Arabe Meridionale: Societe Geologique de France Memoir 14, new ser., tome 6, p. 32, 33.

_____1930b, Nature et extension des depots secondaires dans l'Arabie, l'Ethiopie, et les pays Somalia: Societe Geologique de France Memoir 14 new ser., tome 4, p. 49–55.

Lamare, Pierre, and Carpentier, C.A., 1932, Vegetaux fossiles du Yemen: Societe Geologique de France Bulletin, ser. 5, v. 2, p. 83–92.

Laurent, D., 1976, A perlite deposit at Jabal Shama: [France] Bureau des Recherches Geologiques et Minieres Open-File Report 76–JED–24, 18 p., sketch map.

Le Maitre, R.W., 1976, The chemical variability of some common igneous rocks: Journal of Petrology, v. 17, pt. 4, p. 589–633.

Lenz, H., Bender, F., Besang, C., Harre, W., Kreuzer, H., Muller, P., and Wendt, I., 1972, The age of early tectonic events in the zone of the Jordan Geosuture: International Geology Congress, 24th, Montreal, Proceedings, sec. 3, p. 371–379.

Letalenet, J., 1974, Geology and mineral exploration of the Jabal al Murdamah quadrangle, sheet 23/43A: [France] Bureau des Recherches Geologiques et Minieres Open-File Report 74–JED–10, 35 p., map, scale 1:100,000.

_____1979, Geologic map of the Afif quadrangle, sheet 23F: Saudi Arabian Directorate General of Mineral Resources Geologic Map GM–47–A, scale 1:250,000, *with* text, 20 p.

Liddicoat, W.K., 1975, A review of Wadi Sawawin diamond drill corelogs and interpretation (Interim report 1): Saudi Arabian Directorate General of Mineral Resources Technical Record TR–1975–5, 13 p.

Lopoukhine, M., and Stietjes, L., 1976, Geothermal reconnaissance in the Kingdom of Saudi Arabia: [France] Bureau des Recherches Geologiques et Minieres Open-File Report 76–JED–18, 39 p., 11 figs., 3 tables, 4 app.

Luce, R.W., Bagdady, A.Y., and Roberts, R.J., 1976, Geology and ore deposits of the Mahd adh Dhahab district, Kingdom of Saudi Arabia: U.S. Geological Survey Open-File Report 76–0865, 28 p., 1 pl., 13 figs.

McClure, H.A., 1977, Radiocarbon chronology of late Quaternary lakes in the Arabian desert: Nature, v. 263, no. 5580, p. 755, 756.

_____1978a, Ar Rub' al Khali, *in* Al-Sayari, S.S., and Zotl, J.G., eds., Quaternary period in Saudi Arabia: Vienna and New York, Springer-Verlag, p. 252–263.

_____1978b, Early Paleozoic glaciation in Arabia; Paleogeography, Paleoclimatology, Paleoecology, v. 25, p. 315–326.

_____1980, Permian-Carboniferous glaciation in the Arabian Peninsula: Geological Society of America Bulletin, pt. 1, v. 91, p. 707–712.

McDougall, I., Morton, W.H., and Williams, M.A.J., 1975, Age and rates of denudation of Trap Series basalts at Blue Nile Gorge, Ethiopia: Nature, v. 254, p. 207–209.

Madden, C.T., Naqvi, I.M., Whitmore, F.C., Jr., Schmidt, D.L., Langston, Wann, Jr., and Wood, R.C., 1980, Paleocene vertebrates from coastal deposits in Harrat Hadan area, Aṭ Ṭā'if region, Kingdom of Saudi Arabia: U.S. Geological Survey Open-File Report 80–0227, 32 p., 5 figs., 4 tables.

Mandaville, J.P., Jr., 1973, A contribution to the flora of Asir, southwestern Arabia: Miami, Field Research Publications, 13 p.

Masoli, Mario, 1969, The Mukawwar Formation ostracofauna (Upper Cretaceous–Paleocene) of the Maghersum well 1 (Sudan): African Micropaleontological Colloquium, 3d, National Information and Documentation Center, Cairo, 1969, Proceedings, no. 5, p. 329–340.

Megrue, G.H., Norton, E., and Strangway, D.W., 1972, Tectonic history of the Ethiopian rift as deduced by K-Ar ages and paleomagnetic measurements of basaltic dikes: Journal of Geophysical Research, v. 77, no. 29, p. 5744–5754.

Meissner, C.R., Jr., and Ankary, A.O., 1972, Phosphorite deposits in the Sirhan-Turayf basin, Kingdom of Saudi Arabia: Saudi Arabian Directorate General of Mineral Resources, Mineral Resources Report of Investigations 2, 27 p.

Merghelani, H.M., and Irvine, J.I., 1981, Seismicity of the Yanbu region: Available from Saudi Arabian Directorate General of Mineral Resources, 32 p.

Meunier, M.S., 1888, Fossiles noveau provenant d'Arabie: Le Naturaliste 10, p. 204, 205.

_____1891, Charles Huber, Journal of a Journey in Arabia (1883–1884): Paris National Press.

Michelson, H., 1978, Stratigraphy of the lake area, *in* Serruya, C., ed., Lake Kinnert: The Hague, W. Junkby, Pub., p. 17–23.

Ministry of Petroleum and Mineral Resources, 1977, Annotated bibliography 1970–1975 A.D.: Saudi Arabian Directorate General of Mineral Resources Bulletin 20, 98 p.

_____1980, Annotated bibliography pre-1970 A.D.: Saudi Arabian Directorate General of Mineral Resources Bulletin 19, 126 p.

_____1981, Annotated bibliography 1396–1400 A.H. (1976–1980 A.D.): Saudi Arabian Deputy Ministry for Mineral Resources Bulletin 27, 102 p.

Miyashiro, Akiho, 1974, Volcanic rocks series in island arcs and active continental margins: American Journal of Science, v. 274, no. 4, p. 321–355.

Moltzer, J.G., and Binda, P.L., 1981, Micropaleontology and palynology of the middle and upper members of the Shamaysi Formation, Saudi Arabia: Bulletin of the Faculty of Earth Sciences, King Abdulaziz University, no. 4, p. 57–74, app.

Mooney, W.D., 1980, IASPEI workshop: Seismic modeling of laterally varying structures: EOS, Transactions of the American Geophysical Union, v. 62, no. 2, p. 19, 20.

Moore, J.M., 1979, Tectonics of the Najd Transcurrent Fault System, Saudi Arabia: Journal of the Geological Society of London, v. 136, p. 441–454.

Musil, Alois, 1926, The Northern Hegaz, *in* Oriental explorations and studies, v. 1, no. 1: New York, American Geographical Society, 215 p.

Nasseef, A.D., and Gass, I.G., 1977, Granitic and metamorphic rocks of the Taif area, western Saudi Arabia: Geological Society of America Bulletin, v. 88, no. 12, p. 1721–1730.

Nebert, Karl, 1969, Geology of the Jabal Samran and Jabal Farasan region: Saudi Arabian Deputy Ministry for Mineral Resources Bulletin 4, 32 p., 51 figs., 4 pls., 2 tables.

Nebert, K., Alshaibi, A.A., Awlia, M., Bounny, I., Nawab, Z.A., Sharief, O.H., Sherbini, O.A., and Yeslam, A.H., 1974, Geology of the area north of Wadi Fatima, Kingdom of Saudi Arabia: Centre for Applied Geology [Jiddah] Bulletin 1, 31 p., 38 figs., 5 pls.

Neuman Van Padang, M., 1963, Catalogue of the active volcanoes of the world including solfatara fields: Part 16, Arabia and the

Indian Ocean: International Association of Volcanology, p. 3.1–14.

Overstreet, W.C., 1973, Contributions to the prehistory of Saudi Arabia, 1: Miami, Field Research Projects, 11 p., 99 figs., 3 tables.

Overstreet, W.C., Overstreet, E.F., and Goudarzi, G.H., 1973, Mineralogical and chemical investigations of the laterite in the As Sarat Mountains, Kingdom of Saudi Arabia: U.S. Geological Survey Saudi Arabian Project Report 46, 66 p.

Overstreet, W.C., Stoeser, D.B., Overstreet, E.F., and Goudarzi, G.H., 1977, Tertiary laterite of the As Sarat Mountains, Asir Province: Saudi Arabian Directorate General of Mineral Resources Bulletin 21, 24 p., 1 pl., scale 1:100,000, 11 figs.

Pallister, J.S., 1983, Reconnaissance geologic map of the Harrat Tuffil quadrangle, sheet 20/39B, Kingdom of Saudi Arabia: U.S. Geological Survey Open-File Report 83–332, 3 pls., scale 1:100,000, 3 app.

Pallister, J.S., and Hopson, C.A., 1981, Samail ophiolite plutonic suite: Field relations, phase variation, cryptic variation, and layering, and a model of a spreading ridge magma chamber: Journal of Geophysical Research, v. 86, no. B4, p. 2593–2644.

Pellaton, Claude, 1976, Geology and mineral exploration of the Wadi Dahgalah quadrangle, sheet 26/37D, Kingdom of Saudi Arabia: [France] Bureau des Recherches Geologiques et Minieres Report 76–JED–10, scale 1:100,000, *with* text, 24 p.

_____1979, Geologic map of the Yanbu' al Bahr quadrangle, sheet 24C, Kingdom of Saudi Arabia: Saudi Arabian Directorate General of Mineral Resources Geologic Map GM–48–A, scale 1:250,000, *with* text, 24 p.

_____1981, Geologic map of the Al Madinah quadrangle, sheet 24D, Kingdom of Saudi Arabia: Saudi Arabian Deputy Ministry for Mineral Resources Geologic Map GM–52–A, scale 1:250,000, *with* text, 19 p.

_____1982, Geologic map of the Umm Lajj quadrangle, sheet 25B, Kingdom of Saudi Arabia: Saudi Arabian Deputy Ministry for Mineral Resources Geologic Map GM–61–A, scale 1:250,000, *with* text, 14 p.

Peltier, W.R., 1980, Models of glacial isostasy and relative sea level, *in* Bally, A.W., Bender, P.L., McGetchin, T.R., and Walcott, R.L., eds., Dynamics of plate interiors: American Geophysical Union and Geological Society of America, Geodynamic Series, v. 1, p. 111–128.

Powers, R.W., 1968, Lexique stratigraphique international, v. III, fas. 10bl, Arabie Saoudite: Paris, Centre national de la Recherche Scientifique, p. 76.

Powers, R.W., Ramirez, L.F., Redmond, C.D., and Elberg, E.L., Jr., 1966, Geology of the Arabian Peninsula—Sedimentary geology of Saudi Arabia: U.S. Geological Survey Professional Paper 560–D, 147 p.

Prinz, W.C., 1984, Geologic map of the Wādī Ḥalēy quadrangle, sheet 18E, Kingdom of Saudi Arabia: Ministry of Petroleum and Mineral Resources, Geoscience Map GM–74–C, scale 1:250,000, *with* text, 2 figs., 2 tables, 13 p.

Quennell, A.M., 1951, Geology and mineral resources of (former) Trans-Jordan: Colonial Geology and Mineral Resources [London] 2, p. 85–115.

Rathjens, Karl, 1942, Beobachtungen in Yemen: Geologische Rundschau, v. 33, p. 248–279.

Reischmann, Thomas, 1981, Petrographie and geochemie spat-Proterozoischer volkanite der Wadi Lith region, Saudi Arabia: Mainz, Germany, University of Mainz, Unpub. M.S. thesis, 172 p., 3 app.

Richardson, E.S., and Harrison, C.G.A., 1976, Opening of the Red Sea with two poles of rotation: Earth and Planetary Science Letters, v. 30, p. 135–142.

Richter-Bernburg, G., and Schott, W. (Amt fur Bodenforschung, Hannover, Germany), 1954, Geological researches in western Saudi Arabia: Saudi Arabian Directorate General of Mineral Resources Open-File Report 28, 69 p., 25 illus.

Roland, N.W., 1978, Jung palaozoisch Glazialspuren auf dem Arubischen Schild: Eiszeitalter u. Gegen, v. 28, p. 133–138, 4 figs.

Ross, D.A., and Schlee, John, 1977, Shallow structure and geologic development of the southern Red Sea, *in* Red Sea research 1970–1975: Saudi Arabian Directorate General of Mineral Resources Bulletin 22, p. E1–E18.

Sahl, M., and Al Fatawi, B., 1981, Reconnaissance geology of the Tayyibal Ism quadrangle, sheet 28/34B, Kingdom of Saudi Arabia: Saudi Arabian Deputy Ministry for Mineral Resources Open-File Report 01–18, 24 p., 2 figs, 1 pl.

Said, Rushdi, 1962, The geology of Egypt: New York, Elsevier, 377 p., 71 figs., 10 pls.

Sarnthien, M., 1978, Sand deserts during glacial maximum and climatic optimum: Nature, v. 272, p. 43–46.

Saxena, G.N., and Assefa, G., 1983, New evidence on the age of the glacial rocks of northern Ethiopia: Geology Magazine, v. 120(6), p. 549–554.

Schick, A.P., 1958, Marine terraces on Tiran Island, northern Red Sea: Geografiska Annalen Stockholm, heft 1, XL, p. 63–66, 4 figs.

Schmidt, D.L., 1980, Geology of the Wadi al Miyah quadrangle, sheet 20/42B, Kingdom of Saudi Arabia: USGS Saudi Arabian Mission Technical Record 12 (IR352); Saudi Arabian Directorate General of Mineral Resources Map series, scale 1:100,000, *with* text, 87 p., 21 figs., 9 tables, 2 pls.

_____1981a, Geology of the Jabal al Qarah quadrangle, sheet 20/43C, Kingdom of Saudi Arabia: USGS Saudi Arabian Mission Miscellaneous Document 31 (IR367); Saudi Arabian Directorate General of Mineral Resources Map series, scale 1:100,000, 52 p., 12 figs., 4 tables, 3 pls.

_____1981b, Geology of the Yafikh quadrangle, sheet 20/43D, Kingdom of Saudi Arabia: USGS Saudi Arabian Mission Miscellaneous Document 39 (IR397); Saudi Arabian Directorate General of Mineral Resources Map series, scale 1:100,000, 99 p., 14 figs., 14 tables, 2 pls.

_____1985, Reconnaissance geologic map of the Al Junaynah quadrangle, sheet 20/42D, Kingdom of Saudi Arabia: Saudi Arabian Directorate General of Mineral Resources Geologic Map GM 71–A, scale 1:100,000, *with* text, 31 p.

Schmidt, D.L., and Brown, G.F., 1984, Major-element chemical evolution of the late Proterozoic shield of Saudi Arabia: Symposium on Pan-African Crustal Evolution in the Arabian-Nubian Shield, 1st, International Geological Correlation Program Project 164, Faculty of Earth Sciences, King Abdulaziz University Bulletin (Jeddah), no. 6, p. 1–21, 13 figs.

Schmidt, D.L., and Hadley, D.G., 1985, Stratigraphy of the Miocene Baid Formation, southern Red Sea coastal plain, Kingdom of Saudi Arabia: U.S. Geological Survey Open-File Report 85–0241, 49 p.

Schmidt, D.L., Hadley, D.G., and Brown, G.F., 1983, Middle Tertiary continental rift and evolution of the Red Sea in southwestern Saudi Arabia: U.S. Geological Survey Open-File Report 83–0641, 60 p.

Schmidt, D.L., Hadley, D.G., Greenwood, W.R., Gonzalez, Louis, Coleman, R.G., and Brown, G.F., 1973, Stratigraphy and tectonism of the southern part of the Precambrian Shield of Saudi Arabia: Saudi Arabian Directorate General of Mineral Resources Bulletin 8, 13 p.

Schmidt, D.L., Hadley, D.G., and Stoeser, D.B., 1979, Late Proterozoic crustal history of the Arabian Shield, southern Najd Province, Kingdom of Saudi Arabia, *in* Tahoun, S.A., ed., Evolution and mineralization of the Arabian-Nubian Shield: King Abdulaziz

University, Institute for Applied Geology Bulletin 3 (Oxford-New York, Pergamon Press Ltd.), v. 2, p. 41–48.

Schmidt, D.L., Puffett, W.P., Campbell, W.L., and Al-Koulak, Z.H., 1982, Gold placer and Quaternary stratigraphy of the Jabal Mokhyat area, southern Najd Province, Kingdom of Saudi Arabia: U.S. Geological Survey Open-File Report 82–414, 76 p.

Schott, W., 1953, Geologische Studienreise nach Yemen: Zeitschrift der Deutschen Geologischen Geselleschaft, Hannover, bd. 105, pt. 3, p. 548.

Schurmann, H.M.E., 1966, The Precambrian in north Africa: Leiden, E.J. Brill, 351 p., 88 pls.

Scott, Hugh, and Britton, E.B., 1941, British Museum [Natural History] expedition to south west Arabia 1937–38: v. 1, pt. repts. 1-8.

Seilacher, Adolf, 1970, *Cruziana* stratigraphy of "non-fossiliferous" Paleozoic sandstone, *in* Crimes, T.P., and Harper, J.C., Trace fossils: Liverpool, Seel House Press, p. 447–476.

Sestini, Guilano [Julian], 1965, Cenozoic stratigraphy and depositional history, Red Sea coast, Sudan: American Association of Petroleum Geologists Bulletin, v. 49, no. 9, p. 1453–1472.

Shanti, M.S., and Roobol, M.J., 1982, Guide books for an excursion to the Jabal Ess-Ash Shism area of northern Saudi Arabia: International Geological Correlation Program, 1st symposium, project 164, Pan-African Crustal Evolution in the Arabian-Nubian Shield, Facility of Earth Science Research series no. 14, 35 p.

Shapiro, Leonard, 1967, Rapid analysis of rocks and minerals by a single-solution method, *in* Geological Survey research 1967: U.S. Geological Survey Professional Paper 575–B, p. B187–B191.

Shimron, A.E., and Brookins, D.G., 1974, Rb-Sr radiometric age of late Precambrian fossil-bearing and associated rocks from Sinai: Earth and Planetary Science Letters, v. 24, p. 136–140.

Shimron, A.E., and Horowitz, Akaron, 1972, Precambrian organic microfossils from Sinai: Pollen et Spores 14, no. 3 (Museum National d' Histoire Naturelle, Paris), p. 333–342, 15 figs.

Shukri, N.M., and Basta, E.Z., 1955, Petrography of the alkaline volcanic rocks of Yaman; Egyptian University scientific expedition to SW. Arabia: L'Institute du Desert de'Egypte Bulletin, v. 36, p. 129–163.

Silvestri, Alfredo, 1937, Fossile eocenico singolare della Tripolitania: Societa Geologica Italiana Bulletin, v. 56, p. 203–208.

Simlin, Tom, Siebert, Lee, McClelland, Lindsay, Bridge, David, Newhall, Christopher, and Latter, J.H., 1981, Volcanoes of the World: Stroudsburg, Pa., Hutchinson Ross, 232 p.

Skiba, W.J., 1980, The form and evolution of late Precambrian plutonic masses in the Jiddah-Rabigh-Wadi Al-Quaha area, Saudi Arabia, *in* Cooray, P.G., and Tahoun, S.A., eds., Evolution and mineralization of the Arabian-Nubian Shield: Institute for Applied Geology Bulletin 3, Oxford, Pergamon Press Ltd., v. 3, p. 105–120.

Skiba, W.J., and Warden, A.J., 1969, Preliminary report on the geology of selected areas in the southern part of the Arabian Shield: Saudi Arabian Directorate General of Mineral Resources Open-File Report 325, 42 p., 2 maps.

Smith, C.L., 1980, Brines of Wadi as Sirhan, Kingdom of Saudi Arabia: U.S. Geological Survey Open-File Report 80–1261, 30 p., 7 figs., 3 tables.

Smith, J.W., 1980a, Reconnaissance geologic map of the Wadi Mahani quadrangle, sheet 22/40A, Kingdom of Saudi Arabia: Saudi Arabian Directorate General of Mineral Resources Geologic Map GM–35, scale 1:100,000, *with* text, 18 p.

_____1980b, Reconnaissance geology of the At Ta'if quadrangle, sheet 21/40C. Kingdom of Saudi Arabia: Saudi Arabian Deputy Ministry for Mineral Resources Geologic Map GM–56, scale 1:100,000, *with* text, 33 p.

_____1982, Reconnaissance geologic map of the Wadi Hammah quadrangle, sheet 22/40C, Kingdom of Saudi Arabia: Saudi Arabian Deputy Ministry for Mineral Resources Geologic Map GM–65, scale 1:100,000, *with* text, 19 p.

Soliman, M.M., 1981, Petrology and geochemistry of some granitic rocks from the western Al-Quway'iyah region: Arabian Journal of Science and Engineering, F, no. 3, p. 289–297.

Souaya, F.J., 1966, Miocene foraminifera of the Gulf of Suez region, U.A.R.; Part 3, Biostratigraphy: Micropaleontology, v. 12, no. 2, p. 183–202.

Stacey, J.S., Roberts, R.J., Doe, B.R., Delevaux, M.H., and Gramlich, J.W., 1981, A lead-isotope study of mineralization in the Saudi Arabian Shield: Contributions to Mineralogy and Petrology, v. 74, p. 175–188.

Stacey, J.S., and Hedge, C.E., 1984, Geochronologic and isotopic evidence for early Proterozoic crust in the eastern Arabian Shield: Geology, v. 12, p. 310–313.

Steiger, R.H., and Jager, E., 1977, Subcommission on geochronology; Convention on the use of decay constants in geo- and cosmochronology: Earth and Planetary Science Letters, v. 36, p. 359–367.

Steineke, Max, Berg, E.L., and Wadsack, G., 1944, Preliminary map of the water resources and geology of the Jeddah-Usfan-Wadi Fatima area: U.S. Military Mission to Saudi Arabia in cooperation with the Arabian American Oil Co., unpub., scale 1:100,000.

Steineke, Max, Bramkamp, R.A., and Sander, J.J., 1958, Stratigraphic relations of Arabian Jurassic oil, *in* Habitat of oil: American Association of Petroleum Geologists symposium (Tulsa), p. 1294–1329, 6 figs.

Steinitz, G., Bartov, Y., and Hunziker, J.C., 1978, K-Ar age determinations of some Miocene-Pliocene basalts in Israel; Their significance to the tectonics of the Rift Valley: Geographic Magazine, v. 115, no. 5, p. 329–340.

Stoeser, D.B., 1985, Plutonic rock distribution map of the southern Arabian Shield, Kingdom of Saudi Arabia: U.S. Geological Survey Open-File Report 85–264, map, scale 1:500,000.

Stoeser, D.B., and Elliott, J.E., 1980, Post-orogenic peralkaline and calc-alkaline granites and associated mineralization of the Arabian Shield, Kingdom of Saudi Arabia, *in* Cooray, P.G., and Tahoun, S.A., eds., Evolution and mineralization of the Arabian-Nubian Shield: Institute for Applied Geology Bulletin 3, Oxford, Pergamon Press Ltd., v. 4, 168 p.

_____1985, Plutonic rock distribution map of the northeastern Arabian Shield, Kingdom of Saudi Arabia: Saudi Arabian Deputy Ministry of Mineral Resources, USGS-OF-04-52; *also* U.S. Geological Survey Open-File Report 85–0255, map, scale 1:500,000.

Streckeisen, A.L., 1973, Plutonic rocks, classification and nomenclature recommended by the IUGS Subcommission on the Systematics of Igneous Rocks: Geotimes, v. 18, no. 10, p. 26–30.

_____1976, To each plutonic rock its proper name: Earth-Science Reviews, v. 12, no. 1, p. 1–33.

_____1979, Classification and nomenclature of volcanic rocks, lamprophyres, carbonatites, and melititic rocks; Recommendations and suggestions on the systematics of igneous rocks: Geology (Boulder), v. 7, p. 331–335, 1 table.

Stuckless, J.S., and VanTrump, George, Jr., 1979, A revised version of Graphic Normative Analysis Program (GNAP) with examples of petrologic problem solving: U.S. Geological Survey Open-File Report 79–1237, 115 p.

Taylor, H.P., Jr., and Coleman, R.G., 1977, Oxygen isotopic evidence for meteoric-hydrothermal alteration of the Jabal at Tirf igneous complex, Saudi Arabia [abs.]: EOS, Transactions of the American Geophysical Union, v. 58, no. 6, p. 316.

Thatcher, Leland, Rubin, Meyer, and Brown, G.F., 1961, Dating desert ground water: Science, v. 134, p. 104, 105.

Theobald, P.K., and Thompson, C.E., 1966, Geology and geochemistry of a part of the Ablah Formation at Jabal Rumur, Kingdom of Saudi Arabia: U.S. Geological Survey Open-File Report (IR)SA–88, 15 p., 8 figs., 2 tables.

Thorpe, R.S., 1972, Ocean floor basalt affinity of Precambrian schist from Anglesey: Nature (Physical Science), v. 240, Dec. 18, p. 165.

Tothill, J.D., ed., 1948, Agriculture in the Sudan: Oxford, Oxford University Press, 974 p.

Trent, V.A., and Johnson, R.F., 1966, Reconnaissance mineral and geologic investigation in the Maqna quadrangle, Aqaba area, Saudi Arabia: U.S. Geological Survey Open-File Report (IR)SA–51, 5 p., 3 figs.

Tromp, S.W., 1950, The age and origin of the Red Sea graben: Geological Magazine, v. 87, p. 385–392.

Twitchell, K.S., 1958, Saudi Arabia, with an account of the development of its natural resources: Princeton, N.J., Princeton University Press, 281 p.

Uchimizu, Mamoru, 1966, Geology and petrology of alkali rocks from Dogo, Oki Islands: Tokyo University Faculty of Science Journal, sec. 2, v. 16, pt. 1, p. 85–159, illus. (incl. geol. map, scale 1:80,000).

U.S. Geological Survey, 1972, Topographic map of the Arabian Peninsula: Saudi Arabian Directorate General of Mineral Resources Arabian Peninsula Map AP–1, scale 1:4,000,000.

U.S. Geological Survey–Arabian American Oil Company (USGS–ARAMCO), 1963, Geologic map of the Arabian Peninsula: U.S. Geological Survey Miscellaneous Geologic Investigations Map I–270–A, scale 1:2,000,000.

Vail, J.R., 1971, Geological reconnaissance in part of Berber District, northern province, Sudan: Sudan Geological Survey Department Bulletin 18, Khartoum, 76 p., 2 pls., 6 figs., 2 tables, 1 map.

Vesey-FitzGerald, D.F., 1955, Vegetation of the Red Sea coast south of Jeddah, Saudi Arabia: Journal of Ecology, v. 43, p. 477–489.

_____1957, The vegetation of central and eastern Arabia: Journal of Ecology, v. 45, p. 779–798.

Vidal, Gonzalo, 1979, Acritarchs from the upper Proterozoic and lower Cambrian of East Greenland: Grønlands Geologiske Under søgelso, Bulletin 134, p. 8, 34, 35.

Vincent, Gerard, 1968, Geology and mineral resources of the Halaban-Sabhah region (sheet 118, zone 2): [France] Bureau des Recherches Geologiques et Minieres Open-File Report 68–JED–1, 3 app., scale 1:100,000.

Warden, A.J., 1982, Reconnaissance geology of the Markas quadrangle, sheet 18/43B, Kingdom of Saudi Arabia: Available from Saudi Arabian Deputy Ministry for Mineral Resources, 58 p., scale 1:100,000.

Wendorf, Fred, Schild, Romuald, Said, Rushdi, Haynes, C.V., Gautier, A., and Kobusiewicz, M., 1976, The prehistory of the Egyptian Sahara: Science, v. 193, no. 4248, p. 103–114.

Wetzel, Rene, and Morton, D.M., 1959, Contribution a la geologie de la Transjordanie: Museum National d'Histoire Naturelle (Paris), Notes et memoires sur le Moyen Orient, t. 7, p. 107–120.

Whiteman, A.J., 1970, Nubian group: Origin and status [discussion]: American Association of Petroleum Geologists Bulletin, v. 54, no. 3, p. 522–526.

_____1971, The geology of the Sudan Republic: Oxford, Clarendon Press, 290 p.

von Wissman, Herman, 1963, Catalogue of the active volcanoes of the world including solfatara fields (Neumann van Padang, M., ed.): Rome, International Association of Volcanology Catalogue, v. 16, p. 3.1-1—3.1-12.

Worl, R.G., 1978, Ore controls at the Mahd adh Dhahab gold mine, Kingdom of Saudi Arabia, *in* Evolution and mineralization of the Arabian-Nubian Shield: King Abdulaziz University, Institute of Applied Geology Bulletin 3 (Oxford-New York, Pergamon Press Ltd.), v. 2, p. 93–106.

Wyllie, P.J., 1977, Crustal anatexis: An experimental review: Tectonophysics, v. 43, p. 41–71.

Yamani, M.A., 1968, Geology of the oolitic hematite of Wadi Fatima, Saudi Arabia, and the economics of its exploitation: Ph.D. thesis, Cornell University, Ithaca, N.Y., 10 p., 9 figs., 2 pls.

Zak, I., and Freund, R., 1981, Asymmetry and basin migration in the Dead Sea rift: Tectonophysics, v. 80, no. 1-4, p. 27–38.